BIOLOGICAL MOTILITY

New facts and hypotheses

УДК 577.3
ББК 28.07
   В60

Biological motility: new facts and hypotheses. – Pushchino:
ITEB RAS – 2014. – 362 p.

This volume contains the presentations that were made during the International Symposium "Biological motility: new facts and hypotheses". It took place in Pushchino, Moscow region and was devoted to new ashievements and perspectives in this area of knowledge.
Materials of the Symposium are of interest for biologists, medical and other specialists.

ISBN 978-5-903789-22-1

THE PLANT GROWTH REGULATOR – MELAFEN, ACTIONS TO THE BOVINE SERUM ALBUMIN CONFORMATIONS

O.M. Alekseeva

Institute of Biochemical Physics, RAS, Moscow, 119334, Russia
E-mail: olgavek@yandex.ru

Melafen is a plant growth regulator - heterocyclic organ phosphor compound, synthesized at the Arbuzov Institute of Organic and Physical Chemistry of RAS. Melafen is the melamine salt bis (oximethyl) phosphinic acid. It was acquired by one stage with high stepping out of industrially available products. Melafen raises the plants stress-resistance in the conditions of overcooling and drought, increasing the effectiveness of energy metabolism. In this melafen cases the change of the fatty acid composition and the microviscosity of microsome and mitochondrial membranes in vegetable cell [1, 2].

This investigation deals with the influence of melafen, at the wide concentration range of aqua solutions, applied in agriculture, as of plant growth regulator, to the structural properties of soluble pro-tein: bovine serum albumin (BSA) The melafen interactions were tested by the spectral methods. We did not reveal any noticeable dis-tractions action to the BSA structure.

Melafen is a hydrophilic polyfunctional substance (fig. 1). It is the regulator of plants stress tolerance under the bed environment. Aqueous solutions of Melafen at concentration 10^{-11} - $^{-9}$M increased the plant growth, but under the concentration of melafen to 10^{-8}, 10^{-7} M plant's seeds dyed. Therefore, our studies were carried out in a wide range of concentrations (10^{-21} – 10^{-2} M). The main purpose was to determine how the aqueous solutions of melafen in a wide range of concentrations influence to the structure of BSA.

The selection of BSA as of experimental object was determined by the number of causes. First, this is one of the first targets for BAS. Second, BSA is perfect carrier for endogenous, like some free fatty acids, hormones, metal ions, bilirubin and etc. and exogenous materials. Third, its structure is
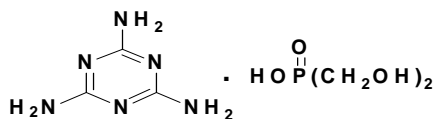

Fig. 1. Structural formula of melafen.

labile, and varies very easily. The molecular interaction of serum albumins with transported materials is determined of their structural mobility, conditioned by the loop stowage of polypeptide chain, composed of 582 amino acid residues. Some changes of serum albumins conformation were registered on change of extent of quenching its intrinsic fluorescence. The numerous works is performed by this time using of this approach for test actions of any BAS on albumins [3].

There is the emission of 2 tryptophane residues in hydrophobic regions of molecule BSA. First residue is located is with close to a surface, second – located at the deep inside of the protein globule. When loosening or molecule unfolding the availability for quencher - oxygen, dissolute in water, increase. The quenching of tryptophane fluorescence was observed at this case.

Results and discussion

When we study on the effect of aqueous solutions of melafen on spectrum patterns of BSA we don't found any important changes in absorption spectrums BSA. These data provides evidence about absence of the covalent linkage of melafen with protein BSA molecule. However, in registration of fluorescence spectrum, presented in figure 2, revealed facts, indicative of great influence of aqueous solution of Melafen over a wide range of concentrations on conformation of BSA. Al solutions under the different concentrations of Melafen was not displaced the wavelength of fluorescence maximum. However the intensity has undergone a change. Was found the great quenching of tryptophane fluorescence when 10^{-4} M of melafen and the burst of fluorescence intensity when 10^{-17} M - 10^{-10} M (fig. 2, 3). The changes of fluorescence tryptophan intensity residues BSA are introduced on fig. 2.
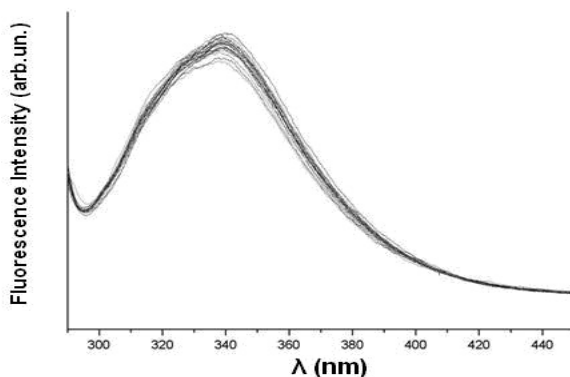
Fig. 2. The influence of Melafen over a wide range of concentrations to the intensity of emission spectra of BSA tryptophane residues.
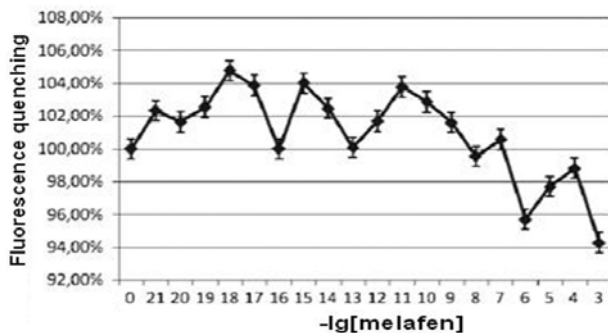
Fig. 3. The Melafen influence to the fluorescence intensity of BSA. The control samples in absentia of melafen have been adopted the fluorescence intensity as 100%. More 100% - is some burst of fluorescence intensity, less - is the quenching of fluorescence intensity.

The fluorescence of BSA tryptophan residues was quenched by Melafen under the wide region of concentration (fig. 3).

As it can be seen from comparison of data, presented at fig. 2 and 3, the shapes of emission spectra were similar. Only the maximal value of fluorescence intensity was change in dependence from the Melafen concentrations. Than, we build a curve of the dependence of value at the maximum of tryptophan emission from Melafen concentration. We obtained the noticeable tendency of the fluorescence quenching by the Melafen large concentrations. And the burst of fluorescence intensity was occurred when low and ultra small concentrations of Melafen presented at the experimental medium. The dose-dependence was polymodal, which is representative for BAS, effectual in ultra small doses [4]. Evidently, conformational rearrangements occurred in BSA molecules. These rearrangements were small, and had the different direction.

Conclusion

Evidently, melafen molecules affected to the albumin so that under the small and ultra small concentrations there was the preserving of the protein tryptophane residues from quenching from oxygen, dissolved in water. And under the large melafen concentrations the change of protein conformation became so essential. At this case the tryptophan residues that deep lying became more available to water (and oxygen, respectively), on that indicated the fluorescence quenching. Occurs "the loosening" of molecule BSA structure. We may conclude that the soluble proteins that unhardened of the membrane lipids were under the melafen actions. Taking into account that melafen is the hydrophilic substance, and

5

it can change the water environment. At this case we may suppose that melafen influence to BSA by two ways: mediated through the water, or directly to the influence to hydrophilic sites of BSA molecules. Mechanism was unknown. These influences were mainly changed in dependence on melafen concentration present in surrounding solution. There were not clear evidences of BSA-melafen linkage existence. However mediated action through the change of water medium appears to occur surrounding the protein's molecules.

Also the water solutions of melafen may be the regulator of transporting function of albumins, as its will be introduced to the animal's body. And it may be take part in extracting fatty acids from any molecules, or bounding of free fatty acids by albumins. As its known the water solutions of melafen change the fatty acid's content of membranes [2].

References
1. Zhigacheva I.V., Fatcullina L.D., Burlakova E.B., Shugaev A.I., Generosova I.P., Fattahov S.G., Konovalov A.I. " Influence of phosphoorganic plant growth regulator to the structural characteristics of membranes plant's and animal's origin" // Biological membrane, 2008, v. 25, №2, P. 150-156.
2. Zhigacheva I.V., Misharina T.A., Trenina M.B., Krikunova N.N., Burlakova E.B., Generosova I.P., Shugaev A. I., Fattahov S.G. "Fatty acid's content of mitochondrial membranes of Pea seedlings in conditions of insufficient moistening and treatment by the phosphoorganic plant growth regulator" // Biological membrane, 2010, v. 27, P. 256-261.
3. Diaz X., Abuin E., Lissi E. "Quenching of BSA intrinsic fluorescence by alkylpyridinium cations its relationship to surfactant-protein association" // Journal of Photochemistry and Photobiology, 2003, № 155, P. 157-162.
4. E.B. Burlakova "Effect of ultrasmall doses". // Vestnik RAS. 1994. V. 64. № 5. P. 425-431.

CHARACTERISTIC OF BONE MARROW MULTIPOTENT MESENCHYMAL STROMAL CELLS ABILITY TO INTERACT WITH ENDOTHELIAL CELLS MONOLAYER

S.A. Alexandrova, A.V. Alexandrova, G.P. Pinaev
*Institute of Cytology RAS, Tikhoretzki pr., 4,
St.Petersburg, 196064, Russia;
Dep. of Medical Physics, St.Petersburg State Polytechnical University,
Polytechnicheskaya str., 29, St.Petersburg, 195251, Russia*

Despite the identified positive therapeutic effect in a number of diseases, many aspects of the clinical using of multipotent mesenchymal stromal cells (MSCs) of bone marrow remain open, in particular, those

related to their migration through the body after injection into the bloodstream. According to preliminary studies, MSCs overcome the endothelial barrier in a similar process with leukocytes - selectin-mediated rolling, integrin-mediated adhesion, transendothelial migration (lateral type). Leukocytes use cytoskeletal protrusions (eg, lamellipodia, pseudopodia and invadosomes) to cross the endothelium through discrete gaps in intercellular junctions or directly through pores in individual ECs. In turn, endothelium generates its own actin-dependent protrusions that embrace the leukocytes. This process occurs with the assistance of a number of specific adhesion molecules whose expression level is increased at the lesion site under the influence of pro-inflammatory factors in both cell types. In addition, there is evidence in the literature that there are other mechanism that some cells use to migrate from high speed - amoeboid type of movement, which is typical for metastatic tumor cells and embryonic germ cells. However, the molecular and cellular details of process MSCs trafficking have not been well-resolved.

The literature data show that bone marrow MSCs expanded *ex vivo* and introduced into the bloodstream quickly migrated through the body to reach the damaged area. The authors also noted such features as the accumulation of the cells in the lung microvascular endothelium, disability of big part of cell population to overcome the endothelial barrier, the low efficiency of tissue penetration. It is known that bone marrow MSCs, expanded in culture, look like as fibroblasts and are highly adhesive, capable of slow lateral migration of mesenchymal type. We can assume that microenvironment have a big influence on MSCs migration during bloodstream trafficking, in particular, the cells can be exposed to different factors such as plasma proteins and factors produced at the site of injury (proinflammatory cytokines, such as tumor necrosis factor α, TNFα). Importantly, the process of MSCs extravazation will also directly affect the endothelial cells (ECs) lining the capillaries. Normally, the endothelium has a smooth surface coated by a layer of glycocalyx lumen having anti-adhesive properties and prevent sticking of platelets and other cells. Under the influence of pro-inflammatory factors ECs express cell adhesion molecules that bind the cell, migrating to the lesion and promote its movement in the tissue. So transendothelial migration is a complex process, which is attended by at least two types of cells and a number of soluble factors. The aim of our work was to characterize the population of primary cultures of rat bone marrow MSCs based on the organization of the actin cytoskeleton before and 1 h after exposure to intact and TNFα-activated endothelial cells.

Materials and Methods

We used a population of bone marrow MSCs from outbred rats 3-4 passage cultivation and ECs from EA.hy 926 cell line. ECs were cultured on glass slides placed in wells of 12-well plates until forming a confluent monolayer, in some wells were TNFa (200 U/ml), rat plasma (10 %), or both during 1 day. The suspension of bone marrow cells (200 thousand cells) stained by vital fluorescent dye CFSE was added to the wells and incubated with ECs for 1 h. Also MSCs were added on clean glass into the growth medium with supplements and incubated for 1 hour with goal to examine non-specific adhesion (controls). Non-adherent cells were removed by means PBS, remaining cells were fixed, treated with a solution of Triton X-100 and stained with rhodamine-phalloidin (Invitrogen, USA). Finished products were analyzed using a fluorescence microscope LSM 5 Pascal.

Results and Discussion

When MSCs were attached to glass under standard culture conditions, about half of the population of MSCs has seen as weak sprawled rounded cells (58±2%). Among them there were the cells of different size, border cells were uneven, were visible surface "bulge". Cells contained either submembrane network actin or large round actin aggregates (often only one pole of the cell). Some of these cells had structure for contact with the surface - basal microvilli or small lamella. 36±2% of MSCs were presented more spreaded cells with a broad lamella edge. Lamella could be noncontinious or could surround the cell by wide layer around. Actin network was poorly observed, present at the edge of the lamella, but the majority of actin microfilaments was concentrated in the center of the cell. The number of such cells was significantly increased in the presence of TNFa (59±3%) and 10 % plasma (69±9%). Also we could noticed single well spreaded cells that were elongated in one or several directions. They formed numerous lamellipodia with several fillopodia. Actin cytoskeleton of that cells was represented by a network of microfilaments. Clusters of radial filaments were visible in filolopodia forming focal contacts with the surface.

When MSCs were attached to the ECs monolayer - number of weak spreaded rounded cells was also about half the population of MSCs and varied slightly depending on the conditions (45±5%). Unlike the cells cultured on glass, there were no cells with broad lamella, surrounded the cells. The most spreading cells looked like rounded cells containing large aggregates of actin and small bulges on the surface of

cells. And such cells were surrounded around by narrow lamella with jagged edges, sometimes forming fillopodia or microvilli. Most of these cells were attached to the surface of endothelium treated with TNFa (67±2%). Also there were small round cells, the surface of which was covered with swellings - most likely there has been a so-called nonapoptotic membrane blebbing. These cells did not form any adhesive structures with ECs or surface. Sometimes it was possible to observe them in gaps between ECs. Also, could be met well-flattened elongated bone marrow cells, contacting with ECs using focal contacts. The greatest number of such cells were observed in preparations where the endothelium was incubated in the presence of TNFa and plasma simultaneously (14±3%). These cells were located mainly in the gaps between the ECs, linking them with each other.

It can be concluded that may be several explanations for why only a small number of MSCs capable to transmigrate from the bloodstream into the tissues. It may be related to the fact that a significant part of the MSCs population does not capable of adhesive interactions with the ECs. At first, it may be associated with a reduction in their viability after changing their microenvironment. If earlier it had been part of the monolayer of cells growing on a extracellular matrix, that for infusion into bloodstream it must be converted into a single cell form, and moreover there it can be exposed to the new microenvironment (different cells and soluble factors). At second, in this process an important role play peculiarities of the interaction between MSCs and ECs. Probably, migration cells can use mechanism of slow lateral migration, forming small fillopodia, or use mechanism of fast amoeboid migration with participation of membrane blebbing. Currently it is impossible to distinguish of the part of the population of these cells that is not able to transendothelial migration. With the greatest certainty it can be argued that the part of MSCs population, that were able to form focal contacts with the ECs, will not capable to migrate anyway. The number of such cells were increased in the presence of proinflammatory cytokine TNFa and blood plasma, which contributed to the formation of gaps between the ECs, as well as the expression of adhesion molecules. This phenomenon may be connected as with varying degrees of differentiation cells in MSCs population, so with different functions of different populations of MSCs partitioning in degree of maturity and expression of adhesion molecules.

PRIMARY CULTUTER OF RAT CORTICAL NEURONS AS A MODEL TO INVESTIGATE CENTRAL MECHANISMS OF EPILEPTIC SEIZURES

S.M. Antonov

Sechenov Institute of Evolutionary Physiology and Biochemistry RAS, Torez prosp. 44, Saint-Petersburg, 194223, Russia

Embryonic development of brain cortex engages significant changes of neuronal network. During this period brain is very vulnerable to the generation of epileptiform activity. Even later in postnatal period the epileptic focus is often located in cortex. Similar state of neuronal network exists in neurons at 12 days of *in vitro* culturing (DIV). The primary culture of cortical neurons is a convenient model to study the physiology of neuronal network. Glial deficiency and flat topology of culture determine some specific functional features different from brain slices. Nevertheless primary cultures of cortex and hippocampus demonstrate epileptiform spiking activity of neurons that is similar for those in brain slices. Recording using extracellular microelectrode arrays from the cortical culture treated with magnesium free medium reveals recurring spontaneous epileptiform discharges lasting up to several days after treatment. Short-time (few minutes) block of inhibitory synaptic transmission with bicuculline triggers self-maintained epileptiform spiking of neurons in brain slices and in brain tissue explants. Both mentioned approaches to induce epileptiform activity trigger periodic increase in intracellular calcium concentration ($[Ca^{2+}]i$). Despite of numerous investigations of mEPSCs in hippocampus cultures, there are only few studies concerning postsynaptic currents in cortical culture. In fact, epileptiform postsynaptic currents in primary culture of rat cortical neurons were not studied and described previously.

In this study we demonstrate that the primary culture of rat cortical neurons is a convenient model for investigations of epileptogenesis mechanisms and specifically, of the postsynaptic epileptiform currents (EC) reflecting periodical asynchronous glutamate release. Starting from 12 DIV in neurons of rat primary cortical culture spontaneous excitatory waves are recorded. These waves arise from massive neurotransmitter release resulting in high amplitude inward currents (up to 5 nA) (fig. 1) with the decay phase up to 5 seconds. The generation of such waves is possible in both magnesium containing (fig. 1A) and magnesium free medium (fig. 1B). However in magnesium-free solution the probability of generation of these currents was much higher. These ECs were periodic and resulted from overlapping multiple mEPSCs (fig. 1C). EC produced significant depolarization of neurons (fig. 1D) promoting action poten-

tials generation. Whereas in some of neurons ECs were completely suppresses with 0.5 μM TTX, in 12 of 24 neurons ECs were resistant to its action. Apparently EC generation is only partly dependent on action potentials. In turn ECs can trigger action potentials. Recordings in current clamp mode demonstrate that action potentials appear in response to strong (up to 30 mV) depolarization caused by ECs.

In magnesium-free medium the block of NMDA receptors (NMDARs) with the specific antagonist, AP5 (50 μM) completely inhibited EC generation in all 14 cells tested. Similar effect was observed after adding of 1 mM MgCl$_2$ to perfusate (n = 12). Competitive inhibitor, AP5 prevents NMDARs activation as well as Mg^{2+}, which is a noncompetitive inhibitor blocking the NMDAR channels. Thus, both agents suppress Ca^{2+} entry into neurons via NMDARs, demonstrating that NMDAR functioning to be critical for the EC generation. AMPA receptors antagonist, CNQX (30 μM) in magnesium-free solution decreased mEPSC's amplitude, but did not affect ECs in 9 of 11 cells tested. Thus, the EC generation is mostly independent of AMPA-receptors, despite of their key role in excitatory synaptic transmission.

In one fifth of experiments ECs could be provoked by block of GABA$_A$ receptors with bicuculline. Bicuculline (20 μM) application increased spontaneous mEPSC's frequency, which was followed by mEPSC synchronization and appearance of ECs lasting even after bicuculline washout. Bicuculline triggered ECs were completely inhibited with TTX, that distinct them from spontaneous ECs. Taking into account that [Ca^{2+}]$_i$ controls vesicular neurotransmitter release and then the generation of all types of postsynaptic currents, we have tested the possibility of EC modulation by pharmacological treatments increasing or decreasing [Ca^{2+}] in cytoplasm. Spontaneous ECs were completely inhibited with receptor saturating concentration of NMDA (30 μM + 30 μM glycine as NMDARs co-agonist) causing stable inward current (n = 22). This current promoted [Ca^{2+}]$_i$ elevation in neurons, which was accompanied with mEPSC's frequency increase. In two of experiments NMDA wash-out partially restored the EC generation. The accelerated accumulation of free calcium in cytoplasm could also be produced by calcium ionophore, ionomycin (2 μM). This kind of [Ca^{2+}]$_i$ elevation desynchronized ECs and gradually reduced EC's amplitude until complete vanishing. At the same time ionomycin significantly increased mEPSC's frequency.

Physiological [Ca^{2+}]$_i$ elevation may also result from activation of IP$_3$-sensitive calcium channels located at the membrane of intracellular calcium stores and secondary free calcium release. In neurons this process
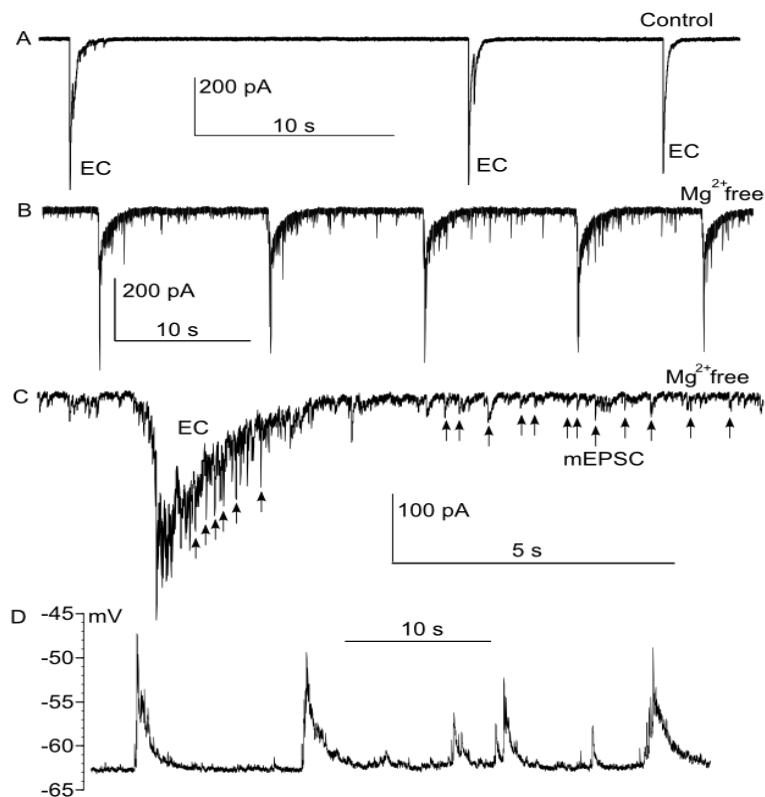
Fig. 1. Epileptiform currents (ECs) in neurons of rat primary cortical culture recorded by patch clamp in whole-cell configuration at -70 mV. Repeated spontaneous ECs in control (A) and in magnesium-free medium (B). The composition of EC (C) as an overlay of multiple mEPSCs. Cell membrane depolarizations recorded in current clamp and produced by ECs (D).

is involved in vesicle's release synchronization. The block of IP$_3$-receptors with membrane permeable inhibitor, 2-APB (4 μM) desynchronized ECs ($n = 6$). The concentration of 2-APB used in our experiments was enough to block IP$_3$-receptors. Whereas this concentration is insufficient to perform 2-APB's nonspecific pharmacological properties like: inhibition of TRP-channels, activation of TRPV-channels or suppression of some calcium-permeable channels of mitochondria or endoplasmatic reticulum. In the presence of 2-APB high amplitude ECs dissipated into multiple events of smaller amplitude with further gradual decrease of

amplitude to the level of mEPSCs. Thus, Ca^{2+} release from intracellular stores is required to synchronize mEPSCs and to form ECs.

Cytoplasmatic free calcium clearance with Na^+/Ca^{2+}-exchanger is critically important mechanism of neuronal calcium homeostasis. Recently we have found, that ouabain at subnanomolar concentrations does not affect Na/K-ATPase pumping function, but interact with Na/K-ATPase in ligand-receptor manned and triggers several intracellular pathways. The fastest of these pathways increases the effectiveness of calcium removal with Na^+/Ca^{2+}-exchanger, which can even save neurons from glutamate receptor hyperactivation induced calcium overload. This effect manifests only in calcium overloaded states, but does not affect $[Ca^{2+}]_i$ in control. Ouabain at 1 nM did not influence spontaneous mEPSC's frequency in control ($n = 9$). When studies on ECs ($n = 9$) ouabain (1 nM) application decreased the number of mEPSCs inside of each EC in a min. In 5 min 1 nM ouabain treatment caused desynchronization and gradual fading of ECs.

Thus, generation of ECs by cortical neurons in primary culture can appear in a spontaneous manner or can be provoked either by removal of magnesium block of NMDA receptors, or by inhibition of GABAergic synaptic transmission. Most likely ECs depend on oscillations of $[Ca^{2+}]_i$ which in turn depends on the NMDA receptor activation and the secondary release of Ca^{2+} from intracellular depots. Treatments causing calcium overload (NMDA, ionomycin) or calcium shortage (BAPTA, ouabain) suppress the EC generation. Thus, ECs in neurons are activated by intracellular periodic calcium waves within a limited concentration window.

EFFECTS OF STABILIZING SUBSTITUTIONS IN THE MIDDLE PART OF TROPOMYOSIN, D137L AND G126R, ON THE DOMAIN STRUCTURE OF ITS MOLECULE

Natalia V. Artemova[1], Alexander M. Matyushenko[1,2], Nikolai N. Sluchanko[1] and Dmitrii I. Levitsky[1,3]

[1] *Bach Institute of Biochemistry, Russian Academy of Sciences, Moscow, Russia;*
[2] *Department of Biochemistry, School of Biology, Moscow State University, Moscow, Russia;*
[3] *Belozersky Institute of Physico-Chemical Biology, Moscow State University, Moscow, Russia*

Recent studies have revealed two non-canonical residues in the middle part of tropomyosin (Tm), Asp137 and Gly126, whose substitu-

tions with canonical residues (mutations D137L and G126R) stabilized the Tm coiled-coil in this region [1, 2]. We applied differential scanning calorimetry (DSC) in combination with other methods and approaches to investigate and compare the effects of these mutations on the domain structure of Tm. Moreover, we for the first time analyzed the structure of Tm carrying both these substitutions within the same molecule (mutation D137L/G126R). It has been shown that all these mutations in the middle part of Tm significantly alter the thermal unfolding of its molecule. The most surprising effect was observed with the double Tm mutant (Tm G126R/D137L): this mutant protein demonstrated a new high-temperature thermal transition at 63.5°C, which has never been observed in the previous DSC studies on Tm.

In order to examine the effects of the stabilizing amino acid substitutions in the middle part of Tm on the domain structure of Tm molecule, it was reasonable to identify the thermal transitions (the so-called "calorimetric domains") observed on the DSC profiles, i.e. to assign them to the certain parts of the molecule. For this purpose, we applied two special approaches. One of them utilized a combination of DSC studies with measurements of temperature dependence of pyrene excimer fluorescence, whose decrease reflected the dissociation of two Tm chains in the vicinity of a cysteine SH-group to which the label was attached. Another approach was based on a cross-linking of the two Tm chains by formation of a disulfide bond between Cys residues of the Tm dimer in the non-reducing conditions. It has been shown in the previous DSC studies that the cross-linking at the single Cys residue of Tm WT at position 190 strongly increases the thermal stability of the Tm C-terminal domain where Cys190 is located [3]. Obviously, the presence of single Cys residue in different parts of the Tm molecule was required in both these approaches. For this purpose, a number of Tm mutants containing the single Cys residue in different parts of Tm was produced: Tm with Cys36 in the N-terminal part (mutation S36C/C190A), Cys123 in the middle part (mutation S123C/C190A), as well as Tm WT containing Cys190 in the C-terminal part of the molecule. All these Tm mutants were used to investigate effects of D137L, G126R, and D137L/G126R substitutions in the middle part of Tm on the domain structure of its molecule.

Preliminary results showed that the investigated substitutions may stabilize not only the middle part of Tm, but also some other parts, including its N- and C-terminal domains, suggesting long-range effects. For example, the unusual high-temperature thermal transition at 63.5°C,

which was observed on the DSC profile of Tm G126R/D137L, was assigned to the N-terminal domain strongly stabilized by the mutations in the middle part of Tm. In conclusion, our results indicate that the stabilization of the middle part of Tm by replacement of non-canonical residues Asp137 and Gly126 (and especially both of them simultaneously) by canonical ones can be transmitted along the Tm coiled-coil, by this means stabilizing even remote parts of its molecule.

References

1. Sumida J.P., Wu E., and Lehrer S.S. (2008) "Conserved Asp-137 imparts flexibility to tropomyosin and affects function". J. Biol. Chem. 283, 6728–6734.
2. Nevzorov I.A., Nikolaeva O.P, Kainov Y.A., Redwood C.S., and Levitsky D.I. (2011) "Conserved noncanonical residue Gly-126 confers instability to the middle part of the tropomyosin molecule". J. Biol. Chem. 286, 15766–15772.
3. Kremneva E., Boussouf S., Nikolaeva O., Maytum R., Geeves M.A., and Levitsky D.I. (2004) "Effects of two familial hypertrophic cardiomyopathy mutations in α-tropomyosin, Asp175Asn and Glu180Gly, on the thermal unfolding of actin-bound tropomyosin". Biophys. J. 87, 3922–3933.

EFFECTS OF INTRA-SESSION ENDURANCE AND STRENGTH TRAINING ON THE EXPRESSION OF OXIDATIVE AND PROTEOLYTIC GENES

A.V. Bachinin[1], D.V. Popov[1,2], E.A. Lysenko[1], T.F. Miller[1], O.L. Vinogradova[1,2]

[1] *Institute for Biomedical Problems, Russian Academy of Sciences, Khoroshevskoye sh. 76A, Moscow, 123007, Russia;*
[2] *Faculty of Fundamental Medicine, Lomonosov Moscow State University, Lomonosovsky prosp. 31-5, Moscow, 117192, Russia*

Endurance exercise induces activation of mitochondrial biogenesis by activation of AMP-dependent protein kinase (AMPK) and p38 mitogen-activated protein kinase. This leads to activation of peroxisome proliferatior-activated receptor gamma coactivator 1 alpha (PGC-1α) – a master regulator of mitochondrial biogenesis, and induces expression of oxidative genes (*TFAM, CS*) as well as *PGC-1a* gene. On the other hand,

aerobic exercise is known not to increase the postexercise fractional synthesis rate of myofibrillar proteins. Moreover, it might be followed by muscle protein breakdown induced by expression of E3 ubiquitin ligases. The aim of the present study was to examine possibility to eliminate the negative effects of endurance exercise on the expression of oxidative and proteolytic genes by using the sequence of endurance exercise session followed by strength exercise.

Nine amateur endurance trained males carried out test sessions: endurance exercise (70 min) and endurance exercise followed by strength exercise. Biopsy samples from m.vastus lateralis were taken before, 40 min, 5 h and 21 h after termination of endurance exercise. Expression of oxydative (*PGC-1a, TFAM, CS*) and catabolic (*Myostatin, Atrogin-1, MuRF*) genes was evaluated by real-time PCR.

Endurance exercise alone and in combination with strength exercise was accompanied by significant accumulation of capillary blood lactate level. Expression of oxidative genes was increased after both exercise sessions, while expression of the markers of exercise-induced catabolism was different in two groups. Thus intra-session endurance and strength training may be used to optimize the effect of endurance exercise.

Ca-DEPENDENT ENZYMES AS REGULATORS OF SYNAPTIC PLASTICITY IN MOTOR SYNAPSES
O.P. Balezina

Department of Human and Animal Physiology, Moscow State University, Leninski gory, MSU, 119992, Russia

The phenomenon of synaptic plasticity means the ability of synapses to potentiate or diminish their efficacy due to specific pattern of stimulation or regulatory influences. Ca-dependent enzymes calcium/calmodulin-dependent protein kinase II (CaMKII), proteinkinase C (PKC) and others are known to take part in postsynaptic plasticity in central synapses [Nichols et al., 2001].

Similar Ca-dependent enzymes have been recently identified in presynaptic nerve terminals of peripheral neuro-muscular synapses [NaoCheng at al., 2006; Wang, 2008; Shakiryanova et al., 2011 Besalduch et al., 2011]). Numerous presynaptic Ca-inputs are also present in these nerve terminals, including different types of Ca channels, presynaptic ryanodine receptors

(RyRs) and Ca-conducting channels of alpha7-nicotinic acetylcholine receptors (alpha7nAChRs) [Catteral et al., 2013]. Which of these presynaptic calcium inputs do participate in activation of individual Ca-dependent enzymes, regulating mediator release, is poorly understand.

The aim of our work was to study selective Ca-dependent activation of three Ca dependent enzymes – PKC, CaMKII and PP2B -phosphatase calcineurin (CaN) in mouse motor nerve terminals, and to clear their role in regulation of mediator secretion . As probable enzyme activators calcium ions were tested entering nerve terminals through different pathways. There were:1) voltage dependent Ca-channel of P/Q- and L-type, 2)channels of alpha7 -nAChRs 3) Ca release from ryanodine receptors.

The electrical activity of neuromuscular synapses of *m.diaphragma* of adult mice (20-30 g) were tested. The isolated neuro-muscular preparation was pinned on a Sylgard-coated Plexiglas chamber and bathed in a physiological solution, containing 135 mM NaCl, 1.0 mM $MgCl_2$, 4 mM KCl, 0.9 mM NaH_2PO_4, 2.0 mM $CaCl_2$, 11 mM glucose, 16 mM $NaHCO_3$, pH 7.2. Electrical activity of neuro-muscular junctions of *m.diapgragma* was recorded using traditional intracellular microelectrode technique. *Nervus phrenicus* was stimulated via silver bipolar electrodes with square pulses at 0.3 Hz to evoke single endplate potentials (EPPs) or at 50 Hz to create rhythmical bursts of evoked EPPs. The muscle fibers were crushed [Barstad, Lilly, 1968] to prevent twitch response to stimulation. All recordings were performed at room temperature (22-24°C). Data were analyzed using Mini Analysis software (by Justin Lee). Data are presented as mean ± standard error of the mean (SEM). Mann-Whitney test was used to evaluate the differences, $p<0.05$ was regarded as significant. Specific inhibitors of PKC –(cheleritrin, GF109203X и Ro320432), of CaMKII (KN 62), calcineurin (CysA, CaN-inhibiting peptide CN412), of L-type Ca-channels(nitrendipin) and of alpha7 nAChRs (metyllicaconitine) from *Sigma* were used.

Activation of PKC and its influence on mediator secretion were studied by testing the effects of PKC inhibitors (cheleritrin, GF109203X , Ro320432) as well as of PKC activator phorbol-12-myristate-13-acetate (PMA) on EPPs amplitude and quantal content. This was tested when different Ca-inputs of nerve terminal were active(opened) - namely P/Q- and/or L- type Ca channels, alpha7 nAChRs, ryanodine receptors of Ca-stores. We discovered for the first time the presence of basal PKC activity in motor nerve terminals, which is aimed to potentiate the evoked ACh release. This PKC activity was found to be independent on Ca-input per P/Q-type Ca-channels. Ca-input via alpha7nAChRs was also not able to

activate PKC and involve it in regulation of mediator secretion. But when Ca-input through latent presynaptic L-type of Ca channels of nerve terminals was implicated, additional activation of presynaptic pool of PKC took place. This induced increase of EPPs quantal content to 30% .The effect can be prevented by cheleritrin or Ca -buffer EGTA-AM. This allow us to suggest that Ca-input per L-type of Ca channels can create a local Ca-signal, which selectively activates a pool of Ca-dependent PKC in motor nerve terminals participating in presynaptic potentiation of transmission. We have also used a direct Ca-independent activation of PKC with the help of phorbol-12-myristat-13acetate (PMA, 10 nM). This led to increase quantal content of EPPs to 30% recorded during single and rhythmical synapse activity. Nitrendipine (5 μM), a specific inhibitor of L-type Ca-channel and ryanodine (2 μM) a specific blocker of Ca-release from Ca stores were able to block this potentiating effect of PMA. It allows us to suggest, that in the case of PMA induced PKC activation enzyme activity is directed to activation (disinhibition) of latent L-type of Ca-channels and implication of L-type Ca-current in activity of nerve terminals. This in turn induced activation of RyRs, Ca-release from Ca-stores and potentiation of transmission (fig. 1).

Activation and role of calcineurin (CaN) in nerve terminals were studied using specific CaN inhibitors - *cyclosporin A* and *CaN-inhibiting peptide CN412*. In the presence of these inhibitors disinhibition of L-type channels activity takes place and significant increase of EPPs quantal content of single and rythmically evoked EPPs for 25-30%. We found for the first time that this potentiation is also coupled with RyRs activation/Ca release from Ca-stores and can be blocked by RyRs inhibitor ryanodine (2 μM) and by Ca-buffer EGTA-AM. It is noteworthy, that potentiation of transmission by CaN inhibitors was also accompanied by additional activation of PKC in nerve terminals and can be blocked by PKC inhibitor cheleritirin.

Role and pattern of CaMKII activation. Application of CaMKII inhibitor KN 62 (3 μM) does not induce any changes in EPPs parameters of active motor synapses of mice m.diaphragma. Nevertheless we revealed for the first time a new pattern of CaMKII activation and its regulatory role in motor synapses. We found, that application on muscle of exogenous choline (100 μM), known as a selective agonist of alpha7nAChRs, can induce significant depression of evoked ACh release for 25%. This was seen in quantal content of single EPPs and in bursts of rhythmically evoked EPPs. Depression of synaptic transmission induced
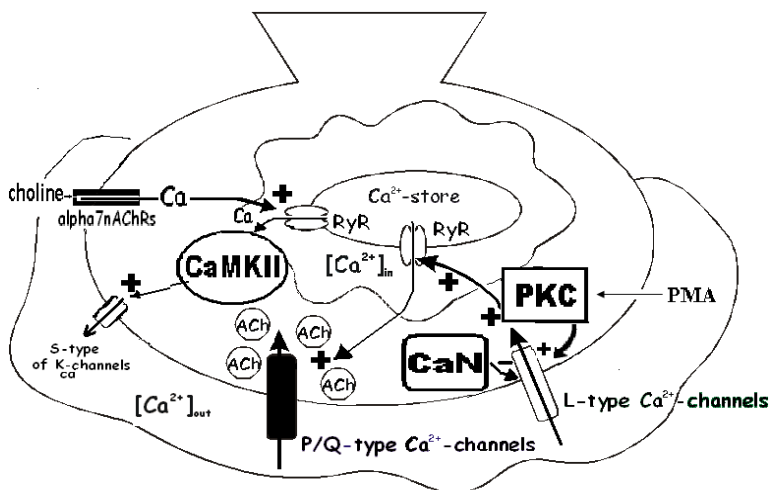
Schematic drawing of Ca-inputs of motor nerve terminal, which participate in selective activation of presynaptic PKC, CaMKII and CaN. Role of Ca, entering nerve terminal per alpha7 nAChRs/RyRs in activation of CaMKII is shown. Important role of Ca, entering nerve terminal per disinhibited L-type Ca-channels in activation of PKC and RyRs is also shown. A consequence of additional PKC activation by PMA is marked, causing disinhibition of latent L-type channels and potentiation of transmission. Role of constitutive CaN activity in inhibition of L-type channels is also mentioned.

by choline, can be prevented by selective inhibitor of alpha7nAChRs metyllicaconitine(20 nM). Besides it this depression can successfully prevented by ryanodine (an inhibitor of RyRs) and apamine (5 µM) –a selective blocker of Ca-dependent potassium channels of SK-type. Furthermore, it was found for the first time, that selective calmodulin blocker calmidazol R2457 (1,2 µM) и CaMKII inhibitor KN-93 (3 µM) fully prevent depression of synaptic transmission, induced by presynaptic action of choline. While the blockade of PKC (using cheleritrin, 4 µM) or PKA (using H89) does not change the depression. The events following activation of presynaptic alpha7-nAChR by choline is seen in figure.

Figure demonstrates the hypothetical intracellular cascades which come next to activation of alpha7-nAChR by presynaptic choline. It is seen that calcium input activates calcium release from Ca-stores per RyRs channels and subsequent CaMKII activation. This enzyme in turn causes activation of small-conducting Ca-dependent K channels of SK-type. The outgoing transmembrane potassium current per SK-type of K_{Ca}-channels causes hyperpolarization of presynaptic membrane. This inhibits

activity of potential-dependent Ca-current through P/Q-channels, causing reduction of Ca-dependent release of cholinergic vesicles.

Thus, our studies revealed new mechanisms of presynaptic plasticity taken place in motor nerve terminals, when three different Ca-dependent enzymes are activated . There are presynaptic potentiation in the case PKC activation and inhibition in the case of specific CaN and CaMKII activation. The still unknown ways of Ca-signals formation in nerve terminals are also discovered, created with the help of L-type of Ca-channels, RyRs, alpha7nAChRs, which are able to activate individual Ca-dependent enzymes, providing different patterns of short term synaptic plasticity of motor synapses.

PRESYNAPTIC CHOLINE EFFECTS IN MOUSE REGENERATING MOTOR SYNAPSES

O.P. Balezina, P.O. Bogacheva
Moscow State University, Faculty of Biology, Lenin Hills 1/12, Moscow, 119234, Russia

Choline, a precursor of acetylcholine (ACh) and a product of acetylcholine hydrolysis by acetylcholinesterase (AChE), acts as an efficient and relatively selective agonist of alpha7-nicotinic acetylcholine receptors (nAChR) in neurons and synapses [6,7]. In central synapses choline is able to activate presynaptic alpha7-nAChRs, which results in increased release of mediator secretion in different types of chemical synapses [1]. Our previous studies of peripheral cholinergic neuromuscular synapses of diaphragmal muscle have shown, that presynaptic alpha7-nicotinic cholinoreceptors are also present there, but their activation by choline or nicotine causes decrease of ACh release and depression of synaptic transmission [2,3]. The aim of this study was to compare the reactivity to choline of mature and immature regenerating motor synapses of mouse hind limb muscle. The activity of regenerating motor synapses was studied at early stages of skeletal muscle reinnevation after motor nerve crush.

Materials and methods

Data presented were obtained from the fast-twitch extensor digitorum longus muscle (*m.EDL*) of adult mice (20-30g). Mice were anesthetized with diethyl ether and *n. peroneus communis* was aseptically crushed approximately 10 mm from its entrance into the muscle. Animals were allowed to recover for 11 days prior to testing the activity of newly formed synapses in isolated neuromuscular preparation. Animals were sacrificed by decapitation. The isolated neuromuscular preparation was

pinned on a Sylgard-coated Plexiglas chamber and bathed in a physiological solution, containing 135 mM NaCl, 1.0 mM $MgCl_2$, 4 mM KCl, 0.9 mM NaH_2PO_4, 2.0 mM $CaCl_2$, 11 mM glucose, 16 mM $NaHCO_3$, pH 7.2. Electrical activity of neuromuscular junctions was recorded using standard intracellular microelectrode technique. Spontaneous miniature end plate potentials (MEPPs) and evoked end plate potentials (EPPs) were recorded. Nerve was stimulated via silver bipolar electrodes with square pulses at 50 Hz for 1 second to record the bursts of rythmically evoked EPPs. The isolated muscle fibers of *m.EDL* were dissected to prevent twitch response to nerve stimulation [4]. All recordings were performed at room temperature (22-24°C). Data were analysed using MiniAnalysis software (by Justin Lee). All data are presented as mean ± standard error of mean (SEM). Mann-Whitney test was used to evaluate the differences, $p < 0.05$ was regarded as significant.

Results and discussion

In the first series of experiments choline (100 microM) was applied on mature intact isolated *m.EDL* preparation. Perfusion of choline solution in course of 60 minutes did not change the membrane potential of dissected muscle fibers (37,8±1,1, mV in control, 38,1±1,2 in presence of choline), mean frequency and amplitude of MEPPs.

To further examine possible choline influences on spontaneous activity, choline (100 microM) was applied to neuromuscular preparation with undissected muscle fibers. Still choline did not significantly change MEPPs amplitude, frequency or time course and, therefore, had no postsynaptic effects.
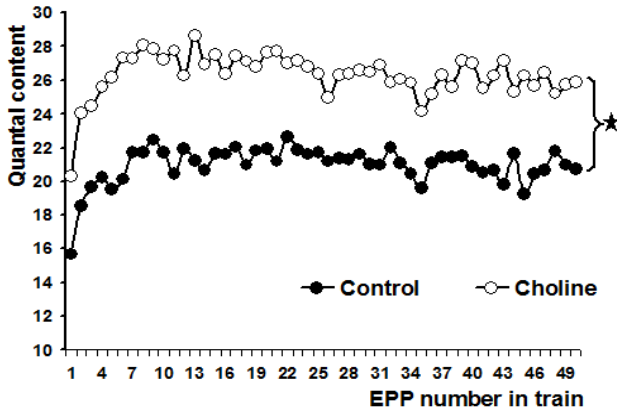
During short rhythmic train of stimuli (50 Hz), a special pattern of synaptic activity is observed: short initial facilitation and subsequent depression of synaptic transmission (fig. 1).

Application of choline to mature neuromuscular preparation caused a significant 26% decrease of each of the 50 recorded EPPs quantal content and amplitude throughout all train of 50 stimuli. The pattern of synaptic activity was not affected. Decrease in amplitude and quantal content of EPPs without altering MEPPs parameters indicates presynaptic inhibitory action of choline.

Blocker of alpha7-nAChR methyllicaconitine (20 nM) had no effects of spontaneous or evoked activity of mature neuromuscular junctions. But it fully prevented choline effects: being applied after metyllicaconitine, choline (100 microM) was not able to decrease amplitude and quantal content of EPPs. This indicates that choline caused reduction of evoked synaptic transmission by acting on its presynaptic alpha7-nAChR.
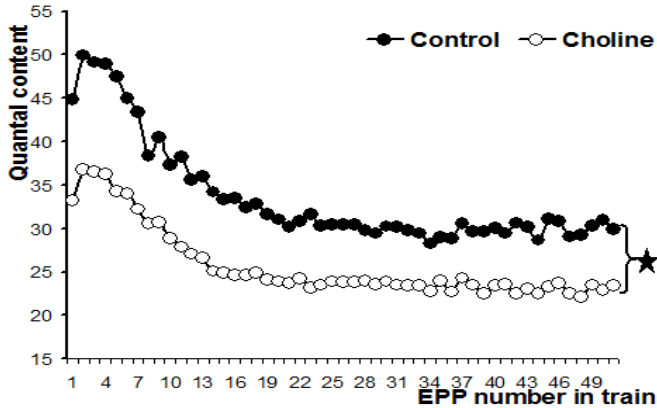
Fig. 1. Changes in EPPs quantal content of mature neuromuscular junctions throughout short rhythmic train of stimuli (50 Hz, 1 s) in control and after choline (100 microM) application. ★- p<0,05.

Fig. 2. Changes in EPPs quantal content of reinnervated neuromuscular junctions throughout short rhythmic train of stimuli (50 Hz, 1 s) in control and after choline (100 microM) application. ★- p<0,05.

In regenerating neuromuscular junctions choline also did not alter the parameters of spontaneous quantal ACh secretion: amplitude, time course or frequency of MEPPs, and thus showed no postsynaptic effects.

During short rhythmic trains of stimuli (50 Hz, 50 s), newly-formed reinnervated neuromuscular junctions show a different pattern of activity than the mature junctions. Initial facilitation is not followed by

depression of transmission. Instead, EPPs amplitudes reach plateau level, which is usually 20-30% higher than first EPP in train.

Application of choline (100 μM) caused a significant 22% enhancement of synaptic transmission in newly-formed junctions: amplitude and quantal content of each EPP in short train were increased comparing to control.

The pattern of synaptic activity in train was not affected (fig. 2). Thus, in neuromuscular junctions on early stage of reinnervation choline causes pronounced enhancement of transmission and this effect is presynaptic.

Ability of exogenous choline to modulate synaptic activity was described only in mature synapses and presynaptic choline effects on ACh release were inhibitory [2,3,5]. We showed that these choline effects are mediated via activation of presynaptic alpha7-nAChR.

Our present data demonstrate for the first time ever, that in regenerating cholinergic neuromuscular junctions exogenous choline is able to enhance synaptic transmission, potentiating the release of ACh. This allows us to suggest that choline can be involved in positive feedback autoregulation of cholinergic synaptic transmission on early stages of synaptic formation in skeletal muscles.

References

1. Alkondon M *et al*. // Eur J Neurosci. (1997) 9(12): 2734-42.
2. Balezina O.P. // Priroda. (2012) 9: 14-20.
3. Balezina OP, Fedorin V, Gaydukov AE // Bull Exp Biol Med. (2006) 142(1): 17-21.
4. Barstad JA, Lilleheil G // Arch Int Pharmacodyn Ther. (1968) 175(2): 373-90.
5. Prior C, Singh S. // Br J Pharmacol. (2000) 129(6): 1067-74.
6. Sun F, Jin K, Uteshev VV // PLoS One. (2013) 8(8).
7. Uteshev VV, Meyer EM, Papke RL. // J Neurophysiol. (2003) 89(4): 1797-806.

SIZE AND LOCALIZATION OF THE MYOCARDIAL ISCHEMIA – WHAT CAN ONE SEE ON ECG? COMPUTER MODELING

O.V. Baum, V.I. Voloshin, L.A. Popov

Institute of Theoretical and Experimental Biophysics, RAS, Pushchino, 142290, Russia

Introduction. One of the problems of coronary heart disease is the development of biophysically-based methods for early diagnostics of this pathology of the cardiac muscle, including identification of localization

and extensiveness of the ischemic foci. When there are a significant number of hypotheses and certain difficulties of interpretation of some facts in this field of knowledge, an important place in scientific studies takes electrocardiography with its potential reserves at the extended interpretation of the method as well as methods of mathematical and computer modeling of the heart electrical activity.

Aim. The purpose of the present work was to investigate with the method of computer simulation the influence of localization and extensiveness of ischemia on repolarization parameters of the electrocardiosignal (ECS), as well as examine some hypotheses about information relation of these parameters with electrophysiological state of the cardiac muscle.

Methods

The work was carried out with the help of a model of the ECS genesis, previously developed in the ITEB RAS [1]. When calculating the ECSs in the given lead points there is a possibility for modification of the spatial orientation of the model ventricles by means of rotating the heart around its own anatomical axis through angles α_X, α_Y, α_Z [2].

To investigate the influence of localization and extensiveness of the ischemic zone on the ECS parameters a method of segmentation for the ventricles of the model heart was used, and to estimate contributions of the "ischemic" segments in the total signal of the different leads a method of partial curves was applied [3].

Foci of ischemia in the selected area of the ventricles were simulated by specific changes of such characteristics of the transmembrane action potential (AP) as the resting potential, AP amplitude, duration of the plateau phase, and steepness of the final phase of rapid repolarization (Fig. 1a) in accordance with literature data [4, 5], while also taking account of the preliminary results obtained in [3]. Numerical values of the AP parameters under norm and ischemia are shown in Fig. 1b. The degree of deviation of prescribed parameters of the AP from their physiologically normal values was considered as an "internal" severity (or intensity) of the simulated ischemia, the concept of which was suggested by us in [3]. The "external" severity of ischemia can be considered in this case only as visible changes in the pattern of ST-T interval compared to "conventional norm" of the model electrocardiogram, which corresponds to the initial parameters of the model, taken as normal. Approximately in such "external" terms, not related directly with electrophysiological state of the cardiac muscle, some ischemic ECG changes in practical electrocardiography are described ("expressed shift of the ST segment", "high positive symmetric, or coronary, T wave", and so on). Internal expression of pathological changes, in this case
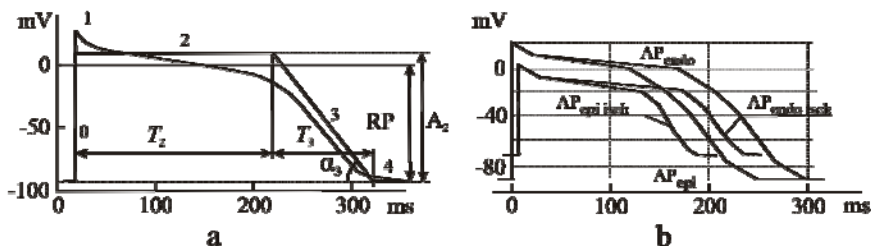
Fig. **1**. Cardiac transmembrane action potential (AP) and its main characteristics. a – Schematic representation of the AP: RP – resting potential; A_2 – amplitude, T_2, T_3 – durations of the AP phases; α_3 – slope of the final repolarization phase. b – Forms of the AP used in the study on boundary surfaces of the ventricles: AP_{endo}, AP_{epi} – endocardial and epicardial APs on the surfaces of the normal myocardium; $AP_{endo\ isch}$, $AP_{epi\ isch}$ – APs on the proper surfaces of the "ischemic" sectors of the ventricles.

– myocardial ischemia, is hidden from an observer who is being "on the outer side with respect to recording electrodes", and in such conditions is essentially a «black box», i.e. concept with which the cybernetics [6] operates. One of the tasks of modeling is just searching for causal quantitative relation between internal and external "expressions" of ischemia what should, on the one hand, to promote the understanding of mechanisms of pathological changes in ECS and, on the other hand, to assist in the development of new diagnostic algorithms.

In this study, as the object for observation when you change localization and extensiveness of the ischemic focus the following parameters of the cardiocycle were chosen: ssST80 – shift of the ST segment in the moment of 80 ms after J point; Gr – relative ventricular gradient; Kg – modified ventricular gradient, parameter which is calculated as the ratio of the area under the curve of the ECG signal on a generalized interval JT to the area under the curve of the signal in modulus on the QRS interval, and also some other parameters, including several indices for estimating a symmetry of the T wave – βT , Asym_1, Asym_2, Asym_3 (see in [3]). The index Asym_3 is considered for the present as a trial estimate. Essentially, it is a certain analogue of the concept of "asymmetry" in the mathematical statistics under formal consideration of the T wave as some conditional distribution of a random variable. Measurement and calculation of the listed ECS parameters was performed for twelve signals of the standard lead system and for three signals of the orthogonal system (taking into account assumptions made in [2]). For the model ECS a "medical" evaluation for changes on the ST-T interval in terms of Minnesota

Code (MC) was also carried out under selected anatomical position of the heart and localization of the "ischemic" zone.

Results and Discussion

To study effects of localization and extent of the ischemic focus a segmentation of the ventricles into separate compartments (segments) was executed for a coordinate binding the "ischemic focus" to geometry of the model. The left ventricle is divided by horizontal layers and their internal division on 17 sectors (fig. 2a), each of which (except the apex of the heart) has inner (endo) and outer (epi) surfaces. Two more surfaces belong to the right ventricle.

In computer experiment on examination of influence of ischemia localization on ECS parameters all the segments of the second layer of the model (7, 8, … 12 on fig. 2b) were, one after another, "affected with an ischemia", i.e. the normal parameters of AP on endo- and/or epi-surfaces of the proper sectors were replaced by pathological ones, as described in the "Methods" section. Then, for each of the versions the sets of ECS were calculated in all the leads.

The results obtained have shown that when simulating subendocardial ischemia the parameters of symmetry in the limb leads, as well as in the chest leads V1-V3, vary only slightly compared to changes in the group of leads V4-V6, what is explained by the "projection" effect. The statistical index Asym_3 in the chest leads varies slightly and irregularly. Values of Asym_1 and Asym_2 are practically coincide, indicating that their equivalence. Behavior of the "amplitude" parameters ccst80, Gr, and Kg in the chest leads one can also explain by positional factors.

When modeling subepicardial ischemia it turned out that parameters Gr and Kg (fig. 3b) vary in opposite phases, which is natural, and
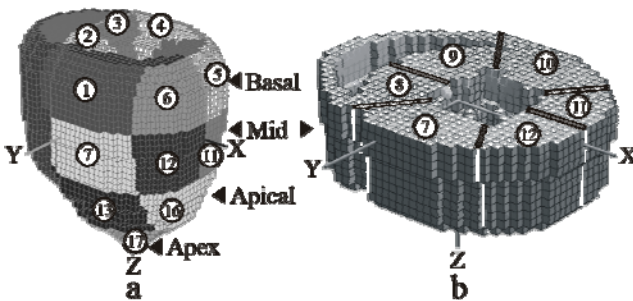
Fig. **2**. Segmentation of the heart model (in circles are given numbers of the segments). a – General view of the model ventricles; b – Middle layer of the model.
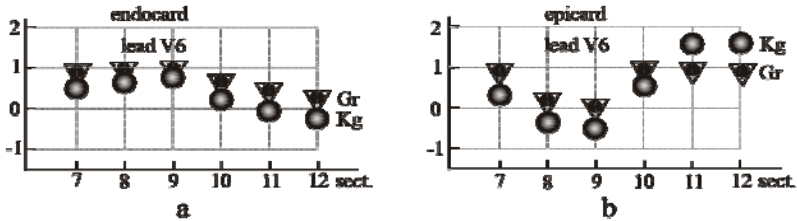
Fig. 3. Values of the relative ventricular gradient Gr and modified ventricular gradient Kg in the lead V6 depending on the number of "ischemic" sector under subendocardial (a) and subepicardial (b) localization of the pathology.

more considerably, than for subendocardial ischemia (Fig. 3a). The latter is connected, apparently, with two factors. For the chosen method of segmentation the areas of epicardial surfaces of sectors are more than areas of endocardial ones (see Fig. 2b), and the distances from the chest electrodes to the external and internal surfaces of the different sectors, as well as their ratio, vary from sector to sector. In each concrete case the given internal expression of ischemia in the model allows, due to the correctness of the direct problem, explain the behavior of the ECS parameters obtained in different leads. But unpredictable combination of all the mentioned factors, considering also the possible dispersion of the heart rotational from patient to patient, suggests that the use of the parameters examined to identify localization of ischemia is hardly possible.

Study of the influence of the ischemia extensiveness on repolarization parameters in different leads was carried out by increasing the area of ischemic focus on the endocardium of the left ventricle according to the following scheme: On the first step of the experiment the endocardium of the sector 12 turned "ischemic", and then endocardial surfaces of sectors 6, 11, 5, 7, 1, 16 were involved in this process sequentially. When increasing the area of "ischemia", i.e. the amount of pathological elements, one can express a general considerations about character of the curves obtained depending on the total area of the pathology with due regard for mutual orientation of the lead axes and normals to the surfaces of elements constituting the segment at the given orientation of the model, as well as taking into account the curvature of the endocardial and epicardial surfaces.

Conclusion. Thus, with the aid of the computer model effects of localization and extensiveness of simulated ischemia on patterns of ST-T interval of electrocardiosignal and its calculated characteristics have been examined and some complexities of solving the corresponding inverse problem has been explained. Results of the work have shown importance

of the choice of an interval and its borders for calculation of indicators of symmetry and allowed to put a question on expansion of the concept of symmetry in electrocardiology from symmetry of the T wave up to some "symmetry" of the process of repolarization, which corresponds to a generalized interval JT on the ECS. Additional complex studies on verified samples of real electrocardiograms for norm and pathology with involving models of ECS genesis are needed for searching new informative parameters of the cardiac electric field and for choice of an optimum strategy of identification of the electrophysiological state of the heart. For this purpose, an illustrated interactive electronic archive for sets of the model input data and results of modeling is being worked out now in the ITEB RAS.

References

1. Baum O.V., Voloshin V.I. and Popov L.A. Biophysical Models of Cardiac Electrical Activity // Biophysics (Biofizika). December 2006, Volume 51, Issue 6, pp 940-954. DOI 10.1134/S0006350906060133.
2. Baum O.V., Voloshin V.I., Popov L.A. Realization of Biophysical Models of Cardiac Electrical Activity // Biophysics (Biofizika). January 2009. Volume 54, Issue 1. P. 72-84. DOI 10.1134/S0006350909010138.
3. Baum O.V., Voloshin V.I., Popov L.A. Electrocardiographic Image of Myocardial Ischemia: Real Measurements and Biophysical Models. Part II // Biophysics (Biofizika). October 2012. Volume 57. Issue 5. P. 668-675. DOI: 10.1134/S0006350912050028.
4. Dolabchyan Z.L. Myocardial infarction and the electromechanical activity of the heart. // M.: Medicine, 1981.
5. Macfarlane P.W., Oosterom A., Pahlm O., Kligfield P., Janse M., Camm J. (Eds.) Comprehensive Electrocardiology (2nd Edition). // Springer, 2010. ISBN 978-1-84882-045-6.
6. W. Ross Ashby. An introduction to cybernetics. London: Chapman & Hall, 1956. ISBN 0-416-68300-2.

STUDY OF THE INFLUENCE OF INCUBATION MEDIA COMPOSITION AND MEMBRANOTROPIC AGENTS ON THE LIPID PALMITATE/Ca^{2+}-INDUCED PORE OPENING IN MITOCHONDRIA AND UNILAMELLAR LIPOSOMES

N.V. Belosludtseva, K.N. Belosludtsev, M.N. Belosludtsev, G.D. Mironova

Institute of Theoretical and Experimental Biophysics RAS, Institutskaya st., 3, Pushchino, 142290, Russia

Free fatty acids (FFAs) exert a diverse array of biological effects and have been implicated in a number of pathophysiological conditions

such as ischemia–reperfusion injury, apoptosis, obesity, diabetes and others. In the presence of Ca^{2+}, FFAs are able to induce the mitochondrial pore opening of two types: cyclosporin A (CsA)-sensitive protein pore (supercomplex consisting of ADP/ATP antiporter, cyclophilin D, porin and other mitochondrial membrane proteins – mitochondrial permeability transition (MPT) pore) and CsA-insensitive lipid pore induced by long-chain saturated FFAs acids and Ca^{2+}.

As shown earlier, the nonselective pore induced by palmitic acid and Ca^{2+} can be considered as fast-tightening lipid pore formed due to chemotropic phase transition in the membranes of different types [1]. The pore opening was observed not only in mitochondria, but also plasma membrane of erythrocytes, as well as artificial lipid membranes (black lipid membranes and unilamellar liposomes) [2-3].

Considering the mechanism of the palmitate/Ca^{2+}-induced pore (PalCaP) formation in lipid bilayer, it is obvious that it is not regulated by known modulators of MPT pore. Previously we have studied some physiological and regulatory aspects of the pore [4]. All these results were obtained using sucrose medium incubation. However, it is not clear whether similar effects can be observed in an incubation medium, which is closer to the intracellular one where K^+ and Cl^- are the main ions. It is known that K^+ ions can influence the surface potential of the membrane, leading to the conductive properties changes of the lipid bilayer. For example, an increase in the amount of positive chargers on mitochondrial membrane results in an acceleration of rates of the substrate transport by some mitochondrial carriers. Additionally, lipophilic agents such as the anionic surfactant sodium dodecyl sulfate (SDS) and the cationic surfactant cetyltrimethylammonium bromide (CTAB) that can modulate the surface properties of membranes are also found to change the membrane permeability [5]. In this regard, it is important to study the possible effects of the agents affected the surface potential on the permeability of artificial and biological membranes.

Thus, the aim of this work was to study the influence of the ionic composition of incubation medium and membranotropic agents on palmitat/Ca^{2+}-induced lipid pore formation in mitochondria and unilamellar liposomes.

Materials and Methods

Mitochondria were isolated from the liver or heart of Wistar rats using a standard differential centrifugation technique. Mitochondrial swelling was measured as a decrease in A540 in a stirred cuvette at room temperature using an USB-2000 spectroscopy fiber-optic system (Ocean Optics Inc., USA). The incubation medium contained 210 mM mannitol,

70 mM sucrose, 5 mM succinate, 5 μM EGTA, 1 μM rotenone 1 μM CsA, and 10 mM Hepes/KOH buffer (pH 7.4) or 120 mM KCl, 5 μM EGTA, 1 μM rotenone 1 μM CsA, and 10 mM Tris/HCl buffer (pH 7.4). The concentration of the protein in the cuvette was 0.4 mg/ml or 0.2 mg/ml (liver and heart mitochondria correspondingly).

Large unilamellar lecithin liposomes loaded by fluorescent dye sul-forhodamine B (SRB) were obtained by a conventional extrusion technique [1]. The release of SRB from liposomes was evaluated by the increase in fluorescence intensity, as described previously [1]. The buffer contained 40 mM KCl, 50 μM EGTA and 10 mM Tris-HCl (pH 8.5) or 80 mM sucrose, 50 μM EGTA and 10 mM Tris-HCl (pH 8.5).

Results

Influence of the incubation medium composition on the CsA-insensitive mitochondrial permeability induced by palmitic acid and Ca^{2+}. Fig. 1 shows the CsA- insensitive swelling of rat liver (*a*) and heart (*b*) mito-chondria induced by 15 μM of palmitic acid and 30 μM Ca^{2+} in media containing sucrose/mannitol or KCl as osmoregulatory agents.

As can be seen, the amplitude and the rate of swelling of liver mito-chondria were significantly higher in the medium with sucrose/mannitol. When 120 mM KCl was added instead of sucrose/mannitol, the mitochon-drial swelling rate was markedly decreased. Moreover, under these conditions the liver mitochondria after the high-amplitude swelling reveals a tendency to their contraction. As shown in fig. 1b, rat heart mitochondria after their swelling induced by palmitic acid and Ca^{2+} in KCl medium fully restored their volume in a few minutes.

Effect of ionic composition of the buffer on the permeability of sul-forhodamine-loaded liposomes induced by palmitic acid and Ca^{2+}. It was
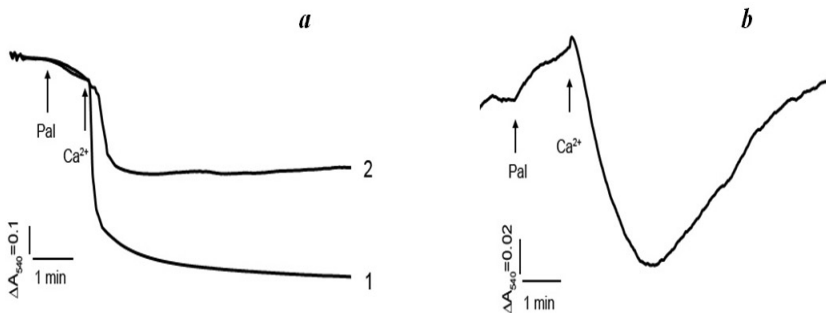
Fig. 1. Palmitate/Ca^{2+}-induced swelling of rat liver (a) and heart (b) mito-chondria in sucrose/mannitol (1) and KCl (2) media.
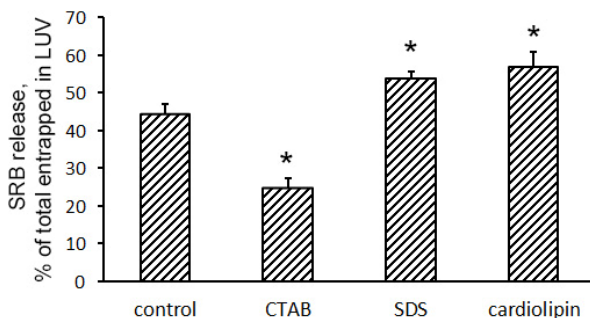
Fig. 2. Effects of the membrane surface potential-modulated agents on the palmitate/Ca^{2+}-induced permeability of liposomes.

found that the release of fluorescent probe SRB from lecithin liposomes induced by 15 μM of palmitic acid and 1 mM Ca^{2+} was considerably (30%) greater in sucrose buffer than in KCl one. In the case when the incubation buffer was prepared from salts of other monovalent cations (Li^+, Rb^+), the permeability of the liposomes was the same as in KCl buffer.

Influence of membranotropic agents on the palmitat/Ca^{2+}-induced lipid pore opening in mitochondria and liposomes. Fig. 2 shows the effect of the cationic detergent CTAB, the anionic detergent SDS and the anionic phospholipid cardiolipin on the palmitate/Ca^{2+}-induced liposome permeability to fluorescent probe SRB. As can be seen from the figure, CTAB (10 μM) significantly inhibited the membrane permeabilization caused by Ca^{2+} in the palmitate-containing liposomes, while SDS (50 μM) facilitated it. It should be noted that 50 μM SDS itself did not affect the permeability of the liposome membrane, whereas 10 μM CTAB itself induced the release of SRB from the liposomes by 20%. Liposomes that were prepared from a mixture of phosphatidylcholine/cardiolipin (25 mol.%) were less resistant to the inducers of the membrane permeabilization that liposomes formed from phosphatidylcholine only.

Fig. 3 shows the influence of CTAB (10 μM) and SDS (10 μM) on the rate of CsA-insensitive palmitat/Ca^{2+} -induced swelling of rat liver mitochondria. As in the case with the liposomes, CTAB inhibited the PalCaP opening in the mitochondria. At the same time, SDS slightly stimulated the rate of mitochondrial swelling.

Discussion

In this paper we showed that the presence of K^+ ions in the incubation medium suppressed the palmitate/Ca^{2+}-induced membrane permeabi
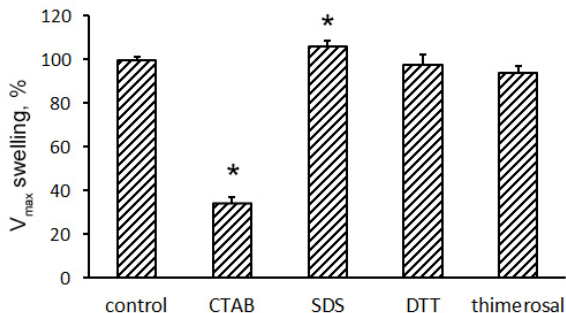
Fig. 3. Influence of membranotropic agents on the cyclosporin A-insensitive rat liver mitochondria swelling induced by palmitic acid and Ca^{2+}.

lization of mitochondria and unilamellar liposomes. The data obtained can be explained by the influence of K^+ on the membrane surface potential. The quenching of the negative charges on membrane surface by K^+ ions is supposed to prevent the binding of fatty acid anions to Ca^{2+} in membrane. Since the lipid pore was found to tighten and close by reason of energetic utility [1], the mitochondria after their swelling in KCl incubation medium is expected to restored their initial volume owing to K^+/H^+ exchange system functioning. Inhibitor of K^+/H^+ exchanger quinidine blocked the mitochondrial contraction stage but did not affect prior swelling. It was shown that the cationic detergent CTAB inhibited the PalCaP opening in mitochondria and liposomes, while the anionic detergent SDS activated the formation of the pore. One can be supposed that SDS being incorporated into the lipid bilayer increases a total negative charge of the membrane surface and thereby facilitates the PalCaP formation. The important role of the negative membrane surface charge in the modulation of the lipid pore formation can be also confirmed by our results that incorporation of anionic phospholipid cardiolipin in liposomes facilitates the PalCaP opening in lipid bilayer.

Thus, the data obtained are in line with our proposal that the membrane surface potential can modulate the lipid pores formation both in artificial lipid bilayers and mitochondrial membranes.

References

1. Agafonov A.V. et al. (2003) Biochem Biophys Acta 1609: 153-160.
2. Sultan A., Sokolove P. (2001a, b) Arch Biochem Biophys 386:31–51, 52–61.

3. Belosludtsev K.N. et al. (2010) J Membr Biol 55(6):1038-1047.
4. Belosludtsev K.N. et al. (2009) J Bioenerg Biomembr 41(4):395-401.
5. Vaidyanathan S. et al. (2014) Phys Chem B. 118(8):2112-23.

CLONE FORMATION REPRESENTS ONE THE MAIN MECHANISMS OF MYOCARDIAL SELF-RENEWAL AND REGENERATION IN THE MAMMALIAN HEART

G.B. Belostotskaya[1,2], T.A. Golovanova[2], I.V. Nerubatskaya[1,2]

[1]*Sechenov Institute of Evolutionary Physiology and Biochemistry, Russian Academy of Sciences, Thorez av. 44, St.-Petersburg, 194223, Russia*
[2]*Federal Almazov Medical Research Centre, Akkuratova str. 2, St.-Petersburg, 197341, Russia*

Current *in vitro* and *in vivo* data suggest that cardiomyogenesis is achieved via the activation and differentiation of endogenous progenitor cells. However, little information is available on the details of this process. We have previously shown that newborn rat heart-derived Sca+, c-kit+ and Isl1+ resident cardiac stem cells (CSCs) are able to form large contracting colonies in the primary culture [Belostotskaya and Golovanova, 2014]. Here we present evidence that CSCs can also generate colonies in the culture of myocardial cells of 20- and 40-day-old rats. Although these colonies were shown to be similar in size and morphology to those grown from CSCs of newborn heart, they were non-contracting and exhibited early signs of cardiac differentiation only, including expression of GATA-4 and α-sarcomeric actin. Presumably the inability of young and adult rat CSCs to undergo full differentiation in culture is due to the lack of direct contact between CSCs and mature cardiomyocytes because of the poor attachment of the latter to substrate. However, compact CSC clones consisting of both undifferentiated and α-sarcomeric actin-, sarcomeric α-actinin- and troponin T-positive cells were identified in the suspension of freshly isolated cardiac cells obtained from age-matched rats and adult C57BL mice. In addition, mononuclear mature cardiomyocytes stemming from CSCs were found *ex vivo* in adult mouse myocardium. These results suggest that resident CSCs are able to produce mature cardiomyocytes by proliferation and differentiation inside the colonies (clones) both *in vitro* and *in vivo*. Thus, clone formation appears to be one of the main mechanisms of cardiomyogenic CSC differentiation contributing to myocardial self-renewal and regeneration after injury.

EFFECT OF THE PEPTIDE DRUG SEMAX ON SYMPATHETIC INNERVATION OF RATS HEART AND VESSELS AFTER EXPERIMENTAL MYOCARDIAL INFARCTION

**A.B. Berdalin, S.A. Gavrilova, A.D. Nikogosova, D.A. Bazhenova,
A.M. Gorbacheva, G.F. Gubaidullina, E.O. Lebedeva,
A.M. Romanyuk, A.N. Stulova, S.V. Buravkov, V.B. Koshelev**

*Faculty of Basic Medicine, Moscow State University,
Lomonosovsky prosp. 31/5, Moscow, 119192, Russia*

After the development of myocardial infarction due to ischemia or ischemia-reperfusion, activation of the sympathetic part of the autonomic nervous system taken place as a result of stress reactions to pain and decreased blood pressure. Increased activity of the sympathetic nervous system leads to an increase of pre- and afterload on the damaged myocardium. Stimulation of β_1-adrenergic receptors may contribute directly in calcium overload and lead to apoptotic death of cardiomyocytes. Due to this unfortunate effects on the progression of myocardial infarction β-blockers became widespread, this drugs, however, do not affect the overall activity level of the sympathetic nervous system.

We have previously shown presence of cardioprotective activity at the peptide drug Semax (AKTG4-7 + Pro-Gly-Pro) (Gavrilova, 2008; Berdalin, 2011). This effect of the peptide is probably associated with lowering of overall activity of the sympathetic nervous system.

Goal of this study consist of investigation of influence of the peptide drug Semax on the amount of sympathetic nerves and adrenergic receptors in the heart and blood vessels in rats with experimental myocardial infarction.

Materials and methods

Study was performed on male rats weighing 300-400g with irreversible ischemia or ischemia-reperfusion after 2.5 hour ischemia with Selye method. There are 5 experimental groups: intact control, irreversible ischemia, irreversible ischemia with administration of Semax, ischemia-reperfusion, ischemia-reperfusion with Semax administration. Semax administered intraperitoneally at 150 mg/kg after 15 minutes and 135 minutes from the start of the coronary occlusion at first day and one time a day at 2-7 experimental days. Control animals received sterile physiological saline solution in the same manner and dose as Semax.

28 days after the operation interventricular septum, segments of femoral, renal, mesenteric and tail artery were taken. Sympathetic nerves in the interventricular septum and arteries were stained by condensation of catecholamines with glyoxylic acid and subsequent fluorescence of the complex. We made series of randomly oriented micrographs (at least 20-

30 on one sample). Sympathetic innervation density was evaluated by the number of intersections of the sympathetic nerves with the grid bundles superimposed on micrograph with the Paint. NET version 3.5.8. program. Data are presented as the number of intersections on 100 grid bundles.

Immunohistochemical staining for α_1-adrenoreceptors were performed on segments of the tail artery. Material were fixed in 10% neutral buffered formalin. Paraffin embedding were performed according to standard histological procedures. Primary rabbit polyclonal antibody were applied on 5 µm slices, then secondary antibody conjugated with peroxidase. Intensity of staining was evaluated in the program Image-Pro Plus followed by counting the relative area of stained sections.

Statistical analysis was performed using STATISTICA 6.0 program with nonparametric Mann-Whitney test with Bonferroni correction.

Results

In the intact control mean relative density of sympathetic nerve fibers, as measured by fluorescence of catecholamines in the condensation with glyoxylic acid, was 0.0 194 ± 0,004. Myocardial infarction in the model of irreversible ischemia did not lead to an increase in the relative density of sympathetic nerves. Semax also had no effect on this value. In ischemia-reperfusion group relative density was 0.0334± 0,004 and were significantly higher than in the control (p = 0.006). Semax administration resulted in a statistically significant (p = 0.01) reduction in the density of sympathetic nerves to 0.0202 ± 0.005. Thus, in ischemia-reperfusion infarction model increased density of fluorescence of the sympathetic nerves were taken place, and Semax administering reduces this index to intact group level. That is that drug somehow reducing effect of factors reinforcing nerve growth after infarction. On the other hand, the decrease in the density of sympathetic innervation may itself be the cause of this decrease in activity of the autonomic nervous system in the postinfarction period.

Relative density of the sympathetic nerves in intact rats in the femoral and renal arteries were 14 ± 3, in mesenteric artery - 29 ± 12, and in the tail artery - 22 ± 6. At 28 days after ischemia-reperfusion innervation of the femoral artery did not change, renal artery innervation (19 ± 6), mesenteric (33 ± 6) and tail (33 ± 9,5) arteries were significantly higher. This likely reflects an overall central activation of the sympathetic nervous system as a result of myocardial infarction. Semax administration in the acute phase at 28 days resulted in an increase of relative density of sympathetic nerves in the femoral artery (18 ± 5,5), renal (18 ± 3,5) and tail artery (30 ± 9) did not changed. Innervation of the mesenteric artery was increased even more - up to 46 ± 5. At irreversible ischemia group we observed an increase in mesenteric (37 ± 8) and tail

(29 ± 9) artery innervation density, which is similar to changes in ische-mia-reperfusion. Semax influence in irreversible ischemia group were especially significant in mesenteric artery, where we observed a statisti-cally significant increase in the density of innervation to 41 ± 8. In gen-eral, the multidirectional effect of the drug on the sympathetic innervation of the arteries can be explained by differences in vascular function and general modulating effect of the peptide, normalizing the autonomic nervous system response to a pathological condition.

To clarify the changes in the sympathetic innervation of blood ves-sels after myocardial infarction and investigate mechanisms of this Se-max effect, we assesed density of α_1-adrenergic receptors in the wall of the tail artery, which plays an important role in thermoregulation in rats.

The average relative density of α_1-adrenergic receptors in intact rat tail artery was $0,39 \pm 0,28$. With the development of myocardial infarc-tion in irreversible ischemia model adrenoceptor density did not change - $0,42 \pm 0,31$, in the model of ischemia-reperfusion changes also were not statistically significant $(0,39 \pm 0, 15)$. Semax significantly increased the density of α_1-adrenoceptors in the rat tail artery in irreversible ischemia model - $0,56 \pm 0,29$, and in ischemia-reperfusion model - $0,59 \pm 0, 31$.

Thus, after the development of myocardial infarction in both models there is an increase of density of the sympathetic nerves in the tail artery, at the same time, the amount of α_1-adrenoceptors did not changed. As long as main function of the tail artery is thermoregulation, these changes reflects the thermoregulation disturbance in the infracted rat caused by heart weak-ening and blood circulation slowing. Increasing the density of sympathetic nerves may be due to the need to reduce heat loss in these conditions.

Semax did not influence on the density of sympathetic nerve ter-minals in tail artery after myocardial infarction, but increase the density of adrenergic receptors. This is consistent with the hypothesis of central decrease of the overall activity of the sympathetic nervous system under the influence of the drug, which led to an increase in adrenergic receptors amount in rat tail artery.

FLAG-TAGGING METHOD FOR ARCHAELLIN IDENTIFICATION IN *HALOBACTERIUM SALINARUM* ARCHAELLA

S.N. Beznosov, M.G. Pyatibratov and O.V. Fedorov
Institute of Protein Research, Russian Academy of Sciences,
Institutskaya st. 4, Pushchino, Moscow Region, 142290, Russia

The movements of both bacteria and archaea in aqueous media are accomplished through the rotation of flagella. Because archaeal flagella are

principally different from their bacterial analogues it has recently been proposed to call archaeal flagella as archaella, and proteins consisting archaella as archaellins [1]. A single archaellum has the appearance of a right-handed helical filament, 4–10μm long and 10 to 20 nm thick. Archaellins have no homology to bacterial flagellins, but at the same time, they are homologous in N-termini to type IV bacterial pilins and are processed in a similar manner, with the removal of the leader peptide before incorporation into supramolecular structure. Archaellins in the archaellum are often glycosylated. Archaella filament of haloarchaea *Halobacterium salinarum* consists of five archaellins - A1, A2, B1, B2 and B3 (FlgA1-FlgB3), which are encoded by genes located in the *flgA* and *flgB* operons. Archaellins A1 and A2 are major filament components, while B1, B2 and B3 are synthesized in much smaller quantities. Earlier by deletion of archaellin genes it was shown that the helical filaments may be formed only from A-proteins, and in the absence of A archaellins, B2 archaellin can form structures similar to the archaellum hook [2-4]. However, the complete picture of the distribution of archaellins within filaments is still not clear.

In this work we have developed a method of directed modification of *H. salinarum* archaellins by insertion of various peptides into a selected region of the archaellin sequence. Since the detailed structure of any archaellin is not known, hence we have selected the insertion site using the following reasons. *H. salinarum* archaellins are N-glycosylated and each of them contains 3 glycosylation sites NXT(S). It is known that glycosylation takes place on the cell surface after the archaellum assembly. This suggests that archaellin glycosylation sites have to be exposed on archaella surface and, consequently, the additional peptide loop introduced nearby glycosylation site will be exposed outside as well [5]. We decided that one of the most suitable sites is between two alanines, located about midway between the two glycosylation sites ***NLT*VRQAxAGADNI*NLS***. Three types of transformed cells synthe-sizing archaella, containing A1, A2, or B2 archaellin modified with FLAG peptide (DYKDDDDK) are obtained [6]. Electron microscopy of archaella has demonstrated that in each case the FLAG peptide is available for the specific anti-FLAG antibody binding. It was shown at first time that B2 archaellin like A1 and A2 is found along the whole filament length, and it is demonstrated that the archaellin modification method is useful for the identification of proteins within archaellum.

Also by this method of archaellin modification we obtained *H. salinarum* archaella, where the gold-binding peptide LKAHLPPSRLPS [7] was inserted into archaellin A2 [6]. The modified archaella were incubated with colloidal gold nanoparticles (5 nm) and then analyzed by electron

microscopy. The gold particles also bound along the whole length of the filaments. So, depending on the introduced peptide, the method of archaellin modification can be used not only in studying the archaella composition, but also as a way to produce new multifunctional nanomaterials.

References

1. Jarrell K.F., Albers S.V., The archaellum: an old motility structure with a new name, Trends Microbiol., 2012, 20, 307-312.
2. Tarasov V.Y., Pyatibratov M.G., Tang S.L., Dyall-Smith M., Fedorov O.V., Role of flagellins from A and B loci in flagella formation of Halobacterium salinarum, Mol. Microbiol., 2000, 35, 69-78.
3. Tarasov V.Y., Pyatibratov M.G., Beznosov S.N., Fedorov O.V., On the supramolecular organization of the flagellar filament in archaea, Dokl. Biochem. Biophys., 2004, 396, 203-205.
4. Beznosov S.N., Piatibratov M.G., Fedorov O.V., On the multicomponent nature of Halobacterium salinarum flagella, Microbiology (Russ.), 2007, 76, 435-441.
5. Beznosov S.N., Pyatibratov M.G., Fedorov O.V., Archaeal flagella as matrices for new nanomaterials, Nanotechnol. (Russ), 2009, 4, 373-378.
6. Beznosov S.N., Pyatibratov M.G., Veluri P.S., Mitra S., Fedorov O.V., A way to identify archaellins in Halobacterium salinarum archaella by FLAG-tagging. Central European Journal of Biology, 2013, 8, 828-834.
7. Nam K.T., Kim D.W., Yoo P.J., Chiang C.Y., Meethong N., Hammond P.T., et al., Virus-enabled synthesis and assembly of nanowires for lithium ion battery electrodes, Science, 2006, 312, 885–888.

STUDY ON INTERACTION OF FULLERENE C_{60} WITH BRAIN Aβ(1-42)-PEPTIDE

A.G. Bobylev[1], Y.V. Shatalin[1], L.G. Bobyleva[1], A.D. Ulanova[1,2], Z.A. Podlubnaya[1,2]

[1]Institute of Theoretical and Experimental Biophysics, Russian Academy of Sciences, Pushchino, Moscow Region, 142290, Russia
[2] Pushchino State Institute of Natural Sciences, Pushchino, Moscow Region, 142290 Russia;
E-mail: bobylev7@rambler.ru

Fullerenes are molecular compounds belonging to the class of allotropic forms of carbon and representing by themselves polycyclic structures of spherical shape consisting of carbon atoms bound into six- and five-membered cycles. Originally a possibility of existence of a structure

consisting of 60 carbon atoms (fullerene C_{60}) was substantiated theoretically. The discovery of fullerenes belongs to Kroto and Smalley [1] who, using a laser beam setup, had fixed special stability of C_{60} and C_{70}, and then proposed the first structural pictures of these molecules.

Fullerene C_{60} is an electronegative molecule, which can be easily reduced, but oxidizes with difficulties. Therefore the main types of reaction appear as nucleophilic, radical or cyclo-additions [3–5]. Because the molecule is electrophilic, it presents a strong acceptor of electrons and free radicals. For this reason fullerenes have even been called «radical sponges» [6]. Fullerenes have other biological properties: inhibition of HIV-1 protease, photomodification of DNA, neuroprotection and so on [7–9]. Fullerenes are insoluble in polar solvents. For studying biological properties of fullerenes use stable colloid solutions in water [10], noncovalent complexes of fullerenes with hydrophilic organic molecules (for example, complexes of fullerene C_{60} with polyvinylpyrrolidones and cyclodextrins), and also synthesized water-soluble derivatives of fullerenes.

Earlier we have shown that fullerene C_{60} and a series of its derivatives destroyed amyloid fibrils of the brain $A\beta(1-42)$-peptide and muscle X-protein [11-14]. A conclusion was made that fullerene C_{60} and its derivatives can be regarded as potential antiamyloid substances.

In this work we investigated the interaction of fullerene C_{60}-polyvinylpyrrolidone (C_{60}/PVP) complex with brain $A\beta(1-42)$-peptide in water.

Using a the spectrophotometric assay we have analyzed the changes occurring in a solution containing $A\beta(1-42)$-peptide and C_{60}/PVP. The peptide in a concentration of 5 µM is low absorbance at wavelengths (228, 264, 344, 524 nm). Fullerene C_{60}, polyvinylpyrrolidone, and the formed their aggregate $A\beta(1-42)nC_{60}kPVPm$ have significant absorption coefficient. For calculating the stoichiometric coefficients we use the formula $-lg(D_{mixture} - D_{reagent}) = f(-lgC_{reagent})$, where $D_{mixture}$ − absorbance of the solution containing all three components, $D_{reagent}$ and $C_{reagent}$ − optical density and the concentration of the titrant containing complex C_{60}/PVP.

It has been found by us that the structure of the aggregate formed in the solution had the following stoichiometric composition $A\beta(1-42)$-$(C_{60})_{1,69-1,82}PVP_{0,22-0,35}$. Using the Method Bent-French relative binding constants of fullerene C_{60} with $A\beta(1-42)$-peptide and PVP with $A\beta(1-42)$-peptide were determined, which amounted to $4,92 \cdot 1013$ and $3,00 \cdot 106$, respectively. The data obtained suggest that $A\beta(1-42)$-peptide interacts with complex $C_{60}kPVPm$, displaces polyvinylpyrrolidone and form a new three molecular aggregate.

References

1. H. W. Kroto, J. R. Heath, S. C. O'Brien, et al., Nature 318, 162 (1985).
2. A. Hirch, I. Lampart, H. R. Karfunkel, Angew. Chem. Int. Ed. 33, 437 (1994).
3. A. Hirch, Synthesis 8, 895 (1995).
4. A. Hirch, Topics in Current Chemistry 199, 1 (1996).
5. A. Hirch, J. Phys. Chem. Solids 58, 1729 (1997).
6. C. N. McEwen, R. G. McKay, B. S. Larsen, J. Am. Chem. Soc. 114, 4412 (1992).
7. A. W. Jensen, S. R. Wilson, D. I. Schuster, Bioorg. Med. Chem. 4, 767 (1996).
8. T. Da Ros, M. Prato, Chem. Commun. 663 (1999).
9. S. R. Wilson, K. Kadish, R. Ruoff, Wiley, New York P. 437–4652000.
10. G. V. Andrievsky, V. I. Bruskov, A. A. Tykhomyrov and S. V. Gudkov, Free Radic. Biol. Med. 47 (6), 786 (2009).
11. L G. Marsagishvili, A. G. Bobylev, M. D. Shpagina et al., Biophysics 54 (2), 135 (2009).
12. A. G. Bobylev, L G. Marsagishvili, M. D. Shpagina et al., Biophysics 55 (3) 353 (2010).
13. A. G. Bobylev, L G. Marsagishvili and Z. A. Podlubnaya, Biophysics 55 (5), 699 (2010).
14. A. G. Bobylev, A. B. Kornev, L. G. Bobyleva, et al., Organic & Biomolecular Chemistry 9, 5714 (2011).

PRESUMABLE ROLE OF SPHINGOLIPID MECHANISMS IN DISUSE ATROPHY OF SKELETAL MUSCLE

I.G. Bryndina, M.N. Shalagina, S.V. Ovechkin
Izhevsk State Medical Academy, Kommunarov St., 281, Izhevsk, 426034, Russia

The role of diverse sphingolipid species in cell signaling is a subject of growing interest in physiology, molecular biology and medicine in two last decades. Sphingolipid derivative ceramide plays a pivotal role in many processes including cell arrest, apoptosis, generation of free oxygen species, inhibition of some intracellular signaling pathways, etc. Ceramide is produced in cell by three main pathways: sphingomyelin hydrolysis by sphingomyelinases, de novo synthesis from serine and palmitoyl-CoA and so-called salvage pathway. Being the important structural component of cell membrane, ceramide is discovered to be also the one of the evolution-

arily conserved cellular factor generated in response on different stress stimuli (inflammatory mediators, heat, UV radiation, hypoxia, chemotherapeutics, and oxidative stress). It is demonstrated that all these stimuli increase ceramide production in diverse type of cells (Bickman et al., 2011).

Now there is much evidence that skeletal muscle may be a target of ceramide and other sphingolipid species effects. Ceramide is considered by some authors as a key factor of insulin resistance in adipose and muscle tissue, particularly in 2 type diabetes mellitus, high fat diet and increased plasma free fatty acids. Some intracellular targets of ceramide in muscle are revealed last years: the pathway of PI-3K and Akt/PKB is among them. It is well known that this pathway is involved in the mechanisms of insulin and IGF action. Furthermore, it has been shown that ceramide induces the apoptosis in skeletal muscle myotubes (S.M. Turpin et al., 2006). Another important sphingolipid molecule is sphingosin-1-phosphate that exerts the opposite (positive) influence on some processes targeted by ceramide.

The problem of ceramide impact on disuse changes in skeletal muscle is of great importance taking into account the prevalence of diseases leading to immobility, strong bed rest and restraint. On the other hand, only few and conflicting data exist regarding the effect of exercise training on ceramide metabolism in skeletal muscle (decreased, increased ceramide level or no effect). The problem of ceramide impact on disuse changes in skeletal muscle is also actual due to intensive exploration of space with necessity of long-term being of cosmonauts in microgravity environment. Space flight (especially of long duration) is accompanied by atrophy and dysfunction of skeletal muscles and changes of their myosin heavy chain phenotype (mainly in slow postural muscle like m. soleus). But sphingolipid impact on muscles changes in microgravity is "terra incognita" now, although we can speculate some possible effects of space flight in this aspect. We have shown previously (I.G.Bryndina et al., 2009-2012) that 30-day antiorthostatic hindlimb suspension in mice leads to accumulation of ceramide in unloaded m. soleus without significant change of its level in forelimb muscle (m. biceps brachii). So, we hypothesized that unloading exerts some sphingolipid pathways generating ceramide or limiting its degradation. Our new experiments have demonstrated the effects of short-term and long-term hindlimb unloading on a number of enzymes involved in ceramide metabolism processes, e.g., sphingomyelinase and serine palmitoyltranspherase (unpublished data).

Thus, we can conclude that exploration of sphingolipid impact on cellular signaling in microgravity is perspective approach in space physiology.

References

1. Bikman B.T., Summers S.A. Ceramides as modulators of cellular and whole-body metabolism // J. Clin. Invest. – 2011. – V. 121, N 11. – P. 4222-30.
2. Брындина И.Г., Багаутдинов М.Р., Васильева Н.Н., Кривоногова Ю.А., Шалагина М.А. Церамиды скелетных мышц, печени и легких грызунов при хроническом эмоциональном стрессе и моделированной невесомости // Вестник Уральской медицинской академической науки. – 2012. - № 2(39).- С.108-109.

DEPENDENCE OF THE 1-st ELECTROCARDIOGRAM LEAD PARAMETERS ON HEART POSITION: REAL MEASUREMENTS AND BIOPHYSICAL MODELING

I.A. Chaikovsky[1], O.V. Baum[2], L.A. Popov[2], V.I. Voloshin[2], N.N. Budnyk[1], Yu. A. Frolov[1], I.O. Syropyatov[1]

[1] *Glushkov Institute for Cybernetics, National Academy of Science of Ukraine, prosp. Glushkova, 40, Kiev, 03680, Ukraine;*
[2] *Institute of Theoretical and Experimental Biophysics, RAS, Institutskaya, 3, Pushchino, 142290, Russia*

Coronary artery disease (CAD), i.e. cardiac muscle ischemia, in last decades has been pandemic in behavior. In the USA almost 17 millions people suffer from CAD. In developed countries CAD is the cause of about 20% of deaths. According to prognostic estimations of the World Health Organization (WHO), the death-rate due to CAD will reach 23.4 millions in 2030 [1]. Due to high morbidity and mortality of CAD and the economic aspects of the disease, early diagnosis of cardiac muscle ischemia is one of the fundamental targets in daily cardiological routines.

Electrocardiography remains the basic, the most widespread diagnostic method in cardiology. In recent years, electrocardiography experienced a number of important innovations. One of them is development of miniature portable electrocardiographic devices, which can be used by patient to some extent by oneself outside doctor's office. This tendency is within the current trend in medical industry, called point-of-care testing (POCT) i.e. medical test conducted immediately in patient's whereabouts, outside doctor's office.

The main idea underlying the use of portable ECG devices, that are generally single-channel, is life-threatening heart rhythm disorders diagnosis (high gradation premature ventricular beats, ventricular and supraventricular paroxysmal tachycardia and so on). There are a number of publications, wherein authors assert that single-channel ECG has value in

myocardial ischemia diagnosis, with even routine amplitude analysis of ECG waves and intervals [2, 3]. Especially the value of such analysis increases if more sensitive parameters are applied. Earlier on we thoroughly analyzed the capability of the 1-st lead electrocardiogram T wave symmetry to be such parameter, including biophysical modeling [4]. Nevertheless, while discussing the diagnostic value of the 1-st lead ECG a set of theoretical considerations emerges inevitably, one of the most important among them is the question about dependence of the parameters of electrocardiogram in one lead on the direction of electrical axis of heart. In other words, changes of which parameters of the 1-st lead electrocardiogram are in fact liable to reflect pathological processes in myocardium, and which one are determined by extracardiac factors, primarily by anatomic characteristics of subjects.

The purpose of given article is to investigate the relations between main amplitude-time parameters of electrocardiogram in the 1-st lead and electrical heart position both in the group of healthy volunteers and with the help of a biophysical model, in the framework of long-term collaboration between Glushkov Institute of cybernetics and Institute of theoretical and experimental biophysics.

Materials and methods

Examination of the group of healthy volunteers. 71 healthy volunteers (medial age 35 ± 7 years), without history of cardiac pathology, with normal outcome of physical examination and 12-lead electrocardiogram in resting state, which was evaluated by applying the Minnesota code, were examined. Electrocardiogram was recorded by production digital electrocardiograph. By means of custom designed software package angle αQRS and a set of amplitude-time parameters of electrocardiogram were routinely calculated. Afterwards Pearson's linear correlation coefficient was calculated between the αQRS angle and 9 parameters of the 1-st lead electrocardiogram, more specifically R and T wave amplitudes, T wave symmetry, evaluated in two various ways, ratio of R amplitude to S amplitude, ST segment displacement in 0.08 sec after J point, spatial angle QRS-T, QRS complex duration, ratio of interval duration JT_{apex}/JT.

Biophysical modeling. Computer experiments were executed on a system for 3D-modeling of the cardiac electrical activity with the aid of earlier developed model of ECG genesis (cellular automaton of about a million elements of the Myocardium-His-Purkinje type), the parameters of which are electrophysiological, anatomical, and biophysical characteristics of the heart muscle. Processing of the model ECG was carried out with original specially designed program [5, 6].

Rotation of heart in frontal plane from 25 to 65 degrees with the step of 5 degrees was performed. Thus, 9 positions of the heart were obtained. In each of these positions the model generated electrocardiograms in 12 standard leads. On these electrocardiograms above-mentioned 10 amplitude-time parameters of the 1-st lead were calculated. Finally, linear correlation coefficient between heart position angle in the frontal plane and calculated parameters was evaluated.

Results

The results of reckoning of correlation coefficients of mentioned parameters and αQRS angle (real measurements) and position of heart in the frontal plane (biophysical model) are represented in tables 1 and 2 accordingly.

Table 1. Linear correlation coefficient between αQRS angle and amplitude-time parameters of the real electrocardiogram in the 1-st lead

R	T	$Tsym_1$	$Tsym_2$	R/S	$ST_{displ.}$	$QRS-T_{ang.}$	$QRS_{dur.}$	JT_{apex}/JT
0,84	0,65	0,42	0,36	0,88	<0,2	<0,2	<0,2	<0,2

Table 2. Linear correlation coefficient between the angle of heart position in frontal plane and amplitude-time parameters of the model electrocardiogram in the 1-st lead

R	T	$Tsym_1$	$Tsym_2$	R/S	$ST_{displ.}$	$QRS-T_{ang.}$	$QRS_{dur.}$	JT_{apex}/JT
0,91	0,84	0,11	0,41	0,95	0,31	0,92	<0,2	0,81

As the tables show, there is a strong relation between the main waves' amplitudes and position of the heart. This fact is confirmed by both analysis of real measurements and modeling. The symmetry of T wave, QRS duration, and ST segment displacement are far less related to heart position. These have average or weak correlation relationships. Concerning these parameters there is also a "consensus" between results of real measurements and model measurements. As regards such parameters as QRS-T angle and ratio of interval duration JT_{apex}/JT there is a difference of the results, obtained from real measurements and modeling: no correlation relationship with heart position in the first case, and strong correlation in the second case.

This is connected, most likely, with several factors: effect of the heart rate variability on time intervals of the cardiocycle for the real electrocardiograms; relationship between the cardiac electric axis and the angles of the heart rotation about its anatomic axes in the model, which is of

a complicated nature, but can be explained physically and expressed analytically in terms of functions for the family of αQRS-curves where the angle of rotation about of axis is the argument and the values of angles of rotation about the two other axes are the parameters of the family. Additional study is needed.

Discussion and Conclusion

There are approximately 10-15 types of portable electrocardiographic devices in the market at the present day, mainly single-channel electrocardiographs. Here are some of them: OMRON (Japan), Health frontier (Canada), Instant Check (United Kingdom), ReadMyHeart (USA), FP-80 (China), MB-100 и MB-100A1 (China), Dimetek (China), Vitaphone (Germany), Gnom (Russia), Fasagraf (Ukraine), Cardiovisor (Russia), Cardioplus(Ukraine) and others.

These devices have already become widespread and this segment of medical device market presents great growth prospects. According to Global Industry Analyst Inc. analysts, portable electrocardiographs market volume in the USA totals US$1.1 billion. Portable electrocardiographic hardware-software complexes (HSC) feature diminutiveness, great looking, eye-catching design, along with easiness and accessibility of tests conduction – there is no need of chest electrodes application. To carry out a measurement one should just place fingers on built-in electrode. It is of utmost importance to position "pocket" electrocardiographic HSCs correctly, i.e. to formulate optimal niche of application as well as criteria of data analysis.

Thus, it is arguable that while analyzing electrocardiogram in the first lead it is necessary to orient with reserve towards waves' amplitudes (especially R wave), as they depend heavily on such factor as position of heart in thorax, i.e. on anatomic features of subjects. At the same time such important parameter of T wave form, as its symmetry much less depends on position of heart in thorax. Also, independent of subjects' anatomic features are such physiologically based informatory indexes as ST segment displacement and QRS complex duration. The results obtained are of interest for theoretical and applied aspects of the cardiac muscle science.

References

1. Cassar A., Holmes D., Charanjit S. at al. Chronic coronary artery disease: diagnosis and management. Mayo.Clin.Proc.2009; 84(12):1130-46
2. Lochen M.L., Rasmussen K., Macfarlene P.W. Can single-lead computerized electrocardiography predict myocardial infarction in young and middle-aged man? The Tromso study. // J. Cardiovasc. Risk.- 1999.- V.6.- P. 273-278.

3. Schweize M.W.F., Jooss M., Gillessen W. at al. Multicenter validation study of an easily applicable cybernetic prototype device that assesses electrocardiographic abnormalities. // Computers in Cardiology. – 1999.- V.26. -P. 531-534.
4. Chaikovsky I. Analysis of electrocardiogram in one, six, and twelve leads in terms of information value: electrocardiographic cascade. Clin. informatics and telemed., 2013; 9(10): 54-65.
5. Baum O.V., Voloshin V.I., Popov L.A. Realization of biophysical models for the cardiac electrical activity. Biofizika, 2009; 54(1): 97-113.
6. Baum O.V., Chaikovsky I.A., Popov L.A., Voloshin V.I., Fainzilberg L.S., Budnik M.M. Electrocardiographic image of myocardial ischemia: Real measurements and biophysical models. Biofizika, 2010; 55(5): 925-936.

SWITCHING BETWEEN DIFFERENT TYPES OF CELL MIGRATION IS ADAPTIVE ADVANTAGE OF TUMOR CELLS

A.S. Chikina, A.Y. Alexandrova

Blokhin Cancer Research Center, Russian Academy of Medical Sciences, Moscow, 115478 Russia

The two main types of migration used by individual cells are mesenchymal and amoeboid modes of motility. Mesenchymal migration normally is used by fibroblasts and fibroblast-like cells. In mesenchymal motility, cells coordinate actin-based protrusion with the formation of actomyosin-associated focal adhesions (FAs) through which contractile forces are transduced to the underlying substrate. Thus the main features of mesenchymal mode of motility is formation of two types of protrusions - lamellipodia and ruffles by Arp 2/3 dependent actin polymerization. In this process Arp2/3 complex binds to lateral side of initial actin filament and initiates the polymerization of new actin filament with 70 degrees to the previous one. Thus the growing network of actin filaments creates the pushing force applied to the plasma membrane, which leads to lamellipodia formation. When substrate is sufficiently adhesive FA are formed and cell attaches to substrate, forms stress fibers and could effective moved by contraction. If the substrate is non-adhesive, cells is not able to attached. Thereby protrusions will recline, back to the cell. This type of protrusions calls ruffles. Consequently all types of protrusions formed during mesenchymal migration develop by the same mechanism, morphological differences between them are due solely anchorage efficiency of the cell.

Amoeboid type of cell migration is normally used by lymphocytes. The main feature of this migration mode is blebbs formation which occurs by

totally different mechanism than it was describe above. For cells demonstrated amoeboid migration mode cortical actin network underlying cell membrane and connected with it by linker proteins is typical, while actin bundles and stress fibers are practically absent. At the first stage of protrusion formation linker proteins which connect cortical actin cytoskeleton and plasma membrane disintegrate. Acto-myosin interaction cause cell contractility what lead to increase of cytoplasmic pressure. Cytoplasm flows to the gap between cortical actin and plasma membrane, cortex disassemblies and new protrusion (blebb) forms at this region. After blebb expansion cortical actin restores by formin-dependent polymerization of actin filaments, then cell contracts. Thereby stabilization of blebbs should occur by physical-support from outside, for instance either by collagen fibers of extracellular matrix or between endotheliocytes during extravasation of intravasation. Thus protrusion stabilizes by high cytoplasmic pressure therein and physical cell-substrate interaction during amoeboid migration.

Normally cells migrate by one of these mechanisms, but undifferentiated and tumor cells could demonstrate plasticity of migration, what means that cell can choose those type of migration which is more effective in microenvironmental condition where migration occurs. Transition from mesenchymal to amoeboid mode of migration calls mesenchymal-to-amoeboid transition, from amoeboid to mesenchymal mode calls amoeboid-mesenchymal transition. Plasticity of cell migration allows cells to migrate effectively through different tissues barriers, for example basal membrane or dense extracellular matrix, possible helps to prolong the time of cell re-circulating into blood flow, proceeds extra- and intravasation and thus probably leads to enhance of effectiveness of invasion and metastatic formation.

Objective of our investigation was analysis of migration plasticity of normal and tumor cells. Human subcutaneous fibroblasts (1036 cell culture) and human fibrosarcoma (HT1080 cell culture) were used for experiments. It was shown that tumor cells when they couldn't migrate by mesenchymal mechanism (due to impairment of substrate adhesiveness or due to Arp2/3- inhibition) switch to amoeboid type of cell migration whereas normal fibroblasts just stop and didn't demonstrate plasticity of cell migration.

However transition to amoeboid mode does not mean increasing in efficiency of cell migration in any cases. Efficiency of cell migration highly depends on structural and dimensional organization of extracellular matrix. On the 2-dimensional substrate (glass) mesenchymal migrating tumor cells demonstrate higher velocity ($0,24 \pm 0,011$ µm/min) than

amoeboid migrating cells (0,18±0,017 μm/min), while in three-dimensional substrates (agarose gel) the situation was reversed: cells, which used amoeboid type of migration moved three-fold faster (**0,625**±0.04 μm/min) then mesenchymally migrated cells (0,18±0,017 μm/min).

Using ImageJ software by kimograph analysis we investigated the dynamics of the leading edge of mesenchymal and amoeboid-migrating cells. It was shown frequency of lamellipodia formation was more rare compare to blebb formation, but their living time was longer. In addition to differences in the dynamics of the formation of protrusions it was shown big differences in the entire life cycle of these types of protrusions. Blebb`s phase of expansion is faster then retraction phase (3.87 ± 0,004 μm/s vs 0.68 ± 0,002 μm/s), there practically absent stationary phase (less than 2 seconds). The reverse situation was demonstrated during lamellipodia formation: expansion is much slower than retraction (0,15 ± 0,001 μm/s vs 0,27 ± 0,004 μm/s), the stationary phase took from 15 seconds to a minute.

	Frequency of protrusion formation, 1\5min	Velocity of expansion, мкм/s	Velocity of retraction, мкм/s	Duration of stationary phase, s
Blebbs	11,8 ± 0,7	3,87 ± 0,004	0,68 ± 0,002	≤ 2
Lamellipodias	1,6 ± 0,1	0,15 ± 0,001	0,27 ± 0,004	45 ± 0,5

The basis of these differences is likely in the fundamentally different mechanisms underlying formation of lamellipodia and blebb described above.

Furthermore, lamellipodia formation occurs in a plane of cell contacts with a substrate (practically 2D interactions) while blebbing can occur at different levels ("tiers") of cell (3D formation). This fact may explain the dependence of the efficiency of cell migration on the spatial organization of the substrate. The mesenchymal motility mode is more efficient for 2D substrate, because of forming a flat lamellipodia, which is attached to it with the FA. In 3D matrix the formation of FA reduced significantly, so lamellipodia is not so effective type of protrusion to support cell motility.

In the case of amoeboid movement situation is reversed: the two-dimensional substrate for cell moves extremely inefficient, since, firstly, blebbs form to all directions, and hence the effective area of interactions with the substrate is markedly reduced , and secondly , the cell does not form FAs, and thus could not attach properly to substrate. But in the

three-dimensional matrix ~~of~~ the cells migrating by amoeboid mode have several advantages : blebbs distributed at multi levels allow the cell to increase the effective area of interaction with the substrate and anchor inside it. The mechanism of blebbs formation suggests the stage of blebbs by "fullness" of the substrate gaps, which can be effectively only in three-dimensional systems.

We also show that cells with amoeboid morphology more effective migrated trough filter in Boyden chambers. Increasing the efficiency of migration in Boyden chambers with mesenchymal- amoeboid transition may also indicate that formation of blebbs on different layers allows the cell to find the way of migration (in this system - the membrane pores) more effectively, compared with mesenchymal - migrating cells.

Thus improvement the efficiency of tumor cell migration is provided apparently not so much by the transition from mesenchymal to amoeboid motility mode, as the acquisition of migratory plasticity mechanisms and the ability of cells to choose the most effective type of motion depending on the spatial organization of the substrate.

INTERACTIONS BETWEEN THE IL-6-174G>C GENE POLYMORPHISM AND CARDIAC AUTONOMIC RESPONSES IN RELATION TO PRECLINICAL ATHEROSCLEROSIS: THE YOUNG FINNS STUDY

N. Chumaeva[1,2], L. Pulkki-Råback[1], T. Lehtimäki[3],
O.T. Raitakari[4,5], L. Keltikangas-Järvinen[1]
[1]Institute of Behavioural Sciences, University of Helsinki,
PO Box 9, 00014 Helsinki, Finland;
[2]Institute of Cell Biophysics RAS, Institutional Street 3,
Pushchino, Moscow region 142290, Russia;
[3]Department of Clinical Chemistry, Fimlab Laboratories,
Tampere University School of Medicine, Finn-Medi 2,
PO Box 2000, Tampere FI-33521, Finland;
[4]Research Centre of Applied and Preventive Cardiovascular Medicine,
University of Turku, PO Box 52, 20521 Turku, Finland;
[5]Department of Clinical Physiology and Nuclear Medicine,
Turku University Hospital, PO Box 52, 20521 Turku, Finland

Functional interleukin-6 (IL-6) -174G/C single nucleotide poly-morphism (SNP) may be responsible for individual's vulnerability to stress-related cardiovascular diseases mediated by negative immune response. The IL-6G174C SNP regulates IL-6 production [1,2] and re-

lates to stress coping [3]: the C allele is related to lower IL-6 levels and to better stress coping while the G allele - to increased IL-6 concentration and less stress coping capability [1-3]. Acute mental stress leads to elevated IL-6 release [4-6] inducing stress-evoked activation of immune system [5]. We suggest that the IL-6-174G allele would be associated with increased cardiac autonomic reactivity and/or with delayed recovery after brief laboratory stress. We also hypothesized interactions between the G allele in combination with unfavorable cardiac responses related to increased risk of atherosclerosis. Thus, we examined associations of the IL-6G174C SNP (rs1800795) with cardiac autonomic responses after acute stress and interactive effect of cardiac reactivity and the IL-6 gene SNP to preclinical atherosclerosis in 45 middle-aged healthy participants. Atherosclerosis was assessed non-invasively by measuring the carotid intima-media thickness (IMT).

Methods and participants

The participants were 24-39 years old adults derived from the epidemiological Young Finns study [7]. The study was established to investigate the development of cardiovascular risk factors in children, adolescents and young adults at intervals of 3 or 5 years (a total N in 1980 = 3596). In 2001, clinical and ultrasound measurements were taken from 2109 participants; genotyping for the IL-6G174C SNP (rs1800795) was performed in 2228 subjects. In 1999, physiological stress experiment was administered for 95 participants. The final sample of the present study consists of 45 men and women. The study was conducted with an agreement of local ethics committees and according the guidelines of the Helsinki Declaration. All subjects gave their written, informed consent in 1999 and in 2001.

Ultrasound imaging: Ultrasound investigations were carried out using Sequoia 512 ultrasound mainframes (Acuson, Mountain View, CA, USA) with 13.0 MHz linear array transducer [8]. Carotid IMT was measured on the posterior (far) wall of the left carotid artery; at least four measurements were taken approximately 10 mm proximal to the bifurcation to derive mean carotid IMT. The between-visit coefficient of variation of IMT measurements was 6.4% and the intra-observer coefficient of variation was 3.4% [8].

The IL-6-174G>C genotyping: Genomic DNA was extracted from whole blood using a commercially available kit (Qiagen Inc., Hilden, Germany). The IL-6-174G>C genotyping (rs1800795) was performed using the 5'-nuclease assay and fluorogenic allele-specific TaqMan probes and primers [9]. PCR was performed in 384-well plates in a total volume of 5μl, using

ABI Prism 7900HT Sequence Detection System (Applied Biosystems, Foster City, CA, USA) as described in our previous study [10].

Clinical characteristics: Blood pressure was measured with a random-zero sphygmomanometer [11]. Average of three measurements was used in the analysis. Standardized enzymatic methods were used for measuring levels of triglycerides and HDL-cholesterol [11]. Serum LDL-cholesterol concentration was calculated by the Friedewald formula [8,11]. Serum insulin was measured by microparticle enzyme immunoassay kit (Abbott Laboratories, Diagnostic Division, Dainabot, Japan) [11].

Psychophysiological experiment: Cardiac autonomic responses: heart rate (HR, an index of sympathetic/parasympathetic autonomic balance), respiratory sinus arrhythmia (RSA, an indicator of parasympathetic drive), and pre-ejection period (PEP, indicates sympathetic activity level) after brief laboratory stressors were quantified by impedance electrocardiography, as previously described [12]. In the current study, the mental arithmetic and the speech tasks were used for calculating cardiac reactivity; and two resting periods (after the mental arithmetic and after the speech) – for computing stress recovery. Average of two tasks reactivity levels and average of two rests after the tasks were used in the statistical analyses. Details of the experiment, data treatment and reactivity/recovery scores calculations were previously described [12].

Statistical analyses: Associations between cardiac autonomic responses and the IL-6-174G/C SNP as well as interactions between cardiac reactivity or recovery and IL-6 gene SNP in relation to IMT were tested by regression analyses using PASW Version 18.0. Clinical measurements were used as covariates.

Results and discussion

Associations between the IL-6-174GG genotype and delayed HR recovery were found. PEP reactivity x IL-6 gene SNP interactive effect on IMT and PEP recovery x IL-6 gene SNP interactive effect on IMT were shown after adjusting for clinical measurements: serum insulin, serum lipid levels and blood pressure. Among the G allele carriers, elevated PEP reactivity was related to increased IMT; among the GG genotype individuals, slower PEP recovery was related to greater IMTs. High HR is an index of sympathetic dominance [13]; in addition, elevated PEP reactivity and delayed PEP recovery found in our study suggest high sympathetic nervous system (SNS) activation induced by stress [14]. Unfavorable PEP and HR responses were found in our study only in the IL-6-174G allele carriers. Our results are in line with the recently found mechanism providing links between SNS beta-adrenergic norepinephrine-dependent activation of GATA1

transcriptional factor that results in IL-6 gene expression related to diseases risk [15]. GATA1 is sensitive to the IL-6-174G allele only in adverse social-environment conditions, whereas the C allele carriers are protected from elevated stress-induced inflammation response by blocking the SNS/GATA1 signaling [15]. Previous studies have also reported the IL-6-174G allele (or GG genotype) associations with increased IMT in healthy adults [16-18] or in diseases populations [19,20]. Some studies have found conflicting results providing the IL-6-174C allele and increased atherosclerosis risk associations or no associations between the IL-6-174G/C SNP and atherosclerosis [21,22]; however, in these studies, socio-environmental preconditions were not taken into account. Complicated transcriptional regulation of the IL-6 gene SNP [15,23,24], complex, not fully investigated effect of the IL-6-174G/C SNP on IL-6 expression [23,24] and different biochemical mechanisms participating in the realizing of the IL-6 effects [24] may also explain contradictory findings and suggest that the effect of one SNP on diseases risk cannot be exaggerated. IL-6 protein may be involved both in atherogenesis and in stress reactions by influencing sympathetic-parasympathetic balance resulted from the hypothalamic-pituitary-adrenocortical axis activation [25] and from increasing catecholaminergic neurotransmitters production in the brain [26].

Conclusions

The IL-6-174GG genotype (or G allele) may be responsible for genetic predisposition to elevated prolonged sympathetic stimulation and, therefore, to increased risk of stress-related atherosclerosis.

References

1. Fishman D., et al. The effect of novel polymorphisms in the interleukin-6 (IL-6) gene on IL-6 transcription and plasma IL-6 levels, and an association with systemic-onset juvenile chronic arthritis. J Clin Invest 1998; 102: 1369-1376.
2. Bonafe M., et al. A gender-dependent genetic predisposition to produce high levels of IL-6 is detrimental for longevity. Eur J Immunol 2001; 31: 2357-2361.
3. Sjögren E., et al. Interleukin-6 levels in relation to psychosocial factors: Studies on serum, saliva, and *in vitro* production by blood mononuclear cells. Brain Behav Immun 2006; 20: 270-278.
4. Goebel M.U., et al. Interleukin-6 and tumor necrosis factor-alpha production after acute psychological stress, exercise, and infused isoproterenol: differential effects and pathways. Psychosom Med 2000; 62: 591-598.
5. Steptoe A., et al. The effects of acute psychological stress on circulating inflammatory factors in humans: a review and meta-analysis. Brain Behav Immun 2007; 21: 901-912.

6. von Kanel R., et al. Delayed response and lack of habituation in plasma inter-leukin-6 to acute mental stress in men. Brain Behav Immun 2006; 20: 40-48.
7. Raitakari O.T., et al. Cohort profile: The Cardiovascular Risk in Young Finns study. Int J Epidemiol 2008; 37: 1220-1226.
8. Juonala M. Cardiovascular risk factors and their associations with markers of subclinical atherosclerosis in young adults. The Cardiovascular Risk in Young Finns Study. Annales Universitatis Turkuensis, D645; 2005.
9. Livak K.J. Allelic discrimination using fluorogenic probes and the 5' nucle-ase assay. Genetic Analysis: Biomolecular Engineering 1999; 14: 143-149.
10. Chumaeva N., et al. Interleukin-6-174G>C polymorphism, chronic stress and risk of early atherosclerosis in the Cardiovascular Risk in Young Finns Study. J Psychosom Res 2014. In Press.
11. Raitakari O.T., et al. Cardiovascular risk factors in childhood and carotid artery intima-media thickness in adulthood: the Cardiovascular Risk in Young Finns study. JAMA 2003; 290: 2277-2283.
12. Chumaeva N., et al. Interactive effect of long-term mental stress and cardiac stress reactivity on carotid intima-media thickness: The Cardio-vascular Risk in Young Finns study. Stress 2009; 12: 283-293.
13. Palatini P. Elevated heart rate as a predictor of increased cardiovascular morbidity. J Hypertens 1999; 17: S3-S10.
14. Cacioppo J.T., et al. Individual differences in the autonomic origins of heart rate reactivity: The psychometrics of respiratory sinus arrhythmia and pre-ejection period. Psychophysiol 1994; 31, 412-419.
15. Cole S.W., et al. Computational identification of gene-social environ-ment interaction at the human IL6 locus. Proc Natl Acad Sci USA 2010; 107: 5681-5686.
16. Rauramaa R., et al. Stromelysin-1 and interleukin-6 gene promoter pol-ymorphisms are determinants of asymptomatic carotid artery atheroscle-rosis. Arterioscler Thromb Vasc Biol 2000; 20: 2657-2662.
17. Rundek T., et al. Carotid intima-media thickness is associated with allelic variants of stromelysin-1, interleukin-6, and hepatic lipase genes: The North-ern Manhattan Prospective Cohort Study. Stroke 2002; 33: 1420-1423.
18. Giacconi R., et al. The -174G/C polymorphism of IL-6 is useful to screen old subjects at risk for atherosclerosis or to reach successful age-ing. Exper Gerontol 2004; 39: 621-628.
19. Pola R., et al. The -174G/C polymorphism of the IL-6 gene promoter and essential hypertension in an elderly Italian population. J Human Hyprtens 2002; 16; 637-640.
20. Bamoulid J., et al. The interleukin-6 gene promoter polymorphism -174 and atherosclerotic events in overweight transplanted patients. J Trans-plant 2011; 2011: 803429. In Press.
21. Riikola A., et al. Interleukin-6 promoter polymorphism and cardiovascular risk factors: the Health 2000 Survey. Atherosclerosis 2009; 207: 466-70.

22. Chapman C.M., et al. Association of an allelic variant of interleukin-6 with subclinical carotid atherosclerosis in an Australian community population. Eur Heart J 2003; 24: 1494-1499.

23. Tso A.R., et al. Interleukin-6 174G/C polymorphism and ischemic stroke: a systematic review. Stroke 2007; 38: 3070-3075.

24. Shanker J., Kakkar V.V. Implications of genetic polymorphisms in inflammation-induced atherosclerosis. Open Cardiovasc Med J 2010; 4: 30-37.

25. Juttler E., et al. Interleukin-6: a possible neuromodulator induced by neuronal activity. Neuroscientist 2002; 8: 268-275.

26. Capuron L., Miller A.H. Immune system to brain signaling: neuropsychopharmacological implications. Pharmacol Ther 2011; 130: 226-238.

TWO SOURCES FOR THE ENDOGENOUS WATER AND THEIR POSSIBLE ROLE IN THE FAT METABOLISM IN THE HUMAN ORGANISM

N.P. Deshcherevskaya, N.O. Deshcherevskaya
*Institute of Biochemistry and Physiology of Microorganisms RAS;
E-mail: deshchere@rambler.ru*

A "global epidemic" of obesity that is increasing in recent years, according to WHO, is a serious threat to humanity. Effectiveness of the use of high doses of water in the fight against obesity leads to the hypothesis of chronic dehydration as one of the causes of overweight and raises the question about the role of water in fat metabolism [1, 2].

Continuous process of removing water from the living body during metabolism is compensated not only due to ingested food and drink, but also due to endogenous water that is produced within the organism. It is generally assumed that the main source of the endogenous water is the biochemical reactions of the catabolism of nutrients. It is known, that the most important part of these reactions occurs in the mitochondria. However on this way, the synthesis of water occurs only at the last stage - in the mitochondrial respiratory chain, which uses the reducing equivalents derived in the biochemical reactions of β- oxidation of fatty acids as well as in the citric acid cycle, which is the final stage of the oxidation of carbohydrates and of the hydrocarbon skeletons of the protein. Thus, the intensity of the synthesis process water is directly related to the efficiency of the operation of the mitochondrial respiratory chain that is largely determined by the ratio of the concentrations of ADP and ATP.

At the same time in the human organism there is the other source of endogenous water - in the biochemical reactions of the fats biosynthe-

sis. Under certain conditions, when the rate of ATP hydrolysis in cells is insufficient and the concentration of ADP in the mitochondria is small (for example, if there are the excessive eating and the lack of exercise), the mechanism of respiratory control leads to inhibition of the electron transport in the respiratory chain of the mitochondria. This slows down the process of oxidation of NADH to the NAD. The large value of the NADH / NAD ratio leads to inhibition of the citric acid cycle. This reduces the possibility of the production of the endogenous water by the biochemical reactions of the catabolism of nutrients and increases the role of the second method of producing endogenous water - by means of the biosynthesis of fats. In this case, a chronic lack of fluid in the human body can lead to an increase in body fat stores. A discussed mechanism may underlie the phenomenon of morbid obesity, arising as a consequence of chronic shortages of fluid in the human body.

References

1. Deshcherevskaya N.P. How to drink water, to be slim. Guide for those who want to normalize your own weight without outside assistance (Vuzovskaya kniga, M., 2011), (in Russian).
2. Deshcherevskaya N.P., Deshcherevskaya N.O. New hypotheses of the water role in the mechanism of the pathological obesity formation. Proceed. Int. Symp. "Biological Motility: Fundamental and Applied Science" (Pushchino, 2012), Scientific Program, p.9, http://normalizuj-ves. narod.ru/ (in Russian).

LEFT VENTRICLE CARDIOMYOCYTES ULTRASTRUCTURE OF YOUNG AND OLD JAPANESE QUAILS *COTURNIX JAPONICA*

M.S. Dukhinova, T.V. Lipina, N.B. Serezhnikova, L.S. Pogodina
Biological Faculty, Lomonosov Moscow State University,
Leninskie gori, 1, Moscow, 119991, Russia

Although aging is an inevitable process, a lot of studies aim at postponing it as late as possible. Search of animal models for aging studies is one of urgent problems in this field of biology. Japanese quail *Coturnix japonica* is characterized by quick natural aging. One year of quail life is supposed to be equal to 70 years of human life. *Coturnix japonica* is a perspective object for retina age-related changes research because its retina structure is similar with human one. Recently subcellular aging markers of retina were described, which are general both for quails and mammals [1]. Like retinal cells, heart ventricle cardiomyocytes undergo heavy oxidative

stress that is the background of human age-related cardiovascular diseases [2]. New data demonstrated possible connection between eye and heart pathologies [3], so comparative studies of aging in these organs have become more interesting. Therefore, Japanese quail's heart can serve as a potential model for investigation not only for retina age-related changes research, but for heart age-related alterations as well. But there is lack of data about myocardium and cardiomyocytes structure of the quail and other birds at senescence.

So in our work the structure of left ventricle myocardium of young (9–12 weeks of age) and old (47–52-weeks) quails (four birds in each group) was studied with light and transmission electron microscopy with subsequent morphometric analysis. The birds were kindly provided by Department of Photochemistry and Photobiology at Emanuel Institute of Biochemical Physics of Russian Academy of Sciences.

Age-related changes were not found at light-microscopic level: cardiomyocytes of young and old birds were long narrow cells about 3 µm in diameter, which is much less than mammalian heart cells, cardiomyocytes had thin sheets of connective tissue between them.

Electron-microscopic study revealed, that in young quails cardiomyocyte nucleus is singular, situated in center and has elongate shape and invaginated borders. These facts correspond to data concerning other birds cardiomycytes [4]. But similar nuclei were described in mammals myocardium only under pathology conditions [5].

Morphometric analysis revealed that the main part of cytoplasm in left ventricle quial cardiomyocytes (about 43% of relative volume) was occupied by myofibrils that organized in parallel rows, the same pattern and volume is typical for mammalian cardiomycytes. In old quails' cardiomyocytes this type of myofibrils' organization was sometimes damaged and myofibrils' volume was decreased. At the same time the particular zones where contractile apparatus was hypertrophied could be seen in cells of old birds. Similar signs are considered as atrophy features in mammals heart and described in humans during cardiomyopathy and hypokinesia [6]. In addition ratio of thick filaments (myozin)\ thin filaments (actin) in cardiomyocytes cross-sections was 1:6 regardless of age, identical to myofilament arrangement in mammals ventricle cardiomyocytes.

Mitochondria in young birds heart are localized between myofibrillar rows as chains or small groups and as clusters in perinuclear region. It should be noted that subsarcolemmal groups of mitochondria, typical for mammalian cardiomyocytes, were absent in quails left

ventricle cardiomyocytes. Mitochondria volume was 30% of cytoplasm at the average and was increased in the cells of old birds. So, the decrease of myofibrils/mitochondrial volumes' ratio happened in left ventricle during aging of quails.

Mitochondria ultrastructure in cardiomyocytes was not altered at aging period, but morphometric analysis revealed several changes. The number density of long mitochondria, longer than 2 μm, was increased by 60% from 9 to 52 weeks age (3.6%±0.12 и 5.7±0.5% from total mitochondria number, respectively). The maximal length of mitochondrion's profile measured in the old birds' cardiomyocytes was twice as much than in young ones: 6.6 μm and 3.3 μm, relatively. Similar ultrastructural change of mitichondria was described also during cardiovascular disease and in human senescent heart cells [7]. Such mitochondria elongation can be considered as earlier intracellular aging marker of quail cardiomyocytes. In retinal pigment epithelium of the same birds change of mitochondrial shape also serves as intracellular aging marker [1], although in those cells ring-shaped and dumbell-like but not elongated organelles number increased with quail age.

Both in interfibrillar and perinuclear zones in quail left ventricle cardiomyocytes lipid drops can be seen, they have close connections with mitochondria rather often. Relative volume of lipids was increased from 2.1±0.1% to 2.9±0.2% during analyzed period. Such growth was likely due to slower lipid peroxidation in mitochondria, which is typical feature of pathological process in mammal myocardium, such as cardiomyopathy [5].

Lipofuscin is a well-known cell aging marker. But against all expectations lipofuscin granules can be easily detected in left ventricle cardiomyocytes of both young and old quails, its quantity slightly increased in old birds cardiomyocytes. Lipofuscin granules in quail's cardiomyocytes are heterogeneous electron-dense structures of different shape and size scattered in cytoplasm. Our recent data showed [1] that in retinal pigment epithelium of the same quails at the age of 47-52 weeks lipofuscin granules were increased significantly. So rate of lipofuscin accumulation differs considerably in left ventricle and in retina, appearing in retina earlier. This fact is in good agreement with data obtained by Flammer and co-authors that retinal vascular changes predict, to some extent, cardiovascular events [3].

So, Japanese quail's left ventricle cardiomyocytes have some similar features with mammalian ones. Our ultrastructural research showed that left ventricle cardiomyocytes of 47-52 weeks old Japanese quail *Coturnix japonica*, in comparison with 9-12 weeks old birds, have

several differences: increased mitochondria\myofibril ratio, also increased number of long mitochondria and lipid drop volume. The described aging process in quails' cardiomyocytes can reflect earlier changes in mammalian and human heart during aging and some cardiovascular pathologies. It shows that quail *C. japonica* could be proposed as one of the models for myocardium aging research. But further studies, including older quails and other heart chambers, are necessary for testing this model.

References

1. N. B. Seryozhnikova, P. P. Zak, L. S. Pogodina, N. N. Trofimova, T. V. Lipina, M. A. Ostrovsky. // Moscow University Biological Sciences Bulletin, 2013, Vol. 68, No. 4, pp. 149–155.
2. Terman A., Kurz T., Gustafsson B. and Brunk U.T. // Current Cardiology Reviews. 2008. V.4. P.107–115.
3. J. Flammer, K. Konieczka, R. M. Bruno, A. Virdis, A.s J. Flammer, S. Taddei. // European Heart Journal. 2013. 34, 1270–1278.
4. McKenzie B.E., Easterday B.C., Will J.A. // Am J Pathol. 1972. V.69. P.239–254.
5. Lushnikova Ye.L., Nepomnyaschih L.M., Klinnikova M.G., Sviridov Ye.A. / / SB RAMS. 2008. V.134. № 6. (in Russian)
6. Kakturski L.V. Sudden heart death (clinic morphology). Moscow: Medicina dlya vseh. 2000. 127 pp. (in Russian).
7. Hom J., Sheu S.S. / / J Mol Cell Cardiol. 2009. V.46. №6. P. 811–820.

THE CALCIUM-SENSING RECEPTOR IN CARDIAC HYPERTROPHY

E.A. Dyukova[1,2], R. Schreckenberg[1], G.F. Sitdikova[2], K.-D. Schlueter[1]

[1]*Institute of Physiology, Justus Liebig University, Ludwigstaße 23, 35390 Gießen, Germany;*
[2]*Institute of Fundamental Medicine and Biology, Kazan Federal University, Kremlyovskaya 18, Kazan, 420008, Russia*

Ca is an important second messenger and plays crucial role in many intracellular signaling steps. Ca is required for the electromechanical coupling of myocytes. This process can be activated by voltage-dependent calcium channels or by recently shown calcium-sensing receptors (CaSR). Via these receptors Ca acts as an important first messenger leading to intracellular signaling pathways which in turns activates calcium release from its intracellular stores.

Recently it was possible to demonstrate the expression of CaSR in many organs among them is heart [1]. It has also been shown, that alongside calcium, CaSR has other direct agonists, whose affinity is directly correlated with positive charges they carry. Among them polyamine putrescine which have been tested in our study [1, 2].

It is also supposed that CaSR may act as a compensatory mechanism in some pathological cases such as hypertrophy. The role of CaSR in cardiac hypertrophy was investigated here in more details.

Experiments were performed in isolated ventricular cardiomyocytes and heart muscle strips. Wistar and SHR male rats were used. Heart muscle strips contraction was measured using special equipment (Biopac Systems, Inc., USA) with isometric transducers (0-50 gr range). Preparation was stimulated with 2 silver plated electrodes with 0.1 Hz frequency.

To isolate cardiomyocytes, heart was perfused with buffer containing collagenases, then choppered and centrifuged carefully increasing Ca concentration. Then cells were plated to Petry dishes and incubated [3]. Cell shortening was measured with special cell-edge-detection system. Culture was stimulated with 2 silver electrodes, contraction was measured in percents comparing to cells diastolic length.

In experiments we used CaSR agonist putrescine (300 µM on strips and 10 µM on cell culture), CaSR inhibitor NPS (100 µM on strips and 3 µM on cell culture), prohypertrophic stimuli endothelin (ET) (10 µM).

Application of putrescine on heart muscle stripes increased contraction as well as on cardiomyocytes culture (fig. 1). Inhibition of CaSR led to the decrease of shortening on cell culture and muscle strips (fig. 2).

Functional role for CaSR in electromechanical coupling is verified.
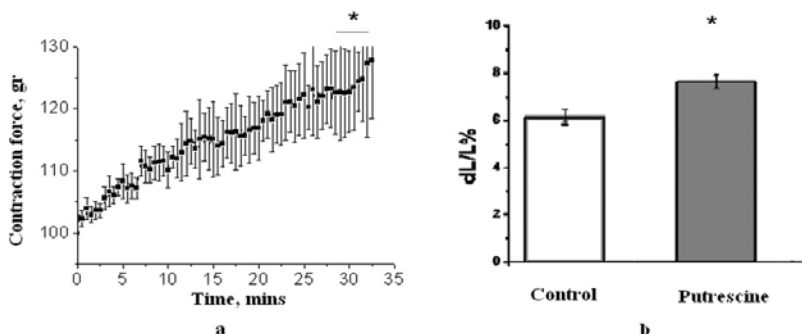
Fig. 1. Effects of putrescine on heart muscle strips (a: $n=10$) and cell culture (b: $n=36$) contraction, *$p<0,05$.
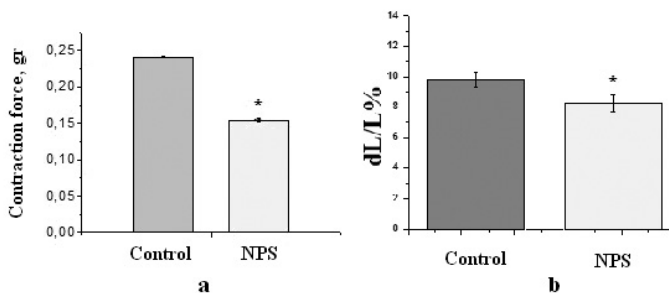
Fig. 2. Effects of CaSR inhibition on heart muscle stripes (a: *n*=10) and isolated cardiomyocytes (b: *n*=72), *p<0,05.
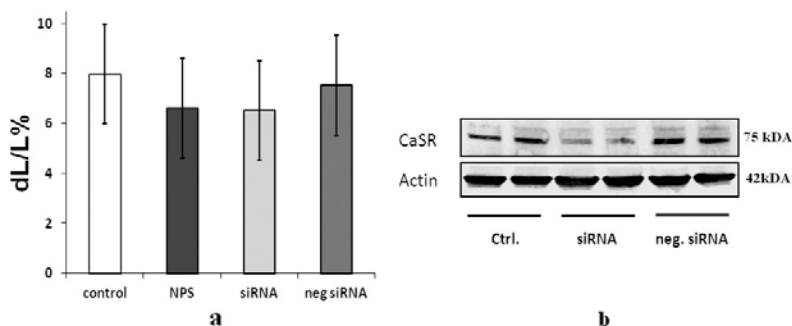
Fig. 3. Downregulation of CaSR over night (a – cell contractility, b – level of CaSR protein under the same conditions), *n*=144, *p<0,05.
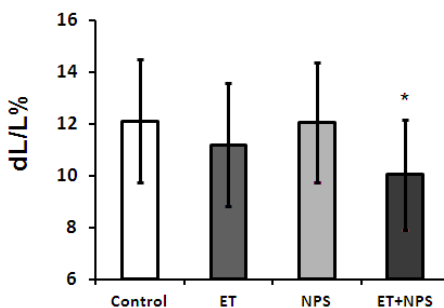
Fig. 4. Effects of prohypertrophic stimuli on cardimyocytes shortening, *n*=72, *p<0,05.

We were also able to downregulate the CaSR using NPS (3 µM) and siRNA (0.05 µM) over night for more confirming the relevance of our findings (fig 3).
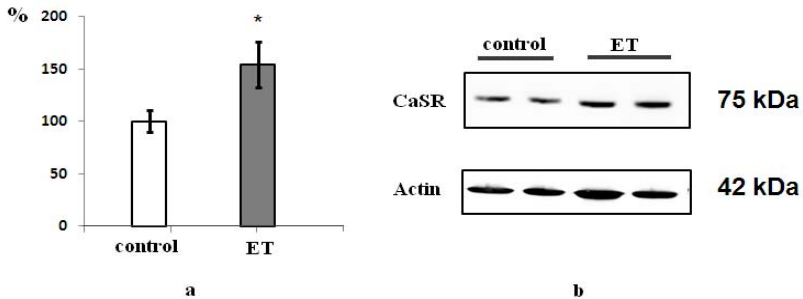
Fig. 5. Level of CaSR protein in control and with addition of prohypertrophic stimuli, *n*=2, **p<0,05*.
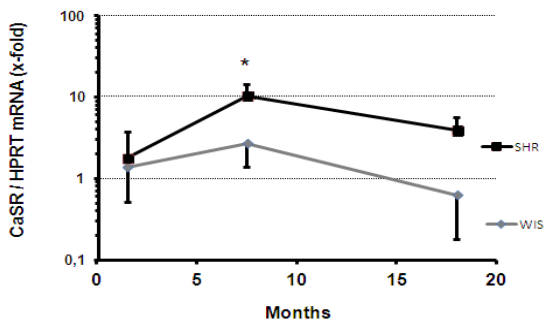
Fig. 6. Levels of mRNA of CaSR in the cell in Wistar and SHR rats, *n*=6; **p<0.05* vs. WIS 1.5 Months; ANOVA; Student-Newman-Keul's post hoc.

To identify the role of CaSR in pathology we used prohypertrophic stimuli (fig 4, fig. 5) and spontaneously hypertensive rats (SHR) (fig. 6). Addition of prohypertrophic ET (over night) decreased cell shortening if CaSR activity is blocked (fig. 4) and increased CaSR protein level (fig. 5).

As ET *in vitro*, SHR express higher levels of CaSR in cardiac tissue *in vivo*.

CaSR affects contractile activity and contributes to the electromechanical coupling of ventricular cardiomyocytes. Its expression is induced in hypertrophic cells. So it's supposed to compensate for loss of function normally seen in cardiac hypertrophy.

References

1. Wang, R. Calcium and polyamine regulated calcium-sensing receptors in cardiac tissues / R. Wang, C. Xu, W. Zhao // Biochem. - 2003. - Vol. 270. - P. 2680-2688.

2. Quinn, S.J. The calcium-sensing receptor: a target for polyamines / S.J. Quinn, C.P. Ye, R. Diaz, O. Kifor, M. Bai, P. Vassilev // Am J Physioogy. – 1997. – Vol. 273. – P. 1315-1323.

3. Schlueter, K-D. Adult ventricular caediomyocytes: isolation and cilture / K-D. Schlueter, D. Schreiber // Methods Mol Biol. – 2005. – Vol. 290. – P. 305-314.

MECHANICAL PROPERTIES OF FIBROBLASTS DEPEND ON LEVEL OF CANCER TRANSFORMATION

Yu.M. Efremov[1], M.E. Lomakina[2], D.V. Bagrov[1], P. I. Makhnovskiy[1], A.Y. Alexandrova[2], M.P. Kirpichnikov[1], K.V. Shaitan[1]

[1] *Lomonosov Moscow State University, Faculty of Biology, Leninskie Gory 1/12, Moscow, 111991, Russia*

[2] *Institute of Carcinogenesis, Blokhin Cancer Research Center, Kashir-skoye shosse 24, Moscow, 115478, Russia*

Many facts point at the importance of cell mechanical properties in tumorigenesis and cancer progression. Recently, it was revealed that tumor cells are significantly softer than normal cells. Although this phenomenon is well known, it is connected with many questions which are still unanswered. Among these questions are the molecular mechanisms which cause the change in stiffness and the correlation between cell mechanical properties and their metastatic potential.

It was shown that mechanical properties of cells are mainly defined by actin cytoskeleton structure. The actin cytoskeleton is a network of microfilaments responsible for cell shape, protrusion formation and motility. Cancer cells show distinct alterations in morphology and actin cytoskeleton structure compared to normal cells. They generally have a reduced number of stress fibers, the residual microfilament bundles are in disorder, maturation of focal adhesions is disturbed. Presumably, cytoskeleton characteristics of cancer cells play an important role in their migration activities, abilities of intravasation and extravasation and thus determine their metastatic potential. The same cytoskeleton characteristics may lead to essential changes in the mechanical properties of tumor cells. Ability of cancer cells to migrate and produce metastasis is one of the main reasons of tumor mortality.

We studied mechanical properties of cells with different level of cancer transformation. Three cell systems consisting of non-transformed cells and their derivates with different level of cancer transformation (by oncogene *N-RAS*, viral and cells of tumor origin – from mildest to strong-

est) were investigated. The first system was the Ras-transformation system: it included 10(3) cells, which are immortalized mouse fibroblasts, as a control cell line and 10(3)RAS cells obtained by the transfection of 10(3) cells with a construct containing constitutively active *N-RAS*[asp13] gene. The second system (SV40-transformation system) included non-transformed MRC-5 cells (human fetal lung fibroblasts) and their derivatives – the transformed cells MRC-5V1 and MRC-5V2 obtained by infection of the initial MRC-5 cells with SV40 virus. The third system included 1036 human dermal fibroblasts as control and HT-1080 fibrosarcoma (malignant mesenchymal tumor derived from fibrous connective tissue) cell line.

All studied cell lines were characterized according to their morphology, actin cytoskeleton and focal adhesions organization. Transformation led to reduction of cell spreading and thus to decrease of cell area, disorganization of actin cytoskeleton, loss of actin stress fibers and decline in the number and size of focal adhesions. But while in case of N-Ras-transformation one could see some residual actin bundles, there are significantly less of them for SV40-transformed cells and for tumor fibrosarcoma cells there are no bundles at all. For all cell systems significant decrease of focal adhesion size was noticed (by 50-60%). This reduction occurs due to disappearance of large matured focal adhesions and by appearance of new small focal complexes. Violation of maturation of the focal adhesions as well as disappearance of the stress fibers and cell area reduction were shown in tumor cells earlier. It should be noticed that in our systems the changes associated with transformation increased from cells with mono-oncogene transformation (Ras-transformation) to cells after viral transformation (SV40-transformation system) and cells of tumor origin (HT1080 fibrosarcoma).

Force spectroscopy by AFM with spherical probes was carried out to measure the Young's modulus of cells. In all cases the Young's moduli were fitted well by log-normal distribution. It may result from the log-normal distribution of actin cytoskeleton density or its level of crosslinking. The reduced Young's modulus of transformed cells was registered in all the studied systems (by ~40% for 10(3)RAS, ~80% for MRC-5V1 and MRC5V2, ~70% for HT-1080). For the cell system with a low level of transformation the difference in stiffness was less pronounced than for the two other systems. Thus, the reduction of the Young's modulus in three studied cell systems correlated with the morphological alterations.

This data suggests that cell mechanical properties change upon transformation, and acquisition of invasive capabilities is accompanied by
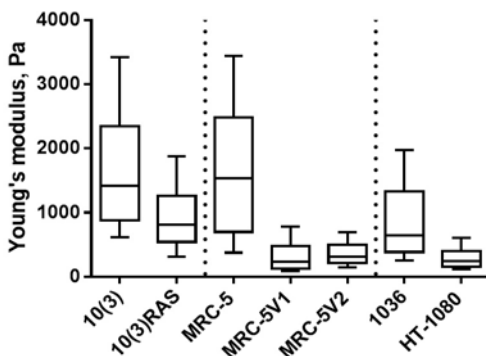
Boxplot for Young's moduli calculated for the cell lines. The percentiles are 10%, 25%, 50%, 75% and 90%.

significant softening. Cell stiffness measured by AFM can be regarded as a biomarker for determination of cells at early stages of tumor progression. High compliance of cancer cells can be a consequence of the faster mitosis rate and dedifferentiation. On the other hand, reduced stiffness could help cancer cells to move within interstitial cavities, crawl through extracellular matrix and through vascular walls during invasion, intra- and extravasation.

INFLUENCE OF THE LOW-TEMPERATURE ARGON PLASMA ON HUMAN STEM AND CANCER CELLS

A.M. Ermakov, A.L. Popov

Institute of Theoretical and Experimental Biophysics RAS, Instituskaya str., 3, Pushchino, Moscow Region, 142290, Russia; E-mail: ao_ermakovy@rambler.ru

It is known that the low-temperature gas plasma has high biological activity. In particular, it is known as a universal sterilizer. Previously, we have shown that it is capable of activating the regenerative processes in planarians by activation of stem cell proliferation. Also in the literature there is evidence of possible influence of the low-temperature gas plasma on normal and cancerous epithelial cells. The aim of this work - study of the effects of low-temperature argon plasma (LTAP) on the proliferation and viability of human stem and cancer cells. We used primary culture of

dental pulp stem cells (Th1), and the cancer cell line MNNG. Cells in the culture medium of a 96 well plate LTAP irradiated for 5, 10, 15 and 20 min. Further every day (for 5 days.) using plate reader determined the dynamics of change of the surface area occupied by the cells in the wells. On day 5, cell viability as determined by MTT test. Irradiation and Th1 cells MNNG for 5 and 10 minutes did not lead to significant differences in proliferative activity in viable cell count during the entire experiment. Impact LTAP for 15 minutes caused some reduction in the proliferative activity (25-30%) cells MNNG 2 and subsequent days of the experiment, and the proliferation of Th1 cells was increased by 30% for 3 days. 20 minute exposure LTAP MNNG cells resulted in a significant decrease in the rate of cell proliferation at day 2 already, and the experiment to decrease (50-65%) in the number of viable cells at day 5 of the experiment (results of MTT-test). At the same time such a regime does not lead to cell death Th1, but not growth stimulation effect was observed during the observation period after irradiation. Thus, we have shown that cancer stem cells and react differently to the impact of LTAP. Further research in this area may be useful in terms of the possibility of using LTAP in regenerative medicine and oncology.

THE ROLE OF PROTEIN PHOSPHATASE 1 IN PLANARIAN REGENERATION

O.N. Ermakova, A.M. Ermakov, A.N. Skavulyak
*Institute of Theoretical and Experimental Biophysics RAS,
Instituskaya str., 3, Pushchino, Moscow Region, 142290, Russia;
E-mail: ao_ermakovy@rambler.ru*

Planarian - freshwater flatworms, have the unique ability to regenerate due to the proliferation and differentiation of stem cells - neoblasts. Comparative genome analysis of planarians and some regulatory mechanisms of regenerative and morphogenetic processes indicate a strong resemblance to those of the higher animals, so planarian can serve as an adequate model for research in the field of stem cell biology. Activity control neoblasts provided, in particular, a system of ERK mitogen-activated protein kinases. These proteins are responsible for the speed and direction of the proliferation and differentiation of stem cells and planarians in regulating the activity of these kinases in a mammal, in particular

MEK, protein phosphatase involved, which have not been investigated flatworms. Therefore, the aim of this work - exploring the role of protein phosphatase 1 in the regulation of planarian regeneration. Work carried out on laboratory freshwater planarian asexual race Schmidtea mediterranea. In the genome of these animals we have detected orthologs 3 isoforms of protein phosphatase 1 - α, β and γ have 100% homology to those in humans and other mammals. Using RNA interference by dsRNA injection isoforms of protein phosphatases to the assay was carried out by us knockout expression of these genes. After 3 successive injections (1 injection per day) were performed after decapitation and screening the resulting regeneration phenotype. We have found that RNA interference of each isoform 1 protein phosphatase inhibition leads to substantial regeneration planarians, which affects the size blastema (five day recovery on the difference reached 300%). Using immunohistochemistry to H3P was found that inhibition of regeneration is achieved due to significant suppression neoblasts proliferative activity (inhibition of the proliferation reached 100%). Thus, we have been found in planarians all isoforms of protein phosphatase 1 inherent mammalian cells and demonstrated their important role in the regulation of stem cell proliferation flatworms.

PHOSPHORYLATION REGULATES ACTIN-BINDING AND CROSS-LINKING ACTIVITY OF THE MYOSIN LIGHT CHAIN KINASE

V.A. Fediunin, A.Y. Khapchaev, V.P. Shirinsky
Institute of Experimental Cardiology, Russian Cardiology Research and Production Center, Moscow, 121552, Russia

Ca^{2+}/calmodulin (Ca/CaM)-dependent long and short myosin light chain kinases (MLCK) are involved in a large variety of motile events in cells through phosphorylation and activation of smooth muscle and non-muscle myosin II. In the central part of long MLCK, there are five DFRxxL motifs which are responsible for high affinity binding to actin. In short MLCK, only three DFRxxL motifs are present, so short MLCK binds to actin less tightly. Due to multiple actin binding sites, MLCK is able to bundle actin filaments. Phosphorylation of MLCK isoforms modulates its enzymatic activity and was suggested to regulate MLCK subcellular localization. Recently, in biosamples taken from cancer patients, Ser[947] and

Thr^{978} of long MLCK (corresponding to Ser^{25} and Thr^{56} of short MLCK) were identified as phosphorylation sites. Interestingly, these sites are located within the DFRxxL-rich actin binding domain of MLCK.

Here, using recombinant human MLCK fragments and mass-spectrometry technique, we show that both Ser^{25} and Thr^{56} are effectively phosphorylated by SAPK2 and p44^{erk1} protein kinases *in vitro*. Modification of these sites attenuated MLCK binding to F-actin and abolished bundling of actin filaments by MLCK *in vitro*. Our findings suggest that phosphorylation within the MLCK high affinity actin-binding domain may 'switch off' at least one of DFRxxL motifs to fine-tune MLCK binding to actin-containing stress fibers and/or MLCK localization in cells during cell cycle or in response to stimulation. Currently we are constructing full-length MLCK phosphorylation imitating mutants to address the effects of MLCK phosphorylation at Ser^{25}(Ser^{947}) and Thr^{56} (Thr^{978}) in cultured cells.

REDOX-DEPENDENT FERRIC OXIDE NANOPARTICLES LOADED WITH DOXORUBICIN AND THEIR INFLUENCE ON THE FUNCTIONS OF MITOCHONDRIA

T.A. Fedotcheva[1], A.G. Akopdjanov[1], N.L. Shimanovskii[1], P.G. Min-galev[2], V.V. Banin[3], V.V. Teplova[4], N.I. Fedotcheva[4]
[1]Pirogov Russian National Research Medical University, Moscow, 117997, Russia;
[2]Lomonosov Moscow State University, Department of Chemistry, Moscow, Russia;
[3]All-Russian Research Institute of Medicinal and Aromatic Plants, Moscow, Russia;
[4]Institute of Theoretical and Experimental Biophysics, Russian Academy of Sciences, Pushchino, Moscow Region, 142290, Russia;
E-mail: nfedotcheva@mail.ru

Mitochondria are one of important targets for anticancer chemotherapy [1, 2]. Chemotherapeutic drugs acting on the mitochondrial apoptotic pathway inhibit the respiratory function or stimulate the production of reactive oxygen species (ROS), thereby inducing the cell death. Anthracyclines, in particular doxorubicin (DOX), act in this way owing to its capacity to enter the redox cycle via one-electron transfer reactions [2, 3]. Mitochondrial changes induced by DOX involve membrane depolarization, which precedes alterations in the mitochondrial respiration, the cellular ATP level, and enzymatic activities [3]. It is known that the cyto-

toxic action of DOX enhances in the presence of iron [4]. This is due to the fact that DOX directly binds iron and cycles in the presence of oxygen between the iron (II) and iron (III) states, producing ROS. Iron is an essential transition metal, which is required for normal cell physiology and plays a prominent role in cell metabolism, heme synthesis, and enzyme activity. However, owing to strong reactivity, iron also participates in the Fenton reaction as an electron donor for hydrogen peroxide with production of a potent ROS, the hydroxyl radical [5]. This highly reactive species can create chain reactions that lead to cell death. These effects of iron, DOX, and of their complex occur not only in tumor cells but also in normal tissues, producing cytotoxic side effects on the heart, skeletal muscles, and liver. This challenges the problem of developing various nanocarriers to transport drugs specifically to tumor sites.

Pharmaceutical nanocarriers possess a broad variety of properties, such as longevity in the blood, enhanced intracellular penetration, and stimulus sensitivity, which allows the release of drugs from the carriers under certain physiological conditions [6, 7]. Due to various targeting ligands attached to the surface of the nanocarriers, they can deliver the drug to specific sites. In addition, the nanoparticle-based drug delivery system is an important strategy for overcoming drug resistance, which is inherent in tumor cells. DOX-loaded nanoparticles (NP) were found to move across the membranes of resistant cells via active endocytic pathways and to be transported to lysosomes, mitochondria, and the endoplasmic reticulum [8]. Magnetic NP based on ferric oxide, especially magnetite (Fe_3O_4), have been explored as sensitive probes for magnetic resonance imaging and therapeutic applications [9-11].

In the present work, we synthesized and characterized ferric oxide and ferric hydroxide nanoparticles loaded with DOX and stabilized with citric acid or lysine. All preparations contained 5–10 mg of ferrite and 1–5 mg of DOX in 1 ml of a colloidal solution of NP. The spectral and fluorescence characteristics of resulting NP were compared with those of free DOX, and their influence on the mitochondrial functions was examined. The measurements were carried out on a USB400 Ocean Optic spectrophotometer and a HITACHI7000 fluorimeter. The membrane potential of mitochondria was recorded by a TPP$^+$-selective electrode with computer registration.

Fig. 1 shows the spectral properties of DOX and DOX-loaded NP of ferric hydroxide in comparison with those of free DOX and of DOX in the presence of added bivalent iron ($FeSO_4$). As seen in Figs. 1A and 1B, the absorption spectra of all three species strongly differ: the high ampli-
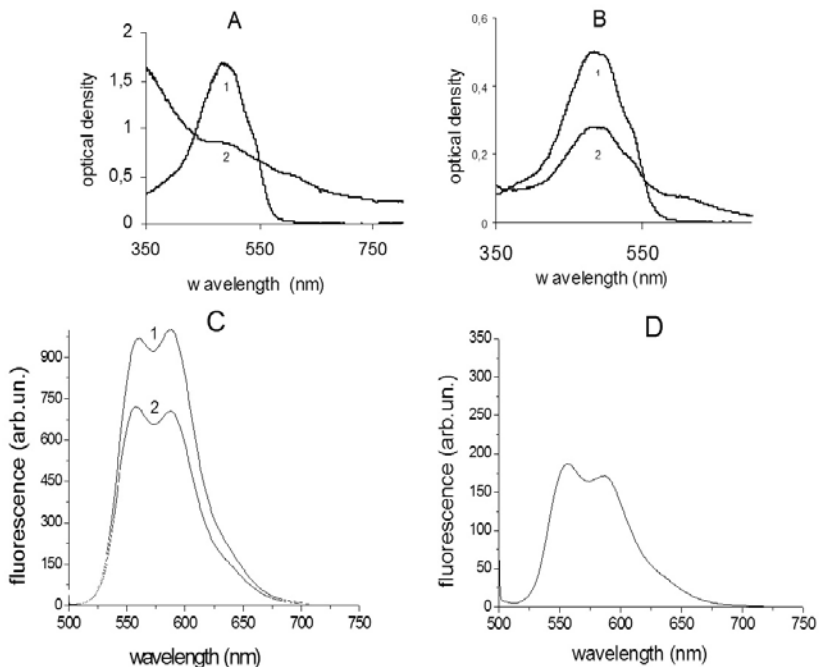
Fig. 1. Spectral properties of DOX and ferric hydroxide nanoparticles (NP) loaded with DOX. A. Absorption spectra of 200 μM DOX (1) and NP (2). B. Absorption spectra of 50 μM DOX (1) and 50 μM DOX in the presence of 50 μM FeSO4 (2). C. Fluorescence spectra of 20 μM DOX (1) and 20 μM DOX in the presence of 50 μM FeSO4 (2). D. Fluorescence spectrum of NP (10 μl into 2 ml).

tude at 480 nm, which is typical of free DOX, abruptly falls after the addition of bivalent iron and is almost not detected in nanoparticles. The decrease in the peak at 480 nm is accompanied by an increase in absorption in the range of 600–620 nm, which increases with increasing concentration of iron. The fluorescent properties of DOX in the composition of NP and in the presence of iron also change (Figs. 1C and 1D). The peak of emission at 580 nm, which is typical of free DOX, though decreases in the presence of iron but does not disappear, as it occurs in the absorption spectrum. The peak of the fluorescence of DOX-loaded iron NP is retained and depends on the concentration of NP.

These data indicate that, from changes in the absorption and fluorescent properties of DOX, it is possible to determine whether DOX is free or bound to NP. The spectrophotometric analysis reveals the absence of free
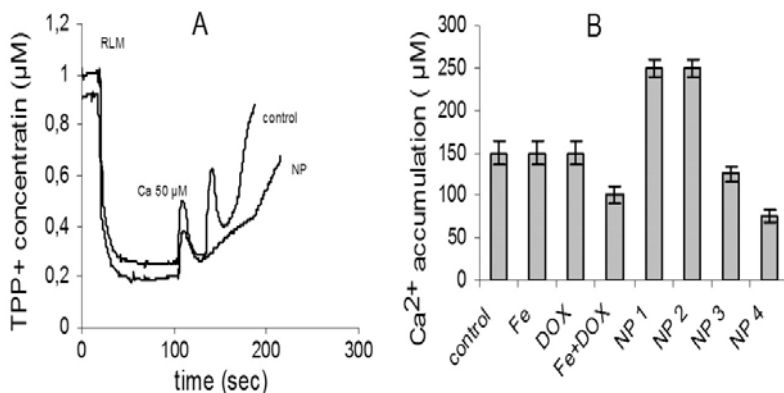
Fig. 2. Effect of nanoparticles on the accumulation of calcium ions in mitochondria. **A**. Original curves of changes in the membrane potential of mitochondria in response to sequential additions of CaCl2 at a final concentration of 50 μl in the control and in the presence of 10 μl of a colloidal NP solution, loaded with DOX and stabilized with lysine. **B**. A comparison of the effect of NP and their components, iron and DOX, on the accumulation of calcium ions: Fe (FeSO4 50 μM); DOX 50 μM; NP1 (ferric oxide–DOX–citric acid); NP2 (iron oxide–citric acid–DOX); NP3 (iron oxide nanoparticles); NP4 (iron oxide–DOX–lysine) (each NP 10 μl into 1 ml).

DOX in NP, whereas the fluorescence shows the concentration of DOX bound to NP. As it follows from the data obtained, the concentration of DOX incorporated in NP is about 400 μM in an initial colloid solution.

The effects of NP on the membrane potential and the accumulation of calcium ions in mitochondria are shown in Fig. 2. As compared with the control, NP loaded with DOX and stabilized with lysine decreased the Ca^{2+} capacity of mitochondria more than twofold at a concentration of DOX of 2 μM, which was recalculated by the above-described method. NP stabilized with citrate increased the Ca^{2+} capacity, which is due to the known ability of citrate to bind calcium ions. Control experiments with NP components (DOX and iron) show that they by themselves do not affect, and in complex decrease, the accumulation of calcium ions in mitochondria (Fig. 2B). The data obtained indicate that the effect produced by ferric oxide- and ferric hydroxide-loaded NP on mitochondria depends in particular on the type of stabilizer.

The methods used in the work enable one to determine the presence or absence of free DOX in NP and estimate the concentration of

bound DOX, as well as to develop, by changing the type of stabilizing compound, novel NP constituents that enhance or weaken the direct or side effects of DOX. Because both components of NP are redox-sensitive, the effects of NP and the release of DOX from NP can be regulated by the redox states of mitochondria and redox-dependent stimuli, which is the subject of further studies.

References

1. Szewczyk A, Wojtczak L. (2002) Mitochondria as a pharmacological target. Pharmacol Rev. 54(1): 101-127.
2. Costantini P., Jacotot E., Decaudin D., Kroemer G. (2000) Mitochondrion as a novel target of anticancer chemotherapy. J Natl Cancer Inst 92: 1042-1053.
3. Kuznetsov A.V., Margreiter R., Amberger A., Saks V., Grimm M. (2011) Changes in mitochondrial redox state, membrane potential and calcium precede mitochondrial dysfunction in doxorubicin-induced cell death. Biochim Biophys Acta 1813: 1144-1152.
4. Xu X., Persson H.L., Richardson D.R. Molecular pharmacology of the interaction of anthracyclines with iron. Mol Pharmacol. 2005,68(2):261-71.
5. Rines A.K, Ardehali H. Transition metals and mitochondrial metabolism in the heart
J Mol Cell Cardiol. 2013, 55:50-7.
6. Torchilin V.P. Multifunctional nanocarriers. Advanced Drug Delivery Reviews 64 (2012) 302–315.
7. Yu S., Wu G., Gu X., Wang J., Wang Y., Gao H., Ma J. Magnetic and pH-sensitive nanoparticles for antitumor drug delivery. Colloids Surf B Biointerfaces. 2013, 103:15-22.
8. Zeng X., Morgenstern R., Nyström A.M. Nanoparticle-directed subcellular localization of doxorubicin and the sensitization breast cancer cells by circumventing GST-Mediated drug resistance Biomaterials 35 (2014) Biomaterials 35 (2014) 1227-1239.
9. Lehner R., Wang X., Wolf M., Hunziker P. Designing switchable nanosystems for medical application. J Control Release. 2012 Jul 20;161(2):307-16.
10. Xu C., Sun S. New forms of superparamagnetic nanoparticles for biomedical applications. Advanced Drug Delivery Reviews 65 (2013) 732–743.
11. Fedotcheva T.A., Fedotcheva N.I., Teplova V.V., Akopdjanov A.G., Shimanovskii N.L., Dryagina M.A., Odinzova E.V., Banin V.V. Cytostatic effects of nanoparticles of ferric oxide. Voprosy biologicheskoi medicinskoi i farmacevticheskoi himii, 2013, №11, 158-163.

DYNACTIN VERSUS RHOA AS PHOSPHORYLATION TARGET FOR LOSK KINASE DURING GUIDE OF DIRECTED CELL MOVEMENT

A.I. Fokin[1], T.S. Klementjeva[1,2], E.S. Nadezhdina[1,2], A.V. Burakov[1]

[1] *Belozersky Institute for Physico-Chemical Biology, Lomonosov Moscow State University, Moscow, 119991, Russia;*
[2] *Institute of Protein Research, Russian Academy of Sciences, Moscow, 117334, Russia*

Directed migration of animal cells is a fundamental process, crucial for the development and maintenance of multicellular organisms. This process is determinative for tissue formation during embryogenesis, for angiogenesis, wound healing and immune response. Defects in cell migration leads to the serious consequences, including intellectual disability, vascular disease, tumor formation and metastasis. The mechanisms of animal cell migration includes a reorganization of the cytoskeleton elements – the actin filaments and the microtubules. Soluble actin monomers rapidly polymerise at the cell's front to form filaments, which pushes the leading front forward and is the main motile force for advancing the cell's front. Microtubules are required to provide directionality to cell movement, for tail retraction and modulation of cell adhesion. Both actin and microtubules are important for establishing and maintaining the cell's polarity. The key regulators of cell motility are small GTPases, which transmit signals from membrane receptors to the cytoskeleton. One of the most studied member of small GTPases is RhoA protein, which is responsible for the formation of focal contacts and stress fibers. But despite the progress made in the study of cell migration, many participants in signaling pathways still remain unknown.

The protein kinase LOSK/SLK was described in our lab as a protein associated with the centrosome and microtubules (Zinovkina et al., 1997). It was shown that LOSK/SLK is crucial for the processes of cell polarization (Burakov et al, 2008) and migration (Roovers et al., 2009; Burakov and Nadezhdina, 2010). It was shown that LOSK can relax the vascular smooth muscle cells by phosphorylation of RhoA (Guilluy et al., 2008). Another substrate for LOSK was demonstrated recently in our lab: LOSK phosphorylates the p150Glued subunit of dynactin and thus targets it to the centrosome (Zhapparova et al, 2013). Hovewer, the LOSK-dependent signaling pathways, regulating cell motility, have yet to be determined.

In present study we investigated the migration of fibroblasts into experimental wound depending on phosphorylation of RhoA and

p150Glued by kinase LOSK. Using site-directed mutagenesis, we construct the series of fluorescent proteins, mimicking the phosphorylated and non-phosphorylated status of p150Glued and RhoA proteins in LOSK phosphorylation site. Such mimicking constructs were transfected in the cells one at a time or co-transfected with dominant-negative LOSK. The movement of transfected cells into experimental wound was documented then using time-lapse video microscopy. Analysis of obtained data allow us to determine, phosphorylation of which protein is crucial for the directional migration of fibroblasts.

STIMULATION OF MECHANO-GROWTH FACTOR EXPRESSION IN MYOBLASTS AND MYOTUBES BY MYOFIBRILLAR PROTEINS

V. Furalyov [1], I. Kravchenko [1], S. Chatziefthimiou [2], M. Wilmanns [2], V. Popov [1]

[1]*Bach Institute of Biochemistry, Russian Academy of Sciences, Leninskiy prospect 33, 119071, Moscow, Russia;*
[2]*European Molecular Biology Laboratory, Hamburg Unit, c/o DESY, Notkestraße 85, 22603 Hamburg, Germany*

Mechano-growth factor (MGF) is a product of alternative splicing of the insulin-like growth factor 1 (IGF-1) mRNA. MGF is known to stimulate myoblast proliferation and protect neurons and cardiomyocytes from apoptosis. MGF exerts its action through the receptors other than IGF-1. The possibility to use MGF for the improvement of muscle activity indicators of the aged people, patients with distinct forms of myodystrophia and sportsmen is the subject of wide speculation. The mechanisms of induction of MGF expression are as yet poorly understood. The mechanical load and some cellular stress factors including hyperthermia and acidification induced MGF expression in myoblasts in culture. Recently a second messenger, cAMP, was shown to be implicated in the synthesis of both splice forms of IGF-1 mRNA, IGF-1Ea and MGF, in human and murine myoblasts and differentiated myotubes. In an earlier investigation it was shown that the damaged muscle release some proteins stimulating MGF expression in myoblasts.

The aim of this work was to isolate and purify these protein inductors of MGF expression, to identify them, to study the ability of their individual domains to induce synthesis of IGF1 splice forms, MGF in particular, and to investigate the respective signalling pathways.

The protocol of purification of myofibrillar proteins able to stimulate MGF expression was worked up. This protocol includes such stages

Table 1. Identification of myofibrillar proteins stimulating MGF expression in myoblasts and myotubes

Protein peak	NCBI gi	identified protein	expected molecular mass	score	matched peptides/ measured peptides	sequence coverage, %
1	gi|145279198	myomesin 1	175 342	586	77/100	44
2	gi|81910387	myosin-binding protein C, fast-type	127 273	419	52/76	52
3	gi|123232573	titin	912 959	131	88/126	12

as several extractions and precipitations of proteins with different buffer solutions, anion exchange chromatography, gel filtration and native gradient gel electrophoresis. Three electrophoretically pure proteins able to activate MGF as well as IGF-1Ea expression were isolated.

To identify the purified proteins mass-spectra were obtained and submitted to the NCBI database using MASCOT. Probability based MOWSE scores greater 71 were deemed significant ($p < 0.05$). Three protein inductors of MGF expression were identified as myomesin 1, myosin-binding protein C and titin fragment (table 1).

To verify the nature of MGF-inducing proteins the immunoblotting of three purified protein samples with commercially available antibodies to titin, myomesin and myosin-binding protein C was carried out. Antibodies to titin were shown to stain the band of protein identified by MALDI as fragment of titin and didn`t stain the bands of two other proteins. Similarly, antibodies to myomesin 1 stained the band of protein identified as myomesin 1 only, whereas the antibodies to myosin-binding protein C stained the band of this protein but not the other two bands.

Several recombinant proteins corresponding to distinct titin and myomesin domains were kindly provided by Spyros Chatziefthimiou and Matthias Wilmanns from European Molecular Biology Laboratory, c/o DESY, Hamburg, Germany. They include titin domains (TA166-167 with a. a. 31648-31848, TA170 with a. a. 32047-32143 and TM4 with amino acid residues 33294-33395) and myomesin domains (My2 with a. a. 273-374, My3 with a. a. 409-502, My4 with a. a. 503-605, My5 with a. a. 635-731, My7-My9 with a. a. 935-1227, My11-My13 with a. a. 1352-1666) respectively (Titin_HUMAN, Q8WZ42 and MYOM1_HUMAN, P52179). All proteins were tested for the ability to activate the expression of MGF and IGF-1. From the tested constructs, My2, My3, My4, My7-9

and TA166-167 were not able to stimulate neither MGF nor IGF-1 synthesis, whereas My5 and TA170 (composed of Fn III domains) and My11-13, TM4 (Ig domains) were shown to activate the expression of MGF and IGF-1 (Table 2). This effect was manifested both on mRNA and protein levels and for both splice forms of IGF-1.

To find out if protein fragments containing different structural protein domains compete for the same or different receptors, the following set of competition binding experiments was performed: binding of the ^{125}I-labeled myomesin 5 fragment (Fn III) with myoblast membrane in the presence or absence of unlabeled myomesin 11-13 (Ig), titin A170 (Fn III) and titin M4 (Ig) was investigated. It was shown that the fragments containing the other domain type, i.e. Ig, did not compete with My5 since neither My11-13 nor TM4 at 20 μg/ml (0.56 μM and 1.76 μM, respectively) had any effect on binding of the ^{125}I-labeled My5, at 50 ng/ml (4.83 nM) with membrane receptors. On the contrary, the protein fragment containing the same domain type was a potent inhibitor of My5 binding. The unlabeled TA170 (Fn III) at the same concentration inhibited binding 4.8-fold (figure).

The same inhibition pattern was obtained with the protein fragments comprising Ig domains. Binding of the ^{125}I-labeled titin M4 fragment (Ig domain) with myoblast membrane was inhibited 10.5-fold by My11-13 (same Ig domain) but was not affected by the fragments containing Fn III domains – My5 and TA170.

Linear Scatchard plots of specific binding were obtained for both My5 (Fn III) and TM4 (Ig), (correlation coefficients 0.943 and 0.952, res-

Table 2. Effects of individual domains of myofibrillar proteins on MGF and IGF-1 expression in myoblasts

protein fragment	domain(s)	relative MGF mRNA levels, fold	relative IGF–1Ea mRNA levels, fold	MGF, pcg/mg of total protein	secreted IGF-1, pcg/ml
My2	Ig-like	1.1±0.2	0.9±0.2	6±4	48±15
My3		0.9±0.1	1.0±0.2	4±3	41±18
My11-13		**8.6±1.2**	**5.4±0.6**	**61±5**	**221±17**
TM4		**7.0±1.3**	**5.6±0.6**	**54±8**	**202±17**
My4	Fn type III	1.0±0.2	1.0±0.2	4±2	33±14
TA166-167		1.4±0.4	1.2±0.3	7±6	39±16
My5		**13±1.3**	**9.2±0.8**	**84±6**	**305±24**
TA170		**9.8±1.2**	**6.9±0.7**	**79±7**	**258±21**
My7-9	Ig-like and Fn type III	1.1±0.3	1.1±0.2	5±3	41±17
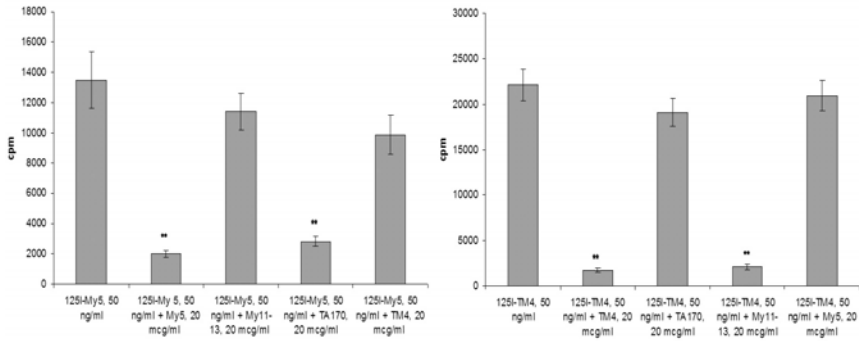
Specific competition of the binding of 125I-labeled recombinant proteins by unlabeled ones to human myoblasts.

pectively), suggesting thus a unique class of binding sites for each recombinant protein. My5 binding was characterized by an apparent dissociation constant (Kd) of 71 ± 38 nM, whereas the Kd for the TM4 was of similar value (56 ± 31 nM).

To investigate a possible difference in the mechanisms of intracellular signaling via two signaling pathways employing Ig and Fn III domain types, the effect of several inhibitors of regulatory protein kinases and Ras protein on MGF and IGF-1 induction were studied.

Adenylyl cyclase inhibitor dideoxyadenosine (DDA) and protein kinase A inhibitor Rp-cAMPS were more potent inhibitors of both the MGF and IGF-1 induction processes (both on the protein and mRNA levels) by Ig domains than by Fn III containing protein fragments. The inhibitory effects were always 2-2.8 fold more profound in the case of Ig domains compared to Fn III domains.

The opposite phenomenon was observed with Ca^{2+}/calmodulin dependent protein kinase II inhibitor KN93. This inhibitor was more effective in retarding activation processes induced by Fn III domains, compared to the constructs comprising Ig domains. In this case, the difference varied in the same range (1.7-2.9 fold).

In this study we report that individual subfragments of titin and myomesin composed of Fn type III and Ig-like domains can activate MGF expression in human myoblasts both at protein and mRNA level. The expression of the regular splice form of IGF-1 gene, IGF-1Ea, as well as IGF-1 protein was also stimulated by these protein fragments. Each of the domain-type, Ig or Fn III, was shown to bind to its own receptor on the myocyte surface. Competition between domains of the same type was observed

but not between domains belonging to different classes. Stimulation of MGF and IGF-1 expression induced by domains of two types showed different sensitivity to inhibitors of regulatory cascades. The effect of Fn type III domains was more sensitive to inhibition of Ca^{2+}/calmodulin dependent protein kinase activity, whereas the effect of Ig-like domains showed greater sensitivity to the inhibition of adenylyl cyclase – cAMP – PKA pathway. Endogenous stimulation of MGF expression in response to a specific external stimulus could be a viable alternative to therapeutic administration of exogenous recombinant protein or its fragments. The present study may serve as a step towards this ultimate goal.

EFFECT OF MUTATIONS IN SALMONELLA FLAGELLIN-SPECIFIC CHAPERONE FliS AND ANTI-SIGMA FACTOR FlgM ON THEIR INTERACTION AND STRUCTURE

A.V. Galeva[1], M.G. Pyatibratov[1], F.A. Samatey[3], A.S. Kostyukova[1,2]

[1]*Institute of Protein Research, Russian Academy of Sciences, Pushchino, Moscow Region, 142290, Russia;*
[2]*Voliand School of Chemical Engineering and Bioengineering, Washington State University, Pullman, WA;*
[3]*Trans-Membrane Trafficking Unit, Okinawa Institute of Science and Technology, Okinawa, Japan*

Flagella are extracellular organelles that propel bacteria to the most favorable environment (1). The flagellum of *Salmonella enterica* serovar Typhimurium is a self-assembled nanomachine; its assembly requires a complex, tightly regulated machinery that involves more than 60 proteins that are expressed in hierarchical order (2). Each flagellum consists of basal body, a long filament, and a hook connecting them. The major protein of filament is flagellin that has to be exported through the hollow core of the filament to be assembled at its distal end.

The flagellum-specific export system is evolutionarily related to a specialized type 3 secretion (T3S) system found in pathogenic bacteria that is used for bacterial toxin export (3). In this system, special proteins that facilitate the export, so-called T3S chaperones, are necessary. It is known, that the N- and C-terminal regions of flagellin molecules are disordered in solution and become structured during polymerization (fila-

ment assembly) (4). To prevent premature polymerization of newly synthesized flagellin molecules, FliS, the flagellin-specific T3S chaperone, binds in 1:1 stoichiometry to the C–terminal region of flagellin and facilitates its export (5).

Completion of the hook-basal body and induction of flagellin gene expression coincide with the secretion of FlgM, an anti-σ^{28} factor, from bacterial cells. Role of FlgM is to inhibit the function of FliA, a flagellar-specific σ^{28} RNA polymerase responsible for transcription of late flagellar genes including flagellin (6).

We were the first to demonstrate and characterize the interaction between FlgM and FliS from S. Typhimurium. Using gel-shift analysis, we demonstrated that these proteins specifically interact to form a 1:1 complex. We studied competition for FlgM binding between FliS and FliA and showed that there is no formation of a triple complex, but FliA displaces FliS from the complex with FlgM (7). We suggested that FliS binds to FlgM to keep it stable before FliA is expressed in cells.

Using several different approaches: fluorescence, limited proteolysis and circular dichroism (CD) we suggested that the FlgM and FliS proteins interact via their C-terminal regions (7). According to data obtained for crystal structures of FliS (in a complex with an FliC fragment) (8) and FlgM (in a complex with FliA) from *Aquifex aeolicus* (9), the C-terminal regions of FlgM and FliS participate in these interactions.

To find residues that participate in FliS/FlgM interaction without affecting binding to their other partners we have introduced point mutations in these regions. The residues were chosen by alignment of FliS and FlgM from different bacteria. For FlgM we have removed eight C-terminal residues by introducing stop codon instead of Ala90. The truncated FlgM [1-89] was purified and its interaction with FliS and FliA was tested. No complex band was formed when FlgM [1-89] was mixed with FliS indicating the drastic decrease in affinity. The truncation had no effect on formation of the complex with FliA (7). We conclude that while binding sites for FliS and FliA in FlgM overlap, their exact localization differ.

In FliS we have replaced Ile64 by Asp (I64D), the same replacements were made at position 65 (I65D) and 108 (I108D). The mutated FliS proteins were purified and tested in gel-shift binding assay. We were unable to visualize the mutant proteins on native gels. We concluded that these mutations lead to protein missfolding accompanied by aggregation of FliS proteins.

References

1. Berg H. C. and Anderson R. A. 1973, Nature 245: 380-382.
2. Chevance F. F. and Hughes K. T. 2008, Nat. Rev. Microbiol. 6: 455-465.
3. Blocker A., Komoriya K., Aizawa S. 2003, Proc. Natl. Acad. Sci. U. S. A. 100: 3027-3030.
4. Kostyukova A. S., Pyatibratov M. G., Filimonov V. V., Fedorov O. V. 1988, FEBS Lett. 241: 141-144.
5. Muskotal A., Kiraly R., Sebestyen A., Gugolya Z., Vegh B. M., Vonderviszt F. 2006, FEBS Lett. 580: 3916-3920.
6. Ohnishi K., Kutsukake K., Suzuki H. and Iino T. 1992, Mol. Microbiol. 6: 3149-3157.
7. Galeva A., Moroz N., Yoon Y. H., Hughes K. T., Samatey F. A., Kostyukova A. S. 2014, J. Bacteriol. 196: 1215-1221.
8. Evdokimov A. G., Phan J., Tropea J. E., Routzahn K. M., Peters H. K., Pokross M., Waugh D. S. 2003, Nat. Struct. Biol. 10: 789-793.
9. Sorenson M. K., Ray S. S., Darst S. A. 2004, Moll. Cell 14: 127-138.

THE ROLE OF PANNEXIN 1 IN THE REGULATION OF ARTERIAL FUNCTION

Dina Gaynullina, Oxana O. Kiryukhina, Olga S. Tarasova, Valery I. Shestopalov, Yury V. Panchin

Faculty of Biology, M.V. Lomonosov Moscow State University, Leninskie Gory 1/12, Moscow, 119234, Russia

Vertebrate pannexins were discovered as homologs to invertebrate gap junction proteins (innexins; Panchin et al., 2000). Pannexin family consists of three members, Panx 1, 2 and 3, which are structurally very similar to connexins, the vertebrate gap junction proteins. Panx1 is ubiquitously expressed in vertebrate tissues and was shown to participate in numerous physiological functions, including calcium waves generation and purinergic signaling.

In murine systemic arterial network Panx1 is the primary expressed isoform. Panx1 is abundant in endothelium of all arteries and capillaries, but the pattern of Panx1 expression depends on the vessel size. In contrast to larger conduit arteries where Panx1 is expressed primarily in the endothelium, in smaller resistance arteries it is also expressed in smooth muscle cells (Lohman et al., 2012). In arterial smooth muscle Panx1 was shown to mediate ATP release, thereby potentiating arterial contractile response to alpha$_1$-adrenoceptor agonist (Billaud et al., 2011). However, the role of Panx1 in the functioning of endothelium has never been studied before.

Thus, we tested the hypothesis, that Panx1 may regulate vascular tone not only by affecting smooth muscle cell contractility, but also via endothelium-dependent mechanisms.

Methods

Since truly selective pharmacological blockers of the Panx1 channel currently are not available, we utilized Panx1$^{-/-}$ mice as the ultimate test model for investigating functional significance of Panx1 activity in vascular system regulation. Wild type (WT) animals were age-matched (2-3 months old) male mice of the C57BL/6 background.

The experiments were performed using the preparations of the endothelium-denuded mesenteric and endothelium-intact or –denuded saphenous arteries, representing different patterns on Panx1 expression: in relatively small mesenteric arteries Panx1 is proposed to be expressed in both smooth muscle and endothelium, while in relatively large conduit saphenous artery Panx1 is expressed only in endothelium. For force recording, 2-mm ring preparations were mounted in isometric myograph. qPCR was used for gene expression analysis.

Results

In order to identify the role of Panx1 in the modulation of smooth muscle cell functioning, we studied contractile reactions of mesenteric arteries. Despite previous findings, showing that Panx1 potentiates smooth muscle contraction to alpha$_1$ – adrenoceptor agonist phenylephrine (Billaud et al., 2011), we didn't observed any difference in the contractile responses to phenylephrine in mesenteric arteries of Panx1$^{-/-}$ and WT mice. However, the difference between the reactions of mesenteric arteries of Panx1$^{-/-}$ and WT mice appeared, when the vessels were incubated with ecto-ATPase inhibitor ARL67156. ARL67156 augmented the contractile responses to phenylephrine in mesenteric arteries of WT mice, but didn't affect the responses of Panx1$^{-/-}$ mice. Importantly, ARL67156 didn't modify the contractile responses to thromboxane A2 analogue U46619 neither in Panx1$^{-/-}$ nor in WT mice.

The role Panx1 plays in the functioning of endothelium was tested in the saphenous arteries of Panx1$^{-/-}$ and WT mice. We found that the ablation of endothelium caused significant reduction of the transcripts of Panx1 and endothelial marker CD31. Thus, Panx1 is expressed predominantly in endothelial cells of murine saphenous artery. Phenylephrine-induced contractile responses of endothelium-denuded arteries did not differ in WT and Panx1$^{-/-}$ mice, which is in good agreement with predominantly endothelial localization of Panx1in murine saphenous arter-

ies. However, the contractile response to phenylephrine in endothelium-intact arteries of Panx1$^{-/-}$ mice was stronger than of WT mice, indicating that in saphenous arteries of Panx1$^{-/-}$ mice the anticontractile role of endothelium is impaired. Similar observations were found for contractile responses to another alpha$_1$ – adrenoceptor agonist methoxamine and non-receptor activation by high-K$^+$ depolarization. Thus, Panx1 modulates anticontractile effect of the endothelium.

Another strong evidence for functional role of Panx1 in the endothelium was obtained by comparing the acetylcholine-induced relaxations of endothelium-intact arteries in WT and Panx1$^{-/-}$ mice. We found that the response to acetylcholine was significantly weaker in Panx1$^{-/-}$ vs. WT saphenous arteries, indicating that Panx1 participates in the regulation of the endothelium-dependent dilatory mechanisms.

Conclusions

Our data show that Panx1 may modulate arterial smooth muscle contractile responses to agonist of alpha$_1$-adrenoceptors, but these modulatory influences could be masked by the activity of ecto-ATPases. Moreover, we demonstrate for the first time that Panx1 is involved in the regulation of anticontractile effect of endothelium and endothelium-dependent relaxation of conduit arteries.

ISOFLURANE COMPLETELY SUPPRESSES GAMMA AND SPINDLE BURSTS DURING THE FIRST POSTNATAL WEEK

E.V. Gerasimova[1], G.F. Sitdikova[1], J.A. Lebedeva[1], A.V. Zakharov[1,3], R.N. Khazipov[1,2]

[1]Kazan Federal University, Kremlevskay 18, Kazan, 420012, Russia;
[2]INMED, INSERM U-901, Marseille, France;
[3]Kazan State Medical University, Butlerov st., 49, Kazan, 420012 Russia

General inhalation anesthetics such as isoflurane reversibly induce deep coma and are widely used in clinical practice. In the adult brain, their effects are associated with the so-called burst-suppression pattern of electroencephalogram (EEG), which is characterized by hyperexcitability of the cortex manifested by intermittent, highly synchronized neuronal discharges (bursts) separated by silence periods (suppression).[1-3] Volatile anesthetics are also widely used in pediatric patients that require anesthesia for surgery. However, recent studies raised concern about the safety of general anesthetics in neonates and infants.[4-6] Prolonged (2–6 h) exposure to general anesthetics including isoflurane at minimal alveolar concentration (MAC) (1.9–2.3% isoflurane in P2–9 rats[7]) and

even at sub-MAC (1.5%) concentrations causes widespread apoptosis and neurodegeneration in the developing brain, and results in long-lasting neurological and behavioral deficits in rodents and nonhuman primates.[8-13] It has been hypothesized that apoptosis is triggered by suppression of neuronal activity by these agents.[14, 15] While this hypothesis is compatible with neuroapoptotic effects of the drugs that suppress the activity of glutamate receptors, sodium channels or enhance GABAergic inhibition, its consistence with the effects of isoflurane and other volatile anesthetics on brain activity is less clear. Indeed, if volatile anesthetics induce a hyperexcitable state and burst-suppression pattern in the neonates as they do in adults, the neurotoxic effects of these agents would not support this hypothesis. Hence it is important to determine the effects of volatile anesthetics on the brain activity in immature animals.

Material and methods

Twenty Wistar rats of both sexes from the second day after birth [P2] (P0 = day of birth) till postnatal day 69 were used. Surgery was performed under isoflurane anesthesia. In brief, the skull of the animal was cleaned of skin and periosteum.

During recordings, the head was fixed to the frame of the stereotaxic apparatus by the attached bars; animals were surrounded by a cotton nest and heated via a thermal pad (35–37°C). A chlorided silver wire, placed in the cerebellum or visual cortex, served as a ground electrode. Isoflurane (0.5–2%, 0.2–0.4 L/min) was administered via mask adapted to the animal head leaving an access to the whiskers at the contralateral whisker pad.

Extracellular local field potentials (LFP) and multiple unit activity (MUA) were recorded using 16-site linear silicon probes (100 μm separation distance between recording sites, Neuronexus Technologies, Ann Arbor, MI) placed vertical into the barrel cortex to the depth of 0–1.5 mm from the cortical surface to trace the columnar activity from all cortical layers. The principal whisker (PW) was identified by the shortest latency MUA responses in layer 4. Single whiskers were stimulated by piezo actuators (2–10 msec pulse duration, backward direction of whisker deflection, from 2 to 10 sec interstimulus intervals depending on the animal's age to avoid depression).

Raw data were preprocessed using a custom-developed suite of programs in Matlab analysis environment.

Results

During the first postnatal week, temporal organization of activity in barrel cortex was highly discontinuous with intermittent bursts occurring at
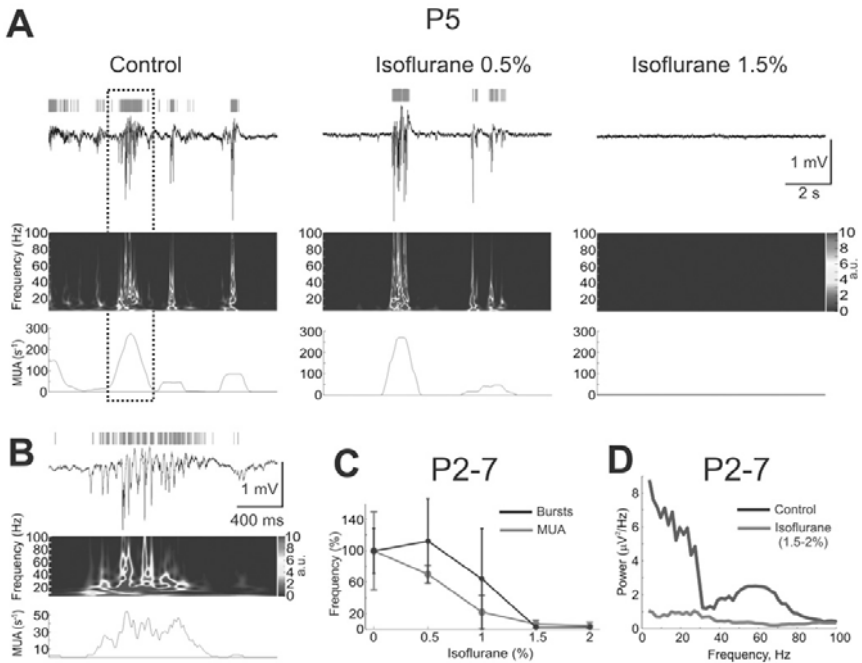
Effects of isoflurane on spontaneous activity in a cortical barrel column of neonatal rats. (A) Example traces of spontaneous electrical activity in L4 of a cortical barrel column of a P5 rat (LFP-black traces; MUA-red bars above) in control conditions and after inhalation of 0.5% and 1.5% isoflurane. Below are shown corresponding wavelet spectrograms and MUA frequency plots. Note that isoflurane (1.5%) completely suppresses ongoing LFP and MUA activity. (B) Individual oscillatory burst outlined by dashed box on panel (A) is shown on expanded time scale. (C) Dependence of spontaneous bursts frequency and MUA frequency on isoflurane concentration. (D) Power spectrum of LFP in control conditions (blue) and in the presence of isoflurane (1.5%) (red). (C–D): pooled data from six P2–7 rats.

frequency 5.6 ± 1.6 bursts/min (n = 6; P2–7; figure). Bursts were associated with intermittent LFP oscillations at spindle- and gamma frequency that were maximal in the L4 and were evident during LFP wavelet analysis and MUA spectral analysis (Fig. 1A, B, and D) [24, 36, 46]. Isoflurane suppressed spontaneous gamma and spindle bursts in a concentration-dependent manner (Fig. 1A and C). While at 0.5% of isoflurane, the frequency of bursts and MUA were not significantly modified, at surgical anesthesia levels (1.5–2%) isoflurane completely suppressed spontaneous spindle

bursts and EGO, that were associated with a reduction in alpha-beta (8–30 Hz) and gamma (30–80 Hz) LFP power from $21 \pm 4\,\mu V^2/Hz$ to $3 \pm 1\,\mu V^2/Hz$ and $2.6 \pm 0.7\,\mu V^2/Hz$ to $0.6 \pm 0.1\,\mu V^2/Hz$, respectively ($P < 0.05$; n = 6). Suppression of LFP activity was accompanied by almost complete suppression of neuronal firing with a drop in MUA frequency from $5.5 \pm 2.3\,s^{-1}$ to $0.1 \pm 0.1\,s^{-1}$. While EEG was completely flattened in P2–5 animals, by the end of the first postnatal week rare ($0.7 \pm 0.3\,min^{-1}$]) spontaneous sharp activity (amplitude of $226 \pm 123\,\mu V$; half-duration of 20 ± 10 msec) associated with occasional unit firing were apparent under 1.5–2% isoflurane anesthesia (n = 2 rats). Main sinks and MUA associated with these sharp potentials were located in L4.

In addition to a suppression of spontaneous activity, isoflurane also completely blocked sensory-evoked oscillatory responses during the first postnatal week. In control conditions, brief deflection of the PW evoked a characteristic oscillatory response consisting of EGO followed by spindle-burst in the corresponding cortical barrel column in P2–7 rats. In keeping with previous studies, the activity during EGO and spindle bursts was essentially restricted to the granular and infragranular layers of the corresponding barrel column without any significant activation of the supragranular layers.[23] Major sinks of the troughs of the evoked oscillatory patterns were located in L4, where the majority on neuronal firing during sensory-evoked responses occurred. Induction of isoflurane anesthesia was associated with a reduction in the power of sensory-evoked oscillations (both EGO and spindle bursts) in a concentration-dependent manner and these oscillatory responses were completely blocked at 1.5–2% of isoflurane. Fourier analysisof the 500 msec time window following the SEP revealed that isoflurane (1.5–2%) causes a reduction in a power the evoked gamma and alpha-beta oscillations from $46 \pm 17\,\mu V^2/Hz$ to $0.8 \pm 0.2\,\mu V^2/Hz$ and $237 \pm 96\,\mu V^2/Hz$ to $8 \pm 3\,\mu V^2/Hz$, respectively; this was accompanied by a reduction in spikes count from 35.6 ± 13.8 units to 0.9 ± 0.5 units (n = 6, P2–7 rats). While gamma and spindle-burst oscillations were completely suppressed, SEPs persisted in the presence of isoflurane without any change in SEP amplitude: SEP amplitudes in control conditions and in the presence of isoflurane were of $601 \pm 158\,\mu V$ and $700 \pm 154\,\mu V$, respectively. Spike count during SEP was also unchanged (control values, 3.4 ± 1.8 units and isoflurane, 4.0 ± 1.4 units (n = 6). In the presence of isoflurane, SEPs were often followed by a second small amplitude trough at 75 ± 10 msec after the stimulus. Stimulation of adjacent whiskers, as well as auditory or visual stimuli failed to evoke responses in both control conditions and in the

presence of isoflurane in P2–7 rats (data not shown). Thus, although SEPs persisted in the presence of isoflurane, there was complete suppression of sensory-evoked and spontaneous gamma and spindle bursts during the first postnatal week.

During the first postnatal week isoflurane completely suppressed spontaneous cortical activity and eliminated sensory-evoked early oscillatory patterns (EGO and spindle bursts).

References

1. Kroeger D, Amzica F. Hypersensitivity of the anesthesia-induced comatose brain. J Neurosci 2007;27:10597–10607.
2. Ferron JF, Kroeger D, Chever O, et al. Cortical inhibition during burst suppression induced with isoflurane anesthesia. J Neurosci 2009;29:9850–9860.
3. Swank RL, Watson CW. Effects of barbiturates and ether on spontaneous electrical activity of dog brain. J Neurophysiol 1949;12:137–160.
4. Patel P, Sun L. Update on neonatal anesthetic neurotoxicity: insight into molecular mechanisms and relevance to humans. Anesthesiology 2009;110:703–708.
5. Jevtovic-Todorovic V. Developmental synaptogenesis and general anesthesia: a kiss of death? Curr Pharm Des 2012;18:6225–6231.
6. Flick RP, Katusic SK, Colligan RC, et al. Cognitive and behavioral outcomes after early exposure to anesthesia and surgery. Pediatrics 2011;128:e1053–e1061.
7. Orliaguet G, Vivien B, Langeron O, et al. Minimum alveolar 8. concentration of volatile anesthetics in rats during postnatal maturation. Anesthesiology 2001;95:734–739.
8. Jevtovic-Todorovic V, Hartman RE, Izumi Y, et al. Early exposure to common anesthetic agents causes widespread neurodegeneration in the developing rat brain and persistent learning deficits J Neurosci 2003;23:876–882.
9. Wise-Faberowski L, Zhang H, Ing R, et al. Isoflurane-induced neuronal degeneration: an evaluation in organotypic hippocampal slice cultures. Anesth Analg 2005;101:651–657.
10. Ikonomidou C, Bittigau P, Ishimaru MJ, et al. Ethanol-induced apoptotic neurodegeneration and fetal alcohol syndrome. Science 2000;287:1056–1060.
11. Leveille F, Papadia S, Fricker M, et al. Suppression of the intrinsic apoptosis pathway by synaptic activity. J Neurosci 2010;30:2623–2635.
12. Istaphanous GK, Ward CG, Nan X, et al. Characterization and quantification of isoflurane-induced developmental apoptotic cell death in mouse cerebral cortex. Anesth Analg 2013;116:845–854.
13. Stratmann G, May LD, Sall JW, et al. Effect of hypercarbia and isoflurane on brain cell death and neurocognitive dysfunction in 7-day-old rats. Anesthesiology 2009;110:849–861.

14. Olney JW, Young C, Wozniak DF, et al. Anesthesia-induced developmental neuroapoptosis. Does it happen in humans? Anesthesiology 2004;101:273–275.
15. Mennerick S, Zorumski CF. Neural activity and survival in the developing nervous system. Mol Neurobiol 2000;22:41–54.

HYDROGEN PEROXIDE AND PAIRED-PULSE FACILITATION OF NEUROTRANSMITTER RELEASE AT THE FROG NEUROMUSCULAR JUNCTION

A.R. Giniatullin, U.N. Garifullina

Kazan State Medical University, Butlerov st. 49, Kazan, 420012, Russia

A ubiquitous property of synapses is the ability to keep track of the history of activity. This history is encoded in various forms of activity-dependent plasticity that shape synaptic output and may form the basis of learning and memory. Short-term plasticity lasts from tens of milliseconds to several minutes and is thought to underlie information processing. It can lead to bidirectional changes in synaptic strength, which can be reduced for hundreds of milliseconds to seconds (depression), or it can be enhanced for hundreds of milliseconds to seconds (facilitation), to tens of seconds to minutes (augmentation and post-tetanic potentiation). Net plasticity at synapses reflects an interaction between multiple forms of plasticity.

The traditional view in the field of free radical biology is that free radicals and reactive oxygen species (ROS) are toxic, mostly owing to direct damage of sensitive and biologically significant targets. However, recent workers in this and in related fields are exploring the view that superoxide radical and reactive oxygen species exert beneficial effects. Thus, such ROS are viewed as involved in cellular regulation by acting as redox signals, and their harmful effects are seen mostly as a result of compromised signaling, rather than due to direct damage to sensitive targets. Reactive oxygen species (ROS) such as superoxide anion, hydroxyl radical, and hydrogen peroxide (H_2O_2) are continuously produced by mitochondrial respiration, the membrane-associated NADPH oxidase complex, or by the action of hormones, neurotransmitters and neurotrophins. H_2O_2 is of particular interest among other ROS because H_2O_2 is the most stable and long-lived ROS; being a mild oxidant, H_2O_2 application for <30 min does not produce non-specific peroxidation of membrane lipids, H_2O_2 passes through cell membranes, and H_2O_2 is more stable in extracellular than in intracellular space and it might serve, therefore, not only as an intracellular but also as an intercellular messenger. In our pre-

vious study we showed that low physiological ($\leq$1-50 μM) concentrations, H_2O_2 facilitated Ach secretion, while at high concentrations, the action of H_2O_2 resulted in synaptic depression. While the genome of the motoneuron is very susceptible to attack by ROS, this data represent fast, presumably non-genomic, action of H_2O_2 on motoneuron terminals.

In the current study we analyzed the effect of low concentrations of H_2O_2 and some reagent which change red/ox status in the cell, on synaptic enhancement that is prominent on the hundreds of milliseconds time scale is referred to as facilitation.

Experiments were carried out on frog sartorius muscle preparations *in vitro* at room temperature. Briefly, muscles were dissected from tricaine-anaesthetized frogs in accordance with the European Communities Council Directive (24th November 1986; 86/609/EEC). To prevent muscle contractions we used the transverse cutting ('cut preparation') of muscle fibres. Ringer solution contained (mM): NaCl 113, KCl 2.5, CaCl$_2$ 1.8, NaHCO3 2.4, pH adjusted to 7.3 with NaOH. The holding potential for cut preparations was kept at -40 mV while for all other preparations it was -70 mV. On cut preparations the voltage dependence of the peak amplitudes of the evoked end-plate currents (EPCs) was linear in the range from 0 to -100 mV, indicating the effectiveness of the voltage clamp. The motor nerve was stimulated with electrical pulses of suprathreshold amplitude and 0.1–0.2 ms duration. Stimuli were initially applied to the motor nerve at 0.05Hz to establish the baseline quantal content and the amplitude and time-course parameters of the EPC. Subsequently, paired-pulse stimulation (interpulse intervals (Δt): 5,7,10,20,50, 100,200,300,500 ms) was applied, three to five pairs in cell for each Δt. EPC quantal content was determined as the ratio of averaged EPC and averaged MEPC amplitudes. The paired-pulse facilitation ratio (PPF) was calculated for each Δt as 100%. (A2$-$A1)/A1, where A1 and A2 denote the average amplitudes of EPCs elicited by first (conditioning) and second (test) stimuli in the pair, respectively.

First of all on cut preparations of sartorius muscle, we tested the action of H_2O_2 on multiquantal EPCs elicited at a frequency of 0.05 Hz. H_2O_2 at a low (3 μM) concentration reversible enhancement the amplitude of EPCs (20$\pm$3.2%; *n*=9; *P*<0.05). This reversible facilitation was stabilized after 15–20 min in the presence of H_2O_2. Our data indicate that the motor nerve terminal is the preferential target for the fast action of exogenous (and potentially endogenous) H_2O_2. This was confirmed by the fact that the amplitude and decay of MEPCs were unchanged by H_2O_2. The EPCs amplitude increase effect of the H_2O_2 application (10 μM) was more weak and sometimes the moderate decrease in the amplitude was observed.
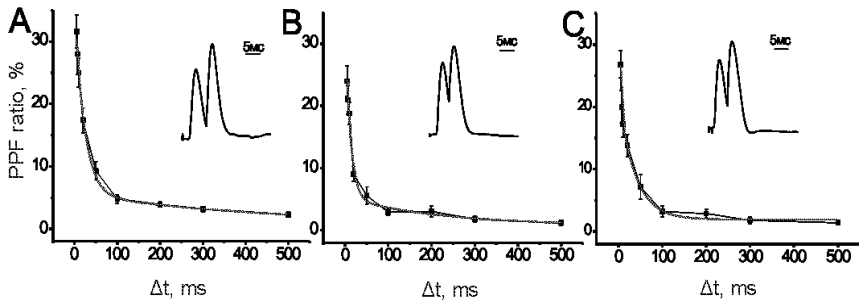
Fig. 1. The facilitation of EPC with paired pulses in control (A) or in the presence of H_2O_2 3μM (B) and 10μM (C). The original EPC traces were obtained with Δt of 5 ms.

Paired-pulse stimulation in control resulted in a significant increase of EPC amplitude (fig. 1A), reflecting the enhancement of the neurotransmitter release. In experiments with 3 and 10 μM H_2O_2 the motor nerve was stimulated with 0,05 Hz during the 10-11 minutes of the oxidant application and the effect dynamics was monitored, then turned to the pair stimulation without cleaning. These results (Fig. 1B,C) indicate that H_2O_2 significantly decrease the intensity of the facilitation , that is the transmitter release during pair stimulation.

In many cases the biological action of H_2O_2 is related to the generation of hydroxyl radicals. It is known that in the presence of Fe^{2+}, H_2O_2 is readily converted into the hydroxyl radical and this provides a reliable tool for ascertaining the mechanism of action. In our experiments the PPF ratio also was reduced after 100 μM $FeSO_4$ и 130 μM L-buthionine-sulfoximine (used to induce experimental glutathione deficiency). When the muscle was pretreated with 50-100 μM paraquat dichloride, PPF ratio also was reduced. Paraquat toxicity is primarily generated by ROS elicited by redox-cycling with molecular oxygen and NADH-dependent formation of superoxide anions. Superoxide can be further converted to H_2O_2 by the antioxidant enzyme superoxide dismutase. The peroxide is converted to water and oxygen by glutathione peroxidase and catalase. When the muscle was pretreated with 1200 Uml^{-1} catalase or 300 Uml^{-1} PEG catalase, the action of H_2O_2 on PPF ration was abolished ($n=6$; $P>0.05$) in accordance with the selective activity of this enzyme for this type of ROS.

Short-term synaptic plasticity represents an increase (facilitation) or decrease (depression) of synaptic strength, which lasts from hundreds

of milliseconds to seconds and is crucial for information processing. Short-term synaptic plasticity is Ca^{2+}-dependent and predominantly pre-synaptic, although postsynaptic mechanisms may also contribute. Several mechanisms have been proposed to account for facilitation One proposed mechanism for facilitation involves residual calcium (Ca_{res}) that persists in the presynaptic terminal following synaptic activation. At the calyx of Held, linear summation of Ca_{res} (hundreds of nanomolar) with the high local calcium levels at a release site evoked by an action potential (Ca_{local} of tens to hundreds of micromolar) will not lead to sufficient enhancement of synaptic transmission. It has therefore been hypothesized that Cares increases the probability of release by binding to a sensor distinct from synaptotagmin, the sensor for synchronous release, and activating a site distinct from the low affinity sites on synaptotagmin that are responsible for vesicle fusion. At present no such calcium sensor has been identified. Another potential mechanism for facilitation involves calcium-binding proteins within presynaptic terminals that normally intercept calcium ions between calcium channels and release sites, thus reducing the initial probability of release. In our previous study we showed that 3 μM H_2O_2 changed neither the Na^+ nor the Ca^{2+} phase of the complex action potential, implying that the increase in EPCs produced by H_2O_2 was located downstream from presynaptic depolarization and Ca^{2+} influx. Another potential mechanism for facilitation involves calcium-binding proteins within presynaptic terminals that normally intercept calcium ions between calcium channels and release sites, thus reducing the initial probability of release. If the first stimulus leads to calcium occupying some of these calcium-binding proteins, then more calcium will reach the release site in response to the second stimulus, and the probability of release will be elevated. This mechanism of facilitation has been demonstrated at some neocortical synapses that contain a high concentration of the calcium binding protein calbindin D-28k.

The obtained data suggest that endogenous H_2O_2, in the low physiological concentrations, decrease the intensity of the facilitation phenomena, perhaps via changing the red/ox station of the effectors molecules or processers of the transmitter release facilitation. These investigations for the identification of the obtained effects of the low H_2O_2 concentrations will be continued.

THE MECHANISMS OF DISSEMINATION
OF CARCINOMA CELLS

N.A. Gloushankova, I.Y. Zhitnyak, S.N. Rubtsova

*Institute of Carcinogenesis, N.N. Blokhin Cancer Research Center
of the Russian Academy of Medical Sciences, Kashirskoe shosse 24,
Moscow, 115478, Russia*

Advances in surgery, radiation therapy and chemotherapy have rendered most tumors largely curable if they are treated before dissemination. However, if the tumor cells migrate from their original site into adjacent or distant tissue and organs, the tumors become highly morbid. There are two forms of tumor dissemination: 1) invasion into tissue surrounding the tumour and 2) metastatic dissemination with colonization at distant sites. Epithelial–mesenchymal transition (EMT), a process by which epithelial cells acquire characteristics of mesenchymal cells, plays an important role in invasion and metastasis. There is much evidence that, using EMT, tumor cell gain migratory and invasive properties. During EMT, epithelial cells lose cell polarity, diminish cell-cell adhesion, acquire mesenchymal markers (N-cadherin, vimentin) and motile phenotype. In the course of invasion and metastasis tumor cells can use mesenchymal or ameboid type of movement. They can migrate as single cells or as groups of cells preserving cell-cell contacts with adjacent malignant cells (collective migration). Studying transformed IAR epithelial cell lines established from rat liver, we found that malignant cells that preserved expression of E-cadherin can assemble dynamic E-cadherin-based adherens junctions. Plasticity of E-cadherin-based AJs is very important for migration of neoplastic cells. In cultures of IAR1170 and IAR-6-1 cells, cell-cell contacts in the islands were unstable. Transformed IAR1170 and IAR-6-1 cells could break contacts and migrate individually forming new contacts with neighboring cells. We found that E-cadherin-based adherens junctions play an important role in maintenance of effective collective migration of neoplastic cells. In comparison with single cells, cell groups moved more directionally.

Recently we also demonstrated the importance of E-cadherin-based adherens junctions in dissemination of neoplastic cells in epithelial structures. We found that transformed IAR-6-1 cells were able to form hybrid E-cadherin-mediated cell-cell contacts with non-transformed IAR-2 epithelial cells. Transformed IAR-6-1 can migrate across the top of monolayer of non-transformed cells. More often, however, (20-40%), transformed cells invaded the continuous monolayer of non-transformed IAR-

2 epithelial cells and migrated across the glass substrate underneath IAR-2 cells. In the majority of cases, neoplastic cells traversed the monolayer at the borders between cells where they destructed cell-cell contacts of normal cells. IAR1162 cells that lost E-cadherin expression in the course of neoplastic transformation and IAR6-1 cells stably transfected with construct of dNE-cadherin were less successful in the adhesion and penetration of epithelial monolayer. It is tempting to speculate that retention of expression of E-cadherin in some cases of neoplastic transformation may be important for carcinoma cell dissemination.

RELATIONSHIP BETWEEN MITOCHONDRIA-ASSOCIATED FLUORESCENCE AND HEMOCYTE MOTILITY IN GROMPHADORHINA PORTENTOSA

E.A. Grebtsova, A.A. Prisny
Belgorod State University, Pobedy str., 85, Belgorod, 308015, Russia

In recent years, fluorescent dyes for measuring the mitochondrial membrane potential ($\Delta\psi$m) have become commonly used tools for monitoring changes in this important physiologic mitochondrial parameter as it relates to cells' capacity to generate ATP by oxidative phosphorylation. As such, the $\Delta\psi$m is a key indicator of cell health or injury, and cell activity. An increase or a decrease in DeltaPsi(m) (that depends on the fluorescence intensity) consequently followed an increase or a decrease in the cellular ATP contents [4, 5].

Insects hemocytes compose the cellular army of their innate immune system. Plasmatocytes, putative homologues to mammalian macrophages, and granulocytes in *Gromphadorhina portentosa*, represent, 70% of the migratory hemocyte population in circulation and are responsible for the phagocytosis of bacteria and apoptotic tissues that arise during metamorphosis [1]. It is not known as to how hemocytes become activated from a sessile state in response to such infectious and developmental cues.

We used noninvasive fluorescence method to determinate and monitoring the fluorescence intensity, using rhodamine B. Rhodamine B distributes across biological membranes in response to the electrical transmembrane potential. Hemolymph of adult insects was collected using standard methods. The collected hemolymph incubated in physiological solution, in hypo- and hyper medium, and with cells of *Saccharomyces cerevisiae.*

Hemocytes of *G. portentosa* are motile, phagocytic cells that are present at all stages of the life cycle and represent the cellular component

of the animal's innate immune system at postembryonic life stages [3]. The most common cell types are plasmatocytes and granulocytes. Accordingly, the main function of post-embryonic hemocytes is to clear infection from invading microorganisms as well as debris from apoptotic cells by performing phagocytosis [2, 3].

As a brief description, the most common morphology of untreated hemocytes (incubated in physiological solution for insects) – "normal spread" represented a fully adhered cell with a uniformly protruding and retracting cell membrane (at all angles surrounding the central region). Normal spread represented the quiescent sessile behavior of these hemocytes. The two active morphological classes, "non-polarized" and "polarized", are predominant at medium with *S. cerevisiae*. Both of "non-polarized" and "polarized" morphology are typical for granulocytes, and only "non-polarized" characteristic for plasmatocytes.

Both classes represent a fully adhered cell that exhibits an extremely active cell membrane that protrudes and retracts at varied angles to the cell central region producing multiple membrane ruffles. The essential difference between these two classes is that polarized cells produce a visual lamellopodium and trailing edge during random migration

Ex vivo hemocytes exhibited 100% normal membrane spread. Rizopodium are uniformly distributed over the surface of the membrane, and their length was no higher 1,5 µm. The fluorescence intensity equals 249±51 for granulocytes and 212±51 for plasmatocytes.

Both of granulocytes and plasmatocytes activity rapidly decreased in hypotonic medium. But energy needs to maintain membrane integrity under the conditions of low osmotic pressure were conducive to growth in fluorescence intensity, which equals 314±28 and 387±40 for granulocytes and plasmatocytes, respectively. Over a period of time rizopodium length shorten to 0,9 µm in hypertonic medium. The rate of spreading was decreased considerably. These hemocytes have maximum fluorescence intensity among the cells incubated in different solutions which attains 554±48 for granulocytes and 420±36 for plasmatocytes. Experiments in medium with high osmotic pressure revealed no changes in the hemocytes activity as compared with cells incubated in physiological solution.

S. cerevisiae addition to hemocytes in physiological solution led to appearance 34% of normal spread granulocytes, 40% -"polarized" and 26% "non-polarized". Among the plasmatocytes no some of polarized, 92% non-polarized and 8% normal spread cells. Beyond the rhizopodium (which ramification was at the elongation of 1 µm), has came up long filopodium about 3,5 µm in length. Both of pseudopodia types located irregu larly on the membrane surface leading in the direction of the yeast cells.

Granulocytes			Plasmatocytes	
normal spread	non-polarized	polarized	normal spread	non-polarized
346±60	581±67	596±82	245±48	425±54

Hypertonic medium and non-self objects identically affect the fluorescence intensity. Moreover, fluorescence intensity of normal spread phagocytes higher in medium with *S. cerevisiae,* and had maximal value for "non-polarised" and "polarized" hemocytes. High values of fluorescence intensity enables us to speak of great needs of energy to recognize non-self objects and kill them.

References

1. Гребцова Е.А., Присный А.А. Определение мембранного резерва гемоцитов Periplaneta americana и Blaberus craniifer и изучение влияния гипоосмотической нагрузки на объем клеток // «Научные достижения биологии, химии, физики»: материалы международной заочной научно-практической конференции. – Новосибирск: Изд. «Сибирская ассоциация консультантов». – 2012. – 114 с.
2. Holz A., Bossinger B., Strasser T., Janning W., Klapper R. The two origins of hemocytes in Drosophila. – Development. – 2003– V.130. – P.4955–4962.
3. Lanot R., Zachary D., Holder F., Meister M. Postembryonic hematopoiesis in Drosophila. – Dev. Biol. – 2001 – V. 230. – P.243–257.
4. Russell C. Scaduto, Jr., Lee W. Grotyohann. Measurement of mitochondrial membrane potential using fluorescent rhodamine derivatives. Biophysical Journal. – 1999. – V.76 – P.469–477.
5. Seth W. Perry, John P. Norman, J. Barbieri, E. B. Brown, Harris A. Gelbard Mitochondrial membrane potential probes and the proton gradient: a practical usage guide. Biotechniques. – 2011 – V.50(2): – P. 98–115.

GENE EXPRESSION AND TITIN CONTENT IN STRIATED MUSCLES OF CHRONIC ETHANOL-FED RATS

Yu.V. Gritsyna[1], I.M. Vikhlyantsev[1], N.N. Salmov[1], A.D. Ulanova[1,2], A.G. Bobylev[1], Z.A. Podlubnaya[1,2]

[1]Institute of Theoretical and Experimental Biophysics, Russian Academy of Sciences, Pushchino, Moscow region, Russia;
[2]Pushchino State Institute of Natural Science, Pushchino, Moscow region, Russia;
E-mail: gri23.86@mail.ru

It is known that chronic alcoholic intoxication results in the development of symptom complex of alcohol-induced injury both of the skeletal (alcoholic myopathy) and cardiac (alcoholic cardiomyopathy) muscles

[1,2]. The main characteristics of alcohol-induced damages in the muscles are successfully modeled on animals, in particular on rats. It has been shown, that development of alcoholic myopathy/cardiomyopathy in man and animals is accompanied by atrophy and skeletal muscle weakness, damages of cardiac muscular contractility [1,3]. A decrease of total quantity of RNA, DNA and proteins (for example, heavy chains of myosin, actin, desmin, troponin-I) [3-5], as well as damages of functional properties of contractile proteins, in particular a decrease ATPase activity of myosin [6] activated by actin, make contribution to these changes. A molecular mechanism of the development of alcohol-induced damages in the muscles is unclear, however, it has been shown that ethanol and, mainly, the product of its oxidation, acetaldehyde, participate both in suppression of protein synthesis and activation of proteolysis [2,7,8].

Titin (connectin), a giant elastic protein forming the third type of the filaments in myofibrils (for reference see [9]), is an important component of striated muscles of sarcomeres in the vertebrates. It has been shown that titin is a scaffold for assemble thick filaments and sarcomere, participates in the maintenance highly-ordered sarcomere structure and, consequently, in contracting function of the muscle; contributes to passive tension at muscle stretch and develops restoring force at contraction of sarcomere; participates in triggering and regulation of actin-myosin interaction and regulation of intracellular signaling processes. In striated muscles of the mammals and a man titin is presented by several isoforms: NT, N2A, N2BA and N2B with molecular weight of their isoforms ~3000-3700 kDa (for reference see [9]).

In this study, changes of titin gene expression, as well as the content of its NT, N2A, N2BA and N2B-isoforms in myocardium (left ventricle) and skeletal (*m. soleus, m. longissimus dorsi*) muscles of chronically alcoholized rats are investigated. Since it has been recently shown that heat shock protein Hsp90 changes stability of titin molecule [10], study the changes of gene expression of proteins Hsp90 and Hsp70 was an additional goal of the work.

Materials and methods

Chronic alcoholization of the rats was carried out for 6 months according to [11]. The rats were divided into two groups: the control one ("Control", n=8): animals were fed standard food, 1% agarose and drinking water; and the test one: chronically alcoholized rats were fed standard food, 1% agarose with the ethanol content 30% and 10% ethanol solution in water as a single source of liquid for 6 months. The daily alcohol consumption was about 20-25 g/kg.

Investigation of the changes of isoform composition and the content of huge proteins titin in sarcomeric skeletal (molecular mass 2000-3700 kDa) and nebulin (700-900 kDA) in rats' muscles was perfomed using the method of SDS electrophoresis in 2.1% polyacrylamide gel with 0.5% agarose content according to the method [12] with our modifications [13]. Titin and nebulin content relative to the content of myosin heavy chains was estimated by densitometry (program Total Lab v.1.11). Phosphorylation of titin was carried out according to the method described in [14] with slight modifications. The level of protein phosphorylation was estimated by using fluorescent dye Pro-Q Diamond (Invitrogen) in a gel for phosphoproteins. For this purpose the gel was fixed in solution with 50% ethanol and 10% acetic acid for 12-18 hours. The stained gel was washed in Pro-Q Diamond phosphoprotein gel destaining solution (Invitrogen). The protein bands with phosphogroups were viewed by using system Pharos ("Bio-rad"); the gels were stained with Coomassie Brilliant Blue (G-250 and R-250), mixed in a 1 : 1 ratio to make control estimation of the protein content.

Total RNA was extracted from the muscle tissue of rats using the Aurum^{TM} Total RNA Fatty and Fibrous Tissue Kit (Bio-Rad, United States) according to the manufacturer's instructions. cDNA was synthesized using M-MLV reverse transcriptase (Eurogen, Russia). RT-PCR was performed with DT-322 amplifier (DNA-Technology, Russia) with Taq DNA polymerase (Eurogen, Russia) and SYBR Green I fluorescent dye (Invitrogen). The quantity of titin mRNA relative to the amount of mRNA housekeeping gen GAPDH was determined according to the method $2^{-\Delta\Delta Ct}$. In the work we used the following primers: forward primer 5'- cagcagccaagaaggccgct-3', reverse primer 5'-gtcccgcagtctcatagtctcaccac-3' for gene *ttn* N2A-isoform; forward primer 5'-ccaagctcactgtgggagaaa-3' and reverse primer 5'-cttaactcgggaaccttcatcg-3' for the gene *ttn* N2B and N2BA exons 49-50; forward primer 5'-acgccaacggcatcctgaac-3', reverse primer 5'-ggcggactcgttcctcctct-3' for gene Hsp70; forward primer 5'-ctttcccgtcaagatgcctgag-3', reverse primer 5'-agagattacgaagtctacgggacc-3' for gene Hsp90. PCR was performed using the following regime: hot start at 95°C for 5 min, denaturation at 95°C for 15 s, annealing with primers at 60°C for 20 s, elongation at 72 for 20 s (35 cycles). The PCR products were then analyzed by electrophoresis in 7% polyacrylamide gel. Data were statistically processed using the Manna–Whitney nonparametric U-criterion. In our study, differences were considered significant at $p < 0.01$.

Results and discussion

A decrease (by ~30%) of mass *m. soleus* in chronically alcoholized rats and a tendency to decreased mass of cardiac muscle relative to the

body mass has been revealed. These results indicate the development of atrophic changes in the muscles of animals from the Alcohol group, which agrees with the published data [15].

In case of atrophic changes in *m. soleus* of chronically alcoholized rats, a slight increase gene expression of titin (3-4 times) and decreasing the content of this protein (NT- and N2A-isoforms) by 1.4 times was observed (figure). Decreasing of content titin, the most important protein of sarcomeric cytoskeleton, involved in maintaining highly-ordered sarcomeric structure and contracting capability of the muscles, is a proof of the development of alcohol-induced pathological changes in *m. soleus*. Such a decreasing of titin content followed by the damages of sarcomeric structure and contractile capability of the muscles was observed in our earlier experiment in human and rat's *m. soleus* at development of atrophy under conditions of gravitation unload and in *m. soleus* of patients with post-apoplectic muscle spasticity [9]. It is interesting that at the development of pathological changes indicated above in human and rat's "slow" muscle *soleus* the increase in the content of "rapid" isoform IIa of heavy myosin chains was observed [9]. Such a shift of myosin phenotype was revealed also in *m. soleus* of chronically alcoholized rats [16]. Hence, changes of isoform composition and the content of important sarcomere titin and myosin proteins in *m. soleus* of chronically alcoholized rats point to the development of pathological process in this muscle.
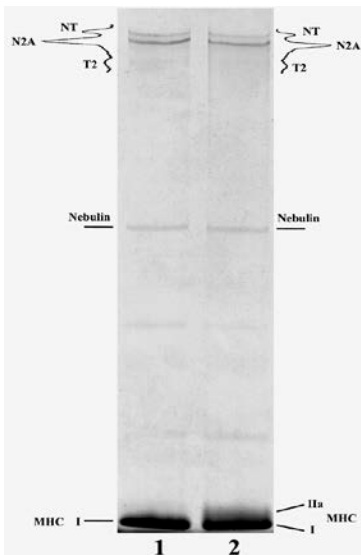
Composition of titin isoforms in *m. soleus* of control (1) and (2) chronically alcoholized rats. Electrophoresis was performed in 2.1% polyacrylamide gel strengthened with agarose. MHC – myosin heavy chains. I – "slow" isoform of MHC. IIa – "fast" isoform of MHC. T2 – proteolytic fragment of titin. Nebulin content (a giant protein of actin filaments) remained unchanged in *m. soleus* of chronically alcoholized rats.

No statistically significant changes in titin content were found in myocardium of chronically alcoholized rats. However, in a number of cases at electrophoretic studies of the samples in myocardium of "Alcohol" group rats, a significant decrease (~1.7 times) of the titin content (N2B-, N2BA- and NT-isoforms) was observed. These evidences, as well as data about a decrease of titin gene expression by 9 times in cardiac muscle chronically alcoholized rats, indicating the development of pathologic changes also in cardiac muscle of these animals.

What is the cause of the decreased titin content in muscles of chronically alcoholized rats? It is known that titin is a substrate for calcium-dependent calpain proteases [17]. It is assumed that the turnover of proteins in the sarcomere is initiated by the cleavage of titin and other proteins of myosin and actin-containing fibrils by calpains, which then degrade by the ubiquitin-proteasome pathway [17]. Taking into account the recently published data that ethanol contributes to the enhanced degradation of muscle proteins via the ubiquity-proteasome pathway [18], one may suppose that the activity of calpain proteases increases in alcoholized rats. Nevertheless, this hypothesis requires verification.

In *m. longissimus dorsi* rats of the "Alcohol" group we observed neither decrease of titin content nor changes of gene expression. However, a two-fold increasing of phosphorylation level of T2-fragment titin connected with myosin filaments in sarcomere A-disk was revealed. In earlier investigations *in vitro* it has been shown, that an increase of titin phosphorylation leads to a decreasing of actin-activated ATPase activity of myosin [19]. Based on these data it is possible to claim that an increasing of the level of titin phosphorylation in spinal muscle of chronically alcoholized rats has a pathologic character that will contribute to decreasing contractility.

Since it has been recently shown that heat shock protein Hsp90 changes the stability of titin molecule [10], another research problem was to study changes of gene expression of proteins Hsp90 and Hsp70 in the muscles chronically alcoholized rats. Taking into account data obtained about decreasing of titin content in *m. soleus* and cardiac muscle of these rats we expected to observe a decreasing of gene expression of heat shock proteins. However, no significant changes in the content of mRNA Hsp90 and Hsp70 in muscles under study were observed. Thus, it may be supposed that the main reason of decreasing titin content in the muscles of chronically alcoholized rats is increased activity

of Ca^{2+}-dependent calpain proteases. A decrease of titin content simultaneously with the increased level of its phosphorylation will, undoubtedly, contribute to the development of alcohol-induced damages in the muscles of the rats.

References

1. Lang C.H., Frost R.A., Summer A.D., Vary T.C. 2005. Molecular mechanisms responsible for alcohol induced myopathy in skeletal muscle and heart. Int. J. Biochem. Cell Biol. 37, 2180–2195.
2. Oba T., Maeno Y., Ishida K. 2005. Differential contribution of clinical amounts of acetaldehyde to skeletal and cardiac muscle dysfunction in alcoholic myopathy. Curr. Pharm. Des. 11, 791–800.
3. Patel V.B., Sandhu G., Corbett J.M., Dunn M.J., Rodrigues L.M., Griffiths J.R., Wassif W., Sherwood R.A., Richardson P.J., Preedy V.R. 2000. A comparative investigation into the effect of chronic alcohol feeding on the myocardium of normotensive and hypertensive rats: an electrophoretic and biochemical study. Electrophoresis. 21, 2454–2462.
4. Preedy V.R., Peters T.J. 1988. The effect of chronic ethanol ingestion on protein metabolism in type-I and type-II fibre-rich skeletal muscles of the rat. Biochem. J. 254, 631–639.
5. Vary T.C., Deiter G. 2005. Long-term alcohol administration inhibits synthesis of both myofibrillar and sarcoplasmic proteins in heart. Metabolism. 54, 212–219.
6. Reddy Y.S., Beesley R.C. 1990. Effects of acute and chronic ethanol on cardiac contractile protein ATPase activity of Syrian hamsters. Biochem. Med. Metab. Biol. 44, 259–265.
7. Lang C.H., Frost R.A., Deshpande N., Kumar V., Vary T.C., Jefferson L.S., Kimball S.R. 2003. Alcohol impairs leucine_mediated phosphorylation of 4E_BP1, S6K1, eIF4G, and mTOR in skeletal muscle. Am. J. Physiol. Endocrinol. Metab. 285, E1205–1215.
8. Preedy V.R., Crabb D.W., Farrйs J., Emery P.W. 2007. Alcoholic myopathy and acetaldehyde. Novartis Found Symp. 285, 158–177; discussion 177–182, 198–199.
9. Vikhlyantsev IM, Podlubnaya ZA. New titin (connectin) isoforms and their functional role in striated muscles of mammals: facts and suppositions // Biochemistry (Mosc). 2012 Dec; 77(13):1515-35. doi: 10.1134/S0006297912130093. Review.
10. Donlin L.T., Andresen C., Just S., Rudensky E., Pappas C.T., Kruger M., Jacobs E.Y., Unger A., Zieseniss A., Dobenecker M.W., Voelkel T., Chait B.T., Gregorio C.C., Rottbauer W., Tarakhovsky A., Linke W.A.

Smyd2 controls cytoplasmic lysine methylation of Hsp90 and myofilament organization // Genes Dev. 2012 Jan 15; 26(2):114-9. doi: 10.1101/gad.177758.111. Epub 2012 Jan 12.

11. Lysenko E.A., Turtikova O.V., Morozkina E.V., Khotchenkov V.P., Popov V.O., Shenkman B.S. Effects of recombinant mechano-dependent growth factor against the background of chronic alcoholisation in rats // Ross. Fiziol. Zh. Im I.M. Sechenova. 2012 Feb; 98(2):283-92.

12. Tatsumi R., Hattori A. Detection of giant myofibrillar proteins connectin and nebulin by electrophoresis in 2% polyacrylamide slab gels strengthened with agarose // Anal. Biochem. 1995 Jan 1; 224(1): 28-31.

13. Vikhlyantsev I.M., Podlubnaya Z.A., Kozlovskaya I.B. New titin isoforms in skeletal muscles of mammals // Dokl. Biochem. Biophys. 2004 Mar-Apr; 395:111-3.

14. Borbély A., Falcao-Pires I., van Heerebeek L., Hamdani N., Edes I., Gavina C., Leite-Moreira A.F., Bronzwaer J.G., Papp Z., van der Velden J., Stienen G.J., Paulus W.J. Hypophosphorylation of the Stiff N2B titin isoform raises cardiomyocyte resting tension in failing human myocardium // Circ. Res. 2009 Mar 27; 104(6):780-6. doi: 10.1161/CIRCRESAHA.108.193326. Epub 2009 Jan 29.

15. Otis J.S., Guidot D.M. 2009. Procysteine stimulates expression of key anabolic factors and reduces plantaris atrophy in alcohol_fed rats. Alcohol Clin. Exp. Res. 33, 1450–1459.

16. Yu.V. Gritsyna, N.N. Salmov, I.M. Vikhlyantsev, A.D. Ulanova, M.G. Sharapov, V.V. Teplova, and Z.A. Podlubnaya Changes in Gene Expression and Titin (Connectin) Content in Striated Muscles of Chronically Alcoholized Rats // Molecular Biology, 2013, Vol. 47, No. 6, pp. 871–878.

17. Goll D.E., Neti G., Mares S.W., Thompson V.F. 2008 Myofibrillar protein turnover: the proteasome and the calpains. J. Anim. Sci. 86 (14 Suppl), E19–35.

18. Vargas R., Lang C.H. 2008. Alcohol accelerates loss of muscle and impairs recovery of muscle mass resulting from disuse atrophy. Alcohol. Clin. Exp. Res. 32, 128–137.

19. Vikhlyantsev I.M., Okuneva A.D., Shpagina M.D., Shumilina Y.V., Molochkov N.V., Salmov N.N., Podlubnaya Z.A. Changes in isoform composition, structure, and functional properties of titin from Mongolian gerbil (Meriones unguiculatus) cardiac muscle after space flight // Biochemistry (Mosc.). 2011 Dec; 76(12):1312-20. doi: 10.1134/S0006297911120042.

EFFECT OF BIOLOGICALLY RELEVANT ANIONS ON THE GENERATION OF REACTIVE OXYGEN SPECIES IN WATER UNDER THE ACTION OF PHYSICAL FACTORS

S.V. Gudkov [1,2], V.E. Ivanov [1], O.E. Karp [1], D.A. Kulikov [1,3], A.M. Usacheva [1], A.B. Gapeev [2,4], N.R. Popova [1], M.E. Astashev [2,4], E.A. Galochkina [1,5], A.V. Chernikov [1], V.I. Bruskov [1,2]

[1] Institute of Theoretical and Experimental Biophysics of RAS, Institutskaya street 3, Pushchino, Moscow region, 142290, Russia

[2] Pushchino State University, Nauki prosp. 3, Pushchino, Moscow region, 142290, Russia

[3] Moscow Regional Research and Clinical Institute "MONIKI", Schepkina street 61/2, Moscow, 129110, Russia

[4] Institute of Cell Biophysics of RAS, Institutskaya street 3, Pushchino, Moscow region, 142290, Russia

[5] Lobachevsky State University of Nizhni Novgorod - National Research University, Gagarin prosp. 23, 603950, Nizhni Novgorod, Russia

Today it is known that a number of pathologies including those related to the biological mobility are associated with the development of oxidative stress. In this work, the influence of biologically relevant anions on the generation of reactive oxygen spicies under the action of non-ionizing factors is investigated. Non-ionizing physical factors under study include heat, laser radiation and modulated electromagnetic radiation of extremely high frequency (EHF EMR).

The influence of biologically relevant anions at a concentration of 1 mM on the formation of hydrogen peroxide in water under the action of laser radiation with a wavelength of 632.8 nm (0.7 mW/mm^2, 5 min) was studied. It is shown that laser radiation under the chosen conditions of exposure produces about 5.5 nM of hydrogen peroxide. It is found that organic anions such as succinate, acetate, citrate and nitrite lead to reduced formation of hydrogen peroxide by the action of laser radiation with a wavelength corresponding to the maximum absorption of one of the lines of molecular oxygen by about 25-40%. Chloride anions at a concentration of 1 mM do not, in fact, affect the formation of hydrogen peroxide. Nitrate anions as well as mono- and dibasic phosphate anions increase the production of hydrogen peroxide by the action of the laser radiation by approximately 50%. Bicarbonate anions increase the formation of hydrogen peroxide about two-fold. The impact of biologically relevant anions at a concentration of 1 mM on the generation of hydroxyl radicals in water under the action of laser radiation with a

wavelength of 632.8 nm (0.7 mW/mm^2, 5 min) was investigated. It is established that under the action of laser radiation (a) succinate, acetate, citrate anions lead to a reduction in the formation of hydroxyl radicals, (b) chloride and nitrate anions do not substantially affect the generation of hydroxyl radicals, and (c) nitrite as well as mono- and dibasic phosphate anions increase the production of hydroxyl radicals.

The influence of biologically relevant anions at a concentration of 1 mM on the formation of hydrogen peroxide in water under the action of heat (4 h, 40°C) was studied. It is shown that heat under the chosen conditions of exposure produces about 4 nM of hydrogen peroxide. It is found that organic anions such as succinate, acetate, citrate lead to reduced formation of hydrogen peroxide by the action of heat by about 30-50%. Chloride anions at a concentration of 1 mM do not, in fact, affect the formation of hydrogen peroxide. Bicarbonate and nitrate anions increase the formation of hydrogen peroxide by about 30%. The impact of biologically relevant anions at a concentration of 1 mM on the genera-tion of hydroxyl radicals in water under the action of heat was investigated. It is established that under the action of heat (a) succinate, acetate anions lead to a reduction in the formation of hydroxyl radicals, (b) citrate, chloride and nitrate anions do not substantially affect the generation of hydroxyl radicals, and (c) nitrite as well as bicarbonate, mono- and dibasic phosphate anions increase the production of hydroxyl radicals 1.3-2.5 times.

The influence of biologically relevant anions at a concentration of 1 mM on the formation of hydrogen peroxide in water under the action of EHF EMR (42.2 GHz, modulation 16 Hz, 100 µW/cm^2, 20 min) was studied. It is shown that EHF EMR radiation under the chosen conditions of exposure produces about 11.5 nM of hydrogen peroxide. It is found that organic anions such as succinate, acetate, citrate lead to reduced formation of hydrogen peroxide by the action of EHF EMR by about 50%. Mono- and dibasic phosphate, nitrate anions lead to reduced formation of hydrogen peroxide by the action of EHF EMR by about 20-35%. Chloride anions at a concentration of 1 mM do not, in fact, affect the formation of hydrogen peroxide. Bicarbonate as well as nitrate anions increase the production of hydrogen peroxide by the action of the laser radiation by approximately 20-30%. The impact of biologically relevant anions at a concentration of 1 mM on the generation of hydroxyl radicals in water under the action of EHF EMR was investigated. It is established that under the action of EHF EMR (a) succinate, acetate, citrate anions

lead to a reduction in the formation of hydroxyl radicals by about 30-35%, (b) chloride and nitrate anions do not substantially affect the generation of hydroxyl radicals, and (c) nitrite as well as mono- and dibasic phosphate anions increase the production of hydroxyl radicals.

Thus, it was shown that reactive oxygen species are formed in the water upon exposure to radiation of a helium-neon laser, heat and EHF electromagnetic radiation. Anions are capable of influencng this process to a large extent.

SEASONAL EXPRESSION OF Ca^{2+}-ATPase ISOFORM IN MYOCARDIUM OF GROUND SQUIRREL *Spermophilus undulatus*

E.V. Karaduleva[1], I.M. Santalova[2], N.M. Zakharova[1]

[1] *Institute of Cell Biophysics of the Russian Academy of Sciences, Pushchino, Moscow Region, 142290, Russia;*
[2] *Institute of Theoretical and Experimental Biophysics of the Russian Academy of Sciences, Pushchino, Moscow Region, 142290, Russia*

Hibernating animals demonstrate perfect adaptation to hypothermal conditions, at which non-hibernating animals and human would die. For example, contraction rate of the myocardium in hibernating animals occur at body temperature near zero and reverts to normal euthermal level at every interbout arousal without any pathological alterations [Johansson, 1996].

It is known that the main reason of pathological alterations of myocardium functioning during hypothermia is imbalance of calcium homeostasis [Wang et al., 2002]. Ca^{2+}-ATPase of sarcoplasmic reticulum (SR) of the myocardium is responsible for deletion of Ca^{2+} from cytoplasm to cisterns of SR for its recycling during further contraction-relaxation cycles and for avoiding calcium overloads. Decrease of body temperature in non-hibernating animals leads to decrease of rate of excess calcium removal from cytosol by Ca^{2+}-ATPase of the reticulum. In hibernating animals, no such effect was observed [Liu et al., 1997; Belke et al., 1991]. Up to today, a large amount of data is accumulated on morphological, physiological and biochemical changes related to functioning of Ca^{2+}-ATPase of the SR [Rubtsov, 2005; Giroud et al., 2013], whereas molecular features of regulation of the synthesis of cardiac isoform of Ca^{2+}-ATPase are not clear yet. Beside that, in studies on hibernation mecha-

nisms, torpor phase is usually compared to summer or interbout activity, without paying much attention to other conditions of an animal during hibernation season. Meanwhile, we have earlier shown in our laboratory that preparation for hibernation begins long before actual hibernation, in late summer or early autumn. In this period, titin expression and its isoform composition in the heart of ground squirrel are altering [Karaduleva E.V. et al., 2010], and an increase in calcium capacity of cardiac SR along with decrease of blood calcium level are being revealed [Zakharova et al., 2009]. These data brought in the tasks of the current work: ultrastructural analysis of the myocardium in order to reveal alterations in relative area of SR (summer, autumn) and investigation of ATP2A2 gene expression in myocardium of ground squirrels at different stages of hibernation (entrance into torpor, torpor, arousal from torpor, interbout activity) in comparison to summer and autumn activities.

For morphological and molecular analysis, tissue samples were obtained from subendocardial part of left ventricle. Expression level of cardiac isoform of SR Ca^{2+}-ATPase gene was determined during entrance into torpor and arousal from torpor at equal heart temperatures around 16°C according to the suggestion that the highest value of Q_{10} quotient for heart rate during entrance into torpor was detected for heart tempetature around 15°C - 20°C [Ignat'ev et al., 2001]. The identical temperature for arousing ground squirrels was taken for comparison. Treatment of tissue samples and estimation of relative sarcoplasmic reticulum area were carried out as described earlier [Santalova et al., 2008]. For comparative analysis of ATP2A2 gene expression level, a real-time polymerase chain reaction method (qRT-PCR) was used as described earlier [Karaduleva E.V. et al., 2010]. The statistical analysis was carried out by means of non-parametric Mann-Whitney U-test and Student t-test. The probability of randomness between the samples was $p < 0.05$.

The results of ultrastructural analysis showed that relative area of the SR significantly increased in autumn compared to summer period.

The qRT-PCR data showed that expression of cardiac isoform of Ca^{2+}-ATPase gene dramatically decreases in myocardium of ground squirrels in autumn period compared to active summer period. The mRNA level of ATP2A2 gene remains low during entering hibernation and during torpor without significant difference between these two states. During active interbout state and arousal, a tendency for restoration of mRNA level to normal euthermal level of active summer animals is observed.

It is most possible that expression of cardiac isoform of of Ca^{2+}-ATPase gene alters in active autumn animals in response to the need for

myocardial functioning in torpor mode. It is not the only case of decrease of gene expression during entering hibernation shown in our laboratory. Our earlier study on expression of titin gene in the myocardium of hibernating ground squirrels showed significant changes in expression of this protein's isoforms already in autumn activity [Karaduleva E.V. et al., 2010]. The revealed suppression of ATP2A2 gene expression in myocardium of ground squirrels during preparation for torpor state, as well as during the whole hibernation period, could have its cause in minimization of energy consumption, because transcription process is quite energy-consuming. Maintenance of relatively stable mRNA level in hibernation period could facilitate rapid protein synthesis during arousal from torpor [Epperson & Martin, 2002].

It is interesting that in torpor period, when the level of ATP2A2 gene expression is small, cardiomyocytes of hibernating animals are accumulating larger amount of Ca^{2+} in internal cisterns of SR compared to active summer animals [Tang et al., 1995 Wang et al., 2002], while the enzymatic activity of SR Ca^{2+}-ATPase is not being altered during hibernation [Belke et al., 1991]. It is supposed that the increase of calcium consumption in SR in torpor period is related to the increase of number of Ca^{2+}-ATPase molecules along with increase of the area of SR [Tang et al., 1995].

Western-blot analysis showed that the level of SERCA2a protein during hibernation increases by 3 times [Yatani et al., 2004]. Thus, at lower levels of SERCA2a mRNA the number of SR Ca^{2+}-ATPase molecules is increasing. The difference between mRNA and protein levels could be due to translation regulation and/or posttranslational modification. A similar case has been already described by us on the example of one of titin isoforms in myocardium of hibernating ground squirrels [Karaduleva E.V. et al., 2010]. Accumulation of Ca^{2+}-ATPase can occur during pre-hibernation period, particularly during entering hibernation. The results of our work, showing increase of sarcoplasmic reticulum area, are also giving evidence on the increase of SR capacity, approving the earlier results of electrophysiological tests on papillary muscles [Nakipova et al., 2007; Zakharova et al., 2009].

Our data on ATP2A2 gene expression during torpor and arousal do not accord to data obtained by other authors. In studies of SERCA2a gene expression, an increase of its mRNA amount in the heart of marmot during hibernation compared to active summer animals was observed [Yatani et al., 2004]. The increase of SERCA2a expression during hibernation was also detected in myocardium of thirteen-lined ground squirrel

[Brauch et al., 2005]. A study on arctic ground squirrel [Yan et al., 2008] showed significant decrease of ATP2A2 during arousal compared to torpor. Such contradictory data could be explained by use of non-equal physiological states of animal during hibernation cycle and/or non-identical methods of studying gene expression, and/or by choice of housekeeping genes for data normalization. The contradictions of data require adequate approaches for their solution and for the search of alternative ways to avoid technical errors.

References

1. Belke D.D., Milner R.E. and Wang L.C.H. Cryobiol. 1991. 28, 354 - 363.
2. Brauch K.M., Dhruv N.D., Hanse E.A., Andrews M.T. Physiol Genomics. 2005. 23, 227–234.
3. Epperson L.E., Martin S.L. Physiol. Genomics. 2002. V. 10(2), 93-102.
4. Giroud S., Frare C., Strijkstra A., Boerema A., Arnold W., Ruf T. 2013. PLoS ONE. 8, Issue 5, e63111. doi:10.1371/journal.pone.0063111.
5. Ignat'ev D.A., Sukhova G.S., Sukhov V.P. Zh Obshch Biol. 2001. 62(1):66-77.
6. Johansson B.W. Cardiovasc. Res. 1996. 31, 826 - 832.
7. Karaduleva E.V., Vikhlyantsev I.M., Tutukina M.N., Podlubnaya Z.A. 2010. 6, №4, 5−12.
8. Liu B., Belke D.D. and Wang L.C.H. Am. J. Physiol. 1997. 272, R1121 - R1127.
9. Nakipova O., Zakharova N., Andreeva L., Chumaeva N., Averin A., Kosarskii L., Anufriev A., Dirk von Lewinski, Jens K., Burkert P. Cryobiology. 2007. 55, 173–181.
10. Rubtsov A.M. Ross Fiziol Zh Im I M Sechenova. 2005. 91(2):141-51.
11. Santalova I.M., Zakharova N.M., Khramov R.N., Kraev I.V., Murashev A.N., Averin A.S., Fakhranurova L.I. Biofizika. 2008. 53(5):879-85.
12. Tang Y.J., Wang S.Q. and Zhou Z.Q. Acta Physiol. Sinica 1995. 547, 478 -483.
13. Wang S.Q., Lakatta E.G., Cheng H., Zhou Z.Q. J. Exp. Biol. 2002. 205, 2957–2962.
14. Yan Jun, Barnes Brian M., Kohl Franziska, and Marr Thomas G. Physiol Genomics. 2008. 32, 170–181.
15. Yatani A., Kim S.J., Kudej R.K., Wang Q., Depre C., Irie K., Kranias E.G., Vatner S.F., Vatner D.E. Am J Physiol Heart Circ Physiol 2004. 286: H2219–H2228.
16. Zakharova N.M., Nakipova O.V., Averin A.S., Tikhonov K.G., Solomonov N.G. Dokl Biol Sci. 2009. 424:21-4.

STOCHASTIC DYNAMICS OF INTRANEURONAL TRANSPORT

A.V. Kargovsky*, Y.M. Romanovsky*, V.P. Trifonenkov**,
A.V. Trifonenkov**

* Faculty of Physics, Moscow State University, Leninskiye Gory 1-2,
GSP-1, Moscow, 119991, Russia,
E-mail: yuromanovsky@yandex.ru;
** National Research Nuclear University MEPhI,
Kashirskoye shosse 31, Moscow, 115409, Russia

Coordinated functioning of neuronal networks depends on the uninterrupted reproduction and transport of neurotransmitters, various proteins, mitochondria, etc. within the neuron. In this paper we consider mathematical models of molecular motors (MM): kinesin and myosin V (MV) that play the leading role in the transport of these ingredients in vesicles in the direction from the nucleus of the neuron to synaptic endings and in the opposite direction with their disintegration products created during synaptic transmission of signals to the cell-targets [1]. The mathematical models take into account fluctuations of various kinds. Models of regular dynamics of kinesin and kindred MM - F1ATPase were presented in [2–4]. The result of this work was a system of equations (1) for kinesin walking along the tubulin microtubule (MT) and similar equations for MV walking along actin filament (AF).

The torques in the heads of kinesin (HK) and their elastic deformations are produced by sorption of ATP molecules in their active sites (AS) by turns. Force bond between HK is created by the "necks" connecting them and produce torque moving load along the MT. System (1) describes the step of kinesin:

$$\varsigma\dot{\beta}_1 = M(\beta_1) - \tau_1 + \varepsilon\dot{\beta}_2 \qquad \varsigma\dot{\beta}_2 = M(\beta_2) - \tau_2 - \varepsilon\dot{\beta}_1$$
$$\mu\dot{\tau}_1 = k\beta_1 - \tau_1 \qquad \mu\dot{\tau}_2 = k\beta_2 - \tau_2 \qquad (1)$$

Here: $\beta_1(t)$ and $\beta_2(t)$ - angles describing the closing "pockets" of AS during the sorption of ATP molecules in them, $\tau_1(t)$ and $\tau_2(t)$ - the elastic tensions produced by deformations of the HK. $\tau_1(t)$ and $\tau_2(t)$ are delayed relatively to the elastic forces $k\beta_1$ and $k\beta_2$ due to ATP hydrolysis (disintegration) processes in the AS. $M(\beta_1)$ and $M(\beta_2)$ - torques that are created in the AS "pockets" deformated . Note that variation $\Delta\beta \sim \pi/6$ corresponds to movement of kinesin per one step ~ 8 nm. The values of ς are determined by Stokes resistance to cargo transported, the value of μ is time of ATP hydrolysis, and k - elasticity of the HK. Torques produced by forces of ATP molecules sorption or hydrolysis products in the AS are defined by the expression:

$$M(\beta) = M_0(\beta - \beta^n / n) \qquad\qquad n = 3, 5, 7 \dots \qquad (2)$$

There are some examples of simulation results below.
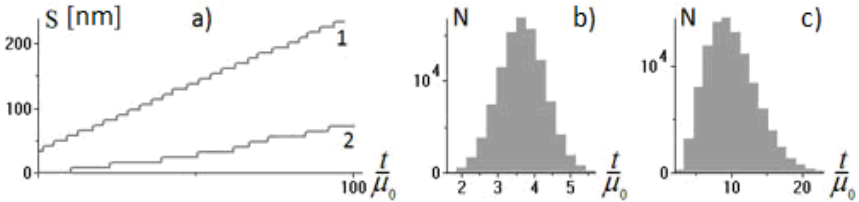
Fig. 1. a) "stairs" of kinesin steps depending on fluctuations of μ and ATP molecule waiting time (ATP concentration values: line 1 - 1 mMol / l, line 2 - 0.1 mMol / l); histogram of duration of time intervals between kinesin steps at ATP concentrations: b) 1 mMol / l, c) 0.1 mMol / l ($\mu_0 = 0.5$ ms).
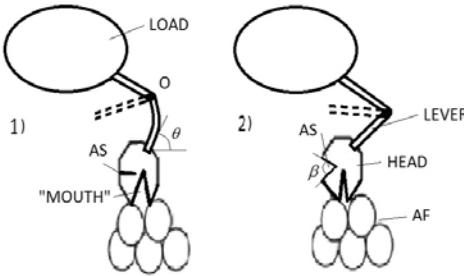
Fig. 2. Scheme of MV front head interaction with AF (by [7]). 1) head with an open "mouth" in contact with the AF, lever is elastically deformed. 2) there is no ATP and reaction products in the AS of the head, "mouth" is closing and stimulating the rotation of the lever and the movement of load.

Similar models are considered for myosin V (MV) walking along the actin filament (AF). However, there are significant differences. Fig. 2 shows the scheme of interaction MV and AF (by [7]).

Sorption of ATP in the AS "pocket" closes it (the angle β decreases), that causes opening of the "mouth" and disconnecting of the MV head from AF. In order to close the "mouth" again with turning the lever to its original position, ATP hydrolysis must occur in the AS and products of reaction must exit from AC. During ATP sorption into AS the energy of elastic deformation is stored. But the energy is not expended for moving of a cargo. Time interval required for these events is substantially greater than the time of pulling of the load that determined by the torque and Stokes resistance. Then cycle repeats in the case of a new contact of head with the AF. Solutions of system (1) for both kinesin and MV are represented in the phase planes (β, τ).

Other approaches to modelling of MM stochastic dynamics are considered in [5, 6]. We would like conclude theses by the following statement. MM mathematical models considered as well as FitzHugh - Nagumo equations, and many other models of active systems in biophysics can be reduced to systems of two or three generalized Rayleigh equations. Of course, their parameters are identified from the experimental data [4, 8].

References

1. Biofile. Scientific Inform. Magazine // http://biofile.ru/bio/9918.html
2. Romanovsky Yu. M., Tikhonov A.N. Molecular energy transducers of the living cell. Proton ATP synthase: a rotating molecular motor // Physics Uspekhi, 180, 931-956, 2010.
3. Yu.M.Romanovsky , A.V.Kargovsky , A.V. Priezzhev , V.P.Trifonenkov . Intracellular autowawe hidrodynamics and molecular motors// in "Optical methods of streams investigation" : Proceedings of the XII International Scientific and Technical Conference June 25-28, 2013, NIU "ME". - M. PERO, 2013.
4. Yu.M. Romanovsky, A.V. Kargovsky and W. Ebeling. Models of active Brownian motors based on internal oscillations // Eur. Phys. J. Special Topic 2013 , 222, 1-15.
5. A. Pogrebnaya, Yu. Romanovsky and F. Tikhonov. Rotation of ATPase: The stochastic model. // Fluctuation and noise Letters, 2005 , 5 , N 2 , L217-L224.
6. Jianhua Xing, Jung-Chi Liao and George Oster. Making ATP // PNAS 2005 , 102, P. 16539-16546.
7. Kubasova N.A., Tsaturian A.K. Molecular mechanism of actin-myosin motor in muscle // Biological Chemistry Uspekhi , 2011, 51, C. 233-282.
8. Lavrova A.I., Postnikov E.B., Romanovsky Yu.M. Brusselator: an abstract chemical reaction? // Physics Uspekhi, 179, 1327-1332 , (2009).

THE ROLE OF TROPOMYOSIN POSITION IN THE MOLECULAR MECHANISM OF THE REGULATION OF ACTIN-MYOSIN INTERACTION DURING THE ATPase CYCLE

O.E. Karpicheva[1], N.A. Rysev[1], S.V. Avrova[1], A.O. Simonyan[2], C.S. Redwood[3], Y.S. Borovikov[1]

[1]Institute of Cytology, Tikhoretsky Pr., 4, Saint Petersburg, 194064, Russia;
[2]Saint Petersburg State University, Universitetskaya nab., 7-9, Saint Petersburg, 199034, Russia;
[3]University of Oxford, John Radcliffe Hospital, Oxford OX3 9DU, United Kingdom

The regulation of striated muscle contraction involves cooperative interactions between actin filaments, myosin heads, tropomyosin, troponin,

and calcium. The critically important factor of this regulation is calcium-dependent azimuthal movements of tropomyosin strands over the surface of the actin filament induced by the binding of either S1 or troponin I to actin. The polarized fluorescence technique allows us to characterize concordant conformational changes of actin, myosin head and tropomyosin occurring in a reconstituted ghost fiber at several simulated stages of the ATPase cycle. Each transition between the intermediate stages of the cycle is characterized by definite interdependent conformational changes of F-actin and myosin heads. The overall change is interpreted as a right-hand rotation of actin subdomain-1 relative to the thin filament axis and an oppositely directed azimuthal movement of myosin SH1 helix (or myosin head) at transition from the weak- to strong-binding states. The actomyosin conformational state at each step of the ATPase cycle is shown to be strictly correlated to a definite conformation and specific position of tropomyosin strands on the surface of the thin filament. Tropomyosin shifts towards the center of the thin filament (to the "open" position) at strong-binding and towards the periphery of the thin filament (to the "blocked" position) at weak-binding states thereby increasing the amplitude of myosin SH1 helix movement and actin subdomain-1 rotation. Troponin modulates those movements in a Ca^{2+}-dependent manner.

Mutations in tropomyosin are able to stabilize its strands in the "open" position and to increase the proportion of the strong-binding actomyosin states, as was shown for the Glu180Gly and Asp175Asn α-tropomyosin mutations, associated with hypertrophic cardiomyopathy. On the other hand, these mutations prevent the formation of the weak-binding state of the myosin head thus causing the incomplete relaxation of the actomyosin system and leading to the enhanced contractility. The mutations Glu40Lys in α-tropomyosin and Glu117Lys in β-tropomyosin, on the contrary, prevent the shifting of tropomyosin strands to the "open" position stabilizing them at the periphery of the thin filament (closer to the "blocked" position) and inhibiting tropomyosin ability to move relative to actin. This behavior of the mutant tropomyosin causes a significant inhibition of the strong-binding actomyosin states formation and of the conformational changes of actin monomers and the myosin heads. The effect of the Glu40Lys and Glu117Lys mutations may explain the muscle weakness observed in dilated cardiomyopathy (DCM) and congenital fiber type disproportion, respectively.

Anomalous positioning of mutant tropomyosin close to the periphery of actin filaments may also disturb the coordination of the conforma-

tional changes of actin and the myosin head during the ATPase cycle, as was observed with DCM-causing Glu54Lys mutation in α-tropomyosin, that prevents the transition of actin to the weak-binding structural state inhibiting the conformational changes of actin, but has a little impact on the work of the myosin head. The aberrant position of the mutant tropomyosin close to the center of actin filament in the case of Gln147Pro mutation in β-tropomyosin affects the weak-binding state of actomyosin increasing the proportion of strong-binding actomyosin states in the presence of ATP. This mutation associates with cap-myopathy and probably causes enhanced contractility. Defined alterations of tropomyosin position are likely to underlie the contractile deficit or vice versa gain of muscle function, which initiates the disease remodeling.

NEW ASPECTS OF ACTIN-TROPOMYOSIN INTERACTION
S.Yu. Khaitlina

Institute of Cytology RAS, Tyhoretsky prosp. 4,
St.Petersburg, 194064, Russia

Tropomyosin is a major regulatory protein of contractile systems and cytoskeleton, which lateral position along actin filaments modulates actin-myosin interaction (Perry, 2001). Tropomyosin isoforms have been also revealed in a variety of cytoskeleton systems, not necessarily connected with actin-myosin interaction and contraction. Thereby, in many cases the diversity of tropomyosin isoforms is paralleled by a diversity of cytoskeleton functions, i.e. many functions of the actin cytoskeleton are related to spatial segregation and non-redundant functional diversity of tropomyosin isoforms (Gunning et al. 2008; 2013). These aspects of tropomyosin biology have been extensively studied using cell biology and molecular genetics approached (reviewed in: Gunning et al. 2008; 2013; Wang, Coluccio, 2010; Lees et al., 2011). However, at the molecular level, the mechanisms underlying the tropomyosin functions are still unclear. To reveal these mechanisms it is important to understand how tropomyosin interacts both with actin and actin-binding proteins that are involved in the regulation of actin dynamics. Here we present biochemical data on the effects of tropomyosin on actin assembly and dynamics, as well as on the modulation of these effects by actin-binding proteins.

We show that in proteolytically modified F-actin where the turnover of subunits is strongly enhanced, tropomyosin slows down polymerization of

this actin but did not stabilize it against the disruptive effects of centrifugal forces and shear stress. Instead of this, tropomyosin inhibited the steady-state ATP hydrolysis of proteolytically modified actin in a cooperative manner, with half-maximal and maximal effects observed at TM:actin molar ratios of about 1:50 and 1:8, respectively. Since the sites of F-actin-tropomyosin interaction do not interfere with the actin-actin contact sites, our data suggest that tropomyosin regulates dynamics of actin filaments by allosterically modifying the subunit conformation and thereby strengthening intermonomer contacts both along and across the filament strands.

Tropomyosin can also be involved in the regulation of actin dynamics by modulating activity of other actin-binding proteins. Previously tropomyosin has been shown to slow down depolymerization of actin with DNase I (Hitchcock et al., 1976), protect actin filaments from disassembly by ADF/cofilin (Ono, Ono, 2002; Mazur et al., 2010) and from branching by Arp2/3 (Blanchoin et al., 2001). Tropomyosin can also function as an activator of formin as a processive capper of the fast-growing actin filament end: binding of tropomyosin to formin enhances actin filament elongation and prevents association of formin with the filament sides. These reactions may also be associated with tropomyosin-induced conformational changes within actin filaments.

Earlier works showed also that both skeletal tropomyosin partially protected F-actin from gelsolin-induced fragmentation (Ishikawa et al., 1989; Nyakern-Meazza et al., 2002). On the other hand, the presence of tropomyosin either along actin filaments or at their barbed ends did not prevent binding of gelsolin to actin (Gonsior, Hinssen, 1995; Michels et al., 1998; Nyakern-Meazza et al., 2002). To re-investigate the influence of tropomyosin on the actin filament severing activity of gelsolin we measured both the F-actin viscosity and the relative number concentrations of filaments after fragmentation by either gelsolin alone or by gelsolin/tropomyosin complexes. Our results show that the association of muscle tropomyosin with F-actin did not significantly protect the filaments from being severed by gelsolin. On the other hand, preceding interaction of gelsolin with tropomyosin reduced the severing activity of gelsolin by up to 80%. These results suggest that tropomyosin is involved in the modulation of actin dynamics not via the protection of the filaments against severing, but rather by binding gelsolin in solution to prevent it from severing.

Cellular actin isoforms differ from each other in polymerization kinetics, filament dynamics and in their affinity for tropomyosin. Combination of these properties with the modulating activity of tropomyosin

may provide at least some mechanisms underlying the regulatory role of tropomyosin in cytoskeleton dynamics. Thereby the experimental approaches used here may be useful to distinguish the effects of different tropomyosin isoforms on actin dynamics.

STUDY OF THE RESPONSE OF CONTRACTING MUSCLE FIBRE TO THE RAMP STRETCH

P.V. Kochubey and S.Y.Bershitsky

*Institute of Immunlogy and Physiology, Ural Branch of RAS,
Yekaterinburg, 620049, Russia*

When isometrically contracting muscle fibre is subjected to a ramp stretch, its tension increases in two phases. At first it rises linearly and rather quickly, than velocity of the rise decreases either smoothly or with an overshoot. Intersection of linear regressions of these two slopes gives a point called critical tension, or P_c. This type of tension transient in muscle is known for a long time however underlying mechanism(s) is still unclear. There are different views on the nature of this phenomenon: some authors suppose the change in the tension rise velocity is due to a re-attachment of myosin heads to actin filaments (1) while others attribute it to a transition the heads from powerstroke to pre-powerstroke state (2,3), the third view is a combination of these two (4).

We studied this phenomenon in single fully activated permeabilized fibre from rabbit *psoas* muscle. Ramp stretches of 5% muscle length at 1.7 muscle length per second (L/s) and 5 L/s were applied to the fibre contracting at ~3ºC and ~28ºC. High temperature was achieved with temperature jump (5). Changes in tension and stiffness were monitored as well as sarcomere length with the use of a laser diffractometer. Fibre stiffness was measured with small-amplitude sinusoidal oscillation of changes its length and subsequent detection of changes in tension (*ibid*). The ratio of myosin heads in powerstroke and pre-powerstroke states was disturbed by temperature and adding blebbistatin (6).

Results

Fig. 1 shows a typical run of experimental protocol and traces of changes in tension, sarcomere length and stiffness. It is seen that during ramp stretch fibre tension rises in two phases with clearly distinct slopes while stiffness increases in one phase (occasionally with a modest overshoot) and sets at new level several milliseconds before tension achieves P_c.

Effects of temperature, velocity of stretch and blebbistatin on tension and stiffness collected from three muscle fibres are shown in table.
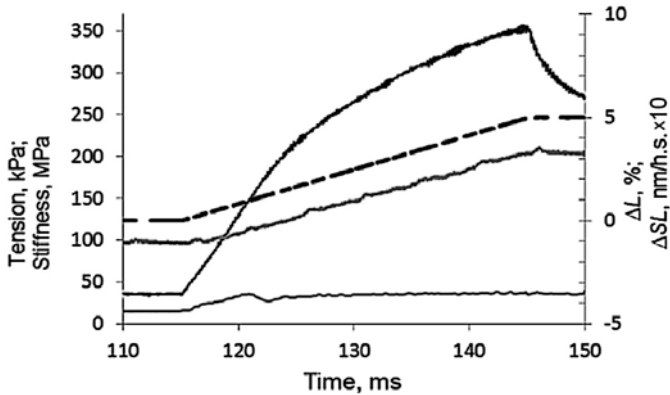
Fig.1. Example of experimental record. Isometrically contracting muscle fibre was stretched with linear motor (5) by 5% for 30 ms. Dashed black trace shows change in fibre length, ΔL (right scale). Solid black trace is fibre tension (left scale), bold grey trace is change sarcomere length, ΔSL (in nanometers per half sarcomere; right scale) and thin grey is fibre stiffness (left scale). Fibre dimentions: length 3.12 mm, cross-section area 5,284 μm^2, sarcomere length 2.5 µm, temperature 3°C.

In the absence of blebbistatin increase of temperature from 3ºC to 28ºC led to a six-fold rise in isometric tension and ~30% increase in stiffness similar to that described earlier (5). It also increased P_c by 35-45% but had little or no effect on the velocity of tension rise in both phases as well as on stiffness rise during the ramp stretch. Increase in the velocity of stretching from 1.7 L/s to 5 L/s mostly affected the velocity of tension rise during the first phase (3.3- 5-fold) and in less extend during the second phase (1.5- 2.5-fold). At this P_c rose by 15-25% and increase in stiffness did not depend on the velocity of the ramp stretch.

With 5 µM blebbisratin added both isometric tension and stiffness were suppressed. Isometric tension decreased ~1.5-fold at low temperature and ~3.5-fold at higher temperature, stiffness dropped to a steady level and became completely temperature insensitive. Change in temperature virtually did not affect the velocities of tension rise in both phases and stiffness during the ramp stretch. Temperature dependence of P_c virtually disappeared. Velocities of the first and second phases of tension rise followed changes in the velocity of the ramp stretch. Note that adding of blebbistatin suppressed the velocity of the first phase of tension rise but accelerated the velocity of the second phase at high temperature. Change in P_c at three-fold change of the ramp velocity was less than 20%.

113

Dependence of tension, stiffness and critical tension on temperature, velocity of fibre stretch and blebbistatin

Temperature; stretch velocity, %/ms	Isometric tension, kPa	Isometric stiffness, MPa	Stiffness during stretch, MPa	Velocity of tension rise in phase 1, kPa/ms	Velocity of tension rise in phase 2, kPa/ms	Pc, kPa
No blebbistatin						
3°C; 0.17	42.3± 9.3	16.6± 1.1	32.7± 3.6	20.8± 3.8	5.8± 1.7	262± 34
3°C; 0.50			30.2± 2.4	68.8± 13.3	8.7± 2,1	328± 25
28°C; 0.17	255± 65	21.8± 3.0	30.0± 4,1	14.2± 4.2	4.3± 0.6	383± 21
28°C; 0.50			35.8± 7.3	72.2± 16.18	10.5± 2.7	435± 93
5 µM blebbistatin						
3°C; 0.17	28.9± 12.8	9.9± 3.2	26.2± 5.5	13.7± 3.2	5.2± 1.8	209± 68
3°C; 0.50			24.5± 5,0	45.3± 8,6	15.4± 4.2	240± 65
28°C; 0.17	74.8± 25.5	10.1± 4.6	22.5± 6.9	10.9± 3.1	6.0± 1.7	181± 55
28°C; 0.50			30.8± 8.9	37.5± 7.7	16.3± 4.6	216± 68

Significant suppression of fibre tension and rather moderate decrease in stiffness at high temperature in the presence of blebbistatin indicates a reduction in force generating ability of myosin heads. This observation is in a good agreement with the explanation by Allingham *et al.* (6) that blebbistatin biases myosin heads into myosin-actin-ADP state(s) thus preventing their transition to power stroke state. The decrease of tension rise velocity in the first phase and the acceleration of the second phase also indicate a re-distribution of cross-bridges in favour of non-stereo-specifically attached states including pre-force generating state.

Taken together, our results can explain the mechanism of change in the velocity of tension rise during ramp stretch on the base of recently suggested model (7) with two assumptions. Fig. 2 illustrates this explanation. Assumption **1** is that strength of binding of stereo-specifically attached myosin head is such high that the ramp stretch first bends its lever arm domain and only after that pulls out the head from stereo-specific bin-
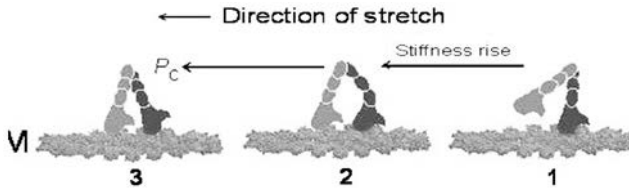
Fig. 2. Schematic model of the behavior of myosin heads upon ramp stretch of muscle that explains our data. During isometric contraction (state 1) only one (black) of two heads of myosin molecule is stereo-specifically bound to actin. Stretch first bends its lever arm domain thus promoting non-stereo-specific attachment of the second (gray) head (state 2) and then unlocks the bound head to a non-stereo-specifically attached state 3. As both heads are bound non-stereo-specifically, their resistance to the stretch becomes weaker and velocity of tension rise decreases.

ding. In this case bending of the lever arm may allow non-stereo-specific attachment of the second head that would increase both stiffness and tension (transition 1→2 in fig. 2). Further stretching leads to the break of stereo-specific bond (2→3) and both heads become non-stereo-specifically attached. Assumption **2** is that the non-stereo-specific bond is mechanically weaker than the stereo-specific bond. This means that during stretching they will show lower force when both heads are non-stereo-specific than when one of them is stereo-specific.

This explanation does not contradict to the X-ray data obtained during ramp stretching of contracting muscle fibre (7) which showed a decrease in the intensity of the first actin layer line, A1, in the diffraction pattern at high stiffness of the fibre. Interpretation of the results was that the stiffness during the stretch provided largely by non-stereo-specifically attached heads, which contribute to A1 intensity significantly less than stereo-specifically bound heads.

References

1. Bagni MA, Cecchi G, Colombini B. 2005. Crossbridge properties investigated by fast ramp stretching of activated frog muscle fibres. J Physiol 565: 261-268.
2. Nocella M, Bagni MA, Cecchi G, Colombini B. 2013. Mechanism of force enhancement during stretching of skeletal muscle fibres investigated by high time-resolved stiffness measurements. J Muscle Res Cell Motil 34: 71-81.
3. Roots H, Offer GW, Ranatunga KW. 2007. Comparison of the tension responses to ramp shortening and lengthening in intact mammalian muscle fibres: crossbridge and non-crossbridge contributions. J Muscle Res Cell Motil 28: 123-139.

4. Minozzo FC, Rassier DE. 2010. Effects of blebbistatin and Ca2+ concentration on force produced during stretch of skeletal muscle fibers. Am J Physiol Cell Physiol 299: C1127-1135.
5. Bershitsky SY, Tsaturyan AK. 2002. The elementary force generation process probed by temperature and length perturbations in muscle fibres from the rabbit. J Physiol 540: 971-988.
6. Allingham JS, Smith R, Rayment I. 2005. The structural basis of blebbistatin inhibition and specificity for myosin II. Nat Struct Mol Biol 12: 378-379.
7. Ferenczi MA, Bershitsky SY, Koubassova NA, Kopylova GV, Fernandez M, Narayanan T, Tsaturyan AK. 2014. Why Muscle is an Efficient Shock Absorber. PLoS One 9: e85739.

VALIDATION OF BETA-ACTIN AS A REFERENCE GENE IN SINGLE-CELL GENE EXPRESSION ANALYSIS

A. Kolesnikova, A. Cherkashin, A. Khokhlov, M. Bystrova

Institute of Cell Biophysics RAS, Institutskaya ulitsa 3, Pushchino, 142290, Russia

Beta-actin is one of the six different but highly conserved actin isoforms in vertebrates, which are involved in cell structure, motility, integrity, and cohesion. Beta-actin protein is present at a constant level in different types of normal and pathological tissues and under different treatment conditions, thus representing a useful loading control in Western blot analysis to verify that the gel lanes have been evenly loaded. Beta-actin is also commonly used to normalize molecular expression studies due to its high conservation as an internal reference marker. It is known as an endogenous housekeeping gene, which shows stable, unregulated, high-level expression in all cell types. Housekeeping genes are used to normalize mRNA levels between different samples in quantitative RT-PCR analysis to account for sample handling, loading and experimental variation. Quantification of the mRNA of the target and the housekeeping gene in the sample ensures that the changes in transcript levels will influence both genes equally. However, the important question remains whether beta-actin can be used as a reference gene for normalization purposes in single-cell gene expression studies. Therefore, the aim of this study was to evaluate the invariance in the expression level of beta-actin gene among individual cells of the same type. We performed single-cell RT-PCR analysis of beta-actin in individual olfactory neurons isolated from olfactory epithelium of transgenic OMP-GFP mice.

Materials and methods

Isolation of single cells. Olfactory epithelium was dissected from adult OMP-GFP mice (a kind gift from Prof. H. Breer (Germany)). Olfactory epithelial turbinates were soaked in an extracellular solution (in mM: 135 NaCl, 5 KCl, 1 MgCl$_2$, 1 CaCl$_2$, 10 glucose, and 10 HEPES, pH 7.4 with NaOH) to remove superficial blood and debris. The turbinates were rinsed 3 times at 3 min intervals. Olfactory epithelium was dissociated for 15 min in a solution containing 0.05% tripsin, 140 mM NaCl, 5 mM KCl, 1 mM EGTA, 1 mM EDTA, 10 mM Hepes (pH 7.0) at room temperature. The tissue was then removed and rinsed 3 times with the extracellular solution. To isolate individual cells, a piece of the olfactory epithelium was first shredded by a steel needle and then gently triturated by a fire-polished glass pipette. Dispersed cells were then plated on dishes. Cells that were adhered to the dish were carefully rinsed with the bath solution containing 140 mM NaCl, 2.5 mM KCl, 1mM MgCl$_2$, 1 mM CaCl$_2$, and 10 mM HEPES (pH 7.4 with NaOH) to minimize possible contaminations with RNA from lysed cells. Dissociated cells were visualized under a Ziess Axioscope-2 microscope and identified by their characteristic morphology. A single olfactory neuron was sucked into a firepolished glass micropipette with an opening of 4-10 μm, expelled into a PCR tube filled with a solution for first-strand cDNA synthesis, snap-frozen, and stored at -70°C. Cell lysis was subsequently performed at 70°C.

Single-cell RT-PCR analysis. The cellular material was utilized for the SMART (switching mechanism at the 5' end of RNA templates) cDNA synthesis using Mint cDNA synthesis kit (Evrogen) based on slightly modified protocols described in the user manual. Specifically, a modified oligo-dT primer containing a T7 promoter sequence was used in reverse transcription reaction. First-strand cDNA was synthesized directly from cell lysate harvested via glass micropipette and expelled into a PCR tube containing 3.3 pmol T7- oligo(dT)$_{15}$ oligonucleotide and 5 pmol template-switching primer in water. As negative control, the bath solution with no cell was sucked into a pipette and expelled into a PCR tube. The sample (2.3 μl) was incubated at 70°C for 2 min, cooled to 42°C, and then a 2,7 μl RT mixture was added (1 μl 5X RT buffer; 0.5 μl 0.1 mM DTT; 0.5 μl 10 mM dNTPs; 8 U RNaseOUT Inhibitor (Invitrogen); 0.5 μl Mint Reverse Transcriptase). The reaction mixture was incubated at 42°C for 30 min, and after the addition of the 2.5 μl IP solution for incorporation of template-switching primer (Evrogen), it was additionally incubated at 42°C for 1 h 30 min. For global cDNA amplification, 67.5 μl PCR mixture (7.5 μl 10X buffer; 1.5 μl 10 mM dNTP mix; 1.5 μl 10 μM (each) oligonucleotides (5'-

AAGCAGTGGTATCAACGCAGAGT-3' and 5'-AAACGACGGCCAGTGAATTGTAATACGACTCAC-3'), 1.5 µl Encyclo Polymerase Mix; 54 µl water) was added to the tube, and a 20-cycle PCR amplification was performed according to the schedule from the kit user manual. After completion, the sample was purified using a High Pure PCR Cleanup Micro Kit (Roche). The subsequent antisense RNA (aRNA) amplification of the sample by *in vitro* transcription from the T7 promoter sequence was carried out in 100 µl reaction mixture for 4 h with the use of T7 RNA polymerase (Promega) following the manufacturer's instructions. After aRNA amplification, DNA template was removed by incubation of the reaction with 4 U DNase I (Sigma) for 15 min. Amplified aRNA was purified using RNeasy MinElute Kit (Qiagen) and reverse-transcribed with SuperScript III (Invitrogen) and random hexanucleotides in a 20 µl reaction at 50°C for 1h. The globally amplified cDNAs of an individual cell was used as templates in sequence-specific PCR. Intron-spanning primers for beta-actin were designed to amplify cDNA but not genomic DNA. PCR products were analyzed on a 1.4% agarose gel electrophoresis using GeneRuler 1 kb DNA ladder (Fermentas) to assess amplicon sizes.

Results

Single cells present specific challenges for gene expression profiling because their mRNA is not readily accessible by conventional methods of isolation. Another problem is minute amount of mRNA present in individual cells. It is generally assumed that a single cell contains approximately 10-20 pg of total RNA, 1-3% of which represent mRNA. The problem of limiting RNA can be resolved with the use of RNA amplification techniques that enable generating sufficient targets from sub-picogram quantities of starting sample (Eberwine et al. 1992). Another challenge for single-cell analysis is the procedure of cell isolation from a tissue and correct identification of the type of an isolated cell. The procedure of mechanical and enzymatic dissociation of the tissue enables liberation of individual cells of various types, however dissociated cells lose their native shape and distinct morphology and their cellular identity cannot be established visually with certainty based on generally accepted criteria. To obtain the homogeneous cell population from the tissue containing diverse cell types we used here a transgenic reporter mouse whose olfactory sensory neurons express green fluorescent protein (GFP) driven by the olfactory marker protein (OMP) promoter.

In OMP-GFP mouse, GFP is strongly expressed throughout the cytoplasm of the mature olfactory sensory neurons labeling them in living cells (Steve M. Potter et al, 2001). The olfactory sensory neurons reside
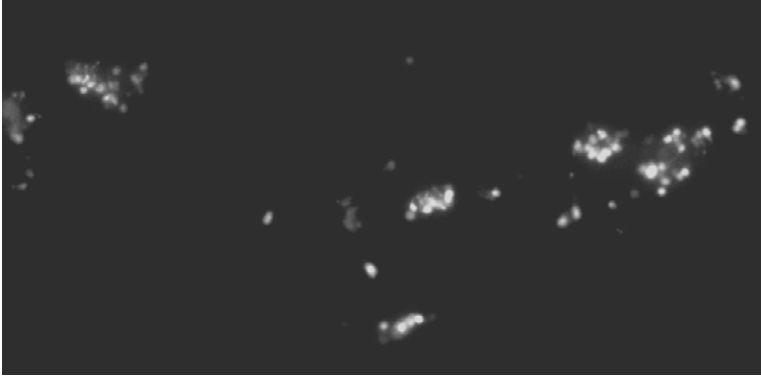
Fig. 1. Fluorescent image of dissociated olfactory neurons isolated from OMP-GFP mice.
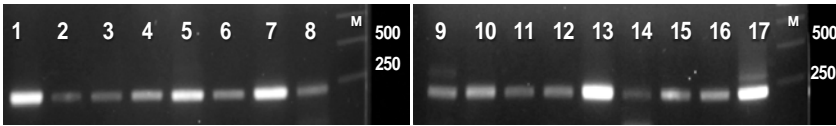
Fig. 2. RT-PCR analysis of the beta-actin gene expression in individual olfactory neurons isolated from OMP-GFP mice.

in the olfactory epithelium tissue. The olfactory epithelium contains three major cell types: olfactory neurons, sustentacular cells, and basal cells. The mature olfactory neurons from OMP-GFP mice are easily identified among other cell types following the procedure of mechanical and enzymatic dissociation by green fluorescence (fig. 1).

The approach we used here for single-cell gene expression analysis relied on a combination of SMART PCR and T7 polymerase-based amplification techniques. It involved: (1) first-strand cDNA synthesis using T7-oligo-dT primer and 3'- tailing of the single-stranded cDNA by template switching mechanism; (2) first-round amplification of single-cell cDNA by a sequence non-specific SMART-PCR protocol; 3) second-round amplification with T7 RNA polymerase leading to conversion of cDNA to aRNA; (4) removal of DNA template by digestion with DNase I; (5) reverse transcription of the total aRNA pool of a single cell followed by sequence-specific PCR. With this approach, we analyzed 17 individual neurons and succeeded in the amplification of beta-actin PCR products from each of them (fig. 2).

The results of single-cell RT-PCR analysis presented here demonstrate cell-to cell variation in the beta-actin expression level. The intensities of the RT-PCR bands are different in samples processed from individual cells (Fig.2). Note that all cells with green fluorescence express olfactory marker protein. Therefore, they represent the subpopulation of mature functionally active olfactory neurons with the established synaptic contacts in the olfactory bulb. The molecular analysis of individual olfactory neurons demonstrated clear heterogeneity in the expression level of beta-actin within homogeneous cell population.

Conclusion

To be used as a reference, a gene should show invariable expression level in the analyzed samples. Our work provides evidence that beta-actin is not a reliable marker for internal control in single-cell gene expression analysis.

ROLE OF ISOFORMS OF CARDIAC CONTRACTILE AND REGULATORY PROTEINS IN CALCIUM REGULATION OF ACTIN-MYOSIN INTERACTION

G.V. Kopylova, D.V. Shchepkin, L.V. Nikitina

Institute of Immunology and Physiology of the RAS, Laboratory of Biological Motility, Pervomayskaya ul., 91, Yekaterinburg , 62004, Russia

Contractile function of heart depends on pattern of contractile and regulatory proteins of cardiomyocytes. Changing conditions of the working heart leads to change of sarcomere proteins of cardiomyocyte. Thus Izumo et al. [1] shown that at pressure overload of the heart an expression of certain proteins (β-chain of tropomyosin, skeletal actin, β- myosin heavy chain) is increased. Research with dilated cardiomyopathy mutant tropomyosin mice demonstrated an increased expression of both β-myosin heavy chain and skeletal α-actin [2]. Previously we shown that α-actin isoforms affect calcium regulation of actin-myosin interaction in myocardium and this is specific for the isoforms of cardiac myosin [3].

The experiments with overexpression of β-tropomyosin in the adult murine hearts showed that the increase of β-chain up to 50-60% increased calcium sensitivity of "pCa-force" relationship, decreased the maximum rate of relaxation and resulted in diastolic dysfunction [4]. Further increase of β-tropomyosin expression up to 75-80% led to animal death shortly after birth [5].

The aim of this work was to study the role of β-tropomyosin for functioning of myocardium. For this Ca^{2+}-regulatory effect of tropomyosin isoforms (with different content of α- and β-chains) on actin-myosin interaction was studied in the *in vitro* motility assay with cardiac myosin and α-actin isoforms.

Homodimer of α-chains of tropomyosin (αα-TM), cardiac actin and troponin were obtained from left ventricles of euthyroid rabbit. Heterodimer of α- and β-chains of tropomyosin (αβ-TM) was isolated from left ventricles of bovine heart and contained 10% β-chain. Skeletal actin was prepared from *m. psoas* of rabbit. V1 and V3 cardiac myosin isoforms were obtained from left ventricles of hyper- and hypothyroid rabbit, respectively. Myosin from the left ventricles of hyperthyroid rabbits contained 90% α- and 10% β- heavy chain, myosin from hypothyroid rabbits contained 10% and 90% α- and β-heavy chain, respectively. The *in vitro* motility assay was performed as described previously [6]. We obtained the dependence of sliding velocity of the regulated thin filaments on calcium concentration in
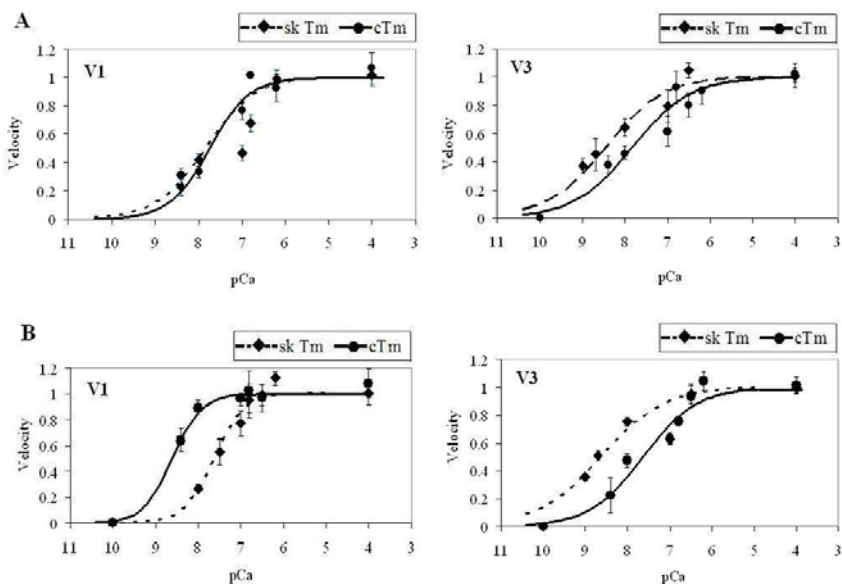
Fig. 1. The "pCa–velocity" relationships for regulated thin filaments consisting of skeletal (A) and cardiac (B) α-actin with αα-TM (circles, solid line) or αβ-TM (diamond, dashed line) tropomyosin over V1 and V3 isomyosins. The data were fitted with the Hill equation. Each data point represents mean ± SD of three experiments.

the flow cell (fig. 1). The data obtained were fitted to the Hill equation: $V = V_{max}(1+10^{h(pCa-pCa50)})^{-1}$, where V and V_{max} are velocity and maximal velocity obtained at saturating calcium concentration, respectively, pCa_{50} (i.e. calcium sensitivity) is pCa at which half maximal velocity was achieved, and h is the Hill coefficient.

The maximal sliding velocities of the regulated thin filaments containing both cardiac and skeletal actin for V1 but not for V3 isomyosin depends on ratio of α/β-chains of TM (table 1 and 2). The maximal sliding velocities over V1 isomyosin were higher for the regulated thin filaments with αα-TM. The Hill coefficient of "pCa-velocity" relationship did not depend on ratio of α/β-chains of TM for cardiac isomyosins withboth cardiac and skeletal actin (fig. 1; table 1 and 2). The Hill coefficient was higher for V1 as compare V3 isomyosin (table 1 and 2).

Calcium sensitivity of sliding velocities was markedly different for the regulated thin filaments with αα-TM and αβ-TM in the case of V3 myosin with both actin isoforms. Presence of β-chain of TM increased pCa_{50} of "pCa-velocity" relationships for V3 myosin (fig. 1; table 1 and 2).

Table 1. Data obtained in the *in vitro* motility assay with skeletal α-actin

isoforms		parameters of Hill equation		
myosin	TM	V_{max}, µm/s	pCa_{50}	h
V1	αα-TM	5.28 ± 0.25	7.75 ± 0.09	0.94 ± 0.22
V1	αβ-TM	4.24 ± 0.20*	7.63 ± 0.06	0.76 ± 0.30
V3	αα-TM	3.70 ± 0.13	7.80 ± 0.26	0.63 ± 0.11
V3	αβ-TM	3.90 ± 0.20	8.47 ± 0.10*	0.63 ± 0.12

The velocities and parameters of Hill equation are represented as mean ± S.D. * is denoted statistical significance of differences of Hill equation parameters with αβ-TM from αα-TM with appropriate isomyosin ($P<0.05$).

Table 2. Data obtained in the *in vitro* motility assay with cardiac α-actin

isoforms		parameters of Hill equation		
myosin	TM	V_{max}, µm/s	pCa_{50}	h
V1	αα-TM	4.81 ± 0.40	8.52 ± 0.33	1.29 ± 0.54
V1	αβ-TM	4.23 ± 0.07*	7.68 ± 0.13*	1.25 ± 0.29
V3	αα-TM	3.47 ± 0.07	7.69 ± 0.17	0.68 ± 0.02
V3	αβ-TM	3.40 ± 0.10	8.63 ± 0.02*	0.58 ± 0.10

The velocities and parameters of Hill equation are represented as mean ± S.D. * is denoted statistical significance of differences of Hill equation parameters with αβ-TM from αα-TM with appropriate isomyosin ($P<0.05$).

Noteworthy, presence of β-chain of TM had opposite effect on calcium sensitivity of "pCa-velocity" relationship for V1 and V3 isomyosins in case of cardiac actin (fig. 1B; table 2).

Thus, the ratio of α/β-chains of TM effect on maximal sliding velocities of the regulated thin filaments over V1 isomyosin, calcium sensitivity of "pCa-velocity" relationship for V3 isoform, and calcium sensitivity for V1 with cardiac F-actin. Switching of the expression of sarcomere proteins isoforms can be one of the mechanisms of adaptation of the working heart to changing conditions of functioning.

References

1. Izumo S, Nadal-Ginard B, Mahdavi V. Protooncogene induction and reprogramming of cardiac gene expression produced by pressure overload (1988) Proc Natl Acad Sci U S A. 85: 339-343.
2. Rajan et al. Dilated cardiomyopathy mutant tropomyosin mice develop cardiac dysfunction with significantly decreased fractional shortening and myofilament calcium sensitivity (2007) Circ Res. 101(2):205-14.
3. Shchepkin DV, Kopylova GV, Nikitina LV. Contrubtion of actin isoforms and cardiac myosin isoforms to calcium regulation (2012) International Symposium "Biological Motility: Fundamental and Applied Science", Pushchino, May 11-15: 183-6.
4. Muthuchamy M. et al. Molecular and physiological effects of overexpressing striated muscle beta-tropomyosin in the adult murine heart (1995) J Biol Chem. 270: 30593-603.
5. Muthuchamy et al. Beta-tropomyosin overexpression induces severe cardiac abnormalities (1998) J Mol Cell Cardiol. 30: 1545-57.
6. Kopylova et al. The *in vitro* motility assay to study the calcium-mechanical relationship in skeletal and cardiac muscles (2006) Biofizika. 51(5):781-5.

STUDY OF AGONISTS AND ANTAGONISTS OF CANNABINOID RECEPTORS ON SYNAPTIC TRANSMISSION IN THE MOUSE NEUROMUSCULAR JUNCTION

L.S. Korolyova, Y.A. Lebedeva, E.V. Gerasimova, G.F. Sitdikova

Institute of Fundamental Medicine and Biology, Kazan (Volga Region) Federal University, Kremlyovskaya st., 18, Kazan, 420008, Russia

Cannabinoids are a group of substances related to derivatives of the plant Cannabis sativa, which exert potent pharmacological effects on the

nervous system [1]. These effects are produced by the interaction of these compounds with the cannabinoid membrane receptors named CB_1 and CB_2 [2]. The actions of cannabinoids have been shown to be related to the inhibition of transmitter release in different synapses of the central nervous system and in smooth muscle [3,4]. The mechanism by which cannabinoids affect transmitter release is thought to work through the activation of potassium channels (Ia) or by blocking voltage-dependent Ca^{+2} channels or both [5]. The inhibition of N-type calcium channels decreases neurotransmitter release in several tissues [6,7].

CB$_1$ agonists are useful for the prevention of nausea, vomiting and for stimulate appetite. Also they display neuroprotective properties because of inhibition of mediator release in glutamatergic synapses. The effects of CB_1 receptors agonists have been shown in periphery nervous system. At the neuromuscular junction of cold-blooded animals the addition of the CB_1 receptor agonist decreased the frequency and amplitude of the miniature end-plate potentials (MEPPs) [2].

Both receptor subtypes are involved in many physiological functions, which are well studied in the central nervous system. However, their effects at the peripheral nervous system of warm-blooded animals still not researched. Therefore, the aim of this work was to determine the effects of agonists and antagonists of cannabinoid receptors on synaptis transmission in the mouse neuromuscular junction.

The experiments were performed on neuromuscular preparations of diaphragm of white mouse using extracellular microelectrode recording
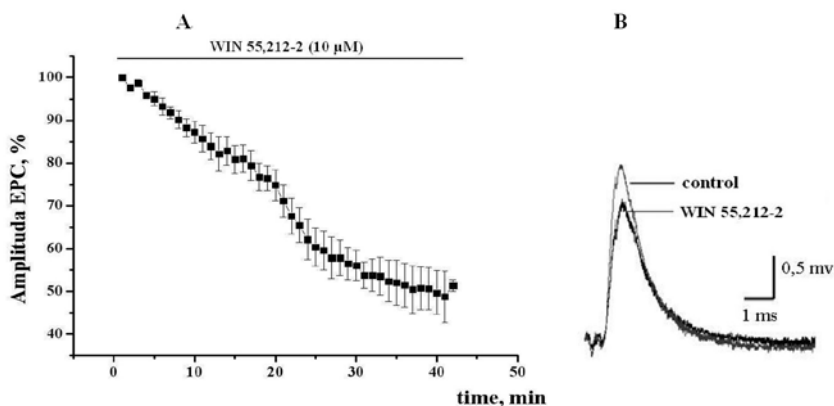
Fig. 1. A. Eeffect of 10 µM WIN on evoked transmitter release. B. Potentials of the end-plate currents (10 realizations) in the control and after adding WIN 55,212-2 in a separate experiment.

of end-plate currents (EPCs). All the experiments were performed under conditions of constant perfusion of the preparation by Kreps solution.The motor nerve was irritated by the electrical stimuli of the supramaximal amplitude at a frequency of 0.2 imp/s. To eliminate the muscular contraction the 1-2 µM d- tubocurarine was added into.

To examine whether cannabinoids modulate transmitter release in the neuromuscular junction of the mouse, we used the cannabinoid agonist WIN 55,212-2, which binds to both types of cannabinoid receptors. As antagonist we used AM 281 (1 µM), which binds with CB_1 of cannabinoid receptors. The results were processed by using standard methods.

The analysis of influence of WIN 55,212-2 (10 µM) of evoked transmitter release showed that the agonist of cannabinoid receptors reversibly reduces the amplitude of the EPCs. The average duration of the effect was 40 minutes (fig. 1). The mean value of EPCs amplitude was $49{,}7 \pm 5\%$ ($n = 4$; $p < 0.05$).

The addition of 1 µM of AM 281, the CB_1 receptor antagonist, into the external media resulted to increase of the end-plate currents. The amplitude of the EPCs for 40th minute of the experiment reached $127{,}1 \pm 9{,}1\%$ ($n = 6$; $p < 0.05$) (fig. 2).

The present results show that the cannabinoid agonist WIN 55,212-2, at micromolar concentrations, inhibits the evoked release of mediator exerting the presynaptic effects in the neuromuscular junction of the mouse diaphragmatic muscle. However, the presence of the CB_1-selective antagonist AM 281 at 1 µM has the opposite effect by facilitating the secretion
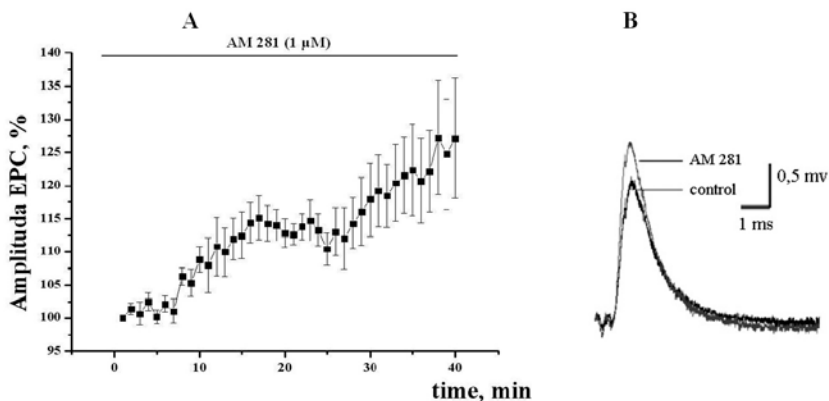
Fig. 2. A. Eeffect of 1 µM AM 281 on evoked transmitter release. B. Potentials of the end-plate currents (10 realizations) in the control and after adding AM 281 in a separate experiment.

of neurotransmitter in the mouse neuromuscular junction. The same results were obtained in the experiments in a cold-blooded animals. It was shown that in the neuromuscular junction of the frog cutaneous pectoris muscle the addition of WIN 55,212-2 reduced the quantal content, amplitude and frequency of the miniature end plate potentials, and the presence of the CB_1-selective antagonist AM 281 inhibited these effects [5,6].

Thus, we can suppose that the cannabinoid system is involved in endogenous modulating of the acetylcholine release at the motor nerve ending of the mouse.

References

1. Pertwee R.G. Ligands that target cannabinoid receptors in the brain: from THC to anandamide and beyond // Addict Biol. - 2008. - V. 13. - P. 147–159.

2. Howlett A.C. XXVII classification of cannabinoid receptors / Barth F, Bonner T.I, Cabral G, Casellas P, Devane W.A, Felder C.C, Herkenham M, Mackie K, Martin B.R, et al // International Union of Pharmacology, Pharmacol Rev. - 2002. - V. 54. - P. 161–202.

3. Ishac E.J. Inhibition of exocytotic noradrenaline release by presynaptic cannabinoid CB1 receptors on peripheral sympathetic nerves / Jiang L, Lake K.D, Varga K, Abood M.E, Kunos G // Br J. Pharmacol. - 1996. - V. 118. - P. 2023–2028.

4. Engler B. Effects of exogenous and endogenous cannabinoids on GABAergic neurotransmission between the caudate-putamen and the globus pallidus in the mouse / Freiman I, Urbanski M, Szabo B // J. Pharmacol Exp Ther. - 2006. - V. 316. - P. 608–617.

5. Elphick M.R, Egertovra M. The neurobiology and evolution of cannabinoid signalling // Philos Trans R Soc Lond B Biol Sci. - 2001. - V. 356. - P. 381–408.

6. Liang Y.C. Cannabinoid-induced presynaptic inhibition at the primary afferent trigeminal synapse of juvenile rat brainstem slices / Huang C.C, Hsu K.S, Takahashi T // J. Physiol (Lond). - 2004. - V. 555. - P. 85–96.

7. Szabo B. Analysis of the effects of cannabinoids on synaptic transmission between basket and Purkinje cells in the cerebellar cortex of the rat / Than M, Thorn D, Wallmichrath I // J. Pharmacol Exp Ther. - 2004. - V. 310. - P. 915–925.

8. Enrique S-P. Effects of Cannabinoids on Synaptic Transmission in the Frog Neuromuscular Junction / Xrochitl T, Miguel H, Felipa A // The journal of pharmacology and experimental therapeutics. - 2007. - V. 321. - N. 2. - P. 439–445.

9. Priscila E.S. Opposing effects of cannabinoids and vanilloids on evoked quantal release at the frog neuromuscular junction / Naiara A.S., Veronica de C. M, et al // Neuroscience Letters. - 2010. - V 473. - P. 97-101.

Tl^+ STIMULATES THE ION PENETRABILITY AND INDUCES THE MITOCHONDRIAL PERMEABILITY TRANSITION IN THE INNER MEMBRANE OF RAT HEART MITOCHONDRIA

S.M. Korotkov, V.P. Nesterov, I.V. Brailovskaya, V.V. Furaev

Sechenov Institute of Evolutionary Physiology and Biochemistry,
the Russian Academy of Sciences, Thorez pr. 44,
St. Petersburg, 194223, Russia

We showed earlier that Tl^+ did induce opening mitochondrial permeability pore (MPTP) in the inner membrane (IMM) of Ca^{2+}-loaded rat liver mitochondria (CaRLM) incubated in a medium containing $TlNO_3$ and nitrates (NH_4NO_3 or KNO_3) or $TlNO_3$ and sucrose (Korotkov, Saris, 2011). This MPTP was shown as the increase in both swelling and dissipation of mitochondrial membrane potential as well as in the decrease of state 4, state 3, or 2,4-dinitrophenol(DNP)-stimulated respiration. On the other hand, effects of Tl^+ on isolated rat heart mitochondria (RHM) are pure researched. Therefore we studied RHM in the use of 400 mOsm medium containing $TlNO_3$ and the nitrates or $TlNO_3$ and sucrose. Our experiments showed that permeability of the IMM of these mitochondria to K^+ and H^+ ions was visible increased by Tl^+ ions that manifested as an stimulation in swelling of nonenergized RHM in the lot of sucrose $< K^+ < NH_4^+$, accordingly. Following succinate administration did induce potent contraction of the RHM preswollen in the medium containing $TlNO_3$ and NH_4NO_3. Both the swelling stimulation and the decrease in basal and DNP-stimulated respiration after administration of Ca^{2+} into medium containing $TlNO_3$ and KNO_3 suggest about opening of the Tl^+-induced MPTP in the IMM of Ca^{2+}-loaded RHM as well. Activation of these Tl^+ effects was found in the presence of the MPTP inducer (carboxyatractyloside) or the mitochondrial K_{ATP} channel (mitoK_{ATP}) inhibitor, 5-hydroxydecanoate. Therewith, MPTP inhibitors (cyclosporine A, ADP, bongkrekic acid, and *n*-ethyl-maleimide) did suppress the MPTP. We propose that the greater sensitivity of heart muscles versus liver, to thallium salts *in vivo* can be resulted in more vigorous Tl^+ effects on muscle cell mitochondria.

COMPETITION BETWEEN TROPOMODULIN ISOFORMS IN MUSCLE AND NON-MUSCLE CELLS.

Alla S. Kostyukova

Voiland School of Chemical Engineering and Bioengineering,
Washington State University, Pullman, WA 99164, USA

Tropomodulin is an actin-capping protein that binds to two tropomyosin molecules at the pointed end of the actin filament in order to prevent further actin polymerization and depolymerization. Understanding the role of tropomodulin is very important when studying actin filament dependent processes such as muscle contraction or neuritogenesis. Tropomodulin /tropomyosin interactions are isoform-dependent. There are four Tmod isoforms (Tmod1-4). Tmod1, Tmod3, Tmod4 are expressed in skeletal muscles, and Tmod1, Tmod2 are expressed in neurons. We altered affinity of tropomodulin to tropomyosin by point mutations in the binding sites and tested the mutants *in vitro* and in cell-based experiments. Two types of cells were used, primary chicken skeletal myocytes and PC12 cells, a model system for neuronal differentiation.

Assembly of Tmod1 at the pointed ends of thin filaments in sarcomers was studied in myocytes. The mutations R11K, D12N and Q144K were chosen because they decreased the affinity of Tmod1 to striated muscle α-tropomyosin (stTM), making it similar to that of Tmod3 and Tmod4. Significant reduction of inhibition of actin pointed-end polymerization in the presence of stTM was shown for Tmod1 [R11K/D12N/Q144K] in pyrene-actin polymerization assays as compared with wild-typeTmod1. When GFP-Tmod1 and mutants were expressed in myocytes, decreased assembly of Tmod1 mutants was revealed. This indicated a direct correlation between tropomyosin-binding and actin-capping abilities of Tmod.

Assembly of the actin cytoskeleton is an important part of neuritogenesis, or formation of neurites (future dendrites and axons), in developing neurons. Tropomodulin is one of the key players in this process. GFP-Tmod1 overexpressed in PC12 cells did not affect formation of neurites; while cells expressing ChFP-Tmod2 showed a significant reduction in the number and the length of neurites. Both tropomodulins bind short α-, γ- and δ-tropomyosin isoforms but with different affinity. We introduced two mutations, A21K and E33V, in one of the tropomyosin-binding sites of Tmod1 to increase its affinity to short γ- and δ-tropomyosin isoforms and make it similar to that of Tmod2. The mutations caused a 2-fold decrease in the length of

neurites. Our data confirmed the hypothesis that competition between tropomodulin isoforms for assembly at the pointed-end of actin filaments in different types of cells depends on their tropomyosin-binding properties.

MODELING THE STRUCTURE OF THE THICK FILAMENTS OF TARANTULA MUSCLE USING ELECTRON MICROSCOPY AND X-RAY DIFFRACTION

N.A. Koubassova[1], L. Alamo[2], A.K. Tsaturyan[1], R. Padrón[2]

[1]Institute of Mechanics, Moscow State University,
Mitchurinsky prosp. 1, Moscow, 119992, Russia;
[2]Centro de Biología Estructural, Instituto Venezolano de Investigaciones Científicas (IVIC), Caracas, Venezuela

Tarantula muscle is an outstanding system for understanding the molecular organization of the myosin filaments. 3D reconstruction of tarantula filaments based on cryo-EM images and single particle image processing revealed that in the relaxed state, myosin molecules undergo intra-molecular head-head interactions, explaining how head activity is switched off [1,2]. A model (PDB code 3DTP) was obtained by fitting a tilt-corrected 3D electron density map [2] with an atomic model built from a human cardiac myosin subfragment 2 (S2) crystal structure [4], a homologue atomic model of tarantula (*Avicularia*) myosin regulatory light chain [2], and atomic models of an essential light chain and myosin heads from chicken smooth muscle [3].

It is known that 3D reconstruction based on cryo-EM technique with negative staining may not reproduce the distances between the objects. For the correct positioning of myosin heads on the backbone of myosin filament we used direct modeling approach developed for the analysis of X-ray diffraction data from contracting rabbit muscle fibres [5]. We considered one myosin filament with 4-stranded helix of myosin molecules, distances between the crowns of myosin heads were taken as 14.5 nm, single unit cell contained 6 crowns or 48 heads.

First six myosin layer lines (M1 to M6) were calculated and compared with low angle x-ray diffraction pattern from live tarantula muscle obtained at DESY synchrotron radiation source (data provided by R. Padrón). The position of the main peak on the M1 layer line indicates that the radial position of the centre of mass of the myosin heads in the model should be shifted by 1 nm to increase the effective radius of myosin heads halo.

Currently we are calculating the X-ray pattern from the *Aphonopelma* quasi-atomic model including also the ring of 12 subfilaments of myosin tails and the 12 paramyosin rods core to refine the model of the backbone of the tarantula thick filaments.

References

1. Woodhead J. L., Zhao F. Q., Craig R., Egelman E. H., Alamo L., Padrón, R. (2005). Atomic model of a myosin filament in the relaxed state. Nature 436, 1195-1199.
2. Alamo L., Wriggers W., Pinto A., Bartoli F., Salazar L., Zhao F. Q., Craig R., Padrón, R. (2008). Three-dimensional reconstruction of tarantula myosin filaments suggests how phosphorylation may regulate myosin activity. J. Mol. Biol. 384, 780-797.
3. Liu J., Wendt T., Taylor D., Taylor K. (2003). Refined model of the 10S conformation of smooth muscle myosin by cryo-electron microscopy 3D image reconstruction. J. Mol. Biol. 329, 963-972
4. Blankenfeldt W., Thoma N. H., Wray J. S., Gautel M., Schlichting I. (2006). Crystal structures of human cardiac beta-myosin II S2-Delta provide insight into the unctional role of the S2 subfragment. Proc. Natl. Acad. Sci. U. S. A103, 17713-17717.
5. Koubassova N.A., Bershitsky S.Y., Ferenczi M.A., Tsaturyan A.K. (2008) Direct modeling of X-ray diffraction pattern from contracting skeletal muscle. Biophys J. 95, 2880–2894.

DELIVERY OF siRNA TO CULTURED MYOTUBES BY CONJUGATE OF ARGININE-CONTAINING OLIGOPEPTIDE WITH FS2 VENOM

I.V. Kravchenko, V.A. Furalyov, V.O. Popov

Bach Institute of Biochemistry, Russian Academy of Sciences, Leninskiy prospect 33, Moscow, 119071, Russia

siRNAs are considered as promising drugs for the therapy of various pathological states. However there are still no publications describing development of drugs based on siRNA to genes of muscle proteins. siRNAs to myostatin and also to its receptor seem to be the most promising for development of such drugs. RNA interference was successfully applied to decrease the content of myostatin mRNA and mRNA of its receptor in murine cell culture. Nonetheless, the standard methods for transfection of skeletal muscles in living organisms have noticeable drawbacks. Viral vectors pro-

vide high efficiency of transfection, but their use can generate tumors. The methods of electroporation, hydrodynamics-based transfection, and use of liposomes and complexes with polycations are almost safe, but nucleic acid penetrates into muscle tissue with low efficiency. Methods of the targeted delivery of nucleic acids into tissues using antibodies to tissue-specific proteins or low molecular weight ligands specifically binding to surface receptors seem to be more efficient. The multicomponent systems including a specific molecule recognizing cell surface, a substance providing nucleic acid penetration through membrane (polycations or liposomes with the positively charged lipids), and siRNA itself are most promising for siRNA delivery. However, such multicomponent systems for specific delivery have not yet been developed for application to skeletal muscles. A ligand binding to protein on muscle surface is the most important component of delivery systems. In this respect, Ca^{2+} channels of L-type (dihydropyridine receptors) are of specific interest among various membrane muscle proteins. Small cationic oligopeptides containing arginine, lysine, or ornithine residues are often used as a component providing penetration of siRNA through the membrane. The goal of the present work was to develop a system of siRNA delivery to muscle cells based on the ligand of dihydropyridine receptors FS2 venom and cationic oligopeptide R(7)-K-R and study of its efficiency *in vitro*.

For development of the delivery system, we used siRNA to the myostatin gene with proven capacity to induce RNA interference – 5`-AAGAUGACGAUUAUCACGCUA-3` (Magee, T R. et al., 2006, J. Gene Med., 8, 1171-1181). Peptide R(7)-K-R was conjugated with FS2 venom from Sigma (USA) using sulfosuccinimidyl-pyridyldithiopropionamido-hexanoate (sulfo-SPDP) according to the producer's instructions. The resulting conjugate was purified on the column HiTiap CM FF from GE Healthcare (UK). To prepare complexes, siRNAs were mixed with conjugate or peptide in DMEM and incubated for 15 min. The complexes were added to 60 mm Petri dishes with differentiated myotubes in DMEM containing l0% FCS to the final volume 5 ml, incubated for 24 h and then the RNAs were isolated for analysis of myostatin expression.

The conjugation of R(7)-K-R oligopeptide with FS2 venom was carried out. To analyze peptide/venom molar ratio in the resulting conjugate, it was reduced with β-mercaptoethanol, released R(7)-K-R and FS2 were separated by gel filtration, and their amounts were estimated by Lowry. Peptide/venom molar ratio in the conjugated appeared to be ~ 2 : 1.

Then we studied the efficiency of siRNA delivery to the differentiated myotubes at various conjugate/siRNA ratios; efficiency of siRNA de-
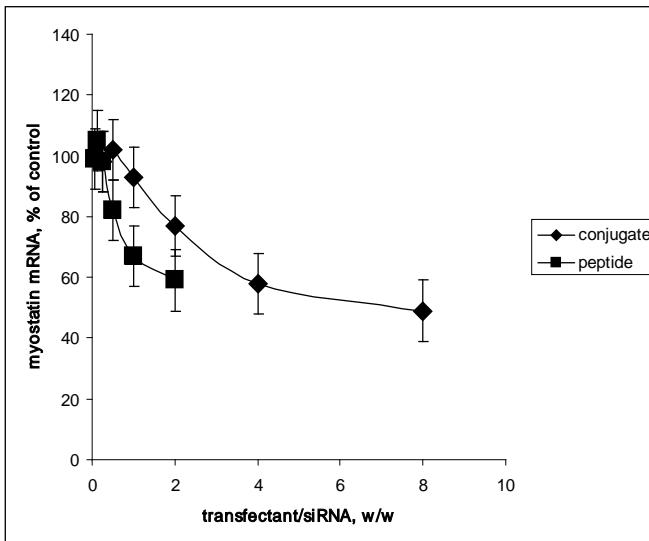
Fig. 1. Effect of transfectant/siRNA ratio on efficiency of myostatin mRNA interference.

livery by non conjugated peptide at various peptide/siRNA was also studied as a control (fig. 1).

It appeared that the maximal efficiency of transfection was observed at the conjugate/siRNA mass ratio 8 : 1, expression of myostatin mRNA being ~ 2-fold decreased compared with control cells. Reliable decrease of myostatin mRNA level was observed beginning with ratio 2 : 1. In the case of transfection of myotubes with complexes of non-conjugated peptide and siRNA the optimal mass ratio was 2 : 1, expression of myostatin mRNA being ~1.7-fold decreased compared with control. In this case reliable decrease of myostatin mRNA level was observed beginning with the ratio 0.5 : 1. Incubation of cells with non-conjugated peptide and also with conjugate at all studied concentrations resulted no noticeable change in expression of myostatin mRNA. When conjugate/siRNA mass ratio was increased to 16 : 1, no further increase in efficiency of transfection was observed, whereas cytotoxicity of the complex significantly increased. Analogous increase in toxicity without increase in efficiency of delivery was observed on increase in peptide/siRNA mass ratio to 4 : 1.

The dependence of suppression of expression of myostatin mRNA on concentration of siRNA complexes with conjugate and the non-conjugated peptide was also studied (fig. 2). For this, we used complexes
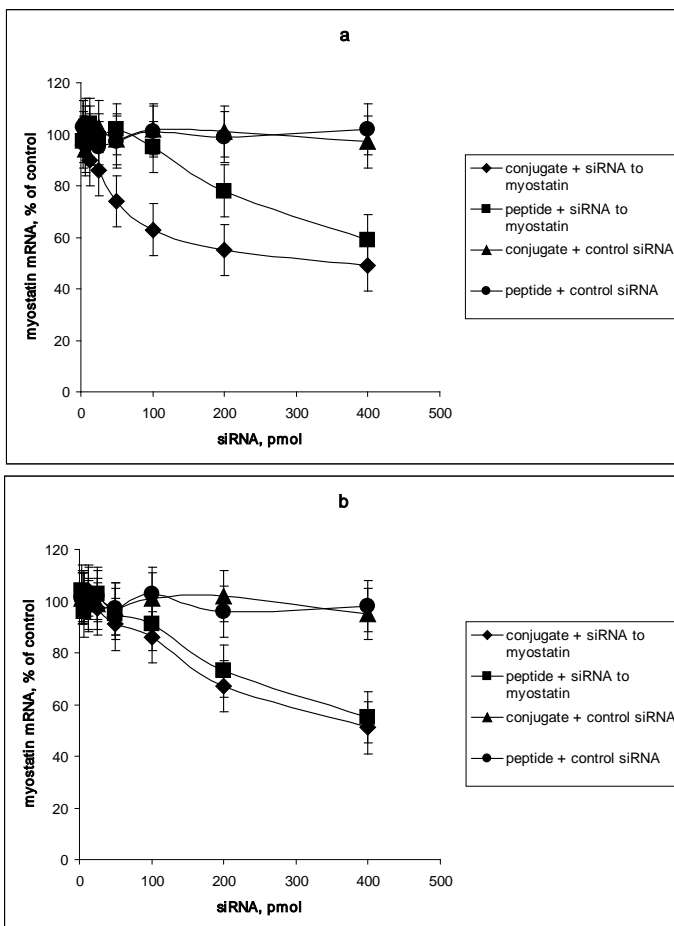
Fig. 2. Dependence of efficiency of myostatin mRNA interference on amount of transfectant/siRNA complex. Differentiated myotubes (a) and non-differentiated myoblasts (b) were used for transfection.

with the optimal transfectatnt/siRNA ratios, that is 8 : 1 on transfection with conjugate and 2 : 1 on transfection with peptide.

It was found that when complexes of siRNA to myostatin with conjugate were used for myotube transfection, a reliable decrease in expression of myostatin was observed already at transfection with 12.5 pmol siRNA, whereas transfection with siRNA/non-conjugated peptide complexes caused statistically reliable effect of myostatin mRNA interference only when 200 pmol of siRNA were used.

Efficient siRNA doses causing decrease in myostatin mRNA level to 2/3 of control also varied significantly. On transfection with siRNA/conjugate complexes, 33% decrease in mRNA-target expression was observed on addition of 74 pmol of siRNA, whereas transfection with siRNA/peptide complexes caused the same effect only on addition of 313 pmol of siRNA.

To test specificity of siRNA delivery using the synthesized conjugate, analogous experiments were performed using non-differentiated myoblast culture. It was found that when these cells were used, the complexes of siRNA to myostatin with conjugate demonstrated almost the same transfection efficiency as complexes of siRNA with the non-conjugated peptide: in both cases statistically reliable decrease in myostatin mRNA level was observed only on addition of 200 pmol siRNA. Efficient siRNA doses causing decrease in myostatin mRNA level to 2/3 of control were also practically equal.

Transfection of myotubes with siRNA/conjugate complexes caused decrease in myostatin expression not only on mRNA level, but also on protein level.

We produced conjugate of cationic arginine-containing oligopeptide and FS2 venom allowing successful transfection of siRNA to myostatin in differentiated myotubes *in vitro*. It should be noted that transfection was performed in the presence of serum proteins, that is, under conditions more corresponding with the *in vivo* situation than transfection in serum free media, which is required when classical liposome based reagents such as Lipofectamine, Oligofectamine, and others are used. Activity of these reagents significantly decreases in the presence of l0% FCS, that is, under the usual conditions for cell culture.

The developed conjugate exhibited significantly higher transfecting potential for cultures of differentiated myotubes than the non-conjugated cationic oligopeptide. The interference effect of myostatin mRNA when siRNA/conjugate complexes were used manifested itself at siRNA concentrations an order of magnitude lower than those when siRNA/peptide complexes were used. On transfection with the maximal nontoxic siRNA doses, use of complexes with conjugate also produced a larger interference effect. So, we conclude that the produced conjugate is promising for study of siRNA transfection in models *in vivo*.

MORPHOLOGICAL FEATURES OF *FASCIOLA HEPATICA* MUSCULATURE IDENTIFIED BY TRITC-PHALLOIDINE FLUORESCENCE

[1]N.D. Kreshchenko, [2]O.O. Tolstenkov

[1]Institute of Cell Biophysics RAS, Pushchino; Moscow region;
[2]Center of Parasitology of Severtsov Institute of Ecology
and Evolution RAS, Moscow

Musculature of the body in representatives of phylum Platyhelminthes is carrying out of a supporting function for cells in the whole organism, forming a shape of the body, as well as takes part in different types of muscle activity - locomotion, food intake, reproduction. In free-living flatworms (class Turbellaria) the musculature is also used for searching, capturing and holding the prey, food uptake and for the accomplishment of reproductive behavior repertoire. In numerous parasitic representatives of classes of Trematode, Cestode and Monogenea the musculature serve for the penetration into host species, attachment to the host tissue, and for locomotion and swimming of their free-living larval stages during their life cycle. For the visualization of the morphological structure of flatworm's musculature the histochemical and immunocytochemical methods are used with conjunction with fluorescent and confocal laser scanning microscopy. Specific fluorescently labeled antibodies or fluorescently labeled phalloidin are usually employed. The rationale behind the last method is that F-actin filaments, which occur predominantly in muscle fibres, specifically bind phallotoxins [1]. In the present study the investigation of musculature organization using staining with fluorescently (TRITC) labeled phalloidin has been performed in parasitic flatworm *Fasciola hepatica* (Trematoda, Platyhelminthes).

Methods

Animals 15-20 mm in length were recovered from a bile duct of the infected cows, rinsed in physiological solution for 2 hrs, flat fixed in freshly made 4% paraformaldehyde in 0.1 M phosphate-buffered saline (PBS, pH 7.4) for 24 hrs at 4ºC, transferred to Ependorffs tube in fresh paraformaldehyde solution for next 6 hrs at 4ºC. Than samples were immersed in 10% sucrose in PBS for 3-5 days, embedded in Tissue Tek, frozen and sectioned frontally on 16-18µm sections by Shandon cryotom (Termoelectron Corporation, UK) at -20ºC. Sections were collected on Polysine or Gold Super Frost Plus microscope slides (Menzel-Glaser, Germany) and dried on air for 2 hrs. For histochemical staining the sec-

tions were washed 3 times for 5 min in PBST (containing PBS with 0,3% of Triton X-100, Sigma) and stained for 12 hrs by TRITC-(tetramethyl-rhodamine isotiocyanat)-labeled phalloidin (Sigma), in solution containing 200 ng/ml of phallodin using wet chamber in strict horizontal position. After final wash slides were mounted in PBS/glycerol (1:9) under the cover slips and examined with fluorescent Leica DM600 microscope connected with digital photo camera Leica DFC 490 or with Leica TCS SP5 (Germany) confocal laser scanning microscope.

Results and discussion

The present study provided the information on muscle system organization in parasitic trematode *Fasciola hepatica* (fig.1, A-D). The data revels that body wall musculature of *F. hepatica* situated underneath of the epidermis comprises of three muscular layers: the outer circular, the inner longitudinal (running perpendicular an parallel to the main body axes, respectively) and the intermediate layer of diagonal muscle fibres running in two directions. The three body wall musculature's layers are tightly packed and hardly distinguishable on the frozen sections from each other. Regularly situated transversal bundles composing of several muscle fibres have been found connecting the dorsal and the ventral body sides (fig.1, B,C). The oral and the ventral suckers display similar organization, they consist of densely packed circular, radial and longitudinal muscle fibres. The pattern of musculature in cylindrical pharynx is constituted of the inner circular and the outer longitudinal muscle fibres (fig.1, B). Branches of the blind intestine are underlying with much more loosely packed thin circular and diagonal muscle fibres easily distinguished (fig.1, C, D). Tubular structures of the complex reproductive apparatus of *F. hepatica* are supplied with circular and diagonal muscle fibres (see the egg-laying chamber on fig.1, C), as well as with irregularly organized and running in different directions thin muscle filaments.

Until last two decades a little was known about the organization and the functioning of the muscle system in representatives of Platyhelminthes. Because of their high economical and medical importance, the numbers of the investigations on parasitic flatworms infecting of human being and their life stocks are now essentially raised. Thus, the morphology of the body musculature had been described for free-living turbellaria *Dugesia tigrina* [2], *Dugesia japonica* [6], *Girardia tigrina* [3] and *Polycelis tenuis* [4]. For paprasitic worms the data had been revealed for *Schistosoma mansoni* [5], *Apatemon cobitidis proterorhini*, *Cotylurus erraticus* and *Bucephaloides gracilescens* [7,8], *Echinostoma caproni* [9]; *Echinoparyphium aconiatum* [10], *Cercaria parvicaudata*, *Maritrema sub-*
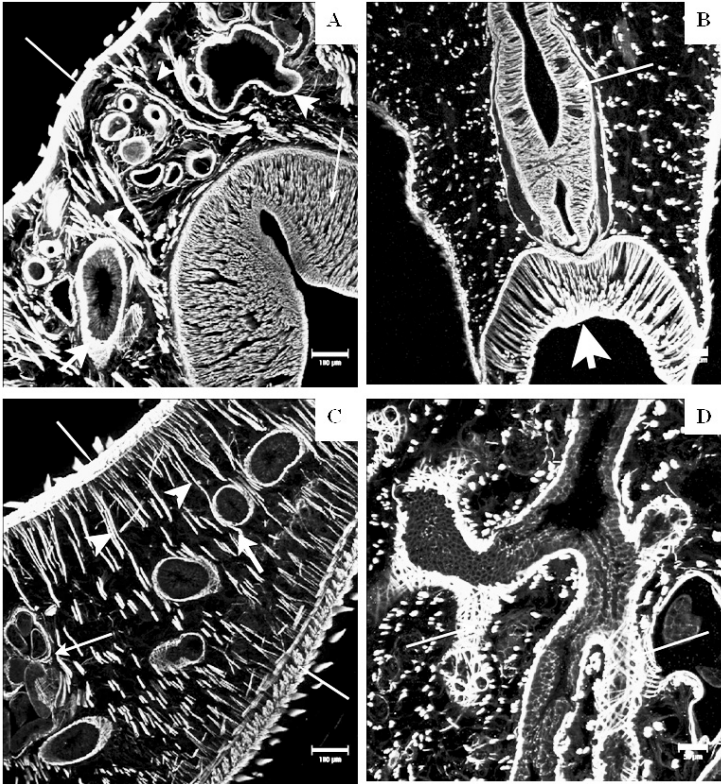
Fig. 1. Musculature of *Fasciola hepatica* stained with TRITC-labeled phalloidin.
A – Ventral sucker in the middle part of the body part with densely packed numerous myofibres (thin arrow), branches of blind intestine surrounding with myofibrils (thick arrows) and thick bundles of muscle fibres (arrowheads) connecting dorsal and ventral side of the body; stick point out on dorsal side of the body with tightly packed body wall myofilaments. **B** – Musculature of the oral sucker (thick arrow) and pharynx (thin arrow) in anterior body area. **C** - Regularly situated bundles of transverse muscles connecting the dorsal and the ventral sides of the body (arrowheads), thick body wall musculature comprised of longitudinal, diagonal and circular layers of muscle fibres (white sticks) situated underneath of epithelia and tegument, in the left upper corner the egg-laying chamber of the female reproductive apparatus (thin arrow), comprised by thin circular and diagonal muscle filaments, thick arrow indicate gut diverticula. **D** – The intestine branches on sagittal section with loosely packed circular and diagonal muscle fibres (arrows). Scale bars: on A, B - 100µm, on C, D – 50µm.

subdolum and *Himasthla elongate* [11], and for a number of larval stages of trematodes (see [12,13]). Our results indicate that the pattern of musculature in *F.hepatica* share similarity with previously studied species and retain conserved features in representatives of phylum Platyhelminthes. The data on musculature organization in basal flatworm species is accumulating and can be useful for better understanding of major principles of organization and evolution of muscle system in animal kingdom. The physiological studies are now the actual for obtaining the essential information on muscles function in flatworms and development of novel anthelmintic drugs using musculature as a target.

References

1. Wieland T. (1977). Modification of actin by phallotoxins. Naturwiss., 64(6): 303-309.
2. Bueno D., et al. (1997). Cell-, tissue-, and position-specific monoclonal antibodies against the planarian Dugesia (Girardia) tigrina. Histochem. Cell Biol., 107(2): 139-149.
3. Kreshchenko N.D. (2010). Organization of musculature in planarian Girardia tigrina monitored by TRITC-conjugated phalloidin and confocal laser scanning microscopy. "Biological motility: from fundamental achievements to nanotechnologies". Pushchino, P. 142-145.
4. Kreshchenko N.D. (2012). Details of morphological structure of the muscle system in planarian Polycelis tenuis. "Biological Motility: Fundamental and Applied Science", Pushchino, P. 93-96.
5. Mair G.R., et al. (2000). A confocal microscopical study of the musculature of adult Schistosoma mansoni. Parasitology. 121 (Pt 2): 163-170.
6. Orii H., et al. (2002). Anatomy of the planarian Dugesia japonica. I. The muscular system revealed by antisera against myosin heavy chains. Zool. Sci., 19(10): 1123-1131.
7. Stewart M.T., et al. (2003a). Development in vitro of the neuromusculature of two strigeid trematodes, Apatemon cobitidis proterorhini and Cotylurus erraticus. Int. J. Parasitol., 33: 413–424.
8. Stewart M.T., et al. (2003b). Neuroactive substances and associated major muscle systems in Bucephaloides gracilescens (Trematoda: Digenea) metacercaria and adult. Parasitol. Res., 91: 12–21.
9. Sebelova S., et al. (2004). The musculature and associated innervation of adult and intramolluscan stages of Echinostoma caproni (Trematoda) visualised by confocal microscopy. Parasitol. Res., 93: 196–206.
10. Terenina N.B., et al. (2006). The spatial relationship between the musculature and the NADPH-diaphorase activity, 5-HT and FMRFamide immunoreactivities in redia, cercaria and adult Echinoparyphium aconiatum (Digenea). Tiss. Cell., 38: 151–157.

11. Tolstenkov O.O., et al. (2011). The neuro-muscular system in cercaria with different patterns of locomotion. Parasitol Res., 108(5): 1219-1227.
12. Tolstenkov O.O., et al. (2012a). The neuro-muscular system in freshwater furcocercaria from Belarus. I Schistosomatidae. Parasitol Res., 110(1): 185-193.
13. Tolstenkov O.O., et al. (2012b). The neuromuscular system in freshwater furcocercaria from Belarus. II Diplostomidae, Strigeidae, and Cyathocotylidae. Parasitol Res., 110(2): 583-592.

FUNCTIONAL INTERACTIONS OF Na,K-ATPase WITH MOLECULAR ENVIRONMENT

I.I. Krivoi

St. Petersburg State University, St. Petersburg, Russia

The Na,K-ATPase is a P-type ATPase which catalyzes the active transport of K^+ into and Na^+ out of the cell, thereby maintaining the steep Na^+ and K^+ gradients that underlie the resting membrane potential and electrical excitability of cells. A Na^+ gradient ensures the work of coupled transporters of Ca^{2+} and H^+, glucose, amino acids, neurotransmitters, vitamins and reabsorption of Na^+. Thus Na,K-ATPase plays the main role in regulation of water-salt exchange, presents an important factor resisting hypoxia and fatigue.

The Na,K-ATPase consists of alpha-catalytic and beta-glycoprotein subunits as well as a FXYD subunit which modulates enzyme activity. Presently mammals are known to have four isoforms of alpha subunit, three isoforms of beta subunit of Na,K-ATPase, and also seven proteins of the FXYD family. It is generally accepted that the ubiquitous alpha1 isoform plays the main "house-keeping" role while the other isoforms are expressed in a cell- and tissue-specific manner and possess additional regulatory functions which are still poorly understood.

Owing to specific structural domains the Na,K-ATPase may form multimolecular complexes with membrane, intracellular and cytoskeletal proteins and take part in formation of functional microcompartments of the cells and in intercellular interactions. An important role in compartmentalization and regulation of Na,K-ATPase is played also by membrane lipids, in particular cholesterol, which participates in control of fluidity and curvature of cell membrane. Cholesterol also is an essential component of membrane mobile heterogeneous domains – lipid rafts, participating in formation of functional cell microcompartments. In addition, Na,K-ATPase

forms multimolecular complexes in specialized microdomains of the membrane called caveolae. They are the invaginations of the plasma membrane characterized by specific lipid composition, in which some proteins are localized performing a signal function in the cell.

It is shown that in neurons, astrocytes and myocytes cardiotonic steroids (CTS) cause Ca^{2+} oscillations only in special microcompartments where Na,K-ATPase coordinates with Na^+,Ca^{2+} exchanger (NCX), various Ca^{2+} channels and receptors of the plasma membrane in proximity to sarco(endo)plasmic reticulum. In accordance with this «PLasmERosome» model inhibition of a part of Na,K-ATPase leads to Na^+ accumulation in these narrow near-membrane spaces. This is accompanied by accumulation of Ca^{2+} as a result of a decrease in its extrusion by NCX. It is established that the Na,K-ATPase $\alpha2/\alpha3$ isoforms have specific structural domains that are responsible for their ability to clusterize in these microdomains. It is supposed that CTS-evoked slow Ca^{2+} oscillations affect not only muscle contractility but also genome and expression of proteins, proliferation, differentiation, etc. In this local Ca^{2+} handling there also involved SERCA, ryanodine and IP_3-receptors of sarco(endo)plasmic reticulum. It was shown that CTS may liberate Ca^{2+} from depot as a result of conformations changes of the Na,K-ATPase alpha subunit N-end interacting with the IP_3-receptor of sarcoplasmic reticulum. In the formation of such Ca^{2+} microdomains an important role is played by various proteins, including ankyrin.

Many proofs has been shown for additional function of Na,K-ATPase as a signal molecule. This function is realized due to functional and direct molecular interactions of Na,K-ATPase with different neighboring proteins. Major of such proteins appears to be Src kinase, which forms a functional complex with Na,K-ATPase, activating upon binding CTS a series of signal intracellular cascades. It is supposed that signal function is actualized by Na,K-ATPase in caveolae of the plasma membrane («Signalosome» model). According to this model, Na,K-ATPase alpha subunit is involved in a signal complex with Src kinase. These complexes also include NCX, Ca^{2+} channels, phospholipase C, IP3 receptor, caveolin etc. Due to such molecular organization of signal transmission even ultralow concentrations of CTS, without inhibition of Na,K-ATPase activity, are capable of regulating most diverse cellular functions: protein synthesis, proliferation and differentiation, processes of apoptosis, contractile properties and others, influence cell survivability and death, exert anticancer and neuroprotector action. It is supposed that physiological stimuli triggering such a signal complex a presented by endogenous CTS.

Functional specialization and peculiarities of the Na,K-ATPase alpha2 regulation isoform are studied more precise. The alpha2 Na,K-ATPase of astrocytes is involved in clearance of the intercellular space from accumulated potassium ions. In addition, alpha2 isoform participates in glutamate level control due to functional and molecular interaction with the glutamate transporter, which is considered to be an important factor in the pathophysiology of migraine.

In a vertebrates body Na,K-ATPase predominantly located in muscle tissues where the alpha1 and alpha2 isoforms of alpha subunit are expressed. In skeletal muscle the Na,K-ATPase is critically important for excitability, electrogenesis and contractility. It was shown that skeletal muscle use and disuse differently regulates the alpha1 and alpha2 isoforms however mechanisms of this regulation remain to be elucidated. Numerous evidences suggest that the Na,K-ATPase alpha2 isoform play key role as regulator of calcium balance and contractile properties of cardiac and smooth muscles due to functional interaction with NCX and co-localization with sarcoplasmic reticulum. It is established that it is the alpha2 isoform that plays the main role in realization of positive inotropic action of cardiac glycosides in cardiac, smooth and presumably skeletal muscles.

In sum, data obtained from different cells and tissues indicates that the Na,K-ATPase alpha2 isozyme is the more regulated subunit compared to alpha1. Regulation of alpha2 Na,K-ATPase is determined by its functional and molecular environment, localization in specific cellular microdomains. These peculiarities of the alpha2 Na,K-ATPase are accompanied with its less stable integration into the cell membrane compared to other Na,K-ATPase alpha isoforms. Instability of the alpha2 isoform is explained by its solely inherent peculiarities of transmembrane domains M8–M10, responsible for interaction with phospholipids, and also by weaker association with subunit FXYD1.

References

1. Blaustin M.P. Livin' with NCX and lovin' it: a 45 year romance. Adv. Exp. Med. Biol. 2013. 961: 3–15.
2. Clausen T. Quantification of Na^+,K^+ pumps and their transport rate in skeletal muscle: Functional significance J. Gen. Physiol. 2013. 142 (4): 327–345.
3. Kapri-Pardes E., Katz A., Haviv H., Mahmmoud Y., Ilan M., Khalfin-Penigel I., Carmeli S., Yarden O., Karlish S.J.D. Stabilization of the a2 isoform of Na,K-ATPase by mutations in a phospholipid binding pocket. J. Biol. Chem. 2011. 286 (50): 42888–42899.

4. Krivoi I.I. Regulatory function of the Na,K-ATPase a2-isoform. Biophysics. 2012. 57 (5): 592–606.
5. Lingrel J.B. The physiological significance of the cardiotonic steroid/ouabain-binding site of the Na,K-ATPase. Annu. Rev. Physiol. 2010. 72: 395–412.
6. Radzyukevich T.L., Neumann J.C., Rindler T.N., Oshiro N., Goldhamer D.J., Lingrel J.B., Heiny J.A. Tissue-specific role of the Na,K-ATPase a2 isozyme in skeletal muscle. J. Biol. Chem. 2013. 288: 1226–1237.
7. Reinhard L., Tidow H., Clausen M.J., Nissen P. Na$^+$,K$^+$-ATPase as a docking station: protein–protein complexes of the Na$^+$,K$^+$-ATPase. Cell. Mol. Life Sci. 2013. 70: 205–222.

EVOLUTION OF INDIVIDUAL CONTRACTILE EVENTS DURING TETANIC STIMULATION OF FAST- AND SLOW-TWITCH RAT MUSCLES

I.V. Kubasov, R.S.Arutyunyan, E.V. Matrosova

Sechenov Institute of Evolutionary Physiology and Biochemistry RAS, 194223, 44, Thorez av., St-Petersburg, Russia

The purpose of this study was to evaluate behavior of individual contractile components (ICC) of muscle response to a tetanic stimulation. To achieve this, we analyzed characteristics (peak amplitude and half-relaxation time) of the last ICC (force transient) in the tetanic constraction evoked by train of 5, 10, 20, 30, 40, 50 or 100 stimuli delivered at 20 or 50 Hz rate (m. Soleus and m. EDL, respectively). In each set of stimulating conditions, Nth ICC was isolated by point-by-point subtraction of di-
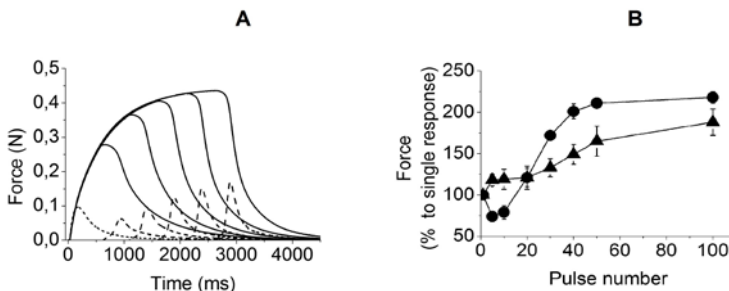
Fig. 1. Effect of duration of tetanic stimulation on global and last ICC muscle contractile responses . A, Representative record of global and last ICC responses of m. Soleus to a trains of 10 -50 stimuli (delivered at 20 Hz intra-train rate). B, Mean amplitude of last ICC of m. Soleus (circles, n=7) and m. EDL (triangles, n=6).

gitally recorded profiles of tetanic contractions evoked by stimulation with N and N-1 pulses-long trains. The results of this analysis were used to estimate the effect of duration of tetanic stimulation on characteristics of individual twitch as an elementary unit of overall tetanic contractile response of a muscle. Our data demonstrate a significant effect of prolonged stimulation on both amplitude and half- relaxation of ICC. With an increase in duration of tetanic stimulation, ICC of m. EDL showed progressive potentiation, while changes in ICC of m. Soleus were transient. The amplitude of ICC elicited by first 5 to10 pulses in the train was decreased by 30-40% but this effect was attenuated and eventually replaced with potentiation of ICC with prolongation of the tetanus. Fig.1A shows the representative example of global (solid lines) and last stimulus ICC (dotted lines) of m. Soleus's contractile response to a 5 - 50 pulses-long tetanic stimulation. Unlike that for slow, m. Soleus (fig. 1A and B, circles), ICC of fast, EDL muscle show potentiation with the increase in duration of tetanic stimulation (fig. 1B, triangles).

In addition to the effect on amplitude of ICC duration of tetanic stimulation had also affected the time characteristics of ICCs. Duration of half- relaxation of ICC decreased from 224 ± 8 ms to 115 ± 12 ms in m. Soleus and from 31 ± 4 ms to 24 ± 3 ms in m. EDL (fig. 2). These effects of prolongation of tetanic stimulation could be interpreted as the result of activation of Ca^{2+}-ATPase.

As it is shown in fig.3, for both types of muscles, latency of ICC increases with an increase in duration of tetanic train from nearly zero for single twitch response to 26 ± 9 ms in m. EDL ($n=6$) and 157 ± 12 ms in m. Soleus ($n=7$) at the end of 100 pulses-long tetanic stimulation. Probably, this increase in latency of ICC reflects changes in the dynamics of
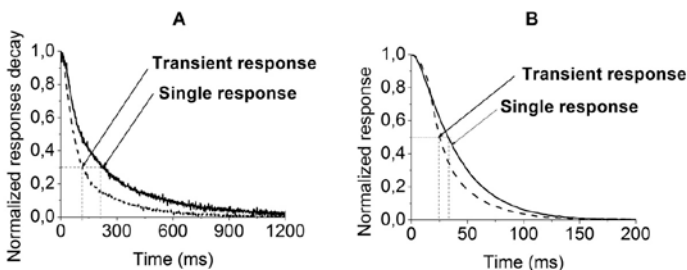
Fig. 2. Post-peak decline of single muscle twitch (solid trace) and ICC (dashed trace) at the end of tetanic train with 100 pulses. Averages of recordings collected in 7 and 6 independent experiments are shown in panels A (m. Soleus) and B (m EDL), respectively.
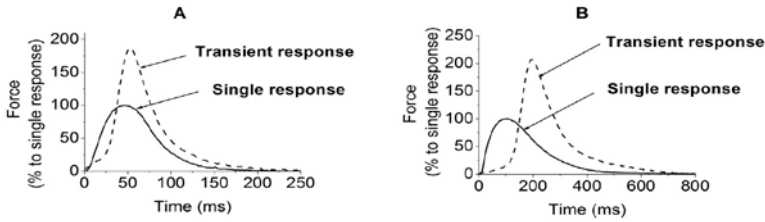
Fig. 3. Single muscle twitch response (solid trace) and ICC (dashed trace) at the end tetanic train with 100 pulses. Averages of recordings collected in 6 (m EDL, panel A) and 7 (m Soleus, panel B) independent experiments are shown. All recordings were normalized to the peak amplitude of respective muscle twitch response.

occupation by Ca^{2+} of troponin C binding sites situated close to points of Ca^{+2} release. As to the difference between latencies of m. EDL and m. Soleus ICCs, it could be attributed to a different sensitivity of fast and slow muscle fibers to Ca^{2+}.

The potentiation of ICCs during tetanic train is not associated with any detectable changes in either amplitude or duration of muscle fiber action potentials (APs). Therefore, it seems reasonable to speculate that changes in operation of other mechanisms such as mechanisms of intracellular Ca^{2+} release, binding and/or uptake are responsible for this potentiation. To test the possibility of activation of Ca^{2+}-indused Ca^{2+}-release (CICR) we evaluated behavior of ICCs during tetanic stimulation of caffeine-treated muscles. In experiments in m. EDL, application of 10 mM of caffeine in bath solution led to prolongation and potentiation of single twitch and tetanic muscle responses but it decreased amplitude of ICCs to about half of that of the first twitch in the tetanus (fig. 4).

The same picture was observed in experiments with caffeine-treated m. Soleus (data not shown). Thus initialy activated by caffeine CICR does
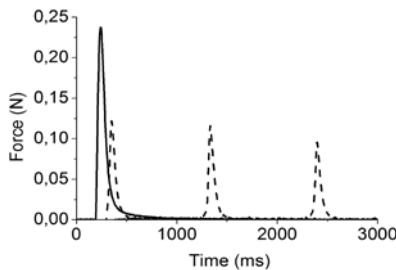
Fig. 4. Single twitch response (solid trace) and 10th, 50th and 100th ICCs (dash traces) during tetanic stimulation at 50.

not support subsequent ponentiation of ICCs during tetanic stimulation. In tetanus decrease in amplitude of ICCs may be associated with depletion in intracellular Ca^{2+} stores in sarcoplasmic reticulum. Potentiation of tetanic force is likely conditioned by initialy prolongated by caffeine of ICCs decay phases only. Part of our finding are similar to that has been shown by B.R. MacIntosh et al. in surgically isolated in situ gastrocnemius muscle for train stimulation consisned of 1-5 pulses [MacIntosh et al., 2006]. Potentiation contractile events during tetanic stimulation and its elimination by caffeine can be evidence of increasing of Ca^{2+}-release during tetanuses development. But in experiments with fluorscent indicators was shown decline of the amount released in repeated action potentials. The fifth depolarization in high-frequency train (50 Hz) of action potentials released only the amount of calcium corresponding to one-fifth of calcium released by the first action potential in slow and one-six in fast fiber (Baylor, Hollingworth, 2003). In our experiments we observed only short-lasting decreasing in transient responses (by 30-40 %) in slow but not fast muscles. Reasons of this disparitet is not clear and need in further study.

References

1. Baylor S.M., Hollingworth S. Sarcoplasmic reticulum calcium release compared in slow-twitch and fast-twitch fibres of mouse muscle // J. Physiol. 2003. 551(1):125–138.
2. Celio M.R., Heizmann C.W. Calcium-binding protein parvalbumin is associated with fast contracting muscle fibres // Nature. 1982. 297: 504–506.
3. MacIntosh B.R., Jones D., Devrome A.N., Rasser D.E. Prediction of summation in incompletely fused tetanic cuntracnions of rat muscle // J. of Biomechanics. 2006. 40:1066-1072.
4. Periasamy M., Kalyanasundaram A. SERCA pump isoforms:their role in calcium transport and disease // Muscle Nerve. 2007. 35: 430–442.
5. Schiaffino S., Reggiani C. Fiber types in mammalian skeletal muscles // Physiol. Rev. 2010. 91: 1447-1531.
6. Stephenson D.G., Williams D.A. Effects of sarcomere length on force-pCa relation in fast-and slow-twitch skinned muscle fibres from the rat // J.Physiol. 1982. 333:637–653.

LOAD PARAMETERS TO PRESERVE THE POWER OF ENDURANCE IN THE PROCESS OF RESISTANCE TRAINING OF ASTRONAUTS IN WEIGHTLESSNESS

T.B. Kukoba, E.V. Fomina

Institute of Biomedical Problems of the Russian Acad. Sci., Moscow, 123007, Russia

The Russian physical countermeasure system is a complex training with the use of both active and passive methods. Among the active meth-

ods is the NASA ARED that allows a vast variety of resistive exercises for the main groups of muscles. These are NASA coaches who develop and introduce the ARED training programs to cosmonauts. According to the US partners' concept, astronauts perform a high-intensity resistive training, i.e. the "loading weight" amounts to 70 - 90% of a rep max and number of repetitions, 3 to 10. Russian instructors give preference to a less intensive regimen; they ease the force loading and increase the number of repetitions and attempts instead. For the ISS Russian crewmembers, resistive sessions are scheduled on days 2 and 4 of the training microcycle so that cosmonauts exercise with the ARED two or three times a week.

In order to evaluate effectiveness of the resistive training with different levels of loading, the strength endurance of cosmonauts' femoral muscles was tested pre and post flight.

The experiment involved 11 cosmonauts who were on 145 to 167-day long ISS missions. Depending on the ARED resistive loading, the cosmonauts were distributed into 2 groups. One group trained with heavy loading that reached about 60% of a rap max; each exercise was done in 4 attempts with 12 to 16 repetitions. The other group performed the same set of exercises but with a moderate loading that is the "weight" did not change, attempts reduced to 3 and the number of repetitions was no more than 12.

Evaluation was performed on pre-launch days 60 and 30, and on day 4 post recovery. Strength endurance of the femoral muscles was estimated by the results of isokinetic testing. The subject fulfilled 22 cyclic maximal contractions (flexion/extension of the knee joint) at the angular velocity of 120°/s without break. The strength endurance of knee flexors and extensors before and after space flight was estimated.

The groups showed significant differences in the parameters of strength endurance of the knee flexors ($P<0.04$) and extensors ($P<0.03$).

Data analysis evidenced that the group of cosmonauts who applied greater loads for resistive training increased strength endurance of equally the knee flexors and extensors. Endurance of the flexors gained 10% to 50% and extensors, 11% to 59%. One cosmonaut made an exception in the group as his flexors lost 17% of the strength endurance.

In the group where cosmonauts trained with moderate loads the parameters under study degraded in each one without exception, i.e. the flexor endurance dropped by 22% to 55% and extensors, 2% to 61%.

It was brought out that the resistive training with heavy loading in microgravity is favorable to maintenance of the strength endurance of cosmonauts.

POSSIBLE EFFECTS OF HYPOXIA INDUCED BY EXOGENIC NITRITE ON RAT HEART AND SKELETAL MUSCLE PROTEINS

N.V. Kuleva, D.S.Aleksejeva, T.E. Shumilova

Departments of Biochemistry and General Physiology,
St.-Petersburg State University, Universitetskaya nab. 7-9,
St.Petersburg,199034, Russia

Nitrite anion is an oxidative breakdown product of nitric oxide (NO), a labile biological mediator from group of gasotransmitters. This gas was firstly discovered in the late 1700s and during two next centuries was considered to be as toxic and dangerous for environment (Calvert J., Lefer D., 2009). The importance NO on the field of biology and medicine was not fully appreciated until the 1980s when several independent research groups found that NO is generated in mammals including human, by nitric oxide syntases (NOSs) and plays a prominent role in controlling blood pressure via regulation of vascular tone (Ignarro L., 1999). The localization of NOS in the vascular epithelium (eNOS) is of particular importance for cardiovascular system , as eNOS maintains basal vascular tone trough its release of low levels of NO (Loscalso J.,Welch G.,1995). The synthesis of NO is significantly influenced by numerous cofactors such as tetrahydrobiopterin, flavin mononucleotide and flavin adenine dinucleotide, the presence of reduced thiols and endogenous NOS inhibitor asymmetric dimetylarginine , as well as substrate and oxygen availability. During ischemia the ability of eNOS to generate NO is severely reduced because of inadequate delivery of oxygen and cofactors (Becker B.F. et al., 2000). But it is a hypoxic state when the main role in NO formation nitrite begins to play. Recently there has been a paradigm shift in nitrite biology with discovery that nitrite is a physiologically relevant storage reservoir of NO in the blood and tissues that can be readily reduced to NO under pathological conditions such as ischaemia and hypoxia (Zweier J.L. et al., 1995). Nitrite reductase activity in mammalian tissues has been linked to mitochondrial electron transport system, non-enzymatic acidic disproportionation, deoxyhemoglobin, xanthine oxidase, and more recently myoglobin (Gladwin M.T. et al., 2005).

So, nitrite injected to animals in hypoxic conditions is able to produce NO that regulates vasodilatation and blood pressure. It means that nitrite represent a novel salvage pathway for NO equivalents that are biologically important and appear to be attractive targets for therapeutic purposes. The diseases include heart ischaemia-reperfusion injury (Gladwin M.T.et al., 2005), pulmonatory hypertension (Zuckerbraun et al., 2011),

chronic ischaemic tissue disease (Patillo E.B. et al., 2011) and other. However, several key questions remain: What signaling mechanisms does nitrite influence? How nitrite cellular uptake is regulated, and is it compartmentalized upon entry into cell? What are the molecular and biochemical targets of nitrite- mediated protection in disease-models? Are there adverse consequences of low levels of nitrite besides carcinogenesis at high concentrations?

In this study we have made an attempt to answer the question about adverse consequences of low levels of exogenic nitrite for rat hearts and skeletal muscle and to look for oxidative modifications of water-soluble proteins at nitrite injection into rates in doses of 1-5 mg 100 gm of body weight. These injections resulted in hemic hypoxia induced by methemoglobinonemia. In our experiments the content of blood plasma methemoglobin was increased to mean value of 10 % of total hemoglobin content. Circulation parameters of nitrite hypoxia are characterized by fast and significant decrease of arterial pressure, bradycardia development, decreasing of heart output and heart stroke volume as well as total peripheral resistance decreasing. After 1-1 ,5 hours the indexes of systemic and peripheral hemodynamics became near to original values. At this moment there were taken blood samples and samples of skeletal and heart muscles. The tissues were homogenized in 10 volumes of 0,01 M phosphate buffer, pH 7,4, and supernatant formed at centrifugation (at 5000g , for 15 min) was used to study oxidative modifications in proteins. As the hypoxic state there may be conditions for free radicals formation followed by oxidative modifications of cardiac and muscle proteins, so, we have considered a possibility of reversible modifications, transformation sulfhydryl groups into disulfide, and non-reversible modifications, protein carbonylation. In the first case, for registration so called "diagonal electrophoresis" was used (Eaton J. et al., 2006), in the second one, thespectrophotometric registration of interaction of carbonylated proteins with 2,4-dinitrophenyl hydrazine was (Dalle-Donne I. at al., 2003).

The reversible oxidative modifications were found in proteins with molecular masses 38, 43 and 79 kDa of skeletal muscle and in those with 37, 48, 52, 95 kDa of heart, but significant differences between density of stained spots on electrophoregrams for normal and hypoxic animals were not found. The same situation of absence of significant differences was found in carbonylation of water-soluble proteins of heart and skeletal muscle of control animals and animals with nitrite hypoxia. This result may be considered as an evidence of absence of harmful action of nitrite

in the doses 1-5mg for 100gm of body weight of rats. But for the using nitrite as a remedy for blood pressure decreasing further investigations are necessary to get answers for questions formulated in this paper.

THE INVOLVEMENT OF ARP2/3 COMPLEX IN GLUTOXIM AND MOLIXAN EFFECT ON INTRACELLULAR Ca^{2+} CONCENTRATION IN MACROPHAGES

L.S. Kurilova, Z.I. Krutetskaya, A.A. Naumova,
N.I. Krutetskaya, S.N. Butov, V.G. Antonov
Department of Biophysics, Saint-Petersburg State University,
University emb. 7/9, Saint-Petersburg, 199034, Russia

Currently, a great number of disulfide-containing drugs altering the redox status and having a physiologically significant effect on cells have been developed and introduced into clinical practice. The pharmaceutical agent glutoxim®, disodium salt of oxidized glutathione (GSSG) with a platinum nanoadditive (PHARMA VAM, Moscow, Russia) is used as an immunomodulator and a hemostimulant in the integrated therapy of bacterial and viral diseases, psoriasis, as well as radio and chemotherapies of cancer. Another disulfide containing agent, molixan (a complex of glutoxim and inosine nucleoside), has a similar application. However, the mechanisms of the cellular and molecular effects of these drugs are not completely understood.

Earlier we found for the first time that GSSG, glutoxim, and molixan increase the intracellular Ca^{2+} concentration ($[Ca^{2+}]_i$) due to Ca^{2+} mobilization from the thapsigargin-sensitive Ca^{2+} stores and subsequent Ca^{2+} entry in rat peritoneal macrophages [1]. Using a wide range of agents affecting the components of signaling systems in cells, we have demonstrated that tyrosine kinases and tyrosine phosphatases [1], phosphatidylinositol kinases [2], the most important enzymes of the phosphoinositide system of signal transduction (phospholipase C and protein kinase C) [3] and the components of cyclooxygenase and lypoxygenase pathways of arachidonic acid metabolism [4] are the key players in the signaling cascade triggered by GSSG and glutoxim and leading to an increase in $[Ca^{2+}]_i$ in macrophages. It has also been found that elements of the actin cytoskeleton [5] and microtubules [6], small G proteins of the Ras family and vesicular transport [7], are involved in the effects of glutoxim and molixan on $[Ca^{2+}]_i$ in macrophages. Moreover it is found that glutoxim and molixan themselves induce actin cytoskeleton reorganization in macrophages: the cortical layer becomes wider and "looser" and actin clusters appear in the cytosol [5].

Arp2/3 (Actin-Related Proteins) complex, consisting of 7 conservative proteins, is one of the key participants in the procesess of actin filament formation from G-actin monomers. It stabilizes intermediates, consisting of two actin monomers, stimulating F-actin filament branching [8]. Therefore, Arp2/3 complex is the factor enhancing actin filament nucleation. Arp2/3 complex consists of two subunits Arp2 and Arp3, which are stucturally similar to the actin monomers, and five additional subunits [8]. Assembled Arp2/3 complex interacts with existing actin filament and line up in the way how actin is located in dimer. Thus Arp2/3 complex is the key player in the formation of new filaments, which line up at 70^0 angle to already existing filaments and form dense F-actin network [8].

Arp2/3 complex is involved in different cellular processes, which need actin filament reorganization, such as cortical layer reorganization, fillopodia formation, endosome transport regulation, endo- and exocytosis processes [9]. Arp2/3 complex can be activated via tyrosine kinase receptors, G-protein coupled receptors and integrin receptors.

Therefore, for further investigation of the role of actin filaments, actin-binding proteins, vesicular transport processes and exocytosis in signalling cascade, induced by glutoxim and molixan, the possible involvement of Arp2/3 complex in glutoxim and molixan effect on $[Ca^{2+}]_i$ in rat peritoneal macrophages was studied.

The procedure of macrophage culturing and an automated system for $[Ca^{2+}]_i$ recording with the use of the fluorescent probe Fura-2AM
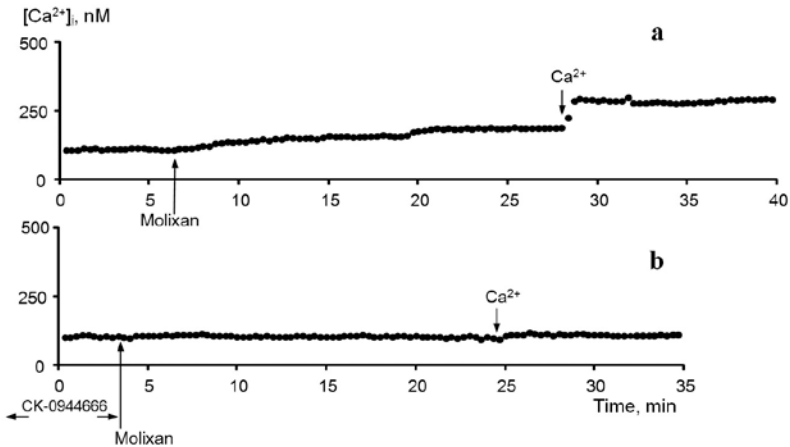
Fig. 1. The effect of CK-0944666 on Ca2+-responses induced by molixan in macrophages.

were described earlier [1]. The experiments were performed at a room temperature of 20–22°C on the second or third day of cell culturing. In order to elucidate Arp2/3 complex involvement in molixan or glutoxim effect on $[Ca^{2+}]_i$ we used effective Arp2/3 complex inhibitor compound CK-0944666 [10].

It has been demonstrated in control experiments that incubation of macrophages in the presence of 100 μg/ml molixan (fig. 1a) or 100 μg/ml glutoxim (not shown) for 20 min in a medium without calcium causes a significant increase in $[Ca^{2+}]_i$, which reflects mobilization of Ca^{2+} from intracellular Ca^{2+} stores. Addition of 2 mM Ca^{2+} to the external medium induces entry of Ca^{2+} into the cytosol, which is apparently mediated by depletion of the Ca^{2+} store (fig. 1a).

It has been found for the first time that preincubation of the macrophages with 100 µM CK-0944666 for 1 hour induces significant (about 80-100 %) inhibition of Ca^{2+}-mobilization and Ca^{2+} entry, evoked by molixan (fig. 1b) or glutoxim. The results suggest the involvement of Arp2/3 complex in the effect of molixan or glutoxim on $[Ca^{2+}]_i$ in macrophages.

The data of this and our earlier works [1-7] suggest that in signaling cascade, induced by molixan or glutoxim in macrophages the signaling proteins and complexes, which are connected with exocytosis prosesses are involved: tyrosine kinases, small G-proteins, vesicular transport mechanism, actin and tubulin cytoskeleton. Also, we have shown that molixan or glutoxim themselves cause actin cytoskeleton reorganization [5], in which Arp2/3 complex can be involved. Actin reorganization can mediate macrophage activation and facilitate the processes of endo- and exocytosis.

The abscissa axis shows time, min; the ordinate axis, Ca^{2+}-concentration in the cytosol, nM.

a – Macrophages were treated with 100 µg/ml molixan in Ca^{2+}-free medium, 21 min later Ca^{2+} entry was induced by addition of 2 mM Ca^{2+} to the external medium;

b – Cells were preincubated with 100 µM CK-0944666 for 1 hour in Ca^{2+}-free medium, after that 100 µg/ml molixan was added, 19 min later Ca^{2+} entry was induced by addition of 2 mM Ca^{2+} to the external medium.

Each recording is obtained for 40–50 cells and is typical of six experiments.

References
1. Kurilova L.S., Krutetskaya Z.I., Lebedev O.E., Antonov V.G. The effect of oxidized glutathione and its pharmacological analogue glutoxim on intracellular Ca^{2+} concentration in macrophages. Cell Tissue Biol. 2008. V. 2. P. 322-332.

2. Krutetskaya Z.I., Lebedev O.E., Kurilova L.S., Antonov V.G., Nozdrachev A.D. Possible involvement of phosphatidylinositol kinases in the effect of the oxidized glutathione and glutoxim on the intracellular Ca^{2+} concentration in macrophages. Doklady Biol. Sci. 2008. V.422. P. 296-297.

3. Krutetskaya Z.I., Lebedev O.E., Kurilova L.S., Antonov V.G., Nozdrachev A.D. The role of the key enzymes of the phosphoinositide signaling pathway in the effect of oxidized glutathione and glutoxim on intracellular Ca^{2+} concentration in macrophages. Doklady Biol. Sci. 2009. V. 428. P. 407-409.

4. Крутецкая З.И., Курилова Л.С., Антонов В.Г., Ноздрачев А.Д. Ингибиторы циклооксигеназ и липоксигеназ модулируют эффект глутоксима и моликсана на внутриклеточную концентрацию Ca^{2+} в макрофагах. ДАН. 2013.Т. 452. N 6. С. 690-693.

5. Kurilova L.S., Krutetskaya Z.I., Lebedev O.E., Krutetskaya N.I., Antonov V.G. The involvement of actin cytoskeleton in glutoxim and molixan effect on intracellular Ca^{2+}-concentration in macrophages. Cell Tissue Biol. 2012. V. 6. P. 240-247.

6. Krutetskaya Z.I., Kurilova L.C., Antonov V.G., Nozdrachev A.D. Involvement of microtubules in the effects of glutoxim and molixan on the intracellular concentration of Ca^{2+} in macrophages. Doklady Biol. Sci. 2013. V. 451. P. 196-198.

7. Курилова Л.С., Крутецкая З.И., Лебедев О.Е., Наумова А.А., Антонов В.Г. Участие процессов везикулярного транспорта в действии глутоксима и моликсана на внутриклеточную концентрацию Ca^{2+} в макрофагах. В сб. «Рецепторы и внутриклеточная сигнализация». Пущино. 2013. Т. 1. С. 213-217.

8. Duleh S.N., Welch M.D. WASH and the Arp2/3 complex regulate endosome shape and trafficking. Cytoskeleton. 2010. V. 67. P. 193-206.

9. Rouiller I., Xu X.P., Amann K.J., Egile C., Nikell S., Nicastro D., Li R., Pollard T.D., Volkmann N., Hanein D. The structural basis of actin filament branching by the Arp2/3 complex. J. Cell Biol. 2008. V. 180. P. 887-895.

10. Nolen B.J., Tomasevic N., Russel A., Pierce D.W., Jia Z., Mc Cormick C.D., Hartman J., Sakowicz R., Pollard T.D. Characterization of two classes of small molecule inhibitors of Arp2/3 complex. Nature. 2009. Vol. 460. P. 1031-1034.

DIFFERENT WAYS OF FOOT STIMULATION
FOR THE PREVENTION OF MUSCLE ATROPHY
CAUSED BY ANTIORTHOSTATIC HANGING IN RATS

M.V. Kuznecov, M.E. Baltin, A.A. Eremeev, T.V. Baltina
Kazan Federal University, Kremlevskaya str., 18, Kazan, 420008, Russia

It was previously suggested by other authors that unloading effects could be explained by the decrease in the supporting afferentation. For

explanation of the unloading effects in the literature is discussed of decrease afferentation support, which plays a role in the regulation of posture and locomotion. The aim of our study was to check the influence of the foot zones vibrostimulation on the functional state of the lower leg muscles in rats after 14 days of gravitational unloading. Stimulation of the sciatic nerve and increased electrical responses of muscle electromyogram was performed by the firm "Medicor" (Hungary), the intensity of stimulation ranged from 0.35 to 60 V and 0.5 ms duration. The studied parameters were the threshold, latency and maximum amplitude of the detected H-and M-responses, as was determined the ratio of maximum amplitudes of these responses (Hmax/Mmax).The experiments were performed in compliance with bioethical norms.

Differential testing of the heads of triceps tibia showed that the amplitude of the M-response of the lateral (LRM), medial gastrocnemius (MGM) and soleus muscle (SM) are reducedunder the conditions of modulated gravitational unloading as compared to the control. Moreover, this reduction is more pronounced in the SM. Bilateral vibratory stimulation of foot under these conditions prevented the decrease of the M-response amplitude in LRM, as compared to MGM and SM. These results indicate that vibrostimulation of the supporting zones of foot can prevent the atrophy of gastrocnemius (most of fibrils in this muscle are represented by muscle fibers of type II). One possible explanation of the observed effects is that the vibration leads to the activation of Ruffini endings and Pacinian corpuscles. Unilateral vibratory stimulation of foot (during the gravity discharge) also prevents decreasing of the amplitude of M-response in the muscles (ipsi-and contralateral side). However, the effect was less pronounced. The effect shows that in this process are involved the adaptive changes of central regulatory mechanisms after vibratory stimulation. Thus, our results showed that vibratory stimulation of supporting zones on the foot reduces the negative effects of exposure to gravity discharge. However, this effect is not the same for functionally different muscles.

A SIMPLE AND EFFECTIVE METHOD FOR THE ISOLATION OF CALPONIN FROM MOLLUSCAN SMOOTH MUSCLE

S.S. Lazarev, N.S. Shelud'ko

Zhirmunsky Institute of Marine Biology, Far Eastern Branch of the Russian Academy of Sciences, Palchevsky str. 17, Vladivostok, 690059 Russia

Calponin is a protein contained in the smooth muscle and non-muscle cells. In smooth muscle cells, calponin is found both in contractile

and in cytoskeletal domain [1]. The function of this protein is not clear. Initially, calponin was considered as a structural component of the contractile apparatus, because it binds to actin and inhibits Mg^{2+}-ATPase activity of actomyosin [2]. It is also assumed that it may be involved in stabilization of actin filaments of the cytoskeleton [3].

The standard method for isolating calponin involves heat treatment. However, this method proved to be ineffective for the isolation of calponin from the catch muscle of the mussels *Crenomytilus grayanus*, in whose muscle calponin was identified [4]. We have developed an essentially different method for isolating calponin from these muscles.

A key step in our method is the extraction of thin filaments (figure, lane 2) from myofibrils (figure, lane 1) with a solution containing (in mM): 75 KCL, 5 $MgCL_2$, 5 EGTA, 15 ATP, 5 sodium pyrophosphate, 0.5 DTT, 0.1 PMSF, 2.5 µg/ml LPN and 20 imidazole-HCL, pH 6.5.

The protein composition of the extract (figure, lane 2) is similar to protein composition of thin filaments [4]. Ultracentrifugation of the extract precipitates the complex of "natural" F-actin and tropomyosin, leaving calponin in the supernatant (figure, lane 3). The supernatant is fractionated with ammonium sulfate in the range from 0 to 30% (figure, lane 4). The ammonium sulphate precipitate is dissolved in 6 M urea and 1 M KCL, diluted with 0.5 M KCl to the original volume of the extract, and isoelectric precipitation is performed at pH 4.9. As a result, actin passes into the precipitate (figure, lane 5), while calponin remains in the
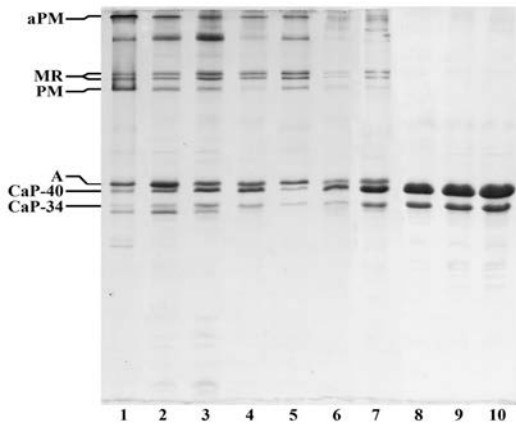
Stages of calponin isolation from smooth muscle of Crenomytilus grayanus: aPM - aggregated paramyosin; MR - myorod; PM - paramyosin; A - actin; CaP-40 - calponin-40 kDa; CaP-34 - calponin-34 kDa.

154

supernatant (figure, lane 6). After removal of actin by low-speed centrifugation, the preparation is concentrated by adding 40% ammonium sulfate, the pellet is dissolved in a minimal volume of 6 M urea, 1 M KCL (figure, lane 7) and dialyzed against of column buffer: 30 mM KCL, 6 M urea, 0.2 mM EGTA, 2 mM NaN_3, 0.5 mM DTT, 20 mM imidazole-HCL, pH 6.5. The dialyzed sample is applied to a CM Sephadex C-50, preequilibrated with column buffer. The column is eluted with a linear gradient produced by 120 ml of column buffer containing 500 mM KCL.

This method allows obtaining about 100 mg of chromato-graphically pure calponin from 100 g of the catch muscle of the mussel *Crenomytilus grayanus* (figure, lanes 8-10). Also, the method makes it possible to simultaneously obtain from this muscle of "natural" actin, tropomyosin, and the fraction of Ca^{2+}-sensitive proteins.

References

1. North A. J., Gimona M., Cross R. A., Small J. V. Calponin is localized in both the contractile apparatus and the cytoskeleton of smooth muscle cells. // J. Cell Science. 1994. V. 107. P. 437-444.
2. Abe M., Takahashi K., Hiwada K. Effect of calponin on actin-activated myosin ATPase activity. // J. Biochem. 1990. V. 108(5). P. 835-838.
3. Rozenblum G. T., Gimona M. Calponins: Adaptable modular regulators of the actin cytoskeleton. // J. Biochem. and Cell Biol. 2007. V. 40(2008) P. 1990-1995.
4. Dobrzhanskaya A. V., Matusovskaya G. G., Matusovsky O. S., Shelud'ko N. S. Thin filaments of bivalve smooth muscle may contain a calponin-like protein. // Biophysics. 2010. V. 55(5). P. 785-789.

NUCLEOTIDE-INDUCED INTERACTION BETWEEN MOTOR AND REGULATORY DOMAINS IN THE MYOSIN HEAD

Dmitrii I. Levitsky[1,2], Denis Markov[1], Olga Nikolaeva[2], Daria Logvinova[1,3], and Nikolai Padalko[1,4]

[1]*Bach Institute of Biochemistry, Russian Academy of Sciences, Moscow, Russia;*
[2]*Belozersky Institute of Physico-Chemical Biology, Moscow State University, Russia;*
[3]*Department of Biochemistry, School of Biology, Moscow State University, Moscow, Russia;*
[4]*Department of Biophysics, School of Physics, Moscow State University, Moscow, Russia*

In the previous works [1, 2], we compared thermally induced denaturation and aggregation of two isoforms of the isolated myosin head

(myosin subfragment 1, S1) containing different "essential" (or "alkali") light chains, A1 or A2. We applied differential scanning calorimetry (DSC) to investigate the domain structure of these two S1 isoforms. For this purpose, a special calorimetric approach was developed to analyze the DSC profiles of irreversibly denaturing multidomain proteins [1]. In the absence of nucleotides, two calorimetric domains were revealed in the S1 molecule, the more thermostable domain denaturing in two steps. Comparing the DSC data with temperature dependences of intrinsic fluorescence parameters and S1 ATPase inactivation, we have identified these two calorimetric domains as motor domain and regulatory domain of the myosin head, the motor domain being more thermostable. Some difference between the two S1 isoforms was only revealed by DSC in thermal denaturation of the regulatory domain, within the temperature range of 35–45 $^{\circ}$C [1]. The irreversible thermal denaturation of S1 is accompanied by its aggregation, and a significant difference between the two S1 isoforms was revealed in the temperature dependencies of their aggregation measured at low ionic strength. Under these conditions, the aggregation of S1 containing light chain A1 (but not A2) was strongly dependent on protein concentration, the increase of which (from 0.125 to 2.0 mg/ml) shifted the aggregation curve by ~10 $^{\circ}$C towards the lower temperatures. It was concluded that the aggregation properties of this S1 isoform at low ionic strength are basically determined by intermolecular interactions of the N-terminal extension of the A1 light chain (which is absent in the A2 light chain) with other S1 molecules, and these interactions seem to be independent of the S1 thermal denaturation as they may take place even at low temperature. It was proposed that these intermolecular interactions reflect the ability of the A1 N-terminal extension to form intramolecular interactions with the motor domain of the same S1 molecule (e.g., during the ATPase reaction, which is accompanied by considerable conformational changes in the myosin head) [2].

It was predicted in the previous works that the rotation of the regulatory domain (Lever arm) relative to the motor domain of the myosin head during the ATPase cycle can be accompanied by a rather tight interaction between the motor domain and the essential light chain associated with the regulatory domain [3–5]. To check this assumption, we compared thermal denaturation and aggregation of the S1 isoforms S1(A1) and S1(A2) in their ternary complexes S1-ADP-V_i and S1-ADP-BeF$_x$, which mimic the S1 ATPase intermediate states S1**-ADP-P$_i$ and S1*-ATP. DSC results showed that formation of these complexes leads to significant increase in the thermal stability of both S1 domains, and the

thermal transition corresponding to the regulatory domain shifts by more than 10 ^{o}C towards higher temperature, from 42–44 ^{o}C to 52–55 ^{o}C. Furthermore, no appreciable differences in the aggregation properties were observed between the two S1 isoforms in their ternary complexes S1-ADP-V$_i$ and S1-ADP-BeF$_x$. These results suggest that nucleotide-induced conformational changes in the myosin head are accompanied by a rather tight interaction of the regulatory domain (predominantly its essential light chain) with the motor domain, which decreases the probability of intermolecular interactions of the A1 N-terminal segment thus preventing unusual aggregation of the S1(A1) isoform at low ionic strength.

References

1. Markov D.I., Zubov E.O., Nikolaeva O.P., Kurganov B.I. & Levitsky D.I. (2010) «Thermal denaturation and aggregation of myosin subfragment 1 isoforms with different essential light chains». International Journal of Molecular Sciences 11, 4194–4226.

2. Markov D.I., Nikolaeva O.P. & Levitsky D.I. (2010) "Effects of myosin "essential" light chain A1 on the aggregation properties of the myosin head". Acta Naturae 2(2), 77–81.

3. Dominguez R., Freyzon Y., Trybus K.M. & Cohen C. (1998) "Crystal structure of a vertebrate smooth muscle myosin motor domain and its complex with the essential light chain: visualization of the pre-power stroke state". Cell 94, 559–571.

4. Borejdo J., Ushakov D.S. Moreland R., Akopova I., Reshetnyak Y., Saraswat L.D., Kamm K. & Lowey S. (2001) "The power stroke causes changes in the orientation and mobility of the termini of essential light chain 1 of myosin". Biochemistry 40, 3796–3803.

5. Lowey S., Saraswat L.D., Liu HJ., Volkmann N. & Hanein D. (2007) «Evidence for an interaction between the SH3 domain and the N-terminal extension of the essential light chain in class II myosins». J. Mol. Biol. 371, 902–913.

THE ROLE OF HYDROGEN SULFIDE IN REGULATION OF MOUSE ATRIUM CONTRACTILITY

A.S. Lifanova, N.N. Khaertdinov, A.R. Latfullina, G.F. Sitdikova

Institute of Fundamental Medicine and Biology, Kazan (Volga Region) Federal University, Kremlyovskaya st., 18, Kazan, 420008, Russia

Hydrogen sulfide (H$_2$S), along with nitric oxide and carbon monoxide refers to endogenously synthesized gaseous molecules. H$_2$S has a number of effects in the cardiovascular system, both in normal and in various pathological conditions [3, 5, 7]. In various tissues H$_2$S is synthe-

sized from L-cysteine by enzymes cystathionine γ-lyase, cystathionine β-synthase and 3-merkaptosulftransferase[4, 7]. There are available data on the cardioprotective role of H_2S, expressed in reducing myocardial damage in ischemia / reperfusion *in vitro* and *in vivo* [8].In the myocardium of the frog H_2S has a negative inotropic effect, which is mediated by the activation of the ATP-dependent K-channels (K (ATP) channel) and a decrease of the cAMP level in the cell [5]. In a rat aorta smooth muscle the relaxing effect of H_2S is mediated by activation of potassium conductance [2]. The aim of our work was to investigate the effects of exogenous and endogenous H_2S in mouse atrium, and to reveal the role of K-channels in the effects of H_2S.

Methods

The object of the study was the mouse Musmusculus. Mice were decapitated under ether anesthesia and dissection was performed. Experiments to determine the myocardium contraction were carried out usingBiopac Systems, Inc. (USA) set up equipped with isometric force transducers MLT 050 / D or TSD 125C with a measuring range of 0-50 grams. During the experiment, the preparation was perfused by Krebs solution of the following composition (in mM): NaCl - 154; KCl - 5; $CaCl_2$ - 2, $MgSO_4$ - 1, glucose - 11 ($t = 20$ºC, pH 7.2-7.4). Krebs solution was bubbled with carbogen during the entire experiment. The preparations were stimulated via two platinum electrodes (stimulator ESL-2 (Russia)) with a frequency 10 Hz, the signal amplitude of 40 mV, duration of the stimulus - 5 ms. NaHS was used as H_2S donor, which is widely used in research, as it dissociates to ions (Na^+) and anion hydrosulphide (HS-)in aqueous solution, which reacts with protons (H^+) to form H_2S. It is known that the physiological solution contains one third of the H_2S in the undissociated form, and the remaining two thirds exist in the form of HS-[6]. Also L-cysteine, β-cyano-L-alanine, tetraethylammonium (TEA), glibenclamide, diazoxide were used (Sigma).

Results and discussion

To reveal the effects of exogenous H2S on myocardial contractility, NaHSwas cumulatively applied in concentrations of 100, 200 and 300mkM Application NaHS at concentrations of 100, 200 and 300 mkM resulted in a significant decrease in the force of contraction to the 15 minute to $91 \pm 2\%$ ($n = 14$, $p < 0.05$), $71 \pm 4\%$ ($n = 14$, $p < 0.05$) and $49 \pm 4\%$ ($n = 15$, $p < 0.05$), respectively. Thus, NaHS has a negative inotropic effect in the atrium of the mouse.A similar effect of NaHS was observed previously in the myocardium of the frog, where it had more

pronounced effect already in concentration 100 mkM [5], which indicated on much more sensitivity of frog tissue.Tto identify the possible endogenous H2S synthesis in the atria of the mouse L-cysteine – substrate and β-cyano-L-alanine – inhibitor of H_2S synthesis. L-Cysteine at concentrations of 1, 10, 50 mkM resulted in a significant decrease in force contraction to $95 \pm 1\%$ ($n = 7$, $p < 0.05$), $89 \pm 1\%$ ($n = 5$, $p < 0.05$), $87 \pm 2\%$ ($n = 5$, $p < 0.05$), respectively whereas the use of higher concentrations of L-cysteine (1 mM) resulted in no significant change in the force of contraction, which was $103 \pm 6\%$ ($n = 3$, $p > 0.05$). Possibly, L-cysteine at low concentrations serves as a substrate of H_2S synthesis, but in high concentrations doinhibition of H_2S synthesis through mechanism of substrate-enzyme inhibiting. Application of β-cyano-L-alanine in a concentration of 1 mM led to significant increase of myocardial force of up to $112 \pm 5\%$ ($n = 5$, $p < 0.05$). Thus, the substrate of synthesis of H_2S - L-cysteine caused a reduction in the amplitude of myocardial contractions like the donor of H2S - NaHS, whereas blocker of cystathionine γ-lyase had the opposite effect - the increase in the amplitude of contraction. Our results suggest that, in mouse myocardium, as with other classes of vertebrates, there is a system of H_2S synthesis, which involves its modulatory effect on the myocardium. One of the mechanisms of muscle relaxation is activating potassium conductance [2]. TEA (2 mM) nonspecific inhibitor of different potassium channelswas used to investigate the involvement of the potassium channel in the effects of H_2S. Application of TEA resulted in an increase of contraction force to $140 \pm 11\%$ ($n = 8$, $p < 0.05$). In the background of TEA application of NaHSin concentrations of 100, 200, 300 mkM decreased the force of contraction to$96 \pm 1\%$ ($n = 8$, $p < 0.05$), $81 \pm 2\%$ ($n = 8$, $p < 0.05$), $65 \pm 1\%$ ($n = 8$, $p < 0.05$). It is known that K(ATP)-channels are widely distributed in the myocardium, and their activation is an important endogenous mechanism of cardioprotection during ischemic reperfusion injury and hypoxia[8]. According to the literature K(ATP)-channels are involved in the negative inotropic effect of NaHS in the myocardium of the frog [5]. It is also shown that in the myocardium of the rat NaHS led to a decrease in the duration of the action potential of cardiomyocytes, and this effect was partially blocked by an inhibitor of K (ATP) channels –glibenclamide [1]. Glibenclamide, an inhibitor of K(ATP)-channels, in the concentration of 50 mkM increased the contraction to $121 \pm 5\%$ ($n = 6$, $p < 0.05$) from control level, which is apparently due to the inhibition of K(ATP)-channels, membrane depolari-
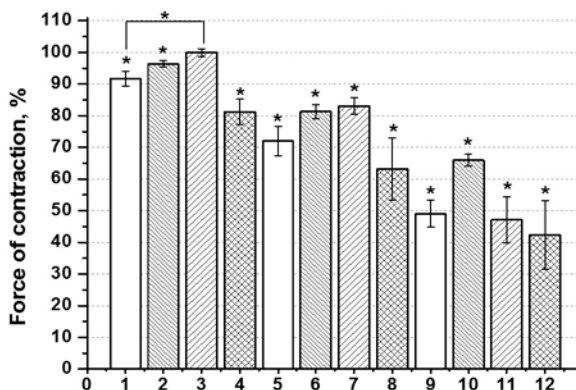
1, 5, 9- NaHS effect at concentrations 100, 200, 300 mkM in the control, 2, 6, 10- NaHS effect at concentrations 100, 200, 300 mkM after application of TEA, 3, 7, 11- NaHS effect at concentrations 100, 200, 300 mkM after application of glibenclamide, 4, 8, 12- NaHS effect at concentrations 100, 200, 300 mkM after application of background diazoxide.

zation and increased Cainward currents.On the background of glibenclamideNaHS at a concentration of 100, 200 and 300 mkM did not result in a significant reduction decrease force, which amounted to 99 $\pm$ 1% ($n = 6$, $p > 0.05$), which was significantly different from control values. In concentration of the effect NaHS was preserved and was 83 $\pm$ 2% ($n = 6$, $p < 0.05$), 47 $\pm$ 7% ($n = 6$, $p < 0.05$), respectively.

Diazoxide was used as an activator of K(ATP)-channels at a concentration of 100mkm, which application led to a significant decrease in the force of contraction to 96 $\pm$ 2% ($n = 7$, $p > 0.05$). On a background of diazoxide effect of application NaHS in concentrations of 100, 200, 300 mkM was 81 $\pm$ 4% ($n = 7$, $p < 0.05$), 63 $\pm$ 9% ($n = 5$, $p < 0.05$), 42 $\pm$ 10% ($n = 4$, $p < 0.05$).

The analysis of the effects of NaHS in different conditions was made by one-way ANOVA test followed by Bonferroni comparison and it was shown that only in glibenclamide condition the effect of NaHS in low concentration was different from others.

Thus, our results suggest that, in mouse myocardium, as with other classes of vertebrates, there is a system of H_2S synthesis, which has a modulating effect on cardiac contractile function. It was shown that the activation of K(ATP)-channels is mediated by effects NaHS in low concentrations, whereas at higher concentrations, apparently, other mecha-

nisms are involved. It is also assumed that the effect of the donor is not associated with H$_2$S other types of K-channels. Indeed, the mechanism of action of H$_2$S in the myocardium of mammalian is ambiguous and may comprise accordant with different facts and depending on the animal species, the K-channels, adenylate cyclase system and voltage-sensitive L-type Ca channels [9, 10, 11].

References

1. Abramochkin D., Moiseenko V., Kuzmin V. 2009. The effect of hydrogen sulfide on electrical activity of rat atrial myocardium. Bulletin of experimental biologe and medicine. 147 (6), 683–687

2. Baskakov M.B., Gusakova S.V., Zheludeva A.S. 2010 Effect of hydrogen sulfide on the contractile activity of smooth muscle cells from the rat aorta Bulletin of Siberian Medicine, № 6. 12-17

3. Zefirov A.L., Sitdikova G.F. 2010. Ion channels of excitable cells (structure, function, pathology). Kazan: Artkafe, 271 p.

Sitdikova GF Zefirov AL 2010. Hydrogen sulfide: from the Paris sewers to the signal molecule. Nature. 9, 29-37.

4. Haertdinov N.N., Ahmetshina D.R., Zefirov A.L., Sitdikova G.F. 2012. Hydrogen sulfide in the regulation of frog myocardial contractility. Biological membranes, 2012, Volume 29, № 4, p. 231-237

5. Abe K. The possible role of hydrogen sulfideasan endogenous neuromodulator/K.Abe,H.Kimura // J. Neurosci.-1996.-V.-16.-P.1066–1071.

6. Gadalla M., Snyder S. 2010. Hydrogen sulfide as gasotransmitter. J. Neurochem. 113, 14–26.

7. Geng B. H2S generated by heart in rat and its effects on cardiac function / B.Geng, J.Yang, Y.Qi, J.Zhao, Y.Pang, J.Du, C.Tang // Biochem. Biophys. Res. Commun.-2004.-V.313.-P.362-368.

8. Sun Y., Cao Y., Wang W., Ma S., Yao T., Zhu Y. 2008. Hydrogen sulfide is an inhibitor of L-type calcium channels and mechanical contraction in rat cardiomyocites. Cardiovasc. Res. 79 (4), 632–641.

9. Xu M. Electrophysiological effects of hydrogen sulfide on guinea pig papillary muscles / M.Xu, Y.M.Wu, Q.Li, F.W.Wang, R.R.He // Acta Physiol. Sin.-2007.-V.59.-P.215-220.

10. Yang G. H2S as a physiologic vasorelaxant: hypertension in mice with deletion of cystathion in eγ-lyase / G.Yang, L.Wu, B.Jiang, W.Yang, J.Qi, K.Cao, Q.Meng, A.K.Mustafa, W.Mu, S.Zhang, S.H.Snyder, R.Wang // Science.-2008.-V.322.-P.587–590.

THE USE OF FLUORESCENTLY LABELLED MYOSIN "ESSENTIAL" LIGHT CHAINS AS A NEW APPROACH TO STUDY INTER-DOMAIN INTERACTIONS IN THE MYOSIN HEAD

Daria Logvinova[1,2], Olga Nikolaeva[3], Denis Markov[1], Nikolai Sluchanko[1], Dmitry Ushakov[4], and Dmitrii I. Levitsky[1,3]

[1]*Bach Institute of Biochemistry, Russian Academy of Sciences, Moscow, Russia,*
[2]*Department of Biochemistry, School of Biology, Moscow State University, Moscow, Russia*
[3]*Belozersky Institute of Physico-Chemical Biology, Moscow State University, Russia*
[4]*King's College, London, United Kingdom*

It is generally accepted that functioning of the myosin head as a molecular motor is based on the rotation of the regulatory domain (Lever arm) relative to the motor domain of the head, which occurs during the ATPase cycle. It was predicted in the previous works that this rotation can be accompanied by a rather tight interaction between the motor domain and the essential light chain (ELC) associated with the regulatory domain [1–3]. We applied differential scanning calorimetry (DSC) to investigate the domain structure of the isolated myosin head (myosin subfragment 1, S1) both in the absence of nucleotides and in the ternary complexes S1-ADP-V_i, S1-ADP-AlF_4^- and S1-ADP-BeF_x which mimic the S1 ATPase intermediate states $S1^{**}$-ADP-P_i and $S1^*$-ATP. DSC results showed that formation of these complexes leads to significant increase in the S1 thermal stability, and the thermal transition presumably corresponding to the regulatory domain shifts by more than 10 ^{o}C towards higher temperature. It was proposed from these results that the nucleotide-induced increase in the thermal stability of the regulatory domain is caused by the interaction of this domain (predominantly its essential light chain) with the motor domain. However, this assumption was based on indirect data obtained from comparison of the DSC data with temperature dependences of fluorescence parameters of the tryptophan residues which are located only in the S1 motor domain, but not in the regulatory domain [4]. To obtain direct evidence for the above assumption, it was necessary to identify on the S1 DSC profile the calorimetric domain corresponding to thermal unfolding of the regulatory domain. For this purpose we applied a new approach based on the use of ELC fluorescently labeled at single Cys residue.

Several ELC mutants containing single Cys residues at different positions in the C-terminal half of the protein (mutations T127C/C180A, G142C/C180A, and E160C/C180A), as well as ELC WT containing Cys180, were obtained as recombinant proteins containing His tag at the C-terminus of ELC as described earlier [5]. Native ELC (without His tag) we prepared from skeletal muscle myosin. The isolated ELC were fluorescently labeled with 1,5-IAEDANS at single Cys residues, and fluorescently labeled ELC was exchanged into S1 as described in [6]. The thermally induced changes in the fluorescence parameters of these ELC associated with the S1 regulatory domain were recorded at the same heating rate (1°C/min) as for DSC experiments, and temperature dependences of fluorescence obtained in this way were compared with corresponding DSC data and with the changes in tryptophan fluorescence that reflect the thermal unfolding of the S1 motor domain.

It was shown that in the absence of added nucleotides the changes in fluorescence parameters of any labeled ELC studied to date (i.e. ELC with single Cys residues at positions 180, 142, and 127) does not significantly differ from those of the tryptophan fluorescence (half-transition at ~48°C) and from the maximum temperature of calorimetric domain corresponding to the melting of the S1 motor domain on the DSC profile. This can be explained, at least for ELC with Cys180 or Cys142, by literature data showing that C-terminal part of ELC can interact with the S1 motor domain under these conditions [7, 8]. In contrast, in the ternary complexes S1-ADP-V_i, S1-ADP-AlF_4^- and S1-ADP-BeF_x the changes in fluorescence parameters of labeled ELC were observed at lower temperatures (by 2–4 $^{\circ}$C) than the changes in the tryptophan fluorescence, but within the temperature range of 49–54 $^{\circ}$C, which is just the range where the thermal unfolding of the S1 regulatory domain is proposed from the DSC data (i.e. at much higher temperatures, by ~10°C, than in the absence of nucleotides). These nucleotide-induced changes in the temperature dependences of fluorescence parameters were generally similar for all S1 samples studied to date, although some differences were observed in half-maximal transitions depending on the position of the fluorescently labeled Cys residue in ELC.

It should be noted that these effects were observed for both recombinant ELC WT (with Cys180) containing His tag at the C-terminus and native ELC (without His tag). This means that the presence of the His tag at the C-terminus of ELC has no appreciable influence on the thermally induced changes in the fluorescence of a label specifically attached to Cys180.

Overall, the results obtained using fluorescently labeled ELC corroborate the DSC data with respect to a significant increase in the thermal stability of the S1 regulatory domain caused by formation of the ternary complexes S1-ADP-V_i, S1-ADP-AlF_4^- and S1-ADP-BeF_x. This is in favor of the proposed nucleotide-induced interaction between the motor domain and ELC associated with the regulatory domain, which leads to significant increase in the thermal stability of the S1 regulatory domain.

References

1. Dominguez R., Freyzon Y., Trybus K.M. & Cohen C. (1998) "Crystal structure of a vertebrate smooth muscle myosin motor domain and its complex with the essential light chain: visualization of the pre-power stroke state". Cell 94, 559–571.

2. Borejdo J., Ushakov D.S. Moreland R., Akopova I., Reshetnyak Y., Saraswat L.D., Kamm K. & Lowey S. (2001) "The power stroke causes changes in the orientation and mobility of the termini of essential light chain 1 of myosin". Biochemistry 40, 3796–3803.

3. Lowey S., Saraswat L.D., Liu HJ., Volkmann N. & Hanein D. (2007) «Evidence for an interaction between the SH3 domain and the N-terminal extension of the essential light chain in class II myosins». J. Mol. Biol. 371, 902–913.

4. Markov D.I., Zubov E.O., Nikolaeva O.P., Kurganov B.I. & Levitsky D.I. (2010) «Thermal denaturation and aggregation of myosin subfragment 1 isoforms with different essential light chains». International Journal of Molecular Sciences 11, 4194–4226.

5. Ushakov D.S., Caorsi V., Ibanez-Garcia D., Manning H.B., Konitsiotis A.D., West T.G., Dunsby C., French P.M., and Ferenczi M.A. (2011) "Response of rigor cross-bridges to stretch detected by fluorescence lifetime imaging microscopy of myosin essential light chain in skeletal muscle fibers". J. Biol. Chem. 286, 842–850.

6. Zaager S. and Burke M. (1988) "Temperature and ionic strength dependence of the subunit interactions in vertebrate skeletal myosin. A comparison of the interaction between the alkali light and heavy chains of mammalian and avian myosin". J. Biol. Chem. 263, 13891–13895.

7. Rayment I., Rypniewski W., Schmidt-Base K., Smith R., Tomchick D., Benning M., Winkelmann D., Wesenberg G. and Holden H. (1993) «Three-dimentional structure of myosin subfragment 1: A molecular motor». Science 261, 50–58.

8. Milligan R.A. (1996) "Protein-protein interactions in the rigor actomyosin complex". Proc. Natl. Acad. Sci. USA 93, 21–26.

EVOLUTION OF CELL MOTILITY
DURING TUMOR PROGRESSION

M.E. Lomakina, A.S. Chikina, A.Y. Alexandrova

*Blokhin Russian Cancer Research Center of the Russian Academy
of Medical Sciences, Moscow, Russia*

Oncological transformation leads to alterations of migration properties of tumor cells and gives them opportunity to invade surrounding tissues and to form distant metastases. The alterations of actin cytoskeleton structure and their regulation make a considerable contribution to acquisition of these capacities. In the course of tumor progression the more aggressive clones are selected, they could change their morphology and the mode of migration depending on the environmental conditions. The switching between different migration modes makes cell migration more effective.

One of the characteristically features of tumor progression is gradual transition from collective to individual migration. At first steps of tumor progression cells could migrate by group without the destruction of cell-cell adhesions (collective migration). Collective migration usually provides tumor cell invasion into surrounding tissues. Further, epithelial cells lose their cell-cell adhesions, dissociate from each other, gain polarized fibroblast-like morphology and migrate individually [1]. Individually migrating cells usually are involved into the formation of distant metastases.

Two major modes of individual cell migration are distinguished: mesenchymal migration (cells migrate in fibroblast-like manner, using lamellipodium and ruffle formation) and amoeboid migration (cells squeeze like amoebas, using the formation of specific structures called blebbs) [2, 3]. These modes of migration can occur in both normal and tumor cells. They are based on different molecular mechanisms. Each mode of migration is characterized by specific cell morphology and actin architecture.

Normal cells which show mesenchymal mode of migration usually have elongated morphology. They are polarized and have front active edge (leading edge) and stable contractive back. Actin cytoskeleton of such cells consists of strong actin stress-fibers, which are connected with extracellular matrix (ECM) by adhesive structures, called focal adhesions. Mesenchymal cells could secret matrix metalloproteinases (MMP) in the region of focal adhesions. It leads to degradation of ECM and facilitates cell migration. Zone of active Arp2/3-induced actin polymerization, which provides the generation of dense actin network and formation of lamellipodia and ruffles is localized at leading cell edge [3–5].

Cells migrating by amoeboid mode usually have rounded morphology. Their actin cytoskeleton consists mainly of cortical actin network

and lacks actin bundles. Formation of specific protrusions named blebbs is characteristic for amoeboid migration [6]. This formation is based on intracellular hydrostatic pressure generated by actomyosin contraction which causes rupture of either the actin cortex itself [7] or the linkage between actin and plasma membrane [8]. Afterwards the actin cortex is reassembled by formin dependent polymerization and blebb structure is stabilized. Cells using amoeboid mode of migration do not form focal adhesions with ECM. This mode of movement is a kind of squeezing upon substratum and is usually observed in 3D matrixes. Amoeboid migration is typically used by leucocytes [9].

Some authors distinguish the intermediate mode of migration, called amoeboid-fillopodial migration. In this case cell migrates using a lot of filopodia and it seems to be transitional stage between mesenchymal and amoeboid migration modes [10]. The capacity to switch from one mode of migration to another is called plasticity. Plasticity is typical mainly for tumor cells, but some types of normal leucocytes and stem cells could also undergo such transitions from one mode of migration to another [11,12].

Mesenchymaly migrating tumor cells have all features typical for this mode of migration (formation of lamellipodium, formation of focal adhesions), but steel their movement is quite different from the movement of normal mesenchymal cell. This is determined by differences in cytoskeleton structure of normal and oncologically transformed cells [13]. Transformed cells usually can't form mature focal adhesions (focal contacts) with ECM, they have only small dot-like focal complexes. These cells lack strong actin bundles and have no tight actin bundle along lateral sided of the cell, which normally protect lateral edge from protrusion formation. Thus, in tumor cells protrusive activity is redistributed and lamellipodia could be formed not only at the leading edge, but also all over the cell perimeter [14]. It gives cell the opportunity for easy turn, and facilitates effective search of ways of invasion to surrounding tissues or intravasation. Moreover, during tumor progression cells could increase secretion of matrix metalloproteinases (MMP), which destroy the proteins of ECM. This also facilitates tumor cell migration and their dissemination.

The architecture of actin network also undergoes essential alterations during tumor progression: sufficiently large holes appear in dendritic network, it becomes less regular. On the model of neoplastic transformation (SV-40 virus transformed human fibroblasts), which consists from cells with different level of malignization, we found that even on 2D substratum transformation causes alterations of actin cytoskeleton leading to initiation of mesenchymal-amoeboid transition (MAT). Cells of less transformed line

have a lot of filopodia (like in transitional filopodial-amoeboid stage) and cells of more transformed line form numerous protrusions with irregular actin network and well pronounced blebb-like thickenings. By our opinion these formations could be prototype of blebbs on 2D substratum. Therefore, cytoskeleton organization of neoplastic cells is very mobile and it provides an intermediate phenotype between mesenchymal and amoeboid cell. The characteristics of actin cytoskeleton gained in course of tumor progression provide capacity for plasticity of tumor cells. The variety of migration modes available to the cell and the ability of the cell to switch between this modes of migration facilitates cell passing through tissue barriers, gives possibility to intravasate to blood or lymph vessels, to overcome considerable distances and to form distant metastases.

Dominance of one or another mode of migration depends on the balance of small GTPases of Rho protein family [9, 15]. Small GTPase Rac activates WASP (Wiscott Aldridch Syndrome Protein), which consequently activates Arp2/3-complex, providing actin network polymerization and formation of lamellipodia at the leading cell edge [16,17]. Small GTPase Rho mediates light myosin chain phosphorylation leading to enhancement of actomyosin interaction and cell contraction. This way stimulates blebb formation [8]. Thus, predominance of active form of Rac stimulates mesenchymal cell migration and predominance of Rho stimulates amoeboid cell migration. Our studies revealed that as the result of Arp2/3-complex (Rac induced way) inhibition in HT1080 cells (human sarcoma cell line) significant amount of cells overcome transition from mesenchymal migration, which is more typical for them, to amoeboid migration. Moreover, lower concentration of inhibitor causes enhanced filopodia fortmation and higher concentration induces amoeboid morphology: cells gain rounded morphology and form blebbs. We could not see this effect on normal human subcutaneous fibroblasts 1036, Arp2/3 inhibition stopped their migration at al. Therefore, we can stand that under inhibition of lamellipodia formation normal fibroblasts could not proceed MAT. This experiment confirms that plasticity is a specific characteristic of tumor cells. Normally plasticity is typical only for leucocytes, which need to migrate in vessels and invade into inflammatory tissues, overcoming tissue barriers, and also for stem cells. Acquisition of capacity of tumor cells to undergo mesenchymal-amoeboid (MAT) and amoeboid-mesenchymal transition (AMT) gives them opportunity to adapt their type of migration to architecture and stiffless of surrounding tissue and to choose the most effective way to move through the barriers.

References

1. Yamazaki D., Kurisu K/ and Takenawa T. 2005. Regulation of cancer cell motility through actin reorganization. Cancer. Sce. 96 (7), 379-386.
2. Wolf K., Muller R., Borgmann S., Brocker E., Friedl P. 2003. Amoeboid shape change and contact guidance: T-lymphocyte crawling through fibrillar collagen is independent of matrix remodeling by MMPs and other proteases. *Blood*. 102, 3262–3269.
3. Ridley A. 2011. Life at the leading edge. *Cell*. 145, 1012–1022.
4. Svitkina T., Borisy G. 1999. Arp2/3 complex and actin depolymerizing factor/cofilin in dendritic organization and treadmilling of actin filament array in lamellipodia. *Cell Biol*. 31, 1009–1026.
5. Pollard T., Borisy G. 2003. Cellular motility driven by assembly and disassembly of actin filaments. *Cell*. 112(4), 453–465.
6. Charras G., Paluch E. 2008. Blebs lead the way: how to migrate without lamellipodia. *Nature*. 9(9), 730–736.
7. Tinevez, J.Y., U. Schulze, G. Salbreux, J. Roensch, J.F. Joanny, and E. Paluch. 2009. Role of cortical tension in bleb growth. *Proc. Natl. Acad. Sci. USA*. 106:18581–18586.
8. Charras, G.T., C.K. Hu, M. Coughlin, and T.J. Mitchison. 2006. Reassembly of contractile actin cortex in cell blebs. *J. Cell Biol.* 175:477–490.
9. Lämmermann, T., M. Sixt. *2009. Mechanical modes of 'amoeboid' cell migration. Curr. Opin. Cell Biol. 21:636–644.*
10. Friedl P., Wolf K. 2010. Plasticity of cell migration: a multiscale tuning model. *Cell Biol*. 188, 11–19.
11. Cougoule C., Goethem E., Le Cabec V., Lafouresse F. 2012. Blood leukocytes and macrophages of various phenotypes have distinct abilities to form podosomes and to migrate in 3D environments. *Eur. J. Cell Biol.* 91, 938–949.
12. Otto A., Collins-Hooper H., Patel A., Dash P., Patel K. 2011. Adult skeletal muscle stem cell migration is mediated by a blebbing/amoeboid mechanism. *Rejuvenat. Res*. 14(3), 249–260.
13. Vasiliev J.M. 2004. Cytoskeletal mechanisms responsible for invasive migration of neoplastis cells. *Int. J. Dev*. Biol. 48, 425-439.
14. Lomakina M.E., Alexandrova A.Y. 2009. Analysis of changes induced by oncogene N-RAS expression in pattern and distribution of pseudopodial activity of fibroblasts. *Ontogenez*. 40(4):282-93.
15. Chan A., Coniglio S., Chuang Y., Michaelson D., Knaus U., Philips M., Symons M. 2005. Roles of the Rac1 and Rac3 GTPases in human tumor cell invasion. *Oncogene*. 24, 7821–7829.
16. Bergerta M., Chandradossa S., Desaia R., Palucha E. 2012. Cell mechanics control rapid transitions between blebs and lamellipodia during migration. *Proc. Natl. Acad. Sci. USA*. 109(36), 14434–14439.
17. Friedl P., Wolf K. 2003. Tumour-cell invasion and migration: diversity and escape mechanisms. *Nat. Rev. Cancer*. 3, 362–374.

ARPIN AS A NOVEL REGULATOR OF CELL MOTILITY AND ITS ROLE IN TUMOR INVASION

M. E. Lomakina[1], I. Dang[2], V. D. Ermilova[1], T.A. Chipysheva [1], A. Gautreau[2], A. Y. Alexandrova[1]

[1] Blokhin Russian Cancer Research Center of the Russian Academy of Medical Sciences;

[2] Laboratoire d'Enzymologie et Biochimie Structurales, CNRS

Enhanced migration activity is an important aspect of metastatic development. Nowadays several molecular mechanisms which underlying cell migration and dissemination are known. One of main mechanisms is the formation of protrusion at the active cell edge based on Arp2/3-induced polymerization of branched actin network. Currently the active search of proteins and other agents which could regulate cell migration is carried out. A group of French scientists in the laboratory of A. Gautreau have found out a new protein, which was characterized as the inhibitor of Arp2/3-complex activity and called Arpin (Arp Inhibitor). It was shown that Arpin could play as a brake in the process of protrusion formation and could play as a "steering wheel" regulating cell migration *in vitro* [1]. Thereby, in seems to be very interesting to analyze the role of Arpin in regulation of cell migration *in vivo* in the process of tumor progression and metastasis.

The aim of our work was to study the role of Arpin in the process of tumorogenesis in the context of human breast tumors.
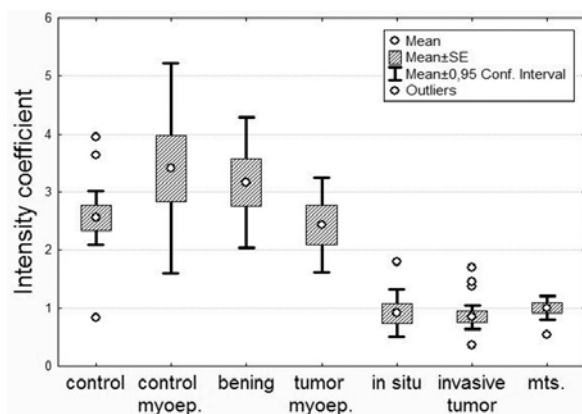
Quantitative analysis of Arpin level in normal tissues of human mammary gland, benign proliferation, different breast cancers and metastases to lymph nodes.

We performed the immunohistochemistry of mammary gland tissue and studied the distribution of Arpin. We studied the frozen sections of human breast tumors after mastectomy provided on the base of Blokhin Cancer Research Center. There were benign fibroadenoma, carcinoma in situ, breast cancer of luminal type and tumor metastases to lymph nodes between our samples. The sections of normal tissue taken from mammary gland near the tumor were used as a control. The antibodies to keratin 8 (marker of luminal epithelium), keratin 17 (marker of myoepithelium), laminin (marker of basal membrane), smooth-muscle actin and some others were used as additional markers for detection of mammary gland structures and determination of tumor type [2].

It was shown that Arpin is expressed both in luminal and myoepithelium cells of normal mammary gland ducts and lobules. The level of Arpin in myoepithelium cells were higher than in the cells of luminal epithelium. Arpin was frequently colocalised with actin bundles in myoepithelium cells (marked by antibodies to alpha-smooth actin). Level of Arpin in benign fibroadenomas did not significantly changed in comparison with its level in normal luminal epithelium of ducts and lobules and was rather high. However, level of Arpin in tumor cells of carcinoma in situ, invasive carcinomas of luminal type and metastases in lymph nodes was significantly reduced, compared to normal tissue. Therefore, the malignant stage of tumor transformation was associated with decrease of Arpin level in tissue, which could denote that Arpin inhibits tumor invasion.

To understand better the dependence of Arpin level of motile status of cells we also analyzed the level of Arpin in different non-transformed and transformed cells lines from the collection of our institute using immunofluorescent staining and western blot analysis. Cells with different Arpin level were detected. We found three cell lines, than lack Arpin (MRC-5V2, HT-1080, K562) according to the Western blot analysis. All three of them are transformed and have strong alterations in morphology and migration characteristics, compared to their homologous more normal counterparts (MRC-5, MRC-5V1, 1036 and others), that express Arpin. It was shown that all these three Arpin-free cell lines could invade 3D matrigel. This data is consistent with our data archived from immunohistochemistry of biopsic material and gives evidence of eventual inhibitory role of Arpin in regulation of invasion.

References

1. I. Dang et al. 2014. Nature. 4; 503(7475):281-284.
2. Trojanovsky et al. 1989. J. Cell Sci. 93: 419-426.

EFFECT OF NIFEDIPINE ADMINISTRATION ON PROTEOLYTICAL EVENTS IN RAT SOLEUS MUSCLE UNDER 3-DAY OF HINDLIMB SUSPENSION

Y.N. Lomonosova[2], S.P. Belova[2], T.L. Nemirovskaya[1,2]

[1]Faculty of Basic Medicine, Lomonosov Moscow State University,
117191 Lomonosovsky pr. 31/5, Moscow, Russia;
[2]Institute for Bio-Medical Problems, RAS,
Khoroshevskoe Highway 76a, 123007 Moscow, Russia

We tested the hypothesis that prevention of cytoplasmic calcium influx via L-calcium channels during 3 days of rat hindlimb suspension could lead to decrease of μ-calpain level, and calcium leakage to cytoplasm could serve a triggering mechanism, which activated the work of ubiquitin-proteosomic pathway in rat soleus. It have been demonstrated earlier that L-channels blocking diminished the calcium level in muscle fibers during hindlimb suspension (Mukhina A.M. et all, 2008). 21 male Wistar rats were divided into 3 groups: Control group (C, n=7), Hindlimb suspended rats during 3 days (HS, n=7), HS+nifedipin administration (in m.soleus twice a day (7 mg/kg in 0,3% DMSO, HSN, n=7). M.soleus weight and MHC protein content haven't been changed after HS. We didn't reveal neither μ-calpain level increase, nor desmin destruction in HSN group in contrast to HS group. However MuRF-1 и MAFbx mRNA levels were both increased and pAkt content was decreased in both hidlimb suspended groups. In conclusion: μ-calpain content under soleus unloading could be regulated by calcium level modulation, destruction of the cytoskeletal protein desmin occurs up to reduce the contractile proteins and noticeable muscle atrophy. The dihydropyridin channel blocking (calcium level modulation in the cytoplasm of muscle fibers) doesn't prevent decrease of pAkt content and MuRF-1 and MAFbx elevated level.

ACTIVATION OF EUKARYOTIC ELONGATION FACTOR 2 KINASE IN SKELETAL MUSCLE UNDER HINDLIMB UNLOADING

Yu.N. Lomonosova, B.S. Shenkman

Institute for biomedical problems, Khoroshevskoye shosse, 76a,
Moscow, 123007, Russia;
E-mail: ylomonosova@mail.ru

Profound decrease of postural (mostly antigravitational m.soleus) and locomotor skeletal muscle mass and/or decrease of functional load-

ing to the muscles is typical not only for humans and animals exposed to zero gravity but also for patients with traumatological and neurological pathology. Muscles being unloaded and/or immobilized under some period show decrease of contractile characteristics, protein mass and fiber size (atrophy) [Thomason et al., 1990; Chopard et al., 2001]. Decrease of protein synthesis rate and increase of proteolysis were shown under functional unloading of skeletal muscle [Loughna et al., 1986; Kandarian et al., 2002]. There is deficiency in studies analyzing mechanisms of protein synthesis rate decrease. Works exploring polypeptide elongation rate in skeletal muscle under the unloading are absolutely absent. It was shown that eukaryotic elongation factor 2 phosphorylation (eEF2) by its specific kinase (eEF2k) 10-100 fold decreases eEF2 affinity to ribosome, which leads to drop of protein synthesis rate [Carlberg et al., 1990]. We have supposed that protein synthesis rate decrease occurred due to eEF2k activation in m. soleus under functional unloading. Male Wistar rats were divided into 4 groups: control group («C», n=7), hindlimb unloaded group during 3 days («3HS», n=7), 7 («7HS») and 14 days («14HS»). Hindlimb unloading was carried out according to Novikov-Ilyin's technique with Morey-Holton's modification. The rats were sacrificed by overtin overdose (75 mg/kg body wt), each m. soleus was weighted, immediately frozen in liquid nitrogen and stored 80°C below zero until analysis. Atrophy of m. soleus was found in 7 and 14 days hindlimb unloaded group. Total and phosphorylated levels of p70S6-kinase downstream of mTOR remained unchanged in skeletal muscle after 3 and 7 days of hindlimb unloading. Eukaryotic elongation factor 2 (eEF2) is one of the important member of eEF family catalyzing simultaneous translocation tRNA and mRNA on a 80S ribosome [Taylor et al., 2007]. eEF2 expression didn't change under hindlimb unloading, but degradation of eEF2 was found after 7 days of the unloading and reached 50% to the 14 days of unloading. It's known that eEF2 phosphorylation by its specific eEF2-kinase leads to prevention of translation elongation [Browne et al., 2002]. We showed that P-eEF2 content increased by 60% as early as after 3 days unloading. When analyzing eEF2k expression we observed two-fold increase of eEF2k mRNA level in m. soleus after 3 days of unloading as compared to control group. It is concluded that increase in eEF2 phosphorylation is sufficiently associated with the activation of eEF2-kinase in rat m. soleus under long period of hindlimb unloading.

TIME-COURSE CHANGES OF THE KEY ANABOLIC MARKERS DURING EARLY PERIOD OF HINDLIMB UNLOADING

Yu.N. Lomonosova, B.S. Shenkman

State Scientific Center RF Institute of Bio-medical Problems, RAS, Khoroshevskoye Shosse, 76A, Moscow, 123007, Russia

The unloading-induced muscle atrophy is known to be developed due to decrease of protein synthesis as well as to increase of protein degradation. But it is still unknown impairment of which anabolic signaling pathway is mostly involved in the atrophy development. As a matter of fact the alteration of protein synthesis could be associated with the mTOR downstream S6 kinase decline, decrease of Akt-dependent GSK3β phosphorylation or increase of eukaryotic elongation factor-2 phosphorylation. At the same time the protein synthesis intensity is believed to be partially associated with the ribosomal biogenesis i.e. ribosomal RNA expression.

The study was purposed to analyze some of the above mentioned anabolic signaling molecules during the early period of the unloading-induced rat soleus muscle atrophy development.

It was previously established that after 3 days of hindlimb unloading the intensity of protein synthesis in rat soleus muscle was found to be 20% declined. But we didn't find any changes in the content of the phosphorylated p70S6K in rat soleus neither after three nor after 7 days of hindlimb unloading. However the content of phosphorylated (inactivated) eukaryotic elongation factor – 2 is 1.5-fold increased after 3 and 7 days of unloading. We also observed the increased (2-3 fold) expression of eef-2 kinase mRNA at the same time points.

Thus we ascribe the early drop of the protein synthesis rate to the impairment of the elongation process. But during these early time points of the fiber atrophy development we also observed the sufficient decrease of the 28S ribosomal RNA content.

It is concluded that although the mTOR-dependent ribosomal kinase activity is not altered during the early period of hindlimb unloading, the protein synthesis intensity decreased due to the impairment of the elongation machinery and decline of ribosomal biogenesis.

THE EFFECTS OF ACUTE ENDURANCE EXERCISE FOLLOWED BY AMINO ACIDS FEEDING ON MOLECULAR RESPONSE IN HUMAN SKELETAL MUSCLE

E.A. Lysenko[1], A.V. Bachinin[1], D.V.Popov[1,2], T.F.Miller[1], O.L.Vinogradova[1,2]

[1] *Institute for Biomedical Problems of Russian Academy of Sciences, Moscow, Russia;*
[2] *Lomonosov Moscow State University, Moscow, Russia*

Endurance exercise results in pronounced metabolic changes in skeletal muscle and activates AMP-dependent protein kinase (AMPK), Ca-calmodulin-dependent protein kinase and mitogen-activated protein kinase p38. This leads to activation of peroxisome proliferatior-activated receptor gamma coactivator 1 alpha (PGC-1α) a master regulator of mitochondrial biogenesis. On the other hand, aerobic exercise is known not to increase the postexercise myofibrillar fractional synthesis rate probably because of negative regulation of mTORC1 pathway by AMPK. Moreover, it might be followed by muscle protein breakdown by activation of ubiquitin proteasome system. The aim of present study was to examine the possibility to eliminate the negative effects of endurance exercise by essential amino acids feeding during postexercise recovery. Nine amateur endurance trained males carried out test sessions: endurance exercise (70 min) and endurance exercise followed by branched-chain amino acids (0.2 g/kg of body weight) feeding. Biopsy samples from m.vastus lateralis were taken before, 40 min, 5 h and 21 h after termination of endurance exercise. Expression of metabolic (PGC-1a, TFMs) and catabolic (Myostatin, Atrogin-1, MuRF) genes were evaluated by real-time PCR. Expression of anabolic and catabolic signaling regulators (p70, FOXO1) as well as PGC-1 alpha in cytoplasmic and nuclear fraction were measured by Western blot.

Endurance exercise alone and combined with amino acids feeding was accompanied by significant accumulation of capillary blood lactate level. Expression of mitochondrial biogenesis genes was increased as well as activation of their upstream kinases. Expression of the exercise-induced catabolism markers was different in two groups. Thus administration of amino acids may be used to optimize the effect of endurance exercise.

AMINO ACID NEUROTRANSMITTERS OF CNS AS SIGNALING MOLECULES AT THE VERTEBRATE NEUROMUSCULAR JUNCTION: FACTS AND HYPOTHESES

A.I. Malomouzh

Kazan Institute of Biochemistry and Biophysics, Russian Academy of Sciences, P.O. box 30, Kazan, 420111, Russia

In neurobiology for decades the 'Dale's principle' dominated, according to which, one neuron synthesizes, stores, and releases a single transmitter liberated from all axon terminals. In this regard, vertebrate motoneuron for a long time was considered as a cell capable to release acetylcholine only. However, by the early 90's, a large amount of experimental data was obtained, the analysis of which led to the formation of the modern theory of 'co-transmission'. According to this theory, one or several types of synaptically active molecules, co-transmitters (coexisting transmitters) are released from the neuron together with basic mediator. These co-transmitters are capable of exerting their own effects in the target cell, regulating the release of primary neurotransmitter (presynaptic modulation) or modulating the physiological response in the postsynaptic cell (postsynaptic modulation). At present, it can be stated that the phenomenon of co-release of several neurotransmitters from the nerve endings is the rule rather than the exception for the entire nervous system, including peripheral part. Some signaling molecules that do not meet the definition of 'co-transmitters' are involved in the functioning of the synaptic apparatus too. They are released from either neuron, but independently of the primary neurotransmitter, or have a glial origin or they are released from the postsynaptic cell and, along with co-transmitters, exert their modulating and/or neurotrophic effects.

Investigations during the last two decades indicate a role for glutamate (which is the most abundant excitatory neurotransmitter in the CNS) as a signalling molecule at the neuromuscular junction of vertebrates. So, it has been established that glutamate is present in the cytoplasm of motoneurons, is associated with synaptic vesicles and can be released from motor nerve ending. Furthermore, glutamate receptors and glutamate transporters have been found at the neuromuscular junction directly. It appeared that this amino acid is able to influence the processes of acetylcholine release from motor neuron, and modulatory mechanisms of glutamate action in mammalian and amphibian neuromuscular junctions are different. Moreover, in the latter it varies apparently during ontogeny. It was shown that in the early stages of establishing and maturing

of amphibian neuromuscular junction glutamate facilitates quantal acetylcholine release, whereas in adult animals, the amino acid inhibits the quantal secretion of primary neurotransmitter, and this effect is more pronounced at higher frequencies of nerve stimulation. At the same time, at the mammalian neuromuscular junctions any effects of glutamate on quantal acetylcholine release have not been established yet. However, the inhibitory action of this amino acid on the non-quantal acetylcholine release was revealed. Since a majority of data indicates that tonic neurotransmitter release is one of the neurotrophic control factors then glutamate can be considered as a regulator of neurotrophic influence. Due to the fact that glutamate receptors activation (both at amphibian and mammalian endplates) may be accompanied by the elevation of nitric oxide (NO) synthesis, and the contribution of NO-mediated signaling in metabolism and contraction of muscle fibers was revealed, glutamate might be assumed to participate in a wide range of physiological functions.

Gamma-aminobutyric acid (GABA), in contrast to glutamate, is the major inhibitory neurotransmitter in the synapses of CNS and plays a key role in the development, maturation and functioning of brain modulating neuronal activity. Research conducted in the 70's to the present day, demonstrated that GABAergic signaling is not restricted to the CNS, and this amino acid can play the role of signaling molecule at peripheral synapses too. Functional GABA receptors have been detected on sympathetic and sensory neurons, on unmyelinated axons in vagal and sympathetic nerve trunks, on myelin-producing Schwann cells and on embryonic skeletal muscle cells. Furthermore, it was shown that GABA reduces the release of acetylcholine from the preganglionic fibers in the rat cervical ganglion and in the bullfrog sympathetic ganglion. At the same time, at the neuromuscular synapse no effects of GABA on the parameters of the quantal acetylcholine release and muscle contraction have been shown. However, recently we have shown that metabotropic $GABA_B$ receptors are localized (apparently presynaptically) at mature rat neuromuscular synapse and that their activation leads to a decrease in the intensity of non-quantal acetylcholine release.

Thus, currently the neuromuscular synapse must be regarded as a rather complex and highly plastic morphological and functional structure with a number of multiple-intercellular signaling pathways which can involve directly amino acids, previously considered only as CNS mediators.

INVOLVEMENT OF PHOSPHATIDYLINOSITOL 4,5-BISPHOSPATE-BINDING PROTEINS IN THE CONTROL OF CONTRACTILE OSCILLATIONS IN *PHYSARUM POLYCEPHALUM* PLASMODIUM

N.B. Matveeva, S.I. Beylina, A.A. Klyueva, V.A. Teplov

Institute of Theoretical and Experimental Biophysics, Russian Academy of Sciences, Pushchino, Moscow region, 142290, Russia

Phosphatidylinositol 4,5-bisphospate (PIP$_2$) is responsible for a wide range of membrane-related phenomena as a source of three second messengers: inositol 1,4,5-trisphosphate (IP$_3$), diacylglycerol (DAG), and phosphatidylinositol 3,4,5-trisphosphate (PIP$_3$). It is also a site of binding of phosphatidylinositol-3phosphatase (PTEN) and PH-domains of proteins controlling the cell contractile apparatus. As a substrate of phospholipase C (PLC), PIP$_2$ is a key regulator of the intracellular Ca^{2+} concentration and is responsible for calcium fluctuations and waves. The concentration of free PIP$_2$ in the membrane is important for these processes. The release of this phospholipid from membrane clusters formed by PIP$_2$-binding proteins causes the phosphorylation of their regulatory domains by protein kinase C (PKC) or interaction with Ca^{2+}/calmodulin (Ca^{2+}/CaM) [1]. Because the activation of PKC is provided by the products of PIP$_2$ hydrolysis DAG and IP$_3$, which releases Ca^{2+} from internal stories, PIP$_2$-binding proteins form in the membrane pools of PIP$_2$, mobilized during the activation of the IP$_3$ receptor (IP$_3$R), which appears to be capable to maintain, through PKC and Ca^{2+}/CaM, the membrane concentration of free PIP$_2$ and thereby its activity.

The goal of the work was to elucidate the mechanism of the regulation of the membrane concentration of free PIP$_2$ in the *Physarum polycephalum* plasmodium, a giant ameboid cell, which exhibits regularities of motile behavior common with those of tissue cells. The plasmodium generates auto-oscillations of the intracellular Ca^{2+} concentration, the contractile activity, and the membrane potential and responds to receptor stimulation by attractants with an increase in their frequency. In tensiometric experiments, which are difficult to realize on tissue cells, contractile oscillations were monitored by changes of the longitudinal force generated by isolated plasmodial strands about 5 mm in length and 0.4 mm in diameter under isometric conditions at temperature 22^{0}C.

The presence of feedbacks regulating the activity of IP$_3$R, which plays a crucial role in the plasmodial oscillator [2], suggests the possibil-

ity of oscillatory changes in the level of PIP_2 and its participation in the regulation of the cytoskeleton dynamics not only through Ca^{2+} but also through phospholipids. It was shown using neomycin as a substrate inhibitor of PLC and the aminosteroid U73122, an effective blocker of receptor-induced PLC activation without inhibition of the enzyme per se, that the activation of PLC is a necessary condition for the generation of autooscillations and the motile response of plasmodium to signal molecules secreted by the cell itself [3, 4]. U73122 changed the period of autooscillations but did not abolish autooscillations.

As opposed to U73122, neomycin led to the termination of autooscillations; however, their damping might continue for hours. The response to the inhibitor depended not only on the physiological state of the plasmodium and the concentrations used but also on the pH of medium. For example, at pH 4.6, an optimal value for the plasmodium cultivation, neomycin at concentrations of 0.1-1 mM at first induced a transient rise in the isometric force, which was accompanied by an increase in the period and amplitude of its oscillations, but the strand stiffness did not change [3]. The duration of the oscillatory regime, which was retained in the presence of neomycin, corresponded to the conception about the development of its effect in membranes of living cells. Neomycin, as a substrate inhibitor of PLC, reduced its activity by gradually binding PIP_2, which was released during oscillations. The process was accompanied by the appearance of hyaloplasm-filled membrane blebs typical of PIP_2-blocking agents [5]. These blebs resulted from the local detachment of the membrane from cytoskeleton, which was accompanied by a decrease in the magnitude of the force, as well as the amplitude and period of its oscillations. These changes in the cell stress and consequently in the intracellular pressure determine, according to our mathematical model, the conditions of excitation of the plasmodial oscillator and its parameters [6]. On the retention of the cortex, an increase in the pressure may result from the enhancement of depolymerization of cytoplasmic actin during the PIP_2 blockade by neomycin [7]. This confirms that PIP_2 is the major target of the inhibitor and a regulator of the state of the *Physarum* cytoskeleton.

The probability of the formation of a complex of neomycin with PIP_2 and its competition with PLC for free PIP_2 should substantially depend on the dynamics of the association–dissociation of PIP_2-binding proteins during the contractile cycle and on the possibility of the phosphoinositide resynthesis, which evidently determines the duration of decay of oscillations. The efficiency of neomycin abruptly increased with increasing pH of

medium, which is probably due to a strong pH dependence of the membrane potential of plasmodium, which increased from -50 mV at pH 5 to -120 mV at pH 7 [8]. The gradient of the membrane potential is surely important for the penetration of neomycin to the target in the cytoplasmic leaflet of the plasma membrane, primary PIP_2 location in eukaryotic cells.

The neomycin concentration at pH 7, which causes the arrest of auto-oscillations on strands similar to the effect of 2-APB, an inhibitor of the IP_3 receptor [2], decreased from 3–5 mM at pH 4.6 (which was observed only on microplasmodia [3]) to 100 µM (fig. 1a). The response of period at the initial stage of the restoration was by ~25% shorter than in the control and then increased due to the elongation of the contraction of plasmodium to the inhibitor was two-phasic: after the termination of auto-
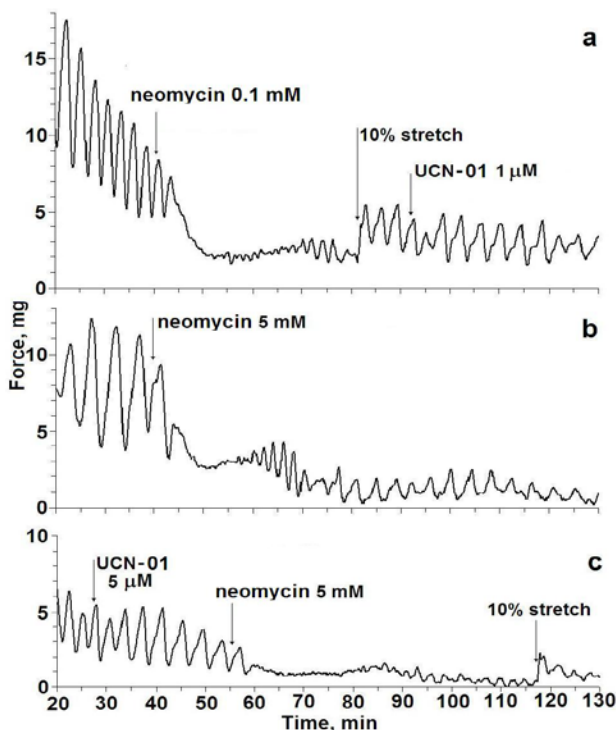
Fig. 1. Comparative effects of neomycin at concentrations of 0.1 mM (a) and 5 mM (b) and under the combined action of neomycin with the PKC inhibitor UCN-01 at concentrations of 1 µM (a) and 5 µM (c) on the regime of isometric force auto-oscillations of protoplasmic strands (explanations in text).

oscillations for 10–30 min, they gradually resumed; the oscillation phase. As it was shown on preparations of cardiocyte sarcolemmes, the binding of PIP_2 by neomycin stimulates the activity of phosphatidylinositol 5-kinase, which catalyzes the synthesis of PIP_2. The significant increase in PIP_2 concentration was also induced by the expression in PC12B cells of the protein MARCKS but not its mutant form devoid of the effector domain binding to PIP_2. Probably the restoration of autooscillations in plasmodium is also related to the stimulation of PIP_2 resynthesis, although this question undoubtedly requires further studies with the use of the inhibitors of 4- and 5-inositolkinases. In favor of the activation of resynthesis of PIP_2 upon its binding by neomycin is the acceleration of the restoration of autooscillations with increasing initial frequency at higher concentrations of the inhibitor. At a neomycin concentration of 5 mM, the oscillations resumed within 10 min (fig. 1b) and were accompanied by a more intensive formation of protoplasm-filled blebs than at pH 4.6, which prevented the increase in ectoplasm tension.

To determine whether PIP_2-binding proteins similar to MARKS are involved in the regulation of the concentration of free PIP_2 in the membrane of plasmodium, we examined the effect of the PKC inhibitors staurosporine, UCN-01 (7-hydroxystaurosporine), and Ro-31-8220 separately and in combination of these inhibitors with the Ca^{2+}/CaM inhibitor calmidazolium (1 μM) and with neomycin on the mode of autooscillations of the contractile activity. The main criterion for the assessment of the effect of PKC inhibitors was the duration of the termination of autooscillations induced by neomycin in comparison with the effect of their combined action in parallel experiments.

The inhibitors of PKC in combination with calmidazolium induced a slow decay of autooscillations. They also induced a twofold increase in the duration of the termination of autooscillations in response to neomycin added in their presence. It should be noted that the addition of calmidazolium (1 μM) diminished the effect of the PKC inhibitors. This is probably related to its influence on other targets, which led to an increase in the intracellular calcium concentration. The most pronounced neomycin-like effect was induced by UCN-01, a selective inhibitor for conventional and novel PKC isotypes. At a concentration of 5 μM, UCN-01 increased the period and amplitude of autooscillations and enhanced the effect of neomycin added in its presence, which manifested itself as an increase in the duration of the absence of autooscillations (30–40 min) (fig. 1c). When used upon the restoration of autooscillations in the pres-

ence of neomycin, all PKC inhibitors accelerated the increase in the period of restored autooscillations due to the elongation of the contraction phase, which coincides in time with the increase in the concentration of free calcium in the cytoplasm [8]. The results count in favor of the assumption that the plasmodial membrane contains MARCKS-like proteins and PKC-controlled pools of PIP_2; however, further studies are needed to confirm this assumption.

References

1. McLaughlin S., Murray D. // Nature 2005. 438: 605-611.
2. Matveeva N.B., Teplov V.A., Beylina S.I. // Biochemistry (Moscow) Suppl. Ser. A: Membrane and Cell Biology. 2010. 4: 70–76.
3. Matveeva N.B., Beylina S.I., Teplov V.A. // Biol. Membrany. 2006. 23: 306-315. (in Russian).
4. Matveeva N.B., Teplov V.A., Beylina S.I. // Biochemistry (Moscow) Suppl. Ser. A: Membrane and Cell Biology. 2012. 6: 255–264.
5. Raucher D. et al. // Cell. 2000. 100: 221-228.
6. Teplov V.A. // Protoplasma (Suppl.1). Cell Dynamics 1. 1988: 81-88.
7. De Corte V., Gettemans J., Vandekerckhove J. // FEBS Lett. 1997. 401: 191-196.
8. Kuroda R. et al. // Protoplasma (Suppl.1). Cell Dynamics 1. 1988: 72-80.

STRUCTURAL AND FUNCTIONAL EFFECTS OF TWO STABILIZING SUBSTITUTIONS, D137L AND G126R, IN THE MIDDLE PART OF α-TROPOMYOSIN MOLECULE

Alexander M. Matyushenko[1], Natalia V. Artemova[1], Daniil V. Shchepkin[2], Galina V. Kopylova[2], Sergey Y. Bershitsky[2], Andrey K. Tsaturyan[3,4], Nikolai N. Sluchanko[1], Dmitrii I. Levitsky[1,5]

[1] *Bach Institute of Biochemistry, Russian Academy of Sciences, Moscow, Russia*
[2] *Institute of Immunology and Physiology, Russian Academy of Sciences, Yekaterinburg, Russia*
[3] *Institute of Mechanics, Moscow State University, Moscow, Russia*
[4] *Blagonravov Institute of Machines Science, Russian Academy of Sciences, Moscow, Russia*
[5] *Belozersky Institute of Physico-Chemical Biology, Moscow State University, Moscow, Russia*

Tropomyosin (Tm) is an α-helical coiled-coil protein that binds along the length of actin filament and plays an essential role in the regulation of muscle contraction. There are two highly conserved non-canonical residues in the middle part of the Tm molecule, Asp137 and Gly126, which are thought to impart conformational instability (flexibility) to this

region of Tm which is considered crucial for its regulatory functions. It was shown previously that replacement of these residues by canonical ones (Leu substitution for Asp137 and Arg substitution for Gly126) results in stabilization of the coiled-coil in the middle of Tm and affects its regulatory function [1, 2]. We extended these studies employing various methods and approaches (such as CD, limited proteolysis by trypsin, ATPase measurements, *in vitro* motility assay, *etc*.) to compare structural and functional features of recombinant human striated muscle α-Tm mutants carrying stabilizing substitutions D137L and G126R. Moreover, we for the first time analyzed the properties of Tm carrying both these substitutions within the same molecule. The results show that both substitutions similarly stabilize the Tm coiled-coil structure, and their combined action leads to further significant stabilization of the Tm molecule. This stabilization has no appreciable influence on the actin affinity for Tm, but it makes the Tm-actin complexes more stable as was shown by measuring the temperature dependences of thermal dissociation of these complexes monitored with light scattering. The stabilizing substitutions in the middle part of Tm increase the ATPase activity of the myosin heads upon their interaction with actin filaments containing Tm and enhances maximal sliding velocity of regulated actin filaments containing Tm and troponin in the *in vitro* motility assay at high Ca^{2+} concentrations; moreover, this stabilization increases Ca^{2+}-sensitivity of the actin-myosin interaction underlying this sliding. We propose a possible explanation for the physiological effects of these substitutions in the middle part of Tm, according to which their effects on the Ca^{2+}-regulated actin-myosin interaction can be accounted for not only by decreased flexibility of actin-bound Tm, but also by the influence of these substitutions on the interactions between the middle part of Tm and certain sites of the myosin head [3, 4].

References

1. Sumida J.P., Wu E., and Lehrer S.S. (2008) "Conserved Asp-137 imparts flexibility to tropomyosin and affects function". J. Biol. Chem. 283, 6728–6734.
2. Nevzorov I.A., Nikolaeva O.P, Kainov Y.A., Redwood C.S., and Levitsky D.I. (2011) "Conserved noncanonical residue Gly-126 confers instability to the middle part of the tropomyosin molecule". J. Biol. Chem. 286, 15766–15772.

3. Shchepkin D.V., Matyushenko A.M., Kopylova G.V., Artemova N.V., Bershitsky S.Y., Tsaturyan A.K., and Levitsky D.I. (2013) "Stabilization of the central part of tropomyosin molecule alters the Ca2+-sensitivity of actin-myosin Interaction" Acta Naturae 5, № 3(18), 126–129.
4. Matyushenko A.M., Artemova N.V., Shchepkin D.V., Kopylova G.V., Bershitsky S.Y., Tsaturyan A.K., Sluchanko N.N., and Levitsky D.I. (2014) "Structural and functional effects of two stabilizing substitutions, D137L and G126R, in the middle part of α-tropomyosin molecule". FEBS Journal (in press; doi: 10.1111/febs.12756).

VESICULAR TRANSPORT INHIBITOR BREFELDIN A AND MICROTUBULE DISRUPTER NOCODAZOLE SIMILARLY MODULATE THE EFFECT OF GLUTOXIM ON Na+ TRANSPORT IN FROG SKIN

A.V. Melnitskaya, Z.I. Krutetskaya, S.N. Butov,
N.I. Krutetskaya, V.G. Antonov
Saint-Petersburg State University, 7/9 University emb.,
Saint-Petersburg, 199034, Russia

The amphibian skin and other isolated epithelial systems are classical model objects for studying the mechanisms of transepithelial ion transport. Na^+ transport in osmoregulatory epithelia is a complex multi-component system providing the establishment and maintenance of electrolytic and water homeostasis. The key Na^+-transport proteins, such as amiloride-sensitive epithelial Na^+ channels (ENaCs), Na^+/K^+ ATPases, and Na^+/H^+ exchangers, are targets for oxidative stress [1]. However, the mechanisms underlying the effect of oxidants and reducing agents on individual components of the Na^+ transepithelial transport are still unknown. Recently, new disulfide containing agents with d-metals as nanoadditives, altering cell redox state, have been widely used. In particular, the drug glutoxim® (disodium salt of oxidized glutathione, GSSG, with platinum nanoaddition; PHARMA-VAM, Moscow, Russia) has been introduced into clinical practice as an immunomodulator and a hemostimulant in the integrated therapy of bacterial and viral diseases, psoriasis, as well as radio and chemotherapies of cancer [2].

We earlier demonstrated that the Na^+ transport in the frog skin was modulated by various oxidants. This was the first finding to demonstrate that GSSG and glutoxim applied to the basolateral frog skin surface imitate the effect of insulin and stimulate Na^+ transeptithelial transport [3]. Later, we have shown that tyrosine kinases, phosphatidylinositol kinases

183

[4], protein kinase C [5], serine/threonine protein phosphatases PP1/PP2 [6], actin filaments [6] and microtubules [7] are involved in the glutoxim regulation of Na^+ transport in the frog skin.

It is also known that processes of exo- and endocytosis play an important role in modulation of the activity of various Na^+-transporting proteins. Moreover, in the processes of deletion/insertion and delivery of ENaC subunits to the membrane various structural and signaling elements, such as microtubules and microfilaments [8], protein synthesis regulators [9] and components of vesicular transport [10] are involved. Therefore, it was interesting to investigate the possible involvement of vesicular transport and microtubules in the modulation of glutoxim effect on Na^+ transport in frog skin. Nocodazole (microtubule depolymerizer) and brefeldin A, a specific inhibitor of vesicular transport, were used in the experiments.

Materials and methods

Experiments were performed on frog *Rana temporaria* males. The skin from the frog abdomen was removed and placed in Ussing chamber (World Precision Instruments, Inc., Germany) with 12 mm inner orifice. Frog skin electrical parameters were measured with the automatic device for voltage-clamp and registration of current-voltage relations (I-V relations). To measure I–V relations, transepithelial potential V_T was changed periodically to a series of nonzero values. From skin I–V relations the electrical characteristics of frog skin were determined: the short – circuit current (I_{SC}), the open – circuit potential ($V_{OC} = V_T$ at the total transepithelial current $I_T = 0$), and transepithelial conductance (g_T). The transepithelial Na^+ transport was measured as amiloride – sensitive short – circuit current (I_{SC}). Nocodazole and brefeldin A were added 30 - 40 min before glutoxim application. Statistical analysis was performed using Student's t-test. The data are presented as $x \pm s_x$. Fig. 1 illustrates the results of typical experiments.

Results and discussion

The mean values of frog skin electrical characteristics in control (from 10 experiments) are: $I_{SC} = 39.16 \pm 3.45$ µA, $V_{OC} = -110.65 \pm 12.41$ mV, and $g_T = 0.35 \pm 0.02$ mS. Glutoxim, applied to the basolateral surface of the intact frog skin, stimulated Na^+ transport. After glutoxim application I_{SC} increased in average by $31.24 \pm 8.32\%$; V_{OC} – by $38.04 \pm 5.15\%$; and g_T did not change (the data from 10 experiments).

It has been also found that nocodazole and brefeldin A modulate the effect of glutoxim on Na^+ transport (fig. 1). On average (the results of 10 experiments), after the preincubation of skin apical surface with 50 µM nocodazole for 30 min before application of 100 µg/ml glutoxim to
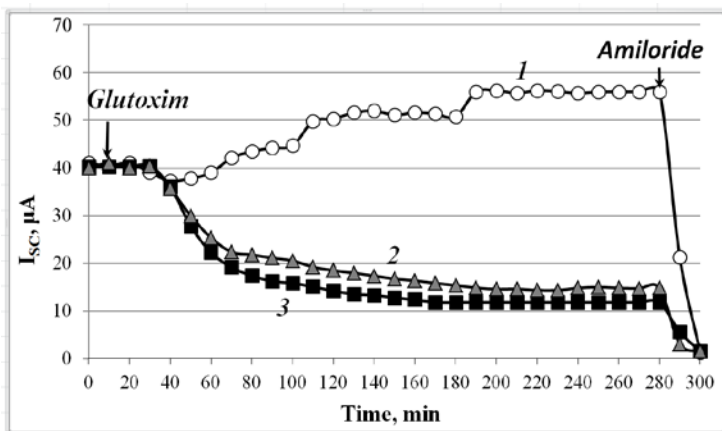
Fig. 1. Dependence of the changes in short-circuit current, ISC, through the frog skin in response to glutoxim: (1) ISC after applying 100 μg/ml glutoxim to the basolateral surface of intact frog skin; (2–3) ISC after applying glutoxim to the frog skin pretreated (for 30 min) from the apical side with 50 μM nocodazole (2) or 50 μM brefeldin A (3); at the end of each experiment, the solution bathing the apical skin surface was supplemented with 20 μM amiloride, an ENaC blocker.

the frog skin basolateral surface, I_{SC} decreased by 35.46 ± 7.09 %, and V_{OC} decreased by 29.15 ± 6.34 %, g_T – by 18.03 ± 6.38 %. Similarly, if the apical surface of frog skin was preincubated with 50 μM brefeldin A, I_{SC} decreased after glutoxim application by 41.62 ± 9.35 %, V_{OC} – by 35.45 ± 8.34 %, and g_T – by 20.81 ± 6.34 %.

We have earlier demonstrated that glutoxim applied to the basolateral frog skin surface imitated the effect of insulin and stimulated Na^+ transport, inducing a biphasic increase in I_{SC} [4]. The figure shows the changes in the I_{SC} through the frog skin after applying 100 μg/ml glutoxim to the basolateral surface of intact skin (fig. 1, *curve 1*), as well as the skin pretreated (for 30 min) from the apical side with 50 μM nocodazole (fig. 1, *curve 2*) or 50 μM brefeldin A (fig. 1, *curve 3*). It is evident that nocodazole and brefeldin A completely inhibit both phases of the glutoxim stimulatory effect on the Na^+ transport in frog skin.

It is known that various Na^+- transporting proteins contain numerous cysteine residues which are the targets for intra- and extracellular oxidizing and reducing agents. In reabsorbing epithelia ENaC play a critical role in the Na^+ transport. Numerous cysteine residues localized in various ENaC segments determine its redox sensitivity and are the targets

for intra- and extracellular oxidizing and reducing agents. Addition of 20 µM amiloride, a ENaC blocker, into the solution washing the apical surface of the frog skin at the end of each experiment almost completely inhibited I_{SC} (fig. 1). It implies that glutoxim affects Na^+ transport primarily by modulation of ENaC activity.

Our results suggest that microtubules and vesicular transport are involved in the glutoxim effect on the Na^+ transport in frog skin. It's also evident that microtubule disrupter nocodazole and vesicular transport inhibitor brefeldin A similarly modulate the glutoxim effect on Na^+ transport in frog skin. Both agents almost completely attenuated glutoxim stimulatory effect on Na^+ transport and also considerably decreased the skin electrical characteristics. Hence, it is possible to suggest that brefeldin A action on the glutoxim effect may be realized through cytoskeleton elements.

References

1. Firsov, D., Robert-Nicoud, M., Gruender, S., et al., J. Biol. Chem., 1999, vol. 274, pp. 2743–2749.
2. Zhukov, O.B., Zubarev, A.R., Mezentseva, M.V., et al., Vracheb. Soslovie, 2004, vol. 5/6, pp. 51–56.
3. Krutetskaya Z.I., Lebedev O.E., Melnitskaya A.V., et al., Doklady Biol. Sci, 2008, vol, 421, pp. 235-238.
4. Melnitskaya A.V., Krutetskaya Z.I., Lebedev O.E., et al., Cell Tissue Biol., 2010. vol. 4, pp. 273-279.
5. Melnitskaya A.V., Krutetskaya Z.I., Lebedev O.E., Biochemistry (Moscow) Supplement Series A: Membrane Cell Biol., 2009, vol. 3, p. 323.
6. Melnitskaya A. V., Krutetskaya Z. I., Lebedev O. E., et al., Cell Tissue Biol., 2010, vol. 6, pp. 248-253.
7. Krutetskaya Z.I., Mel'nitskaya A. V., Antonov V. G., et al., Doklady Biol. Sci, 2012, vol. 445, pp. 696–698.
8. Verrey F., Groscurth P., Bolliger U., J. Membr. Biol, 1995, vol. 145, pp. 193 - 204.
9. Brown D., Stow J., Physiol. Rev, 1996, vol. 76, pp. 245 - 297.
10. Fisher R.S., Grillo F.G., Sariban-Sohraby S., Am. J. Physiol, 1996, vol. 270, pp. C138 - C147.

INHIBITORY ANALYSIS OF PROTEIN SYNTHESIS SIGNALING PATHWAYS IN RAT POSTURAL MUSCLE DURING RECOVERY AFTER FUNCTIONAL UNLOADING

T.M. Mirzoev, O.V. Turtikova, B.S. Shenkman
SSC RF - Institute of Biomedical Problems of RAS,
123007, Khoroshevskoe shosse 76A, Moscow, Russia

Restoration of muscle mass after functional unloading is an urgent problem both in space and rehabilitation medicine. The most important

role in the recovery of atrophied muscle belongs to the protein synthesis. However, the work of intracellular signaling pathways that regulate protein synthesis in mammalian postural muscle during the period of readaptation after functional unloading remains poorly studied.

One of the effective ways of studying intracellular anabolic signaling systems is an inhibitory analysis that allows us to assess the contribution of different signaling molecules in the regulation of protein synthesis. In the present study we used inhibitors wortmannin and 1-butanol in order to determine the role of PI3K-dependent (PI3K - phosphoinositide-3 kinase) and PA-dependent (PA - phosphatidic acid) signaling pathways in rat m.soleus in the period of readaptation after disuse. The aim of the study was also to evaluate the rate of protein synthesis and analyse anabolic signaling pathways in rat m.soleus on the 3rd day of recovery after 14 days of simulated gravitational unloading. Wistar male rats weighing 190-210g were divided into the following groups: 1) «Control» (n=7), 2) «14HS» (n=7) - a group of hindlimb suspension for 14 days, 3) «14HS+3R+placebo» (n=7) - 3-day readaptation with introduction of placebo, 4) «14HS+3R+wort» (n=7) - 3-day readaptation with introduction of wortmannin, 5) «14HS+3R+but» - 3-day readaptation with introduction of 1-butanol. Gravitational unloading was simulated by hindlimb suspension of rats. All procedures with the animals were approved by the Committee on Bioethics of SSC RF - IBMP RAS. The intensity of the protein synthesis in m.soleus was determined by SUnSET technique. Content of phosphorylated ribosomal protein kinases p70S6K and p90RSK was assessed by Western blotting.

Two-week gravitational unloading induced a 33% decrease of protein synthesis in m.soleus ($p<0.05$) compared to «Control». However, after a period of 3 day readaptation we observed an increase of protein synthesis by 40% ($p<0.05$) compared to «14-HS». In rats that were treated with wortmannin and 1-butanol during recovery period there was a decrease in the rate of protein synthesis vs. «14HS+3R+placebo» by 35.6% and 38.5% ($p<0.05$) respectively. After 14-day gravitational unloading the content of the phosphorylated ribosomal kinase p-p70 did not significantly differ from the «Control». Following 3 days of readaptation we observed a significant increase of p-p70 content in m.soleus vs. «14-HS». In «14HS+3R+but» the p-p70 content was lowered by 57.7% ($p<0.05$) vs. «14HS+3R+placebo». There was 84.5% ($p<0.05$) decrease of the phosphorylated p-90 RSK in «3R+placebo» compared to «Control». Administration of inhibitors during the period of readaptation didn't induce any significant changes in p-p90RSK content in m.soleus.

The obtained results suggest that the decrease in the protein synthesis rate caused by wortmannin could be associated with the mTORC1-independent pathway such as AKT-GSK3β-eIF-2b. Thus, the increased rate of protein synthesis during the early recovery after gravitational unloading is most likely caused by both PA-dependent activation of mTORC1 and mTORC1- independent pathway.

LIFETIME OF ACTOMYOSIN COMPLEX MEASURED WITH OPTICAL TRAP

S.R. Nabiev[1], D.A. Ovsyannikov[1], A.K. Tsaturyan[2], S.Y. Bershitsky[1]
[1]*Institute of Immunology and Physiology, Ural Branch of RAS,*
Yekaterinburg, 620049, Russia
[2]*Institute of Mechanics, Moscow State University,*
Moscow, 119992, Russia

During eccentric contraction muscle works against a load which exceeds its force-generating ability. Such type of contraction is widely used for athletic training in order to increase the mass and force capacity of skeletal muscles. Mechanism underlying eccentric contraction was studied in numerous works on whole muscles [e.g. Cole *et al*., 1996, Abbott, Aubert, 1952] and isolated muscle fibres [e.g. Piazzesi *et al*., 1992, Bagni *et al*., 1998; Ferenczi *et al*., 2014]. Here we reproduced the conditions of eccentric contraction at single molecule level and studied the effects of load and ATP concentration on the lifetime of myosin cross-bridge using an optical trap.

Methods

Actin and myosin were obtained from fast skeletal muscles of the rabbit with standard methods [Margossian, Lowey, 1982; Pardee, Spudich, 1982]. Protein purity was checked with SDS-PAGE. Experiments were done at two ATP concentrations: 3 µM and 6 µM.

The experiments were carried out using three bead assay [Finer *et al*., 1994]. Two polystyrene beads of 1 µm in diameter were trapped and held by two well-focused laser beams. Actin filament of ~5 µm in length was attached to the beads with N-ethylmalimide-modified myosin [Veigel *et al.*, 1998] forming dumbbell-like probe (fig. 1) and prestretched by 3-5 pN. The probe was put above the third (silica) bead 2 µm in diameter very rarely coated by myosin molecules and the surface of this bead was scanned in search of events of interaction between actin filament and a myosin molecule.
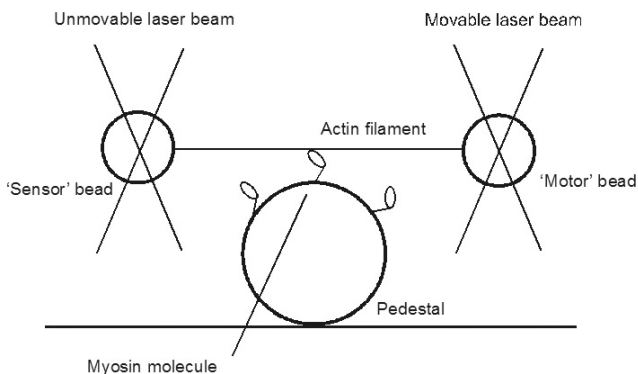
Fig. 1. Diagram of the three bead assay.
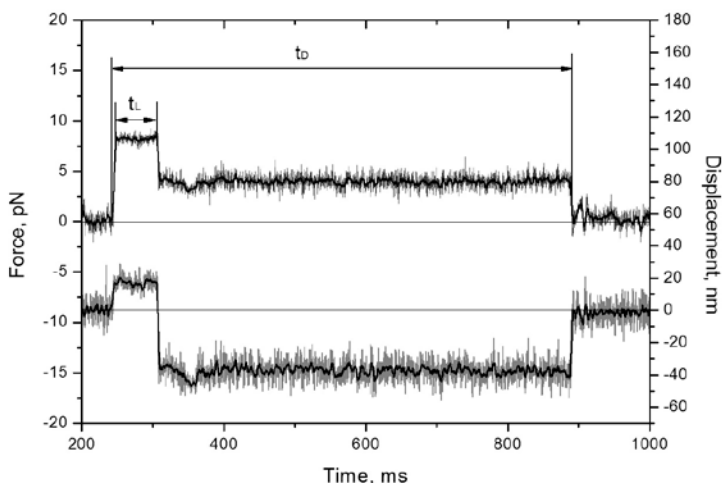
Fig. 2. Example of a record obtained with the experimental protocol described in the text. Upper trace is signal of the 'motor' bead position with respect to trapping beam, which is proportional to applied force at a constant trap stiffness, lower trace is the signal of the 'sensor' bead position with respect to the trapping beam, which is proportional the its displacement; t_D is the total time of experimental protocol until the feedback is switched on again; t_L is lifetime of actomyosin complex at load.

To apply a certain load to a single myosin molecule the following protocol was used (fig. 2). One of the probe beads, 'sensor', was held by static beam and its displacement indicated the step of myosin molecule attached to actin filament. The second bead, 'motor', was held by the

189

beam which position was controlled by an acousto-optical deflector feed-backed by the 'sensor' signal [Takagi *et al.,* 2006]. The feedback compensated the displacement of the 'sensor' bead by deflection the beam in the direction opposite to the step thus increasing force applied to the myosin molecule. When force achieved preset level, the feedback was switched off and the actin-bound myosin molecule was left at a defined load for 0.7 s, a period of time certainly exceeding the lifetime of actomyosin complex, t_L, which was measured from the moment of achievement of the defined level of load to the detachment the molecule from the actin filament.

Results

The whole range of applied loads (1-15 pN) was divided into three intervals: <6 pN, 6-10 pN and >10 pN. The distribution of the number of events against t_L was plotted at both used ATP concentrations and different load as well as in the experiments carried out with no feedback used as a control (fig. 3). The distribution for all levels of load as well as for non-loaded conditions had similar shape and was fitted by a sum of two exponentials: $P(t) = A \cdot (e^{-k_s \cdot t} - e^{-k_f \cdot t})$, where $P(t)$ is the probability density of the events with duration t, k_s and k_f are the rate constants of the slow and fast exponentials, respectively (fig. 3).
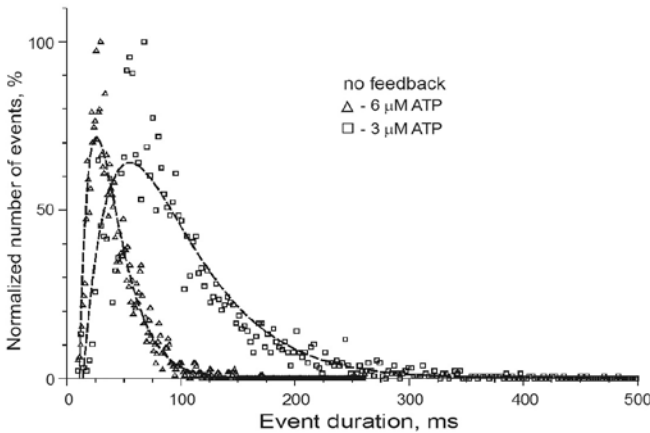
Fig. 3. The distribution of the number of events against their duration at two ATP concentrations without the feedback control.

The rate constants calculated from the fits are shown in table and plotted in fig. 4. It is seen that both rate constants rose with the increase
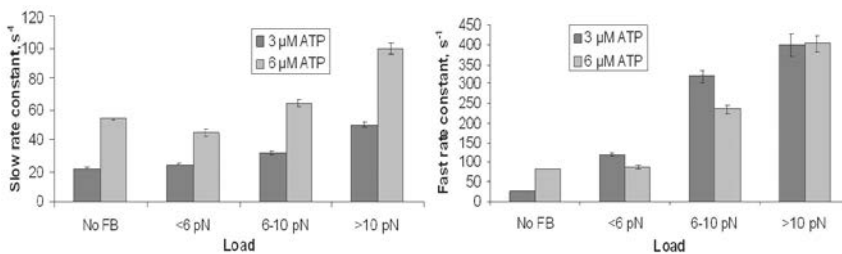
Fig.4. The dependence of the slow (left panel) and fast (right panel) rate constants on the applied load and ATP concentration.

Rate constants at different ATP concentration and applied loads

ATP concentration	Load	k_s, s^{-1} (mean±SD)	k_f, s^{-1} (mean±SD)
3 µM	No FB	21.9±0.6	26.7±0.8
	<6 pN	24.0±1.3	118.3±10.8
	6-10 pN	32.2±1.6	316.5±36.3
	>10 pN	50.1±3.3	398.4±57.1
6 µM	No FB	54.4±1.3	80.7±2.3
	<6 pN	45.4±4.7	87.3±10.9
	6-10 pN	64.0±4.1	235.3±23.0
	>10 pN	99.1±6.3	401.6±40.6

of load. Slow constant, k_s, was directly proportional to ATP concentration within the used range, doubling the concentration led to two-fold increase in the rate constant. Fast rate constant, k_f, did not depend on ATP concentration but was more sensitive to the load, at doubled load the constant increased by about four times.

The apparent sensitivity of the slow rate constant to ATP concentration is easily explainable by a decrease in diffusion time at higher ATP. The rate limiting step is ATP binding, not product release as the slow rate constant is proportional to ATP concentration. However the behavior of the fast rate constant is quite puzzling and at the moment we cannot attribute it to a particular step of the mechano-chemical cycle of the actin-myosin interaction.

Acnowledgemens

Li$^+$ IN Na$^+$- DEPENDENT PROCESSES OF EMC IN MYOCARDIUM AND SKELETAL MUSCLE OF *RANA TEMPORARIA* FROG

V.P. Nesterov, I.V. Shemarova, S.V. Nesterov

Sechenov Institute of Evolutionary Physiology and Biochemistry, Russian Academy of Sciences, Toreza pr. 44, St. Petersburg, 194223, Russia

It is known that the excitation of the plasma membrane (PM) of cardiomyocytes (CM) and skeletal muscle fibers (SMF) of vertebrates arise transmembrane incoming currents I_{Na+} and I_{Ca2+} , the value of which depends on the electrochemical gradient of Na$^+$ and Ca^{2+} on the PM. These currents initiated increase $[Ca^{2+}]_i$ in the cells, activating the contractile proteins – is performed electromechanical coupling (EMC) in the muscles. Important role of these cations in providing EMC processes due to their unique and stable physico-chemical properties and high content in biosphere. As a result of technological development in our environment in large quantities are envolved and therefore act in living organisms and all other inorganic cations (Li$^+$, Ni^{2+}, Y^{3+}, etc.), the content of which is initially in the biosphere was a thousand times smaller. Penetrating into living cells, they according to their physico-chemical properties can play an important and useful regulatory role in cellular processes or, conversely, become dangerous toxicants.

Li$^+$ ions, getting into muscle of vertebrates, including human, can replace Na$^+$ in various processes, for example Li$^+$ is the only cation able to replace the Na$^+$ in membrane electrogenesis. At the same time it was found that Li$^+$ accumulation in the body greater than the natural level of concentration, can alter metabolism and lead to dysfunction of the internal organs, the cardiovascular system and central nerve system. This research is devoted to a comparative study of the effects of replacing Na$^+$ by Li$^+$ in EMC processes in the myocardium and skeletal muscle of the frog. As an integral test were studied inotropic effects of such replacement. In the study of SMF we based on the model of direct Na$^+$-induced Ca^{2+} release from the sarcoplasmic reticulum (SR). According to this model, the Na$^+$ ions, forming I_{Na+} at the excitation of PM, rapidly accumulating in the slit-like space gap between T-tubules and SR and neutralizing fixed negative charges of ryanodine receptor 1 (RyR1) of SR activate the interaction between these «foot» part of RyR1 and dihydropyridine receptor (DHPR) in the L-type Ca^{2+} channel of PM, and thereby open Ca^{2+}-channels of SR. When studying the CM we came from the fact that the excitation of the PM (I_{Na+}) opens L-type Ca^{2+}-channel and occurs I_{Ca2+}, inducing the release of

Ca^{2+} from the SR through RyR2-channel. Entered in myoplasm Na^+ ions increases the concentration of free Ca^{2+} ions in myoplasm in result of reverse entry Ca^{2+} through Na^+/Ca^{2+}-exchanger in the PM. Experiments were performed *in vitro* on isolated heart preparations (myocardium ventriculi) and skeletal muscles (m. sartorius) of *Rana temporaria* frog males. The incubation medium were normal Ringer solution (Na^+-R) and salt mediums in which Na^+ is completely or half replaced equimolar amount LiCl - Li^+-R and Li^+ (50 %)-R respectively. Contraction of muscles evoked by electrical stimulation and recorded them in conditions that guarantee the establishment of a homogeneous distribution of cations throughout the extracellular medium. Processing and analysis of rhythmic isometric contractions of muscle preparations were performed using a special computer programs. The muscles efforts with regard the cross-section of the muscle preparation in its middle part – (Fn, g/mm^2), the maximum speed of effort development (V_{max}, g/s), the time of effort development (tc , c) and the its decrease of half ($t_{1/2R}$, s) were evaluated. We used the standard methods of statistical data processing.

The incubation of muscle preparations in Li^+-salt media for 10 minutes had almost no effect on contractile parameters of the skeletal muscle, but had a significant negative effect on all parameters characterizing inotropic function of the heart muscle, particularly at the transition from Li^+ (50 %)-R to Li^+-R. Such tissue specificity of effect of replacing Na^+ by Li^+ reflects the structural and functional features of EMC organization in these muscles. On the basis of new and last published data (Nesterov et al., 1985-2002; Wei Liu et al., 1998) can come to the following conclusion. In the Li^+-R incubation medium for CM: 1) entrance of Li^+ ions in the CM through L-type Ca^{2+}-channels, have a negligible effect on the Ca^{2+}-binding sites of RyR2, activating the opening of Ca^{2+} - channels in the SR membrane; 2) Li^+ ions receive the competitive advantage against Ca^{2+} in the Ca^{2+}-binding sites of RyR2, inactivating the channel Ca^{2+} conductance of the SR membrane; 3) Li^+ ions reduce the contractions of CM because blocked reverse entry of Ca^{2+} through highly specific with respect to the Na^+ - Na^+/Ca^{2+}-exchanger in the PM. The obtained data demonstrate the importance of maintaining the functional Na^+-gradient on PM in striated muscles and the dangers of Li^+ contamination for human. The initial absence of a negative or appearance even a positive inotropic effect as a result of replacement of sodium by lithium ions in the medium for skeletal muscles (even in the absence of Ca^{2+} in medium) indicates a direct effect of Na^+ and Li^+, as a positive charge carriers, on the

193

fixed negative charges of RyR1 "foot", opening Ca^{2+}-release SR channels. After 1-1.5 hours after the start of incubation in the Li^+-R lithium ions start to displace the K^+ ions and the contractile ability of the muscles is rapidly reducing. We believe that the described processes are not unique to frog skeletal muscle, but also for skeletal muscles of high vertebrates, including human.

EFFECT OF URIDINE ON THE ENDURANCE DEVELOPMENT OF ANIMALS WITH DIFFERENT RESISTANCE TO PHYSICAL TRAININGS: THE ROLE OF THE MITOCHONDRIAL ATP-DEPENDENT POTASSIUM CHANNEL

V.I. Nosar[1], O.S. Gorbacheva[2,3], O.A. Gonchar[1], B.L. Gavenauska[1], L.V. Bratus[1], I.N. Mankovskaya[1], G.D. Mironova[2,3]

[1]*Bogomolets Institute of Physiology NASU, Kiev, Ukraina;*
[2]*Institute of theoretical and experimental biophysics RAS, Universitetskaya str. 3, 142290, Pushchino, Russia;*
[3]*Pushchino State University, Pushchino, Moscow region, 142290, Russia*

In the last decades the participation of mitochondrial ATP-dependent potassium channel (mito K_{ATP} channel) in cardioprotection and adaptation of the organism to hypoxia has been found (Gross G. et al., 1992 ; Garlid K. et al., 1997; Grover G., Garlid K., 2000). Administration of the metabolic precursor of natural activator of mito K_{ATP} channel - uridine before the myocardial ischemia simulating protects the heart against ischemic injury, restoring the heart rhythm and reducing the infarction zone, and moreover, preventing the changes in energetic and oxidative metabolism (Krylova I. et al., 2006, Mironova G.et al., 2007, Krylova et al., 2012).

The aim of our work was to determine the ability of uridine to affect the animal endurance to physical trainings and to establish whether its influence is mediated by modulation of the mitochondrial K_{ATP} channel activity in the development of the hypoxic a.

Endurance to physical activity was measured by recording the time during which the male Wistar rats swam with a load of 20% of body weight in water at $32^{\circ}C$ to exhaustion (sinking on the pool bottom for 15 s). It was determined that the tested rats reacted differently to the introduced load. Into the experimental groups were included only the animals with high endurance (HE), swimming to exhaustion on average 7.40 ± 0.35 min, and the animals with low endurance (LE) whose swimming time to exhaustion was 2.07 ± 0.10 min. Activity of mito K_{ATP} channel in both groups was

determined at rest. The animals were decapitated under light ether narcosis, the liver was placed into the chilled incubation medium (70 mM sucrose, 210 mM D-mannitol, 2 mM EDTA , 10 mM HEPES; pH 7.2). Then, the liver was grinded up and homogenized in a glass homogenizer with a teflon pestle in a 6- fold volume of isolation medium relatively to the weight of the tissue. For mitochondria isolation, homogenate was centrifuged for 7 min at 700g (4°C), then the supernatant was centrifuged for 15 min at 11,000g (4°C). The precipitate was suspended in a small volume of medium without the addition of EDTA and stored at 4°C. The energy-dependent K^{+} influx into mitochondria was determined spectrophotometrically by the swelling magnitude of mitochondria according to the change in light absorbance at 520 nm (ΔA_{520})/min per mg of mitochondrial protein, assuming that the swelling reflects the accumulation of cation in mitochondria (Jaburek M. et al., 1998). The medium contained: 50 mM KCl, 5 mM Na_2HPO_4, 0.5 mM $MgCl_2$, 0.1 mM EGTA, 5 mM HEPES; pH 7.2. Mitochondrial protein concentration in the cuvette was 0.2 mg / ml. The swelling of mitochondria was initiated by the introduction of 5 mM succinate in the presence of 2 µM rotenone.

The ATP-dependent DNP-induced efflux of K^{+} from mitochondria, which also reflects the work of mitochondrial K_{ATP} channel but in an opposite direction (Baranova et al., 2000), was measured by using of the K^{+} - selective electrode in a 1 ml cell at constant stirring and thermostating (26°C). The medium contained: 170 mM sucrose, 80 mM D- mannitol, 5 mM Na_2HPO_4, 10 mM tris-HCl, 1 µg/ml oligomycin (pH 7.2); mitochondrial protein concentration in the cuvette was 0.9 - 1.1 mg / ml. The rate of K^{+} efflux from mitochondria was expressed as the change of potassium ions concentration in the medium ($\Delta[K^{+}]$)/min per mg of mitochondrial protein.

The mitochondrial K^{+} was conducted with a K^{+} -selective electrode after the addition of detergent (0.05 % Triton X-100) to the suspension of mitochondria in a 1 ml cell at constant stirring and thermostating (26°C). The amount of K^{+} in mitochondria was calculated from the amount of potassium ions appearing in the incubation medium after the destruction of mitochondria by added Triton X-100.

The analysis of the obtained data indicates that the rate of K^{+} influx into mitochondria of HE animals, determined by the mitochondria swelling at rest, was higher compared to that of LE animals (figure).

Administration of uridine to LE animals resulted in an increase of the rate of ATP-dependent K^{+} influx into mitochondria almost to the level of its values in HE rats, and combined insertion of uridine and inhibitor 5-HD reduced it almost to the control level.
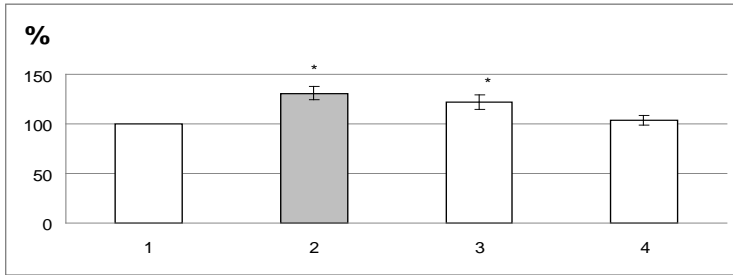
The swelling rate of liver mitochondria in rats with high and low endurance to physical trainings at rest.
Note: 1 - LE (control); 2 - HE (control); 3 - LE (60 min after the insertion of uridine (30 mg / kg); 4 - LE (60 min after the insertion of 5-HD (mg / kg) 10 min before the insertion of uridine (30 mg / kg). P<0.05 comparing with control LE.

Table 1. Effect of uridine on the swimming time of the rats until exhaustion

Experiment conditions	Time, min	
	HE	LE
Swimming	7.40 ± 0.35	2.07 ± 0.10
Uridine+swimming	$4.11 \pm 0.18^*$	$4.28 \pm 0.25^*$
5-HD+swimming	$3.26 \pm 0.25^*$	$1.08 \pm 0.34^*$
5-HD+uridine +swimming	$2.35 \pm 0.45^*$	2.15 ± 0.24

Note: * - the differences are statistically significant compared to control ($p < 0.05$).

ATP-dependent K^+ efflux from mitochondria induced by 2,4 -DNP was also higher in HE than in LE animals (39.7 ± 3.7 and 27.9 ± 2.9 µmol/ min / mg, respectively, $P < 0.05$). While measuring the amount of K^+ in the rat liver mitochondria the larger K^+ content was found in LE compared to HE animals (56.5 ± 8.3 and 42.3 ± 5.4 µmol / mg, respectively, $p < 0.05$). Our presented data are consistent with our previous results obtained in animals with different resistance to hypoxia (Mironova G. et al., 2010).

The following objective was to determine the influence of uridine on the physical endurance in HE and LE animals. Uridine is the metabolic precursor of the natural activator of mito K_{ATP} channel - uridine diphosphate (UDP). It has a low toxicity and, unlike UDP, can penetrate through the biological membranes, forming UDP in a cell. At intraperitoneal injection of uridine (30 mg / kg) 60 min before the swim-

ming, the differences in its effect on the swimming time of tested animals until exhaustion were identified (table 1).

It was found that the swimming time until exhaustion under the uridine administration was increased twice in LE animals reaching the HE level, while in HE it decreased to 44%.

The established marked changes in the mitochondrial ATP-dependent K^+ transport while swimming, accompanied by the load hypoxia (Gavenauskas B., 2005), served as the basis for the investigation of the effect of the selective channel blocker 5-hydroxydecanoate (5-HD) at a dose of 5mg/kg administrated before 60 min to swimming. It was found that under the mito K_{ATP} channel blockade the physical endurance was significantly decreased both in LE and HE animals (see table 1). It was also shown that 5-HD administrated at a dose of 5mg/kg 10 min before uridine reduced the swimming time to exhaustion in LE animals to the control level, which indicates the elucidation of the positive effect of uridine by 5-HD. We can see that 5-HD administration also reduced the swimming time to exhaustion in HE animals (see table 1).

The investigation of K^+ transport in mitochondria in LE animals at rest (60 min after the uridine administration) has showed that mitochondria swelling as well as DNP- induced transport of K^+ was increased compared to control (see fig. 1 and table 2), and the quantity of K^+ did not almost differ from the control value (table 2).

The registration of the liver mitochondria swelling in the LE rats at rest after 5-HD + uridine administration also testified that the inhibitor removed the effect of uridine (see table 2, fig. 1).

Analysis of the obtained data indicates that endurance to physical trainings is strongly connected with the activity of mito K_{ATP} channels. In rats with high endurance, the K^+ transport rate in mitochondria is higher and the amount of K^+ is lower than in rats with low endurance. Admini-

Table 2. Effect of uridine on the rate of DNP- induced efflux of K^+ from the liver mitochondria and the amount of K^+ in mitochondria in rats with low endurance to physical trainings.

Experiment conditions	K^+ efflux, µmole/min/mg of protein	K^+ amount, µmole/mg of protein
Control	27.90 ± 2.91	56.50 ± 8.71
Uridine	33.61 ± 3.74	53.30 ± 5.61
5-HD + uridine	30.62 ± 2.88	48.22 ± 6.41

stration of uridine to LE animals led to an increase of the physical endur-ance while, on the contrary, uridine reduced this parameter in HE ani-mals. However, an inhibitor of mito K_{ATP} channel (with and without uridine administration) reduced the physical endurance in both groups of animals, indicating a positive role of mitoK_{ATP} channel in the forming of endurance to physical trainings.

ORGANIZATION OF CORTICAL CYTOSKELETON IN FIBERS OF MOUSE POSTURAL MUSCLES AND CARDIOMYOCYTES AFTER BEING EXPOSED TO 30-DAY SPACE FLIGHT ON BOARD BION-M1 BIOSATELLITE

I.V.Ogneva[1,2], M.V.Maximova[1,3], I.M.Larina[1]

[1] *Department of Molecular and Cell Biomedicine, State Scientific Center of Russian Federation Institute of Biomedical Problems of the RAS, 123007, Khoroshevskoyoe shosse, 76a, Moscow, Russia;*

[2] *Sechenov First Moscow State Medical University;*
[3] *Moscow Institute of Physics and Technology (State University)*

At the moment, pathways involved in mechanotransduction in cells have not been fully studied yet. Also, there have not been found answers to the questions what the primary receptor is and in what way the cell differ-entiates increase/decrease of load (particularly, gravitational load) on it.

The latter seems to be extremely important for implementing long-term space flights, as spending prolonged time in microgravity has negative effects on all body systems, particularly on the musculoskeletal and cardio-vascular systems. In order to develop efficient methods of protection, a detailed study of mechanisms of gravity stimuli realization in the cells of the skeletal muscles and myocardium is required. It is possible to simulate microgravity conditions on the ground using a number of models, particu-larly the «dry» immersion model in humans and the model of rodent antiorthostatic suspension (Grigoriev A.I., Shulzhenko E.B., 1978; Morey-Holton E. et al., 2005). Under terrestrial conditions the direct impact of gravitation cannot be avoided. Thus, the only most effective tool to study the effect of weightlessness on living beings is a real space flight.

However, all previously obtained experimental data is related mainly to the state of the contractile apparatus of skeletal muscles and myocardium cells. But it has not been made clear yet what induces negative changes in muscle cells, resulting in further decrease in their functional properties. We

have obtained evidence from a series of our earlier studies, suggesting the role of the submembranous cytoskeleton in primary mechanoreception in the skeletal muscle and myocardium cells (Ogneva et al., 2009-2013). It should be noted, however, that these results have been obtained not under zero gravity conditions, but under conditions of changes in cell orientation with respect to the Earth's gravity field. Thus, implementation of studies under the influence of natural microgravity (during a space flight) will allow us to identify the precise mechanisms in the development of skeletal muscle and myocardium cell responses when being exposed to the space flight, as well as the role of non-muscle isoforms of actinin in provision of mechanotransduction in these cells.

Materials and methods

Experiments were performed on the left ventricular myocardium (LV), soleus muscle (Sol) and tibialis anterior muscle (TA) samples obtained from C57 black mice, sacrificed within 13–16.5 hours after the BION-M1 biosatellite landing (the space flight lasted 30 days). There were 6 animals ($n = 6$) in this main study group designated as group F. During the space flight, the animals were provided with paste-like feed with an energy value of 361.4 kcal per 100 g of dried feed.

The following control groups were formed.

There were 8 animals in control groupV1 ($n = 8$), which were housed in the animal breeding facility (vivarium) during the space flight of the BION-M1 biosatellite.

Control group S consisted of 7 animals ($n = 7$), which served as synchronous control animals left under the 3-month surveillance (since the date of the biosatellite launch). These animals were housed in a model of a space flight vehicle and underwent the entire cycle of pre-launch preparation tests (including the 72-hour pre-launch housing of the animals in the spacecraft with all conditions of a space flight artificially reproduced, including the dietary pattern and gas composition of the air inflated). The age of the animals at the start of the synchronous experiment was similar to the age of the animals of the main study group. They were provided with the same feed as the group F animals.

Group V2 consisted of 7 animals ($n = 7$) and served as the vivarium control group (in relation to the animals in control group S). The formation of this group was justified by the necessity to avoid the effects of seasonal fluctuations on the studied parameters.

All animal experimental procedures were approved by the Commission on Biomedical Ethics of the State Scientific Center of the Russian Federation - Institute for Biomedical Problems, the Russian Academy of Sciences.

The transversal stiffness measurements were performed using the atomic force microscopy in accordance with the technique, which had been described in detail earlier (Ogneva I.V., 2010).

Determination of relative proteins content were performed using gel electrophoresis-immunoblot analysis with specific primary antibodies for each protein. Real-time PCR (RT-PCR) was used for mRNA quantification with specific primers for each gene.

Results

Left ventricular cardiomyocytes. The data obtained in all studied groups indicated that the transversal stiffness of the cortical cytoskeleton did not differ from the control level (groupV1). The content of beta-actin in the membranous fraction of proteins was found to be similar across the study groups. But in group F the relative content of beta-actin within the cytoplasmic fraction of proteins reduced by 38% (p < 0.05) as compared with group V1. Similarly, expression rates of the gene encoding beta-actin were found to be decreased by 26% in comparison to the corresponding control value (p < 0.05).The content of gamma-actin in both protein fractions (as well as expression rates of the corresponding gene) did not differ between groups F, V2, and S and the reference value registered in group V1. Alpha-actinin-1 concentrations within both protein fractions of the left ventricular cardiomyocytes did not differ between all study groups and control level. At the same time, expression of the corresponding gene appeared to be elevated by 34% (p < 0.05) in group F as compared with group V1. Within the membranous fraction of proteins of the left ventricular cardiomyocytes the content of alpha-actinin-4 was reduced by 28% in mice of group F (p < 0.05) as compared with group V1. No differences were detected for the content of alpha-actinin-4 within the cytoplasmic fraction of proteins. Alpha-actinin-4 gene expression rates changed exclusively in group F, where it was shown to be reduced by 18% (p < 0.05) in comparison to group V1.

Soleus muscle fibers. The values of the transversal stiffness registered across all study groups did not differ from the control value obtained in groupV1. Beta-actin content within the membranous fraction of proteins of the soleus muscle did not differ from its content in group V1 either. But within the cytoplasmic fraction of proteins the content of beta-actin was decreased by 16% in group F as compared with group V1 (p < 0.05). The content of gamma-actin did not differ from its reference value across all study groups. In group F alpha-actinin-1 concentration dropped by 55% within the membranous fraction of proteins (p < 0.05) compared with

groupV1. Conversely, it elevated by 62% within the cytoplasmic fraction of proteins. In mice of study groups F, V2, and S the content of alpha-actinin-4 within both protein fractions of the soleus muscle remained similar to the reference value registered for the animals of group V1.

Tibialis anterior muscle fibers. The transversal stiffness of the tibialis anterior muscle fibers did not change across the study groups, except for group F where it was found to be increased by 12% ($p < 0.05$). Beta-actin levels, as well as expression rates of the gene encoding this protein were similar within all control groups of animals. In group F the content of beta-actin was found to be elevated by 55% ($p < 0.05$) within the membranous fraction of proteins and reduced by 24% ($p < 0.05$) within the cytoplasmic fraction of proteins accompanied by a reduction in beta-actin gene expression rate by 36% ($p < 0.05$) compared with the values of the corresponding parameters registered in group V1.Gamma-actin levels did not change within both protein fractions across all study groups. However, in group F the expression rate of the gene encoding gamma-actin was found to be reduced by 15% ($p < 0.05$) as compared with groupV1. In groups F, V2 and S contents of alpha-actinin-1 and alpha-actinin-4 within both (membranous and cytoplasmic) protein fractions did not differ from their relative content within the corresponding protein fractions in group V1. The same situation was reported for the expression rates of the corresponding genes.

Conclusion

In general, some experimental data has been obtained for the first time after completion of the abovementioned studies held after the 30-day flight of the BION-M1 biosatellite (particularly, data concerning changes of the organization of the cortical cytoskeleton of different types of muscle cells under conditions of a space flight and during the following 13–16.5-hour period of readaptation). These data allowed to suggest the existence of various signaling pathways, integrated within the cortical cytoskeleton and determining possible pathways of mechanoreception. The latter allows to approximate the solution of the fundamental problem of modern cell biology and biophysics, related to interactions between physical field and a cell. In its turn, solution of this problem will allow to elaborate fundamentally new protective measures for different tissues of the body from the negative effects of space flights, as well as rehabilitation methods after long-term exposure to weightlessness.

THE PHOSPHORYLATION STATE
OF TRANSDUCIN BETA-SUBUNIT

**D.N. Orlov, A.R. Nezvetsky, T.G.Orlova,
O.V. Petrukhin, N.Ya. Orlov**

*Institute of Theoretical and Experimental Biophysics Russian Academy
of Sciences, Pushchino, Moscow region, 142290 Russia*

The ability β-subunit (Gtβ of transducin (Gt), G protein of vertebrate retinal rod outer segments (ROS), to form an intermediate phosphorylated state was studied. This state reflects the capacity of this subunit (which we have predicted earlier) to play the role of a phosphotransferase which phosphorylates GDP in the active center of the transducin α-subunit (Gtα) [1] thus participating in the activation of transducin [2].

Currently, the capacity for phosphorylation has been demonstrated both for Gtβ [3–7)] and for β-subunits of other heterotrimeric GTP-binding proteins (G proteins) [8]. Also, it has been shown that the process of phosphorylation of Gtβ is not autophosphorylation as we suggested before [1] but is catalyzed by an independent component [8].

The role of such a component is assumed to be played by nucleoside diphosphate kinase (NDP kinase). According to the present notions, NDP kinase is a multifunctional enzyme playing a role in many functionally important processes in the cell. In particular, NDP kinase determines the metastatic potential of cancer cells and is also a factor to control processes of cell growth and differentiation (see for instance [9–11]).

This proposal is supported by 1) the ability of α-(but not β−) isoform of NDP kinase to interact with the rhodopsin-transducin complex in the GTP-dependent manner [12–15]; 2) the ability of NDP kinase to act as a protein kinase phosphorylating a number of proteins on histidine residues [16–18]; and 3) the data pointing to that a residue exposed to phosphorylation in Gtβ is a histidine one (His-266) [3,6].

The present study is an attempt to show in model experiments that phosphorylation of Gtβ is just catalyzed by NDP kinase. The reactions were carried out in agreement with a procedure elaborated earlier [3,4,7,8,19]. The enzymes used were recombinant α- and β- isoforms of rat NDP kinases [20] being added to the reaction medium at concentrations 10-100 times lower than those of transducin. As a substrate for phosphorylation, various types of Gtβ-containing preparations were used (transducin and extracts of water-soluble ROS proteins [21,22] as well as the so-called "free" Gtβ [23,24] obtained by our method developed earli-

er [22,25]). These preparations were centrifuged for removing traces of photoreceptor membranes [7]. Samples usually contained 0,1-1µg Gtβ (≈3-30 pmol) whose major part was used for subsequent analysis by the electrophoresis method (SDS-PAGE). The reactions were initiated by adding 10-100 µM [γ^{32}P] ATP or [γ^{32}P] GTP (see below). After completion of the reaction, proteins were separated by SDS-PAGE, the gels were fixed and dried as described earlier [8] and radioautographed for 1-3 days using the X-ray film (RETINA X-ray XBM Blue sensitive).

The calculations showed that the use of [γ^{32}P]ATP or [γ^{32}P]GTP at a specific activity ≈ 1 Ci/mmol would be sufficient to reveal the phosphorylated state of Gtβ. This conclusion was supported by experiments on studying processes of endogenous phosphorylation and autophosphorylation in the preparations of ROS soluble proteins. In accordance with our earlier data (see for example [19]), we observed endogenous phosphorylation (or autophosphorylation) of proteins such as phosducin and rhodopsin kinase whose concentration in the ROS cytoplasm does not exceed that of Gtβ [26].

However, despite the sufficient sensitivity of the method used, we were unable to reveal both the endogenous phosphorylation of Gtβ observed earlier [3–7] and the phosphorylation of Gtβ in the presence of recombinant NDP kinase isoforms. Addition of photoreceptor membranes to the preparations also resulted in no Gtβ phosphorylation.

But what is the origin of our failures? Possibly, it is due to that the major part of Gtβ is already in the phosphorylated state. That is the reason why the phosphorylated state of Gtβ in the preceding studies (see for instance [3– 7,23,24]) could be observed only at very high levels of specific activity [γ^{32}P]ATP or [γ^{32}P]GTP (≈ 5000 Ci/mmol).

An alternate, though less probable, reason may be that in preparations of ROS proteins, there is histidine phosphatase which dephosphorylates Gtβ during the experiment. Such a histidine phosphatase was recently isolated from vertebrate tissues [17] and one of its substrates was Gtβ [27]. The presence of these histidine phosphatase is another evidence that phosphorylation of G-protein β-subunits may play an important functional role.

Thus, in our model experiments we were unable to show that the process of Gtβ-subunit phosphorylation is catalyzed just by NDP kinase. However there are several studies performed at a high specific activity of [γ^{32}P]ATP or [γ^{32}P]GTP which point to that the process of Gtβ phosphorylation indeed takes place and seems to play an important physiological role [3].

If this is really the case, it is quite possible that in ROS the following principal scheme of transducin activation is functioning: 1) NDP kinase phosphorylates Gtβ; 2) The interaction of transducin with activated rhodopsin permits the phosphate transfer from the Gtβ-subunit to GDP bound by the Gtα subunit and, as a result, the activation of the latter. Within this scheme, the surprising fact that the concentration of Gtβ exceeds 5 to 6 times that of Gtα and is about 1 mM [24] seems not to be unexpected. It simply means that the rod contains not only millimolar concentrations of ATP and GTP but also a specific fuel (1 mM of phosphorylated Gtβ) which is used as a source of energy for rapid transducin activation.

Thus, what is the principal physical advantage of trans-phosphorylation over the GDP/GTP exchange? Probably it lies in that instead of a GTP capable of being not only a cofactor of activation but also a source of noise (see for example [11]) the nature employs a much more specific donor, a phosphorylated Gtβ-subunit, that is a protein molecule localized in a molecule of the transducin complex in a specific manner forbidding a spontaneous transport of phosphate. The transfer of phosphate to GDP in the active center of the Gtα-subunit is possible upon conformational rearrangements of the complex, which are realized only during its interaction with rhodopsin. Apparently, only in this manner a rapid and high-level transducin activation can be achieved at an extremely low level of its own noise, thus providing the functioning of the rod as a single photon counter.

References

1. Tishchenkov V.G., Orlov N.Ya. (1984) Mol. Biol. (Moscow) 18, 776-785.
2. Tishchenkov V.G., Grumbkova L.O., Orlov N.Ya. (1982) Dokl. AN USSR 268, 735-738.
3. Wieland T., Ulibarri I., Gierschik P., Jakobs K.H. (1991) Eur. J. Biochem. 196,707–716.
4. Wieland T., Nürnberg B., Ulibarri I., Kaldenberg-Stasch S., Schultz G., Jakobs K.H.(1993) J. Biol. Chem. 268,18111–18118.
5. Cuello F., Schulze R.A., Heemeyer F., Meyer H.E., Lutz S., Jakobs K.H., Niroomand F., Wieland T. (2003) J. Biol. Chem. 278, 7220-7226.
6. Hippe H.J., Lutz S., Cuello F., Knorr K., Vogt A., Jakobs K.H., Wieland T., Niroomand F. (2003) J. Biol. Chem. 278, 7227-33.
7. Klinker J.F., Seifert R. (1999) Eur. J. Biochem. 261, 72-80.
8. Kowluru A., Seavey S. E., Rhodes C. J., Metz S. A. (1996) Biochem. J. 313, 97-107.
9. Steeg P.S., Palmieri D., Ouatas T., Salerno M. (2003) Cancer Lett. 190(1), 1-12.
10. Kimura N., Shimada N., Fukuda M., Ishijima Y., Miyazaki H., Ishii A., Takagi Y., Ishikawa N. (2000) J. Bioenerg. Biomemb. 32, 309-315.

11. Orlov D.N., Orlov N.Ya. (2008) Biophysics (Moscow) 53, 482-487.
12. Orlov N.Ya., Orlova T.G., Nomura K., Hanai N., Kimura N. (1996) FEBS Lett. 389, 186-190.
13. Orlov N.Ya., Orlova T.G., Reshetnyak Ya. K., Burstein E.A., Kimura N. (1997) Biochem. Mol. Biol. Internatl. 41, 189-198.
14. Orlov N.Ya., Kimura N. (1998) Biochemistry (Moscow) 63, 171-179.
15. Orlov N.Ya., Ishijima Y., Orlov D.N., Orlova T.G., Burstein E.A., Kimura N. (2007) Biochemistry (Moscow) 72, 835-842.
16. Srivastava S., Li Z., Ko K., Choudhury P., Albaqumi M., Johnson A.K., Yan Y., Backer J.M., Unutmaz D., Coetzee W.A., Skolnik E.Y. (2006) Mol. Cell. 24, 665-675.
17. Klumpp S., Bechmann G., Maurer A., Selke D., Krieglstein J. (2003) Biochem. Biophys. Res. Commun. 306, 110-115.
18. Klumpp S, Krieglstein J. (2009) Sci. Signal. 2, 1-3
19. Fesenko E.E., Orlov N.Ya., Satina L.Ya (1980) Mol. Biol. (USSR) 14, 787-794.
20. Ishijima Y., Shimada N., Fukuda M., Miyazaki H., Orlov N.Ya., Orlova T.G., Yamada T., Kimura N. (1999) FEBS Lett. 445, 155-159.
21. Kühn H.(1980) Nature 283, 587-589.
22. Orlov N.Ya. (2011) Phototransduction systems of vertebrate retinal rods and cones. Molecular mechanisms. LAP LAMBERT Academic Publishing GmbH & Co KG.
23. Clack J.W., Juhl M., Rice C.A., Li J., Witzmann F.A. (2003) Electrophoresis 24, 3493-3499.
24. Clack J.W., Springmeyer M.L., Clark C.R., Witzmann F.A. (2006) Cell Biol. Int. 30, 829-835.
25. Orlov D.N., Orlova T.G., Nezvetsky A.R., Orlov N.Ya. (2010) Biophysics (Moscow) 55, 986–989.
26. Pugh E.N.,Jr., Lamb T.D. (2000) Handbook of Biol. Physics. Vol. 3. (Eds by D.G. Stavenga, W.J. de Grip and E.N. Pugh, Jr.) Elsevier Science B.V. Chapter 5, pp. 183-255.
27. Mäurer A., Wieland T., Meissl F., Niroomand F., Mehringer R., Krieglstein J., Klumpp S.(2005) Biochem. Biophys. Res. Commun. 334, 1115-1120.

ADVANCES AND PROBLEMS OF CRYO-EM F ACTIN FILAMENT-CONTAINING COMPLEXES

A. Orlova, E.H. Egelman

Dept. of Biochemistry and Molecular Genetics, University of Virginia, Charlottesville, VA 22908

Cryo-electron microscopy is rapidly emerging as a mainstream technology for three-dimensional structural studies of the architecture of cells and macromolecular complexes. Recent developments in microscope design and imaging hardware together with strong image pro-

cessing and automation possibilities are further advancing the effectiveness of cryo-EM methods, allowing for an unprecedented advance in resolution with near-atomic resolution becoming nearly routine.

The preservation of the structure of protein complexes has always been one of the most challenging and crucial issues. Because F-actin is structurally polymorphic, it cannot be described using only one atomic model and must be understood as an ensemble of different states. Using the mechanical forces generated by thin films, we have achieved a near-atomic resolution for one state of F-actin. But studying different actin complexes at high resolution is just started and will become one of most important means for understanding actin function in the cell. Results and unexpected problems in preservation of those complexes for cryo-EM will be discussed.

PROTEOMIC STUDY OF DJ-1 PROTEIN IN CULTURED HUMAN CELLS AND MAMMALIAN MUSCLE TISSUES

N.V. Pashintseva, L.I. Kovalyov, M.A. Kovalyova, L.S. Eryomina, K.V. Lisitskaya, A.V. Ivanov, S.S. Shishkin

Bach Institute of Biochemistry of Russian Academy of Sciences, Moscow, 119071, Russia

First information about the DJ-1 protein was published by Nagakubo D. et al. (1997) [1], who isolated and characterized cDNA encoding the protein in cultured mice embryonal fibroblasts. The authors showed that it is also expressed ubiquitously in many human tissues. Based on analysis of protein features and structure it has been concluded that DJ-1 is involved in cell transformation, and the gene encoding this protein was defined as a new mitogen-dependent oncogene. Recently two groups of authors have analyzed the role of DJ-1 in different types of tumors. They noted increased expression of this protein, and showed that DJ-1 stimulates tumor cells mobility and, thus, tumor invasion [2,3]. Particularly, DJ-1 was detected in neoplasm's of muscle-containing organs of the genitourinary system: in human prostate tissue biopsy samples with benign prostate hyperplasia and prostate cancer [4] as well as in bladder cancer [5]. Recent study showed the presence of DJ-1 in muscles biopsy samples from patients with sporadic myositis and suggested its potential role in pathogenesis of human muscle diseases [6]. However, no data exist on the presence of DJ-1 in muscle tumor cells (rhabdomyosarcoma). In addition, data on DJ-1 protein function is limited. For example, UniProt database contains annotations of DJ-1 in bovine, pork and equine species based only on corresponding transcripts.

However, M. Montowska, E. Pospiech identified DJ-1 using proteomic technology in cattle muscle tissue samples after thermal processing [7].

The study presents the results of DJ-1 proteomic analysis of cultured human cell lines (rhabdomyosarcoma cell line A-204, ATCC® HTB82™) and agricultural animal muscle tissues (pork and bovine).

Extraction and fractionation were carried out by O`Farrell`s two-dimensional electrophoresis as it was previously described [8]. Protein spots on polyacrylamide gels were stained with colloidal Coomassie R-250 and silver nitrate. The gels were scanned on Epson expression 1680 scanner. Spot detection and quantification were performed using ImageMaster 2D Platinum 7.0 software (GE Healthcare, Switzerland). Protein identification after trypsinolysis was performed by matrix-assisted laser desorption/ionization time of flight mass spectrometry (MALDI-TOF MS) and tandem mass spectrometry (MS/MS) using the Ultraflex MALDI-TOF spectrometer (Bruker, Germany). Peptide mass spectra data were searched against Mascot program database (Matrix Science, USA). The results were estimated according to standard «score» and «coverage» criteria, furthermore experimental and estimated MW and pI values were compared.

Typical 2D electrophoregramms (including those of A-204 cells) contained more than one hundred individual protein fractions stained by Coomassie R-250 and 400-500 protein fractions stained by silver nitrate. DJ-1 was also identified, and identification results are presented in table.

Mass spectrometric MALDI-TOF MS identification of DJ-1 protein in rhabdomyosarcoma cultured cells, bovine and pork muscle tissues

Samples	№ in NCBI Protein database	Score	Coverage (%)	MW/pI* experimental	MW/pI** estimated
A-204 cell line	50513593	54	26	22,5/6,90	19,9/6,33
Musculus longissimus dorsi (*Sus scrofa)*	118403904	286	83	20,5/6,07	19,9/6,33
Musculus longissimus dorsi (*Bos taurus)*	62751849	330	42	23,0/6,75	20,0/6,84

* Experimental values of molecular weight (MW, kDa) and isoelectric points (pI). **Estimated values of MW (kDa) and pI recorded in NCBI Protein database.

1	maskralvil	ak**GAEEMETV**	**IPVDVMRRAG**	**IKVTVAGLAG**	KDPVQCSRDV
51	**VICPDASLED**	**AKKEGPYDVV**	**VLPGGNLGAQ**	**NLSESAAVKD**	**ILKEQEKR**kG
101	**LIAAICAGPT**	**ALLAHEIGFG**	**SKVTTHPLAK**	dkmmngshys	ysenrvek**DG**
151	**LILTSRGPGT**	**SFEFALAIVE**	**ALAGKEVADQ**	**VKAPLVLRD**	

Total amino acids sequence of pork DJ-1 protein predicted at the transcript level [Q0R678 UniProt]. Tryptic peptides obtained during MS analysis are marked with title letters.

The total amino acid sequence of pork DJ-1 protein predicted at the transcript level [Q0R678 UniProt] is shown on figure (tryptic peptides obtained during MS analysis are marked with title letters).

The results of our study showed in Table 1 and Fig. 1 suggest the presence of DJ-1 protein both in human rhabdomyosarcoma cultured cells and skeletal muscles of healthy pigs and cattle. Therefore this protein could be considered as a component of normal proteomic profile of muscle cells and DJ-1 expression is altered during malignant cell transformation (which was observed by many authors [2,3,9]).

References

1. Nagakubo D. et al. Biochem. Biophys. Res. Commun. 1997. V.231. P.509-513.
2. Vasseur S. et al. Oncogene. 2012. V.31. P.664-670.
3. Zhu Z.M. et al. Oncol. Rep. 2014. V.31. P.1489-1497.
4. Lisitskaia K.V. et al. Biomed Khim. 2011. V.57. P.392-401
5. Lee, H. et al. Oncol Lett. 2012. V.3. P.507-512.
6. Terracciano C. et al. Free Radic Biol. Med. 2008.V.45. P.773–779.
7. Montowska M., Pospiech E. Food Chem. 2013. V.136. P.1461-1469
8. Kovalyova, M.A. et al. Biochemistry-Moscow 2009. V.74. P.1239-1252.
9. Li Y. et al. Int. J. Med. Sci. 2013. V.10. P.1689-1697.

CHOLESTEROL DEPENDENT REGULATION OF THE SYNAPTIC TRANSMISSION AT NEUROMUSCULAR JUNCTIONS

A.M. Petrov, M.R. Kasimov, A.A. Yakovleva, A.L. Zefirov

Kazan State Medical University, Butlerova st. 49 , Kazan, 420012, Russia

Presynaptic nerve terminals release neurotransmitters by synaptic vesicle exocytosis. When an action potential depolarizes the presynaptic membrane, Ca^{2+} channels open, causing a local increase in the intracellular Ca^{2+} concentration at the active zone thus triggering a fusion event. After the fusion pore opens, synaptic vesicle membrane is recovered

through clathrin-mediated endocytosis. Then, synaptic vesicles are filled with neurotransmitters and supply the synaptic vesicle pool. This mechanism of synaptic vesicle recycling could be observed at the majority of synapses (Zefirov, Petrov, 2012). However, in some cases, synaptic vesicles may recycle via "kiss-and-run" mechanism, where the fusion pore opens and closes and synaptic vesicle undergoes undocking (Alabi, Tsien, 2013). In addition synaptic exocytosis occurs at rest spontaneously. Excitability of neurons, synaptic connections stability and local synaptic protein synthesis are depended on spontaneous neurotransmitter release. Spontaneous exocytosis enhancement may lead to undesirable effects due to emptying a vesicle population, desensitization of neurotransmitter receptors and decrease in a protein synthesis at synapse. Overall there is factors invokes the attenuation of the synaptic transmission efficacy (Kaeser, Regehr, 2013).

Membrane cholesterol is an essential component that is involved in key steps of the synaptic vesicular cycle (Wasser, Kavalali, 2009, Petrov, Zefirov, 2012; Puchkov, Haucke, 2013). Cholesterol can directly interact with different exo- and endocytotic proteins and form together with sphingolipids a membrane microdomains (lipid rafts). Cholesterol arranges a lipid rafts at the synaptic sites that are comprised of quite a number signaling molecules and ion channels (Petrov et al. 2011; Petrov, Zefirov, 2012).

In experiments on a frog (Rana Ridibunda) neuromuscular junction the influence of cholesterol depletion by methyl-β-cyclodextrin (MCD) on the presynaptic vesicular cycle was investigated. Electrophysiological (two electrode fixing of potential) and various optical methods were applied. It was shown that 1 mM methyl-beta-cyclodextrin (MCD) reduced membrane content of cholesterol on ~ 10-15% (fluorescent filipin probe) and decrease raft stability at presynaptic membrane (staining by fluorescent-labeled B-subunit of cholera toxin). If 10 mM MCD was used then level of membrane cholesterol was declined by 40-50% and the ordinary distribution of active zone protein syntaxin (the protein immunofluorescence staining) was disturbed. Depletion of «little» cholesterol (by 1mM MCD) did not change spontaneous neurotransmitter release (frequency of miniature end plant potentials), but application of 10 mM MCD induced the dramatic increase in spontaneous transmission (Petrov et al., 2010, 2011, Tarakanova et al., 2011).

Using registration of evoked postsynaptic currents (indicator of neurotransmitter release) and FM1-43 dye (load and unload from recy-

cling synaptic vesicle) it is shown that extraction of cholesterol by 1mM MCD led to the apparent shifts in recycling of synaptic vesicles during prolong high frequency activity (20 Hz, 3 minutes). Evoked by single and high frequency stimulation exocytosis of synaptic vesicles was decreased, and also the attenuation of synaptic vesicle supply to the exocytotic sites (ready releasable pool) was observed. In addition to above effects the depletion of cholesterol both from external membranes and membranes of recycling synaptic vesicles broke to synaptic vesicles endocytosis and recycling. Thus, in the processes of exocytosis the key role is played by cholesterol of plasma membranes, and the endocytosis critically depends on the amount of cholesterol in the membranes of synaptic vesicles (Petrov et al., 2010, 2011).

Subsequently the stimulatory effect mechanisms of cholesterol depletion (by 10mM MCD) on spontaneous release and exocytosis were studied. It is shown that MCD (10 mM) mediated exhaustion of cholesterol induced the enhancement of a reactive oxygen species (ROS) production (for intracellular ROS detection was used a H2DCF fluorescent dye), which was prevented by antioxidant (N-acetyl cysteine, NAC) and NADPH oxidase inhibitor (apocynin). Increase in ROS level occurred both in extra – and intracellular spaces (as extracellular ROS indicator was applied the compound of Amplex Red reagent and horseradish peroxidase), and it was associated with lipid peroxidation in synaptic regions (it was estimated by IT-lipid peroxidation kit). Cholesterol depletion provoked an intracellular Ca level growth (fluo4 – is a fluorescent Ca indicator), there was hindered by NAC and TRPV channels blockers (ruthenium red and capsazepine). On the other hand the MCD induced [Ca]i rising did not change if Ca release from endoplasmic store was blocked by TMB8. The cholesterol depletion effects on a spontaneous release and an exocytosis were significant reduced by antioxidant, intracellular Ca chelation agent (BAPTA-AM) and blockers of TRPV channels. Calcineurin antagonist (cyclosporine A) applied to bath damped MCD-induced enhancement of spontaneous release / exocytosis, whereas a phosphatases PP1 and PP2A inhibitor (nanomolar concentration of okadaic acid) did not change the MCD effects. It was suggested that cholesterol depletion induced enhancement of spontaneous exocytosis depends on a ROS generation, which in turn leads to an influx Ca via TRPV channels and calcineurin activation.

It has been demonstrated that protein kinase C is involved in the enhancement of spontaneous exocytosis caused by cholesterol depletion

from the surface membranes of cerebellar synapses and synaptosomes (Smith et al., 2010; Teixeira et al., 2012). We investigated the role of protein kinase C in the enhancement of spontaneous exocytosis after cholesterol depletion. As mentioned above both spontaneous neurotransmitter release and unloading FM1-43 dye from synaptic vesicles were increased when cholesterol was removed from the membranes by the 10 mM MCD treatment. However, inhibition of the protein kinase C by myristoylated peptide prevented MCD-induced increases in FM1-43 unloading, whereas the frequency of spontaneous postsynaptic events remained enhanced. The increase in FM1-43 unloading still could be observed if sulforhodamine 101 (the water soluble FM1-43 quencher that can pass through the fusion pore) was added to the extracellular solution. This suggests a possibility that exocytosis of synaptic vesicles under these conditions could occur through the kiss-and-run mechanism with the formation of a transient fusion pore. Inhibition of phospholipase C and calmodulin did not lead to similar change in MCD-induced exocytosis. It is possible that the depletion of cholesterol could lead to the increase in kiss-and-run exocytosis, whereas simultaneous activation of protein kinase C may switch exocytosis to a full mode. There is evidence indicating the tight relationship between cholesterol and the type of exocytosis. We have recently showed that "kiss-and-run" mechanism of neurotransmitter release can be used by vesicles belonging to the recycling pool after the enzymatic oxidation of membrane cholesterol (Petrov et al., 2013).

Thus amount of plasma membrane cholesterol determines the balance between spontaneous and evoked synaptic transmission at the frog neuromuscular junction. Evoked neurotransmitter release / exocytosis and synaptic vesicle traffic to sites of exocytosis are more sensitive to cholesterol content. These are significantly reduced by a slightly cholesterol depletion. Also tightly cholesterol dependent step of vesicular cycle is endocytosis, but this process is specially required abundance of vesicular cholesterol. Therefore depletion of cholesterol form recycling vesicles is blocked endocytosis and led to uncoupling of synaptic vesicle cycles. Natural dynamics of spontaneous exocytosis is altered only in condition of severe depletion of membrane cholesterol. Dramatic decrease in membrane cholesterol arouses the spontaneous exocytosis enhancement. Partly this effect is occurred dye to elevation of NADPH-oxidase activity which generates ROS. In turn ROS facilitates a TRPV channel mediated Ca-ion influx into the cytoplasm and subsequently stimulation of phosphatase PP2B (calcineurin). Calcineurin dependent dephosphorylation

may control a compensatory endocytosis and a number of synaptic vesicles that is easily evolved in exocytosis. In addition heavy cholesterol depletion induces Ca/calmodullin/phospholipase C independent activation of protein kinase C and this kinase switches the mode exocytosis to fully collapse pathway. PKC may promotes full exocytosis through the phosphorylation of exocytosis machinery proteins (e.g., SNAP-25 and Munc18) or direct interaction with these proteins. Thus while slightly cholesterol depletion inhibits the evoked synaptic transmission, the more significant cholesterol lowering leads to increase in spontaneous release and activating of the signaling molecules (NADPH-oxidase, TRPV channel, calcineurin, protein kinase C). In the last situation the over activation of signaling pathway may have a deleterious effect (such as oxidation of membrane lipids, Ca toxicity).

Our work has a nice concordance with data from other research group. Cholesterol depletion by extracellular sequestration with MCD or acute statin-mediated inhibition of de novo cholesterol biosynthesis dramatically reduces evoked neurotransmitter release but at the same time augments spontaneous fusion rates at the crayfish neuromuscular junction, synaptosomes, cerebellar and hippocampal synapses (Zamir, Charlton, 2006; Wasser, Kavalali., 2009; Teixeira et al., 2012).

References

1. Alabi AA, Tsien RW. Annu. Rev. Physiol. 75:393-422. 2013.
2. Kaeser P.S., Regehr W.G. Annu. Rev. Physiol. 76:26.1-26.31. 2014.
3. Petrov AM, Kasimov MR, Giniatullin AR, Tarakanova OI, Zefirov AL. Neurosci. Behav. Physiol. 40(8):894-901. 2010.
4. Petrov AM, Kasimov MR, Giniatullin AR, Zefirov AL. Ross. Fiziol. Zh. 99(2):245-60. 2013.
5. Petrov AM, Kudryashova KE, Odnoshivkina YuG, Zefirov AL. Neurochem. J. 5(1): 13-19. 2011.
6. Petrov AM, Naumenko NV, Uzinskaya KV, Giniatullin AR, Urazaev AK, Zefirov AL. Neuroscience. 186:1-12. 2011.
7. Puchkov D, Haucke V. Trends Cell Biol. 23(10):493-503. 2013.
8. Smith AJ, Sugita S, Charlton MP. J Neurosci. 30(17): 6116-21. 2010.
9. Tarakanova OI, Petrov AM, Zefirov AL. Dokl. Biol. Sci. 438:138-40. 2011.
10. Wasser CR, Kavalali ET. Neuroscience. 158(1):177-88. 2009
11. Zamir O, Charlton MP. J. Physiol. 571(Pt 1):83-99. 2006.
12. Zefirov AL, Petrov AM. Neurosci. Behav. Physiol. 42(2): 144-152. 2012.

THE KINETIC BEHAVIOUR OF CGMP-SPECIFIC PHOSPHODIESTERASE IN BOVINE RETINAL ROD OUTER SEGMENTS ON ITS ACTIVATION WITH LOW GTP CONCENTRATIONS IN A WIDE RANGE OF FREE CALCUIM ION CONCENTRATIONS

O.V. Petrukhin, A.R. Nezvetsky, T.G. Orlova, N.Ya. Orlov

Institute of Theoretical and Experimental Biophysics, Russian Academy of Sciences, Pushchino, Moscow region, 142290 Russia;
E-mail: petrukhinoleg@rambler.ru

Kinetics of cyclic nucleotide hydrolysis by cGMP–specific phosphodiesterase (PDE6) in bovine retinal rod outer segment (ROS) suspension have been studied by the pH-metric method [Yee, Liebman, 1978; Orlov et al., 1988] over a wide range of free calcium ion concentrations ($[Ca^{2+}]$). PDE6 in totally bleached ROS suspensions was activat-ed by low GTP concentration (about 1-2 μM) that were comparable with the concentration of G protein transducin (Gt), which GTP-binding α-subunit (Gtα) is the intrinsic activator of PDE6. The main results are: (1) the amount of cyclic nucleotides hydrolyzed under these conditions by transducin-activated PDE6 was about two times more at high free calci-um ion concentrations ($[Ca^{2+}] > 1$ мкМ) than that at low calcium concen-trations ($[Ca^{2+}] < 100$ nM), whereas the control experiments showed that (2) activation of PDE6 by GTP[S] (a pure-hydrolyzed GTP analog guanosine 5`-O-(3-thiotriphosphate) in totally bleached ROS suspen-sions was calcium-independent.

These results are in agreement with the early data that suggest that the lifetime of transducin active state (determined by the rate of GTP hydrolysis in the transducin active site) is greatly decreased at low Ca^{2+} concentrations (< 100 nM) [Tishchenkov, 1985; Orlov, 2011; Firsov, 2012; Astakhova et al., 2008]. We suggest that: (1) besides the earlier described RGS-system (that consists of RGS9-1, Gβ$_{5L}$ and R9AP proteins involved in the acceleration of GTP hydrolysis when the complex is formed between Gtα and inhibitory γ-subunit of PDE6 [He et al., 1998; Makino et al., 1999; Arshavsky et al., 2002]), ROS contains an additional Ca^{2+}-dependent mechanism that inactivates free transducin in response to a rapid photoinduced drop in Ca^{2+}-concentration in the ROS cytoplasm [Yau, Nakatani,1985; McNaughton et al., 1986; Nakatani, Yau, 1988]; (2) such a system seems to be important for inactivation of a so called "free transducin", that is the transducin molecules that have no

chance to interact with PDE6 within the time of photoresponse generation. In the framework of such an idea, (1) a bleached rhodopsin molecule, during its lifetime, produces a surplus amount of active transducin that seems to be necessary to provide a sharp increase in the photoresponse; (2) the Ca^{2+}-dependent process of free transducin inactivation additionally contributes to the required temporal course of the back front of photoreceptor response.

References

Arshavsky V.Y., Lamb T.D., Pugh E.N., Jr. (2002) G proteins and phototransduction. Annu. Rev. Physiol. 64, 153–187.

Astakhova L.A, Firsov M.L., Govardovskii V.I. (2008) Kinetics of turn-offs of frog Rod phototransduction cascade. J. Gen. Physiol. 132, 587-604.

He W., Cowan C.W.,Wensel T.G. (1998) RGS9, a GTPase accelerator for phototransduction. Neuron 1, 95-102.

Makino E.R., Handy J.W., Li T., Arshavsky V.Y. (1999) The GTPase activating factor for transducin in rod photoreceptors is the complex between RGS9 and type 5 G protein beta subunit. Proc. Natl. Acad. Sci. U S A 96, 1947-1952.

McNaughton P.A., Cervetto L., Nunn B.J. (1986) Measurement of the intracellular free calcium concentration in salamander rods. Nature 322, 261-263

Nakatani K., Yau K.-W. (1988) Calcium and magnesium fluxes across the plasma membrane of the toad rod outer segment. J. Physiol. 395, 695-729.

Orlov N.Ya., Kalinin E.V., Orlova T.G., Freidin A.A. (1988) Properties and content of cyclic nucleotide phosphodiesterase in photoreceptor outer segments of ground squirrel retina. Biochim. Biophys. Acta 954, 325-335.

Orlov N.Ya. (2011) Phototransduction systems of vertebrate retinal rods and cones. Molecular mechanisms. LAP LAMBERT Academic Publishing GmbH & Co KG.

Pugh, E. N., Jr., & Lamb, T. D. (2000). Phototransduction in vertebrate rods and cones: molecular mechanisms of amplification, recovery and light adaptation. In D. G. Stavenga, W. J. de Grip & E. N. Pugh (Eds.), Handbook of biological physics, Vol. 3, Molecular mechanisms of visual transduction (pp. 183-255). Amsterdam: Elsevier.

Tishchenkov V.G. (1983) GTP-binding protein complex of frog retinal rod outer segments. PhD thesis, Pushchino-Moscow-Minsk.

Yau K.-W., Nakatani K.(1985) Light-induced reduction of cytoplasmic free calcium in retinal rod outer segment. Nature 313,579-582.

Yee R., Liebman P.A. (1978) Light-activated phosphodiesterase of the rod outer segments. Kinetics and parameters of activation and deactivation. J. Biol. Chem., 253, 8902-8909.

EXPRESSION OF PGC-1α ISOFORMS AFTER ACUTE EXERCISE IN HUMAN SKELETAL MUSCLE

D.V. Popov[1,2], E.A. Lysenko[1], A.V. Bachinin[1],
T.F. Miller[1], O.L. Vinogradova[1,2]

[1] *Institute for Biomedical Problems, Russian Academy of Sciences, Khoroshevskoye sh. 76A, Moscow, 123007, Russia;*
[2] *Faculty of Fundamental Medicine, Lomonosov Moscow State University, Lomonosovsky prosp. 31-5 Moscow, 117192, Russia*

Peroxisome proliferator-activated receptor gamma (PPARG) coactivator 1 alpha (PGC-1α) is a master regulator of mitochondrial biogenesis in the skeletal muscle. Aerobic exercise induces activation of AMP-activated protein kinase (AMPK) and p38 mitogen-activated protein kinase. These kinases regulate the transcriptional initiation of the PGC-1α promoter as well as the activation of PGC-1α. Activated PGC-1α transits into the nucleus. As a result the coactivation of transcription factors and the increase in mRNA expression of genes involved in mitochondrial function (TFAM, CS) and angiogenesis (VEGFA) take place. Rodent studies showd that skeletal muscle potentially might express at least six transcript variants of PGC-1α mRNA. Full length (FL-) PGC-1α-a mRNA is transcribed from the canonical proximal promoter and FL-PGC-1α-b, -c mRNA are transcribed from the alternative upstream promoter. Additionally N-truncated (NT) isoforms might be express in the skeletal muscle. Recently it was shown that different PGC-1α isoforms induced different gene expression programs. It is not clear what PGC-1α isoforms are expressed in human skeletal muscle. The goal of the study was to investigate expression of different PGC-1α isoform in human skeletal muscle after acute endurance exercise.

Nine male endurance trained amateurs carried out endurance exercise (70 min). Biopsy samples from m.vastus lateralis were taken before, 40 min, 5 h and 21 h after termination of endurance exercise. The expression of PGC-1α was evaluated by real-time PCR. The primer pairs were designed to detect total PGC-1α, FL-PGC-1α-a, -b, -c, and NT-PGC-1α-a, -b, -c transcripts. Activation of PGC-1α protein was evaluated by translocation of PGC-1α to the nucleus. The protein level was measured by immunoblotting.

The acute exercise led to increased phosphorilation of both upstream kinases: AMPK and p38. The exercise session induced expression of PGC-1α mRNA from both canonical and alternative promoter 5 h after termination of exercise. The expression of PGC-1α-a, and NT-PGC-1α-b was

higher than that of another transcripts. The FL-PGC-1α level in nucleus did not increase 40 min post endurance exercise , but PGC-1α total protein content increased at 21 h of postexercise recovery. The expression of different PGC-1α isoforms was compared to expression of their target genes.

VARIETY OF MOLECULAR ORGANIZATION
OF HALOARCHAEAL FLAGELLAR FILAMENTS
M.G. Pyatibratov, S.N. Beznosov, A.S. Syutkin,
A.V. Galeva, O.V. Fedorov

Institute of Protein Research, Russian Academy of Sciences,
Institutskaya str., 4, Pushchino, Moscow Region, 142290, Russia

After the publication of a considerable quantity of archaeal genome sequences (including more than 90 sequences for *Haloarchaea*) it was revealed that the number of flagellin genes and their genomic organization may be substantially different in different organisms. As shown in figure, among the 91 haloarchaeal species analyzed, about 25% of genomes have no flagellin gene, nearly 9% have one flagellin gene, about 43% have two copies and the remainders have three to six copies.
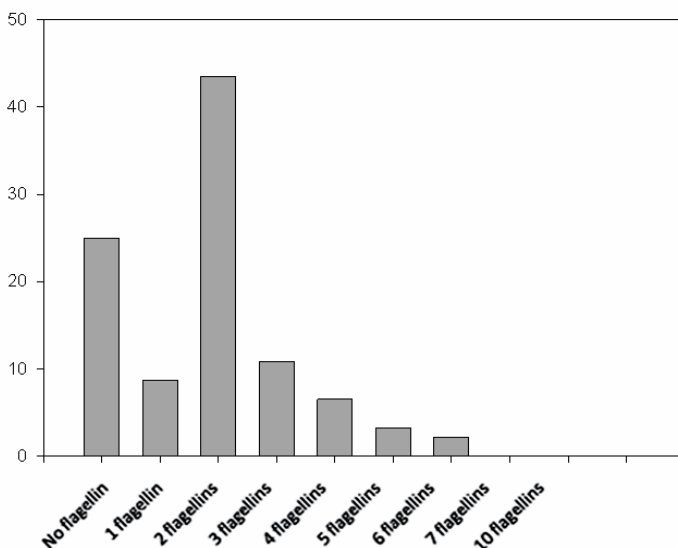
Distribution of flagellin genes per genome among 91 haloarchaeal species analyzed.

216

It can be assumed that these differences are revealed at the level of the mode of flagella construction and lead to varied structural and functional flagella properties in different archaeal species. Until recently it was believed that in Euryarchaeota the functional helical flagellar filaments need at least two flagellin molecules with different amino acid sequences. Mutant *Halobacterium salinarum* strains in which all flagellin genes, except one, have been inactivated were nonflagellated or formed straight nonfunctional flagella (Tarasov et al., 2000; Beznosov et al., 2007). However, recent data suggest that in some haloarchaea the functional flagella could be formed from a single flagellin gene product. We were the first to show that the Antarctic haloarchaea *Halorubrum lacusprofundi,* unlike *H. salinarum,* forms functional helical filaments from a single flagellin gene product (Syutkin et al., 2012). But in this case several flagellin forms, which probably are different post-translational modifications of the same polypeptide, were identified. It is probable that a change in the ratio of these forms results in a variety of structural and functional properties of the formed flagella. We found that *H. lacusprofundi* cultivation at different temperatures results in distinct flagella types differing in the ratio of flagellin forms. This phenomenon may be associated with adaptation of flagellar structure to environmental changes. *H. lacusprofundi* was the first member of the *Halorubrum* genus, which was determined to complete the genomic sequence. Later the genome sequences of 12 more *Halorubrum* species were published including *Halorubrum saccharovorum*. It turned out that unlike *H. lacusprofundi* in other *Halorubrum* genomes, there are two flagellin genes organized into one operon. The amino acid sequences of FlaB1 and FlaB2 flagellins, encoded by these genes are substantially different from each other and FlaB1 has a high homology with single *H. lacusprofundi* flagellin. From our point of view, the lack of the second flagellin gene in *H. lacusprofundi* may be related with unique habitat conditions of this organism (Deep Lake in Antarctica), while the habitat area of the remaining 12 *Halorubrum* species includes warmer salt ponds in the regions of Turkmenistan and Tibet to Chile and Australia. We initiated studies to elucidate the possible FlaB2 role, which may consist of: (I) formation of individual filaments functionally different from FlaB1 filaments, and (II) stabilization of the supramolecular structure of the bicomponent FlaB1/FlaB2 filaments. As an object of the research we selected the *H. saccharovorum* strain isolated from salterns in California evolutionarily closest to *H. lacusprofundi*. We found that when grown on semisolid agar plates *H. saccharovorum* shows higher motility than *H. lacusprofundi*.

When grown in the liquid medium, the *H. saccharovorum* cells, unlike *H. lacusprofundi,* aggregate to form larger granular cell agglomerates and a characteristic biofilm at the inner surface of the glass flask. Upon SDS-electrophoresis *H. saccharovorum* flagella appear as two major bands corresponding to FlaB1 and FlaB2 flagellins.

Another object of our research, haloarchaea *Haloarcula marismortui*, has two flagellin genes located in different replicons. We expected to see both flagellins in the flagella composition, but it turned out that the main flagella component is the only one of flagellins (Pyatibratov et al., 2008; Syutkin et al., 2012). We demonstrated that the external conditions could determine which of the *H. marismortui* flagellin gene products will be used in the flagella assembly (Syutkin et al., 2014).

References

1. Beznosov S.N., Pyatibratov M.G., Fedorov O.V. Microbiology, 2007, 76: 435-441.
2. Pyatibratov M.G., Beznosov S.N., Rachel R., Surin A.K., Syutkin A.S., Fedorov O.V. Can. J. Microbiol., 2008, 54: 835-844.
3. Syutkin A.S., Pyatibratov M.G., Beznosov S.N., Fedorov O.V. Microbiology, 2012, 81: 573-581.
4. Syutkin A.S., Pyatibratov M.G., Galzitskaya O.V., Rodriguez-Valera F., Fedorov O.V. Extremophiles, 2014, 18: 341-349.
5. Tarasov V.Y., Pyatibratov M.G., Tang S.-L., Dyall-Smith M., Fedorov O.V. Mol. Microbiol., 2000, 35: 69-78.

PLANARIANS AS A MODEL SYSTEM
FOR BIOINDICATOR STUDIES POLLUTION LEVELS
AND SOURCES OF FRESHWATER

M.O. Rasgulaeva, A.S. Savinkina
*Municipal budget educational institution gymnasium "Pushchino"
(MBOU Gymnasium "Pushchino"), Pushchino, Russia;
E-mail: chechako-m@rambler.ru*

At the present time, in view of the growing anthropogenic pressure on the environment in the world there is an increasing shortage of fresh drinking water. Now the question becomes urgent fast express determination of the quality of drinking water. Very sensitive method can serve bioindication, not only qualitatively but also quantitatively, which allows a high level of pollution to be reliably determined . Such an object for analysis can be bioindicators freshwater flatworms - planarian, the

regeneration process which is sensitive to the surrounding physical and chemical factors. Thus, the purpose of the work - the study of the toxicological sensitivity Schmidtea mediterranea planarians to salts of heavy metals and detergents. A freshwater planarian flatworms the possibility of using these animals as a highly object to quantify bioindication. In this work we studied the sensitivity of planarian regeneration process and the sustainability of their DNA damage when exposed to heavy metal salts and detergents. It was shown that the detergent sodium dodecylsulfate, plumbum nitrate, and copper sulfate at low concentrations (10^{-7} M and about 10^{-8} M) significantly inhibited the regeneration head portion animals had a copper salt expressed genotoxic properties. Thus, the demonstrated high sensitivity biological system applied to water pollution, which is comparable to the sensitivity of modern analytical instruments.

PLANT MODELS FOR ANALYSIS OF CONTRACTILE ACTIVITY

V.V. Roshchina

Institute of Cell Biophysics, Russian Academy of Sciences,
Institutskaya Str. 3, Pushchino, Moscow region, 142290, Russia

Contractile activity could be studied on plant models. Ten years of our experiments with various cells gave new information having perspectives for the studies in Future that needs to discuss in small review. Among purposes of new investigations in such field are as follows: 1. Participation of contractile proteins in transfer of external signal from plasmatic membrane to cellular compartments such as nuclei, chloroplasts or vacuoles., 2. Biological activities of exogenous contractile proteins, 3. The study of special contractile structures, 4. Effects of toxins and drugs – relaxants and spazmolitics – on the cell and organelles behavior that is usually difficult on animal cells,

Participation of contractile proteins in transfer of external signal. Microspores involved in plant reproduction and pigmented cells were proposed as models to study chemical signal perception and transduction. First objects include chloroplast-containing vegetative microspores of spore-bearing species or generative microspores of seed-bearing species (pollen or male gametophyte) incapable of autotrophic nutrition and lacking photosynthetic structures in mature forms. Involvement of contractile components in chemical signal transduction
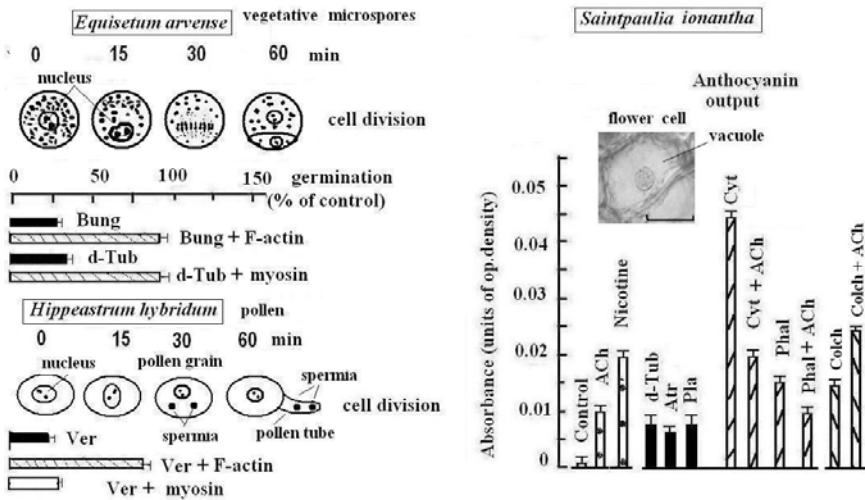
Fig. 1. Examples of cellular models such as vegetative microspores, pollen and pigmented cells of flower (bar = 50 μm) to study effects of contractile proteins, antagonists of acetylcholine and anticontractile reagents. Bung - bungarotoxin10^{-6}M , Tub - d-tubocurarine 10^{-5}M, Ver – verapamil 10^{-5}M l, Cyt - cytochalasin B 10^{-5}M, Phal – phalloidin 2×10^{-6}M, Ach – acetylcholine 10^{-6}M, Atr – atropine 10^{-5}M, Pla – platyphylline 10^{-5}M, Colch-colchicine 10^{-5}M.

from the cell surface to the organelles was studied in unicellular vegetative *(Equisetum arvense)* and generative *(Hippeastrum hybridum* pollen) microspores of plants where the germination served a physiological response to the chemical signal by various natural compounds (fig. 1), in particular acetylcholine and biogenic amines [1, 2]. Both types of microspores exposed to neurotransmitters and their agonists demonstrated growth activation, while neurotransmitter antagonists and ion channel blockers inhibited this process. Pretreatment with ion channel blockers and then by anticontractile agents (cytochalasin B or colchicines) either had no effect or increased the inhibition of microspore growth. The addition of exogenous actin the treatment of the cells with α-bungarotoxin or *d*-tubocurarine or verapamil prevented negative effects [3]. In the experiments potential participation of the actin domains in the work of ionic channels was examined. Neurotransmitters dopamine and serotonin as well as active oxygen species hydrogen peroxide and *tert*-butyl peroxide stimulated microspore germination as chemical signals, but there was no

effect after pretreatment with cytochalasin B or colchicine or even the germination rate was decreased [1,2]. Increased blue fluorescence was observed in certain cell regions. The involvement of actin and tubulin in chemical signal transduction from the cell surface to the nucleus has been also proposed based on experiment blue-fluorescent *d*-tubocurarine and yohimbine (blockers of cholinoreceptor and adrenoreceptor, respectively) decreased the number of the *E. arvense* cells with red fluorescence of chlorophyll at 680 nm [4]. After the addition of the cytoskeleton proteins and cholinesterase to the medium, the decrease of red fluorescence intensity, usually induced by *d*-tubocurarine or yohimbine, was not observed.

Unlike microspores plant pigmented intact cells containing anthocyanins were recommended to study signaling from plasmalemma to vacuole (a membrane-surrounded cavity in a cell, is considered as an organ of osmoregulation and excretion) which demonstrating contractile activity. Microfilaments with actomyosin play important roles in supporting strand structures in the cytosol on the opposite side of vacuoles have been identified as a possible route for cytoplasmic streaming, considered responsible for the intracellular transport of molecules and organelles in vacuolated cells. Recently vacuoles of pigmented intact plant cells started to study as possible biosensors for the investigation of chemosignaling by acetylcholine and histamine from plasmalemma to the vacuole [5]. Among the objects included secreting flower petal cells clear results were received for intact petal cells from common African violet *Saintpaulia ionantha* Wendl (Fig.1). The cell responses based on the absorbance of the anthocyanin-containing secretion released through 0.5 -1 hour after the addition of reagents. In untreated (control) samples there were no pigment release up to 20 h of exposure. Output of anthocyanins was seen only under the addition of acetylcholine into medium (unlike histamine) or its agonists nicotine (bind with nicotinic type of animal cholinoreceptors), muscarine, arecoline, and quinuclidinyl benzilate (bind with muscarinic type of animal cholinoreceptor) as well as cytochalasin B, phalloidin and colchicine. The process was depressed by antagonists of acetylcholine d-tubocurarine, atropine and platiphylline. After more than 1 h of exposure in variant with colchicine, the anthocyanin uptake was also observed that showed on the work of microtubules. The participation of actin and tubulin, possible connecting with cholinoreceptors, in the output of anthocyanin has been proposed.

Biological activities of exogenous contractile proteins. Functions of cytoskeleton as a whole appear to be not limited only to a participation
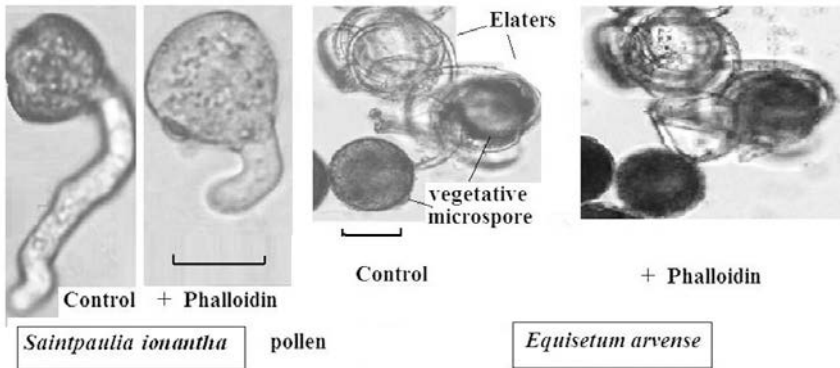
Fig. 2. Examples of cellular models such as pollen tubes (left bar = 50 μm) and elaters of vegetative microspores (right bar = 20 μm) for the study with phalloidin 10^{-4}M stabilizing of F-actin.

in motile reactions inside the cell [6]. In particular, the cytoskeleton protein titin stimulates the mechano-growth factor synthesis as well as protein synthesis in rat or human myoblasts culture [7]. In nature proteins of cytoskeleton being liberated out interact with various cells belonged to majority of different organisms - from microbes to plants and animals - and play certain role in chemosignaling and regulating of growth process. Bioactivity of the cytoskeleton proteins such as actin, myosin and titin that have been extracted from the rabbit muscle was analyzed on plant misrospores as unicellular biosensors [8]. The fibrillar forms of the proteins stimulated the germination of vegetative microspores from horsetail *E. arvense* and generative (pollen) microspores from knight's star *H. hybridum.* In special experiments the proteins tested were able to reverse the blockade of ion channels by drugs d-tubocurarine and α-bungarotoxin, acting on cholinoreceptors, or verapamil, regulating Ca^{2+}-channels.

    Special motile structures as models. The study of special motile structures, like pollen tubes and elaters of vegetative microspores (fig. 2), may be carried out with fluorescent markers binding with contractile proteins: for F-actin fluorescein - phalloidin conjugate (ex. max 496 nm/emission 516 nm) [10] or for tubulin - colchicine (ex. max 360 nm/emission 460 nm) were represented [11]. The compounds are the secretory products of fungi *Amanita phalloides* and plants belonged to genera *Colchicium,* and *Gloriosa*. Green fluorescence of the probe on actin was observed in both models studied, showing the binding within pollen tube and in elaters. Actin in the elaters of vegetative microspores from *E.*

Effects of toxins on the germination of spores

Development of *Saintpaulia* pollen			Development of microspores from *Equisetum arvense*	
Variant	Index of germination	Length of pollen tubes (mm)	Variant	% of ger-minated cells
Control	0.88 ± 0.01	1.05 ± 0.10	Control	100 ± 5
Phalloidin (10^{-4}M)	0.45 ± 0.02	0.04 ± 0.006	Butanol 1:1000 (alcohol/water)	122 ± 3

arvense was not seen earlier. Colchicine binding with tubulin also included in the structures well-seen by any type of luminescence microscopes [11].

Testing of drugs and toxins acting on contractile structures. The use of the plant cells as model systems permits the fast drug testing of damages of living structures related to contractile elements [9], instead experiments with animals, in which a vivisection and fixation procedures are necessary. In high concentrations (about 10^{-4}M) toxin phalloidin depressed both the germination of pollen and pollen tube elongation dealt with the actin polymerization (Table 1) while some muscle spazmolitics papaverine, dehydropapaverine and clofelin either had no effects or weakly inhibited [3]. Known toxin n-butanol which acts on actin-related cell elongation stimulated the microspores development (Table 1).

Based on the above-mentioned experiments plant cellular models may be recommended for the study of contractile activity related to chemosignaling and growth processes.

References

1. Roshchina, V.V. Contractile proteins in chemical signal transduction in plant microspores. Biol.Bull., Ser. Biol. 2005, 33 (3), 281-286.
2. Roshchina, V. V. Chemosignaling in plant microspore cells. Biol. Bull.,Ser.Biol. 2006, 33 (4), 414-420.
3. Roshchina, V. V. and Vikhlyantsev, I. M. Mechanisms of chemosignalling in allelopathy: Role of Ion channels and cytoskeleton in development of plant microspores. Allelopathy J., 2009, 23 (1), 25-36.
4. Roshchina, V.V. , Yashin V.A. and Vikhlyantsev, I. M. 2012.
5. Roshchina, V.V.and Yashin V.A. Secreting cells of Saintpaulia as a model for studies of plant cholinergic system. Biological Membranes 2013, 30 (5-6), 454-461.
6. Pinaev, G. P. Contractile systems of cell: from muscle contraction to regulation of cellular functions. Tsitologia (Cytology, Russia), 2009, 51 (3), 172-181.

7. Kravchenko I.V, Furalyov V.A, Popov V. O. Stimulation of mechano-growth factor expression by myofibrillar proteins in murine myoblasts and myotubes. Mol Cell Biochem 2012. 363 (1-2), 347-355.

8. Roshchina V.V. and Vikhlyantsev I.M. Bioactivity of exogenous cytoskeleton proteins: regulation of development of plant microspores as biosensors. Current Bioactive Compounds 2012, 8 (3), 287-290.

9. Roshchina, V.V. and Karnaukhov, V.N. Fluorescence analysis of the effect of drugs on unicellular biosensors. Farmatsia, 2010, N 3, 43-46.

10. Haugland R.P. Handbook of fluorescent probes and research chemicals. Leiden: Molecular Probes, 2000.

11. Roshchina V.V. Fluorescing world of plant secreting cells. Enfield, Plymouth: Science Publisher, 2008.

STRUCTURAL-FUNCTIONAL RELATIONSHIPS IN RAT MYOCARDIUM UNDER THE CONDITIONS OF STRESS AND HYPOXIA

E.V. Rozova[1], I.N. Mankovskaya[1], G.D. Mironova[2]

[1] *Bogomolets's Institute of Physiology of the Ukrainian National Academy of Sciences, Bogomolets's Street 4, Kiev, Ukraine, erozova@ukr.net;*
E-mail: mankovsk@biph.kiev.ua
[2]*Institute of Theoretical and Experimental Biophysics RAS, Institutskaya st. 3, 142290, Pushchino, Russia,*
E-mail: mironova40@mail.ru

Studying the relationship between structure and function is an important goal, since structural organization of an object often determines its physical and chemical properties, as well as its existence and functioning under extremal conditions. Adaptive reactions in the organism occur immediately after the stimulus, and during this initial phase only a pre-formed physiological mechanism can be launched. At the later stages of adaptation, a so-called "system-structural trail" is formed. Under various hypoxic conditions, for example, the number of mitochondria increases 1.5-2 fold, with the myocardial content of hemoglobin, activity of cytochrome oxidase and other enzymes of the respiratory chain growing as well. Also observed are structural changes of mitochondria (MC) and myocardial histohematic barrier (HHB), consisting of capillary endothelium and inter-capillary space; these changes substantially alter the consumption of oxygen and its transport from the capillary blood to mitochondria. Hence, increased resistance of the organism to various internal and external factors is not only a functional phenomenon but also the result of structural rearrangements in organs and tissues. The objective of

the work was to study how HHB hyperhydration, which was judged by the mean HHB thickness (an integral indicator of tissue hydration), correlates with the morphological and stereometric characteristics of cardiomyocyte mitochondria.

The study was performed on 414 adult male Vistar rats (220-300 g). Hypoxia and stress were modeled by the following techniques. 1) Hypoxic hypoxia (H; $n = 110$) developed under animal's breathing with a gas mixture of 7% O_2 in N_2 for 30 min (with CO_2 being continuously removed). 2) Circulatory-hemic hypoxia (BL; $n = 133$) was modeled by an acute blood loss, amounting to 25-30% of the circulatory blood volume without replenishment, with the examination of animals started 30 min after the blood loss. 3) Acute 6-h immobilization stress (S; $n = 127$) was induced by fixation of animals in the supine position. The control group included 44 intact animals. The conditions of (1), (2) and (3) led to a secondary tissue hypoxia of comparable severity, which was indicated by the ratio of supplied-to-consumed O_2.

The function of the cardiovascular system was examined rheographically, using a 4RG-1A rheograph (Russia), according to the modified Kubicek method. The consumption of O_2 by myocardium (VtO_2) was determined by the modified manometric technique. The activity of mitochondrial ATP-dependent potassium channels (mitoK$_{ATP}$) was modulated under acute hypoxic hypoxia. 15 min before the experiment, one group of rats was intravenously injected with the selective activator of mitoK$_{ATP}$ diazoxide (0.3 mg/100 g of body mass), and another group, with the selective inhibitor of mitoK$_{ATP}$ 5-hydroxydecanoate (5HD; 0.5 mg/100 g of body mass). For control, the activator and inhibitor of mitoK$_{ATP}$ were also introduced under normoxia. To examine the effects, tissue samples were taken from the upper part of the heart. The material was fixed according to the conventional technique. The ultrathin sections (40-60 nm) were examined using an electron microscope JEM 100CX (Japan). The morphometric and stereometric studies were conducted on the basis of Weibel's approach, using the morphometric analysis software Image Tool (USA) – 100-150 fields for each animal group.

The statistical analysis of the data obtained was performed with the software packages Statistica 6.0 and Microsoft Excel 2003, using the Fisher criterion φ, Student coefficient t, Pearson and Spearmen correlation coefficients (when system and tissue characteristics were compared).

The study revealed a high correlation between the rate of blood flow and mean HHB thickness –both in norm and under all the experi-

Table 1. Spearmen coefficients for the correlation between the mean myocardial HHB thickness and the functional parameters of cardiovascular system at different kinds of hypoxia and stress

Parameters	Control group	Acute hypoxic hypoxia	Acute blood loss	6-h immobilization stress
Volumetric rate of blood flow	0,834 *	0,811 *	-0,718 *	0,732 *
Heart rate	*0,436*	0,720 *	0,267	0,798 *
Stroke volume	0,731 *	*0,406*	-0,734 *	*0,478*

Note: *a close relation between the parameters; values in italic indicate the average correlation between the parameters.

mental conditions examined (table 1). Hence, statistically significant changes in the rate of blood flow would indicate structural disorders in the myocardium (at least, in the form of barrier hyperhydration).

We showed that under all the experimental conditions, there were changes in the level of VtO_2: it grew upon hypoxic hypoxia and blood loss and declined upon stress. It was established that VtO_2 was mainly affected by the total surface area of mitochondria of the subsarcolemmal subpopulation (SS MC) per unit of tissue volume and by the number of structurally changed mitochondria of the intramyofibrillar subpopulation (MF MC) (table 2).

Somewhat smaller is the dependence of VtO_2 on the total number of SS MC and diameter of MF MC. The rest of morphological and stereometrical parameters of MC have no substantial effect on the level of O_2 consumption by the myocardium. The data obtained show that the

Table 2. Ratio between the rate of oxygen consumption by the myocardium (VtO2) and major morphological and stereometrical parameters of mitochondria (Pearson correlation coefficient)

Parameters	SS MX	IMF MX
Mean number of MC	*0.545*	0.295
Number of structurally changed MC	-0,214	-0,709 *
Average diameter of MC	0.320	*0.477*
Average area of MC	*0.553*	0.211
Total surface area of MC per unit of tissue volume	0,669 *	0.345

Note: *a close relation between the parameters; values in italic indicate the average correlation between the parameters.

Table 3. The percentage of different types of structural changes in myocardial MC under hypoxic hypoxia, blood loss and stress

Experimental conditions	Types of structural changes in MC, % of total					
	SS MC			IMF MC		
	Apoptotic	Necrotic	MS*	Apoptotic	Necrotic	MS*
Hypoxic hypoxia	29,9	19,8	50,3	43,4	9,4	47,2
Blood loss	20,2	34,7	45,1	31,3	26,4	42,3
Stress	18,2	60,5	21,3	21,4	62,6	16,0

*MS – changes aimed at the support of adequate metabolism (metabolism-supporting)

subsarcolemmal subpopulation of MC affects VtO_2 a bit stronger. As turned out, both under the control and all the experimental conditions, the correlation of oxygen consumption by the myocardium with the parameters of MC is the same.

A comparative study of structural defects in the cardiomyocyte MC under different hypoxic conditions allowed us to obtain important, in our mind, data. They indicate that under hypoxic hypoxia, myocardial MC do not reveal an evident necrotic damage – in contrast to what was observed upon stress (table 3).

At the same time, changes indicating intensification of energy processes under hypoxic hypoxia (MC in the energized and energized-twisted state) are maximal. This can explain the positive effect of hypoxic hypoxia we found: it probably aimed at optimization of energy metabolism.

Under hypoxic hypoxia, we observed ultrastructural rearrangements in MC of the heart tissue, which have been unseen before *in vivo* and could be viewed as a compensatory-adaptive reaction of the mitochondrial apparatus. Many of the structurally damaged mitochondria contain 1-3 small, optically dense formations (10-15 nm in diameter), which resemble intact mitochondria. Such a process was first discovered *in vitro* in the works of Saprunova, Solodovnikova et al. These authors tend to consider the formation of intramitochondrial microMC as a way to maintain the capacity of the mitochondrial apparatus during hypoxia, and we agree with this view. The formation of microMC is observed only under H; it does not occur in case of BL and S. Studying the effects of mitoK$_{ATP}$ modulators, we managed to identify one of the mechanisms involved in the formation of microMC. Modulation of mitoK$_{ATP}$ activity with diazoxide was accompanied by intensive formation of microMC, which is important since activa-
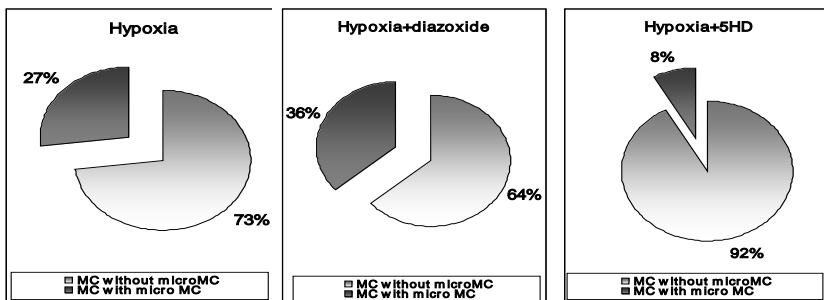
Change in the number of microMC in the cells of heart tissue by modulating the activity of mitochondrial ATP-sensitive K+ channels (changes are reliable in both cases p <0.05).

tion of mitoK_{ATP} is known to protect heart from hypoxia (figure) Introduction of the mitoK_{ATP} blocker 5HD considerably reduced the effect.

The data obtained in the present work indicate that correction of hypoxic conditions of various genesis would require complex approaches aimed simultaneously at normalization of the function of cardiovascular system, myocardium structure as a whole, histohematic barrier in the myocardium and mitochondrial apparatus. It also can be supposed that one of the regulators of the MC morphological state under hypoxic hypoxia is ATP-dependent potassium channel.

E-CADHERIN PLAYS A ROLE IN MIGRATION OF TRANSFORMED EPITHELIAL CELLS

S.N. Rubtsova, I.Y. Zhitnyak, N.A. Glushankova
Institute of Carcinogenesis, Russian Cancer Research Center, Kashirskoye Shosse, 24, Moscow 115478, Russia

Tumor cell dissemination to other regions of the body remains a major problem in experimental and clinical oncology. Cell-cell adhesion, mediated by various specific proteins, holds together cells in a normal tissue, and its loss contributes greatly to the transition between a normal tissue and a disseminating malignant tumor. In epithelial cells, the most prominent cell-cell adhesion structures are adherens junctions (AJ) formed by the protein E-cadherin. However, certain human epithelial tumors (ductal breast carcinomas, colorectal carcinomas and melanomas) retain their E-cadherin expression even in the process of invasion and metastasis. Moreover, E-cadherin expression is often restored in metastases of E-cadherin-negative tumor types.

Contrary to previous data that highlight the tumor suppressor role of E-cadherin, can it be instrumental in tumor dissemination in epithelial tissues? To address this issue, we devised a two layered culture system of transformed and non-transformed epithelial cells. The cells were rat liver epithelial cells IAR-2 (non-transformed) and their transformed derivatives with or without E-cadherin. IAR6-1 (transformed with dimethylnitrosamine) and IAR2-1170 (ras-transformed) expressed E-cadherin while IAR6-1DNE and IAR2-1162 did not.

We discovered that IAR6-1 were able to move across the non-transformed monolayer at approximately the same speed as across glass substrate. We hypothesized that transformed cells may travel across the top of the monolayer attaching themselves briefly to underlying non-transformed cells with E-cadherin-based AJ and using these AJ as anchor points. Our earlier work has demonstrated transitory and unstable nature of the AJ formed between transformed epithelial cells. Indeed, as our current experiments showed, transformed IAR6-1 cells sitting on top of the non-transformed IAR2 monolayer formed transient dot-like AJ with IAR2.

However, our subsequent confocal observations of cells labeled with diffuse red and green fluorescent proteins, showed that while transformed IAR6-1 cells were indeed able to move over the non-transformed monolayer, this was a rather rare event. More often, transformed cells traversed the non-transformed monolayer, attached, spread on and moved across the glass substrate underneath the non-transformed cells. The majority of the attachment and spreading events fell into 12-16 h post-seeding time range. XZY projections of IAR 6-1 cells traversing the monolayers showed that a rounded transformed cell on top of the monolayer first formed a pseudopod that penetrated the monolayer and attached to the glass underneath. Within 1-2 hours, the cell body sunk through the monolayer and attached to the glass surface. The pseudopod could be seen flattening, enlarging and moving under the neighboring cells.

Expression of E-cadherin or lack thereof determined the behavior of various transformed cell lines in this culture system. We used several subclones of the IAR2-1162 cell line transformed by oncogenic ras, as well as with IAR6-1DNE subclones. IAR2-1162 cells lost E-cadherin expression in the course of their neoplastic transformation. The IAR6-1 cell line initially obtained by transforming immortalized cells with dimethylnitrosamine, we transfected with a dominant negative E-cadherin mutant that suppresses formation of AJ. As E-cadherin-positive controls we used subclones of the IAR2-1170 cell line also transformed by oncogenic ras which retain their E-cadherin expression, as well as the original IAR6-1. All E-cadherin-positive cell lines had a clear advantage over all

E-cadherin-negative cell lines in the percentage of the cells that had traversed the non-transformed monolayer, with the difference between those subgroups being statistically significant. Within the E-cadherin-positive and E-cadherin-negative subgroups, the differences were more minor. We conclude that E-cadherin expression is necessary for transformed cells to successfully traverse the monolayer of non-transformed cells.

Observation of transformed IAR6-1 cells traversing a monolayer of IAR-2 cells expressing GFP-E-cadherin showed that all traversing events happened at the borders between two IAR-2 cells, and that the AJ linking those cells were disassembled immediately prior to the traversing.

To determine the mechanism of the AJ disassembly, we used a panel of specific small molecule inhibitors of various targets: metalloproteinases (marimastat and GM6001); EGFR (PD153035); ERK (CI1040); Akt/PIK3 (wortmannin); p38 (rapamycin); Src (SKI-1); mDia (SmifH2); Arp2/3 (CK666); myosin II ATPase (blebbistatin) and ROCK (Y27632).

Of all these, only blebbistatin, Y27632 and SKI-1 reduced the percentage of IAR6-1 cells traversing the non-transformed IAR-2 monolayer. Contractility inhibitors blebbistatin and Y27632 did not prevent pseudopods from penetrating the monolayer and attaching to the underlying glass substrate, however, the cell bodies remained on top of the monolayer for the entire period of observation. The Src inhibitor SKI-1 reverted the transformed morphology of the IAR6-1 cells to nearly normal epithelial phenotype, restoring circumferential actin bundles and AJ. Apparently these cytoskeletal rearrangements hindered the ability of the transformed cells to traverse the monolayer of non-transformed cells.

Taken together, our data demonstrate that transformed epithelial cells retaining E-cadherin expression are able to form AJ with the underlying non-transformed cells. These "mixed" AJ may promote dissemination of the transformed cells in the epithelial tissues.

THE EFFECT OF G126R AND D137L MUTATIONS IN α-TROPOMYOSIN ON THE POSITION AND FLEXIBILITY OF TROPOMYOSIN STRANDS DURING THE ATPase CYCLE

Nikita A. Rysev[1], Alexander M. Matyushenko[2], Natalia V. Artemova[2], Dmitrii I. Levitsky[2] and Yurii S. Borovikov[1]

[1]*Institute of Cytology, Russian Academy of Sciences, St. Petersburg, Russia;*
[2] *Bach Institute of Biochemistry, Russian Academy of Sciences, Moscow, Russia*

Tropomyosin molecule (TM) is a semi-rigid structure which is stiff enough to move across the surface of actin as a unit when perturbed me-

chanically by other actin-binding proteins such as myosin. TM is a two-chain α-helical coiled coil whose periodic interactions with the F-actin helix are critical for thin filament stabilization and the regulation of muscle contraction. It is believed that non-canonical residues Asp137 and Gly126 located in the middle part of TM molecule can destabilize the molecule at these points. Thus recently it has been shown that the Asp substitution for Leu at 137 position and the replacement of Gly126 with Ala or Arg significantly stabilize the middle part of the TM molecule [1, 2, 4]. This stabilization not only enhances maximal sliding velocity of regulated actin filaments in the *in vitro* motility assay at high Ca^{2+} concentrations but also increases Ca^{2+}-sensitivity of the actin-myosin interaction underlying this sliding [3, 4].

To examine the effect of the substitution of Gly126 with an Arg residue or Asp137 with a Leu residue and of both substitutions within the same skeletal α-TM molecule on the position and flexibility of the N-terminus of TM and the spatial arrangement of actin monomers during the ATPase cycle we labelled the recombinant wild type and mutant TMs with 5-IAF at Cys36 (which was introduced into the N-terminal part of TM by mutation C190A/S36C) and F-actin with FITC-phalloidin, incorporated them into troponin-free ghost muscle fibres and studied their polarized fluorescence at different stages of the ATPase cycle. In the absence of myosin subfragment 1 (S1), these mutations shift TM towards the periphery of the filament, dramatically enhance TM strands rigidity, and slightly increase a proportion of the switched-on subunits in F-actin. The binding of S1 to F-actin (in the absence or presence of MgADP) moves all mutant TMs further to the center of the filaments (towards the "open position"), which results in a decreased flexibility of the N-terminus of TM and a pronounced rotation of actin monomers to the periphery of the filaments. The latter indicates an increase in the number of the switched on actin monomers. Under conditions mimicking the weak-binding states, the mutant TMs move further to the periphery of the filament and the amount of the switched on actin monomers extremely decreases compared to that for the wild type TM. We suggest that the observed increase in Ca^{2+}-sensitivity of actin-myosin interaction and maximal sliding velocity of actin filaments in the *in vitro* motility assay induced by Asp137Leu and Gly126Arg substitutions in TM [3, 4] may result from the enhanced efficiency of the cross-bridge work caused by the abnormal TM shift further towards the center and periphery of the filaments at the strong-binding and weak-binding states, respectively.

References

1. Sumida J.P., Wu E., and Lehrer S.S. (2008) "Conserved Asp-137 imparts flexibility to tropomyosin and affects function". J. Biol. Chem. 283, 6728–6734.
2. Nevzorov I.A., Nikolaeva O.P, Kainov Y.A., Redwood C.S., and Levitsky D.I. (2011) "Conserved noncanonical residue Gly-126 confers instability to the middle part of the tropomyosin molecule". J. Biol. Chem. 286, 15766–15772.
3. Shchepkin D.V., Matyushenko A.M., Kopylova G.V., Artemova N.V., Bershitsky S.Y., Tsaturyan A.K., and Levitsky D.I. (2013) "Stabilization of the central part of tropomyosin molecule alters the Ca2+-sensitivity of actin-myosin Interaction" Acta Naturae 5, № 3(18), 126–129.
4. Matyushenko A.M., Artemova N.V., Shchepkin D.V., Kopylova G.V., Bershitsky S.Y., Tsaturyan A.K., Sluchanko N.N., and Levitsky D.I. (2014) "Structural and functional effects of two stabilizing substitutions, D137L and G126R, in the middle part of α-tropomyosin molecule". FEBS Journal (in press; doi: 10.1111/febs.12756).

THE ROLE OF POTASSIUM CHANNELS IN THE EFFECT OF HYDROGEN SULFIDE ON THE SPONTANEOUS CONTRACTILE ACTIVITY OF RAT JEJUNUM

G.I. Sabirullina, M.U. Shafigullin, N.N. Khaertdinov, G.F. Sitdikova

Institute of Fundamental Medicine and Biology , Kazan (Volga Region) Federal University, Kremlevskaya st., 18, Kazan, 420008, Russia

Hydrogen sulfide (H_2S) – a gas, well-known for its toxic effects associated with impaired oxidative phosphorylation in the cell. H_2S endogenously produced in mammalian tissues and plays a major role in physiological and pathological processes. Traditionally known as a toxic gas it is also an important gaseous messenger [1,2]. Like other gasotransmitters, H_2S has a relaxing effect on the smooth muscle in the cardiovascular system, gastrointestinal tract, reproductive system [3,4]. In a number of studies the relaxing effect of H_2S in various parts of the gastrointestinal tract in different animal species was found [5–7]. However, it was also shown that H_2S could produce different effects on smooth muscle motility dependent on concentration [8].

The aim of our study was to determine the effect of H_2S on contractile activity in smooth muscle of rat intestine and identify the role of voltage-dependent and ATP-dependent potassium channels in the effects of H_2S.

232

Materials and methods

Experiments were performed on isolated segments of jejunum from Rattus norvegicus on the equipment of Biopac Systems, Inc. (USA). Animals were anesthetized by using 5% isoflurane (Abbott Laboratories, North Chicago, IL, USA). The abdomen was opened and the mid jejunum was removed and placed in oxygenated Krebs solution. The 7 mm long muscle strip is suspended vertically in a 20-ml tissue chamber, the lower end fixed to the rubber block and the other end was connected to a force transducer (TSD125C, Biopac Systems, Inc USA). During the experiment, the muscle strip was continuously washed with 37°C Krebs solution and aerated with 95% oxygen and 5% carbon dioxide.

Registration and analysis of the parameters of the muscle contraction was performed using the program AcqKnowledge 4.1. Amplitude (force in grams), frequency and the baseline tone were analyzed. The baseline tone was accessed using values of maximum relaxation between contractions.

Sodium hydrosulfide (NaHS) was used as H_2S donor. H_2S in an aqueous solution dissociates to ions (Na^+) and anion hydrosulphide (HS^-), which reacts with protons (H^+) to form H_2S [4]. In aqueous solution, approximately one third of the gas in the nondissociated form. It is known that at pH 7.4 and a temperature of 37°C, only 18% of NaHS is presented in the form of a gas - H_2S [9]. The following drugs were used: L-cysteine, β-cyano-L-alanine, 4-aminopyridine, glibenclamide, diazoxide (Sigma, USA). Substances, insoluble in water, were dissolved in dimethylsulfoxide (DMSO), which at the concentration used (up to 0.01%) had no effect on spontaneous contractile activity of the jejunum.

Results and discussion

In control the jejunum segment spontaneously contracted with average frequency $0,45 \pm 0,01$ Hz and amplitude - $0,57 \pm 0,5$ g ($n = 20$).

To analyze the mechanisms of NaHS action according our previous data we used concentration - 200 μM, which reduced amplitude of contractions to $19,6 \pm 2,8$% (n = 20, p <0,05), baseline tone to $87,7 \pm 2,5$% ($n = 20$, p <0,05), frequency to $90,08 \pm 2,17$% ($n = 21$, p <0,05) compare to control.

Endogenous H_2S is produced from L-cysteine by two enzymes, cystathionine (β) synthase and (CSB) and cystathionine (γ) lyase (CSE). For detection of endogenous synthesis of hydrogen sulfide in the intestinal cells, we used its endogenous donor - L-cysteine and inhibitor of CSE - β-cyano-L-alanine.

L-cysteine in the cumulative addition of 10, 50, 100, 200 μM resulted in dose-dependent decrease of amplitude (after 200 μM) to 80.5 ± 3% ($n = 8$, $p < 0,05$), baseline tone - 74.13 ± 7% ($n = 6$, $p < 0.05$) frequency - 97.11 ± 1.7% ($n = 5$, $p > 0,05$).

β-cyano-L-alanine at 200 μM showed not significant changes in the parameters of spontaneous activity: to 30 minutes of application amplitude of spontaneous contraction was 114.7 ± 9.3% ($n = 4$, $p > 0,05$), frequency - 101.7 ± 0.4% ($n = 4$, $p > 0,05$), baseline tone - 97.48 ± 5.2% ($n = 4$, $p > 0,05$). These results show that the substrate of synthesis of the H_2S — L-cysteine reduced the spontaneous contraction parameters as H2S donor, probably due to endogenous synthesis of gas. Inhibitor of enzyme that catalyzing the synthesis of H_2S - β-cyano-L-alanine resulted in no significant effect on the contractile activity, which can probably be attributed to the presence of other enzymes of the gas synthesis in the tissue or insufficiently concentration of inhibitor.

It is known that K^+-channels play a key role in maintaining of the tone of smooth muscles, are involved in the control of gastrointestinal smooth muscle contraction, affecting the membrane potential, slow waves of depolarization, duration of the action potential (Horowitz, 1999). K^+-channels may be the targets of the effects of hydrogen sulfide.

We investigated the role of voltage-dependent and ATP-dependent potassium channels in our experiments. Previously, we studied the role of Ca^{2+}-activated and voltage-dependent K^+-channels, in which we used nonspecific blocker of these channels tetraethylammonium (TEA) and it was shown that after TEA application the effects of NaHS on the amplitude, baseline tone and frequency were the same as in control.

Inhibitor of voltage-dependent potassium channels 4-aminopyridine (4-AP) at concentrations 200 μM increased the amplitude to 121,4 ± 4,8 % ($n = 7$, $p < 0.05$) relative to a control, wherein the baseline tone and frequency were not changed. In the background 4-AP effect of NaHS on the amplitude baseline tone fully preserved, but the frequency of contractions increased – 103,3 ± 4,9 ($n=5$, $p < 0.05$).

It has been shown, that in vascular smooth muscle cells the effects of NaHS were mediated through activation of $K_{(ATP)}$-channels. In our study to determine the role of $K_{(ATP)}$-channels we evaluated the effects of hydrogen sulfide donor after inhibition or activation of these channels.

Inhibitor of $K_{(ATP)}$-channels by glibenclamide at the concentration 50 μM decreased the amplitude of contractions to 63,84 ± 5,93% ($n = 10$, $p < 0.05$) and frequency to 90,73 ± 1,91% ($n = 10$, $p < 0.05$), baseline tone not significantly changed (103,52 ± 3,07%) ($n = 10$, $p > 0.05$). On the

background of the glibenclamide, effect of NaHS on the amplitude and frequency of contractions completely preserved ($22,60 \pm 4,39\%$ and $86,88 \pm 1,99\%$, respectively), while the baseline tone significantly increased to $111,65 \pm 3,83\%$ ($n = 10$, $p < 0.05$).

$K_{(ATP)}$-channels were activated using diazoxide (100 μM). Application of diazoxide caused the decrease of the force of contraction to $65 \pm 5,1\%$ ($n = 5$, $p < 0.05$) from the control values without changing the frequency of spontaneous contractions and baseline tone. Adding NaHS on the background of the diazoxide decreased the amplitude and frequency of the same abbreviations as in the control, but the effect to baseline tone not manifested.

The results of our study showed that donor H_2S - NaHS endogenously synthesized in the intestinal cells and causes a reduction of the spontaneous contractile activity of rat jejunum segment, reducing the amplitude, frequency and the base tone. The findings suggest that the effects of NaHS on the amplitude of the contractions are not related to its effect on the voltage-dependent potassium and $K_{(ATP)}$-channels, effects to baseline tone mediated by $K_{(ATP)}$-channels of smooth muscle cells, and a decrease in the frequency - by voltage-gated potassium channels of neuronal cells or muscle cells of intestine.

References

1. Wang, R. The Gasotransmitter Role of Hydrogen Sulfide. // Antioxid Redox Signal. - 2003. - V.5(4). - P. 493-501.
2. Sitdikova, G.F. Gaseous mediators in the nervous system / G.F. Sitdikova, A.L. Zefirov // Rus. Physiol . Magazine. - 2006 . - V. 92, № 7. - P. 872-882.
3. Xu, M. Electrophysiological effects of hydrogen sulfide on pacemaker cells in sinoatrial nodes of rabbits. / M. Xu, Y.M. Wu, Q. Li, X. Wang, R.R. He // Acta Physiol Sin.- 2008.- V. 60.- P. 175-180.
4. Lowicka, E. Hydrogen sulfide (H2S) — the third gas of interest for pharmacologists / E. Lowicka, J. Bełtowski // Pharmacol. Rep.- 2007.- V. 59. - P. 4–24.
5. Hosoki, R. The possible role of hydrogen sulfide as an endogenous smooth muscle relaxant in synergy with nitric oxide. / R. Hosoki, N. Matsuki, H. Kimura / / Biochem Biophys Res Commun. - 1997 . - V.237. - P. 527-531.
6. Nagao M. Role of hydrogen sulfide as a gasotransmitter in modulating contractile activity of circular muscle of rat jejunum. / M. Nagao , A.J. Duenes, M. G. Sarr // Gastrointest Surg. - 2012. - V.16(2). - P. 334–343.
7. Kasparek, M.S. Hydrogen sulfide modulates contractile function in rat jejunum / M.S. Kasparek, D.R. Linden, G. Farrugia, M.G. Sarr / / J. Surg Res. - 2012. - V.175. - P. 234-242.

8. Zhao P. Dual effect of exogenous hydrogen sulfide on the spontaneous contraction of gastric smooth muscle in guinea-pig. / X. Huang, Z.Y. Wang, Z.X. Qiu, Y.F. Han, H.L. Lu, Y.C. Kim, W.X. Xu // Eur J Pharmacol. - 2009. - V. 616 (1-3). - P. 223-8.

9. Horowitz, B. Cellular and molecular basis for electrical rhythmicity in gastrointestinal muscles / B. Horowitz, M. Ward Sean., M. Sanders Kenton / / Annu. Rev. Physiol. - 1999 . - V.61. - P. 19-43.

PI3-KINASE (PI3K) PATHWAY IS INVOLVED IN REGULATION OF MIGRATION AND PROLIFERATION IN NIH-3T3 FIBROBLASTS BY MEANS OF REDOX-DEPENDENT MECHANISM

G.D. Sagaradze, N.D. Zhdanovskaya, P.A. Tyurin-Kuzmin, A.A. Sukhova, A.V. Vorotnikov

Department of Biochemistry and Molecular Medicine, Faculty of Fundamental Medicine, Moscow State University, Moscow, Russia

Wound healing is an important physiological process. It attends inflammation associated with reactive oxygen species (ROS) production. It is known that ROS synthesis and damaged tissue regeneration have time and space intersection. Fibroblasts migrate to a damaged area during regeneration process. There they proliferate under the influence of platelet derived growth factor (PDGF). Epithelial cells restore a surface layer of the damaged tissue under the effect of epidermal growth factor (EGF). PI3K and Ras/Erk1/2 MAP-kinase pathways are involved in PDGF- and EGF-stimulated proliferation and migration of fibroblasts. It is shown that hydrogen peroxide (H_2O_2), a main ROS metabolite, can participate in regulation of growth factors' cellular effects as a second messenger. Besides exogenous ROS there is an endogenous H_2O_2 source in fibroblasts: NADPH-oxidase complex (NOX). NOX complex assembly is activated under the influence of different growth factors. This work is dedicated to research of mechanisms of redox-dependent migration and proliferation of NIH-3T3 fibroblasts.

Primarily we researched the influence of PDGF and EGF on migration and proliferation of NIH-3T3 fibroblasts. Obtained results showed that PDGF and EGF stimulate proliferation but only PDGF stimulates migration of fibroblasts. Then we found out pathways involved in PDGF and EGF signaling. Three interesting pathways: NOX/ H_2O_2, PI3K, Ras/Erk1/2 MAP-kinase are involved in PDGF-regulated signaling. By means of an intracellular genetically encoded biosensor sensitive to H_2O_2

we looked after changes of intracellular H_2O_2 level in PDGF-stimulated fibroblasts. Obtained experimental data showed that PDGF activates long-term production of endogenous H_2O_2 and NOX inhibitor apocynin suppresses this effect. At the same time during NIH-3T3 activation EGF does not trigger off H_2O_2 synthesis and PI3K pathway. To understand better NOX/ H_2O_2 relation with PDGF we researched PDGF-stimulated increased production of H_2O_2 influence on PI3K and Ras/Erk1/2 MAP-kinase pathways. Obtained data showed that NOX/ H_2O_2 system activation leads to increase of PI3K-pathway signaling amplitude and duration of its activation. PDGF and EGF activate Ras/Erk1/2 MAP-kinase pathway by means of redox-independent mechanism. PI3K redox-dependent activation takes part in PDGF-mediated regulation of migration and proliferation in NIH-3T3 fibroblasts.

SEASONAL CHANGES IN THE ISOFORM COMPOSITION OF TITIN AND MYOSIN HEAVY CHAINS IN STRIATED MUSCLES OF BEARS

N.N. Salmov[1], A.D. Ulanova[1], I.M. Vikhlyantsev[1], A.G. Bobylev[1], D.S. Kozhevnikova[2], A.P. Saveljev[3], V.V. Makariushchenko[3], G.Yu. Maksudov[4], S.N. Udaltsov[1,5], Z.A. Podlubnaya[1,6]

[1]*Institute of Theoretical and Experimental Biophysics, Russian Academy of Sciences, Pushchino, Moscow region, 142290, Russia;*
[2]*Samara State University, Samara, Russia;*
[3]*Russian Research Institute of Game Management and Fur Farming, Russian Academy of Sciences, Kirov, Russia;*
[4]*Moscow Zoo, Moscow, Russia;*
[5]*Institute of Physicochemical and Biological Problems of Soil Science, Russian Academy of Sciences, ul. Institutskaya 2, Pushchino, Moscow region, 142290, Russia*
[6]*Pushchino State Institute of Natural Science, Pushchino, Moscow region, 142290, Russia*

Hibernation (winter torpor) is evolutionary capability of some mammals representing a temporal reduction in metabolism in order to survive at low temperatures and under conditions of seasonal food shortage. In true (obligate) hibernators (ground squirrels, woodchucks) the dormancy lasts 5-8 months and includes the 2-3 week cycles (torpor bouts) with short-term (several hours) arousal. During torpor bout the animal body temperature falls to 2-4°C, and the heart rate drops to 4-20 beats per minute (bpm) [1]. Bears entering winter sleep are the hibernating animals. The

temperature of the bear's body decreases only by 5-7°C and animals easily come out of torpor into active state, but changes in metabolism are similar to those observed in the true hibernators during winter torpor.

Previously we revealed adaptation changes in the isoform composition of giant protein titin and myosin in striated muscles of an obligate hibernator, the long-tailed ground squirrel *Spermophilus undulatus* during winter dormancy. For instance, in cardiac muscle of ground squirrels during hibernation the increased content of the long (more elastic) N2BA titin isoform and the lowered content of the short N2B-isoform were observed [2]. Similar changes in titin content, the increased content of the long NT-isoform and lowered content of the short N2A-isoform, were recorded in skeletal muscles of these animals during hibernation [2]. Adaptation to these changes contributes to the maintenance of a highly-ordered sarcomeric structure and the necessary level of a contractile muscle activity for different periods of a hibernating cycle in the ground squirrel (entering hibernation, hibernation, arousal, winter interbout activity) [2]. It should be noted that during winter hibernation of the ground squirrel in atrophied skeletal muscles the increased content of the "slow" I isoform and the lowered content of "fast" IIa and IIx/d isoforms of myosin heavy chains were observed [3]. These changes point to the increase in the content of the slow, more endurable fibers with characteristic protein isoforms in muscles of the hibernating animals. Similar changes are adaptive response allowing considerable reduction in energy expenditure during hibernation period. It is necessary for the animal in order to survive under severe conditions of this period.

In this work we explored changes in isoform composition of titin and myosin heavy chains in cardiac and skeletal muscles of Brown (*Ursus arctos*) and Asian Black (*Ursus thibetanus*) bears with the aim of elucidating the role of these changes in adaptation of muscle system to the conditions of winter sleep.

In this study we used following striated muscles of the bears: (1) cardiac and skeletal muscles (*m. longissimus dorsi, m. biceps*) of the hibernating Asian black bear (adult male) trapped in the den on 28 January 2013 in Obluchenski district, the Jewish Autonomous Region in the Upper Ditur River watershed, 90 km west of Birobidzhan; (2) cardiac and skeletal muscles (*m. gastrocnemius, m. triceps, m. biceps, m. longissimus dorsi*) of the hibernating brown bear (adult female) bagged in the den in Yukamensk district, Udmurt Republic; (3) cardiac and skeletal muscles (*m. gastrocnemius*) of active brown bear (six-year old female) shooted

down on 20 April 2013 at biostation of VNIIOZ (Kirov); (4) skeletal muscles (*m. gastrocnemius, m. triceps, m. longissimus dorsi)* of active brown bear (adult male) shooted on 9 September 2013 in vicinity of the village of Katny, Kotelnich district, Kirov region. All animals were legally gained in accord with special permits issued at regional offices of animal health and usage of the animal world objects.

The isoform composition of myosin heavy chains (MHC) was studied by 7% SDS-PAGE as described in [4]. SDS-PAGE of titin isoform was carried out by the method described in [5] with a content of agarose of 0.55% and polyacrylamide of 2.1-2.3%. The densitometry was performed using the program Total Lab 1.11 [2]. The content of titin was estimated relative to the content of MHCs. The statistical processing was carried out using the nonparametric U-test of Mann-Whitney. Differences with a confidence level $p<0.05$ were considered significant.

In skeletal muscles of the hibernating bears the changes in the isoform composition of titin and myosin heavy chains similar to those recorded in the muscles of the hibernating long-tailed ground squirrels were found. For instance, the content of the longer NT-titin isoform increases and the content of the shorter N2A-isoform of this protein declines (fig. 1). In this case in *m. gastrocnemius* and *m. longissimus dorsi* of the hibernating brown bear the content of the "slow" I isoform was higher than that of the "fast" IIa isoform of myosin heavy chains (fig. 2). In *m. longissimus dorsi* and *m. biceps* of the hibernating Asian black bear the contents of "slow" I and "fast" IIa isoforms of myosin heavy chains were nearly equal (~50% each) (data not shown).

It is interesting to note that the observed changes in titin and myosin heavy chains in muscles of the hibernating animals are opposite to those during the development of a series of pathological processes. For
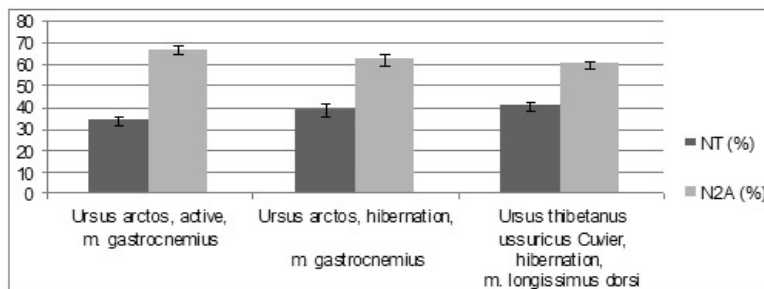
Fig. 1. Seasonal changes in titin isoforms composition in skeletal muscles of the brown bears.
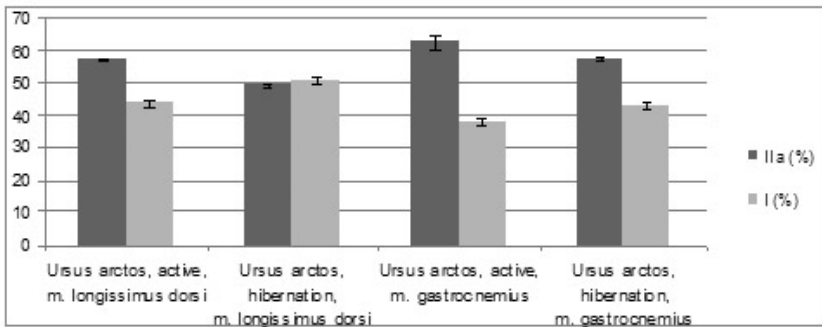
Fig. 2. Seasonal changes in the isoform composition of myosin heavy chains in skeletal muscles of the brown bears.

instance, during pathological and atrophied changes in skeletal muscles of humans and animals the content of NT- and N2A titin isoform decreases, the content of proteolytic T2-fragments of this protein increases and myosin phenotype shifts towards the augmentation of the content of "fast" isoforms of myosin heavy chains [2]. These alterations lead to disruption of a sarcomeric structure and a deterioration of the capacity of muscle contraction [2]. Based on the results obtained we believe that the increase in the content of NT-titin isoform in muscles of the true hibernators (ground squirrels) and in muscles of the bears is adaptive contributing to the maintenance of a highly-ordered sarcomeric structure and the necessary level of a contractile muscle activity in winter period. The decrease in the content of proteolytic T2-titin fragments in bear muscles during hibernation may also be adaptation. It is known that the products of protein catabolism are substrates of gluconeogenesis. Most likely that during hibernation the processes of gluconeogenesis in the liver occur due to the products of protein degradation, in particular, degradation of T2-titin fragments, the decreased content of which we observed in skeletal muscles of the true hibernator [2] and bears as well. The changes in myosin phenotype in skeletal muscles of the winter hibernating animals that directed to the increase in the content of "slow" isoforms of this protein have also a great physiological importance. Taking into account that the main strategy of hibernation is a strict economy of energy resources, it can be stated that transformation of skeletal muscles of the winter hibernating animals towards the increase in "slow" fibers with characteristic isoforms of myosin heavy chains is also an adaptation to hibernation conditions. These changes allow considerable decrease in energy ex-
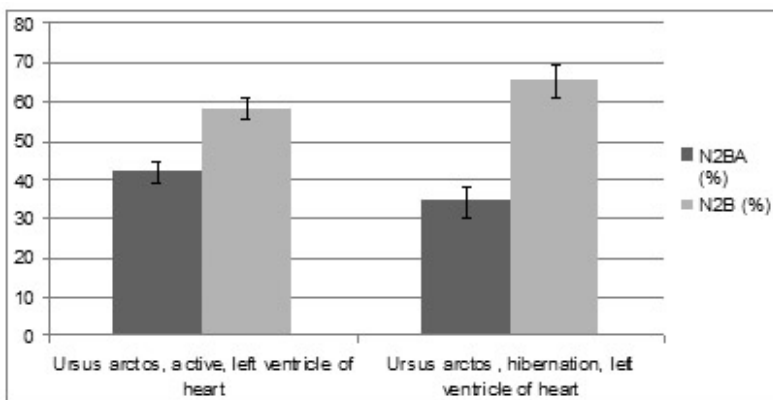
Fig. 3. Seasonal changes in titin isoforms composition in the left ventricle of the brown bear's heart.

penditure during winter dormancy that is necessary for the animal to survive under severe conditions of this period. It should be also noted that "slow" muscle fibers as opposed to "fast" ones are not only energetically more advantageous but more endurable. This property of muscles is vital to keep the postural pose of the animal during hibernation.

In the bear's cardiac muscle the changes in titin isoform composition were opposite to those in the cardiac muscle of the winter hibernating ground squirrel. For instance, as opposed to the increased content of the long N2BA-titin isoform in the cardiac muscle of the hibernating ground squirrel the content of this isoform in the cardiac muscle of the hibernating brown bear was lower than that in the active animal (fig. 3). In the cardiac muscle of the hibernating Himalayan black bear the N2BA to N2B ratio was similar to that one observed in the cardiac muscle of the hibernating brown bear (data not shown). Therefore, it can be stated that seasonal changes in titin isoform composition in the cardiac muscle of bears are directed to the increase in the content of the short N2B-isoforms of this protein while hibernating. The results obtained in our study are in accord with [6] – the increase in the relative content of the short N2B-titin isoform in the cardiac muscle of the hibernating grizzly bears (*U.a.horribilis*). Adaptive response of the changes revealed is presumably in preventing chamber dilation in heart of hibernating bears.

References

1. Hochachka P., Somero J. (1988) Biochemical adaptation 568 p.
2. Vikhlyantsev IM, Podlubnaya ZA. New titin (connectin) isoforms and their functional role in striated muscles of mammals: facts and suppositions // Biochemistry (Mosc). 2012; 77(13): 1515-35. doi: 10.1134/S0006297912130093.
3. Lazareva MV, Trapeznikova KO, Vikhliantsev IM, Bobylev AG, Klimov AA, Podlubnaia ZA. Seasonal changes in the isoform composition of the myosin heavy chains in skeletal muscles of hibernating ground squirrels Spermophilus undulatus // Biofizika. 2012; 57(6):982-7.
4. Tikunov BA, Sweeney HL, Rome LC // J Appl. Physiol. 2001. V. 90(5). P. 1927-1935.
5. Vikhlyantsev IM, Podlubnaya ZA, Kozlovskaya IB. New titin isoforms in skeletal muscles of mammals // Dokl. Biochem. Biophys. 2004; 395: 111-3.
6. Nelson O.L., Robbins C.T., Wu Y., Granzier H. Titin isoform switching is a major cardiac adaptive response in hibernating grizzly bears // Am. J. Physiol. Heart Circ. Physiol. 2008; 295(1): H366-71. doi: 10.1152/ajpheart.00234.2008. Epub 2008 May 23.

DESIGN OF CULTURED CELL-BASED MODELS FOR ELUCIDATION OF THE 210 KDA MYOSIN LIGHT CHAIN KINASE ROLE IN MECHANOPHENOTYPE AND PERMEABILITY OF MICROVASCULAR ENDOTHELIUM

M.V. Samsonov[1], M.M. Khalisov[2], V.A. Penniyaynen[2], O.A. Kazakova[1], A.Y. Khapchaev[1], E.L. Vilitkevich[1], A.V. Nikashin[1], A.V. Ankudinov[3], B.V. Krylov[2], V.P. Shirinsky[1]

[1]Institute of Experimental Cardiology, Russian Cardiology Research and Production Center, Moscow, 121552, Russia;
[2]Pavlov Institute of Physiology RAS, Saint-Petersburg, 199034, Russia;
[3]Ioffe Physical Technical Institute, Saint-Petersburg 194021, Russia

Microvascular endothelium participates in the formation of barrier between blood and tissues and in exchange of nutrients, gases and metabolic products between these compartments. High molecular weight myosin light chain kinase (MLCK210) is the key regulator of endothelial barrier. MLCK210 activation leads to attenuation of microvascular barrier and increased permeability to macromolecules. Acute increase in permeability of microvessels due to insufficiency of their endothelial lining is observed during physiological defence reaction of inflammation as well

as in a number of pathologies, which are accompanied by excessive mechano-chemical stimulation of vascular endothelium.

MLCK210 is considered a key molecular player in realization of endothelial cell mechanical properties that seem important for the reception by endothelium of the natural mechanical stimuli such as shear stress produced by blood flow, stretching of vascular wall and hydrostatic pressure applied on it. In order to study in detail the role of MLCK210 in mechanophenotype of endothelium as well as in regulation of paracellular permeability of endothelial monolayer we design and validate cultured cell-based models.

We utilized mice with genetic knockout of MLCK210 (kindly donated by Prof. D.M. Watterson, Northwestern University, Chicago, IL, USA) as a source of lung microvascular endothelial cells. Using immunoblotting we confirmed that lungs of MLCK-/- mice do not contain MLCK210 while this protein is synthesized in the lungs of wild type mice. Lung microvascular endothelial cells from MLCK-/- mice and from wild type mice of the same strain and age were isolated using immunomagnetic technology and introduced in cell culture.

Using ECIS-z (Applied BioPhysics, USA) apparatus that measures electric impedance across the monolayer of endothelial cells grown on gold electrode we demonstrated that in the presence of natural edemagenic agent thrombin (100 nM) wild type endothelium reversibly loses its barrier properties that is manifested by a decrease in impedance. In comparison, MLCK-/- endothelium exhibited less pronounced decrease in impedance. These findings suggest that intercellular contacts between MLCK-/- endothelial cells are broken to a lesser extent following thrombin challenge which results in a more modest alteration of electric impedance due to ion flow across the monolayer. Additionally, these observations highlight the role of MLCK210 in thrombin-mediated increase of endothelial monolayer permeability. Mechanistically, obtained results may be explained by the failure of MLCK-/- endothelial cells to efficiently contract and form intercellular gaps due to the lack in these cells of the key activator of endothelial myosin.

As an additional model system, we used standard in the field human endothelial cell line EA.hy926 that contains MLCK210 as established by immunoblotting. We confirmed that thrombin (10-100 nM) stimulation of EA.hy926 cells grown in DMEM supplemented with 10% fetal bovine serum results in a decrease of the monolayer electric impedance and simultaneous increase in permeability for FITC-albumin and 70

kDa FITC-dexran. Inhibition of MLCK catalytic activity in these cells by the novel cell-permeable peptide inhibitor PIK2 prevents thrombin-induced increase in permeability for macromolecules. Cultivation of EA.hy926 cells in the special growth medium for endothelial cells EBM (Lonza, Switzerland) supplemented with the set of growth factors and hormones leads to the strengthening of interendothelial contacts in the monolayer, significant reduction of its basal permeability and increase in impedance. Morphologically, these cells look more spread with few intercellular gaps between them. At the same time, thrombin-induced disassembly of intercellular contacts and acute increase in permeability is still reproduced in these cells. Noteworthy, PIK2 exerts much weaker inhibitory action on FITC-dextran permeability in EA.hy926 cultured in EBM suggesting that motile reactions of these cells are less dependent on MLCK210. According to our preliminary data, morphological and functional alterations in EA.hy926 grown in EBM are related to the presence of hydrocortisone in the medium. Apparently, this glucocorticoid changes the expression of various genes in endothelial cells leading to increased synthesis of intercellular contact proteins and, perhaps, to reduced expression of MLCK210.

We employed the method of atomic force microscopy (AFM) and initiated analysis of topography and stiffness of MLCK210-/- and wild type mouse lung microvascular endothelial cells as well as EA.hy926 endothelial cells grown in DMEM and EBM. We used custom-made cantilever that has spherical submicron particle of SiO_2 glued to the end of the needle. Such a design of a cantilever allows multiple rounds of scanning in a contact mode over cell surface without a damage to plasma membrane. Preliminary topographic images of endothelial cells clearly show elevated nuclear region and peripheral cytoplasm with fibrillar structures in it, most likely the components of the cytoskeleton. The stiffness of endothelial cells is lower over the nucleus and much higher in the peripheral cytoplasm where fibrillar structures are located. In AFM images, EA.hy926 cells differ from mouse lung endothelial cells by elongated nuclei and less spread cytoplasm.

Thus, we produced and initially characterized the set of endothelial cell-based model systems to study the role of MLCK210 in mechanophenotype and permeability of endothelium. We also validated several analytical methods to probe endothelial morphological and functional features that are dependent on MLCK210 activity in these cells.

DROSOPHILA SWISS CHEESE, ORTHOLOG OF HUMAN HEREDITARY SPASTIC PARAPLEGIA GENE, NTE, REGULATES MICROTUBULE STABILITY, SYNAPTIC STRUCTURE AND FUNCTION

S.V. Sarantseva, G.A. Kislik, O.I. Bolshakova

Petersburg Nuclear Physics Institute, National Research Centre "Kurchatov Institute", Gatchina, Russia

Hereditary spastic paraplegias (HSPs) comprise a heterogenic group of neurodegenerative diseases, characterized by progressive lower-extremity weakness and spasticity as a result of corticospinal tract axonal degeneration minimal in cervical region with caudal enhancement. It is estimated to affect about 1—7 people per 100,000 worldwide [http://www.ncbi.nlm.nih.gov/books/NBK1509]. The first symptoms of the disease appear within a wide age range. Autosomal-recessive and X-linked forms are mostly early-onset cases of HSP. It was established recently that mutations in catalytic domain of the neuropathy target esterase (*NTE*) cause autosomal-recessive form of HSP (SPG39). Initially NTE was found in human brain homogenates as an enzyme inhibited by organophosphates, leading to development of the organophosphorus compound induced delayed neuropathy (OPIDN). HSP and OPIDN are both characterized by distal degeneration of motor and sensory axons. NTE is a highly conservative protein with a homology among many organisms (from yeast to humans) especially in a catalytic esterase domain. NTE's ortholog in *Drosophila melanogaster* is called *swiss-cheese* (*sws*). All of main *sws* mutants were obtained and described by D. Kretzschmar et al. These mutants develop axonal and glial pathology in the brain and neuron apoptosis. The level of phosphatidylcholine is increased in these mutants. Sws and NTE have a 39%-homology. These proteins are widely expressed in nervous system, localized on endoplasmic reticulum (ER) and are also considered to have esterase activity. Interestingly, sws acts autonomously in neurons and glia: neuropil degeneration could only be rescued by neuronal sws expression and only sws expression in glia could stop formation of abnormal glial hyperwrapping. However, *sws* functions today are poorly understood. In our study we carried out functional studies of *sws in vivo*, using *Drosophila melanogaster* larval neuromuscular junctions (NMJ) as a good system of HSP modeling. We showed that sws is widely expressed in larval nervous system especially in glia. We also established that mutations in *sws* gene alters NMJ morphology, microtubule network formation and axonal transport of mitochondria.

NEW FINDINGS ABOUT THE FUNCTIONAL ROLE OF SMOOTH MUSCLE K CHANNELS IN THE CIRCULATORY SYSTEM

R. Schubert

Cardiovascular Physiology, Medical Faculty Mannheim, University Heidelberg, Ludolf-Krehl-Str. 13-17, Mannheim, 68167, Germany

The circulatory system serves the important task of delivering nutrients and oxygen to all organs of the body and of removing carbon dioxide and metabolites from these organs by matching the blood supply of an organ to its actual demand. An appropriate blood flow is ensured primarily by changes in blood vessel diameter because flow depends on the 4th power of the diameter. One of the major factors determining vessel diameter is the membrane potential of the contractile cells in the vessel wall, the smooth muscle cells. Membrane potential in turn is regulated by a large variety of ion channels with potassium (K) channels providing the major pathway for ion flux thereby having a high impact on the membrane potential. More than 100 different K channels have been identified. They consist of pore-forming α- and auxiliary β-subunits and are classified according to the predicted membrane topology into groups and according to sequence similarity into families and subfamilies. Three K channel groups have been defined: The voltage-gated and Ca-activated K channel group, the leak K channel group and the inward rectifier K channel group.

One member of the voltage-gated and Ca-activated K channel group, the large conductance Ca-activated potassium (BK) channel is of special importance because it is ubiquitously expressed in all vascular smooth muscle cells. This channel combines high potassium selectivity with high conductance and possesses a truly specific inhibitor, iberiotoxin. Since this channel is activated by membrane depolarization and an increase of the intracellular calcium concentration, it has been suggested to serve as a negative feedback mechanism during contractile reactions, i.e. to play an anti-contractile role. Recently, it was found that this channel is also able to prevent vasomotion, i.e. to functionally transform phasic smooth muscle into tonic smooth muscle. Further, the BK channel is activated by a number of protein kinases, in particular PKG, the target of the NO-cGMP pathway suggesting a pro-dilatory role of this channel. New findings show that the NO-cGMP pathway not only activates the BK channel via PKG but also reduces the activator calcium for the BK channel where the latter effect prevails over the former one, establishing an anti-dilatory role of the BK channel.

The inward rectifier K channel group has also attracted a lot of attention recently, especially the Kir2 channel family. Kir2 channels are activated by an increase of the extracellular K concentrations. Such an increase is observed physiologically near brain arterioles when transmitter substances released from active neurons initiate a K release from astrocyte endfeet resulting in a dilation of nearby arterioles. This mechanism helps to match the increased demand of active neurons in blood supply. However, an increased perfusion would result in overperfusion in the case of high blood pressure, e.g. during exercise. Normally, the myogenic response, i.e. the vessel contraction in response to an increase in blood pressure, would prevent overperfusion. But vasodilation evoked by vasoactive hormones and transmitter substances usually weakens or even abolishes the myogenic response. New findings show that such changes in the myogenic response are not observed during vasodilation induced by an activation of Kir2 channels. In contrast to most other K channels, these channels are inhibited by membrane depolarization, a major contributor to the myogenic response. As a consequence, activation of Kir channels by an increase of the extracellular K concentration leads to a strengthening of the myogenic response preventing overperfusion at high blood pressure. Thus, Kir2 channels orchestrate myogenic and metabolic autoregulation in the brain circulation.

THE POTENTIAL ROLE OF PRESENILIN 1 IN REGULATION OF SYNAPTIC FUNCTION

A.L. Schwarzman, S.V. Sarantseva
Petersburg Institute of Nuclear Physics,
Gatchina, Leningrad oblast, 188300, Russia

Alzheimer's disease (AD) is one of the most common forms of primary neurodegenerative disorders. Its clinical manifestation includes progressive memory loss and impairment of cognitive functions eventually resulting in total mental and intellectual degradation. Most models of AD typically mimic the pathogenesis of early onset familial AD that are caused by mutations in the amyloid precursor protein (APP) and presenilin (PS1 and PS2) genes. We examined APP and PS1 intra-and extracellular distribution in cultured embryonic neurons. It was shown that both proteins are localized in interneuronal synapses. PS1 localization in synapses was confirmed by embryonic neuron transfection with *PS1* cDNA containing the sequence of green fluorescent protein (GFP). GFP_immunoprecipitates extracted from transfected neurons contained *N*-cadherin proving that GFP-PS1 formed complex with major neuronal

cell adhesion protein. The density of morphological synapses was significantly lower in cultures derived from *PS1* knockout mice. In addition, L cells, which do not form tight intercellular contacts, formed clusters of adhered cells. For cell sorting (cell segregation) of non-transfected cells and wild type GFP-PS1 transfectants (or PS1 mutants) were mixed in 1:1 ratio, and cultured 16 hours at the presence of 50μM ponastron A, which induced PS1 expression. To distinguish between the two cell lines the cells were differentially labeled using DiO and DiI dyes. Cell cultures were monitoring at different times to follow the progress of cell segregation. After stable transfection with GFP-PS1 cDNA L cells demonstrated a clear preference for independent aggregation in the mixed cultures. However, L cells transfected with mutant GFP-PS1 partially failed to form intercellular contacts. Our results suggest that, the primary effect of *APP*, and *PS1* mutations results in impairment of synaptic functions.

SEASONAL CHANGES OF C-FOS PROTEIN ACTIVITY AS INDICATOR OF BRAIN PLASTICITY IN HIBERNATORS

T.P. Semenova, I.A. Anoshkina

Institute of Cell Biophysics Russian Academy of Sciences,
Institutskaya str. 3, Pushchino, Moscow reg. 142290

Plasticity of the central nervous system (CNS) is provided by structural and biochemical plasticity of cells elements and their interaction. The number of synaptic contacts, receptors density to surface of synaptic membranes and intensification of classic neurotransmitters synthesis, regulatory peptides, the character of interaction with glial elements, the level of expression of immediate early genes in brain structures change under influence of environmental factors. The immediate early genes, especially c-fos, appears as markers of neurons, in what we can await longtime plastic reorganization [1, 9]. The character of changing of hibernators' brain functional activity during annual cycle of their activity represents the simple of such high plasticity [7, 11]. Most of all attention among factors, influencing to processes of structure and biochemical changes of hibernators brain, directs to the circannual rhythms and molecular-genetic mechanisms of their regulation [5, 7, 10, 13, 16]. The control under circadian rhythms and their organization realizes such structures as suprachiasmatic nucleus of hypothalamus [10]. The present experiments were undertaken therefore to determine whether the immediate early genes, in particular, *c-fos* is also activated in suprachiasmatic nucleus by changing of functional state of hibernator during arousal.

Material and methods of investigation

Long - tail Yakutian ground squirrels (*Spermophilus undulatus*), 500-600 g were used in experiments. Animals of one group were in the state of hibernation (Control group I), the animals of other group (Experimental group II) - in state of exit from hibernation. The material for experiments was received from animals of Group I to 14th days of hibernation, the temperature of brain was 4-5°C. From animals of Group II material was received during their exit from hibernation, after 2. 5 hour from warm up beginning. Temperature of brain in this animals was +28-30°C. From each brain it was prepared 100 pair of frontal slices in cryostat, thickness 20 mkm. Each tenth slice was used for experiments. It was counted the number of neurons with expression of *c-fos* protein in suprachiasmatic nucleus (SCN) and paraventricular nucleus (PVN) of hypothalamus and density of distribution of *c-fos* positive neurons in these nuclei to area of one mm^2. Immunohistochemical staining for *c-fos* was carried out via streptavidine - biotin procedure. The results were analyzed by ANOVA.

Results of investigation

The immunohistochemical analysis of experimental data revealed the low level of transcriptional factor *c-fos* in the neurons of hypothalamic nulei during hibernation period of the yakutian ground squirrels (Group I). The number of *c-fos* positive neurons in the SCN was 21.89±8.5, and in PVN of hypothalamus – 21.89±8.5, correspondingly. In the ground squirrels, who are exits from hibernation (Group II), the number of *c-fos* positive neurons in the SCN of hypothalamus was increased to 100,54±31,7 (p<0,0079), but in PVN did not changed significantly with comparison to control (72,7±36,0). The density *c-fos* positive neurons in the ground squirrels SCN hypothalamus during hibernation period (Group I) was 847.2 ± 687.9 to mm^2, and in PVN - 1667.5 ± 855.2 to mm^2, correspondingly. During arousal animals from hibernation (Group II) the significant increasing of the expression density of *c-fos* positive neurons was revealed in SCN of hypothalamus only and was 3484.564 ± 743.1 (p<0,0107) to mm^2 as compared with period of hibernation. Taken together this data indicate that the significant increasing of the number and density of *c-fos* positive neurons during arousal was revealed only in the hibernator' SCN of hypothalamus.

Discussion

Modulation of the early genes transcription provides for harmonious regulation of central and visceral function of the organism in the time of the environment conditions changes [6]. Hypothalamus participates in the

maintenance of homeostasis also, in the control of many physiological functions of organism, which significantly change during hibernation. It was revealed the increase of metabolic activity during exit of animals from hibernation [8]. It was demonstrated that the level of mRNA *c-fos* expression in hypothalamic SCN of hibernators was increased under photo stimulation during arousal period [5]. It is possible to suppose, that activation of gene *c-fos* during the exit of the animals from hibernation state comes by the adrenergic way. It is known, that the increasing of noradrenaline level in several brain structures comes preceds to exit of the animal from hibernation [15, 16]. The activation of the adrenergic system leads to the increasing of the concentration of cyclic AMP in the cells and induces the expression *c-fos* gene [2-4]. Maximal expression of *c-fos* mRNA from group of immediate early gene was noted in SCN of ground squirrel in the period of his arousal at brain temperature $+20^{\circ}C$ already [5].

Agents that stimulated noradrenaline release and restraint stress all led to marked increases in *c-fos* immunoreactivity in the brain. The protein response was localized to the cell nucleus as has been reported previously for any *c-fos* inducing agents [14]. It is demonstrated, that blockers of noradrenergic receptors, propranolol and prazozin produced reduction in neuronal *c-fos* [4], as well as the coagulation of main noradrenergic nucleus locus coeruleus decreased the concentration of noradrenaline in the brain structure [15] and significantly delayed the exit of animal from hibernation and their warm up [12, 17]. The precise mechanism by which adrenoceptor stimulation lead to immediate early gene expression in the SCN of hypothalamus is not completely understood. In the case of *c-fos*, however, a number of studies have suggested that cyclic AMP elevation is responsible since cyclic AMP can mimic the action of beta-agonists and since the promoter region of the *c-fos* gene contains the cyclic AMP responsive element [17]. Furthermore the cyclic AMP response to beta-receptor stimulation is known to be augmented by $alpha_1$-adrenoceptors stimulation acting probably via phosphoinositide hydrolysis [4].

The hibernation presents the unique natural model for study neurotransmitter, molecular and genetic mechanisms of the CNS plasticity regulation. The process of hibernation submit (present) the complicated model of adaptive behavior, which can to reveal the longtime changes in the neurons of SCN of hypothalamus, connected with expression of *c-fos* as their marker.

References

1. Anokhin K.V. Molecular genetic of brain development and learning: on the way to synthesis. // Vestn. Ross. Akad. Med. Nauk. 2001. 4: 30-35.

2. Berridge C.W. Noradrenergic modulation of arousal.// Brain Res. Rev. 2008. 58(1): 1-17.

3. Berridge C.W., Schmeichel B.E., Espana R.A. Noradrenergic modulation of wakefulness/arousal. // Sleep Med. Rev. 2012. 16(2): 187-197.

4. Bing G., Stone E., Zhang Y., Filer D. Immunohistochemical studies of noradrenergic – induced expression of c-fos in the rat CNS. // Brain. Res. 1992. 592(1): 57- 62.

5. Bitting L., Sutin E. L., Watson F. L., Leard L. E., O'Hara B. F., Heller H. C., Kilduff T. S. C-fos mRNA increases in the ground squirrel suprachiasmatic nucleus during arousal from hibernation. // Neurosci. Lett. 1994. 165: 117-121

6. Cohen D. R., Curran T., Transcriptions activation and repression by c-Fos are independent functions. // Mol. Cell. Biol, 1990. 10: 4243-4255

7. Drew K.L., Buck C.L., Barnes B.M., Christian S.L., Rasley B.T., Harris M.B. Central nervous system regulation of mammalian hibernation: implications for metabolic suppression and ischemia tolerance // J Neurochem. 2007 102(6): 1713–1726.

8. Kilduff T.S., Radeke C.M., Sharp F.R., HellerH.C. 14C-2-deoxiglucose uptake in the ground squirrelbrain during entrance to and arousal from hibernation. // J. Neurosci. 1990. 10(7): 2463-2475.

9. Lamprecht R., Dudai Y. Transient expression of c-Fos in rat amigdala during training is required for encoding conditioned taste aversion memory. // Learn. Memory. 1996.3(1): 31-41.

10. O'Hara B.F., Watson F.L., Srere H.K., Kumar H., Wiler S.W., Welch S.K., Bitting L., Heller H.C., and Kilduff T.S. Gene expression in the brain across the hibernation cycle. // The J. of Neuroscience. 1999. 19(10): 3781-3790.

11. Ohe Ch.G., Darian-Smith C., Garner C.C., and Heller H.C. Ubiquitous and temperature-dependent neural plasticity in hibernators. // J. of Neuroscience. 2006. 26 (41): 10590- 10598.

12. Pastukhov Yu.F. REM sleep as a criterion of temperature comfort and temperature homeostasis "well-being" in euthermic and hibernating mammals. // Ann. NY Acad. Sci. 1997. 813: 71–72.

13. Ruby N.F, Dark J, Burns D.E, Heller H.C, Zucker I. The suprachiasmatic nucleus is essential for circadian body temperature rhythms in hibernating ground squirrels. // J. Neurosci. 2002. 22:357–364.

14. Sagar S.M., Sharp F.R., Curran T. Expression of c-fos protein in brain: metabolic mapping at the cellular level. // Science, 1988. 240: 1328-1331.

15. Semenova T.P., Kolaeva S.G. Role of endogenous factors in the regulation of the hibernators CNS functional state. // In: "Essay of ecological physiology". Eds. V.A. Trufakin, K.A. Shoshenko. Novosibirsk. 1999: 213-219.

16. Semenova T.P., Spiridonova L.A. Circadian and circannual rhythms of the effect of monoamine on the plasticity of the central nervous system of

hibernators. // In: «Biological Motility: basic research and practice». Ed. Z.A. Podlubnaya. Pushchino. 2012:177 - 180.

17. Stone E.A., Zhang Y., Filer D., Bing G. Effect of locus coeruleus lesion on c-fos expression in the cerebral cortex caused by yohimbine injection or stress. // Brain Res. 1993. 603(2): 181 – 185.

NAVIGATION RECEPTORS: MOLECULAR MECHANISMS OF CELL GUIDANCE

G.V. Sharonov

Shemyakin-Ovhinnikov Institute of Bioorganic Chemistry RAS,
ul. Miklukho-Maklaya 16/10, Moscow, 117997, Russia;
Faculty of Medicine, Moscow State University,
Lomonosov ave. 31/5, Moscow, 119992, Russia

Cell guidance is a key mechanism of cell positioning in a multicellular organism during development and tissue regeneration in adults. Each cell is continuously exposed to multiple guidance signals including soluble growth factors and cytokines, cell surface ligands such as ephrins, semaphorins, cadherins and selectins and extracellular matrix components. These multiple guidance cues are resolved and integrated into coherent instructions for cell navigation. Guidance signals are integrated and resolved at the stage of ligand receptor binding, receptor spatial rearrangement and downstream phosphorylation cascade. One guidance cue may induce different cell responses depending on coreceptors engaged, receptor localization to lipid microdomains, membrane thickness, and local intracellular phosphatase activity. Mechanisms of guidance signal processing will be discussed with the emphasis on ephrin/Eph signaling.

A134L TROPOMYOSIN MUTATION ALTERS THE FORCE-GENERATING CAPACITY OF MYOSIN MOLECULE

D.V. Shchepkin[1], G.V. Kopylova[1], A.M. Matyushenko[2], S.Y. Bershitsky[1], D.I. Levitsky[2,3]

[1] *Institute of Immunology and Physiology, Russian Academy of Sciences, Ural Branch, Yekaterinburg, 620049, Russia;*
[2] *Bach Institute of Biochemistry, Russian Academy of Sciences, Moscow, 119071, Russia;*
[3] *Belozersky Institute of Physico-Chemical Biology, Moscow State University, Moscow, 119992, Russia*

Tropomyosin (TM) is a key regulatory protein of actin-myosin interaction. TM molecule is a dimer of α-helices forming coiled-coil structure.

The central part of the TM molecule includes conservative non-canonical residues that disrupt its coiled-coil structure – Asp137 [1] and Gly126 [2]. Their presence increases conformational mobility (flexibility) of TM molecule. The peptide bond between Arg133 and Ala134 is the most susceptible site to cleavage by trypsin in the full-length TM [3, 4] indicating that the region around Arg133 is the least stable part of the TM molecule. Replacement of these residues by canonical ones (mutations D137L, G126R, or G126A) results in the stabilization of the central part of TM molecule and prevents trypsin cleavage of TM at the nearby Arg133 [1, 2]. These stabilizations alter the functional characteristics of TM. D137L and G126R mutations increase the actin-activated Mg^{2+}-ATPase of myosin and affect the Ca^{2+}-regulation of the interaction of myosin with regulated thin filaments consisting of actin, troponin, and tropomyosin [2, 5].

Like residues Asp137 and Gly126, residue Ala134 has destabilizing effect on the central part of the TM molecule [6]. It was shown that further destabilization of the central part of the molecule leads to a serious myopathy [7]. The aim of our work was to investigate the functional characteristics of A134L TM. Using the *in vitro* motility assay we studied the effect of A134L/C190A TM on the force generating capacity of myosin molecule and also on the Ca^{2+}-dependent sliding velocity of regulated thin filaments over myosin.

Experiments in the *in vitro* motility assay were done as described previously [8]. To assess the force generating capacity of myosin molecule we used NEM-modified myosin as a load [9]. The minimum concentration of NEM-myosin at which the filaments stopped moving indicated the isometric force. It was assessed effect of A134L mutation on the force of myosin with F-actin-tropomyosin filaments (actin-TM) and regulated thin filaments. Force of myosin molecules with regulated thin filaments was determined at saturated calcium concentration (pCa 4).

The force generating capacity of myosin molecules with actin-TM filaments containing both A134L/C190A TM and C190A TM was lower than that with F-actin alone (fig. 1A). The myosin force with regulated thin filaments was two-fold of the force with actin-TM (fig. 1). The force generating capacity of myosin molecules with regulated thin filaments containing A134L/C190A was significantly lower than that with the filaments containing C190A TM (fig. 1B).

The dependence of sliding velocity of regulated thin filaments on calcium concentration (fig. 2) was fitted to the Hill equation: $V = V_{max}(1+10^{h(pCa-pCa50)})^{-1}$, where V and V_{max} are velocity and maximal veloci-
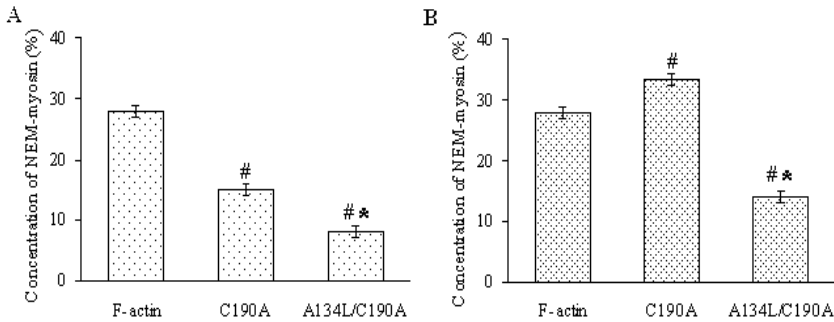
Fig. 1. The force generating capacity of myosin molecules with actin-TM filaments (A) and regulated thin filaments (B) containing A134L/C190A TM assessed in the *in vitro* motility assay. The columns and error bars are mean ± S.D. # indicates significant difference of force generating capacity of myosin molecules with these filaments from F-actin, $p < 0.05$. * is significant difference of force generating capacity of myosin molecules with the filaments containing A134L/C190A TM from these with C190A TM, $p < 0.05$.
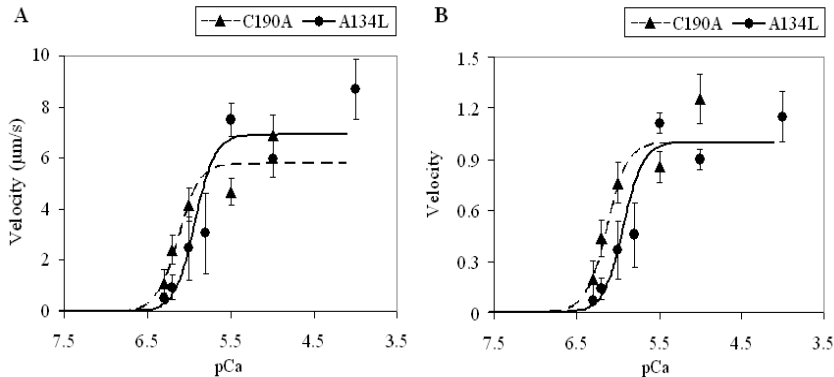
Fig. 2. Effect of the A134L/C190A TM on the Ca2+-dependent sliding velocity of regulated thin filaments in the in vitro motility assay as compared to control C190A TM. (A) Average data of three experiments. (B). The same data normalized for the maximal velocity. The data were fitted with the Hill equation. Each data points represent mean ± SD of three experiments.

ty obtained at saturating calcium concentration, respectively, pCa$_{50}$ (i.e. calcium sensitivity) is pCa at which half maximal velocity is achieved, and h is the Hill coefficient.

Parameters of the Hill equation

	h	$p\mathrm{Ca}_{50}$	V_{max}, µm/s
A134L/C190A	3.62 ± 1.34	5.91 ± 0.08	6.91 ± 0.75
C190A	2.51 ± 1.06	6.06 ± 0.04*	6.05 ± 0.43

A134L mutation of TM slightly enhances the sliding velocity of the thin filaments at saturated calcium concentrations and decreases Ca^{2+}-sensitivity of the velocity by shifting pCa -velocity curve towards higher Ca^{2+} concentrations (table).

We conclude that substitution the Ala134 residue in TM molecule with Leu dramatically affects the force generation capacity of myosin molecule and slightly influences on calcium regulation of actin-myosin interaction.

References

1. Sumida J.P., Wu E., Lehrer S.S. (2008) Conserved Asp-137 imparts flexibility to tropomyosin and affects function. *J. Biol. Chem.* 283, 6728–34.
2. Nevzorov I.A., Nikolaeva O.P, Kainov Y.A., Redwood C.S., Levitsky D.I. (2011) Conserved noncanonical residue Gly-126 confers instability to the middle part of the tropomyosin molecule. *J. Biol. Chem.* 286, 15766–72.
3. Pato M.D., Mak A.S. & Smillie L.B. (1981) Fragments of rabbit striated muscle α-tropomyosin. *J. Biol. Chem.* 256, 593–601.
4. Ueno H. Local structural changes in tropomyosin detected by a trypsin-probe method. (1984) *Biochemistry.* 23, 4791–8.
5. Shchepkin D.V.et al. Stabilization of the central part of tropomyosin molecule alters the Ca^{2+} -sensitivity of actin-myosin interaction. (2013) *Acta Naturae.* 5, No 3(18), 24–7.
6. Hodges R.S. et al. Identification of a unique "stability control region" that controls protein stability of tropomyosin: A two-stranded alpha-helical coiled-coil. (2009) *J Mol Biol.* 392(3), 747-62.
7. Ochala J.et al. Effects of a R133W beta-tropomyosin mutation on regulation of muscle contraction in single human muscle fibres. (2007) *J Physiol.* 581(Pt 3), 1283-92.
8. Kopylova GV, Katsnel'son LB, Ovsiannikov DA, Bershitskiĭ SIu, Nikitina LV. The *in vitro* motility assay to study the calcium-mechanical relationship in skeletal and cardiac muscles. (2006) *Biofizika.* 51(5),781-5.

9. Haeberle JR, Trybus KM, Hemric ME, Warshaw DM. The effects of smooth muscle caldesmon on actin filament motility. (1992) *J Biol Chem.* 267(32), 23001-6.

EFFECTS OF cMyBP-C ON THE CALCIUM REGULATION OF INTERACTION OF CARDIAC ISOMYOSINS WITH THIN FILAMENT. THE *IN VITRO* MOTILITY ASSAY AND OPTICAL TWEEZERS

D.V. Shchepin, G.V. Kopylova, S.R. Nabiev, L.V. Nikitina

Institute of Immunology and Physiology of the RAS, Laboratory of Biological Motility, Pervomayskaya ul., 91, Yekaterinburg, 62004, Russia

According to published studies about a half of familial hypertrophic cardiomyopathies (FHC) occur due to mutations in genes encoding cardiac myosin binding protein-C (cMyBP-C) [1]. cMyBP-C is a large thick filament-associated protein that consist of 11 domains domains (8 immunoglobulin I-like and three fibronectin 3-like) called C0–C10 from N- to C-terminus. Numerous data report cMyBP-C contribution not only to the thick filament structure but also to the regulation of cardiac contractility.

In our previous study, we assessed the modulatory role of cMyBP-C in the regulation of contractility of cardiac muscle using an *in vitro* motility assay [2]. We confirmed regulatory role of cMyBP-C in myocardium. There are two most probable mechanisms of influence of cMyBP-C. First, cMyBP-C slows down cross-bridge kinetics when binding to actin [3]. Second, cMyBP-C may modulate thin filament activity [4].

In ventricles of mammalian heart there are two myosin isoforms: V1 and V3 that have different functional characteristics. It is shown that cardiac myosin isoforms effect on calcium regulation of actin-myosin interaction [5,6]. The aim of our study was to analyze the role of cardiac isomyosins on interaction cMyBP-C with contractile and regulatory proteins of myocardium.

The *in vitro* motility assay with regulated thin filaments was applied. We obtained dependences of sliding velocities of thin filaments on calcium concentration (figure). Rabbit cardiac isomyosins V1 and V3 both with and without cMyBP-C were used. The Hill coefficient and calcium sensitivity estimated as pCa_{50} were assessed for "pCa–velocity" relationships. The effect of cMyBP-C on the interaction of single cardiac myosin molecule with F-actin was tested by the optical tweezers.
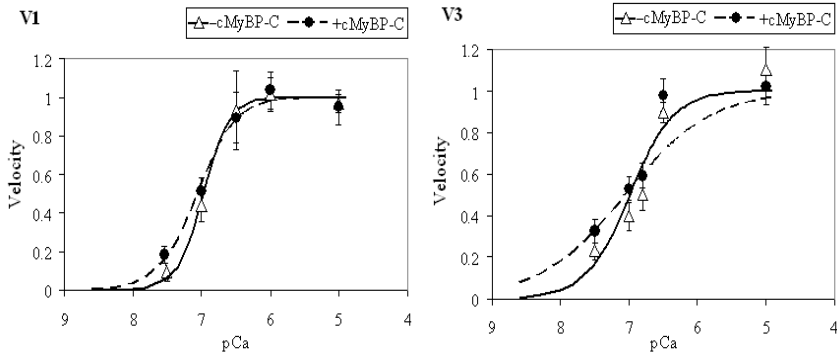
The 'pCa–velocity' relationships for V1 and V3 isomyosins in the presence and the absence of cMyBP-C. The data were fitted with the Hill equation. Each data point represents mean ± SD of three experiments.

We found that addition of cMyBP-C to myosin at physiological proportion (1:5 molar ratio of cMyBP-C/myosin) led to a decrease the sliding velocities of regulated thin filaments at maximal calcium (pCa 4) for both cardiac isomyosins (table 1). The presence of cMyBP-C not effect on calcium sensitivity of "pCa-velocity" relationships for both isomyosins. The Hill coefficient of "pCa–velocity" relationship decreased for V3, but did not change in the case of V1 (figure, table 1).

Adding of cMyBP-C did not affect appreciably mechanical characteristics of the actin-myosin interaction (step size and force developed by myosin head) for both isomyosins (table 2). As for kinetic characteristics of this interaction, the addition of cMyBP-C affected only the duration of force developed by V1.

We can conclude that cMyBP-C effects on calcium regulation of actin-myosin interaction depending on cardiac myosin isoforms. This

Table 1. Parameters of Hill equation

	V_{max} (μm/s)	h	pCa_{50}
V1	3.2 ± 0.1	2.28 ± 0.78	6.97 ± 0.28
1 : 5 cMyBP-C	1.7 ± 0.1*	1.56 ± 1.10	7.06 ± 0.12
V3	2.1 ± 0.1	1.40 ± 0.18	7.20 ± 0.20
1 : 5 cMyBP-C	1.7 ± 0.1*	0.70 ± 0.14*	7.06 ± 0.10

The velocities and parameters of Hill equation are represented as mean ± S.D. * is denoted statistical significance of differences of parameters of Hill equation with cMyBP-C from without cMyBP-C.

Table 2. Parameters of single molecule interaction of V1 and V3 with F-actin

	step size		average unitary force	
	d (nm)	duration (ms)	F (pN)	duration (ms)
V1	8.5 ± 3.0	51.1 ± 4.5	1.4 ± 0.6	55.5 ± 5.0
1 : 2.5 cMyBP-C	11.9 ± 5.0	54.1 ± 3.2	2.0 ± 0.7	$76.9 \pm 8.9^*$
1 : 5 cMyBP-C	10.2 ± 4.2	*N/a*	1.7 ± 50.6	$75.9 \pm 4.5^*$
V3	9.5 ± 4.0	58.5 ± 5.6	1.6 ± 0.7	72.1 ± 4.5
1 : 2.5 cMyBP-C	11.0 ± 5.0	50.5 ± 4.1	2.2 ± 0.9	76.9 ± 8.9
1 : 5 cMyBP-C	10.4 ± 4.1	$68.8 \pm 5.4^*$	1.6 ± 0.5	75.9 ± 4.5

Values *d* and *F* are represented as mean ± S.D. Durations of the events are mean ± S.E.M. Figures in brackets are numbers of the events analyzed. Statistical significance for differences in step durations of V1 and V3 isomyosins with appropriate F-actin is denoted as * (*P*<0.05).

may play a significant role in maintenance of the effective heart work both during ontogenesis and in pathological conditions.

References

1. P. Richard et al. Circulation 107 (2003) 2227–32.
2. Shchepkin et al. Bioch and Bioph Res Com (2010) 401: 159-163.
3. Saber et al. J Mol Cell Cardiol. (2008) 44(6):1053-61.
4. Mun et al. Proc Natl Acad Sci U S A. (2014) 11;111(6):2170-5.
5. Nikitina et al. Biochemistry (Moscow) (2008) 73(2): 178-84.
6. Shchepkin et al. International Symposium "Biological Motility: Fundamental and Applied Science", Pushchino, May 11-15: (2012) 183-6.

NON-STRAUB TYPE G-ACTIN FROM MOLLUSCAN SMOOTH MUSCLE: COMPARISON WITH MYTILUS "NATURAL" F-ACTIN AND STRAUB TYPE RABBIT SKELETAL ACTIN

U.V. Shevchenko, N.S. Shelud'ko

A.V. Zhirmunsky Institute of Marine Biology, Far Eastern Branch of the Russian Academy of Sciences, Palchevsky str. 17, Vladivostok, 690059, Russia

Straub type actin is easily obtained from skeletal muscle of vertebrate animals [1], but really not from all other types of muscles. For exam-
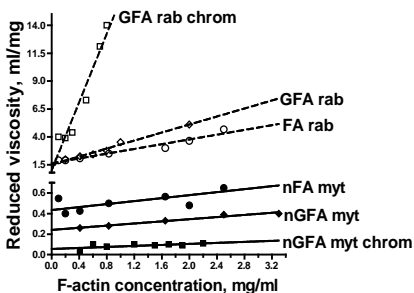
Fig.1. Comparison of different preparations of actin from rabbit skeletal muscle and actin from mussel catch muscle.
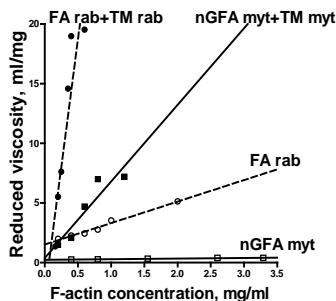
Fig.2. Effect of tropomyosin on the viscosity of actin from rabbit skeletal muscle and actin from mussel catch muscle.

ple, when studing proteins of the smooth muscles of bivalve mollusks, we have to use in the contraction models either actin of the rabbit skeletal muscles, or "natural" F-actin of the mussel, which we extract from molluscan muscles in the polymer form [2].

Although actin is a distinct example of the conservative protein, we have noticed that Straub actin of the rabbit and "natural" F-actin of the mussel differ in a number of properties, in particular in their viscosity characteristics (fig.1, FA rab and nFA myt). It is not clear whether these differences are determined by impurities in preparations, or they depend on the properties of actins *per se*.

To elucidate the nature of the differences, we purified the preparations by sedimentation at high ionic strength with ATP and pyrophosphate and by gel filtration chromatography on a «Sephadex G100» column.

Surprisingly, the "natural" actin of mussel purified in this way (high ionic strength, ATP and pyrophosphate) becomes capable of depolymerization in solutions of low ionic strength, as it is known for Straub actin. The G-actin thus obtained from mussels (nGA myt) was capable of repolymerization as well as actin of the rabbit. The viscosity of the repolymerized mussel actin (nGFA myt) was lower than the viscosity of the starting "natural" F-actin, while a similar treatment of rabbit actin results in an increase of its viscosity (fig.1, GFA rab and nGFA myt). Further, both actins in G-form were subjected to chromatographic purification. In accordance with the literature data, a similar purification of rabbit actin led to increased viscosity (fig. 1, GFA rab chrom). At the same time, chromatographic purification of mussel G-actin led to a

further reduction of its viscosity (fig. 1, nGFA myt chrom). Finally, we have achieved after two purification steps not a decrease, but the opposite - an increase in the differences between the viscosities of the polymeric actins from mussel and from rabbit.

The results of our study indicate that differences in viscosities of the investigated preparations are determined by the properties of the actins *per se*. Apparently, the mussel actin polymers are less rigid. This is also indicated by the reaction of actins to addition of tropomyosin: the viscosity of the mussel actin polymers increased markedly more than the viscosity of rabbit actin polymers (fig. 2).

Thus, despite the conservatism of actin, there is a need for careful use of rabbit actin in the study of mussel proteins.

References

1. A. Szent-Gyorgyi. Chemistry of muscular contraction. Academic Press, New York. 1947.
2. N.S. Shelud'ko, O.S. Matusovsky, T.V. Permyakova, G.G. Matusovskaya. Arch. Biochem. Biophys. 466, 125. 2007.

THE ROLE OF THE CALRETICULINE IN MITOCHONDRIAL ATP-DEPENDENT POTASSIUM TRANSPORT

M.I. Shigaeva[1], E.Y. Talanov[1], N.I. Venediktova[1], Y.A. Horokhovatski[2], M.S. Honcharenko[2], S.V. Murzaeva[3], G.D. Mironova[1,3]

[1] Institute of Theoretical and Experimental Biophysics RAS, Universitetskaya str. 3, Pushchino, 142290, Russia;
[2] Karazin Kharkiv National University, pl. Svobodi 4, Kharkiv, 61022, Ukraine;
[3] Pushchino State Naturally-Scientific Institute, Prospect Nauki 3, Pushchino, 142290, Russia

The key role in the process of potassium transport in mitochondria plays mitochondrial potassium channels, of which the most studied mitochondrial ATP-dependent potassium channel (mitoK$_{ATP}$). It has been shown that activation of the mitoK$_{ATP}$ channels before prolonged myocardial ischemia leads to positive experimental and clinical results such as reducing infarct zone and cardiac rhythm restore (1-4), increase the organism's resistance to acute hypoxic stress (5, 6), and also affects on energy and oxidative exchange (7). However, despite intensive study, the

structure mitoK$_{ATP}$ not completely elucidated. It is believed that mitoK$_{ATP}$ structure similar to the structure of ATP-dependent potassium channel of the cytoplasmic membrane (cytoK$_{ATP}$) and accordingly, is composed of the channel and the regulatory subunits (8-11). This is confirmed by our data immunoelectron microscopy studies using antibodies to KIR6.2. (12). However, according to Inoue (13) and Akopova (14), in the mitochondria, in addition to the channel that is similar in properties to the KIR 6.2, there is probably the ATP-dependent potassium channel of another type, characterized by the action of modulators. We have recently shown that such a channel may be a protein with m.w. 57 kDa, which, according to MALDI-TOF-TOF analysis, is a very high homology with the amino-acid sequence of the protein calreticulin precursor. This fact gives us reason to believe that calreticulin or its derivatives are able to form channels of potassium conductance in the mitochondrial membrane. Indirectly in favor of it electron microscopy data obtained in our laboratory, which demonstrate that calreticulin or homologous protein can be localized not only in the reticulum, but also in the mitochondria (15). According to the latest published data, half of calreticulin is localized at the contact sites of mitochondria and reticulum, the so-called OMM-contacts (16). Identify at calreticulin or its derivatives ability to form a channel structure in the mitochondrial membrane is extremely important: it will take a fresh look at the question of the structure of potassium channels in mitochondria. According to our preliminary data, this protein, reconstructed in the BLM, forms in it potassium channels inhibited by ATP.

The main purpose of our work is evidence of the role of calreticulin in the formation K$^+$ - transporting channels in mitochondria.

For this task we have prepared and purified polyclonal antibodies to calreticulin required for immunochemical and inhibitor assays. Antibodies are prepared by immunizing an animal (rabbit) by commercial bovine liver calreticulin (Sigma, USA). Antibody (IgG) was isolated from the obtained antiserum using immune-affinity chromatography. The antibody was stained in reticulum only one band corresponding to calreticulin. Based on these data, we conclude that the antibodies are specific for calreticulin. Mitochondria and microsomes (reticulum) were isolated from rat liver by differential centrifugation.

Inhibitory analysis of potassium transport in mitochondria was performed using spectrophotometry and potassium selective electrode. Influence derived antibodies on mitochondrial respiration was examined using the method of polarography. For immunohistochemical analysis were taken mitochondria and reticulum from rat liver purified on a sucrose gra-
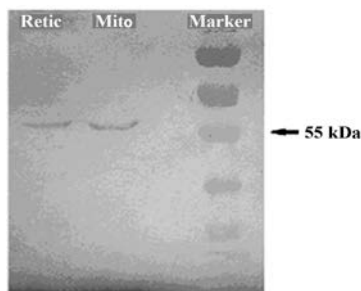
Fig. 1. Immunoassay of homology of mitochondrial potassium-transporting protein m.w. 57 kDa and calreticulin. Mito - purified mitochondrial fraction, Retic - purified reticulum fraction, right - protein markers

dient. It is shown that antibodies to calreticulin interact with only one protein m.w. 57 kDa as in the mitochondria, and in the reticulum (fig. 1).

Consequently, there is a protein m.w. ~ 57 kDa homologous calreticulin in mitochondria, which is likely localized in the contact points of reticulum and mitochondria. And, this protein is capable to forming potassium channels in bilayer lipid membranes.

To prove the role of calreticulin in potassium transport in mitochondria, inhibitory analysis of ATP-dependent potassium transport in mitochondria was performed using antibodies to calreticulin. Work was carried out on two experimental models: 1) the model of energy-dependent swelling of mitochondria in potassium medium reflecting uptake of potassium into the mitochondria, and 2) model of 2,4-dinitrophenol (DNP)-induced efflux of potassium from the mitochondria, reflecting the inverted channel functioning. Antibodies were added into the incubation medium at various concentrations (0.05 - 0.5 mg / ml) before placing in medium the mitochondria. As a negative control, the same antibodies inactivated by boiling were used. In the experiments, was shown to dose-dependent inhibitory effect of antibodies to calreticulin on potassium transport in the mitochondria (table).

Inhibition of DNP-induced potassium efflux from rat liver mitochondria by antibodies to calreticulin

Amount of antibodies in the cuvette, mg/ml	Inhibition of K^+ transport, % from control
0,005	18,49 ± 3,87
0,05	24,87 ± 4,55
0,1	36,12 ± 5,12
0,4	58,39 ± 10,32
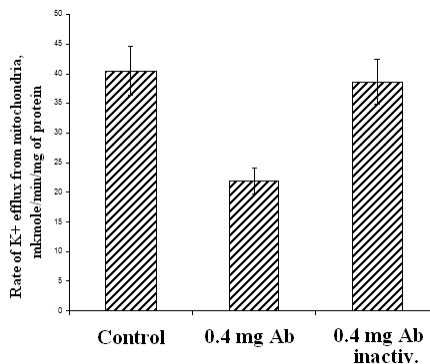
Fig. 2. Effect of native and inactivated by boiling antibodies to calreticulin on rate of DNP-induced potassium efflux from mitochondria.

According to our data, obtained on two models, the maximum value of the inhibitory effect was 55-65%, which is comparable with the magnitude of inhibition of potassium transport in mitochondria by antibodies on mitochondrial potassium-transporting protein (17). The maximum inhibitory effect was shown at a concentration of antibody 0.4 mg / ml of medium. It should be noted that we have not discovered effect of these antibodies on the parameters of mitochondrial respiration and oxidative phosphorylation. Calreticulin antibody on the maximum effective concentration (0,4 mg/ml) inactivated by heating to 98ºC for 5 minutes, almost did not exerted its inhibitory effect (fig. 2).

Based on these data, we can conclude that antibodies to calreticulin directly block the ATP-dependent potassium transport through mitoK$_{ATP}$ in mitochondria. However, the lack of complete inhibition of ATP-dependent potassium transport by calreticulin antibodies indicates the presence of at least another one system of the ATP-dependent potassium transport in mitochondria. Given our earlier data resulting MALDI-TOF/TOF-analyses showing partial homology calreticulin and channel subunit mitoK$_{ATP}$, we hypothesized that the mitoK$_{ATP}$ structure included homolog of calreticulin but not classic calreticulin.

On the results of research, we can suggest that in one of the systems provided the ATP-dependent potassium transport in mitochondria involved the contact of the reticular, outer and inner mitochondrial membranes, the so-called OMM-contacts (16). As was recently shown in mitochondrial ruthenium red-dependent calcium transport I also involved this three membranes (16).

References

1. Gross G., Auchampach J. // Cardiovasc. Res., 1992, 26(11): 1011-6;
2. Krylova I.B., Kachaeva E.V. et al. // Experimental Gerontology., 2006, 41(7): 697-703;
3. Liu Y., Sato T., et al. // Circulation., 1998, 97: 2463-2469;
4. Tsai Ch, Su Sh, et al. // Pharmacol. and Exp. Therap., 2002, 301: 234-440;
5. Миронова Г.Д. и др. // Бюлл. Эксп. Биол. и Мед., 2011, Том 151, №1, с. 30-35;
6. Mironova G.D. et al. // J. of Bioen. and Biomembr., 2010, V. 42, № 6, pp 492-503;
7. Крылова И.Б.. и др. // Бюлл. Эксп. Биол. и Мед., 2012, Том 153, №5, с. 596-599;
8. Bajgar R., Seetharaman S., et al. // J.Biol.Chem. 2001, 276(31):33369-33374;
9. Mironova G, Negoda A, et al., // J. Biol. Chem. 2004, 279(31): 32562-68;
10. Mironova G.D., Skarga Yu. //J Bioenerg Biomembr. 1999, 31(2): 157-161;
11. Foster D.B., Ho A.S. et al. //Circ. Res. 2012, 111(4): 446-54;
12. Павлик Л.Л., Гриценко Е Н. и др. // Биофизика, 2010, т.55, №5, с.809-813;
13. Inoue I., Nagase H. et al. // Nature. 1991, 352: 244-247;
14. Акопова О.В., Носарь В.И. и др. // Биохимия, 2010, т.75, №9, с.1273-7283;
15. Таланов Е.Ю., Павлик Л.Л. и др. // Биол. Мембр., 2013, т.30, № 5-6, с. 474-478;
16. Yi M., Weaver D., et al // Cell Calcium. 2012 Nov;52(5):355-65;
17. Скарга Ю.Ю., Долгачева Л.П. и др. // Укр. Биохим. Журнал, 1987, 59 (6): 54-59.

THE KINETIC MODEL OF MUSCLE CONTRACTION AND ENERGETICS

E.N. Shvorina

Institute of Mechanics, Moscow State University, Mitchurinsky prosp. 1, Moscow, 119992, Russia

Mechanical force generated in a contracting muscle results from cyclic interactions of myosin cross-bridges with actin filaments. The

kinetic scheme of such interaction consists of several states of the myosin head transiently bound to and detached from the actin filament and the transitions from one state to another. The rates of these transitions depend on the microscopic movements of the cross-bridge and on the biochemical and thermodynamic parameters such as temperature and concentrations of ATP, ADP and inorganic phosphate. The corresponding mathematical model is a system of the first order partial differential equations for the density distribution of the concentrations of the myosin bridges in each state. Kinetic models vary the numbers of attached and detached states of the myosin head and the functions describing transitions from one state to another. It is useful to develop a software tool in order to quantitate these models, and compare the results of calculations with experimental data to elucidate the molecular mechanisms of actin-myosin motor.

The goal of this work was to create software for calculations the kinetic models of muscle contraction with arbitrary number of the states and transition between them, with regards to different parameters affecting macroscopic behavior of the muscle fiber. We also have developed a specific kinetic model which reproduces some experimental data.

The Model in details

A myosin cross-bridge cycle includes several biochemical and mechanical transitions. It is known from the experimental data that the myosin head behaves as if it has an element with linear-elasticity, so head attached to actin we assume be linearly elastic without specifying the location of the elastic element in the molecule. Accordingly, we define as mechanical transitions the changes of the myosin head with the displacement of the equilibrium position of the elastic element along the filament axis. Thus, the changes in deformation of the elastic element in the process of mechanical transition do occur without the relative displacement of the filaments.

In our model we have three biochemical (ATP hydrolysis, phosphate release, ADP release) and three mechanical transitions (reverse tilt of the 'lever arm' i.e. the 'neck domain' of the myosin head with respect to its globular catalytic domain, stereo-specific locking on actin and the 'working' tilt of the lever arm) between the 16 possible biochemically and mechanically different states (figure).

In complete working cycle that starts from the attachment of the myosin head to actin and ends during detachment after binding of a 'new' ATP molecule all 6 transitions must occur and define all 7 corresponding 'active', i.e. achievable cross-bridge states in a certain sequence. In our model we postulate the following order of transitions of an attached cross-bridge (figure): reverse tilt of the lever arm with the closing of the ATP-
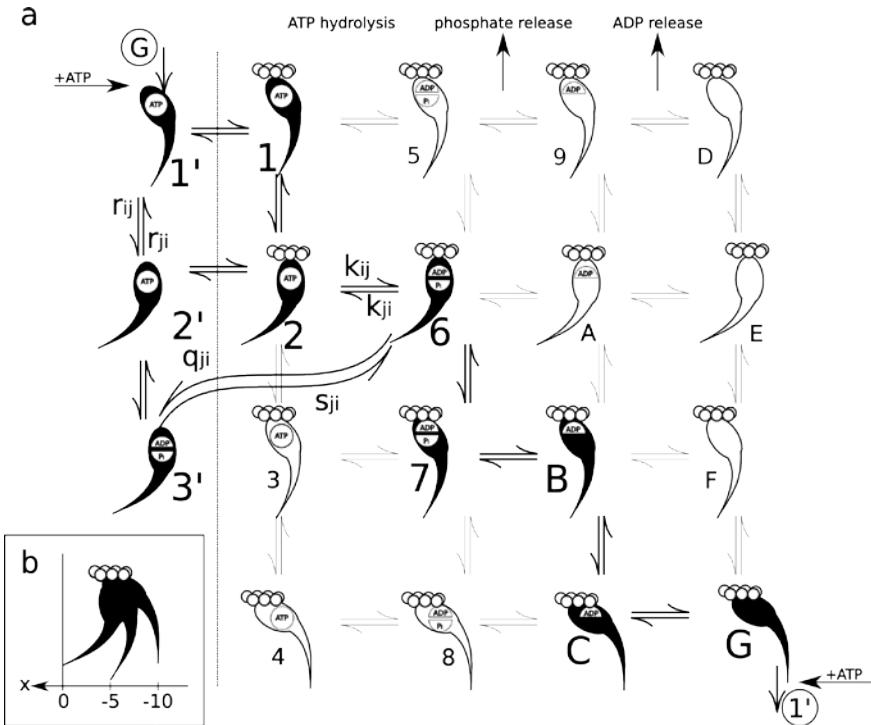
Fig. 1. The scheme of the myosin cross-bridge cycle.

binding 'pocket', ATP hydrolysis, 'roll-and-lock' transition [8], phosphate release, force-generating step (lever arm tilt), ADP release[9]. Furthermore, we assume that the ADP release occurs along with the shift of the equilibrium position by 0.5 nm ([6]). ATP binding to a myosin head is accompanied by conformational changes on its actin-binding surface [9]. In our model, these two processes occur not consequently, but simultaneously.

Transitions between three detached states correspond to the ATP hydrolysis that follows the reverse tilt of the lever arm along with the closing of the ATP-binding pocket. In each of these states myosin head can be reversibly attached to actin and form a weakly bound non-stereospecific complex. Since the weak binding to actin has almost no effect on the rate of transitions between the states of the myosin heads, we assume that the transition rates between the three detached and three weakly attached states are identical. It is also important that while our software tool allows any order or sequence of mechanical and biochemical transitions, a specific model described here matches the best to experimental data.

Results

The above model is a developement and generalization of the model [8], where were the dependences of the rate constants for transitions on micro-displacements of a head, x, were specified. Additionally the transitions corresponding the ADP and phosphate release were introduced to the scheme. Overall, the results of our modeling of a wide range of experiments with the proposed model has shown its ability to describe adequately the dependence of the macroscopic characteristics on temperature ([1,10,13]), fiber shortening velocity ([12,14]) and concentration of ATP ([2,3,7,15]), ADP ([3,5]), and partly inorganic phosphate([3,4,9]). At the same time, our model predicts some structural characteristics of contraction which can be verified by X-ray diffraction, and possibly by other techniques.

References

1. Bershitsky S.Y. The elementary force generation process probed by temperature and length perturbations in muscle fibres from the rabbit / S.Y. Bershitsky, A.K. Tsaturyan // The Journal of Physiology. – 2002. – Vol. 540, No. 3. – P. 971–988.
2. Cooke R. Contraction of glycerinated muscle fibers as a function of the ATP concentration. / R. Cooke, W. Bialek // Biophysical Journal. – 1979. – Vol. 28, No. 2. – P. 241–258.
3. Cooke R. The effects of ADP and phosphate on the contraction of muscle fibers. / R. Cooke, E. Pate // Biophysical Journal. – 1985. – Vol. 48, No.5 – P. 789–798.
4. Coupland M.E. Temperature dependence of active tension in mammalian (rabbit psoas) muscle fibres: effect of inorganic phosphate. / M.E. Coupland, E. Puchert, K.W. Ranatunga / The Journal of Physiology. – 2001. – Vol. 536, No. 3. – P. 879–891.
5. Coupland M.E. Endothermic force generation, temperature-jump experiments and effects of increased [MgADP] in rabbit psoas muscle fibres / M.E. Coupland, G.J. Pinniger, K.W. Ranatunga // The Journal of Physiology. – 2005. – Vol. 567, No. 2. P. 471– 492.
6. Geeves M.A. The molecular mechanism of muscle contraction. / M.A. Geeves, K.C. Holmes // Advances in Protein Chemistry. – 2005. – Vol. 71 – P. 161–193.
7. Ferenczi M.A. The dependence of force and shortening velocity on substrate concentration in skinned muscle fibres from Rana temporaria. / M.A. Ferenczi, Y.E. Goldman, R.M. Simmons // The Journal of Physiology. – 1984. – Vol. 350. – P. 519–543.
8. Ferenczi M.A. The "roll and lock" mechanism of force generation in muscle. / M.A. Ferenczi, S.Y. Bershitsky, N. Koubassova,V.

Siththanandan, W.I. Helsby, P. Panine, M. Roessle, T. Narayanan, A.K. Tsaturyan // Structure. – 2005. – No. 13, Vol 1 – P. 131–141.

9. Geeves M.A. The molecular mechanism of muscle contraction. / M.A. Geeves, K.C. Holmes // Advances in Protein Chemistry. – 2005. – Vol. 71 – P. 161–193.

10. He Z.H. ATP consumption and efficiency of human single muscle fibers with different myosin isoform composition. / Z.H. He, R. Bottinelli, M.A. Pellegrino, M.A. Ferenczi, C. Reggiani // Biophysical Journal. – 2000. – Vol. 79, No. 2. – P. 945–961.

11. Huxley A.F. Muscle structure and theories of contraction. / A.F. Huxley // Progress in Biophysics and Biophysical Chemistry. – 1957. – Vol. 7 – P. 255–318.

12. Linari M. Stiffness and fraction of Myosin motors responsible for active force in permeabilized muscle fibers from rabbit psoas / M. Linari M, M. Caremani, C. Piperio, P. Brandt, V. Lombardi // Biophysical Journal. – 2007. – Vol. 92, No. 7. – 2476–2490.

13. Piazzesi G. Temperature dependence of the force-generating process in single fibres from frog skeletal muscle / G. Piazzesi, M. Reconditi, N. Koubassova, V. Decostre, M. Linari, L. Lucii, V. Lombardi // The Journal of Physiology. – 2003. – Vol. 549, No. 1. – P. 93-106.

14. Rall J.A. Influence of temperature on mechanics and energetics of muscle contraction / J.A. Rall, R.C. Woledge // American Journal of Physiology. – 1990. – Vol. 259, No. 2. – P. R197–R203.

15. Tesi C. Modulation by substrate concentration of maximal shortening velocity and isometric force in single myofibrils from frog and rabbit fast skeletal muscle / C. Tesi, F. Colomo, S. Nencini, N. Piroddi, C. Poggesi // The Journal of Physiology. – 1999. – Vol. 516, No. 3. – P. 847–853.

THE MOLECULAR BASIS OF REGULATION OF ACTIN-MYOSIN INTERACTION BY CALPONIN FROM THE MUSSEL *CRENOMYTILUS GRAYANUS* DURING THE ATPase CYCLE

V.V. Sirenko[1], A.V. Dobrzhanskaya[2]

[1] *Institute of Cytology of the Russian Academy of Sciences, Tikhoretsky pr. 4, St. Petersburg, 194064, Russia;*

[2] *Zhirmunsky Institute of Marine Biology, Far Eastern Division, Russian Academy of Sciences, ul. Palchevskogo 17, Vladivostok, 690059, Russia*

The effects of a calponin (CaP) from the thin filaments of the mussel *Crenomytilus grayanus* on actin-myosin interaction at different stages of the ATP hydrolysis cycle have been studied. In order to study the regulation of actin-myosin interaction by mytilus CaP we specifically modified actin monomers by FITC-phalloidin or 1,5-IAEDANS, myosin subfragment-1 (S-1) by 1,5-IAEDANS and CaP by acrylodan. The proteins were incorporated into ghost muscle fibers. Since the fluorescent

probes are rigidly linked with proteins, absorption and emission dipoles of the probes were sensitive to changes in orientation and mobility of actin monomers, S-1 and CaP. The changes in orientation and mobility of the probes were assessed by polarized fluorimetry. The stages of the ATPase cycle were simulated by the absence of nucleotides and presence of MgADP or MgATP.

It was found that ghost fibers containing F-actin modified with FITC-phalloidin or 1,5-IAEDANS had highly anisotropic polarized fluorescence, and it changed significantly in the presence of CaP or S-1. CaP markedly suppressed the changes in orientation and mobility of the probes bound to actin monomers and S-1 in the absence of nucleotide and in the presence of MgADP (i.e. at simulation of strong myosin binding to actin), but does not affect the corresponding changes in the presence of MgATP (i.e. at simulation of weak myosin binding to actin). CaP labeled with acrylodan changed its mobility and position on thin filaments in response to addition of MgADP or MgATP.

In addition, using skeletal muscle actin and S-1, we investigated the effects of the mytilus CaP on the acto• S-1 ATPase activity. It was shown that as CaP concentration increased, the actin-activated ATPase activity decreased.

The data suggest that mytilus calponin by changing its mobility and position on thin filaments – inhibits formation of the so-called strong actin–myosin bond in the skeletal muscle that is necessary for force generation.

SEARCH FACTORS THAT PREPARE THE PROCESS OF ASEXUAL REPRODUCTION IN PLANARIANS SCHMIDTEA MEDITERRANEA

A. Skavulyak, A. Ermakov, A. Kuchin, N. Kreshchenko
ICB RAS, ITEB RAS, Pushchino

Planarian is free-living flatworms that reproduce by arhitomic dividing and knocking the back of the body (tail zooid). Regenerative capacity provided proliferate activity of stem cells (neoblasts). The process of asexual reproduction in planarians poorly studied. Factors preparing and launching office caudal zooid unknown. We have previously found that when the content of single intact planarians together with tail regenerates division in a mini-group is more intense than the content of intact planarians with head regenerates. The aim of this work was to study the cellular mechanisms that prepare the process of asexual reproduction in planarians Schmidtea mediterranea when kept together one intact and three regenerating

(severed tail fragments in front of the pharynx) planarians. In the experience of selected planarian length about 3 mm. To analyze immunohistochemical staining method was used drugs to antibodies using H3 fosfogiston (proliferating cell marker) and confocal scanning microscopy.

It was found that contained intact and regenerating together individuals change in proliferate activity among them occurs differently. Thus, the relative number of regenerate's mitoses per unit body surface area was significantly higher than in intact planarians throughout the observation period (from the 1st to the 10th day). The maximum number of mitoses regenerates was observed on day 2, after which the number of mitotic cells decreased. Dynamics of changes in mitotic activity in intact animals wore oscillatory character (with a period approximately equal to 24 hours), while the number of mitosis was maximal 1 day observation, gradually decreasing to a minimum value to 10 days. Synchronous fluctuations in the number of mitoses were also observed in a separate study, the tail region of the body. No preparation of the separation characteristics zooid example enhanced mitotic activity in the tail region was found neither in the intact nor regenerating fish. Accordingly, at least 10 days of observation, none of the intact (n = 100) and regenerating (n = 300) animals did not share.

Probably limiting (and challenging) division planarian factor may be the size of the bodies of animals, as there are not yet any details. Possible dependence of the initiation of the process of asexual reproduction of the planarian body size may be the subject of further study.

THE WATER STRUCTURE: BIOLOGICAL ACTIVITY
A.N. Smirnov

Moscow State Technical University of Radiotechnics, Electronisc and Automatics, Vernadsky prosp., 78 Moscow, 119454, Russia; E-mail: a.n.smirnov@mail.ru

In previous studies [1] it was shown that liquid water has a very complex structure. Using optical methods, acoustic emission and by thermal analysis of the water supramolecular complexes sized from 1 to 100 μm (micrometer) were found in "continuous" aqueous systems. Basing on the characteristic properties of these supramolecular formations we have named them "emulons". Sizes and spatial organization of emulons depend on the composition of aqueous solutions, temperature and prehistory of the water. Size specters of emulons reveal five fractions with cha-
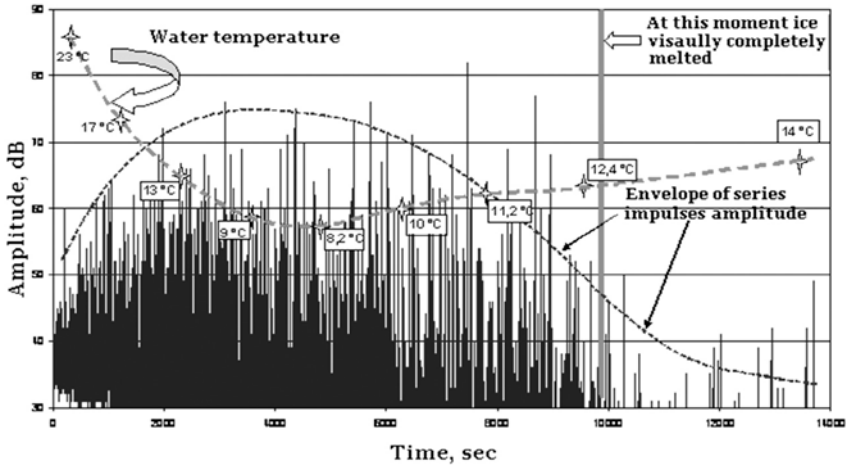
Fig. 1. Alteration of AE signals amplitude and water temperature in a volume during ice melting.

racteristic sizes:1-3 μm,10-12 μm,30-35 μm, 70 μm и100 μm. This means, that acoustic emission method (AE) is a very powerful experimental method for investigate of the water structures, during any kind of chemical reactions and physical-chemical processes. In our experiments we have used modern acoustic emission system ALine32. We have thoroughly investigated AE during ice melting.

An explored fact that AE signals generation process of melt-water figs 1 (AE after the vertical red line) is very interesting. Appearance of AE signals in melt-water can be explained only by structural changes. Experimental results show that melt-water for some time (up to a day) can be in "active" metastable state. The uniqueness of the phase transition ice ↔ water is that despite ice and water (that appeared from it) consist of the same H_2O molecules, but these two phases have for some time equal ionic composition: equal concentration of ions [H^+] and [OH^-], but for the ice this concentration is equilibrium and for the water – not. In melt-water concentration of hydrogen and hydroxyl ions for some time remains nonequilibrium – as it was in the ice. Concentration of [H^+] and [OH^-] ions in ice is $1,4-5,0 \cdot 10-10$ mol/l and in water at $0°C$ it is $0,35 \cdot 10-7$ (three orders higher) [2] We have paid special attention to the crucial role of hydrogen [H^+] and hydroxyl [OH^-] ions in formation of supramolecular complexes – emulons – in water. The reaction of water dissociation: $H_2O \rightarrow H^+ + OH^-$ needs sufficient energy consumption and goes on very slowly. The rate constant of this reaction is only $2,5 \cdot 10^{-5}$ sec^{-1} at $20°C$. That is why relaxation period of water into a normal state theoretically should be around ~10-

17 hours that was proven on practice. We have found in melt-water with the use of optical method only presence emulons fractions with small sizes around 1-3μm. This fact explains the phenomenon of speeding up of all biological processes in living organisms by melt-water.
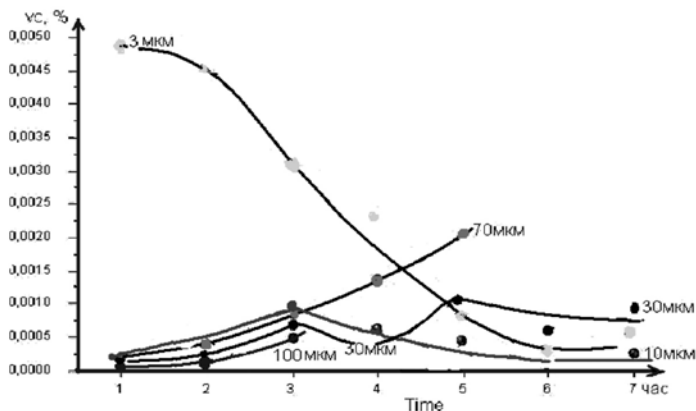
Fig. 2. Contents of the emulons into melt-water.

Complex organization of water structure as a unite ensemble, that includes - emulons, result in the fact that properties of aqueous system are not simply the sum of properties of its different structural elements, but are explained by cooperation phenomenon. The polydisperse structure of the emulons formed of the water, ensuring polymodalnost reply by the external affects, appearance hysteresis, considerable times relaxation.
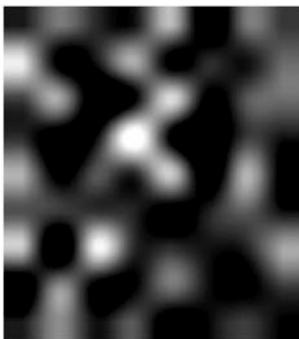
Fig. 3. Spatial distribution of the emulons into the water. Top side of the image is 400 µm.

These images allow to conclude that formation of water structure is not connected with any artifacts (or with dust, or with bubbles, or with laser beam).
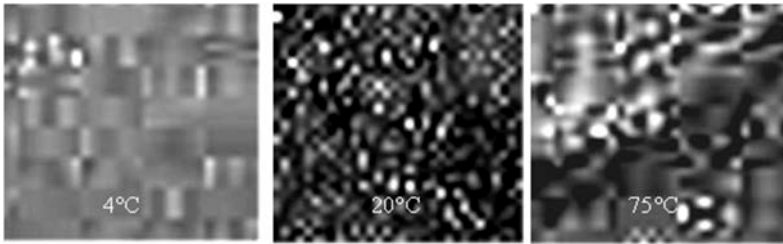
Fig. 4. Influence of temperature on the structure of water.

There are no structures observed in nonpolar liquids.
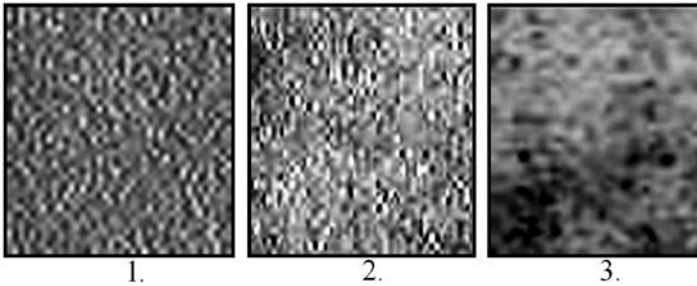
Fig. 5. Structure of different aqueous solutions: 1 – distilled water; 2 – natural mineral water; 3 – alcohol solution.

As it can be seen from fig. 5 spatial organization and distribution of the emulons complexes, their appearance in "continuous" water depends on chemical composition of aqueous solution.
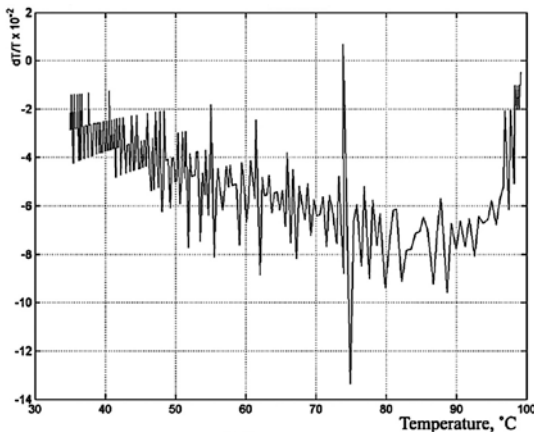
Fig. 6. Relative alteration of the temperature during water heating.

In the sake of proving the real existence of structural formations in water and their significant stability that were detected by the use of optical methods we have used a classical method – thermal differential analyse. Results of one of the experiments are presented on fig. 6. Destroying of emulons can leads to grow up of solitons. This phenomenon can be describe with model "phi-4" with asymmetrical "dubble-pit" potential V(u) [3].
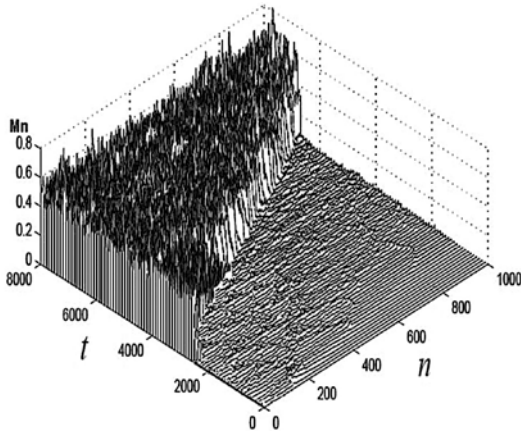
Fig. 7. Dependence on time t state Mn chains n consist of N = 1000 emulons of the temperature is increasing.

This model describes sequence of emulons, who can stay in several stable forms. This transposition is contributed by dispersion of topological soliton due to local changings from one condition to another. The results demonstration on the fig. 7.

Summary
The using optical method and acoustic emission method for the water structure analysis are suggested. The sizes and spatial organization of emulons depend on the composition of aqueous solutions, temperature and prehistory of the water. The polydispersion structure of the water, ensuring polymodality reply by the external affects, appearance hysteresis considerable time relaxation and are explained by cooperation phenomenon.

References
1. Smirnov A.N. Water structure: new experimental date. // Science and Technologies for the industry, 2010, № 4, pp. 41-45.
2. Physical units. Reference book. Energoatomizdat publishing. Moscow. – 1991. – p. 1231.
3. Savin A. V., Tsironis G.P. and Zolotaryuk A.V . Reversal effects in stochastic kink dynamics. //Phys. Rev. E, 56(3):2457-2466, 1997.

MORPHOLOGICAL STRUCTURE OF AORTA AND PULMONARY ARTERY WALL OF ISIAH RATS

L.T. Smoluk[1], E.A. Mukhlynina[1], A.T. Smoluk[1], V.S. Markhasin[1], A.L. Markel[2], Y.L. Protsenko[1]

[1]*Institute of Immunology and Physiology Ural Branch of the RAS, Ekaterinburg, Russia;*
[2]*Institute of Cytology and Genetics Siberian Branch of the RAS, Novosibirsk, Russia*

Inbred rats with genetic stress-induced arterial hypertension are bred at Institute of cytology and genetics SB of the RAS (ISIAH rats) [8]. Today at Institute of immunology and physiology UB of the RAS the integrated study of morphological and biomechanical performances of ISIAH rat myocardium is carried out. Together with changes in myocardial tissue it is significant to take into account the changes of the structure and mechanical properties of aorta and pulmonary artery to understand the process of hypertension forming of ISIAH rats.

It is well known that arteries behave as viscoelastic materials in the dynamic, pulsatile blood flow environment; a characteristic of viscoelastic materials is frequency-dependent behavior [3]. Arterial elasticity describes how much energy is stored (maintained) in each oscillatory deformation, whereas arterial viscosity reflects how much energy is dissipated. Together, viscoelastic properties enable arteries to serve as both conduits and buffers and furthers for the pulsatile blood flow generated by the contracting heart. The structure of connective tissue matrix (CTM) play a crucial role in arterial wall mechanical properties changing especially under hypertension. It often occurs in pathological remodeling such as due to hypertension, alters arterial viscoelasticity. For example proximal pulmonary artery (PA) stiffening is universally observed in pulmonary hypertension is strongly associated with changes in CTM besides the changes of endothelium layer of the vessel [5].

The aorta is the largest artery in the mammalian body. The cardiovascular system is affected by the function of the aorta in many ways. When the stiffness of the aorta is increased, an increased pulse-wave velocity is induced. It causes premature return of reflected pulse waves in late phase of systole. It also increases central pulse load and the myocardial demand of oxygen [7]. The aortic wall is divided into the adventitia layer, the media layer and the intima layer. It contains collagen fibrils, some number smooth muscle cells, and elastic fibers as the primary load-bearing components [9]. The elastin forms elastic lamellae, which is situ-

ated between the smooth muscle cells. Collagen surrounds the smooth muscle cells and the elastic lamellae. Both collagen and elastic fibers are crucial for the determination of the tensile strength and the stiffness of the aorta [4]. Collagen is a key element of the CTM of the aorta and its removal is capable of reducing the local stiffness by up to 50 times, but the remaining aorta connective tissue is still capable to form a coherent network [2]. The mechanical properties of the aorta are depended not only on the amounts of the aortic wall main constituents but also on the spatial organization and the mechanical interactions among these components.

The two main types of collagen found in the aorta and the PA are types I and III. They account for 80-90% of the total collagen present in the aorta [9]. The amount of collagen and the collagen types ratios in the aortic wall change with ageing, sex and pathology. For example, hypertension is associated with structural alterations of main arteries, and arterial wall hypertrophy is a major feature of these changes. Hypertension appears to be one type of insult that enhances vascular connective tissue formation and induced an increased collagen synthesis and an increased total amount of collagen [10]. The study of passive mechanical properties of the aortas showed that in spontaneously hypertensive rats (SHR) the aortas were stiffer compared with aortas of normotensive rats [1]. Thus collagen probably is one of the most important components of the aortic and PA wall. Therefore, the issue of current work is to compare the morphological changes in the wall of the aorta and PA in ISIAH rats and to evaluate the contribution of the collagen tissue matrix into the structure of these vessels.

Investigations were carried out on transverse histological sections of the aorta and PA of control group rats and ISIAH rats with age of 7 months. Sections were stained with pikrosirius red (Direct Red, Sigma-Aldrich) in accordance with standard method [6]. Images were obtained using confocal laser scanning microscope LSM-710, Carl Zeiss with dry objective 20x/0.8; the image resolution was 1024x1024 dots; size of image was 606x606 mkm. Specific λ-mode was used to obtain contrast images by dedicated software ZEN2009 (Carl Zeiss) followed by a linear unmixing of the emission channels. Contrast images of the main structural components (collagen fibers and elastin fibers) of the aortic wall and the PA of ISIAH rats were obtained for the first time (figure). Further processing and calculation of structural morphometric criteria was carried out using specialized software Morphology 5.2 (VideoTesT). The following criteria for assessing preparation structure (relative area of connective tissue collagen matrix, the relative area occupied by elastin fibers as a fraction of the area of the entire histological section preparation) were obtained.
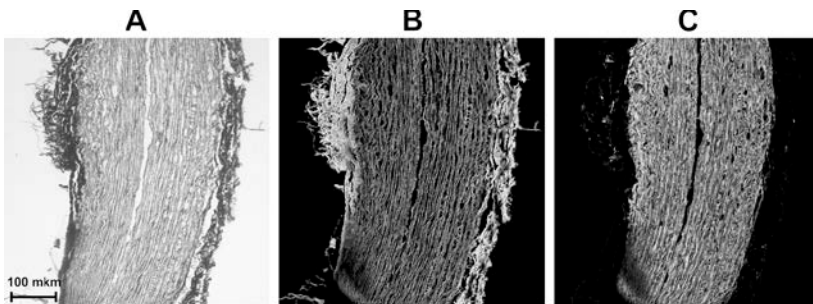
Micrograph of histological cross-section of control rat aorta stained with Sirius Red. (A) the image at transmitted light; (B) confocal image of collagen connective tissue matrix; (C) confocal image of elastin fibers.

For the present example the following data were obtained: in the aortic wall of hypertensive rats the fraction of elastin fibers (52.0%) increased significantly in comparison with normotensive animals (41.5%), with the fraction of collagen fibers decreased (40.4% ISIAH group, 47.4% - control group). In the wall of the PA similar data were obtained: the fraction of elastin fibers in hypertensive rats (34.5%) and normotensive animal (17.4%); the fraction of collagen fibers decreased (49.8% in ISIAH group, 45.7% in control group). Such changes in morphological parameters should be accompanied by significant changes in the viscoelastic properties that can significantly contribute to the pathogenesis of hypertension in ISIAH rats. To verify this hypothesis experiments on comparison of the viscoelastic characteristics of the vascular wall of control group rats and hypertensive ISIAH rats were carried out.

References

1. Bashey R.I., Cox R., McCann J., Jimenez S.A. Changes in collagen bio-synthesis, types, and mechanics of aorta in hypertensive rats. // J Lab Clin Med. 1989. V. 113(5). P. 604-11.
2. Beenakker J.W., Ashcroft B.A., Lindeman J.H., Oosterkamp T.H. Mechanical properties of the extracellular matrix of the aorta studied by enzymatic treatments. // Biophys J. 2012. V. 102(8). P. 1731-7.
3. Bergel D.H. The dynamic elastic properties of the arterial wall. // J Physiol. 1961. V. 156(3). P. 458-69.
4. Bruel A., Oxlund H. Growth hormone influences the content and composition of collagen in the aorta from old rats. // Mech Ageing Dev. 2002. V. 123(6). P. 627-35.

5. Hunter K.S., Albietz J.A., Lee P.F., Lanning C.J., Lammers S.R., Hofmeister S.H., Kao P.H., Qi H.J., Stenmark K.R., Shandas R. In vivo measurement of proximal pulmonary artery elastic modulus in the neonatal calf model of pulmonary hypertension: development and ex vivo validation. // J Appl Physiol (1985). 2010. V. 108(4). P. 968-75.

6. Junqueira L.C., Bignolas G., Brentani R.R. Picrosirius staining plus polarization microscopy, a specific method for collagen detection in tissue sections. // Histochem J. 1979. V. 11(4). P. 447-55.

7. Laurent S., Cockcroft J., Van Bortel L., Boutouyrie P., Giannattasio C., Hayoz D., Pannier B., Vlachopoulos C., Wilkinson I., Struijker-Boudier H. Expert consensus document on arterial stiffness: methodological issues and clinical applications. // Eur Heart J. 2006. V. 27(21). P. 2588-605.

8. Markel A.L., Redina O.E., Gilinsky M.A., Dymshits G.M., Kalashnikova E.V., Khvorostova Y.V., Fedoseeva L.A., Jacobson G.S. Neuroendocrine profiling in inherited stress-induced arterial hypertension rat strain with stress-sensitive arterial hypertension. // J Endocrinol. 2007. V. 195(3). P. 439-50.

9. Silver F.H., Horvath I., Foran D.J. Viscoelasticity of the vessel wall: the role of collagen and elastic fibers. // Crit Rev Biomed Eng. 2001. V. 29(3). P. 279-301.

10. Wolinsky H. Long-term effects of hypertension on the rat aortic wall and their relation to concurrent aging changes. Morphological and chemical studies. // Circ Res. 1972. V. 30(3). P. 301-9.

QUANTITY ANALYSIS OF CONNECTIVE TISSUE MATRIX STRUCTURE DURING MYOCARDIAL REMODELING

L.T. Smoluk, A.T. Smoluk, Y.L. Protsenko

Institute of Immunology and Physiology of the Ural Branch of the RAS, Pervomayskaya str., 106, Ekaterinburg, 620049, Russia

Structural organization of biological tissue (and, in particular, myocardial tissue) is closely connected with the function performed by it. Consideration of structural changes in the myocardium is very important to assess the functional changes in the heart. For example, myocardial remodeling in pressure overload conditions can eventually lead to disturbance of the pumping function of the heart [2, 5]. In this case not only cardiomyocites, but also fibroblasts and connective tissue matrix are influenced by the essential transformation. It is also important to take into account the age-related dynamics of mechanical properties and heart tissue structure, since properties of myocites and connective tissue are known to vary significantly depending on the age [1, 8]. The comprehensive nature of the changes of myocyte sizes, their intracellular properties and structural organization of connective tissue matrix make it difficult to analyze the

impact of structural and functional changes in myocardial contractility depending on the age and the existing data on the subject are rather contradictory. In this study a new approach is proposed to quantify the contribution of connective tissue matrix into the myocardial structure.

The object of the study was the histological sections of the papillary muscles of rats. Sections (about 5 mkm) were stained with pikrosirius red (Direct Red, Sigma-Aldrich) according to the standard method [4]. Images were obtained using confocal laser scanning microscope LSM-710, Carl Zeiss, the immersion lens 40x / 1.3 Oil; image resolution was 1024×1024 pixels; image size was 212×212 mkm. Emission spectra of the connective tissue and the cardiomyocites stained with Picrosirius Red had a sufficiently wide range of overlap. Therefore, specific λ-mode was used to obtain informative images by dedicated software ZEN2009 (Carl Zeiss) followed by a linear unmixing of the emission channels. As a result contrast images of the main structural components of the papillary muscle (collagen connective tissue matrix and cardiomyocytes) were obtained. Further processing supposes the use of specialized software to calculate structural morphometric criteria. To date there are plenty of software solutions for rendering of histological sections. However they focus on the morphometric parameter calculation of the structures representing discrete particles, such as cardiomyocytes. In this case there is a lack of the function allowing for calculation of the parameters of netlike structures such as connective tissue matrix. It is possible to estimate the total area of the netlike structure, but it is not possible to estimate local geometrical parameters of such structure automatically. We have developed numerical algorithm that allows to evaluate the parameter such as the average thickness of the fiber in netlike structure (in this case - the fibers of connective tissue matrix of the myocardium). In our opinion, this parameter is needed to be taken into account when assessing structural changes in the myocardium and comparing them with the changes of mechanical properties, because connective tissue matrix in the myocardium has structural stiffness.

The developed algorithm involves the following steps. After obtaining the contrast image of histological section of the papillary muscle connective tissue mask and cardiomyocyte mask is divided from one another (fig. 1). Defying the both limiting maximum and minimum diameter of cells and cell rotundity fused and damaged cells are excluded from the analysis of cardiomyocyte mask (fig. 1B).

Then relative centers of each cell (the point of intersection of maximum and minimum diameters) should be defined (fig. 2A). After that, using connective tissue mask limiting thickness of connective tissue fi-
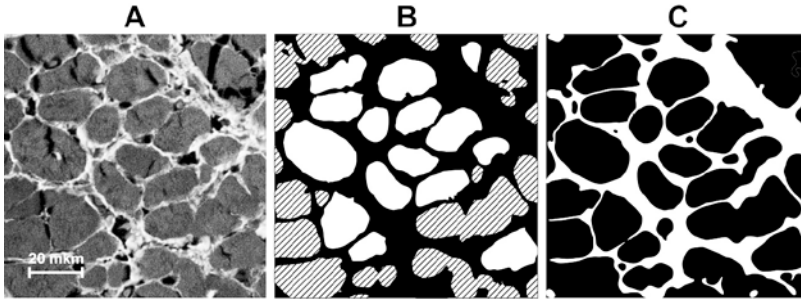
Fig. 1. Micrograph of histological section of rat papillary muscle stained with Sirius Red. (A) The original image, where light fibers represent a net of connective tissue, dark gray - cardiomyocytes; (B) cardiomyocyte mask; particles excluded from the analysis are shaded, (C) connective tissue mask.
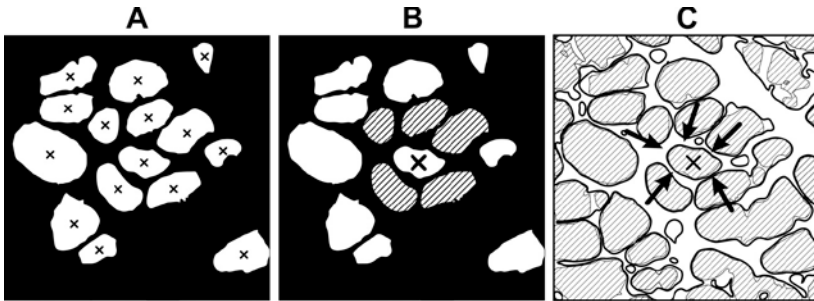
Fig. 2. The steps of calculating the average thickness of the fibers of the connective tissue matrix. (A) Determination of relative centers of cells (marked by crosses); (B) Example of determination of neighboring cells (shaded) for the cells marked with a cross; (C) The extracellular region, in which the thickness of the connective tissue fibers is calculated for cells marked with a cross, is marked by arrows.

bers is defined in order to exclude from analysis thick perymisial fibers and vessel connective tissue matrix trapped in the area of section. On the next step using the cardiomyocyte mask neighboring cells for each myocyte are determined in accordance with the following criterion (fig. 2B). The distance between the centers of neighboring cells shall not exceed the sum of the radii of the corresponding cells and the maximum thickness of connective tissue fibers along the line connecting the relative centers of these cells. Then, on the lines connecting the centers of neighboring cells extracellular regions with connective tissue fibers are marked out (Fig. 2C). On

the final step the thickness of connective tissue fibers along the lines connecting the relative centers of cells is defined using the connective tissue mask. For the present example the following morphometric parameters have been obtained: the fraction of myocites (69%), the fraction of connective tissue matrix (11%), the average diameter of myocites (15.3±3.6), the average thickness of the connective tissue fibers (1.65±0.34) (M±σ, P<0.05). The findings coincide with the size of rat cardiomyocytes [**6**] and the size of the myocardial endomysial fibers of rats [**3**].

The proposed approach allows to compare data on the structural changes during various pathologies or with changes of the mechanical characteristics in the ontogenesis of heart tissue, for example, using a previously developed technique of dividing the impacts from the main structural components of myocardium [**7**]. It should also be noted that the proposed approach can be generalized and applied successfully for the analysis of the morphology of other biological netlike tissues.

References

1. Conrad C.H., Brooks W.W., Hayes J.A., Sen S., Robinson K.G., Bing O.H. Myocardial fibrosis and stiffness with hypertrophy and heart failure in the spontaneously hypertensive rat. // Circulation. 1995. V. 91(1). P. 161-70.
2. Cooper G.t. Cytoskeletal networks and the regulation of cardiac contractility: microtubules, hypertrophy, and cardiac dysfunction. // Am J Physiol Heart Circ Physiol. 2006. V. 291(3). P. H1003-14.
3. Fratzl P. Collagen Structure and Mechanics. 2008. New York. Springer. 506 C.
4. Junqueira L.C., Bignolas G., Brentani R.R. Picrosirius staining plus polarization microscopy, a specific method for collagen detection in tissue sections. // Histochem J. 1979. V. 11(4). P. 447-55.
5. Opie L.H., Commerford P.J., Gersh B.J., Pfeffer M.A. Controversies in ventricular remodelling. // Lancet. 2006. V. 367(9507). P. 356-67.
6. Satoh H., Delbridge L.M., Blatter L.A., Bers D.M. Surface:volume relationship in cardiac myocytes studied with confocal microscopy and membrane capacitance measurements: species-dependence and developmental effects. // Biophys J. 1996. V. 70(3). P. 1494-504.
7. Smoluk L., Protsenko Y. Viscoelastic properties of the papillary muscle: experimental and theoretical study. // Acta Bioeng Biomech. 2012. V. 14(4). P. 37-44.

8. Weis S.M., Emery J.L., Becker K.D., McBride D.J., Jr., Omens J.H., McCulloch A.D. Myocardial mechanics and collagen structure in the osteogenesis imperfecta murine (oim). // Circ Res. 2000. V. 87(8). P. 663-9.

DYNAMICS OF FIBROBLAST MICROCONTACTS WITH A SUBSTRATE

V.V. Smolyaninov[1], A.E. Platonov[2]

[1] *Institute of Theoretical and Experimental Biophysics, Institutskaya str. 3, Pushchino, Moscow region, 142290, Russia;*
[2] *Central Research Institute of Epidemiology, Novogireevskaya str. 3A, Moscow, 111123, Russia*

The adhesion of non-muscle cells plays an essential role in embryogenesis; the adhesive contacts with a substrate are necessary for the movement of tissue cells during wound healing and chemotactic motility of leukocytes. Adhesive characteristics of fibroblasts have attracted a special attention when it had been hypothesized that many tumor cells and transformed cell lines had reduced adhesion.

Dynamics of initial attachment of fibroblasts (cell line L) to the glass has been studied by several methods. Using the interference reflection microscopy, we have found that the primary cell contact with a substrate was formed from a set of discrete point contacts. Each point contact represented probably a contact of small cell surface protrusion. The growing number of point contacts increased the dimensions of contact zone; subsequently the confluence of adjacent point contacts led to the formation of the central zone of large uniform contact. Temporal and geometric characteristics of this process have been described.

The darkest areas of interference reflection microscopy images corresponded to the most firm contact as this was shown by cell detachment from a substrate by the sucker microcapillary with a calibrated force. The specific strength of the cell contact with the glass was 2.5 ± 0.5 nN/μm^2 when cells were incubated in Eagle's culture medium, while the strength of one IC is 4.2 ± 1.7 nN. When 10% serum was added to Eagle's medium, the strength was decreased by 25%, whereas the addition of 1% human serum albumin decreased the strength by 50%.

Determination of adhesion strength is only possible at the early stages of fibroblasts attachment. When attempting to detach cells having a large contact, they were deformed into a long bundle, then bursting at some distance from its place of attachment to the substrate. Bundle tensile strength did not depend on the culture medium composition and was equal to 120 ± 40 nN in our experiments.

When interference reflection microscopy observation and a "standard impulse force" generated by a special device was applied to the attaching cells, it was demonstrated that the initial attachment of cells might be slowed down if the serum was added to Eagle's medium whereas the initial attachment might be slowed down and reduced if human albumin was added. These effects were enhanced with increasing concentration of serum or albumin. When serum and albumin were added together, the attachment was worse than in medium with serum alone and better than in a medium with albumin only.

If serum or albumin were adsorbed on a glass substrate, their effects on initial cellular attachment were qualitatively similar as when added to the medium. Importantly, the effects were restricted locally to an area of adsorption.

The formal mathematical model of initial cellular attachment has been elaborated, in which the attachment was considered as a random multi-step process where a step was the formation of one point contact. The time and the probability of formation or destruction of one point contact have been estimated using the model. These parameters varied also if serum or human albumin were added to the culture medium.

ROLE OF HEAT SHOCK PROTEIN 90 (HSP90) IN MIGRATION OF HUMAN TUMOR CELLS *in vitro*

A.V. Snigireva, V.V. Vrublevskaya, O.S. Morenkov

Institute of Cell Biophysics, Russian Academy of Sciences, Institutskaya str., 3, Pushchino, Moscow Region, 142290, Russia

Heat shock protein 90 (Hsp90) is an intracellular chaperone that plays an important role in cell functioning under normal and stress conditions. Recently, Hsp90 has also been found on the cell plasma membrane and in the extracellular space. Extracellular Hsp90 performs an activating function in processes associated with cell motility, invasion and metastasis of tumor cells. The roles of isoforms Hsp90α and Hsp90β in cell migration processes have not been fully understood. It has not been determined which segments of the Hsp90 molecule are responsible for binding to receptors on the cell plasma membrane and Hsp90-dependent stimulation of migration. It has recently been shown that fragment 236-350 aa of the Hsp90 molecule (fragment F-5) has a stimulating effect on cell migration comparable with the effect of full-length Hsp90 [Li W. et al., Biochim. et Biophys. Acta; 2012; 1823, 730–741]. Despite the data available, a more detailed research is required into the roles of particular Hsp90 domains and fragments in processes related to cell motility and

invasion. Given the above, the aim of this work was to investigate the effect of the total Hsp90 purified from murine brain, consisting of Hsp90α and Hsp90β, on migration of human glioblastoma cells (A-172), as well as to determine the roles of particular Hsp90 isoforms in cell migration processes *in vitro*.

The studies were done using two models, Hsp90-induced cell migration and non-induced Hsp90-dependent migration. In the former case, migration of tumor cells was activated by native Hsp90 followed by inhibition of Hsp90-induced migration of cells by Hsp90-specific polyclonal antibodies. In the latter case, we assessed the effect of Hsp90-specific polyclonal antibodies on non-induced cell migration.

The effects of native Hsp90 and Hsp90-specific polyclonal antibodies on migration were investigated using two methods: determination of the rate of wound healing on the cell monolayer (wound healing assay) and determination of cell migration using inserts with polyethylene terephthalate (PET) membrane. Native Hsp90 was purified from murine brain using the thiophilic chromatography-based method developed earlier at our laboratory. The Hsp90 preparation was of 95–97% purity, it did not affect cell proliferation and possessed no cytotoxicity. Heat shock protein 70 (Hsp70), isolated from murine brain, and BSA were used as controls. Peptides corresponding to N-terminal fragments of Hsp90α and Hsp90β, having no homology between themselves, and a peptide from the region of fragment F-5, the same for both Hsp90 isoforms, were synthesized. The peptides were selected using special programs for prediction of highest-immunogenicity epitopes. Further on, we immunized rabbits with full-length native Hsp90 and conjugates of proteins with the peptides. To purify antibodies to full-length Hsp90 and peptide-specific antibodies, specific sorbents based on agarose gel coupled with native Hsp90 and peptides were prepared. The antibodies were purified from hyperimmune rabbit serum by the method of immunoaffinity chromatography. A high activity and specificity of the antibodies were shown using immunoenzyme assay, immunoblotting and immunofluorescence assay.

In the Hsp90-induced migration model, Hsp90 at concentrations of 0.01–0.1 mg/ml reliably stimulated migration of human glioblastoma cells *in vitro* by 240–280% in the wound healing assay and by 35–50% using PET membrane inserts. Control proteins, Hsp70 and BSA, had no effect on cell migration at concentrations of 0.1 mg/ml. To study the role of particular Hsp90 isoforms in Hsp90-induced migration, Hsp90 (concentration, 0.01 mg/ml) and Hsp90-specific polyclonal antibodies were simultaneously added to glioblastoma cells. Antibodies to fragment F-5 of the Hsp90 molecule and to full-length Hsp90 eliminated the activating effect of Hsp90

virtually completely (86.7 ± 5% using both methods). Antibodies to Hsp90α and Hsp90β inhibited the stimulation of cell migration by 77.5 ± 5% and 82.6 ± 5%, respectively, in the method using PET membrane inserts. In the wound healing assay, the effect of decreasing the activation of cell migration under the action of antibodies was less pronounced, but the tendency of inhibition was preserved. Addition of antibodies purified from nonimmune rabbit serum did not decrease the Hsp90-induced activation of cell migration. These data indicated the involvement of both Hsp90 isoforms in the activation of tumor cell migration process.

In the model of non-induced Hsp90-dependent migration, antibodies to Hsp90α and to Hsp90β inhibited cell migration by 14.0 ± 5.5% (wound healing assay) and by 18.0 ± 6% (PET membrane inserts). Antibodies to fragment F-5 were found to have the greatest inhibitory effects on non-induced migration: using wound healing assay, it was inhibited by 21.0 ± 5%; using PET membrane inserts, by 42.2 ± 5%. The antibodies purified from non-immune rabbit serum did not affect non-induced Hsp90-dependent migration *in vitro*.

These results implicate the involvement of both Hsp90 isoforms in the stimulation of tumor cell migration. The polyclonal antibodies to fragment F-5 of the Hsp90 molecule severely inhibited migration of human glioblastoma tumor cells A-172 both in the model of Hsp90-induced cell migration and in the model of non-induced Hsp90-dependent migration *in vitro*. Cell migration is an essential element in the process of metastasis of tumor cells, which includes migration and invasion of tumor cells through tissue barriers inside the surrounding tissues. In this context, the obtained results suggest that extracellular Hsp90, especially F-5 fragment of the protein, can be considered as a promising molecular target whose inhibition can suppress metastasis of tumor cells.

EFFECTS OF PROBIOTIC PRODUCT
ON MYOCARDIAL CONTRACTILITY
AND ON HEART MITOCHONDRIA SWELLING

C.V. Sobol, S.M. Korotkov, V.P. Nesterov

SechenovInstitute of Evolutionary Physiology and Biochemistry, prosp. Thoreza, 44, St.-Petersburg, 194223, Russia

Cardiac glycosides and catecholamines have long been used for the treatment of cardiac contractile dysfunction in patients with congestive heart failure. However, since the cardiac glycosides have very narrow safety margins and both types of agent can induce arrhythmias and injury to myocardial due to calcium overload, extensive efforts have been made over

the past two decades to develop cardiotonic agents that act via novel mechanisms as replacements for cardiac glycosides and catecholamines.

We examined the influence of new probiotic product (PP) on the myocardial contractile force and on heart mitochondria swelling and mitochondrial potential. We used spontaneous contraction of circular muscle isolated from heart of male frog Rana Redibunda. Mitochondria were isolated from rat heart and swelling was determined in NH_4NO_3, KNO_3 and KAc. PP had dual influence on contractile force. In the presence of PP the contractile force decreased by $22\pm3\%$. However, after wash-out of PP with PP free solution, the contractile force increased considerably ($140\pm15\%$ of basal force, $n=4$). The contractile force remained high for approximately 2 h after wash-out. PP reduced mitochondrial swelling in all milieus both in energized and non-energized mitochondria, thereby reducing permeability of mitochondrial membrane to K^+ and H^+. PP did not change mitochondrial potential. However, PP stimulated mitochondria respiration and exerted a mild uncoupling effect on electronic transport and oxidative phosphorylation in mitochondria (Sobol et al., Biochemistry (Moscow) Supplement Series A: Membrane and Cell Biology, 2013, Vol. 7, No. 4, pp. 294–301).

We suppose that PP may stabilize mitochondria energetics and stimulate contractile properties of heart muscle during hypoxia/ischemia.

DEVELOPMENTAL ALTERATIONS
OF ARTERIAL SMOOTH MUSCLE AND ENDOTHELIUM
IN DIFFERENT VASCULAR BEDS

S.I. Sofronova, A.A. Borzykh, D.K. Gaynullina, O.S. Tarasova
Faculty of Biology, Moscow State University,
Leninskie Gory, 1-12, Moscow, 119234

During maturation the vascular system undergoes structural and functional alterations. We showed recently that saphenous arteries of young rats demonstrate a tonic nitric oxide (NO) production which contribute to lower contractile responses compared to adult rats arteries (Gaynullina et al. Cardiovasc Res 2013, 99:612-21). Along with that, serum content of NO metabolites in young rats was two-fold higher compared to adult rats, which suggest systemic character of the alterations. Here we tested the hypothesis that vasorelaxing NO influence takes place not only in cutaneous circulation but in the majority of vascular beds young rats.

The segments of saphenous, intrarenal, small mesenteric and sural arteries (supplying skin, kidney, small intestine and hindlimb skeletal

muscle, respectively) were isolated from young (14-16 day old) and adult (10-12 wk old) rats and mounted in isometric myograph. Anticontractile effect of NO was evaluated by increases of the response to methoxamine (MX, α_1-adrenoceptor agonist) in the presence of NOS inhibitor L-NNA vs. its inactive analogue D-NNA. Arterial smooth muscle NO-sensitivity was measured in young and adult rats by analyzing the response to NO donor DEA-NO. In addition, we estimated eNOS and Arginase-2 mRNA expression levels in arterial preparations from young and adult rats by quantative PCR. To evaluate the level of arterial pressure (AP) we inserted catheters in the carotid arteries of young and adult rats and recorded AP in conscious state.

In arteries of adult animals the effect of NOS inhibition was minimal in mesenteric arteries and absent in renal, suralis and saphenous arteries. NOS inhibition in renal arteries of young rats did not change their contractile responses to MX. However, in all other arteries of young animals (mesenteric, suralis and saphenous) NOS inhibition caused the significant increase in the sensitivity to MX. Smooth muscle sensitivity to NO donor DEA-NO was smaller in mesenteric and sural arteries of young rats compared to adults and did not differ in saphenous arteries. Thus, in mesenteric, suralis and saphenous arteries of young animals augmented effects of NOS inhibitor on agonist-induced contraction (in comparison to adults) are not associated with the elevated smooth muscle sensitivity to NO. These data show that the NO-dependent regulation of agonist-induced contraction is more pronounced in the majority of the tested arteries of young animals.

To investigate the mechanisms, regulating the dissimilar activity of NO-dependent pathway in endothelium of young and adult animals, we compared expression levels of eNOS mRNA and Arginase 2 mRNA in different arteries of young and adults rats. The eNOS mRNA expression levels were not different in young and adult animals in arteries of all types. However, the expression level of eNOS mRNA was the highest in mesenteric arteries and the lowest in renal arteries, indicating that the NO-dependent regulation of arterial tone is more pronounced in mesenteric arteries and less pronounced in renal arteries. The expression level of Arginase 2 mRNA, which negatively regulates NO pathway by affecting the substrate bioavailability, was decreased in arteries of all types in young animals. Interestingly, the level of Arginase 2 was the highest in renal arteries, pointing to the suppression of NO pathway in kidneys in animals of both ages.

Taking together, these data show that (i) the NO-dependent regulation of agonist-induced contraction decreases during early postnatal development in mesenteric, cutaneous and skeletal muscle vascular beds; (ii) the role of NO in the regulation of vascular tone is more pronounced in mesenteric vascular bed and is minimal in renal arteries; (iii) the developmental regulation of NO production occurs not at the level of eNOS expression, but probably at the level of its activity.

The increased activity of NO-pathway in arteries of young animals may maintain the low blood pressure level during first weeks of postnatal development. Indeed, the mean AP levels were more than twice lower in young rats (50.9 ± 9.0 mmHg) as compared to adults (114.9 ± 3.4 mmHg).

In conclusion, tonic NO production by the endothelium in young rats weakens contractile responses of arteries supplying skin, small intestine and skeletal muscles. Since these organs receive a high proportion of the cardiac output, influence of NO may contribute to lowering AP level in immature circulatory system. With maturation of the circulatory system dilator influence of NO disappears which permits gradual AP rise. Insufficiency of endothelial function early after birth may be the reason of cardiovascular pathologies in adulthood.

THE INFLUENCE OF THE ACUTE HYPOXIA ON THE MOTILITY OF RATS IN THE OPEN FIELD TEST UNDER THE CONDITIONS OF AN ALTERED PHOTOPERIOD

I.Yu. Sopova, I.L. Nemish

Bukovinian State Medical University,
Teatralnaya pl. 2, Chernovtsy, 58002, Ukraine

The influence of the acute hypoxia on the motility of rats under the conditions of an altered photoperiod in the open field test was studied. The study was carried out on the 64 juvenile mail rats. In the open field within 3 minutes the next parameters were registered: horizontal activity, vertical locomotor reactions, mink reflex. After the preliminary passage of the open field test the animals were kept during one week under the conditions of usual (natural conditions of illumination) and altered (constant darkness, constant light) photoperiod. Then the acute hypoxia was simulated by means of imitation of the lifting of rats at a height of 12000 meters. Then the behavior of rats was studied again in the open field test.

Preliminary research has been shown that all 3 groups of animals authentically did not differ in parameters of the behavior reactions: horizontal activity was 20-30 squares, vertical locomotor reactions were 5-10 racks, exploratory activity - 5-10 looks into the minks.

After the experiment the animals from groups with different light conditions have shown the differences in the behavior. Exposure to acute hypoxia of rats that were under the conditions of an ordinary photoperiod was accompanied with the decrease activity in the open field: horizontal activity decreased by 4.8 times; vertical – by 9.6 times, mink reflex – by 5.7 times. In case of combined action of the constant darkness and hypoxia the similar changes in the motility were observed: horizontal activity decreased by 5.6 times; vertical – by 8.0 times, mink reflex – by 5.1 times. In the same time the animals that were kept under the conditions of constant light and hypoxia have shown the horizontal activity similar to intact rats, the vertical activity was lower than the control indices by 2.8 times. Thus, these results suggest that altered photoperiod modulates the influence of the hypoxia on the motility of rats and the character of the photophase change is important. Thus, staying of the animals in the constant darkness after the modeling of acute hypoxia leads to the depression of the locomotive and exploratory components of the behavior. In the same time the animals that were kept under the conditions of constant light show the change in the correlation between the components of motility after the action of hypoxia.

SIMULTANEOUS AXONAL FLOWS
OF OPPOSITE DIRECTION IN NEURITES

O.S. Sotnikov, N.Yu. Vasyagina, S.S. Sergeeva,
L.A. Podolskya, M.V. Smirnova

Pavlov Institute of Physiology, Russian Academy of Sciences,
nab. Makarova, 6, St. Petersburg, 199034, Russia

Every year, hundreds of molecular-biological papers about participation in neural motor function of such proteins as actin, myosin, tubulin, etc. (Fath et al., 2010; Lees et al., 2011; Baas and Mozgova, 2012). But several principal questions concerning mobility of the main, part of neurite at the cellular, microscopy level have remained unanswered so far. Specifically, insufficiently explainable is the mechanism of simultaneous "axonal flow" in the same fiber in opposite directions (Davison, 1970; Skibo, 1980; Salinas et al., 2009; Kramer et al., 2012). Hypotheses proposed on this point remain unproved or broken down (Allen et al., 1985).

The supramolecular, cytological organization and supravital kinetics of the neuronal neurite itself as a motile organ are not taken into account. It seems as if microfilaments, microtubules, "axonal flows" are independently flowing somewhere inside the axon like in a blood vessel, while the wise P. Weiss thought that movement of a "column" of axon together with a liquid layer of axoplasm – this is what axoplasmic flow was. The idea and our research lies in this.

The investigations were carried out on 194 living isolated neurons of 52 molluscs *Limnaea stagnalis* with preserved neurite fragments. The cells were isolated from supraesophageal ganglia by their incubation in 0.4% solution of the pronase. The studies were performed with aid of an inverted phase-contrast microscope. As the natural points of adhesion of preparation in these experiments served additional groups of non-nervous cells located at the end of fiber, neuronal body or the middle part of the contracting neurite. Vector of the object movement was determined by direction of translocation of the preparation ends. The translocation of mass of the axoplasm was recorded from a shift of volumes of the neurite elements.

In experiments with neurite amputation in mononeurite neuron at any way of dissection of conductor, its slow contraction is developing. This unanimously indicates the existence of retractile properties of its axopalsm. In the light microscope, contraction of neurite, a change of its length or mass represents translocation of its axoplasm (the "axonal flow"). The contractile movement of axoplasm is also noted both in the proximal and in the distal stump of the transected neurite. Already this first phenomenon of cutting of the living neurite shows the same axoplasm of the same sectioned fiber to be able in stumps to be retracted into opposite sides. Hence, the "axonal flow", in principle, can indeed be opposite. The neurite often rushes cellulopetally to the head end of preparation. The main axoplasm, by moving cellulopetally, replenishes the cell soma volume. Another part of axoplasm moves into the proximal part of the contracted neurite by increasing its diameter and by partially translocating in sides, in the transverse direction.

If the accidental additional cells remaining from preparation of ganglia are adjacent to the neurite end by providing a new point of its adhesion, the direction of movement of the preparation end is completely changed to the opposite one. Now the neuronal body is translocating to the fiber end. Such experiments imitate situation with a strained band of expanded rubber, in which the cut end will inevitably stream toward the point of rest. It turned out that cut fiber behaved in the same way as a

rubber band. Its both ends are contracted toward the center, to each other, i.e. bidirectionally. Muscle contraction is so far the only example when two fiber points or their organelles during functioning are moving regularly and necessarily in the cytoplasm simultaneously and toward to each other, i.e., in opposite directions.

Thus, at videomicroscopical observation of retraction of fragment of isolated fiber it is detected that its different parts experience complex pathways of translocation of axoplasm. The fraction of isolated nerve outgrowth is clearly seen to be shortened. Meanwhile, it is clear that the peripheral parts of the axoplasm mass is translocated in the direction from periphery of the fragment toward its middle. Diameter of the main part of the fiber is simultaneously thinned. This indicates that the central part of mass of the fragment axoplasm, on the contrary, is translocated in the direction of neurite periphery. That is, some parts of axoplasm are simultaneously translocated sidewise from the center and from each other. This example, in principle, demonstrates once more a possibility of complexly changing directions of "flows" of axoplasm in the same axon.

In our opinion, it is the proof of retractile properties of neurites which is the main explanation of the mysterious phenomenon of bidirectional simultaneous "flow of axoplasm" and its organelles. We think that axoplasm generally does not flow, that no "flows" of liquid axoplasm exist, but the denser substance of neuroplasm, by contracting slowly, is able to transfer the content of the structure, organelles and molecules, i.e., it itself, simultaneously in anterograde and retrograde directions. Meanwhile, expression of some or opposite direction of movement is regulated by the degree of adhesion of a particular site of axon. At some partial (indefinite) or variable degree of adhesion, the mass of axoplasm will be slowly (weakly) translocated in the direction of point of prevailing adhesion.

In the case that in the area of the middle of neurite there are present additional cells left from preparation of glia and forming a new point of adhesion of fiber, mass of axoplasm will be eager both to the neuronal soma and into the area of the end of fiber by increasing its volume, i.e., in two opposite directions. At the same time, these increased axoplasm masses will be approaching by translocation to meet each other. Besides, under such conditions there is noted a thinning of the axon in the middle of the preparation, in the area. This indicates a partial additional translocation of the axoplasm mass from the middle to ends of preparation, to lateral sides.

In varying conditions of experiment, we managed to reveal an unusual form of movement of the axoplasm, which can be called isometric contraction. Sometimes such conditions are emerged when immobile, ad-

hered can become both preparation ends; both the neuronal body and the end of neurite (Fig. 7). In these cases the movement of axoplasm is manifested not as a decrease of the neurite length, but as its thinning, i.e.,, which is translocated a volume decrease of mass of the axoplasm in the middle parts of the fiber, which is translocated to opposite sides of the neurite.

Vector of the axoplasm masses traslacation depends to the significant degree on the position, translocation, and intensity of zones of adhesion of neurite. The phenomenon of simultaneous and opposite, bidirectional translocations of the axoplasm masses is based on the retractile myosimilar peculiar function of nerve outgrowths.

All molecular cytoskeletal mechanisms quite agree with the proposed hypothetical scheme. This model quite agrees with the substrate-cytoskeletal model (Mitchison and Kirschner, 1988). By experimenting on similar, but living preparations, we can specify hypothesis of the pioneers of "flows" of axoplasm. They turned out to have dealt not with the "flowing axoplasm", but with effects of local retraction of the denser contractile axon substance that is connected with bilateral translocation of organelles and enzymes in the central and peripheral stumps of the cut axons.

Based on investigations of behavior of living isolated neurons with preserved neurites, it is possible to formulate statement about the constant contractile tonus of nerve fiber. The tonus is realized not only in the form of retraction of axoplasm at its transaction, but also at any disturbance of environmental homeostasis, which is sensitive for axon and its adhesion.

The presented hypothesis can be summarized by the schematic determination. The neuronal body synthesizing proteins and other vitally important substances are unable to deliver them along the thin fiber to huge distances to terminals with aid of diffusion, mechanical axis pressure, peristalsis of membranes, and other theoretical ways. There are proposed an idea and experimental proofs for the contractile tonus of nerve fiber, which is realized by retraction of axoplasm by engine of its movement, which has natural, obligatory property of simultaneousness and bidirectionality and regulated by owing to variations of adhesion points.

A KINETIC MODEL OF CARDIAC MUSCLE MECHANICS

F.A. Syomin, A.K. Tsaturyan

Institute of Mechanics, Moscow State University,
Mitchurinsky prosp., 1, Moscow, 119192, Russia

There are many kinetic models of muscle contraction based on the schemes of the myosin cross-bridge cycle during muscle contraction.

Most of the models assume that the transition rates for a myosin head in a sarcomere are strain-dependent. Mathematically those models are usually represented by partial differential equations. For this reason, the usage of such model in computer simulations of any complex problem is very time consuming. There is a need in a simple mathematical model capable to describe muscle contraction and its activation with Ca ions including length dependence of the regulation. A possible model of this kind is briefly described below. The model use a scheme of cross-bridge cycle that is similar to those in earlier models, and also exploits an essential assumption that the transition rates depend not on the strain of a particular cross-bridge, but only on the average strain or distortion over the ensemble of all actin-bound myosin heads. That simplification allows us to set the model by the system of ordinary differential equations.

The model for full activation. The model published earlier [1] was described by the system of ODE as follows:

$$
\begin{cases}
\dot{n}_1 = k_{01}(1 - n_1 - n_2) - k_{10}n_1 - k_{12}n_1 + k_{21}n_2 \\
\dot{n}_2 = k_{12}n_1 - k_{21}n_2 - k_{20}n_2 \\
\dfrac{d\left(\delta(n_1 + n_2)\right)}{dt} = (n_1 + n_2)(\dot{L} - c \cdot \dot{F}_{Act}) - \delta(k_{10}n_1 + k_{20}n_2) \\
\dot{L} = \Phi(t) \text{ or } \dot{F} = \Psi(t)
\end{cases}
\quad (1)
$$

where n_1 and n_2 are the probabilities of the cross-bridge to be weakly or strongly bound to actin, respectively, δ is the average cross-bridge distortion, L is the sarcomere length, F_{Act} is force developed by myosin heads in a half-sarcomere, and k_{ij} – the transition rates depending on δ. The last equation was used to set a law of muscle strain or loading depending on simulated experiment. A set of model parameters was chosen to describe a wide range of experiments with maximal activation near plateau or at full overlap of the thick and thin filaments in sarcomeres The experimental data concerned properties of muscle contraction such as developed force, muscle stiffness, and the rate of ATP hydrolysis as function of the shortening (or stretching) velocity at steady-state contraction. Non steady-state experiments included tension responses to step changes in fiber length applied during either isometric contraction of muscle or its ramp stretch.

The model of calcium activation. Contraction of striated muscle is regulated by tropomyosin and troponin, regulatory proteins of actin filament. Tropomyosin monomers bind each other in 'tail to head' manner to form long chains that run along the thin filaments. In the absence

of calcium, they block myosin-binding sites on actin. Troponin consists of three subunits: troponin C (TnC), troponin I (TnI), and troponin T (TnT). When the calcium sensor, TnC, binds Ca^{2+} ions, TnI detaches from actin releasing tropomyosin from the blocked state. Accordingly, we consider the cross-bridge binding probability as a function of the number of Ca-TnC complexes. The reaction that can be used in the model for the complex formation is as follows: $Ca^{2+} + TnC \rightleftarrows CaTnC$. Let us denote the probability of that formation in the region where myosin and actin filaments overlap by A_1 and the probability of the same process in the not overlapped region by A_2. In the model we defined the process by next equations:

$$\dot{A}_1 = \begin{cases} \alpha_{01}(1 - A_1) - \alpha_{101}A_1, & \dot{W}_{ov} \leq 0 \\ \alpha_{01}(1 - A_1) - \alpha_{101}A_1 + \dot{W}_{ov}\dfrac{A_2 - A_1}{W_{ov}}, & \dot{W}_{ov} > 0 \end{cases},$$

$$(2)$$

$$\dot{A}_2 = \begin{cases} \alpha_{01}(1 - A_2) - \alpha_{102}A_2 - \dot{W}_{ov}\dfrac{A_1 - A_2}{1 - W_{ov}}, & \dot{W}_{ov} \leq 0 \\ \alpha_{01}(1 - A_2) - \alpha_{102}A_2, & \dot{W}_{ov} > 0 \end{cases}.$$

We denoted by α_{ij}, α_{jik} the rates of the CaTnC complexes formation and decay, respectively. W_{ov} is a function that characterized the zone of thick and thin filaments overlap. To define model rates of the CaTnC kinetics we took into account a number of experimentally demonstrated facts, which describe the feedback between mechanics and the calcium activation system.They state that the calcium affinity to troponin C was stronger at:

1) longer sarcomeres;
2) larger number of strongly-bound cross-bridges;
3) larger number of CaTnC complexes.

The rate of CaTnC formation α_{01} depended on the concentration of Ca^{2+} ions denoted by C_{Ca}, and we set it by the following equation:

$$\frac{dC_{Ca}}{dt} = I_{Ca}(t) - Y_{Ca}C_{Ca} - C_{Tn}\cdot\frac{d(A_1 W_{ov} + A_2(1 - W_{ov}))}{dt}, \qquad (3)$$

where $I_{Ca}(t)$ is given time course of calcium inflow, Y_{Ca} is the rate constant of calcium diffusion outflow, and C_{Tn} is total troponin concentration. Considering the dependence of the cross-bridge binding probability on the number of CaTnC complexes and using substitutions $n = n_1 + n_2$, $\theta = n_2/(n_1 + n_2)$ we obtained the following ODE:

$$\dot{n} = k_{01}(A_1 - n) - k_{10}n(1-\Theta) - k_{20}n\Theta ,$$

which together with (1), (2), (3) form the closed set of the equations for the model.

A tensor-invariant model of myocardial tissue. In addition to the kinetic model, we set the stress-strain relations for myocardium that was considered incompressible transversal-isotropic nonlinear elastic continuous medium with active tension. We defined elastic strain-energy as the function of the first and the second invariants of right Cauchy-Green tensor $\mathbf{G}$:

$$W = W(I_1(\mathbf{G}), I_2(\mathbf{G})) = a_0 e^{Q}$$

$$Q = a_1 \left(0.25 \cdot (I_1(\mathbf{G}) - 3)^2 - 0.5 \cdot (I_2(\mathbf{G}) - 2I_1(\mathbf{G}) + 3) \right) =$$

$$= a_1 \left(0.25 \cdot (I_1(\mathbf{G}) - 3)^2 - 0.5 \cdot (I_2(\mathbf{G}) - 2I_1(\mathbf{G}) + 3) \right).$$

The basic stress-strain relation was

$$\overset{\square}{\mathbf{T}} = 2 \cdot \left(\left(\frac{\partial W}{\partial I_1} + I_1 \frac{\partial W}{\partial I_2} \right) \cdot \mathbf{F} - \frac{\partial W}{\partial I_2} \mathbf{F}^2 \right) + \mathbf{T_{Act}} + \mathbf{T_T} + \mathbf{T_0} ,$$

where $\overset{\square}{\mathbf{T}}$ is the Cauchy stress tensor, $\mathbf{F}$ is the Finger strain tensor, $\mathbf{T_0}$ is the spherical tensor related to incompressibility, and $\mathbf{T_{Act}}$ and $\mathbf{T_T}$ are tensors of active forces developed by cross-bridges and passive forces of protein titin. Both of the forces act along anisotropic axis, i.e. along cardiac muscle fiber.

Simulation of experiments of calcium activation of cardiac muscle. Model parameters used in the equations for CaTnC formation rates were optimized to fit well a set of steady-state experiments including those, which describe the dependence of calcium sensitivity of muscle on the sarcomere length, or so called length-dependence of the activation. The phenomenon is very important for the heart and is the basis of the Frank-Starling law of the heart: the higher the end-diastolic volume of the ventricle the higher the systolic pressure and ejection fraction. Computation results reproduced the steepness of the force-calcium curves, their shift with increasing sarcomeres lengths, and the change in calcium sensitivity when actin-myosin interaction was inhibited by blebbistatin. The last fact demonstrates the dependence of the TnC affinity to calcium on the number of strongly-bound cross-bridges described above. Also the model allowed us to obtain reasonable results for isometric twitch muscle contraction at various sarcomeres lengths and the phenomenon of load-dependent relaxation.

Modeling contraction of the left ventricle with simple geometry. The model proposed was used to simulate work of the left ventricle. The ventricle was modeled by a hollow thick-walled cylinder made from cardiac tissue with properties which were described above. The muscle fibers were aligned along helices with the helical angle changing linearly from epicardium to endocardium. Non-linear elasticity and large deformations of the ventricular wall were taken into account. The radial and axial stretch and the uniform twist were considered as the only possible deformations of the ventricle. The model equations defining the relation of hemodynamic macroscopic parameters – blood inflow and outflow, ventricular pressure, arterial pressure and the ventricular volume – were based on the 'windkessel' model. To obtain full system of equations we set boundary conditions as the equality of internal stress on the inner wall to the ventricle pressure and the one on the outer wall to zero. Also we set additional integral expressions considering that the force of ventricular pressure equals the total axial internal tensile force of the cylinder base and the integral torque equals zero.

Basic results of the modeling. After initial filling of empty ventricle we 'turned on' the calcium cycle, and the computation of the problem was undertaken until the behavior of such main model variables as ventricular pressure and volume and arterial pressure became periodical. Varying geometrical and hemodynamic parameters we obtain the model behavior being in good accordance with experiment. The results of the modeling show that the model is able to explain basic changes in shape and size of the left ventricle during cardiac cycle. To demonstrate the significance of the muscle fiber orientation and the ventricle twist we changed its geometry to make all fiber be placed in the plane parallel to the cylinder base. In that case the fibers underwent non-physiological strain at the given stiffness and ejection fraction.So results suggest that the twist of the left ventricle during its diastolic feeling and blood ejection in systole leads to more uniform change in sarcomere length across the ventricle wall that is needed to obtain high ejection fraction. The model suggested here can be used for future development of more realistic 2D and 3D models of the left ventricle.

References

1. F. A. Syomin, A. K. Tsaturyan, A simple kinetic model of contraction of striated muscle: full activation at full filament overlap in sarcomeres, Biophysics, Vol. 57, pp 651-657, 2012.

INVESTIGATION OF MOLECULAR ORGANIZATION OF THE *HALOARCULA MARISMORTUI* ARCHAELLAR FILAMENTS

A.S. Syutkin, M.G. Pyatibratov, S.N. Beznosov, O.V. Fedorov

Institute of Protein Research, Russian Academy of Sciences,
Pushchino, 142290, Russia

Many archaeal species live in the most extreme environmental niches represented on the Earth (high temperatures, salinity etc.). Archaea move using archaella, which only functionally appear similar to bacterial flagella, whereas structurally they resemble bacterial type IV pili. The differences are so fundamental, that recently it has been proposed to call archaeal flagella as archaella [5]. One of the most characteristic features of Archaea (mostly Euryarchaeota) is the widely distributed multiplicity of genes encoding the main structural protein of the archaellar filament – the archaellin. In order to elucidate the reasons for the archaellin gene multiplicity and the role of each of the genes in the formation of the archaellum, archaellin gene deletion experiments on a limited range of model archaea species of the phylum Euryachaeota (*Halobacterium salinarum*, *Methanococcus voltae*, *M. maripaludis*) were conducted. Archaellin deletion mutants in the model organisms showed a complete loss or abnormalities in motility [1,3,4,11]. From these results, it was concluded that the archaellin multiplicity is necessary to form functional archaella, unlike bacteria, where only one flagellin forms functional helical flagella. Sulfolobus species representing phylum Crenarchaeota are an exception to this rule. In their genomes, there is only one archaellin gene, despite that they have functional archaella [8].

An interesting object for the study is the halophilic archaeon *Haloarcula marismortui*. In the *H. marismortui* genome there are two archaellin genes, one (*flaB*) is located near the *fla*-locus on the chromosome, while the other (*flaA2*) is on the plasmid pNG100 [2]. Previously, we have identified two *H. marismortui* strains, archaella of which consisted of either FlaB- or FlaA2-archaellin [7], these strains were designated as FlaB and FlaA2 respectively. We have demonstrated that *H. marismortui* strains, FlaA2 and FlaB, actually are a wild-type and plasmid pNG100 deficient strain, accordingly. We have shown that FlaA2 and FlaB filaments significantly differ in antigenicity, thermostability and thickness [7]. In addition we have found that FlaA2- and FlaB-flagellins of *H. marismortui* are the glycoproteins with unusual type of glycosylation [9].

As each of the flagellins of *H. marismortui* can form the functional filament it may seem that this organism has redundant archaellin genes.

Initially we thought that this redundancy could be related to defense against hypothetic viruses interacting with specific sites on the archaella surface [7]. However, after reading the article about the role of the redundancy detected for the *H. marismortui* rRNA genes [6], we put forward a new hypothesis. In the above-mentioned paper the authors demonstrated that the redundancy of rRNA genes is a mechanism of adaptation to environmental changes, namely, thermal changes. For genes, the products of which perform the same function in different environments, the term "ecoparalogs" was suggested (Sanchez-Perez et al., 2008). We assume that in our case the *H. marismortui* archaellin genes also can be ecoparalogs. An indirect confirmation of this assumption is the fact, that, as we have shown earlier, that the filaments composed of the FlaA2-archaellin are essentially more thermostable than the ones composed of the FlaB-archaellin [7]. To test our hypothesis about whether *H. marismortui* archaellin genes are ecoparalogs, we compared the motility of the FlaA2 and FlaB strains on a semisolid agar medium at different temperatures and salinities. The analysis of cell motility on semisolid agar medium showed that the FlaA2 archaellin provides motility under conditions in which FlaB archaellin cannot (high temperature/low salinity). Moreover, no archaella could be isolated from cells growing in liquid under conditions when cells lost motility on semisolid media. We have found that this effect results from the FlaB archaellin's inability to form archaella at these conditions [10].

As already mentioned above, the multiple archaellin genes are a key feature for Archaea. Earlier it was shown that for some archaea, at least two archaellins encoded by different genes are necessary to form a functional helical filament. At the same time, recently it was shown that some of the archaea retain normal motility and functional archaella after knockout of one of the two archaellin genes [12]. Here, we show for the first time that the multiplicity of archaellin genes may also be associated with the adaptation to changing environmental conditions.

References

1. Bardy S.L., Mori T., Komoriya K., Aizawa S.-I., Jarrell K.F. 2002. Identification and localization of flagellins FlaA and FlaB3 within the flagella of Methanococcus voltae. J. Bacteriol., 184:5223–33.
2. Baliga N.S., Bonneau R., Facciotti M.T., Pan M., Glusman G., Deutsch E.W., Shannon P., Chiu Y., Weng R.S., Gan R.R., Hung P., Date SV., Marcotte E., Hood L., Ng W.V. 2004. Genome sequence of Haloarcula marismortui: a halophilic archaeon from the Dead Sea. Genome Res., 14:2221-2234.

3. Beznosov S.N., Pyatibratov M.G., Fedorov O.V. 2007. On the multi-component nature of Halobacterium salinarum flagella. Microbiology (Moscow), 76: 435-441.

4. Chaban B., Ng S.Y.M., Kanbe M., Saltzman I., Nimmo G., Aizawa S.-I., Jarrell K.F. 2007. Systematic deletion analyses of the fla genes in the flagella operon identify several genes essential for proper assembly and function of flagella in the archaeon Methanococcus maripaludis. Mol. Microbiol., 66:596-609.

5. Jarrell K. F. & Albers S. V. 2012. The archaellum: an old motility structure with a new name. Trends Microbiol., 20:307-312.

6. Lopez-Lopez A., Benlloch S., Bonfa M., Rodriguez-Valera F., Mira A. 2007 Intragenomic 16S rDNA Divergence in Haloarcula marismortui Is an adaptation to Different Temperatures. J. Mol. Evol., 65:687-696.

7. Pyatibratov M.G., Beznosov S.N., Rachel R., Tiktopulo E.I., Surin A.K., Syutkin A.S., Fedorov O.V. 2008. Alternative flagellar filament types in the haloarchaeon Haloarcula marismortui. Can. J. Microbiol., 54:835-844.

8. Szabó Z., Sani M., Groeneveld M., Zolghadr B., Schelert J., Albers S.V., Blum P., Boekema E.J., Driessen A.J.M. 2007. Flagellar Motility and Structure in the Hyperthermoacidophilic Archaeon Sulfolobus solfataricus. J. Bacteriol., 189:4305-9.

9. Syutkin A.S., Pyatibratov M.G., Beznosov S.N., Fedorov O.V. 2012. Different mechanisms of helicity formation in haloarchaeal flagella. Microbiology (Moscow), 81:573-581.

10. Syutkin A.S., Pyatibratov M.G., Galzitskaya O.V., Rodríguez-Valera F.E., Fedorov O.V. 2014. Haloarcula marismortui archaellin genes as ecoparalogs. Extremophiles, 18:341-349.

11. Tarasov V. Y., Pyatibratov M. G., Tang S.-L., Dyall- Smith M., Fedorov O.V., 2000. Role of flagellins from A and B loci in flagella formation of Halobacterium salinarum. Mol. Microbiol., 35:69-78.

12. Tripepi M., Esquivel R.N., Wirth R., Pohlschroder M. 2013. Haloferax volcanii cells lacking the flagellin FlgA2 are hypermotile. Microbiology, 159:2249–2258

ALL-BIOLOGICAL, SEXUAL AND INDIVIDUAL AND TYPOLOGICAL REGULARITIES OF FORMATION OF MUSCULAR FIBRES

R.V. Tambovtseva

Russian state university of physical culture, sports, youth and tourism, Sirenevy Boulevard 4, Moscow, 105122, Russia

Age changes of a muscular fabric is first of all formation, growth and development of the main structurally functional units – muscular fiber. We have investigated various muscles: the longest muscle of the head,

m. biceps, m.triceps, diaphragm, rectus femoris , m.gastrocnemius, soleus of rats of males and females of the line Vistar, guinea pigs and human. An age interval – from a 1 days till 2 years at rats, at guinea pigs – in 10 days prior to the birth till 2 years. Muscles of the human considered from 4 months of pre-natal development to 70 years. Histochemical methods of activity of ATPase of a myosin and activity of SDG have been used.

Having analysed a big actual material, by us it has been shown that formation of various types of muscular fibers passes the long period pre-and post-natal ontogenesis. Developments of muscular fibers differentiation depending on a studied muscle and specific accessory of object. The beginning of different- processes all animals is connected with emergence and formation from a pool of not differentiated structures of fibers, on histochemical properties coming nearer to type fiber I with oxidative power supply: at rats this period lasts from 5 to 16 days of life, at guinea pigs in 10 days prenatal till 3rd day of life. Primary differentiation of muscular fiber, on histochemical properties coming nearer to IIA fiber, at a rat for the 16th day, at a guinea pig for the 3rd day, that is exactly in those terms when in muscles formation of fibers I of type generally comes to the end. Final differentiation of fibers II of type is interfaced to processes of puberty which passes in the mixed muscles in two phases: a) begins with secondary increase in number of fibers of the IIA type and strengthening of their oxidative potential at the expense of decrease in relative amount of anaerobic fibers (at rats this process – for the 40th day, at a guinea pig for the 25th day); б) the second phase (at rats from 45th day, at guinea pigs from 35th day) is characterization by rapid growth of relative quantity MBIIB and the maximum increase in the area of their cross-section section. The crucial role in formation of muscular fibers of the IIB type at males is played by a man's sexual hormone – testosterone. Formation of the definity organisation of skeletal muscles is defined by time of complete completion of puberty. The area of cross-section section of various types of muscular fibers before puberty at rats and guinea pigs increases slightly, however during the puberty period intensive growth of a diameter of all fibers, especially MBIIB is observed. Accurate sexual dimorphism comes to light. Before puberty processes of formation of fibers at males and females go synchronously, after – asynchronously. At males by the end of puberty the large relative amount of fibers of the IIB type with anaerobic type of power supply, at females – with oxidative is noted. All processes of formation of various muscular fibers at females come to an end for 5-10 days earlier. The area of cross-section section of muscular fibers at females before puberty it is authentic above, than

at males. After puberty at males the area of a diameter of all fibers authentically above females.

At mature and not mature animals it is possible to explain similarity of development of various types of muscular fibers as biological regularity, showing unity of processes of morphological and functional maturing.

Analyzing a material received on the human, we have come to a conclusion that the basic principles of development of skeletal muscles in the course of individual development of the human completely correspond studied on animals. The first stage of differentiation of tonic fibers with a "slow" myosin is found in the person on the 5-6th month of pre-natal life. Comparison of these results to data of the researches which have been carried out on animals, allows, that at the person development of skeletal muscles passes on type of mature. It is possible to believe that at the person the general type of development peculiar to primacies, being characteristic high possibilities of tonic muscles of extremities at newborns remains. Feature of the human is connected with longer development of the highest of movements. In the first months of post-natal life in many areas of a brain unripe nervous elements and even still prevail. At the same time by the time of the birth there is quite well created a spinal level of regulation. Functionality of this level does not go further realisation of simple movements such as a reflex and its options. However the level of development of motor-neurons is apparently sufficient for initiation of the first wave of muscular differentiations. Thus it should be noted a large number of the fibers beginning differentiation on the I type: in the different mixed muscles their number makes not less than 50-60 % while the relative amount of fibers I of type in the mixed muscles of extremities of small laboratory animals does not exceed 10-15 %. It is possible to believe that the number of fiber I of type is defined by emergence of gravitational loadings. They affect muscles of the human in much bigger degree that is connected with big mass of a body in comparison with small laboratory animals. The general age tendency is shown in decrease in relative amount of fiber I of type. Other accurately being shown regularity is steady increase of quantity MBIIB. The most important period in formation of definity level of the organisation of muscular fiber is the puberty period. The general tendency of gradual increase shares of fast fiber II of type with anaerobic power supply in even bigger degree comes to light with age in the analysis of the sizes of muscular structures. Thus means various growth rates of a diameter of muscular fibers I and II of types that makes additional changes to distribution of the total areas of busy muscular fibers of that other type on cross-section a muscle cut. Before puberty the area of cross-

section section of muscular fibers at girls authentically is more than an area some fibers of boys. However from 12-year age the area of cross-section section of MV of boys authentically exceeds those at girls. It is possible to believe that change of a ratio of amount of muscular fibers goes only at the expense of a redifferentiation of fibers at the age from 14 till 18 years. These processes are substantially supervised by man's sexual hormones. All this allows to emphasise importance of the final stages of puberty for formation of the definity organisation of a power profile of skeletal muscles. The role of the puberty period in reorganisation of power of muscular fibers in even bigger degree was shown at research of age changes of SDG – a marker is mitochondrial oxidation. The comparisons carried out by us show that activity of SDG in various muscular fiber of the studied muscles undergoes, during all post-natal ontogenesis ambiguous changes. Process of decrease in oxidative activity by 18 years more all is expressed in four-head to a muscle of a hip and three-head to a shoulder muscle while in a two-headed muscle of a shoulder high activity of SDG remains practically without changes almost in all fibers. Such regularity is noted also at mature and not mature animals. Among features of development of skeletal muscles of the person it should be noted a special role of MV. If at small laboratory animals this quite stable education keeping the organisation in all subsequent reorganisations of skeletal muscles, at the person of possibility of transition by the main types of muscular fiber is much wider that is apparently connected with considerably bigger flexibility and plasticity of the developing peripheral impellent device.

At comparison of fiber composition of representatives of leptosom and eurisom types of a constitution it has been shown that young men asteno-torakal and muscul types have essential distinctions in fiber structure and the areas of cross-section section. Young men of leptosom type are characterization by existence of large relative amount of fibers with aerobic power, meanwhile representatives of eurisom type of addition have more muscular fibers with anaerobic power supply. However, as show our researches, the final definity version of muscular fibers with this or that power orientation (miotype) is formed during the long period and finally comes to the end after puberty as formation of muscular IIB fibers directly depends on a man's sexual hormone of testosterone. Meanwhile, fibers of an oxidative orientation depend on influence of hormones of a thyroid gland. Thus it should be noted that the difference in relative amount of fibers of different type at representatives of various type can be revealed at earlier age (7-8 years), but during the period puberty there are powerful differentiations

which do not give an objective picture. Besides, growth of a diameter of muscular IIB fibers occurs at a final stage of the puberty period – from 15 by 17-18 years. In puberty there is a continuous reorganisation of an energy potential of muscular fibers. There is only small amount of muscular fibers of type I which really are stable structures. Meanwhile IIA and IIB type fibers constantly change the power profile depending on the hormonal status. And, fibers of the IIA type are as though «a cambial layer». There is very big variety of fibers of this type with high, average, low activity of studied enzymes. And, if ATP-ase activity of a myosin shows us only generally three options of muscular fibers, detection of activity of SDG – a marker of intensity of oxidative processes in an organism show us that the fibers having the same colouring at detection of activity of Atf-aza of a myosin, can be characterization by different SDG activity. Apparently, existence of this big «a cambial layer» also provides high adaptable possibilities of any live organism. We believe that miotype, finally being formed only after puberty, coincides with a morphotype and power type. By our researches it has been shown that miotype at the person coincides with a morphotype in 70 % of cases. Such tendencies are observed at small laboratory animals. At the pure line of rats of the line Vistar the difference in the ratio amounts of fibers in four-head to a muscle of a hip and sexual distinctions between males and females is revealed.

AMPK AS A MASTER CONTROLLER OF SKELETAL MUSCLE METABOLISM AND BLOOD SUPPLY

O.S. Tarasova, G.V. Morgunova, A.A. Borzykh, A.A. Shvetcova, E.K. Selivanova, D.K. Gaynullina, S.I. Sofronova, O.L. Vinogradova

Faculty of Biology, M.V. Lomonosov Moscow State University, Leninskie Gory 1/12, Moscow, 119234, Russia; SRC RF - Institute for Biomedical Problems RAS, Khoroshevskoe shosse 76A, Moscow, 123007, Russia

The adenosine monophosphate-activated protein kinase (AMPK) is a key controller of metabolic processes in skeletal muscle. During exercise, AMPK becomes activated in muscle fibers in response to increased AMP/ATP and creatine/phosphocreatine ratios, and serves to inhibit ATP-consuming pathways, and activate pathways involved in carbohydrate and fatty-acid metabolism to restore ATP levels. Along with that, AMPK is expressed in both endotheial and smooth muscle cells of the vascular wall and can be regulated by hypoxia, fluid shear stress, Ca^{2+}-

elevating agonists, and several hormonal influences. AMPK was recently proposed to participate in functional hyperemia. Functional hyperemia is not manifested uniformly in different vascular beds, being most pronounced in skeletal muscles, moderate in intestine and negligible in kidney and skin. This study tested the hypothesis that the effects of AMPK activation will show similar pattern of tissue specificity.

The segments of small arteries from medial gastrocnemius muscle (GA), mesentery (MA), kidney (KA) and skin (SA) were isolated from male Wistar rats and mounted in wire myograph (DMT A/S, Model 620M). We studied the effects of AICAR (10^{-4} M, 60-min incubation), a metabolic AMPK activator on vessel contraction to α_1-adrenoceptor agonist methoxamine.

The incubation with AICAR greatly reduced the contractile responses of GA and MA, but did not change KA and SA contractions. The relaxatory effects of AICAR was abolished after vessel denudation from the endothelium or after inhibition of the three key pathways of the endothelial influence: NO-pathway, cyclooxygenase/prostacyclin-pathway and the pathway of endothelium-derived hyperpolarising factor (EDHF). L-NNA, a NO-synthase inhibitor (10^{-4} M), given alone or in combination with indomethacine (10^{-4} M) reduced but not abolished the effects of AICAR. Along with that, the inhibition of EDHF-pathway activity either at the level of endothelial cells (by combined blockade of SK_{Ca} and IK_{Ca} channels, the combination of UCL1684 (10^{-7} M) and TRAM-34 (10^{-6} M)) or at the level of smooth muscle cells (by the combination of ouabain (10^{-5} M) and Ba^{2+} ($3*10^{-5}$M)) almost completely abolished the effect of AICAR. The inhibition of hemoxygenase (Sn-Protoporphyrin, 10^{-5} M) did not affect the effect of AICAR, therefore, the activity of EDHF-pathway was not associated with CO production.

In conclusion, AMPK activation results in diminished vasocontractile responses and this correlates with magnitude of functional hyperemia in different organs; the effect is prominent in skeletal muscle and intestine but is absent in kidney and skin, where blood flow is mainly regulated by blood flow autoregulation response and sympathetic influences, respectively. EDHF-pathway activity is the major target of AMPK in the arterial wall.

SOLEUS MUSCLE SATELLITE CELLS POPULATION DURING THE RELOADING AFTER GRAVITATIONAL UNLOADING

O.V. Turtikova, E.G.Altaeva, B.S. Shenkman

Institute of Biomedical Problems RAS,
Khoroshevskoe sh., 76-A, Moscow, Russia

Cellular and molecular mechanisms underlying great skeletal muscle plasticity are of interest for many researchers. Skeletal muscle atrophy during its inactivation in the conditions of hypokinesia, immobilization, paralyses and stay in zero gravity (microgravity) up to now is not an entirely solved problem. Along with the recovery of normal gravity-dependent mechanisms of motor control, it is necessary to increase muscle mass by intensification of protein synthesis.

The transcription intensity depends directly on the number of DNA copy. The additional DNA can be supplied by myosatellite cells (SC) which undergo activation, proliferation and fusion with muscle fibers. The data are known about SC significant role in the recovery of muscle mass during the second week of the reloading [Mitchell P.O., Pavlath G.K., 2001]. There is increasing evidence about inessential role of SC and significance of other mechanisms in the reloading of atrophied muscles after gravitational unloading [Bruusgaard et al., 2011, Jackson et al., 2012]. Also remains unclear whether the transcriptional activity of incorporated nuclei and SC proliferative activity, their ability for self-maintenance, differentiation, and fusion during early reloading period is undamaged.

The goals of the study

1. To estimate the number of myonuclei per myofiber, nuclei/cytoplasm ratio, giving evidence on the incorporation of SC nuclei or reduction in myonuclei number;
2. to analyze changes in SC population (the ratio of proliferation and differentiation) at different time points of the recovery after simulated weightlessness;
3. to reveal the phenomenon of fusion of SCs with muscle fibres in the course of recovery period;
4. to access the IGF-1 concentration in blood and in SC niche.

Results

The number of myonuclei per cross-section of a single muscle fiber decreased as a result of 14-day hindlimb suspension (HS) by 19.1 % as compared with the control group C14, $p<0,05$. Reduction on the first day of recovery compared with C14 amounted to 19 %, $p<0,01$. In groups R1,

R3, R7 and R14 no significant growth of myonuclei was observed in comparison with a group HS14. The reduced number of myonuclei per myofiber cross-section wasn't restored even by the day 14th of recovery. Changes in myonuclear domain (myofiber cross section per one myonucleus) were insignificant. Thus the present work confirms the hypothesis of myonuclear domain constancy, but disproves the point of view about the absence of reducing the myonuclear number during the unloading atrophy. Counting the number of incorporated BrdU+ myonuclei per one myofiber cross-section for 12 hours period (from the BrdU introduction to the animal sacrificing) allow estimating SC fusion with myofiber. After 14 days of HS BrdU+ nuclei were detected in 1 out of 50 myofibers. On the first day there was a sharp increase in the number of fused SC (3,4 times compared to the group HS14). On the day first of readaptation blood levels of IGF-1 increased by 47% as compared to control group ($p < 0.05$). There was no difference in the number of incorporated myonuclei already on the 3rd day of reloading as compared to the HS14 group. *Follistatin* expression was three times increased after 14-day HS, it decreased 1,5 times after the first day of readaptation as compared to unloaded animals. We didn't observe any differences from control level on the day 3 and 7 of reloading. *Mki67* expression was reduced after HS; the expression sharply increased on the day 1 day of recovery, increased twice - on day 3, the peak of expression was observed on day 7 of reloading (28-fold as compared to HS animals). The least *Cdh15* expression was detected after 2 weeks of HS. There was a gradual increase in *Cdh15* expression up to the control level after 7 days of reloading. *Myogenin* expression was not significantly decreased during HS; sharp increase was observed on the 1st day of the reloading and gradual decrease to control by the day 7.

We assume that rapid proliferation, differentiation and fusion took place in SC which respond to the activating stimulus at the time of the return of the muscle to the conditions of normal gravity to respond to activating stimulus (IGF- 1 concentration in the blood, the expression in the muscle). This is indicated by increase the number of BrdU+ nuclei included on the 1st day of recovery, as well as the increase in *myogenin* expression. Then, after 7 days, there is some stabilization of c*dh15* and *myogenin* expression , but high *mki67* indicates active proliferation, which may lead to the introduction of further myonuclei to enhance protein synthesis in late recovery period.

PARTIAL STABILIZATION OF MICROTUBULES SLOWDOWN CELL SPREADING SUPPOSEDLY BY INCREASING CONTRACTILITY OF ACTIN-MYOSIN SYSTEM

A.V. Tvorogova [1], T.A. Smirnova[2], I.A. Vorobjev [1,2]

[1] *Belozersky Institute, MSU, Leninskie Gory 1-40, Moscow, 119992, Russia;*

[2]*MSU, Faculty of Biology, 1-12 Leninskie Gory, Moscow, 119991, Russia*

Microtubules (MTs) are cytoskeleton structures that exhibit dynamic instability (switching between growth and shortening periods). Low concentrations of nocodazole or paclitaxel can inhibit cell migration by suppressing microtubule dynamic instability without depolymerizing the whole MT array [1,2], but the role of the dynamic instability in cell spreading is still poorly understood. In our previous study [3] it was shown that fibroblasts' spreading occurs in two steps: fast initial and slow final spreading. In this study we investigate the role of dynamic instability of MTs in the fast spreading phase.

Fibroblast-like VERO cells were grown in DMEM+F12 with 10% FBS and gentamicin 0.08mg/ml. Combination of nocodazole at 100 nM and paclitaxel (taxol) at 50 nM (NT) was used to suppress MT dynamic instability. Blebbistatin 45 μM (Bl) was used for inhibition of myosin contractility. Inhibitors were added to cell suspension before plating. Time-lapse observations were performed under Nikon TiE inverted microscope (objective 20×/0.45) with Photometrics CoolSnap HQ2 14-bit camera. For immunofluorescence analysis, cells were placed on 170 um thick coverslips, fixed with cold 2.5% glutaraldehyde on PBS for 10 minutes and processed for immunofluorescence. Microtubules were labeled with DM1-A antibody (Sigma-Aldrich, USA), followed by goat Alexa Fluor 488 anti-mouse secondary antibody (Invitrogen, USA). Alexa-555-phalloidin used as actin marker. In order to locate MT ends accurately, super-resolution Nikon N-SIM fluorescent microscopy was employed (objective 100×/1.3). Cell areas were measured once per 2 minutes using ImageJ. Growth rate was characterized as dynamics of current area to zero time-point area ratio for each cell. Distances from ends of MTs to cell edge were determined in ImageJ.

Spreading cells usually demonstrate fast initial growth, which gradually slows down [3,4]. Partial MT-stabilization decreases the spreading rate and the whole process becomes more linear (fig. 1). Cell area duplication occurs approximately on the 8th minute without inhibitors, and on the 55th minute for cells with nocodazole and paclitaxel
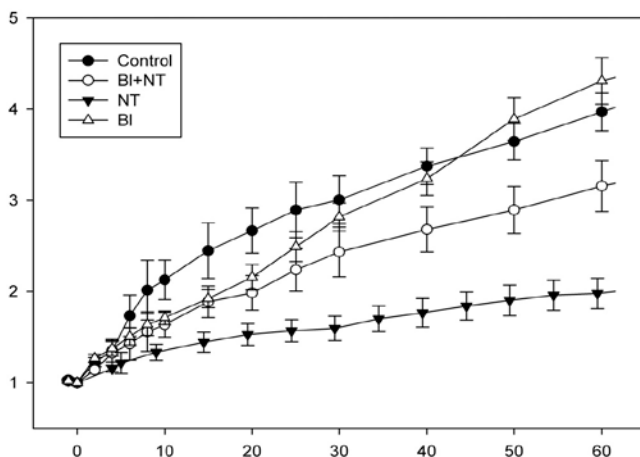
Fig. 1. Spreading of VERO cells on a glass slide. Axis: *x*-time, min; *y*- mean area to zero time-point area ratio. Bars show standard error of mean (SEM).

added. Cell area triplication occurs on the 30th minute for control cells and on the 189th minute for cells with stabilized MTs. Combined treatment with nocodazole and paclitaxel leads to partial suppression of MT dynamics marked by the decrease in comet brightness, track length and speed. Along with this the distance between MT ends and cell edge is also altered. Measurements of the distances from MT ends to cell edge were performed 20 minutes after addition of culture medium with or without inhibitors. The largest cells which had began to spread and formed explicit lamellae were measured in all experimental groups. Normally most MT ends are located close to the cell edge (mean distance ±SEM: 1.99±0.09 um). When dynamic instability was suppressed most ends are located at approximately 3-5 um from the cell edge (mean distance 3.86±0.18 um, see fig. 2). Addition of myosin light chain inhibitor (blebbistatin) to spreading cells does not accelerate spreading (fig. 1) whereas combined with nocodazole+paclitaxel treatment it minimizes their inhibiting effect. So far, cell area duplication in blebbistatin and in blebbistatin+nocodazole+paclitaxel occurs on the 16th and 17th minutes respectively; cell area triplication in blebbistatin and in blebbistatin+nocodazole+paclitaxel occurs on the 34th and 53th minutes respectively. However, in the presence of blebbistatin the distance from MT ends to cell edge in cells treated by blebbistatin+nocodazole+ paclitaxel remains the same as in cells treated by nocodazole+ paclitaxel only (see fig. 2).
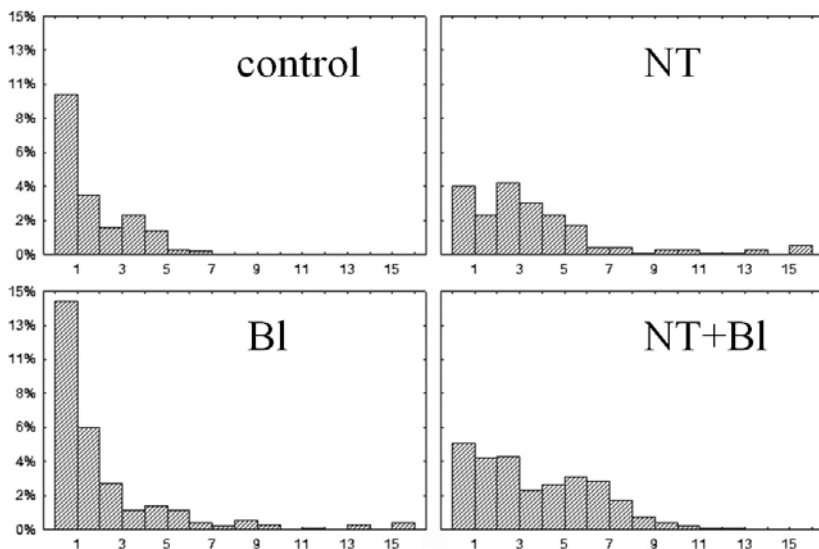
Fig. 2. Histogram of distances from ends of MTs to cell edges. Axis: x-distance from cell edge, um; y-percent of MT ends.

Our data confirms that partial stabilization of MT dynamic instability decreases the spreading rate of cultured cells and the most prominent effect of stabilization is increased distance between MT ends and cell edge. Slowdown of cell spreading may be a result of hypercontractility induced when MTs are not able to follow the advancing cell edge.

References

1. Liao, G., Nagasaki, T., Gundersen, G.G. (1995) Low concentrations of nocodazole interfere with fibroblast locomotion without significantly affecting microtubule level: Implications for the role of dynamic microtubules in cell locomotion. J. Cell Sci. 108:3473–3483.

2. Grigoriev I.S., Chernobelskaya A.A., Vorobjev I.A. (1999) Nocodazole, vinblastine, and taxol at low concentrations affect fibroblast locomotion and saltatory movements of organelles. Biologicheskie Membrany, 16 (1): 21-41.

3. Tvorogova A.V., Vorobjev I.A. (2012) Microtubules suppress blebbing and stimulate lamellae extension in spreading fibroblasts. Tsitologiya. 54 (10) : 742-753.

4. Petrov Yu.P., Negulyaev Yu.A., Tsupkina N.V. (2012) Dynamics of L-929 cell spreading after mitosis. Tsitologiya, 54 (4): 307–312.

REDOX CONTROL OF FIBROBLAST CHEMOTAXIS

P.A. Tyurin-Kuzmin, A.V. Vorotnikov

Faculty of Fundamental Medicine, Lomonosov Moscow State University, Moscow, Russia

Cells produce hydrogen peroxide (H_2O_2) as a part of physiological response to external stimulation with growth factors and cytokines. NADPH oxidases (NOX) generate H_2O_2 downstream of receptor activation. This H_2O_2 acts as a second messenger by transiently oxidizing and altering enzymatic activity of a limited number of target proteins including protein tyrosine kinases and phosphatases. Recent studies have also implicated the lipid phosphatase PTEN and serine/threonine kinase PKB/Akt as the H_2O_2 targets within PI3-kinase signaling module, suggesting that locally produced intracellular H_2O_2 may control migration and chemotaxis.

To test this hypothesis, we used intracellular live biosensors to image the phosphatidylinositol-3,4,5-trisphosphate (PIP_3) and H_2O_2 in both freely moving and chemotacting fibroblasts. We found that in both cases H_2O_2 accumulated in the cell front and formed dynamic gradients in the cytoplasm that always matched those of PIP_3 and oriented along the axis of cell polarization and movement. Inhibitory analysis further suggested that H_2O_2 gradients are caused by a rearrangement of H_2O_2 generating machinery rather than by a *de novo* synthesis of H_2O_2. As such, inhibition of PI3-kinase eliminated both the PIP_3 and H_2O_2 gradients, but had no effect on basal level of H_2O_2 in cytoplasm. On the contrary, NOX inhibitor apocynin dramatically cut down the cytoplasmic level of H_2O_2, but failed to flatten its gradient or to affect the PIP_3 gradients. The cell-permeable catalase eliminated both the basal and gradient signals of H_2O_2, but still did not affect the PIP_3 gradients. These results indicate that PIP_3 acts upstream of H_2O_2, and the latter has two sources in cytoplasm: one provides for the basal level of H_2O_2 and is sensitive to apocinin, whereas the other is liable for H_2O_2 gradients and is apocynin-insensitive.

We next asked if H_2O_2 controls directional sensing or movement velocity of fibroblasts. We tracked paths of cells that freely moved into the wound area in a scrap assay, and determined cell speed and net displacement. Having few hundred cells analysed we found that apocynin or catalase did not significantly affect directionality, but reduced speed of cell movement aproximately 2-fold. These results suggest that H_2O_2 controls activity of the actin propulsion machinery, whereas PIP_3 acts upstream to regulate both the directionality, and speed of fibroblast movement in H_2O_2-dependent manner.

ISOFORM COMPOSITION AND GENE EXPRESSION OF THICK AND THIN FILAMENTS PROTEINS IN STRIATED MUSCLES OF MICE AFTER SPACE FLIGHT

A.D. Ulanova[1,2], Yu.V. Gritsyna[1], N.N. Salmov[1],
I.M. Vikhlyantsev[1], A.G. Bobylev[1], V.V. Rogachevskii[3],
B.S. Shenkman[4], Z.A. Podlubnaya[1,2]

[1]*Institute of Theoretical and Experimental Biophysics, Russian Academy of Sciences, Pushchino, Moscow region, Russia;*
[2]*Pushchino State Institute of Natural Science, Pushchino, Moscow region, Russia;*
[3]*Institute of Cell Biophysics, Russian Academy of Sciences, Pushchino, Moscow region, Russia;*
[4]*SRC, Institute for Biomedical Problems, Russian Academy of Sciences, Moscow, Russia;*
E-mail: a-okyneva@yandex.ru

It is known that the human or an animal exposure to real or simulated microgravity (head-down-tilt bed rest, hindlimb suspension models and "dry" immersion) leads to alteration in all body systems. A complex of these changes in sensorimotor system is called "hypogravitational motor syndrome" (HMS). The alterations are more profound in anti-gravity muscles of legs and the body [1]. A decrease in muscle tone and force of muscle contraction takes place under short-time (up to 5 days) impact of microgravity. Under more longer impact these changes are accompanied with atrophy in slow and fast type muscle fibers [2], destructive changes in thin filaments [2], higher degradation of myosin heavy chains [3], shift in myosin phenotype towards the increase in the content of fast isoforms of heavy chains of this protein [2, 4] and also with a decrease in the content of giant proteins of thick and thin filaments (titin and nebulin) [5-9]. In particular, in gravity dependent muscle soleus of the human and a rat under simulated microgravity was seen a decrease (by 1,5-2 times) in the content of nebulin and NT- and N2A-isofoms of titin, and it was accompanied with a decrease in contractile capability of muscle [7, 9]. But after 12-day space flight a decrease in the content of giant sarcomeric cytoskeletal proteins or a decrease in contractile capability of skeletal muscles of Mongolian gerbil (*Meriones unguiculatus*) were not observed in our experiment [9-11]. No decrease in the content of titin in cardiac muscle of Mongolian gerbil was revealed after exposure to real microgravity [12]. However an increase in the content of the long (more elastic) N2BA-isoform of titin relative to the content of short (stiffer) N2B-isoform of this protein in cardiac muscle of

gerbils (flight group) was registered that is directed to the strengthening of contractile activity of the cardiac muscle [12].

In this work we explored changes in isoform composition and gene expression of titin, myosin heavy chains (proteins of thick filaments) and nebulin (protein of thin filaments) in striated muscles of mice after 30-day space flight. A separate task was to study changes of titin phosphorylation level in mice muscles after space flight.

Materials and methods. The object of the study was mice being onboard the Russian spacecraft "BION-M" №1. All procedures connected with preparation of animals to the experiment, their maintenance and subsequent slaughtering were conducted by the members of State Scientific Centre of Russian Federation – Institute for Biomedical Problems RAS and were approved by Committee on biomedical ethics. Skeletal muscles (*m. psoas, m. tibialis anterior, m. gastrocnemius*) and left ventricle of cardiac muscle of mice from the flight (n=5) and control (n=6) groups were used.

Agarose-strengthened 2,1% SDS-polyacrylamide gels were optimized to detect the changes in isoform composition and the content of titin (molecular mass 2000-3700 kDa) and nebulin (700-900 kDa) in mice muscles as described in [13] with our modifications [14]. Gels were stained with Coomassie brilliant-blue. The content of titin and nebulin relative to the content of myosin heavy chains was estimated with densitometry (program Total Lab v.1.11). Isoform composition of myosin heavy chains (MHC) was studied during SDS-gel-electrophoresis in 7% polyacrylamide gel as described in [15]. Phosphorylation of titin was carried out by the method described in [16] with negligible modifications. A native level of protein phosphorylation was estimated with the help of fluorescent stain Pro-Q Diamond (Invitrogen) for phosphoproteins in gel. For this purpose gel was put into the solution containing 50% of ethanol and 10% of acetic acid for 12-18 hours. The stained gel was washed in prepared solution Pro-Q Diamond phosphoprotein gel destaining solution (Invitrogel). Protein bands containing phosphate were viewed with the help of the system Pharos ("Biorad"). After it gels were stained with Coomassie Brilliant Blue (G-250 and R-250) mixed in a 1:1 ratio for the control estimation of protein content.

Total RNA was extracted from the muscle tissue of rats using the Aurum^{TM} Total RNA Fatty and Fibrous Tissue Kit (Bio-Rad, United States) according to the manufacturer's instructions. cDNA was synthesized using M-MLV reverse transcriptase (Eurogen, Russia). RT-PCR was performed with DT-322 amplifier (DNA-Technology, Russia) with Taq

DNA polymerase (Eurogen, Russia) and SYBR Green I fluorescent dye (Invitrogen). The quantity of titin mRNA relative to the amount of mRNA housekeeping gen GAPDH was determined according to the method $2^{-\Delta\Delta Ct}$. In the work we used the following primers: forward primer 5'-cagcagccaagaaggccgct-3', reverse primer 5'-gtcccgcagtctcatagtctcaccac-3' for gene ttn N2A-isoform; forward primer 5'-ccaagctcactgtgggagaaa-3' and reverse primer 5'-cttaactcgggaaccttcatcg-3' for the gene *ttn* N2B and N2BA exons 49-50; forward primer 5'-acgccaacggcatcctgaac-3', reverse primer 5'-ggcggactcgttcctcctct-3' for gene Hsp70; forward primer 5'-ctttccccgtcaagatgcctgag-3', reverse primer 5'-agagattacgaagtctacgggacc-3' for gene Hsp90. PCR was performed using the following regime: hot start at 95°C for 5 min, denaturation at 95°C for 15 s, annealing with primers at 60°C for 20 s, elongation at 72 for 20 s (35 cycles). The PCR products were then analyzed by electrophoresis in 7% polyacrylamide gel. Data were statistically processed using the Manna–Whitney nonparametric U-criterion. In our study, differences were considered significant at $p < 0.01$.

Results. An expected decrease in the content of IIa isoform of MHC and an increase in the content of "faster" IIx/d isoform of this protein was observed in *m. tibialis anterior* of the flight group of mice (fig. 1).

In other skeletal muscles of mice of the flight group significant changes in isoform composition of MHC were not revealed. However in *m. psoas* of mice from group "flight" a tendency to a negligible increase in the content of IIa isoform of MHC relative to the content of "faster" IIx/d isoform of this protein was recorded.

An expected decrease in the content of NT- and N2A-isoforms of titin and nebulin in *m. psoas* of mice from the flight group was not observed. However in the absence of credible changes in nebulin gene expression, a decrease (by 36 times) in titin gene expression in this muscle was revealed. An expected increase in the content of N2BA-isoform of
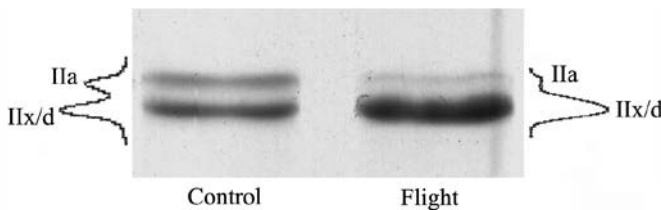
Fig. 1. Changes in isoform composition of MHC in m. tibialis anterior of mice after 30-day space flight.
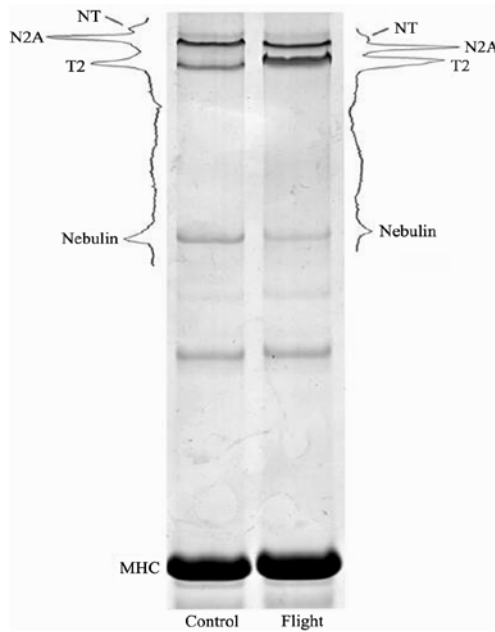
Fig. 2. Changes in the content of titin and nebulin in m. gastrocnemius of mice from the flight group.

titin was not recorded in cardiac muscle of mice from the flight group. However an increase (by 4 times) in titin gene expression in heart of these animals was detected (data not shown).

In *m. tibialis anterior* and *m. gastrocnemius* of the flight group of mice in the absence of significant changes in titin and nebulin gene expression, a considerable decrease (by 1,6-2 times) in the content of nebulin and a decrease (by 1,15 times) in total content of NT- and N2A-isoforms of titin were registered (fig. 2). This changes were accompanied by a 1,5-2 fold increase in the content of proteolytic fragment of titin-2 (T2) in *m. gastrocnemius* of mice from group "flight" (fig. 2).

No changes in phosphorylation level of titin in cardiac and skeletal (*m. psoas, m. tibialis anterior*) muscles of mice from the flight group were observed. However in *m. gastrocnemius* of mice from the flight group a threefold increase in the phosphorylation level of T2-fragment of titin was recorded (data not shown).

Discussion. It is known that the human or animal exposure to real or simulated microgravity leads to atrophied changes in muscles. In this

314

case the content of "fast" isoforms of MHC in skeletal muscles fibrils significantly increases. Such changes we expected to view also in skeletal muscles of mice after 30-day space flight. An expected decrease in the content of IIa isoform of MHC and the increase in the content of "faster" IIx/d isoform of this protein was observed in *m. tibialis anterior* of mice from the flight group (fig. 1). However an uncertain increase in the content of IIa isoform of MHC relative to the content of "faster" IIx/d isoform of this protein was observed in *m. psoas* of mice from the flight group, and that is the evidence of minor shift of myosin phenotype towards "slow" one. The obtained data may point to activation of different signal mechanisms responsible for change in myosin phenotype in the studied muscles of mice under conditions of space flight.

An expected increase in the content of the long N2BA-isoform of titin in cardiac muscle and also a decrease in the content of giant proteins of titin and nebulin in *m. psoas* of mice after 30-day exposure to real microgravity were not observed. The recent result is rather difficult to explain in view of our data on a 36-time decrease in titin gene expression in *m. psoas* of mice from the flight group. Titin in this muscle is most likely less subjected to proteolytic degradation in conditions of space flight. However molecular mechanism of such protection is unknown.

A decrease (by 1,15 times) in the content of NT- and N2A-isoforms of titin was observed in *m. gastrocnemius* and *m. tibialis* of mice from the flight group and that was followed by a significant increase (by 1,6-2 times) in the content of proteolytic T2-fragment of titin in these muscles (Fig.2). Moreover in these muscles of mice from the flight group a significant decrease (in 1,5-2 times) in the content of nebulin was observed (fig. 2). Data obtained and our data on the absence of significant changes in titin and nebulin genes expression point to the increased proteolysis of these proteins in *m. gastrocnemius* and *m. tibialis anterior* of mice in conditions of space flight. These destructive changes will certainly lead to impairments in contractility of the studied muscles. An increased titin phosphorylation level, particularly T2-fragment will also contribute to a decrease in the contractile activity of *m. gastrocnemius*. This conclusion is based on *in vitro* data that was obtained earlier by us and this data indicate that an increase in titin phosphorylation level leads to decrease of actin-activated myosin ATPase activity [12].

References

1. Grigor'ev A.I., Kozlovskaia I.B., Shenkman B.S. The role of support afferents in organisation of the tonic muscle system // Ross. Fiziol. Zh. Im I.M. Sechenova. 2004 May; 90(5):508-21.

2. Riley D.A., Bain J.L., Thompson J.L., Fitts R.H., Widrick J.J., Trappe S.W., Trappe T.A., Costill D.L. Thin filament diversity and physiological properties of fast and slow fiber types in astronaut leg muscles // J. Appl. Physiol. (1985). 2002 Feb; 92(2):817-25.

3. Ikemoto M., Nikawa T., Takeda S., Watanabe C., Kitano T., Baldwin K.M., Izumi R., Nonaka I., Towatari T., Teshima S., Rokutan K., Kishi K. Space shuttle flight (STS-90) enhances degradation of rat myosin heavy chain in association with activation of ubiquitin-proteasome pathway // FASEB J. 2001 May; 15(7):1279-81.

4. Talmadge R.J., Roy R.R., Edgerton V.R. Distribution of myosin heavy chain isoforms in non-weight-bearing rat soleus muscle fibers // J. Appl. Physiol. 1996 Dec;81(6):2540-6.

5. Toursel T., Stevens L., Granzier H., Mounier Y. Passive tension of rat skeletal soleus muscle fibers: effects of unloading conditions // J. Appl. Physiol 2002 Apr;92(4):1465-72.

6. Shenkman B.S., Nemirovskaya T.L., Belozerova I.N., Vikhlyantsev I.M., Matveeva O.A., Staroverova K.S., Podlubnaya Z.A. Effects of Ca2+-binding agent on unloaded rat soleus: muscle morphology and sarcomeric titin content. // J. Gravit. Physiol. 2002 Jul; 9(1):P139-40.

7. Podlubnaia Z.A., Vikhliantsev I.M., Mukhina A.M., Nemirovskaia T.L., Shenkman B.S. Sarcomeric cytoskeletal proteins and myosin phenotype in stretched soleus of hindlimb-suspended rats // Biofizika. 2004 May-Jun; 49(3):424-9.

8. Udaka J., Ohmori S., Terui T., Ohtsuki I., Ishiwata S., Kurihara S., Fukuda N. Disuse-induced preferential loss of the giant protein titin depresses muscle performance via abnormal sarcomeric organization // J. Gen. Physiol. 2008 Jan; 131(1):33-41. doi: 10.1085/jgp.200709888.

9. Vikhlyantsev I.M., Podlubnaya Z.A. New titin (connectin) isoforms and their functional role in striated muscles of mammals: facts and suppositions // Biochemistry (Mosc). 2012 Dec; 77(13):1515-35. doi: 10.1134/S0006297912130093.

10. Lipets E.N., Ponomareva E.V., Ogneva I.V., Vikhliantsev I.M., Karaduleva E.V., Kratashkina N.L., Kuznetsov S.L., Podlubnaia Z.A., Shenkman B.S. Contractile properties of fibers and cytoskeletal proteins of gerbil's hindlimb muscles after space flight // Aviakosm. Ekolog. Med. 2009 May-Jun; 43(3):34-9.

11. Okuneva A.D., Vikhliantsev I.M., Shpagina M.D., Rogachevskiĭ V.V., Khutsian S.S., Poddubnaia Z.A., Grigor'ev A.I. Changes in titin and myosin heavy chain isoform composition in skeletal muscles of Mongolian gerbil (Meriones unguiculatus) after 12-day spaceflight // Biofizika. 2012 Sep-Oct; 57(5):756-63.

12. Vikhlyantsev I.M., Okuneva A.D., Shpagina M.D., Shumilina Y.V., Molochkov N.V., Salmov N.N., Podlubnaya Z.A. Changes in isoform composition, structure, and functional properties of titin from Mongolian gerbil (Meriones unguiculatus) cardiac muscle after space flight // Biochemistry (Mosc.). 2011 Dec; 76(12):1312-20. doi: 10.1134/S0006297911120042.

13. Tatsumi R., Hattori A. Detection of giant myofibrillar proteins connectin and nebulin by electrophoresis in 2% polyacrylamide slab gels strengthened with agarose // Anal. Biochem. 1995 Jan 1; 224(1):28-31.

14. Vikhlyantsev I.M., Podlubnaya Z.A., Kozlovskaya I.B. New titin isoforms in skeletal muscles of mammals // Dokl. Biochem. Biophys. 2004 Mar-Apr;395:111-3.

15. Tikunov B.A., Sweeney H.L., Rome L.C. Quantitative electrophoretic analysis of myosin heavy chains in single muscle fibers // J. Appl. Physiol. 2001 May;90(5):1927-35.

16. Borbély A., Falcao-Pires I., van Heerebeek L., Hamdani N., Edes I., Gavina C., Leite-Moreira A.F., Bronzwaer J.G., Papp Z., van der Velden J., Stienen G.J., Paulus W.J. Hypophosphorylation of the Stiff N2B titin isoform raises cardiomyocyte resting tension in failing human myocardium // Circ. Res. 2009 Mar 27;104(6):780-6. doi: 10.1161/CIRCRESAHA.108.193326. Epub 2009 Jan 29.

STABILIZATION OF FLANINE MONONUCLEOTIDE IN ACTIVE CENTER OF NADH DEHYDROGENASE OF MITOCHONDRIA BY ADENOSINE PHOSPHATES AND GUANOSINE PHOSPHATES

N.L. Vekshin, M.S. Frolova

Institute of Cell Biophysics of RAS,
Institutskaya str., 3, Pushchino, 142290, Russia

In recent years, a number of cases of age-related neuromuscular diseases are steadily grown in the world. One of the main reasons, leading to these diseases, is the disruption of the mitochondrial NADH-dehydrogenase – the most huge and important enzyme in respiratory chain. Perhaps, the disruption can be due that the NADH-dehydrogenase losses its coenzyme – flavine mononucleotide (FMN) – a key link in the transfer of electrons from NADH to respiratory chain. As a result, a cell undergoes by oxidative stress and cannot work well.

The FMN molecule is located in a 50 kDa subunit of NADH-dehydrogenase (this subunit contains a pocket for binding of NADH). FMN is connected to the subunit by non-covalent bond and, therefore, the binding is unstable, especially under different treatments: temperature, detergents (0.001%) and so on. FMN can be released even spontaneously, over time. As a result, a transfer of electrons from NADH to the electron transport chain will be blocked. In this case, electrons will be transmitted directly on molecular oxygen and transform it to superoxide anion. Overabundance of superoxide in cells leads to developing of oxidative stress, which may be a cause of many serious molecular diseases, including neurodegenerative ills, such as Parkinson's disease and so on.

FMN is natural fluorophore and, therefore, it can be detected by own fluorescence, without using of special fluorescent probes. Under incubation of isolated mitochondria at 37°C, the FMN molecule over a time (2 hours) spontaneously releases from mitochondria and goes out into a free solution. This process is accompanied by increasing in the intensity of fluorescence and decreasing in the fluorescence polarization degree of FMN. Using this fluorescence spectroscopy approach, we can monitor the kinetics of releasing of FMN from mitochondrial NADH-dehydrogenase. Previously, we have found that the process of releasing of FMN from NADH- dehydrogenase of mitochondria is prevented by NADH or NAD. Thus, NADH and NAD stabilize the enzyme due to their binding in the pocket of active center. When NADH or NAD penetrates into the binding site, the FMN molecule has not a way to pass through the pocket to aqueous phase. Unfortunately, NADH and NAD are hardly can be used as medicine preparations, since they are difficultly penetrate into cells and also they can hamper in a cell the functioning of others NAD-dependent enzymes.

In the presented study, we tested the ability of adenine derivatives (analogues of adenine part of molecule of NAD) and guanine derivatives (analogues of adenine derivatives) to stabilize FMN in NADH-dehydrogenase in isolated rat liver mitochondria, as a simple comfortable model object. In order to amplify the penetration of the tested substances into mitochondria, we used a moderate-hypotonic buffer, containing only 100 mM sucrose and 10 mM Tris-phosphate (pH 7,0). In this buffer, the mitochondrial membranes become more permeable. Also, we used the mitochondria which were defrosted once. One frosting-defrosting does not destroy organelles, but improves the permeability of their membranes and promotes better penetration for substances.

We added 100 mM NADH, 100 mM p-NTV and tested substances (AMP, ADP, ATP, GDP, guanosine etc.) in excess quantity (up to 300 μM) to suspension of mitochondria. The kinetics of increase in optical density due to formation of formazan was measured during 15 min with spectrophotometer PromEkoLab-5400UF at 540 nm. Spectra of flavine fluorescence were recorded with spectrofluorometer SLM-4800 (SLM, Inc., USA) in 1-cm or 0.4-cm cuvettes at 20°C. Flavine fluorescence was excited at maximum of the absorption band at 450 nm and detection was done at maximum of the emission band at 525 nm. In some experiments, where fluorescence intensity was too low, in particular, in the case of measuring of polarization degree, the flavine fluorescence was registered in a special mirror cuvette, allowing amplify the signal at several times.

To detect the localization of FMN after 2 h of incubation (at 37°C), the suspension of mitochondria was passed through 0,2 micron Millipore filter, and then the flavine fluorescence was measured in the obtained filtrate (mitochondria are rest adsorbed on the filter). In addition to flavines and flavoproteins, also protomitochondria (small immature mitochondrial particles) could penetrate through 0,2 micron pores, but they have almost not flavines and therefore do not affect on measurements. In most experiments, mitochondria itself did not hinder on measurement of fluorescence of free FMN, and that is why they were not removed.

Previously, we have shown that the process of output of FMN from the active center of mitochondrial NADH-dehydrogenase can be accelerated by certain factors, in particular by a little quantity of detergents (about 0,001%), as well as prolonged (1–2 h) keeping at moderate temperature (37°C). This observation is in consistent with well-known fact about complete or partial loss of FMN during isolation and purification of the enzyme. The loss of FMN is accompanied by a fall of NADH: ubiquinone reductase activity, but not NADH: ferricyanide reductase activity. This is related to the fact that the FMN molecule is not involved in the second reaction. Also, FMN is not involved in NADH: tetrazolium reductase reaction.

In the present study, we observed a spontaneous release of FMN from mitochondria after their incubation during 2 hours at 37°C. This process was accompanied by sufficient increasing in the intensity of flavine fluorescence and decreasing in polarization degree. The both parameters were measured at $\lambda_{ex} = 450$ nm and $\lambda_{em} = 525$ nm at 20°C. In addition, we measured a tryptophan fluorescence ($\lambda_{ex} = 286$ nm, $\lambda_{em} = 340$ nm) to determine the output of proteins from mitochondria (most

mitochondrial proteins contain tryptophan residues), and fluorescence of 7-aminoactinomycin (λ_{ex} = 530 nm, λ_{em} = 620 nm) to determine the release of mitochondrial DNA (7-aminoactinomycin is well specifically integrated into the unwound DNA regions). However, release of proteins and DNA from mitochondria into free solution was not observed: the intensity of tryptophan fluorescence and 7-aminoactinomycin fluorescence in solution after the 2 h incubation of mitochondria at 37°C and subsequent removal of mitochondria by 0,2 micron filters was negligible. This means that mitochondrial membranes remained generally intact.

Intensity of flavine fluorescence in control samples was enhanced after 2 hours incubation by 2–3 times. There are two reasons for it, namely: 1) increasing in the absorption of the exciting light by FMN due to releasing from light-scattered particles, 2) increasing in fluorescence quantum yield of FMN due to change in the environment.

It should be noted that some contribution to the total flavine fluorescence of mitochondrial suspension gives flavine adenine nucleotide (FAD), which are tightly covalently associated with several mitochondrial dehydrogenases. But the *change* in the flavine fluorescence intensity belongs mainly due to release of FMN from NADH-dehydrogenase into solution. FAD molecules of mitochondrial flavoproteins do not give any significant contribution to the change of fluorescence, because FAD molecules remain covalently bound with their enzymes. Fluorescence quantum yield of FAD is 2 times low then FMN. Besides, flavine fluorescence of mitochondria is low due to scattering of excitation light on each single mitochondrial particle, i.e. a number of photons cannot be absorbed by FAD. Also, the FAD fluorescence in mitochondria may be particularly quenched by aromatic amino acids and iron-sulfur clusters.

In addition to recording of flavine fluorescence intensity, we measured the polarization degree of flavine fluorescence. This parameter gives us knowledge about rotation of FMN, i.e. a free flavine can be easy differently detected, separately of a bound flavine. Polarization degree of the bound flavine is high due to a short lifetime of the excited state and low rotational mobility of the flavine within the protein. When FMN releases into aqueous solution, the polarization degree is decreased, because the velocity of rotation is greatly increased in aqueous phase (also, the lifetime is increased - due to disappearing of scattering of excitation light on the particles and due to lack of quenching by iron-sulfur clusters). In our experiments, the polarization degree of flavine fluorescence was decreased after incubation at 37°C over 2 hours to 1,5–2 times.

For checking the place, from where FMN emits - from mitochondrial matrix or from external solution – we measured the intensity and polarization degree of filtrates, which were obtained by filtration of mitochondrial suspensions (before and after 2 hours incubation at 37°C) through 0,2 micron Millipore filters. The intensity of fluorescence of the filtrate was strongly increased (after 2 hours incubation of mitochondria) up to 4,5 times. The fluorescence polarization degree of the filtrate was reduced greatly – to 0,06, which corresponds to free rotation of FMN in water. The obtained data clearly indicate that almost all FMN molecules are released (as a free form) from mitochondria to the external solution.

Flavine fluorescence changes in our experiments are not associated with processes of oxidation / reduction of flavines, because incubation of mitochondria during 2 hours in most of our experiments was performed in the absence of NADH, succinate and other reducing or oxidizing agents. Only in one case - the using of NADH – two phenomena during incubation took place at the same time: the reduction of fluorescent FMN to non-fluorescent FMN-H2 and stabilization of FMN in the enzyme. Since the reduced form of flavine FMN-H2 has disintegrating electron clouds and is unstable (electrons are rapidly transferred into respiratory chain), the FMN-H2 quickly returns to FMN – the oxidized fluorescent form. Thus, it is unlikely that any red-ox transitions FMN / FMN-H2 make a significant contribution to the observed changing of flavine fluorescence.

We tested as stabilizers of FMN in NADH-dehydrogenase of mitochondria the following group of substances: adenine, adenosine, ATP, ADP and AMP (they are analogs of adenine part of NAD) and also nicotinic acid and nicotine amide (they are analogs of the nicotine part of NAD). The best stabilizers are AMP, ADP and ATP.

Also, we tested the more distant analogs of NAD: cAMP, caffeine, GMP, GDP, GTP, cGMP, UDP, CDP, inosine and IMP. When adding of GTP, GDP and GMP at a concentration of 300 µM to the suspension of liver mitochondria was done with subsequent cultivation during 2 hours at 37°C, the intensity of flavine fluorescence was increased in 1,6, 1,8 and 1,8 times, respectively (compared to the initial level). It is less in 2,4, 2,1 and 2,0 times comparing to the control. For comparison, the intensity of flavine fluorescence under the same conditions in the presence of ATP, ADP and AMP was changed lesser than in the control experiments, in 1,8, 2,0 and 1,7 times.

The obtained data clearly shows that the used purine phosphates inhibit the release of FMN from NADH dehydrogenase of mitochondria and, therefore, stabilize the enzyme.

Flavine fluorescence polarization degree in the presence of GTP, GDP and GMP in comparison with the control sample (without adding substances) was greater in 1,7; 1,5 and 2,0 times, respectively. This indicates that presence of these substances allow FMN to be remained in association with the enzyme.

We also tested how these substances affect on enzymatic oxidation of NADH. In presence of guanosine phosphates the kinetics has some small decrease in the velocity at the end of the reaction (comparing to the control sample). It can be concluded that GTP, GDP and GMP (unlike of adenine nucleotides) depress at some small degree on the enzymatic activity of NADH-dehydrogenase. In the used concentrations, they a bit compete with NADH for the active centre of the enzyme.

In order to clear the importance of phosphate groups in stabilization of the enzyme, we conducted the investigation with guanine and caffeine (these purines do not contain phosphate). Also, two pyrimidine di-phosphates – UDP and CDP – were tested. When guanine or caffeine was added (in concentration of 300 μM) to suspension of mitochondria, the flavine fluorescence intensity and polarization degree were changed like in the control sample. Thus, it is no influence. After addition of UDG or CDG to mitochondrial suspension under the same conditions, the intensity of flavine fluorescence was also changed like in the control. Thus, it is no influence.

We have also tested cAMP and cGMP. In these cases also the intensity and polarization of flavine emission were changed as in the control sample.

The influence of inosine on the flavine emission of mitochondria was negligible. Action of inosine mono-phosphate (IMP) was not too expressed.

Thus, these tested compounds are hardly could be used as potential stabilizers of NADH-dehydrogenase.

A number of researchers stated that the NADH-dehydrogenase has two binding site. It was assumed that NADH is oxidized to NAD in the first site, but NAD is reduced to NADH in the second one. If so, we can suggest a hypothesis that such analogues of NAD, which stabilize the molecule of FMN in the enzyme (GMP, GDP, GTP, AMP, ADP, and ATP), bind with the second center and stabilize it, mechanically preventing exit of FMN from the enzyme into solution (especially if the first center is oc-cupied by molecule of NADH or NAD). Guanine phosphates and adenine phosphates did not compete with NADH for the first binding site, since binding constant for NADH, as well-known, is very high ($\sim 10^5 \, M^{-1}$). That

is why they do not inhibit the NADH:tetrazolium reaction even at 300 μM concentration. Obviously, guanine and adenosine phosphates interact with the second center or may be they have any own binding site in NADH-dehydrogenase.

In summary, we go to conclusion that guanosine phosphates (GTP, GDP, GMP) as well as adenosine phosphate (ATP, ADP, AMP) effectively prevent the release of FMN from NADH-dehydrogenase of mitochondria.

Because of adenosine phosphates and guanosine phosphates are involved in the energy metabolism, their real content in living cells depends on many biochemical processes. In particular, a balance between amount of phosphorylated and dephosphorylated derivatives may significantly vary, depending on the activity of ATP-ases and other enzymes. Introduction into cells an excess amount of adenosine phosphates or guanosine phosphates will not cause any disorder in intracellular balance, but may temporarily stabilize the mitochondrial NADH-dehydrogenase.

It is no accident that AMP and ATP are currently used in sport medicine, as well as for the treatment of muscular dystrophy, chronic coronary insufficiency and myocardial dystrophy.

Guanosine phosphates are mainly involved in regulatory mechanisms. Therefore, they should be more carefully examined on their effects on the human body in possible treatment of neuromuscular diseases. Also, a number of chemical analogues of AMP and GMP could be synthetized in future and tested for prevention and treatment of mitochondrial aging and neurodegenerative diseases.

Table 1. Influence of NADH and its analogs (300 μM) on the intensity and polarization degree of flavine fluorescence of mitochondria during 2 hours incubation at 37°C. The initial intensity was taken as 100%, the initial polarization degree was 0,32

The substance name	Intensity, %	Degree of polarization
Control	241	0,11
Adenine	307	0,18
Adenosine	256	0,2
AMP	142	0,2
ADP	122	0,21
ATP	133	0,22
NADH	199	0,21
NAD^2	185	0,25
Nicotine amid	336	0,15
Nicotinic acid	322	0,12

Table 2. Influence of NADH and its analogs (300 μM) on the intensity and polarization degree of flavine fluorescence of mitochondria during 2 hour incubation at 37°C. The initial intensity was taken as 100%, the degree polarization was 0,25

The substance name	Intensity, %	Degree of polarization
Control	366	0,11
Guanine	295	0,12
GMP	183	0,19
GDP	178	0,17
GTP	155	0,19
Caffeine	369	0,08
cGMP	348	0,15
cAMP	345	0,15
UDP	214	0,11
CDP	184	0,11
Inosine	366	0,09
Inosine phosphate	317	0,09

MATHEMATICAL MODELING OF RHYTHM DISTURBANCES INDUCED BY ENHANCED I$_{Na}$ IN HETEROGENEOUS MYOCARDIUM

N.A. Vikulova[1], A.D. Vasilyeva[1,2]

[1]*Institute of Immunology and Physiology of the Ural Branch of the Russian Academy of Sciences, 106 Pervomayskaya st., Yekaterinburg, 620049, Russia;*
[2]*Ural Federal University named after the first President of Russia B.N. Yeltsin, Mira str., 19, Ekaterinburg, 620002, Russia*

The most common cause of the heart rhythm disturbances is a disruption of conductivity, which might result in abnormality of cardiac pump function. In some cases, arrhythmia is invoked by disturbances in electrophysiological activity of cardiac cells resulting in local spontaneous excitation of myocardium. An abnormal excitation could originate not only from pacemaker cells, but also from ventricular myocytes. It is recently shown that mechanical events in the heart could contribute to the rhythm disturbances along with electrophysiological conditions. Thus, experimental and theoretical studies confirm that local deformations and loading can change electrophysiological characteristics of cardiomyocytes (Carmeliet et al., 2002). For instance, disorder in mechanical de-

formations of the pathological myocardial tissue during the cardiac cycle can induce rhythm disturbances under calcium overloading resulted from Na^+-K^+ pump attenuation (Sulman et al., 2008).

Using mathematical model we study effects of the mechanical factors on the development of rhythm disturbances induced by an increased density of sodium current (I_{Na}). A gain-of-function mutation in the sodium channel (enhanced I_{Na}) causes distinct clinical syndromes like LQT3 syndrome, heart failure, hypertrophic cardiomyopathy (Moreno et al., 2012).

The heterogeneity as the essential property of the myocardium is considered in our mathematical modeling. Cells from inner subendocardial (ENDO), superficial subepicardial (EPI) and mydmyocardial (MID) layers of the ventricular wall in the normal heart differ in their electrophysiological and mechanochemical characteristics, reaction on heart rhythm changes and on pharmacological exposure (Markhasin et al., 2004).

In our previous studies, we have developed a mathematical model of subendocardial (ENDO model) and subepicardial (EPI model) cells based on the 'Ekaterinburg-Oxford' model (EO model) of isolated ventricular cardiomyocyte (Katsnelson et al., 2011). The ENDO and EPI models allows to reproduce transmural peculiarities of the action potential generation, membrane ion currents and flows, calcium-dependent mechanisms of contraction and force generation (Vasilyeva & Solovyova, 2012).

In the framework of single ENDO and EPI models we have shown that during isometric contractions (force generation under the fixed cell length) the enhanced I_{Na} resulted in early afterdepolarizations (EAD) in the ENDO model, but not in the EPI model. The arrhythmic changes in the action potential (AP) were accompanied by significant force alterations. Rapid fall down of isometric force from twitch to twitch was followed by subsequent recovery in several beats (Vasilyeva et al, 2014).

Then ENDO and EPI models were tested under afterloaded conditions. Isometric (fixed length) and isotonic (fixed load) modes interchanged during afterloaded twitch. Increased I_{Na} induced the similar responses in the ENDO model as like in isometric conditions whatever afterload was applied. Afterload twitch and the AP generation had the same pattern in the EPI model under high loads. However, spontaneous excitations had been only obtained during the low-load mode of contraction. The rhythm disturbance was followed by completely stopped cell shortening (Vasilyeva et al, 2014).

In present study, ENDO and EPI models were used as elements of a continuous 1D mathematical model of a cardiac muscle fiber, in which

mechanical and electrotonic interaction between cells was implemented (Vasilyeva et al., 2013). Under experimental data, we have constructed a virtual fiber of 2 mm length, consisting 40%ENDO-40%MID-20%EPI models imitating the transmural heterogeneity of the ventricular wall. Parameters for MID cells were linearly changed from EPI to ENDO parameters. In agreement with experimental data, the stimulation signal for excitation of the fiber was applied to the ENDO layer of the fiber. The depolarization wave spread along the fiber to the EPI layer with velocity 0.5 m/s (Kanai &Salama, 1995).

The developed 1D model of the transmurally heterogeneous fiber has been used for reproducing rhythm disturbances induced by the enhanced I_{Na}. Isometric (fixed fiber length) and afterloaded (fixed load equal to 0.1 of maximum isometric force) conditions were applied to the fiber similarly to it was made at the single ENDO and EPI models. The density of sodium current I_{Na} was increased in each cell of the fiber. First 11 twitches were considered.

Although the single EPI cell was not susceptible to the enhanced I_{Na} during isometric conditions we have obtained an early afterdepolarization along the whole fiber due to electrotonic interaction between cells of EPI, MID and ENDO layers. The pattern of EADs differed from cycle to cycle interchanging pronounced disturbances of the AP generation with prolonged repolarization, less expressed EADs and underlined instability of mechanical behavior of the heterogeneous fiber under isometric conditions. Amplitude of isometric force generated by the fiber in cycles with pronounced disturbances of APs was higher than in the cycles following them and tended to increase from cycle to cycle.

The abnormalities in the AP generation during the low-loaded isotonic contraction in the fiber were not so significant comparing with isometric conditions. Nevertheless, EADs have arisen in the stimulated ENDO layer and have spread along the fiber. We have not observed the stop of any cell shortening as it was in the case of the single EPI model. Moreover, the amplitude of the fiber shortening during afterload twitches increased from cycle to cycle.

In conclusion, the 1D modeling of transmurally heterogeneous cardiac fiber suggest that the enhanced I_{Na} results in rhythm disturbances and uncoordinated mechanical activity. The appearance of obtained EADs depends on mechanical conditions applied to the fiber. The electrotonic and mechanical interaction between cells within the fiber results in more similar response of the individual ENDO and EPI cells within the fiber than they demonstrate in isolated conditions.

References

1. Carmeliet E., Vereecke J. // Springer. 2002. Vol. 9.
2. Kanai A., Salama G. // Circ Res. 1995, V.77(4), p.784-802.
3. Katsnelson L.B., Solovyova O., Balakin A., Lookin O., Konovalov P., Protsenko Y., Sulman T., Markhasin V.S. // Prog Biophys Mol Biol. 2011, V.107(1), p.81-89.
4. Markhasin V.S., Balakin A.A., Gur'ev V.Yu., Lukin O.N., Konovalov P.V., Protsenko Yu.L., Solov'eva O.E. // Ross Fiziol Zh Im I M Sechenova. 2004 Aug;90(8), PP. 1060-77.
5. Moreno J.D., Clancy C.E. // J Mol Cell Cardiol. 2012, V 52, p. 608-619.
6. Sulman T., Katsnelson L.B., Solovyova O., Markhasin V.S. // Bull Math Biol. 2008, V. 70(3), P. 910-949.
7. Vasilyeva A., Solovyova O., Markhasin V.S. // Biophysical Journal. 2014. Abstracts. San Francisco. P. 731a.
8. Vasilyeva A., Solovyova O. // Comput Cardiol. 2012. V.39: p.453-456.
9. Vasilyeva A.D., Vikulova N.A., Markhasin V.S., Solovyova O.E. // Abstracts. Rostov-on-Don, 2013. P. 34.

EFFECTS OF SHORT-TERM GRAVITATIONAL UNLOADING ON NO-DEPENDENT SIGNALING PATHWAYS IN HUMAN SKELETAL MUSCLE

N.A. Vilchinskaya, T.M. Mirzoev
*SSC RF-Institute of Biomedical Problems, RAS,
Khorochevskoe Shosse 76 a, Moscow, 123007, Russia*

Currently little is known about functioning of NO-dependent signaling systems in human skeletal muscles during early stages of gravitational unloading. It is known that during the initial period of gravitational unloading of skeletal muscles there is an accumulation of calcium ions, resulting in activation of calcium-dependent proteases – calpains (Ingalls et al., 1999; Shenkman., Nemirovskaya 2008, Алтаева Э.Г. и др., 2010). Calpains play a key role in degradation of a number of cytoskeletal proteins (Bartoli et all, 2004). Previously it has been shown that NO can inhibit calpain activity and prevent atrophy of the skeletal muscle (Tidball et al., 1999). The aim of the study was to investigate the mechanisms regulating catabolic signaling pathways in human m.soleus at early stages of gravitational unloading.

The study was conducted on 13 individuals, aged 20-26 years. Dry immersion was used as a ground model of hypogravity. The duration of immersion was 3 days. After immersion, muscle samples of m.Soleus were taken under local anesthesia, using biopsy technique. The content of desmin, total and phosphorylated nNOS, phosphorylated AMPK was determined using western-blotting technique.

After 3-day dry immersion 10% (p <0.05) decrease of cytoskeletal protein desmin was observed in m.soleus compared to pre-immersion level. Also, there was a 43% (p <0.05) decrease of phosphorylated nNOS and 26% decrease of total nNOS compared to pre-immersion value. Besides after 3-day dry immersion we detected a 36% (p <0.05) decrease of phosphorylated AMPK in m.soleus compared to pre-immersion value.

Thus, our data suggest that calpain-dependent processes are likely to develop at an early stage of gravitational unloading. We assume that decrease of AMPK phosphorylation leads to a decrease of nNOS phosphorylation, resulting in reduction of NO-synthesis.

MOLLUSCAN SMOOTH (CATCH) MUSCLE CONTAINS A TROPONIN-LIKE PROTEIN

I.G. Vyatchin, N.S. Shelud'ko

Zhirmunsky Institute of Marine Biology, Far Eastern Branch of the Russian Academy of Sciences, Palchevsky str. 17, Vladivostok, 690059, Russia

The regulation of thin filaments from bivalve smooth muscles is supposed to be caldesmon type [1, 2]. However, we have not confirmed caldesmon presence in smooth muscle of mussel *Crenomytilus grayanus* and managed to get from this muscle a caldesmon-free fraction providing rabbit actomyosin with Ca^{2+}-sensitivity [3]. This fraction contains filamin, actin, calponin, tropomyosin, and several unidentified proteins (fig. 1a). Using chromatographic separation methods proposed for obtaining components of troponin [4], we have isolated from this fraction three components with molecular weights of 19, 20, and 26 kDa (fig. 1), which have the same properties that are known for troponin subunits - inhibiting (TnI), Ca^{2+}-binding (TnC), and tropomyosin binding (TnT) (fig. 2).
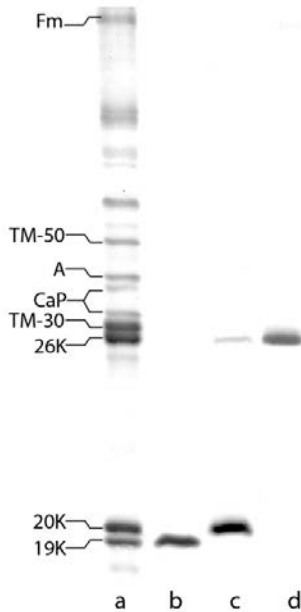
Fig. 1. Composition of Ca2+-sensitive fraction (a) and isolated Tn-like components: 19 kDa (b), 20 kDa (c) and 26 kDa.

The 20 kDa component inhibits actomyosin Mg^{2+}-ATPase activity in the same manner as TnI does [5] (fig. 2). In addition, the 20 kDa component is similar to TnI [5] in its solubility and has the same electrophoretic mobility [6] (fig. 1c).

The calcium-binding component of the mussel thin filaments is an acidic protein of about 19 kDa molecular weight, as TnC also is [7]. Moreover, this protein, like TnC, at the same time relieves the 20 kDa protein inhibitory effect on Mg^{2+}-ATPase activity and confers a moderate Ca^{2+}-sensitivity to actomyosin [8] (fig. 2).

The 26 kDa protein is similar to vertebrate TnT. First, it interacts with actin-tropomyosin complex, as TnT does [9]. Secondly, like TnT [10], this protein per se does not affect the Mg^{2+}-ATPase activity, but enhances the inhibitory action of 20 kDa protein on this activity (Fig. 2). Finally, the 26 kDa protein, like troponin T [11], greatly increases calcium sensitivity confered to actomyosin by 19 kDa and 20 kDa protein complex (fig. 2).

The properties of the protein components isolated in our study and their effect on Mg^{2+}-ATPase activity suggest that these proteins are troponin-
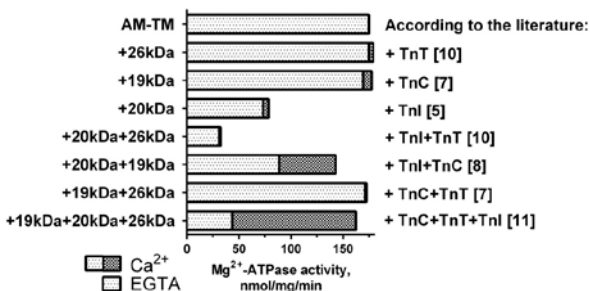
Fig. 2. Effect of 19, 20, 26-kDa proteins and mussel tropomyosin on the Mg^{2+}-ATPase activity of rabbit actomyosin.

like; therefore, thin filaments of the smooth catch muscle of the mussel *Crenomytilus grayanus* possess not caldesmon, but troponin regulation.

References

1. Marston S.B., Lehman W. // Biochem. J. 1985. v. 231, p. 517-522.
2. Bennet P.M., Marston S.B. // J. Muscle Res. Cell Motil. 1990. v. 11(4), p. 302-312.
3. Dobrzhanskaya A.V., Vyatchin I.G., Lazarev S.S., Matusovsky O.S., Shelud'ko N.S. // J. Muscle Res. Cell Motil. 2013. v. 34(1), p. 23-33.
4. Ojima T., Nishita K. // Biochem. J. 1988. v. 104(1), p. 9-11.
5. Perry S.V., Cole H.A., Head J.F., Wilson F.J. // Cold Spring Harb. Symp. Quant. Biol. 1973. v. 37, p. 251-262.
6. Ebashi S., Wakabayashi T., Ebashi F. // Biochem. J. 1971. v. 69, p. 441-445.
7. Ebashi S., Ohtsuki I., Mihashi K. // Cold Spring Harb. Symp. Quant. Biol. 1973. v. 37, p. 215-224.
8. Greaser M., Gergely J., Griaser M. // J. Biol. Chem. 1971. v. 246, p. 4226-4233.
9. Ojima T., Nishita K. // J. Biol. Chem. 1986. v. 261, p. 16749-16754.
10. Eisenberg E., Kielley W. // J. Biol. Chem. 1974. v. 249(15), p. 4742-4748.
11. Ebashi S. // Biochem. J. 1972. v. 72(3), p. 787-790.

EFFECT OF HYPOTHERMIA ON MOTOR RECOVERY AFTER SPINAL CORD INJURY

G.G. Yafarova, L.R. Zaripova, A.R. Hazieva, T.V. Baltina
Kazan Federal University, Kremlevskaya str., 18, Kazan, 420008, Russia

Immediate treatment of acute spinal cord injury with hypothermia may have high potential when used alone or in combination with pharmacological treatment due to reducing energy requirements, apoptotic cell death, and oxidative stress.

Investigation of the functional state of the motor centers in the spinal cord before and after experimental spinal cord injury in dogs using a local intraoperative hypothermia. Injury was applied at a level L1.

Refrigerant is a frozen 0.9% NaCl solution for infusion, which was placed in a decompression window of vertebral dura. Optimal exposure time were selected experimentally, using histological control. All manipulations were performed in compliance with bioethical norms. Electroneuromyographic study was performed before surgery, as well as in acute and early periods of traumatic spinal cord disease. Using needle electrodes were recorded H and M responses of square muscle after stimulation of the tibial nerve with subsequent analysis of their parameters. Stimulation of the tibial nerve and increased electrical responses of muscle electromyogram was performed by the firm "Medicor" (Hungary), the intensity of stimulation ranged from 0.35 to 60 V and 0.5 ms duration. The studied parameters were the threshold, latency and maximum amplitude of the detected H-and M-responses, as was determined the ratio of maximum amplitudes of these responses (Hmax/Mmax). After surgery the rats exhibited movement disorders, neurological status of animals is estimated at 5 points on a scale of Bagley, which corresponds to the least severe spinal cord injury.

The results showed that the using of 20-minute Local hypothermia after experimental spinal cord contusion, the ratio of Hmax/Mmax does not exceed the reference level. It is indicating that we get the inhibition of excitability of spinal motoneurons. At a similar spinal cord injury in dogs without the any interventions, the reflex excitability of spinal motor neurons in the posttraumatic period was increases as well as we observed spasticity of hind limbs. Thus, the use of local hypothermia of the spinal cord during the surgery improves outcomes after spinal cord injury. This research was supported by the Russian Foundation for Basic Research № 13-04-01746 a.

THE SYNAPTIC PLASTICITY OF NEURONS IN LAYER IV OF SOMATOSENSORY CORTEX OF NEWBORN RATS

A.V. Yakovlev, E.A. Minkina, G.F. Sitdikova, R.N. Khazipov
Kazan (Volga Region) Federal University , Russia, Kazan

Sensory experience during early postnatal development modifies cortical connections and form responses of cortical neurons transforming immature neuronal circuits in the well-organized neuronal network of the adult brain. One of the well-studied systems for research development and formation of thalamocortical synaptic plasticity is the cortical

representation of vibrissae (barrels) in the somatosensory cortex of the rat. It is known, that one of the mechanism of synaptic plasticity is the temporal correlation between pre- and postsynaptic neuronal activity. Does this rule in developing thalamocortical synapses during the critical period remains poorly known.

To analysis of synaptic plasticity in the somatosensory cortex of newborn rats experiments were performed on thalamocortical brain slices of rats aged 4 to 8 days after birth. Using extracellular and bipolar stimulation electrodes the evoked synaptic response in IV layers of neurons in the cortex was recorded. To investigate the temporal correlation between pre- and postsynaptic neuronal activity in IV layers of the somatosensory cortex using paired stimulation of thalamic projections (stimulation electrode placed in the VPM thalamic nucleus or white matter of the cortex) and the axons of IV layers neurons (stimulation electrode placed in II/III layers of somatosensory cortex) by driving antidromic action potential.

Long-term synaptic depression in thalamocortical synapses of IV layers neurons was observed when, the antidromic action potentials in axons of principal cells at 5 - 10ms preceded the presynaptic neurotransmitter secretion trigger of the stimulation of thalamic projections. In this case, the amplitude of excitatory postsynaptic potentials decreased to 25-30% of control after paired stimulation. If the activation of thalamic ascending pathways occurred over 10- 15ms before the arrival of antidromic action potential, the cortical IV layer neurons formed long-term synaptic potentiation and the amplitude of synaptic response increased to 40-55 % of control after the paired stimulation.

Thus, we have shown that the IV layers of the somatosensory cortex of the first postnatal week in the formation of synaptic potentiation and depression depends on the time of spikes in the pre- or postsynaptic neuron.

EFFECT OF NITRIC OXIDE ON THE PROCESS OF EXOCYTOSIS OF SYNAPTIC VESICLES FROM MOUSE MOTOR NERVE ENDINGS OF MUSCLES DIAPHRAGM AND SOLEUS

O.V. Yakovleva, E.D. Kurmashova, G.F. Sitdikova
Kazan (Volga Region) Federal University,
Kremlevskaya str., 18, Kazan, 420008, Russia

Nitric oxide (II) (NO) is the first gaseous mediator which functions have been fully explored in various systems of the body. It is known that

NO reduces the transmitter release from in neuromuscular junction of cold-blooded animals and slows down the recycling of synaptic vesicles in warm-blooded animals. The aim of our study was to investigate the action of NO on transmitter release from motor nerve endings in muscles of different types.

Materials and methods

Experiments were performed on isolated neuromuscular preparations of diaphragm and soleus muscles of laboratory white mice. The dye reversibly bounds to the presynaptic membrane and during endocytosis gets ("is loaded") into the newly formed synaptic vesicles. Dye loading is accompanied by the fluorescence of the nerve ending, which reflects the aggregates of the vesicles that have captured the dye. Endocytosis processes were investigated using the following protocols. FM 1-43 was present in the solution for 1 min during the 50 Hz stimulation of the motor nerve and for 7 min after its termination ("full loading"). Then the loaded nerve terminals were stimulated at 50 Hz for 20 minutes and a decrease in the fluorescence intensity was observed ("unloading"). Soleus nerve stimulation was performed for 15 minutes with following pattern: 5 sec at 1 Hz and 10 s at 10 Hz.

The fluorescence of nerve endings was observed using MIKMED-2 (LOMO, St. Petersburg) or AxioScope A1 (Carl Zeiss, Germany) microscopes through water immersion objectives LUMPLFL 60x/0.9-NA (Olympus, USA) and/or Plan-Neofluar 63x/0.9 (Carl Zeiss, Germany). All observations were made only for nerve endings in the most superficial layers of tissues. Fluorescence patterns were recorded with high-speed black-and-white video cameras AxioCam MRm (Carl Zeiss, Germany). The mean fluorescence intensity was estimated in arbitary units (AU), taking the maximum pixel fluorescence of 256 as 1. Then background fluorescence was determined as the mean fluorescence intensity in a 50 x 50 square of pixels in the image area without nerve ending. The background value was then subtracted from each pixel obtained after image averaging. All data were processed by the methods of variation statistics. The quantitative results are presented as the mean value ± standard deviation; n is the number of independent experiments.

In experiments NG-nitro-L-arginine methyl ester (LNAME 100 mkM) the inhibitor of NO synthesis was used.

Results

In control the high frequency stimulation of diaphragm motor nerve induced the decrease of nerve terminals fluorescence which

reflected the process of exocytosis of synaptic vesicles preloaded with FM 1-4. By 30 seconds of stimulation to $79 \pm 3\%$, 1 minute - 64 ± 3 % to 3 min - to $51 \pm 3\%$ to 6 min - to $41 \pm 4\%$ for 20 min - $30 \pm 1\%$. (n = 11) compare to the initial value.

In the presence LNAME (100 mkM) the unloading process was slower than in control and by 30 seconds of high-frequency stimulation the fluorescence intensity was $83 \pm 6\%$, by 60 seconds - $78 \pm 6\%$, 3 min - $64 \pm 5\%$, 6 min - $50 \pm 3\%$, 20 min - to $36 \pm 2\%$.(n = 9) compare to the initial value.

Stimulation of soleus muscle induces the exocytosis of synaptic vesicles followed by unloading of motor nerve terminals by 30 seconds - to $79 \pm 6\%$, by 1 minute - $68 \pm 8\%$ to 3 min - $57 \pm 6\%$, by 6 min - $50 \pm 4\%$, by 15 min - to $46 \pm 4\%$. (n = 9) compare to initial value. In the presence of LNAME (100 mkM) there were no significant differences in unloading process of motor nerve terminals. By to 30 seconds of stimulation the fluorescence intensity was $86 \pm 2\%$, by 60 seconds - $76 \pm 5\%$, by 3 min - $63 \pm 5\%$, byr 6 min - $51 \pm 5\%$, by 20 min - $44 \pm 4\%$.(n = 8) compare to initial value.

Thus it was shown than in diaphragm muscle the inhibition of NO synthesis slowed down the process of exocytosis of synaptic vesicles, which indicated on the participation of this gaseous molecule in regulation of transmitter release in motor nerve ending. In soleus muscle we didn't reveal changes in unloading process of fluorescent dye during inhibition of NO-synthase. It was suggested that these results may be associated with the properties or content of NO-synthase in fast and slow muscle fibres.

AMELIORATION OF RHABDOMYOLYSIS-INDUCED ACUTE KIDNEY FAILURE BY KIDNEY PEPTIDES

I.I. Zamorskii, T.S. Shchudrova
Bucovinian state medical university,
Teatral'naia sq. 2, 58002, Chernovtsy, Ukraine

Rhabdomyolysis is a potentially life-threatening syndrome characterized by the breakdown of skeletal muscle resulting in the subsequent release of intracellular contents into the circulatory system [3]. The causes of acquired rhabdomyolysis are classified as traumatic and non-traumatic. The traumatic ones, such as crush syndrome, accidents, natural disasters, or intense exercise, cause direct muscle injury and rupture of

the sarcolemma. The non-traumatic causes include alcohol abuse, medicines, seizures and coma [2].

Despite the great diversity in the etiology of rhabdomyolysis, the mechanisms involved in the pathogenesis of rhabdomyolysis are direct sarcolemmic injury (trauma) or depletion of ATP within the myocyte, leading to an unregulated increase in intracellular calcium. The increased calcium initiates intracellular processes, such as the activation of phospholipase A2, calcium-dependent neutral proteases, prolonged contraction of muscle cells, mitochondrial dysfunction, and production of reactive oxygen species, which eventually promote disintegration of the myocyte, muscle cell damage and the release of various substances (myoglobin, creatine phosphokinase, potassium, organic acids, and other enzymes and electrolytes) into the systemic circulation, thereby leading to the clinical manifestation of rhabdomyolysis [1, 2].

The complications of rhabdomyolysis include acute renal failure (ARF), cardiac arrhythmias, compartmental syndrome, and disseminated intravascular coagulopathy. It is estimated that 10–40% of cases of rhabdomyolysis leads to ARF, and although interventions have improved, the mortality rate may still be as high as 8% [4]. Myoglobin plays a dominant role in the pathogenesis of rhabdomyolysis-induced ARF include: renal constriction and ischemia, myoglobin cast formation in the distal convoluted tubules, and direct cytotoxic action of myoglobin on the epithelial cells of the proximal convoluted tubules. Recent studies have demonstrated that timely prophylactic and/or early therapeutic interventions ameliorated rhabdomyolysis-induced ARF.

The present study was designed to investigate the renoprotective potential of produced in St.-Petersburg Institute of Bioregulation and Gerontology kidney polypeptide extract and short oligopeptides (T-31, T-35) against rhabdomyolysis-induced kidney dysfunction, oxidative stress and fibrinolysis inhibition. The existing data indicate their regulatory and antioxidant activity, ability to induce cell proliferation and differentiation, reparation of mitochondrial DNA.

Thirty-five non-linear adult white rats were divided into five equal groups: I group - control, II group – modeling of rhabdomyolytic ARF by intramuscular injection of 50% glycerol (8 ml/kg), III group - glycerol (8 ml/kg) and polypeptide kidney extract (300 μg/kg), IV group - glycerol (8 ml/kg) and oligopeptide T-35 (3 μg/kg), V group - glycerol (8 ml/kg) and oligopeptide T-31 (3 μg/kg). Kidney extract and oligopeptides were administered during seven days before glycerol administration. After 24 h

of glycerol administration urine, blood and kidney samples were collected. Data were compared by SPSS Statistica 17.0 software and Mann-Witney test at $p \leq 0.05$. Glycerol administration induced marked renal failure, characterized by increased plasma creatinine and creatinine excretion, reduced diuresis and glomerular filtration rate (GFR), increased protein, titrated acids and ammonium excretion along with high levels of sodium and potassium excretion on the base of inhibition of their reabsorption. This was associated with decrease in the activity of renal glutathione-peroxidase (GPX), catalase (CAT), and increased malondialdehyde (MDA), oxidative modification of proteins (OMP) levels compared with control group. The enzymatic fibrinolytic activity in the kidneys was significantly decreased compared to a control group.

Pretreatment with oligopeptides improved kidney function compared with the untreated group: diuresis increased by 1.25 times in polipeptide extract treated group, by 1.85 times in T-35 treated group and by 1.77 times in T-31 treated group, protein excretion decreased by 3.3, 7.9 and 3.3 times simultaneously. Polipeptide extract and T-31 didn't affect significantly creatinine excretion and GFR while T-35 increased GFR by 3.4-fold. All studied peptides decreased standardized sodium excretion: polypeptide extract by 2.4 times, T-35 by 6.0 and T-31 by 1.9 times, but only T-35 significantly increased absolute sodium reabsorption by 3.0 times, proximal and distal transport of this ion. Decreased titrated acids and ammonium excretion by 1.7-fold and more was seen in all treated groups of animals. The enzymatic fibrinolytic activity in kidneys was increased by 5.3-fold in polypeptide extract treated group, by 4.5-fold in T-35 treated group and by 5.2-fold in T-31 treated group, as compared with untreated animals.

All peptides have shown significant antioxidant effect under the conditions of ARF. Pretreatment with oligopeptide T-35 increased renal CAT activity by 42% and renal GPX activity by 66.5%, decreased MDA content by 22% and OMP content by 49% as compared with those of untreated animals with ARF. Pretreatment with polypeptide kidney extract increased renal CAT activity by 43% along with decrease of MDA content by 40% and OMP content by 54%. T-31 didn't affect markedly kidney GPX activity and MDA content, but increased CAT activity by 32% and decreased OMP content by 46% compared with untreated group.

The obtained results suggest the renoprotective action of kidney peptides under the conditions of rhabdomyolysis-induced kidney failure with more significant effect of oligopeptide T-35 that points out the marked organospecific action of short peptides.

References

1. Bosch X. Rhabdomyolysis and acute kidney injury / Xavier Bosch, Esteban Poch, Josep M. Grau // N Engl J Med. – 2009. - №361. – P. 62-72.
2. Chatzizisis Y. S. The syndrome of rhabdomyolysis: Complications and treatment / Yiannis S. Chatzizisis, Gesthimani Misirli, Apostolos I. Hatzitolios // Eur J of Int Med. – 2008. - №19. – P. 568–574.
3. Khan F.Y. Rhabdomyolysis: a review of the literature / F.Y. Khan // The Neth J of Med. - 2009. - Vol.67. - №9. – P. 272-283.
4. Korrapati M. Recovery from glycerol-induced acute kidney injury is accelerated by suramin // Midhun C. Korrapati, Brooke E. Shaner, Rick G. Schnellmann / The J of Pharm and Exp Ther. - 2012. – Vol.341. – P.126–136.

USE OF STATINS FOR TREATMENT
OF THE MYOGLOBINURIC ACUTE RENAL FAILURE
CAUSED BY RHABDOMYOLYSIS

I.I. Zamorskii, V.G. Zeleniuk, T.S. Shchudrova

Bukovinian State Medical University,
Teatralna Sq., 2, Chernovtsy, 58002, Ukraine

The muscle damage may be caused by medications, drug abuse, infections, vascular interruption, ischemia-reperfusion, crush injury, improper patient positioning, alcohol ingestion, seizures, extreme exercise, electrical injury, infection, hyperthermia, and steroids and neuromuscular blockade (especially in combination). Rhabdomyolysis and its complications are significant problems for those injured in disasters such as earthquakes and bombings. With heightened suspicion for this disorder, non-traumatic causes are being seen with increasing frequency.

Rhabdomyolysis is a condition in which damaged skeletal muscle tissue breaks down rapidly and leads to the release of ruptured muscle cells' products into the bloodstream. When damaged, muscle tissue rapidly fills with fluid from the bloodstream, including sodium ions. The swelling itself may lead to destruction of muscle cells, but those cells that survive are subject to various disruptions that lead to rise in intracellular calcium ions resulting in continuous muscle contraction and depletion of ATP. The persistent contraction of the muscle cell leads to breakdown of intracellular proteins and disintegration of the cell. Neutrophil granulocytes enter the muscle tissue, producing an inflammatory reaction and releasing reactive oxygen species, particularly after crush injury. Crush syndrome may also cause reperfusion injury. Finally, destroyed muscle

cells release potassium ions, phosphate ions, the heme-containing protein myoglobin, the enzyme creatine kinase and uric acid into the blood. Activation of the coagulation system may precipitate disseminated intravascular coagulation [1].

The incidence of acute renal failure (ARF) in rhabdomyolysis is 10-30%. Rhabdomyolysis may cause ARF by several mechanisms. The most important problem is the accumulation of myoglobin in the kidney tubules. Normally, the blood protein haptoglobin binds circulating myoglobin and other heme-containing substances, but in rhabdomyolysis the quantity of myoglobin exceeds the binding capacity of haptoglobin. As the kidneys reabsorb more water from the filtrate, myoglobin interacts with Tamm-Horsfall protein in the nephron to form casts (solid aggregates) that obstruct the normal flow of fluid; the condition is worsened further by high levels of uric acid and acidification of the filtrate, which increase cast formation. Iron released from the heme generates reactive oxygen species, damaging the kidney cells. In addition to the myoglobinuria, two other mechanisms contribute to renal impairment: low blood pressure leads to constriction of the blood vessels and therefore a relative lack of blood flow to the kidney, and finally uric acid may form crystals in the tubules of the kidneys, causing obstruction. Together, these processes lead to acute tubular necrosis, the destruction of the cells of tubules. Glomerular filtration rate falls and the kidney is unable to perform its normal excretory functions. This causes disruption of electrolyte regulation, leading to a further rise in potassium levels [2].

The main goal of rhabdomyolysis treatment is to treat shock and preserve kidney function. While many sources recommend additional intravenous agents to reduce damage to the kidney, most of the evidence supporting this practice comes from animal studies, and is inconsistent and conflicting. Mannitol acts by osmosis to enhance urine production and is thought to prevent myoglobin deposition in the kidney, but its efficacy has not been shown in studies and there is a risk of worsening renal function. The addition of bicarbonate to the intravenous fluids may alleviate acidosis and make the urine more alkaline to prevent cast formation in the kidneys, but there is limited evidence that it has benefits above saline alone, and it can worsen hypocalcemia by enhancing calcium and phosphate deposition in the tissues. Furosemide, a loop diuretic, is often used to ensure sufficient urine production, but evidence that this prevents renal failure is lacking.

It has been found that drugs from a group of statins had a positive effect on renal functions. Specifically, based on some experimental and

clinical research studies its was found that on the occasions of postischemic and toxic ARF the statins were efficient to improve the renal functions of patients due to their effects on inflammatory mechanisms, the NO, fibrinolysis, prooxidant and antioxidant systems [3].

Our research study was targeted at the examination of statin influence on rhabdomyolytic ARF in rats. *In vivo* studies were carried out using 40 white laboratory rats randomly divided into five groups of 8 animals each. Myoglobinuric ARF was modelled after 50% glycerol solution injected intramuscularly with the dose of 10 ml/kg. An administration of statins (atorvastatin, lovastatin, simvastatin) was conducted intragastrically at 20 mg/kg daily during a week after the ARF simulation. The renal functions and other parameters were assessed 7 days after completion of ARF simulation.

As has been found in our experiments, myoglobinuria caused severe loss in renal function, to illustrate: glomerular filtration rate (GFR) decreased by 2.9 times (p≤0,01), creatinine plasma concentration and protein level in the urine increased by 2 times (p≤0,01), and creatinephosphokinase (CPK) activity in the blood plasma by 1.4 times (p≤0,05). Elevation of CPK activity is seen in this disorder and its activity has been seen to correlate with the GFR (r=0.7). It is worthy of note, that mortality rate within a week after ARF simulation in the group of untreated animals was 10.7%, but neither died owing to statin administration.

Under the conditions of ARF statin-treated rats featured improvements in the excretory functions of kidneys. Characteristically, the best results were found with atorvastatin which caused an increase of diuresis by 1.28 times (p≤0,05), GFR by 2.9 times (p≤0,01) and levels of creatinine excretion by 1.4 times (p≤0,05) (in comparison with the group of untreated animals). A significant impact on proteinuria has been shown: an average decrease in urine protein levels by 1.8 times (p≤0,01) by all of the studied statins.

Myoglobinuric ARF caused an increase in the malonic dialdehyde (MDA) concentration in the kidney tissue of untreated animals by 1.7 times (p≤0,05) and the decrease in glutathione peroxidase (GP) activity in the kidney tissue by 1.2 times (p≤0,05) (in comparison with the intact animals). Atorvastatin reduced MDA content in the kidney tissue by 1.7 times (p≤0,01) and increased GP activity in the kidney tissue by 1.2 times (p≤0,05) as compared with a group of untreated rats.

Furthermore, we have found a number of favourable changes concerning the effects of studied medicinal agents on fybrinolytic and

proteolytic systems. To illustrate: the administration of atorvastatin has demonstrated considerably increased enzymatic and non-enzymatic fybrinolytic activity by 1.4 and 1.7 times (p≤0,01) simultaneously and low molecular weight proteins lysis on an average by 1.6 times (p≤0,01).

It should be emphasized that the CPK activity in the blood plasma of statin-treated rats approached the intact animals' levels confirming the absence of myotoxic effects, caused by statins.

Relying on our data, we may conclude that under the conditions of experimental myoglobinuric ARF certain of studied statins (atorvastatin, lovastatin, and simvastatin) at 20 mg/kg did not cause any aggravation of ARF. Renoprotective properties of statins were shown and verified by significant reduction in proteinuria, and increase in GFR. Atorvastatin have featured high renoprotective properties due to improved prooxidant/antioxidant balances and activation of fybrinolytic and proteolytic systems.

References

1. Vanholder R., Sever M. S., Erek E., Lameire N. Rhabdomyolysis // J. Am. Soc. Nephrol. 2000. № 11. P. 1553–1561.
2. Bosch X., Poch E., Grau J. M. Rhabdomyolysis and Acute Kidney Injury // N. Engl. J. Med. 2009. № 361. P. 62–72.
3. Holmqvist G. N. Statins: indications and uses, safety and modes of action. New York: Nova Science Publishers, Inc., 2009. P. 73–84.

WATER DEFICIT AND ACTIVITY OF MITOCHONDRIAL RESPIRATORY CHAIN COMPLEX I OF PEA SEEDLING

Irina Zhigacheva, Elena Burlakova, Tamara Misharina, Mariya Terenina, Natalya Krikunova

Emanuel Institute of Biochemical Physics, Russian Academy of Sciences, ul. Kosygina 4, Moscow, 119334 Russia

The development and, probability, survival of plant in any case are more dependent on availability of water than on any other environmental factors. Metabolism of plants survived even short-term strong drought could not be recovered [4]. Water deficit modified cell membranes, which affected their functions and disturbed cell metabolism [5]. The alterations occur at the level of glycolipids, monogalactosyl-diacyl-glycerol and digalactosyl-diacyl- glycerol [6, 7]. The content of unsaturated fatty acids decreases in these lipids which results in the decreasing the membrane "fluidity", alteration in the lipid - protein ratio, and eventually in the activity changes of the enzymes associated with membrane, first of all enzymes which enter into complex of electron-transport chain of mito-

chondria and chloroplasts [1]. The energy metabolism plays a significant role in adaptive response of the organism. Mitochondria play a key role in the energy, redox and metabolic processes in cell [8]. As known from the literature, regulators of plant growth and development improve their tolerance to biotic and abiotic stresses, to water deficit in particular [2]. One of such growth regulators is melaphen – a melamine salt of bis(oxymetyl)phosphonic acid [3] :
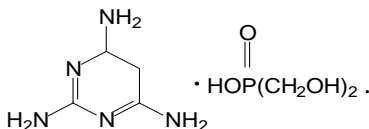
The aim of this work is to study the effect of insufficient watering and the plant growth regulator – melaphen on the fatty acids composition of lipid fraction of mitochondrial membranes and bioenergetical function of 5-day pea seedling mitochondria.

Materials and methods

Plant material. The study was carried out on mitochondria isolated from pea seedlings (Pisum sativum) obtained in standard conditions and in the conditions of insufficient watering. **Pea seeds germination**. The seeds from the control group were washed with soap solution and 0.01 % KMnO4 solution and left in water for 60 min. The seeds from the experimental group were placed in the 2×10^{-12} M melaphen solution for 60 min. After 1-day exposure, half of the seeds from the control group and half of the seeds treated with melaphen were placed onto a dry filter paper in open cuvettes. Two days later the seeds were placed into closed cuvettes with periodically watered filter paper and left for 2 days. On the 5-th day the amount of germinated seeds was calculated and mitochondria isolated.

Isolation of mitochondria from 5-day sprouts epicotyls was performed by a method of [9] in our modification. The isolation medium comprised: 0.4 M sucrose, 20 mM KH_2PO_4 (pH 8.0), 10 mM KCl, 2 mM dithioerythritol, and 0.1% BSA (free of fatty acids).The homogenate was centrifugated at 25000g for 5 min. The second centrifugation was carried out at 3000g for 3 min. The sediment was re-suspended in 2-3 ml of solution contained: 0.4 M sucrose, 20 mM KH_2PO_4 (pH 7.4), 0.1 % BSA (without fatty acids) and mitochondria were precipitated by centrifugation at 11000 g for 10 min.

The rate of mitochondria respiration was measured with the aid of Clarke oxygen electrodes and LP-7 polarograph (Czechia). Mitochon-

dria were incubated in a medium containing 0.4 M sucrose, 20 mM HEPES-Tris buffer (pH 7.2), 5 mM KH_2PO_4, 4 mM $MgCl_2$ and 0.1% BSA, 10 mM mlate + glutamate, pH 7.4. The rate of respiration was expressed in ng-atom O/(mg protein min).

Fatty acid methyl esters (FAMEs) were produced by acidic methanolysis of mitochondrial membrane lipids [10].

FAME identification was performed by gas chromatography-mass-spectrometry (GC-MS) using a Hewlett-Packard-6890 spectrophotometer with a HP-5972 mass-selective detector and the use of retention times [11].

FAME quantification was performed using a Kristall 2000M chromatograph (Russia) with flame-ionization detector and quarts capillary column SPB-1 (50 m x 0.32 mm, a nonpolar phase layer - 0.25 μm). FAME analysis was performed at programmed temperature increase from 120 to 270 oC at the rate of 4 ^{o}C /min. The FAME content in samples was calculated as the ratio of peak area of a corresponding acid to the sum of peak areas of all found FAMEs.

Lipid peroxidation (LPO) activity was assessed by fluorescent method [12]. A fluorescence was recorded in 10-mm quartz cuvettes with a spectrofluorometer (FluoroMaxHoribaYvon, Germany). The excitation wavelength was 360 nm, the emission wavelength was 420--470 nm.

RESULTS. Insufficient watering resulted in 3-fold increase in content of LPO products in pea seedling mitochondrial membranes. The treatment of seeds with a 2 $x10^{-12}$ M melaphen solution decreased the content of LPO products to the control values. Insufficient watering promoted LPO accompanied by modification of the fatty acid composition of pea seedling mitochondrial membranes. Water deficit led to the increase in the relative content of saturated and a decrease in the content of unsaturated fatty acids in mitochondrial membranes of pea seedlings. The relative content of linoleic acid was reduced by 11%, that of linolenic acid -- by 19%. The content of stearic acid increased by 41%, which resulted in the decrease in the total content of C18 unsaturated fatty acids relative to the content of stearic acid from 16.61 ± 0.30 to 10.59 ± 0.20. Similar effect of the water deficit on the fatty acid composition of the mitochondrial membranes from maize, potato, and leaves of *Arabidopsis thaliana* and apricot was observed earlier [6, 13-14]. The authors detected a considerable decrease of the levels of linoleic and linolenic acids and an increase of the level of stearic acid in the membranes. Substantial changes occurred also in the relative content of fatty acids with 20 carbon at-

oms. The pool of 20:2ω6 reduced by 2.7 times, 20:1ω 9 - 1.3 times. At the same time, the content of eicosanoic acid (20:0) increased more than twofold. As a result, the ratio of pool unsaturated fatty acids containing 20 carbon atoms (20:1ω7 + 20:1ω 9) + (20:2ω6) x 2 to eicosanic acid in mitochondrial membrane lipids decreased from 3.65±0.03 to 1.20± 0.16.

The observed alterations possibly influence lipid–protein relation and thus alter the activity of the enzymes associated with the membrane. Indeed, insufficient watering results in a decrease of the maximal rates of NAD-dependent substrates oxidation. The rate of the pair glutamate + malate oxidation in the presence of uncoupling agent (FCCP) drops from 70.0 ± 4.6 down to 48.9 ± 3.2 ng oxygen atom/mg of protein min and the respiratory control rate (RCR) decreases from 2.27 ± 0.1 to 1.7 ± 0.2. The treatment of seeds with a 2×10^{-12} M melaphen solution before germination prevents the alteration of the oxidative phosphorylation efficiency caused by insufficient watering. Besides, the preliminary treatment with melaphen reduces the rates of NAD-dependent substrates oxidation in the presence of ATP or FCCP to the control values. Apparently, the described alterations are related with the physicochemical state of mitochondrial membranes. Indeed the treatment with melaphen protects the unsaturated fatty acid from LPO and prevents thereby from changes in the fatty acid composition of seedling membranes in condition of insufficient watering. In the group of seedlings subjected to insufficient watering combined with melaphen treatment fatty acid composition of mitochondrial membranes was not different from the fatty acid composition of mitochondrial membranes control group. The changes in the fatty acid composition of mitochondrial membranes were accompanied by changes in maximum rates of NAD-dependent substrates oxidation. A decrease in unsaturation coefficient of fatty acids in mitochondrial membranes led to decreasing the rates of NAD-dependent substrates oxidation and efficiency of oxidative phosphorylation.

On the basis of presented data, it may be supposed that a prevention of unsaturated fatty acids peroxidation, in particular C18 and C20 acids in membranes of plant tissues leads to enhancement of plant resistance to insufficient watering. In fact, a close correlation was observed between the unsaturation coefficient of C18 fatty acids in mitochondrial membranes (∑unsaturated C18 fatty acids/ C18:0) and maximum rates of NAD-dependent substrate oxidation (the correlation coefficient r= 0.765). An even greater correlation is observed between the unsaturation coefficient of C20 fatty acids (20:2 ω6) x 2+ 20:1 ω 9+ 20:1 ω 7/20:0) and maximum rates of NAD-dependent substrate oxidation (r= 0.964).

Thus, under condition of insufficient watering, melaphen decreased the intensity of lipid peroxidation in mitochondrial membranes. As a result, the pool of unsaturated fatty acids containing 18 and 20 carbon atoms in the lipid phase of mitochondrial membranes remained unchanged. The prevention of changes in fatty acid composition of mitochondrial membranes affected the bioenergetic indices: there was maintained a high activity of the NADH-dehydrogenase complex of the respiratory chain of mitochondria.

References

1. Shugaeva N.A., Vyskrebentseva E.I., Orekhova S.O., Shugaev A.G.// Plant Physiol. (Rus.), 2007, 54 (3), 373-380.
2. Zhirmunskaya N.M., Shapovalov A.A// Agrokhimiya 1987, 5, 102-119
3. Fattakhov S.G. Reznik V.S., Konovalov A.I// Proceedings of the 13th International Conference on Chemistry of Phosphorus Compounds. Saint-Petersburg. 2002, 80
4. Boyer J.S// Science.1982, 218, 443-448
5. Kizis D., Lumbreras V., Pages M.// FEBS Lett. 2001, 498, 187-189.
6. Junior R.R.M., Oliveira M.S.C., Baccache M.A., de Paula F.M. // Brazilian Arch. Biol. and Technol. 2008, 5, 361-367
7. Sahsah Y, Campos P., Gareil M.// Plant. Physiol. 1988, 104, 577-586
8. Atkin O.K., Macherel D// Ann. Bot. 2009, 103, 581-59.
9. Popov VN, Ruuge E.K., Starkov A.A.// Biohimiya 2003, 68 (7), 910-916
10. Carreau J.P., Dubacq J.P.// J. Chromatogr. 1979, 151б, 384–390.
11. Golovina R.V., Kuzmenko// Chromatogr 1977, 10, 545-546.
12. Fletcher B.I., Dillard C.D., Tappel A.L// Ann. Biochem. 1973, 52, 1–9.
13. Gigon A., Matos A.R., Laffray D., Fodil Y.Z., Thi Anh-Thu Pham//. Ann. Bot. 2004, 94, 345–351
14. Guo Yun-ping, Li Jia-rui.// J. Zhejiang Univ (Agricalt. & Life Sci) 2002, 28, 513–517.

MICROTUBULE DYNAMICS
IN DIFFERENT ZONES OF FIBROBLAST

E.I. Zvorykina, A.V. Tvorogova, T.A. Smirnova, I.A. Vorobjev
Faculty of biology, Moscow State University,
Leninskie Gory 1-12, Moscow, 119991, Russia

Microtubule system is a major component of cytoskeleton. Microtubules have important functions in various cellular processes, such as cell shape formation, cell polarization, and, particularly, motility. Nonetheless, the peculiarities of microtubule dynamics and inner cell space organization are still poorly enlightened. In various cell types microtubules are orga-

nized in a radial array with their minus-ends anchored at the centrosome and their plus-ends extending toward the cell periphery where they are involved in a number of essential cellular events. In mesenchymal cells and neurons microtubules are organized according to cell polarization (Yvon and Wadsworth, 2000 ; de Anda et al., 2010. In fibroblasts and epithelial cells microtubules are radially organized and are known to interact in cell-cell adhesion process (S. Mary et al., 2002 ; Akhmanova et al., 2009). The question of microtubule centers of organization is rather complicated and still unclear. In most cell types the majority of microtubules are formed on centrosome, contrary, previous data showed that low amount of microtubules in fibroblasts are connected with centrosome and are directly nucleated in cytoplasm (Vorobjev et. al., 2000).

In order to reveal details of microtubule dynamical properties we observed microtubules in fibroblasts. The present assay was performed on 3T3 Swiss cell culture. Cells were seeded on glass bottom Petri dishes and transfected with EB1-GFP plasmid. We analyzed microtubule growing plus ends in 10 cells expressing EB1-GFP (70-100 MT tracks in each cell). EB1-GFP movement was analyzed by time-lapse microscopy. All the observed tracks (periods of microtubule growth) were divided into three groups according to their localization in cell's inner space. Tracks that started to grow radially from centrosome were confined as centrosomal region, tracks that started to grow in cytoplasm and ended at 10 µm and more from the cell edges were defined as internal cytoplasm area. Tracks that ended on the leading edge were distinguished to the leading edge area (Figure 1). Tracks that started on the first stack of the video were excluded from further analysis because the beginning of track could not be defined properly. Further analysis of obtained data was performed with imageJ software (NIH imageJ). We determined track length, duration and instantaneous growth rate as dynamic parameters for microtubules.

A portion of tracks that started directly from centrosome grew in a radial way and did not reach the edge of the cell, as well as tracks that started in cytoplasm. Tracks on the leading edge reached the border of the cell and, in some cases, continued growing along the cell's edge. Average parameters±median of dynamic parameters obtained on sedentary cells are presented in table.

The quantification of track length showed relative rates for all the observed cell's areas - 4±3.5 µm. Meanwhile there are some significant variations in velocities and growth period durations measured in the analyzed zones. In 3T3 cells **the most long-lasting tracks** were observed at

Position	Growth period length, µm	Growth rate, µm/min	Growth period duration, sec
centrosomal area	4.1±3.7 (n=103)	12.5±12,1 (n=103)	20.6±20 (n=103)
Internal cytoplasm	3.8±3.4 (n=102)	14.4±4,42 (n=102)	17.6±12 (n=102)
leading edge	5.2±3.9 (n=300)	9.6±14,4 (n=300)	25.7±28 (n=300)

the leading edge (table). Track length was 20% lower in the centrosomal area and 32% lower in the internal cytoplasm (table). The **highest velocity** of microtubule growth was in the internal cytoplasm, growth rates of MTs in centrosomal region are 17% lower and the slowest MT growth rate was at the leading edge (table). The sufficient volume of measurements enabled to obtain significant differences for microtubules in distinguished zones . Significance was evaluated using the Mann - Whitney U-test ($p<0,05$). **Thus we expect different ways of regulation of microtubule dynamics in established zones of fibroblast.**
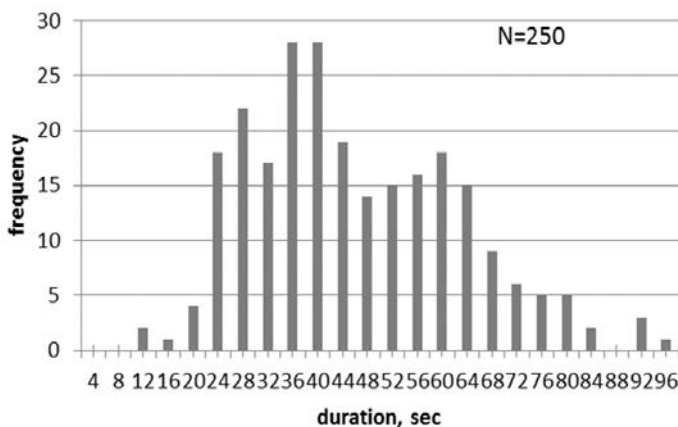
Distribution of MTs growth periods at the leading edge according to their duration. Microtubule growing plus-ends were selectively marked in 3T3 cells. The cells were transfected with EB3-GFP. Transfected protein's movement was visualized by time-lapse microscopy. Stacks were acquired every 4 sec. Microtubules growing directly into the moving lamella were measured. Number of analyzed tracks=250. The histogram of duration distribution in lamella showed two peaks – at 30 sec level and 60 sec level (frequency maximum in these areas). Mean growth period duration is 46.1±36 sec.

Most of the observed cells changed their shape in non-dramatic way, but we've distinguished a group of cells (10 cells expressing EB1-GFP, EB3-GFP or tubulin-GFP) with growing lamella (velocity of retraction over 0.5 µm/min). Using the obtained data we analyzed MT dynamics in protruding lamella by time-lapse microscopy. We observed 10 cells (30-40 tracks in each cell). The mean distance that growing part of the cell passed was 7.35 ±8.2 µm. (Distance was measured during 100 stacks in films). Approximate velocity of protrusion was 0.83±0.9 µm/min. Mean MT growth rate was 11.0±11.3 µm/min that is consistent with the same meaning in sedentary cells (10.8±12.3µm/min respectively). The mean growth period duration rate was 1.5 times higher than in spread-eagled cells (8.0±6.1 µм vs 5.2±3.9 µм). Mean growth period duration was 46.1±36 sec that is 1.7 times higher than in sedentary cells, 25.7±28 sec consistently. **Therefore growing microtubules in protruding lamella demonstrate higher processivity than in sedentary cells despite the same velocity.**

The review of instantaneous growth rate and track allocation showed quite uniform way of distribution, meanwhile track duration distribution demonstrated two peaks – at 30 sec level and 60 sec level (frequency maximum in these areas). (figure).

INDEX OF AUTHORS

TABLE OF CONTENTS

Materials of International Symposium
"Biological motility: new facts and hypotheses"

Научное издание